

**Ecotoxicological and Biodegradation Studies of
Reactive Azo Textile Dyes using Different
Microorganisms**



By

Noshaba Hassan Malik

**Department of Microbiology
Faculty of Biological Sciences
Quaid-i-Azam University
Islamabad Pakistan
2019**

Ecotoxicological and Biodegradation Studies of Reactive Azo Textile Dyes using Different Microorganisms

A thesis submitted in partial fulfillment of the requirements for the
Degree of

Doctor of Philosophy

In

Microbiology



By

Noshaba Hassan Malik

**Department of Microbiology
Faculty of Biological Sciences
Quaid-i-Azam University
Islamabad Pakistan
2019**



*In the name of Allah,
the Most Beneficent,
the Most Merciful*

Dedicated to my

PARENTS

CONTENTS

List of Tables	viii
List of Figures	x
List of Appendices	xiv
List of Abbreviations	xv
Acknowledgements	xvii
Abstract	xix
Chapter 1: Introduction	1
Chapter 2: Literature Review	6
Chapter 3: Organismic-level acute toxicology profiling of reactive azo dyes	44
Chapter 4: Comparison of Immobilized Fungal and Hybrid Activated Sludge Batch Reactors for the Treatment of Metal complex Reactive Azo Dye	81
Chapter 5: Appraisal of different natural bacterial consortia for the treatment of reactive azo dyes	112
Chapter 6: Degradation optimization and kinetics studies for reactive azo dyes by mesophilic and thermophilic bacteria	180
Conclusions	289
Future Prospects	291
References	292
Appendices	321

LIST OF TABLES

Table No.	Title	Page No.
2.1	Classification of dyes based on chromophore group and application	9
2.2	Genotoxicity studies on textile dyes	16
2.3	Cellular and organismic level toxicity studies on textile dyes	18
2.4	Physicochemical methods for dye waste treatment	24
2.5	Studies on dye waste treatment by fungal cultures	34
2.6	Studies on dye waste treatment by bacterial cultures	37
3.1	Chemical structures of reactive azo dyes	46
4.1	Phytotoxic analysis of immobilized fungal reactor samples	102
4.2	Phytotoxic analysis for hybrid activated sludge reactor samples	103
4.3	Acute toxicity analysis for immobilized fungal and hybrid activated reactor	105
5.1	Design factors and coded variables for MBC	118
5.2	Design factors and coded variables for AHBC	119
5.3	Design factors and coded variables for TBC	119
5.4	Barcode and linkers for the natural bacterial consortia	121
5.5	Co-substrate utilization, pH, temperature, dye, and salt tolerance profiles of the natural bacterial consortia	134
5.6	Box-Behnken design layout with observed and actual response values for MBC	138
5.7	Box-Behnken design layout with observed and actual response values for AHBC	139
5.8	Box-Behnken design layout with observed and actual response values for TBC	141
5.9	ANOVA for Quadratic Model of synthetic dye wastewater decolorization by MBC	143
5.10	ANOVA for Quadratic Model of synthetic dye wastewater decolorization by AHBC	143
5.11	ANOVA for Quadratic Model of synthetic dye wastewater decolorization by TBC	144
5.12a	Predicted solutions for model validation and confirmation for MBC	153
5.12b	Predicted solutions for model validation and confirmation for AHBC	153
5.12c	Predicted solutions for model validation and confirmation for TBC	154
5.13	Statistical analysis of pyrosequencing data showing alpha diversity matrices	155
5.14	Dye mixture metabolites detected in GC-MS analysis after treatment with the natural bacterial consortia	167
5.15	Phytotoxic analysis of the reactive azo dye mixture containing synthetic effluent (before and after bacterial treatment)	169
6.1	Bacterial combinations for consortia screening for mesophilic isolates	185
6.2	Bacterial combinations for consortia screening for thermophilic isolates	185

6.3	Design factors and coded variables for mesophilic bacterial coculture	
6.4	Design factors and coded variables for thermophilic bacterial coculture	186
6.5	Strain names for the selected mesophilic and thermophilic isolates	196
6.6	Morphological and biochemical properties of bacterial isolates	198
6.7	Co-substrate utilization, pH, temperature, dye, and salt tolerance profiles of the mesophilic and thermophili bacterial cocultures	210
6.8	Box-Behnken design layout with observed and actual response values for the mesophilic coculture	213
6.9	Box-Behnken design layout with observed and actual response values for the thermophilic coculture	214
6.10	ANOVA for Quadratic Model of synthetic dye wastewater decolorization by Mesophilic coculture	216
6.11	ANOVA for Quadratic Model of synthetic dye wastewater decolorization by Thermophilic coculture	217
6.12	Predicted solutions for model validation and confirmation for the mesophilic coculture	223
6.13	Predicted solutions for model validation and confirmation for the thermophilic coculture	223
6.14	Bacterial Growth and dye degradation constants for the individual dye degradation by mesophilic bacteria	238
6.15	Bacterial Growth and dye degradation constants for the individual dye degradation by the thermophilic bacteria	252
6.16	Bacterial Growth and dye degradation constants for the dye mixture degradation by the thermophilic bacteria	259
6.17	Bacterial Growth and dye degradation constants for dye mixture degradation by the mesophilic bacteria	267
6.18	Dye metabolites detected in GC-MS analysis after treatment with the mesophilic coculture	271
6.19	Dye metabolites detected in GC-MS analysis after treatment with the thermophilic coculture	274
6.20	Phytotoxic analysis of the reactive azo dye mixture containing synthetic effluent (before and after bacterial treatment)	277

LIST OF FIGURES

Figure No.	Title	Page No.
3.1	Dose response curves for <i>P. aeruginosa</i>	54
3.2	Dose response curves for <i>E. coli</i>	55
3.3	Dose response curves for <i>K. pneumoniae</i>	56
3.4	Dose response curves for <i>S. aureus</i>	57
3.5	Dose response curves for <i>L. monocytogenes</i>	58
3.6	Dose response curves for <i>B. subtilis</i>	59
3.7	Effective dye concentrations (EC20, EC50, and EC80)	60
3.8	Dose response curves for <i>T. asperellum</i>	62
3.9	Dose response curves for <i>A. flavus</i>	63
3.10	Dose response curves for <i>F. fujikuroi</i>	64
3.11	Dose response curves for <i>R. solani</i>	65
3.12	Effective dye concentrations (EC20, EC50, and EC80)	66
3.13	Dose response curves for <i>R. sativus</i> seeds	68
3.14	Dose response curves for <i>T. aestivum</i> seeds	69
3.15	Dose response curves for <i>S. bicolor</i> seeds	70
3.16	Dose response curves for <i>P. mungo</i> seeds	71
3.17	Effective dye concentrations (EC20 and EC50)	72
3.18	Dose response curves for <i>A. salina</i> larvae	74
3.19	Effective dye concentrations (EC20, EC50, and EC80)	75
4.1	a) Schematic diagram of immobilized fungal reactor; b) Schematic diagram of hybrid activated sludge reactor	86
4.2	Color removal performance of (a) Immobilized fungal reactor, (b) Hybrid activated sludge reactor	91
4.3	COD removal performance of (a) Immobilized fungal reactor, (b) Hybrid activated sludge reactor	93
4.4	pH variation in the synthetic dye wastewater (a) Immobilized fungal reactor, (b) Hybrid activated sludge reactor	95
4.5	FTIR overlay spectrum of synthetic dye wastewater (before and after treatment), (a) Immobilized fungal reactor, (b) Hybrid activated sludge reactor	97
4.6	(a) suspended and attached bacterial count in the hybrid activated sludge reactor batches, (b) Attached to total bacterial count ratio in the hybrid activated sludge reactor batches	99
5.1	Decolorization performance of the natural consortia under static and shaking conditions	123
5.2	Decolorization performance of MBC, AHBC, and TBC for the synthetic dye effluent, in the presence of different carbon sources (0.1% [w/v])	128
5.3	Decolorization performance of MCB, AHBC, and TBC for the synthetic dye effluent, in the presence of different nitrogen sources (0.1% [w/v])	129
5.4	Decolorization performance of MBC, AHBC, and TBC for the synthetic dye effluent, at different temperatures	130
5.5	Decolorization performance of MBC, AHBC, and TBC for the synthetic dye effluent, at different initial pH	131

5.6	Decolorization performance of MBC, AHBC, and TBC for the synthetic dye effluent, at different initial dye concentrations	132
5.7	Decolorization performance of MBC, AHBC, and TBC for the synthetic dye effluent, at different NaCl concentrations (% [w/v])	133
5.8	The normal % probability vs. studentized residuals plots	145
5.9	Box-Cox plots of model transformation	146
5.10	Response surface plots showing interactions of pH and temperature for the synthetic dye wastewater decolorization by MBC	149
5.11	Response surface plots showing interactions of dye concentration and temperature for the synthetic dye wastewater decolorization by MBC	149
5.12	Response surface plots showing interactions of dye concentration and pH for the synthetic dye wastewater decolorization by MBC	149
5.13	Response surface plots showing interactions of pH and temperature for the synthetic dye wastewater decolorization by AHBC	150
5.14	Response surface plots showing interactions of dye concentration and temperature for the synthetic dye wastewater decolorization by AHBC	150
5.15	Response surface plots showing interactions of salt concentration and temperature for the synthetic dye wastewater decolorization by AHBC	150
5.16	Response surface plots showing interactions of dye concentration and pH for the synthetic dye wastewater decolorization by AHBC	151
5.17	Response surface plots showing interactions of salt concentration and pH for the synthetic dye wastewater decolorization by AHBC	151
5.18	Response surface plots showing interactions of salt concentration and dye concentration for the synthetic dye wastewater decolorization by AHBC	151
5.19	Response surface plots showing interactions of pH and temperature for the synthetic dye wastewater decolorization by TBC	152
5.20	Response surface plots showing interactions of dye concentration and temperature for the synthetic dye wastewater decolorization by TBC	152
5.21	Response surface plots showing interactions of dye concentration and pH for the synthetic dye wastewater decolorization by TBC	152
5.22	Rarefaction plots for natural bacterial consortia	156
5.23	Phylum level relative abundance (%) in natural bacterial consortia	159
5.24	Class level relative abundance (%) in natural bacterial consortia	159
5.25	Genus level relative abundance (%) in natural bacterial consortia	160
5.26	Color reduction performance of the natural bacterial consortia	162
5.27	COD reduction performance of the natural bacterial consortia	162
5.28	pH variation in the synthetic dye wastewater treated by the natural bacterial consortia	162
5.29	FTIR spectra of synthetic dye wastewater	166
5.30	Effect of the synthetic textile wastewater on Brine shrimp larvae (before and after bacterial treatment)	170
6.1	Comparison of mesophilic bacterial isolates for the decolorization of a reactive azo dye mixture containing synthetic textile effluent under static and shaking conditions	195

6.2	Comparison of thermophilic bacterial isolates for the decolorization of a reactive azo dye mixture containing synthetic textile effluent under static and shaking conditions	196
6.3	Neighbor-joining phylogenetic tree of the mesophilic reactive azo dye mixture decolorizing bacterial isolates	199
6.4	Neighbor-joining phylogenetic tree of the thermophilic reactive azo dye mixture decolorizing bacterial isolates	200
6.5	Effect of different coculture combinations of the selected bacterial isolates on the decolorization of reactive azo dye mixture containing synthetic textile effluent under static condition	202
6.6	Decolorization performance of the Mesophilic and Thermophilic bacterial cocultures for the synthetic dye effluent, in the presence of different carbon sources (0.1% [w/v])	206
6.7	Decolorization performance of the Mesophilic and Thermophilic cocultures for the synthetic dye effluent, in the presence of different nitrogen sources (0.1% [w/v])	206
6.8	Decolorization performance of Mesophilic and Thermophilic bacterial cocultures for the synthetic dye effluent, at different temperatures.	207
6.9	Decolorization performance of the Mesophilic and Thermophilic cocultures for the synthetic dye effluent, at different initial pH	207
6.10	Decolorization performance of the Mesophilic and Thermophilic cocultures for the synthetic dye effluent, at different initial dye concentrations (ppm)	208
6.11	Decolorization performance of the Mesophilic and Thermophilic cocultures for the synthetic dye effluent, at different NaCl concentrations (% [w/v])	208
6.12	The normal % probability vs. studentized residuals plots for the Mesophilic and Thermophilic	218
6.13	Box-Cox plots of model transformation for the decolorization of synthetic dye wastewater by the Mesophilic and Thermophilic cocultures	219
6.14	Response surface plots showing interactions of pH and temperature for the synthetic dye wastewater decolorization by the Mesophilic coculture	221
6.15	Response surface plots showing interactions of dye concentration and temperature for the synthetic dye wastewater decolorization by the Mesophilic coculture	221
6.16	Response surface plots showing interactions of dye concentration and pH for the synthetic dye wastewater decolorization by the Mesophilic coculture	221
6.17	Response surface plots showing interactions of pH and temperature for the synthetic dye wastewater decolorization by the thermophilic coculture	222
6.18	Response surface plots showing interactions of dye concentration and temperature for the synthetic dye wastewater decolorization by the thermophilic coculture	222
6.19	Response surface plots showing interactions of dye concentration and pH for the synthetic dye wastewater decolorization by the thermophilic coculture	222

6.20	Growth and degradation by <i>P. aeruginosa</i> NHS1 for RB 221 dye	226
6.21	Growth and degradation by <i>P. aeruginosa</i> NHS1 for RR 195 dye	227
6.22	Growth and degradation by <i>P. aeruginosa</i> NHS1 for RY 145 dye	228
6.23	Growth and degradation by <i>Pseudomonas</i> sp. NHS2 for RB 221 dye	229
6.24	Growth and degradation by <i>Pseudomonas</i> sp. NHS2 for RR 195 dye	230
6.25	Growth and degradation by <i>Pseudomonas</i> sp. NHS2 for RY 145 dye.	231
6.26	Growth and degradation by <i>Escherichia</i> sp. NHS3 for RB 221 dye	232
6.27	Growth and degradation by <i>Escherichia</i> sp. NHS3 for RR 195 dye	233
6.28	Growth and degradation by <i>Escherichia</i> sp. NHS3 for RY 145 dye	234
6.29	Growth and degradation by <i>E. coli</i> NHS4 for RB 221 dye	235
6.30	Growth and degradation by <i>E. coli</i> NHS4 for RR 195 dye	236
6.31	Growth and degradation by <i>E. coli</i> NHS4 for RY 145 dye	237
6.32	Growth and degradation by <i>A. pallidus</i> NHT1 for RB 221 dye.	240
6.33	Growth and degradation by <i>A. pallidus</i> NHT1 for RR 195 dye	241
6.34	Growth and degradation by <i>A. pallidus</i> NHT1 for RY 145 dye	242
6.35	Growth and degradation by <i>Aeribacillus</i> sp. NHT2 for RB 221 dye	243
6.36	Growth and degradation by <i>Aeribacillus</i> sp. NHT2 for RR 195 dye	244
6.37	Growth and degradation by <i>Aeribacillus</i> sp. NHT2 for RY 145 dye	245
6.38	Growth and degradation by <i>Geobacillus</i> sp. NHT3 for RB 221 dye	246
6.39	Growth and degradation by <i>Geobacillus</i> sp. NHT3 for RR 195 dye	247
6.40	Growth and degradation by <i>Geobacillus</i> sp. NHT3 for RY 145 dye	248
6.41	Growth and degradation by <i>Brevibacillus borstelensis</i> NHT4 for RB 221 dye.	249
6.42	Growth and degradation by <i>Brevibacillus borstelensis</i> NHT4 for RR 195 dye.	250
6.43	Growth and degradation by <i>Brevibacillus borstelensis</i> NHT4 for RY 145 dye.	251
6.44	Growth and degradation by <i>A. pallidus</i> NHT1 for the dye mixture.	254
6.45	Growth and degradation by <i>Aeribacillus</i> sp. NHT2 for the dye mixture.	255
6.46	Growth and degradation by <i>Geobacillus</i> sp. NHT3 for the dye mixture	256
6.47	Growth and degradation by <i>Brevibacillus borstelensis</i> NHT4 for the dye mixture.	257
6.48	Growth and degradation by the thermophilic coculture for the dye mixture.	258
6.49	Growth and degradation by <i>P. aeruginosa</i> NHS1 for the dye mixture.	262
6.50	Growth and degradation by <i>Pseudomonas</i> sp. NHS2 for the dye mixture.	263
6.51	Growth and degradation by <i>Escherichia</i> sp. NHS3 for the dye mixture.	264
6.52	Growth and degradation by <i>E. coli</i> NHS4 for the dye mixture	265
6.53	Growth and degradation by the mesophilic coculture for the dye mixture	266
6.54	FTIR spectra of synthetic (dye mixture containing) wastewater	269
6.55	Effect of the synthetic textile wastewater on Brine shrimp larvae (before and after bacterial treatment)	278

LIST OF APPENDICES

Appendix	Page No.
Appendix 1	321
Appendix 2	337
Appendix 3	338
Appendix 4	341

LIST OF ABBREVIATIONS

Abbreviation	Complete form	Abbreviation	Complete form
(NH ₄) ₂ SO ₄	Ammonium sulphate	MnCl ₂ .4H ₂ O	Manganese chloride tetrahydrate
ATR	Attenuated Total Reflectance	MR	Methyl red
C	Celsius	R ²	Determination coefficient
CaCl ₂ .2H ₂ O	Calcium chloride dihydrate	ANOVA	Analysis of variance
CdCl ₂	Cadmium chloride	N. A	Nutrient Agar
CoCl ₂ .6H ₂ O	Cobalt chloride hexahydrate	COD	Chemical Oxygen Demand
CuCl ₂ .2H ₂ O	Cupric chloride dihydrate	Na ₂ HPO ₄	disodium hydrogen phosphate
		Na ₂ MoO ₄ .2H ₂ O	Sodium molybdate dihydrate
Fig.	Figure	NaCl	Sodium chloride
Fe(NH ₄) citrate	Iron ammonium citrate	NaNO ₂	Sodium nitrite
FTIR	Fourier transform Infrared Spectroscopy		
H ₃ BO ₃	Boric acid	OD	Optical density
HgCl ₂	Mercuric chloride		
h.	Hours	ppm	Parts per million
		RB 221	Reactive Blue 221
KH ₂ PO ₄	Potassium dihydrogen phosphate	RR 195	Reactive Red 195
KNO ₃	Potassium nitrate	RY 145	Reactive Yellow 145
L	Liter	OTU	Operational taxonomic unit

RSM	Response surface Methodology	PD	Phylogenetic diversity
mg	Milligram	GC-MS	Gas Chromatography and Mass Spectrometry
MgSO ₄	Magnesium sulphate	MBC	Mesophilic bacterial consortium
mL	Milliliter	AHBC	Alkaliphilic and halotolerant bacterial consortium
UV-Vis spectrophotometer	UV-Visible Spectrophotometer	TBC	Thermophilic bacterial consortium
VP	Voges-proskauer	STW	Synthetic textile wastewater
ZnSO ₄ .7H ₂ O	Zinc sulphate heptahydrate	TSTW	Treated synthetic textile wastewater
λ_{\max}	Lambda maximum	EC	Effective concentration
μm	Micrometer		
T.E. Solution	Trace elements Solution	SIM	Sulfide Indole Motility
TSI	Triple sugar iron	sp.	Species
UV	Ultraviolet	BBD	Box-Behnken design
%	Percentage	OFAT	One factor at a time
rpm	Revolutions per minute	kg	Bacterial growth constant
SD	Standard deviation	kc/ kc'	Degradation constant
cm	Centimeter	t	Time
cm ⁻¹	Per centimeter	h ⁻¹	Per hour

Acknowledgements

“All Praises to Almighty Allah, The Light of Heavens and Earths, the omnipotent, the most compassionate and His Prophet Muhammad (S.A.W) The Most perfect among all human beings ever born on the surface of earth, who is forever a source of guidance and knowledge for the humanity as a whole.

*I feel great pleasure in expressing my ineffable thanks to my encouraging and inspirational supervisor **Dr. Naeem Ali**, Associate professor, Department of Microbiology, Quaid-i-Azam University Islamabad, whose personal interest, thought provoking guidance, valuable suggestions and discussions enabled me to complete this work,*

*I would like to express my deep gratitude to **Dr. Heidi L. Gough**, Associate Research Professor, Civil and Environmental Engineering, University of Washington, Seattle, USA for her valuable and constructive suggestions and guidance during my research stay at the Department of CEE.*

*It is a matter of immense pleasure for me to express my sincerest feelings of gratitude to all the faculty members of the Department of Microbiology, Quaid-i-Azam University Islamabad, especially, **Prof. Dr. Abdul Hameed**, **Dr. Rani Fayal** (Chairperson Dept. of Microbiology) **Dr. Safia Ahmed**, **Dr. Fariha Hasan**, **Dr. Malik Badshah**, **Dr. Muhammad Imran**, **Dr. Muhammad Ishtiaq Ali**, **Dr. Asif Jamal**, **Dr. Rabaab Zahra** for their cooperative attitude and humble guidance throughout my stay in the department of Microbiology.*

*I deem it utmost pleasure to express my heartiest gratitude to my amiable lab fellows at the Dept. of Microbiology, QAU and Dept. of CEE, UW for their kind support, and care which helped me put-up with all the challenges encountered during my research work and for their pleasant companionship. Especially I will not forget the great role of **Hajira Zain**, **Misbah Khan**, **Farhan Ahmed Chisti**, **Elizabeth Guilford**, **Sterling Bath**, and **Keenan Ferar** who facilitated me by helping me with my*

experiments during the lab work, I am indeed humbly grateful to them for their kind attitude, most cooperative affectionate behavior, and moral help.

At the same time, I will pay my special thanks to all my friends and colleagues for their care and honest support that enabled me to complete this hard job. I feel great pleasure in expressing my heartiest thanks to my dearest friends and lab fellows: Abdul Wahab Ajmal, Maliha Ahmed, Anum Munir Rana, Shama Zainab, Mahtwish Malik, Iqra Sharafat, Zargona Zafar, Nicollete Zhou, Bryce Figdore, Shuang Young, Songlin, Chris Callahan, Qurat-ul-Ain Rana, Hammad Ismail, Awais Khan, Sadia Mehmood Satti, Maria Abdul Salam, Leena Mavis Cycil, Zara Razaque, Mohsin Gulzar Barq, Farook Ahmed, Sabba Kyani, Irum Iqrar, Irum Naqvi, and Farwa Rubab, who shared all my sorrows and happiness, and for being there whenever I needed any help. I wish to record my deep sense of gratitude and sincere thanks to them. Special thanks are for the lab attendants, lab managers, and the staff members of both departments.

*Last but not the least, I am highly indebted to my **Parents**, their continuous support, positive attitude and encouragement greatly motivated me throughout my educational career. They prayed for me, shared the burdens and made sure that I sailed through smoothly. Even through the toughest times of their lives, they were always there for me with warmest smiles and utmost love.*

*I thank again **ALMIGHTY ALLAH**, who listens and responds to my every prayer.*

Noshaba Hassan Malik

Abstract

Reactive azo dyes are one of the most extensively used dyeing agents in the textile industry. Representatives of this class of dyes containing sulfonic acid derivatives, are usually more persistent in the aquatic environments due to their high water-solubility and complex polyaromatic nature. Due to the xenobiotic, possible toxic, and recalcitrant nature, these dyes act as one of the major environmental hazards that can adversely affect the aquatic ecology. The assessment of their toxicity in different living systems is therefore vital to document their possible role in the ecological milieu. Biological dye waste treatment strategies, employing pure or mixed microbial cultures in suspended and/or attached forms, is usually deemed as an effective, economically sustainable, and eco-efficient approach. Moreover, for the complex heterogenic natured textile effluents, application of microbes with a more adaptive physiological profile (such as the extremophilic bacteria) could provide a more workable solution. In the present sets of studies, ecotoxicity assessment and biotreatment investigations for three model reactive azo dyes i.e., Reactive Blue 221 (RB 221), Reactive Red 195 (RR 195), and Reactive Yellow 145 (RY 145) (pure and/or mixed form) were carried out using specialized microorganisms from different environmental origins in lab scale attached and suspended reactors. Treatment and detoxification efficiencies were monitored through analytical techniques and toxicity assays.

Organismic-level acute toxicology profile of three reactive azo dyes and their mixture was investigated, by using bacterial (*Pseudomonas aeruginosa*, *Escherichia coli*, *Klebsiella pneumoniae*, *Staphylococcus aureus*, *Listeria monocytogenes*, and *Bacillus subtilis*), fungal (*Trichoderma asperellum*, *Aspergillus flavus*, *Fusarium fujikuroi*, and *Rhizoctonia solani*), plant (*Raphanus sativus*, *Triticum aestivum*, *Sorghum bicolor*, and *Phaseolus mungo*), and aquatic (*Artemia salina* and *Daphnia magna*) specimens. Microbial test organisms (all the six bacteria and two fungi, i.e., *T. asperellum* and *A. flavus*) and *D. magna* were found to be relatively more sensitive towards the reactive azo dyes and their mixture, as the EC₅₀ values were in the range of 80-330, 135-360, and 108-242 ppm for bacteria, fungi, and *D. magna*, respectively (generally the effect was not acutely toxic). Moreover, the dye mixture had a comparable effect to the individual dyes in almost all the tested microbial specimens. For plant seeds, the dye mixture was found to be relatively more inhibitory towards *T. aestivum* and *R. sativus* than the individual dyes. For *S. bicolor* and *P. mungo* seeds, the effect of the dye mixture was almost identical to the individual dyes. However, in all cases, EC₅₀ values were in the range of 950-3500 ppm, which indicates a non-toxic effect on plant seed germination potential. Likewise, the dyes and their mixture were not acutely toxic for the aquatic test specimens.

Efficacy of an immobilized fungal (*Trichoderma asperellum* SI14) and a hybrid activated sludge reactor was evaluated and compared in batch mode for the treatment of RB 221 containing synthetic textile wastewater. Scotch Brite™ was used as support material in both setups; and the reactors' efficacy was tested at 25, 50, and 100 ppm of RB 221 over a period of 144 hours. Both types of reactors showed 90-98% color removal with a relatively faster reduction observed with the immobilized fungal reactor (50-90% reduction in 48 hours of reactor operation in all the three batches). However, the hybrid activated sludge reactor was found to be more efficient in chemical oxygen demand (COD) reduction (79-92%) and demonstrated a smooth decline as compared to the fungal reactor, where 73-83% reduction was observed with spells of highs and lows during the treatment. Moreover, the hybrid activated sludge system showed a stable performance in terms of pH maintenance as compared to the immobilized fungal reactor, where drastic pH alterations were observed. Furthermore, a trend towards increased attached active bacterial biomass on the support material was observed through the successive batches. Biodegradation of the dye was confirmed through FTIR band changes. Both reactors did not produce toxic dye metabolites, as indicated by the phytotoxicity and brine shrimp acute toxicity analyses.

Three enriched natural bacterial consortia (obtained from different locations) with different temperature, pH, and salt tolerance profiles [mesophilic [MBC], thermophilic [TBC], and alkaliphilic-halotolerant [AHBC]], were investigated for the treatment of a reactive azo dye mixture containing synthetic textile effluent. Based on the results of single factor optimization studies, the decolorization potential of the consortia was further optimized using Response Surface Methodology through Box-Behnken design (BBD). The models' adequacy was confirmed through ANOVA, determination constant values and validation experiments. The consortia efficiently removed the dye mixture (100 ppm; glucose [sucrose for TBC], and yeast extract, 0.1% [w/v] each as co-substrates) in 72 (MBC and AHBC) and 120 hours (TBC) from the synthetic effluent under the optimal conditions. For MBC and AHBC, maximum activity was observed around mesophilic temperature conditions i.e., 35.51 and 34.93 °C, respectively; while 50.81 °C was found as the suitable temperature for TBC. The optimal pH for both types of consortia was neutral. However, with AHBC the dye mixture effluent was decolorized, under high pH (10.08) and salinity (10.68% [w/v]) conditions. Additionally, up to 70% COD reduction was observed with all the three consortia in ~144 hours. Through 454-pyrosequencing, a complex community of anaerobic, facultative, and aerobic bacteria with some efficient dye degraders were found in all the three consortia.

Bacteria with different temperature tolerance abilities (mesophilic and thermophilic) were isolated for the treatment of reactive azo dyes. Through the biochemical and molecular

characterization (16S rRNA gene analysis) the mesophilic isolates were identified as: *Pseudomonas aeruginosa* NHS1, *Pseudomonas* sp. NHS2, *Escherichia* sp. NHS3, and *Escherichia coli* NHS4. The thermophilic isolates were: *Aeribacillus pallidus*, *Aeribacillus* sp., *Geobacillus* sp. NHT3, and *Brevibacillus borstelensis* NHT4. Cocultures were designed and optimized through OFAT and RSM using BBD design layout. The mesophilic and thermophilic cocultures decolorized the 100 and 50 ppm dye mixture in the presence of co-substrates (0.1% [w/v] yeast extract and glucose, each) in 24 and 48 hours, respectively. The mesophilic coculture showed optimal performance at temperature: 34.75 °C, pH: 7.69, and dye concentration: 111 ppm. Whereas, 50.25 °C, 7.31, and 60 ppm, were the most suitable temperature, pH, and dye concentration values for the dye removal by the thermophilic coculture. Through first order kinetics, growth and degradation rates for the individual and mixed dyes were computed and modeled, which showed one phasic growth and degradation process except for the dye mixture removal by the mesophilic pure cultures and coculture, where a two-phasic dye removal system was involved. Furthermore, mesophilic bacteria were relatively more efficient and showed a higher dye tolerance than the thermophiles. Biodegradation analysis of the treatment systems involving natural and designed consortia was done through FTIR spectral and GC-MS analyses. With the natural consortia, the dye mixture was converted to low molecular weight long chained aliphatic and aromatic compounds. However, the cocultures (designed consortia) converted the individual dyes and their mixture into low molecular weight aliphatic and aromatic products. The metabolites produced from both the natural and designed consortia were not toxic towards plant seeds and brine shrimp larvae, which confirms the eco-safety of these treatment methods.

Environmental pollution is one of the most critical issues of the modern-day world. To cope with the constantly increasing needs of expanding human population, advancements in agriculture, medicine and various industrial fields are inevitable (Sarayu and Sandhya, 2012; Khan et al., 2013). All such activities, done for the sake of mankind facilitation have some associated pitfalls and result in the generation of different pollutants which mutilate the air, water and soil ecosystems (Ali 2010). Water pollution results from the release of improperly treated municipal and industrial wastewater (Chan et al. 2009). Such wastewaters add organic and inorganic load in receiving water bodies, indicated by different analytical parameters *e.g.*, color, smell, pH, total solid content, Biochemical Oxygen Demand (BOD), Chemical Oxygen demand, Total Organic Carbon (TOC) and various inorganic species (Solís et al., 2012). Industrial effluents are usually referred to as high strength wastewaters because the contaminants concentrations found in such effluents are higher than that found in municipal wastewater (Hamza, Iorhemen, and Tay 2016). The contaminants nature and concentrations vary depending upon the type of industrial operations (Basha et al. 2011). Textile industries hold a very promising position among different industrial units and are among the greatest generators of polluted water due to the extensive water usage during textile processing procedures (Kalyani et al. 2008).

Discharge of untreated and/or inadequately treated colored wastewater from the textile facilities poses serious threats to aquatic community by altering the dissolved oxygen levels, due to the reduced photosynthetic activity resulting from sunlight obstruction (Kuberan et al. 2011). Moreover, most of the textile dyes and their products have been documented to have toxic and mutagenic effects (Pielesz et al. 2002). Compounds like aniline, dioxin and heavy metals such as copper and chromium are frequently used in the manufacture of azo, triphenylmethane and copper complex dyes (Hunger and Wiley-vch 2003). These and variety of other compounds (known as aromatic amines) when released into the environment, following breakdown of the complex dye molecules, can act as toxicants, mutagens as well as hormone disruptors (Beall 2011). Several types of intrinsic and extrinsic factors affect the toxicity profile of dyes. Intrinsic factors include the chemical structure of dyes and their interaction with metabolic machinery of the living systems while oxygen availability, moisture content, availability of light and inorganic electron shuttles are some major extrinsic factors

(Rawat, Mishra, and Sharma 2016). All these factors accentuate the application of toxicity evaluation procedures for the assessment of short and long- term impacts of dye waste on receiving water bodies and living organisms, so that pollutants concentrations in the effluents can be properly regulated (Novotný et al., 2006; Mathur et al., 2012). Toxicity estimation studies are usually conducted at different levels of biological organization *e.g.*, molecular, cellular, and organismic-level to encompass the overarching effect of a given compound in the ecosystem (Ventura-camargo and Marin-morales, 2013; Rawat et al., 2016). Textile dyes have complex structure consisting of polycyclic aromatic rings and different types of functional groups which confer chemical stability. The chemical stability of dye waste makes the treatment process more arduous (Prasad and Rao, 2010). Dye waste treatment can be achieved through physical, chemical and biological means (Wang et al. 2010). Choice of the treatment method depends on factors such as: dye removal efficacy, ecoefficiency and economic and technical feasibility (McMullan et al. 2001). Physical methods include adsorption, filtration, and coagulation-flocculation; while oxidation, photooxidation, electrochemical oxidation, and Fenton process are some of the important chemical dye treatment strategies. These methods have a number of limitations such as elevated cost, inefficiency in terms of complete dye removal in some cases and secondary sludge production that requires additional treatment prior to disposal (Saratale et al. 2011).

Biological transformation of dyes using microorganisms is a method of choice nowadays due to a number advantages over physicochemical treatment procedures (Pearce, Lloyd, and Guthrie 2003). Biological dye removal process is relatively a specific, cost effective, and eco-friendly approach (Pandey, Singh, and Iyengar 2007). Different types of microbial systems utilizing bacteria, fungi, yeast and algae have been explored for textile dye treatment (Ali 2010). These microorganisms can partially and in some cases completely transform the dyes under certain environmental conditions (Ong et al. 2011). Microbial dyes transformation processes involve biosorption and/or enzymatic degradation (R. L. Singh, Singh, and Singh 2015). The process can be aerobic, anaerobic, anoxic or facultative depending upon the type of microorganisms involved. The treatment method can also employ a combination of these conditions for complete and efficient removal of textile dyes (Solís et al., 2012).

Fungi and bacteria are two of the most important microbial agents in the perspective of textile dye treatment (Robinson et al., 2001; Pearce et al., 2003). Fungi contain a diverse enzymatic profile consisting of different non-specific extracellular oxidoreductive enzymes such as oxidases, peroxidases (manganese peroxidase and lignin peroxidase) and laccases that can break down a variety of complex aromatic structures under aerobic environment (Rodríguez Couto 2009). Dead fungal biomass can also be utilized for textile dye removal as in that case nutrition supply is not needed for culture maintenance which makes the overall operation relatively easier and biomass regeneration capability is also improved due to efficient decoupling of adsorbed dye molecules from the dead fungal biomass (Fu and Viraraghavan, 2001). Fungal dye removal efficiency can also be enhanced through immobilization which increases the culture stability and facilitates culture reutilization in repeated treatment cycles, therefore, fungal bioreactors based on attached biomass can perform better than those based on suspended cultures (Moreira, Feijoo, and Lema 2004).

Bacteria are usually considered as a better option for dye waste treatment due to their faster growth rates and more adaptive physiological profile (Ali, 2010). Bacterial dye transformation involves different types of azo-reductases (oxygen sensitive and insensitive) and some oxidative enzymes (Solís et al., 2012). Anaerobic and anoxic conditions usually result in incomplete transformation of dyes to aromatic amines which have toxic and mutagenic effects (Pielesz et al. 2002). Further transformation of such amines require aerobic conditions, therefore requires sequential treatment that can be done by using bacteria with different oxygen requirements or facultative bacteria (Tan 2001). Bacterial bioreactors that employ integrated aerobic and anaerobic conditions using physical or temporal separation strategies can carry out efficient dye removal (Jonstrup et al. 2011). Moreover, bacterial wastewater treatment ability is usually harnessed in bioreactor systems employing suspended [activated sludge process (Kumar et al. 2014), sequencing batch reactors (Mirbolooki, Amirnezhad, and Pendashteh 2017), anaerobic, and aerobic digesters (Hamza et al. 2016)] and attached [immobilized fungal reactors (Moreira et al. 2004), Packed bed reactor {PBR}(Ruiz-Arias et al. 2010) , trickle bed {trickling filter systems}(Irum et al. 2015), fluidized bed reactors {FBR}(Lin et al. 2010), rotating biological contactors {RBCs} (Hassard et al.

2015) and biofilm-based systems (Castro, Bassin, and Dezotti 2017).. In addition to these, hybrid activated sludge reactors

employ a combination of suspended and attached biomass (Riffat, 2013).

Furthermore, mixed and co-cultures of bacteria provide a better solution in this regard as efficient and complete dye removal can be achieved through the community degradation process (Joshi et al. 2010). Bacterial dye degradation processes are affected by various physiological parameters of which pH, temperature, and salinity play a pivotal role in the development of efficient treatment systems (Ali 2010; Sarayu and Sandhya 2012). However, most of the dye degrading bacteria reported in literature, function under neutral pH, mesophilic temperatures and salinity-free conditions. Such bacteria may fail to perform in real textile wastewaters, that have alkaline pH, high temperature, and increased salt load (Amoozegar et al. 2011). This problem can be overcome by the application of extremophilic bacteria that can tolerate harsh environmental conditions. Multiple reports on the application of halotolerant and/or halophilic and alkaliphilic bacteria for the treatment of different types of dyes are available (Khalid et al. 2012; Khalid, Arshad, and Crowley 2008a; Prasad and Rao 2013), though few studies have focused on pure bacterial cultures under combined high pH and saline conditions (Bhattacharya, Goyal, and Gupta 2017). Additionally, thermophilic bacteria are the least explored entities in this regard (Deive et al. 2010). Despite the extensive literature on specialized dye decoloring bacteria, very few studies have focused on the kinetics of dye removal process (Karunya et al., 2014; Durruty et al., 2015; Das and Mishra, 2017; Sudha et al., 2018). Such studies, focusing on temporal monitoring of microbial growth and fate of xenobiotics in batch reactor systems provide a conceptual framework and insight into the degradation process (Kova and Egli 1998). Therefore, such knowledge is necessary to develop and model better treatment approaches. In view of all these aspects regarding the likely toxic effects, heterogenic and complex nature of textile effluents, present set of studies focused on the organismic-level toxicity evaluation, efficiency assessment of an immobilized and a hybrid reactor, followed by the application of indigenous and extremophilic dye decolorizing natural and designed consortia along with the detailed kinetic assessment of the color removal process by the latter.

1.1 Aims and Objectives

Generalized aims of the present study were to assess the ecotoxicity of reactive azo dyes; and evaluate the dye degradation potential of different microorganisms in attached and suspended batch reactor systems. Specific objectives of the present study were:

- To develop the organismic-level toxicology profile of reactive azo dyes (Reactive Blue 221, Reactive Red 195, and Reactive Yellow 145, and reactive azo dyes mixture) via microbial growth inhibition, phytotoxicity, and invertebrate toxicity assays.
- To design, fabricate, evaluate, and compare the performance of immobilized fungal and bacterial bench scale batch reactor for the treatment of reactive azo dye containing simulated textile effluent.
- To optimize the treatment potential of different natural bacterial consortia (mesophilic, alkaliphilic and halotolerant, and thermophilic) for reactive azo dyes using Response Surface Methodology and bacterial community analysis through 454-Pyrosequencing.
- To evaluate the treatment efficiency of different designed bacterial consortia (mesophilic and thermophilic) for the treatment of reactive azo dyes
- To investigate the dye removal kinetics with reference to the bacterial biomass growth and dye degradation rates using first order kinetics.
- To assess the degradation products using analytical techniques (FTIR and GC-MS).
- To evaluate the ecoefficiency of the treatment procedures via different organismic-level toxicity assays.

The increase in human population is associated with a surge in industrialization for the fulfilment of daily needs that is concomitantly leading to environmental deterioration (Aravind et al. 2010). The air-, water-, and soil-based ecosystems are being degraded by the wastes generated by industries. Textile industries hold a very important place among different types of industrial units as clothing is one of the basic needs of human beings (Khan et al. 2013). Textile industries consume large volumes of water during the textile dyeing and finishing processes, *e.g.*, about 200 L of water is consumed by an average sized textile unit for every kg of the fabric processed per day. According to the figures provided by the World Bank, ~17-20% of industrial wastewater is produced from the textile dyeing and finishing procedures (Holkar et al. 2016). Type of machinery, dyeing and processing techniques, raw materials and fabric type are the core factors that determine the final composition of textile effluent (Basha et al. 2011). Textile waste constitutes of myriad of pollutants such as acids, alkalis, hydrogen peroxide, surfactants, starch, metals, high salt load and different types of synthetic dyes, which in most of cases, are not properly treated before release into surface waters (Sarayu and Sandhya 2012). Disposal of inadequately treated textile waste into streams, rivers and other water bodies, pollutes the receiving water systems that damages aquatic communities and hence is a matter of grave environmental concern (Kabra et al. 2011).

2.1 Synthetic dyes

The term dye can be defined as a compound that adheres and imparts color to a given substrate. The use of dyes dates back to 2000 BC when natural color compounds were more common. A breakthrough in the history of dyes was the accidental discovery of a synthetic dye, Mauveine in 1856 by William Henry Perkin. Since then, myriad types of synthetic dyeing agents have been developed that have occupied an integral position in present day socio-economic fabric (Holme 2006). Textile industries are one of the major consumers of synthetic dyes that are mostly obtained from coal-tar and petroleum-based intermediates (Hunger and Wiley-vch 2003). The main structural components of synthetic colorants are chromophores and auxochromes. Chromophores consist of conjugated double bonds with a delocalized electron cloud. These are the absorptive regions for the visible light in the electromagnetic spectrum (400-750nm). Auxochromes are electron withdrawing or donating agents that are responsible for managing the color intensity and adherence to the fabric. -COOH, -NH₃, -OH and -

SO₃H are some common examples of auxochromes (Van Der Zee 2002). Classification of dyes on the basis of chromophore and application is given in the Table 2.1 (Griffiths, 1990; Ali, 2010).

2.1.1 Reactive dyes

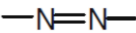
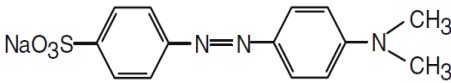
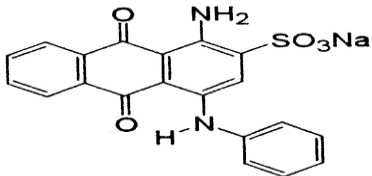
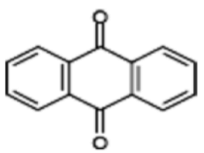
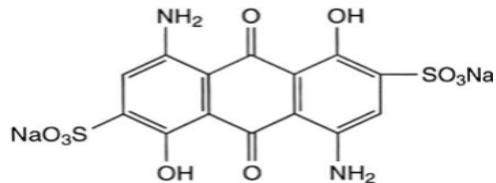
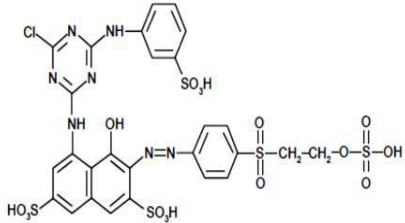
This class of dyes contains one of the most widely used coloring agents in the textile industry. Reactive dyes make ~45% of the annual textile dye production. They are used for cellulose, wool and viscose rayon fibers (Tunç, Tanacı, and Aksu 2009). These dyes contain reactive groups such as chlorotriazine, trichloropyrimidine vinyl sulfone, and difluorochloropyrimidine that form covalent bonds with the hydroxy, amino or sulfhydryl groups of the fabrics. Reactive textile dyes contain different types of chromogenic groups, most important of which are azo, anthraquinone, phthalocyanine and triphenodioxazine (Waring and Hallas 1990). Among these, reactive azo dyes are more extensively used because of their bright hues, high fastness property and easier application. The presence of sulfonic acid groups in the reactive azo dyes structure, enhances water solubility. Moreover, the complex polycyclic aromatic structures make them stable against sweat, light, chemical and microbial attack (Sahasrabudhe and Pathade 2011). Some of the examples of reactive azo dyes include, Reactive Blue 13, Reactive Blue 221, Reactive Red 195, Reactive Red 80, Reactive Yellow 145 and (Wang et al., 2009; Olukanni et al., 2010; Pajot et al., 2011; Al-Amrani et al., 2014).

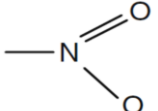
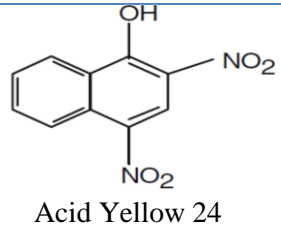
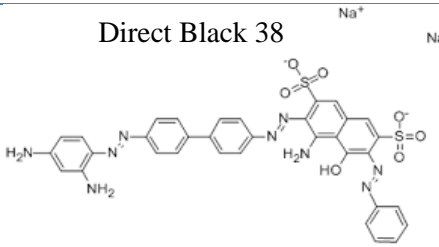
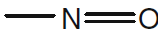
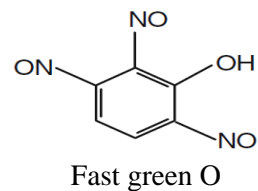
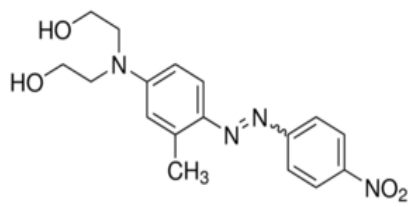
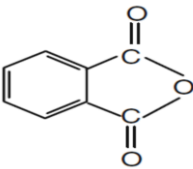
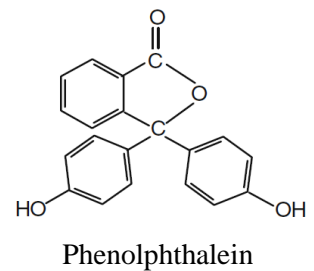
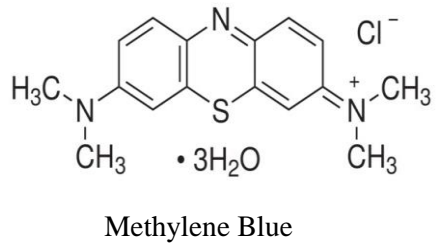
2.2 Environmental impact of textile dyes

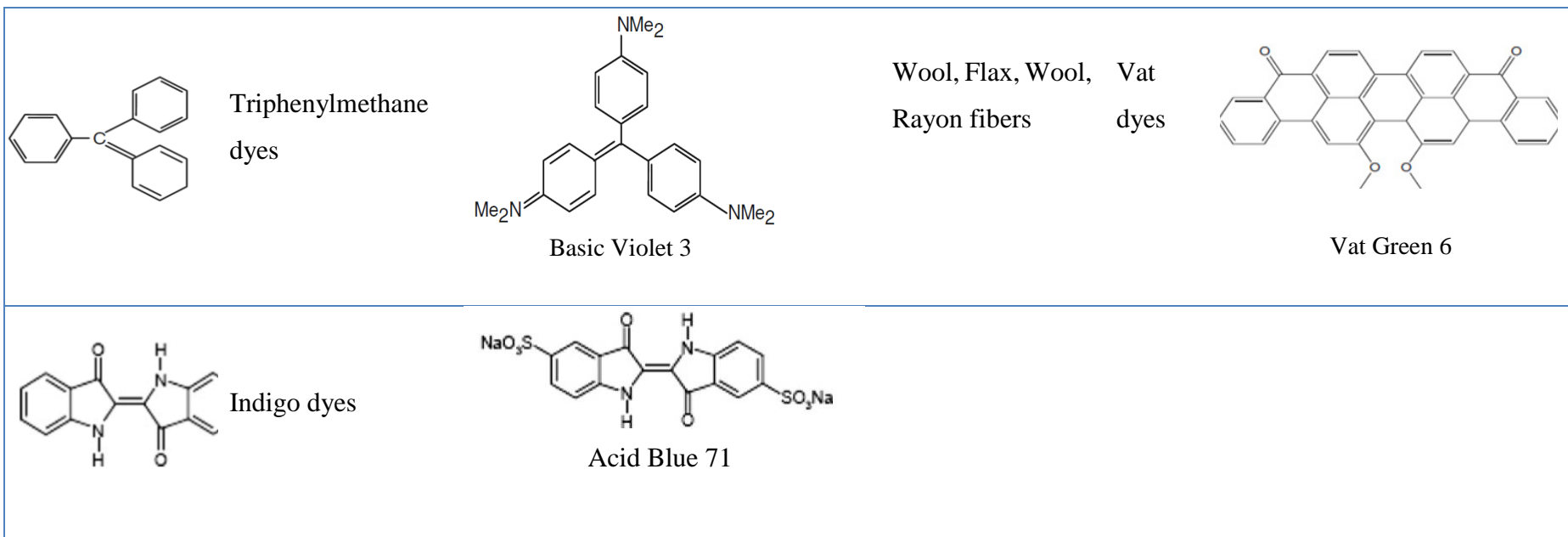
Textile industries release large amounts of colored wastewater due to the high consumption of water during textile dyeing and processing (Babu et al. 2007). Substantial quantities of the applied textile dyes fail to adhere to the fabric and are lost to the waste stream. The loss percentage can range from 2-50%, depending upon the type of dyes. The high-water solubility of reactive azo dyes accounts for their large (up to 50%) release into the effluent (Ali 2010). The discharge of untreated or partially treated textile effluent into the open water systems is one of the major causes of environmental havoc. Textile dyes can be detected in water at a very low amount (1 ppm) due to the striking hues (Pandey et al. 2007). Such effluents are not only a cause of aesthetic mutilation but also endanger the aquatic communities, due to the reduction in the dissolved oxygen levels resulting from lesser sunlight penetration and diminished

photosynthetic activity (Roy et al. 1970). In addition to the color, textile waste adds a chemical load in the receiving waters and results in elevated levels of pollution indicators *i.e.*, pH, salinity (especially in the case of reactive azo dyes), chemical oxygen demand (COD), biological oxygen demand (BOD), total solids (TS) *i.e.*, suspended and dissolved (TSS, TDS). Generally, the BOD/COD values are very low (0.2-0.5), that is indicative of high content of recalcitrant organic matter (Wang et al., 2010; Saratale et al., 2011).

Table 2.1 Classification of dyes based on chromophore group and application

Chromophore	Class	Example	Application	Class	Example
	Azo dyes	 Methyl Orange	Wood, Silk, Nylon, Polyurethane, fibers	Acid dyes	 Acid Blue 25
	Anthraquinone dyes	 Acid Blue 45	Cellulosic, fibers, Wool, Polyamide	Reactive Dyes	 Reactive Red 195

	Nitro dyes	 Acid Yellow 24	Cotton, Wool, Direct Flax, silk, Leather dyes in (alkaline or neutral bath)	 Direct Black 38
	Nitroso dyes	 Fast green O	Polyamide, fibers, Disperse Polyesters, Nylon, dyes polyacrylonitriles	 Disperse Red 17
	Phthalein dyes	 Phenolphthalein	Polyester, Wool, Basic Silk, Mod-acrylic dyes nylon	 Methylene Blue



2.3 Ecotoxicity of azo dyes

2.3.1 Factors affecting the ecotoxicological response of dyes

Azo dyes pose long term challenges to the ecosystems owing to their xenobiotic and recalcitrant nature (Ayyaru and Dharmalingam 2014). Most of the textile dyes and/or their metabolites are toxic and mutagenic in nature. According to EU criteria most of the dyes are not acutely toxic in nature as their LD50 values are high (250-2000 mg/kg of body weight) (Novotný et al. 2006). However, some of the aromatic amines, resulting from the breakdown of textile dyes are a subject of a serious environmental concern due to their mutagenic properties which make them potential carcinogens (Barsing et al. 2011). Different types of intrinsic and extrinsic factors affect the toxicity profile of azo dyes. Intrinsic factors include the chemical structure of dyes and their interaction with metabolic machinery of the living systems. The general mechanism of toxicity assessment of textile is based on toxic impact of the parent dye molecule (Rawat et al. 2016). Some low molecular weight and lipophilic dyes can diffuse into cell membranes and effect the cellular machinery directly (Brown and De Vito 1993). They may also disrupt the genetic material by binding to it through the free amino groups leading to genotoxicity. This usually occurs following metabolic activation of free and N-acetylated amines in living systems, resulting in the formation of nitrenium ions (Ollgaard et al. 1998).

Dyes with some functional groups *e.g.*, sulfonic acid and carboxyl groups, generally have low direct toxicity due to the increased hydrophilicity and steric hindrance which restricts their diffusion into the cell (Chung et al. 2000; Levine 1991). However, such dyes due to their water-soluble nature are more persistent in environment and the likelihood of toxicity could also not be completely ruled out, as the parent dye may not be directly toxic but is still prone to the release of toxic byproducts following breakdown by some microbial agents (Pinheiro, Touraud, and Thomas 2004; Rawat et al. 2016). Ecological fate of dyes is affected by different environmental factors such as oxygen availability, moisture content, availability of light, and inorganic electron shuttles. These extrinsic factors also affect the toxicological nature of dyes (Sharma et al. 2007). Anaerobic environment facilitates the dye decolorization process but the reductive cleavage of azo bond results in the production of persistent and mutagenic

colorless aromatic amines (Coughlin, Kinkle, and Bishop 2003). Some microbes can carry out complete mineralization of dyes under aerobic conditions through =N–C bond cleavage, but this is not a norm for all oxidative removal processes (Stolz 2001). Formation of toxic metabolites following oxidative degradation has also been reported. The oxidative byproducts of food dyes, Amaranth and Sunset Yellow showed high mutagenicity in *Salmonella typhimurium* (Sweeney, Chipman, and Forsythe 1994). Similarly, Johnson et al., (2010) reported mutative and chromosome damaging effects of oxidative metabolites of Sudan I and Para Red.

Moisture content is another factor that can enhance ecotoxicity of azo dyes through hydrolysis. Although hydrolysis is not a major mechanism for dye degradation to aromatic amines but it still can add to the toxicological response of dyes. Reactive Black 5 demonstrated increased toxicity in *Vibrio fischeri* upon hydrolysis (Gottlieb et al. 2003). Although the treatment of hydrolyzed products with *Clostridium butyricum* reduced the toxicity but the metabolites were still more toxic than the parent non-hydrolyzed dye (Ollgaard et al. 1998). Light is another major environmental factor affecting the toxicological response of azo dyes. Although azo dyes are usually stable to photolysis but can undergo photodegradation in upper and lower layers of soil by the activity of oxy-radicals or nascent oxygen (Brown and Casida 1988). Photolysis is also observed in aquatic environments but is affected by the turbidity and UV/visible light ratio. Photodegradation can also induce reduction in dye metabolites but that will not always result in a diminished toxicity level. Dichlorobenzidine (DCB), a major intermediate used in most azo dyes, produces cytotoxic and genotoxic effects in human cells upon photolysis (Wang et al. 2005). Azo dyes degradation doesn't follow a specific pattern in nature. Myriad of factors like types of microbes and enzymes, molecular structure cleavage pathways, redox mediators and other inorganic radicals, decide the final fate of a azo dye molecule resulting in the production of diverse types of degradation products with varying toxicological effects (Chacko and Subramaniam 2011).

2.3.2 Toxicity assessment procedures for textile dyes

Toxicity studies are usually conducted at different levels of biological organization *e.g.*, molecular, cellular and organismic level. However, population and community level studies are seldom found in the literature. Toxicity assessment is based on response of

a given test specimen towards sub-lethal concentrations of dyes. The data collected from such studies can be utilized to get a generalized idea about the possible effects of the azo dyes in a community (Rawat et al. 2016).

2.3.2.1 Genotoxic effects of textile dyes

Textile dyes may induce genotoxic effects in living systems following metabolic activation and release of free radicals that lead to DNA damage through oxidation (Mansour et al., 2009; Carmen and Daniel, 2012), formation of micronuclei (An et al., 2007), DNA adducts (Kojima et al., 1994), direct DNA binding (Wang et al., 2012) and chromosomal aberrations (An et al., 2007; Kojima et al., 1994; Wang et al., 2012; Arun Prasad et al., 2013). Some of the most commonly used genotoxicity assays for dyes and their metabolites are Ames *Salmonella* mutagenicity test, SOS Chromo test (Kwan and Dutka 1992; Szeberenyi 2003), *Allium cepa* assay (Agrawal et al. 2014), Comet (Kadam et al. 2014), and TUNEL assay (Bafana et al. 2009). Table 2.2 summarizes some of the major genotoxic studies carried out for textile dyes. Most of the toxicity studies focus on acute toxic effects of the dyes and their breakdown products, while chronic toxicity assessment and time course detoxification evaluation, following dye treatment by microbial agents is rarely found (Rawat et al. 2016). Bafana et al., (2009) studied time depended detoxification of Direct Red 28 metabolite i.e., benzidine, obtained after treatment with *Bacillus velezensis*. The toxicity of benzidine was reduced after 15 days of bacterial treatment. The reduction in genotoxicity was supported by Comet assay, DNA ladder, TUNEL, and flow cytometric tests.

2.3.2.2 Cellular and organismic toxicity

Textile dyes (purified dyes and industrial effluents) and their breakdown products also poses cytotoxic effects. The cytotoxicity of dyes can be assessed by detection of reactive oxygen species, free radical production, peroxidation of lipids, changes in chlorophyll structure and function and glutathione formation (Jadhav et al., 2010, 2011, 2012). Moreover, in model species, an upsurge in antioxidant enzymes activity and loss of cell viability is also observed (Phugare et al. 2011; Waghmode et al. 2012). The cellular response of dyes is tested in microorganisms, plants and animal models under *in vitro* and *in vivo* conditions (Hensley et al. 2000). In human beings, *in vitro* studies are conducted for testing cellular level toxic effects of dyes. For that, red blood cells

and polymorphonuclear leukocytes are usually used (Mansour et al., 2011; Kumar et al., 2007). Mutagenic and carcinogenic arylamines are usually produced in mammalian gut microbes, due to the anaerobic environment (Ferraz et al. 2012). Biomarker based studies in dye contaminated niches for stress assessment have received least consideration till present. This is due to the low genomic data availability in such environments, however, an overall protein expression analyses could be a better solution in this regard (Monsinjon and Knigge 2007).

Toxicity and detoxification studies at organismic level are conducted on variety of test organisms such as bacterial cultures *e.g.*, *Vibrio fischeri*, *Vibrio harveyi*, *E. coli*, *Bacillus subtilis*, *Rhizobium radiobacter*, *Pseudomonas desmolyticum* NCIM-2112 (Saratale et al. 2010); algae and protozoans *e.g.*, *Selenastrum capricornutum* and *Tetrahymena pyriformis* respectively (Novotný et al. 2006; Wang et al. 2001) animal models *e.g.* *Artemia salina*, *Daphnia* (Franciscon et al. 2012; Leme et al. 2015). Effect of dyes is usually determined by measuring the growth of microbial cultures while reproductive, respiratory and other behavioral disruptions are studied in other small test organisms. Some of the major higher animals used in toxicity testing of textile dyes include fish *e.g.*, zebrafish; frogs *e.g.*, *Silurana tropicalis* and rats (Soriano et al., 2014; Liu et al., 2007; Sharma et al., 2008) where textile dyes can induce developmental issues. In addition to these, dyes can also be phytotoxic in nature. Phytotoxicity studies are usually carried out for monitoring detoxification of dyes after treatment by physicochemical and biological methods. Some of the commonly used plant species in phytotoxicity studies include: *Triticum aestivum*, *Triticum vulgare*, *Phaseolus mungo*, *Sorghum biolor*, *Raphanus sativus*I, etc. In phytotoxicity assay seed the usual procedure is to measure the seed germination rate and length of root and shoot (Ali 2010). Textile dyes and/or their metabolites effect the levels of plant pigments and hormones such as on chlorophyll, carotenoids and abscisic acid which in turn retards the plant growth process (Puvanewari, Muthukrishnan, and Gunasekaran 2006). Some of the cellular and organismic level toxicity studies are summarized in Table 2.3.

Table 2.2 Genotoxicity studies on textile dyes

Test type and conditions	Dyes tested	Tested concentration range	Results	Reference
Ames test (TA98 and TA100 strains of <i>Salmonella typhimurium</i>) with and without S9 metabolic activation	Multiple dyes (53) belonging to different structural groups i.e., azo, anthraquinone, phthalocyanine, acid and basic dyes	15.8-5000 ppm	15 dyes showed positive results (13 with TA98 and 2 with TA100), 7 dyes showed mutagenic effects without metabolic activation while 8 showed a positive response following S9 activation	(Jäger et al. 2005)
Ames test (<i>Salmonella typhimurium</i> T100 strain) without S9 activation	Orange 3R; Brown GR; Blue S1; Violet; Royal blue; Congo red; Bordeaux	2,5,10,50, and 100µL)	All dyes were mutagenic at higher concentrations except Violet	(Mathur, Bhatnagar, and Bakre 2006)
Ames test (TA100 and YG1042 strains for substitution mutation, TA98 and YG1041 for shift mutation testing) With and without S9 activation	Reactive Orange 16, Congo Red (azo dyes), Remazol Brilliant Blue; Disperse Blue 3 (Anthraquinone dyes)	50-400 µg/agar plate and 15-520 µg/agar plate for Disperse Blue 3	Congo Red showed negative response towards all testes strains; Reactive Orange 16 showed mutagenicity, with and without S9 in TA98, while only after S9 activation in TA100; Remazol Brilliant Blue was potentially mutagenic to TA98 and TA100; Disperse Blue 3 showed mutagenicity in all tested strains following S9 activation	(Novotný et al. 2006)
SOS Chromotest (using <i>Escherichia coli</i> PQ37 strain) with and without S9 mix.	Acids yellow 17, Violet 7, Orange 52 (original dyes and biodegradation products obtained after treatment with <i>Pseudomonas putida</i> mt-2 (under static and shaking culture conditions)	100 ppm	Biodegradation products were found to be mutagenic following S9 treatment. Genotoxicity of metabolites obtained after static incubation was higher than that obtained after shaking conditions	(Mansour et al. 2011)

<i>Allium cepa</i> and comet assay	Genotoxic effects of textile effluent (before and after treatment with bacterial consortium)	10-30% (v/v)	Chromosomal aberrations in mitotic cells were observed that were significantly reduced in treated effluent samples. Comet analysis demonstrated DNA damage in root meristems of <i>Allium cepa</i> , in untreated effluent samples.	(Jadhav et al. 2010)
<i>Allium cepa</i> and Comet assay	Red HE3B before and after treatment with bacterial consortium	500 ppm	Red HE3B caused DNA damage and chromosomal aberrations in <i>Allium cepa</i> that were significantly reduced after bacterial decolorization	(Phugare et al. 2011)
Comet assay (DNA damage in lymphocytes)	Textile effluent (containing azo dyes Indigo Blue, Sudan Red and Cypress Green dyes); original and decolorized effluent obtained after treatment with immobilized Horseradish peroxidase (HRP) enzyme	NM	DNA breakage was observed with untreated effluent sample while HRP treated sample showed no such effect on the nuclear DNA	(Karim, Adnan, and Husain 2012)
Ames test (TA98 and YG1041 strains) with and without S9 based activation	Textile effluent samples from a wastewater treatment plant and Quilombo River (containing 6 major dyes viz., Disperse Blue 373, Disperse Blue 291, Disperse Red 1, Disperse Orange 30, Disperse Yellow 3, and Disperse Violet 93).	NM	Disperse Violet 93 and Disperse Blue 373 were found be highly mutagenic with S9 activation in YG1041 strain.	(Vacchi et al. 2017)
<i>Allium cepa</i> assay	Textile dyeing effluents (Blue and pink colored)	0, 20, 40, 60 80 and 100% (v/v)	Effluent at higher concentration (above 40% and above) caused significant chromosomal aberrations and lower mitotic index	(Rahman, Rahman, and Nasirujjaman 2017)
Comet assay and micronucleus test (effects in multiple tissues of swiss male mice)	Disperse Red 1 dye	0.0005-500 mg/kg Bw (single doses)	DNA damage in liver cells at 0.005 mg/kg	(Fernandes et al. 2018)

NM: Not mentioned

Table 2.3 Cellular and organismic level toxicity studies on textile dyes

Test type	Dyes tested	Tested concentration range	Results	Reference
Cellular level toxicity studies				
Oxidative stress assay in zebrafish <i>Danio rerio</i>	Textile effluent (original and pulverized chitosan treated)	NM	Untreated effluent caused increased levels of oxidative stress biomarkers <i>e.g.</i> , acid reactive and lipoperoxidative agents and reduced glutathione. Moreover, catalase activity was diminished. A decrease in oxidative stress markers was observed following treatment with chitosan.	(Grinevicius et al. 2009)
Hematological analysis of Swiss albino rats	Textile effluent (untreated and biologically treated from an effluent treatment facility)	NM	A significant decrease (12-46%) in RBC, WBC, Hb, PCV and MCHC level was observed. Moreover, RBC and WBC size was also affected	(Sharma et al. 2008)
HaCaT (human keratinocyte) cytotoxicity assay	Drimarene Red CL-5B, Drimarene, Blue CL-2RL, Drimarene Yellow CL-2R	12,25,50,100,150,190,380 and 750 ppm	The total protein content of dye exposed HaCaT cells was reduced than that of control. Inhibitory concentrations for the dyes were ($\mu\text{g}/\text{mL}$); Red: 155, Yellow:237, and Blue: 278	(Klemola et al. 2007)
Trypan blue exclusion test using human polymorphonuclear leukocyte cells (PMNL)	Direct Blue-15 (original dye and metabolites obtained biodegradation by bacterial consortium)	50,100, and 250 ppm	PMNL viability was decreased upon treatment with the pure dye solutions. However, decreased toxic response was	(Kumar et al. 2007)

			observed in the case of dye metabolites.	
In vitro butyrylcholinesterase (BuChE) inhibition assay in human plasma	Acid orange 52 (original dye and metabolites obtained after treatment with <i>Pseudomonas putida</i> mt-2 under static and shaking conditions	1,10, and 100 ppm	BuChE activity was reduced in the presence of Acid Orange 52 dye and metabolites obtained after static incubation, while metabolites obtained under shaken condition showed no inhibition	Mansour2011
<i>Allium cepa</i> cytotoxic assay	Textile effluent (before and after treatment with bacterial consortium)	10-30%	Cells exposed to untreated effluent demonstrated high mitotic index, indicative of uncontrolled cell division that was reduced following bacterial treatment.	Jadhav 2010
<i>Allium cepa</i> cytotoxic and oxidative stress assays	Remazol Red, Remazol Orange (original dyes and degradation metabolites (treated with <i>Pseudomonas aeruginosa</i> BCH); Rubine GFL (original dye and metabolites obtained after treatment with <i>Galactomyces geotrichum</i> MTCC 1360; Red HE3B before and after treatment with bacterial consortium	500 ppm; 500 ppm; 1000 ppm; 500 ppm	Dyes induced cell death and lower mitotic index in <i>A. cepa</i> cells, while reduced toxicity was observed with dye metabolites. Pure dyes also caused oxidative stress in <i>A. cepa</i> cells, that was indicated by diminished activity of catalase. Moreover, an upsurge in sulfur oxide dismutase, guaiacol and ascorbate peroxidase activity was observed. Protein and lipid oxidation was increased.	(Jadhav et al., 2011, 2012;Waghmode et al., 2012; Phugare et al., 2011)
Organismic level toxicity Studies				
Microbial toxicity (Bioluminescence) assay using <i>Vibrio fischeri</i>	Processed effluent samples and different dyes and auxiliaries	5-7000 ppm	EC50 values for dyes and auxiliaries were in the range of 9-6930 ppm while one of the processed effluent sample was	(Wang et al. 2002)

			highly toxic, 7 showed moderate toxicity and 9 showed no toxic effects. The respective GL values were: 100, 12-32 and <10.	
Microbial toxicity (Bioluminescence) assay using <i>Vibrio fischeri</i>	Reactive Orange 16, Congo Red (azo dyes), Remazol Brilliant Blue; Disperse Blue 3 (Anthraquinone dyes)	500–5000 ppm (RO16), 625–2500 ppm (CR), 125–2000 ppm (RBBR), and 62.5–1000 ppm (DB3).	EC50 values: 1375 ppm (RO16), 1623 ppm (CR), 813 ppm (RBBR) and 359 ppm (DB3)	(Novotný et al. 2006)
Microbial toxicity (Bioluminescence) assay using <i>Vibrio fischeri</i>	Textile effluent (original and pulverized chitosan treated)	1-100% (v/v)	Original effluent samples were toxic to <i>V. fischeri</i> with an EC50 value (%) of 10.64. Treated samples were not toxic	(Grinevicius et al. 2009)
Microbial toxicity (measurement of zone of inhibition) using <i>Rhizobium radiobacter</i> , <i>Pseudomonas desmolyticum</i> (NCIM-2112), <i>Acinetobacter</i> sp. <i>Cellulomonas biazotea</i> (NCIM-2550), <i>E. coli</i> DH5a, <i>Proteus vulgaris</i> (NCIM-2027) <i>Micrococcus glutamicus</i> (NCIM- 2168)	Green HE4B (pure dye and degradation metabolites obtained after treatment with a bacterial consortium)	100 and 300 ppm	Pure dye samples showed concentration related response and resulted in significant growth inhibition in all test strains. No zone inhibition was observed with dye metabolites at 100 ppm, however, a slight inhibition was recorded for some microbes at 300 ppm	(Saratale et al. 2010)
Microbial toxicity (measurement of zone of inhibition) using <i>S. paucimobilis</i>	Methyl Red (Pure dye and degradation metabolites after treatment with <i>S. paucimobilis</i>)	750 ppm	MR caused growth inhibition (0.9 cm) while the metabolites were non-toxic	(Ayed et al. 2011)
Microbial toxicity using gram positive and negative bacteria, and fungal specimens	Reactive Blue 221, Reactive Red 195, Reactive yellow 145, dye mixture	50-2000 ppm	The dyes and their mixture produced variable toxic effect on bacteria and fungi. The EC50 values were in the range of 80-360 ppm for most sensitive microbial specimens	(Malik, Zain, and Ali 2018) (This study)

Algal toxicity using <i>Selenastrum capricornutum</i>	Reactive Orange 16, Congo Red (azo), Remazol Brilliant Blue; Disperse Blue 3 (Anthraquinone)	0.2–100 ppm	EC50 values: 7.8 ppm (RO16), 4.8 ppm (CR), 81 ppm (RBBR) and 0.5 ppm (DB3)	(Novotný et al. 2006)
Algal toxicity using <i>Chlorella vulgaris</i>	Effluent samples (17) from dye treatment facility	1,10,50, and 100% (v/v)	Most of the tested effluent samples (13) showed acute toxicity	(Sponza 2006)
Protozoan toxicity test using <i>Tetrahymena pyriformis</i>	Reactive Orange 16, Congo Red (azo), Remazol Brilliant Blue; Disperse Blue 3 (Anthraquinone)	500 ppm	Generation time was increased with all the four dyes. Cell size was substantially changed in the case of CR and DB3. All dyes except RO16, reduced the ingestion rate	(Novotný et al. 2006)
Protozoan test using <i>Vorticella campanula</i>	Effluent samples (17) from dye treatment facility	1-100% (v/v)	EC50 values for all samples were higher than that obtained with algae used in that study	(Sponza, 2006)
Aquatic toxicity test using <i>Daphnia magna</i>	10 copper-complexed dyes and Direct Blue 218	0.8-10 ppm	All the tested dyes were highly toxic	(Bae and Freeman 2007)
Aquatic toxicity test using <i>Daphnia magna</i> and <i>Artemia salina</i>	Textile effluent (original and pulverized chitosan treated)	1-100% (v/v)	Untreated effluent showed acute toxicity towards <i>D. magna</i> and <i>A. salina</i> with EC50 (%) values of 48.98 and 12.22. Treated samples were not acutely toxic to both test organisms	(Grinevicius et al., 2009)
<i>A. salina</i> acute toxicity assay	Methyl Red (Pure dye and degradation metabolites after treatment with <i>S. paucimobilis</i>)	2-100% (v/v)	LC50 values (%) for dye before and after degradation were 3.5 and 8.3 respectively	(Ayed et al. 2011)
Aquatic toxicity test using <i>Daphnia magna</i> and <i>Artemia salina</i>	Reactive Blue 221, Reactive Red 195, Reactive yellow 145, dye mixture	25-2000 ppm	EC 50 for <i>A. salina</i> and <i>D. magna</i> were observed in the ranges 516-950 and 108-242 ppm, respectively	(Malik et al. 2018) (This study)

Aquatic toxicity using fish (<i>lepistes-Poecilia reticulata</i>)	Effluent samples (17) from dye treatment facility	1-100% (v/v)	EC50 values as low as 0.2% were obtained with some effluent samples	(Sponza 2006)
Acute toxic effect of dyes on zebrafish (<i>D. rerio</i>) embryos	Vat Green 3, Direct Black 38, (RB15), Reactive Orange 16, and Reactive Blue 15	1-100 ppm	All the tested dyes caused developmental problems at embryonic and larval stages	(de Oliveira et al. 2016)
Acute toxic effect of dye waste on albino rats and mice (male reproductive biology study)	Original and treated textile wastewater from a treatment plant	NM	Reproductive system of test organisms was highly affected. Reduction in body weight, reproductive organ weight, total protein, cholesterol, lipid and spermatozoa content was also observed. Treated samples were found to be less toxic	(Suryavathi et al. 2005)
Phytotoxicity assays (using <i>Triticum aestivum</i> , <i>Trticum vulgare</i> , <i>Phaseolus mungo</i> , <i>Sorghum biolor</i> , <i>Raphanus sativus</i>)	Variety of pure dyes, textile effluents and dye metabolites obtained after biodegradation	Varying concentrations ranging from 25-1000 ppm	In majority of studies reduction in seed germination, and radical and plumule length was observed upon treatment with pure dyes and textile effluents. Biodegradation resulted in reduced toxicity in most cases	(Parshetti et al., 2006; Jadhav et al., 2008; Kalyani et al., 2008; Dawkar et al., 2009; Jadhav et al., 2010.2011, 2013; Hassani et al., 2014; Vijayalakshmidivi and Muthukumar, 2015; Sudha et al., 2018; Malik et al., 2018)

NM: Not mentioned

2.4 Treatment methods of textile dye waste

2.4.1 Physicochemical methods

The harmful effects associated with textile dyes necessitate proper treatment prior to their discharge into the environment (Imran et al. 2014). The available treatment methods involve color concentration (using sludge and concentrating agents) and/or complete removal of dyes (Nguyen and Juang 2013). On industrial scale, textile waste remediation is done by physicochemical or biological methods or a combination of both (Khan et al. 2013). Physicochemical dye removal strategies (given in Table 2.4) include variety of physical and chemical methods such as adsorption, filtration, precipitation, coagulation-flocculation, oxidation (chemical, advance oxidation process and electrochemical oxidation) (Wang et al., 2010; Holkar et al., 2016). However, these methods are relatively expensive (due to the application of costly absorbent materials and chemicals) and in some cases, less efficient in terms of complete dye removal due to the structure complexity of the dye molecules. Additionally, secondary sludge generated during most of these methods needs further treatment that in turn increases the overall expenditures (Vandevivere, Bianchi, and Verstraete 1998; Yeap et al. 2014).

Table 2.4 Physicochemical methods for dye waste treatment

Method	Process	Advantages	Disadvantages	Reference
Adsorption	Activated carbon is the most commonly used adsorbent for dyes. Clay, peat, bentonite, different types of polymeric resins, and agricultural waste (corn cobs and wheat straw) are other low-cost materials tested for this purpose	Activated carbon is the most suitable adsorbent for mordant, cationic and acid dyes (up to 90% removal occurs).	High cost limits the use of activated carbon. It is not effective for reactive, sulfur and vat dyes. Additionally, the low-cost materials investigated as adsorbents fail to remove different dyes, cannot be easily regenerated, and produce excessive sludge.	(Galán et al. 2013; Sadhasivam et al. 2009)
Filtration	Microfiltration, ultrafiltration, nanofiltration and reverse osmosis (depending upon the membrane permeability). Membrane selection depends on the textile effluent composition and process temperature	Efficient method for color, BOD and COD reduction through recycling of variety of dyes and auxiliaries	Prohibitive cost, membrane fouling and secondary waste production	(Chollom et al. 2015; Koyuncu and Güney 2013)
Precipitation (Coagulation-flocculation)	Different types of coagulants are used which coalesce suspended particles that in turn favors settling and subsequent removal by physical methods. This process is affected by the chemical type, pH and system temperature.	This method is highly suitable for sulfur and disperse dyes, while shows less efficacy towards removal of reactive, direct, acid, and vat dyes	Comparatively lower color removal efficiency than other chemical based methods and generation of copious amounts of sludge.	(Vandevivere et al. 1998)
Oxidation	1. Chemical oxidation using oxidizing agents such as: ozone, permanganate and hydrogen peroxide.	Chemical oxidation methods are relatively more effective for dye degradation and easier to apply.	Ozone is an expensive chemical with a short life span. It is also	(Metcalf, 2003)

	Among the different chemicals used, ozone, due to its highly reactive nature, carries out efficient removal of different azo dyes with little or no changes in overall reaction volume.	less effective towards water insoluble and disperse dyes.	
2. Advance oxidation process (AOP, using photocatalytic agents such as Fe, Mn, ZnO, TiO and oxidizing agents that generate OH radicals for dye removal in the presence of a light source).	Advance oxidation process combines different oxidation technologies and hence is a more effective dye removal strategy, for example Fenton's process is very efficient for a variety of soluble and insoluble dyes and shows high COD and color removal rates. H ₂ O ₂ /UV based AOP is another efficient hybrid method, with no sludge generation.	Large quantities of sludge are produced during Fenton's process. Dye degradation with H ₂ O ₂ /UV leads to the formation of hazardous products. This method also fails to treat highly colored effluents containing disperse and vat dyes. Moreover, the process is costly.	(Anjaneyulu, Sreedhara Chary, and Samuel Suman Raj 2005)(R.-C. Wang, Fan, and Chang 2009)
3. Electrochemical oxidation	Very efficient method for organic waste removal with production of non-hazardous end products.	Inflated cost of electricity	(Morawski et al., 2000).

2.4.2 Biological Methods

Microbial transformation of pollutants is one of the most important natural phenomena occurring in different ecosystems. This process is based on the natural acclimation capability of microorganisms to toxic wastes (Kumara, Dastidara, and Sreekrishnanb 2012). The intrinsic adaptive property of microorganisms led to the emergence of different biotechnological remediation technologies, that enhance the naturally occurring process of biotransformation by harnessing different microbial entities such as bacteria, fungi, yeast and algae (Solís et al., 2012). Biologic treatment has many advantages such as cost-effectiveness, eco-efficiency, and less sludge generation, which favor its application over physiochemical methods (Holkar et al. 2016). Microorganism type, dye structure and dye to microbial load ratio are important factors that affect biologic dye waste treatment. Moreover, the process is affected by different ambient conditions most important of which are pH, temperature and oxygen content (Wang et al. 2010). Based on the oxygen requirement of microorganisms, the biologic treatment process can be categorized as aerobic, anaerobic, anoxic and facultative (Khouni, Marrot, and Amar 2012). These conditions can be used alone or in a combination, to develop an eco-efficient treatment strategy because oxygen deficient conditions can result in the formation of aromatic compounds that can tend to be more toxic than the parent molecules (Gonçalves et al. 2005).

2.4.2.1 Basic mechanisms of microbial dye waste removal

Biosorption and enzymatic degradation are two main mechanisms employed by microbes for dye waste removal. These strategies can be utilized by the microbes alone or in a combination. In the case of biosorption, hetero-polysaccharide and lipid containing charged cell walls of live and/or dead microbial biomass take up the dye molecules (Solís et al., 2012). This process has mostly been observed in fungi, yeast, algae and some bacteria (Imran et al. 2014). Temperature, pH, type of the dye, microbe, and their relative concentration as well the contact time are the key factors that influence this process (Saratale et al., 2011; Solís et al., 2012). Depending upon the type of microbe involved, adsorbed dye molecules may or may not be subjected to enzymatic conversion. Through the activity of intracellular and/or extracellular enzymes, microbes break down the dye molecules (Khan et al. 2013). Some of the most common

enzymes involved in the dye degradation are reductases *e.g.*, azo-reductases, which carry out the reductive cleavage of azo bond under oxygen deficient conditions and in the presence of different redox mediators such as NADH, NADPH and FADH (Chacko and Subramaniam 2011; Van der Zee and Cervantes 2009). Because of their need for reducing equivalents, azo-reductases can be classified as NADH-dependent or NADPH dependent, FMN-dependent or independent and NADH-DCIP reductases (Liu et al., 2007; Bürger and Stolz, 2010; Misal et al., 2011). They are mostly found in bacteria, yeast and algae (Solís et al., 2012). Oxidative removal of dyes is brought about by different types of oxidative enzymes such as oxidases, peroxidases (manganese peroxidase and lignin peroxidase), laccase, N-demethylase and tyrosinase which are found in fungi, bacteria, and some yeast (Baldrian, 2006; Bürger and Stolz, 2010; Liers et al., 2010; Martorell et al., 2012; Saratale et al., 2011).

2.4.2.2 Physiological factors affecting microbial dye waste removal

In natural environment, microbial response towards xenobiotics such as textile dyes, is affected by several physiological factors such as pH, temperature, oxygen, dye concentration and structure, chemical constituents, and salinity. These abiotic factors therefore, need be optimized while studying the microbial potential for dye degradation for the development of efficient pilot and industrial scale treatment operations (Solís et al., 2012).

2.4.2.2.1 Additional supplemental compounds

Azo dyes are aromatic, carbon, and electro deficient compounds. Therefore, additional supplemental agents *i.e.*, carbon and nitrogen sources are required for microbial azo dye degradation (Khelifi et al. 2009; Tony, Goyal, and Khanna 2009). Carbon sources such as glucose sucrose, starch, lactose, maltose, fructose, sodium acetate, and potassium acetate provide the microbes with the energy and electrons essential for breakdown of complex azo (Holkar et al. 2016; Ponraj, Gokila, and Zambare 2011). Organic nitrogen sources such as yeast extract enhance the degradation process through the regeneration of redox mediators such as NADH (Saratale et al. 2011; Kalyani, et al. 2009). Other effective nitrogen sources include peptone, beef extract and agricultural waste products such as rice husk and straw (Jin et al., 2007; Jadhav et al., 2008).

2.4.2.2.2 pH and temperature

Optimum pH and temperature for microbial degradation are directly dependent on the environmental niches from where they are isolated (Khan et al., 2012). pH of the medium affects dye degradation, and maximum dye removal is observed at optimum pH that can vary between 3-11 depending upon the type of microbe involved (Ayed et al. 2011; Holkar et al. 2016; Saratale et al. 2013). Fungi show maximum activity in the acidic pH range while bacteria show maximum efficiency at neutral and/or basic pH range (Solís et al., 2012). Very low and high pH values are detrimental for many microorganisms, due to disruption of metabolic activities. pH can also affect the microbial transport system through changes in the cell membrane structure which in turn can limit the influx of small structured dye molecules (Chang et al. 2001; Kodam et al. 2005). Textile effluents mostly have alkaline pH which limits the application of neutral pH dwelling microbes (Willmott 1997). This problem can be solved by the application of alkaliphilic and/or alkali-tolerant microbes (Bhattacharya et al. 2017). Temperature is another crucial factor that affects the overall microbial physiology. Temperature influences microbial growth, biomass yield, enzymatic activity, and reaction kinetics (dos Santos, Cervantes, and van Lier 2004). 25-37 °C is usually the most suitable range for degradation by many microbes (Ali, 2010). At higher temperatures, many microorganisms fail to perform due to loss of cell viability and enzyme denaturation (Pearce et al. 2003). Temperature of textile effluent is usually high, therefore thermophilic and thermotolerant microorganisms can provide a better treatment alternative (Ali et al., 2009; Solís et al., 2012).

2.4.2.2.3 Salinity and oxygen

Textile effluents contain high sodium levels that result from the utilization of sodium hydroxide in the dye bath. About 15-20 % salt concentrations have been recorded in textile wastewaters (Khalid, Arshad, and Crowley 2008b). High salinity (above 3.0 g/L) hampers the microbial growth and hence reduces the decolorization activity. Halophilic and salt tolerant microorganisms can present a promising solution in this regard (Amoozegar et al. 2011). Presence of oxygen can inhibit or favor microbial dye degradation depending upon the type of microbe involved (Solís et al., 2012). Reductive dye degradation by anaerobic and facultative bacteria require anaerobic/anoxic and

static conditions because oxygen is detrimental to anaerobes and being a strong terminal electron acceptor, competes with the electron deficient centers in dye molecules such as the azo bond for the utilization of redox mediators in the medium (Chang et al. 2001). In the case of aerobic bacteria, fungi and yeast, presence of oxygen and shaking conditions facilitate the color removal process through improved oxygen and mass transfer (Olukanni, Osuntoki, and Gbenle 2009).

2.4.2.2.4 Dye structure and concentration

Microbial dye degradation is also affected by the dye structure and concentration. Usually higher dye concentrations result in decreased color removal rate (Charumathi and Das 2013). The toxic effect of dyes towards a given microorganism become more pronounced at higher concentrations (Holkar, Pandit, and Pinjari 2014), moreover, dye to cell ratio imbalance occurs at high concentrations of dyes which in turn can affect the enzymatic activity through active site blockage (Saraale et al. 2011; Kalyani, et al. 2009). Low molecular weight and simple structured dyes are relatively easily removed by microorganisms (Rawat et al., 2016). On the other hand, low color removal rates are observed with high molecular weight (more than 500 g/mol) complex structured dyes (Holkar et al. 2016). Presence of certain electron withdrawing functional groups such as $-\text{SO}_3\text{H}$, and $-\text{SO}_2\text{NH}_2$ in the para location of phenyl ring relative to the azo bond also restricts the microbial dye degradation process (Hsueh, Chen, and Yen 2009). Moreover, sulfonic acid group makes the dyes more toxic and its steric hindrance hampers the access of incoming electrons towards azo bond (Kalyani et al. 2008).

2.4.2.3 Textile dye degradation by different microorganisms

2.4.2.3.1 Algae

Algae can carry out the process of dye degradation through adsorption and/or enzymatic conversion (El-Sheekh, Gharieb, and Abou-El-Souod 2009). The process of adsorption is favored by low pH due to electrostatic attraction between the positively charged cell biomass and anionic dye molecules (Srinivasan and Viraraghavan 2010). Moreover, the dye structure also has a strong influence on dye removal ability of microalgae (Omar 2008). They do not require additional supplemental agents, due to their photosynthetic ability (Kumar Saha et al. 2010). Both reductive and oxidative removal mechanisms

have been found in different types of microalgae (El-Sheekh et al. 2009; Priya et al. 2011a). In addition to the suspension cultures, some immobilized microalgae have also been studied for dye degradation (Chu, See, and Phang 2009). They are among the least explored microbial agents for dye degradation (Ali, 2010). Some of the common examples of algae explored for azo dye degradation include *Chlorella vulgaris* (Lim, Chu, and Phang 2010), *Chlorella ellipsoidea* (Omar 2008), *Spirogyra* sp. (Mohan, Ramanaiah, and Sarma 2008), *Oscillatoria curviceps* (Priya et al. 2011b), *Chroococcus minutus*, and *Phormidium ceylanicum* (Parikh and Madamwar 2005).

2.4.2.3.2 Yeast

Yeast present another microbial alternative for textile dye degradation. They demonstrate faster growth and decolorization rates than filamentous fungi and can withstand unfavorable environmental conditions (Martorell et al. 2012). The color removal mechanism is like that of microalgae, i.e., adsorption and/or enzymatic conversion (Yu and Wen 2005). Acidic conditions favor the adsorption process through enhanced attraction between the yeast cells and anionic dye (Vitor and Corso 2008). Moreover, studies have shown that autoclaved yeast cell biomass exhibit a better adsorption capacity than non-autoclaved biomass (Charumathi and Das 2013). The growth and decolorization process require additional carbon and energy source such as glucose and can be aerobic, anoxic, or aerobic (Waghmode, Kurade, and Govindwar 2011). Dye degradation mechanisms can be reductive or oxidative depending upon the type of dye and yeast (Waghmode, Kurade, Khandare, et al. 2011). Different types of dye specific reductases and oxidases such as NADH-DCIP reductase, MnP, and tyrosinase have been detected in yeast (Aghaie-Khouzani et al. 2012). For some types of yeast, aerobic conditions are more favorable for efficient color, COD, and TOC removal than aerobic or anoxic ones (Waghmode, Kurade, and Govindwar 2011). *Candida albicans* (Vitor and Corso 2008), *Candida tropicalis* (Das, Charumathi, and Das 2011), *T. akiyoshidainum* (Pajot et al., 2011), *Galactomyces geotrichum* (Waghmode et al., 2011b), and *Trichosporon beigelii* (Saratale et al., 2011; Chang, et al. 2009), are some examples of yeast that have been studied for textile dye degradation.

2.4.2.3.3 Fungi

Filamentous fungi are equipped with an array of non-specific oxidative enzymes such as oxidases, peroxidases and laccase, which bring about oxidative removal of textile dyes (Liers et al. 2010; Majeau, Brar, and Tyagi 2010). The non-selective nature of these extracellular enzymes facilitates complete mineralization of various kinds of polyaromatic compounds (Solís et al., 2012). Aerobic environment is more suitable for fungal dye degradation process; moreover, color removal is enhanced under shaking conditions because of increased oxygen and mass transfer (Srinivasan and Viraraghavan 2010). Other culture conditions that affect fungal decolorization process are pH, temperature, nitrogen and carbon supplements, additives, and salts (Bakshi et al., 2006; Kaushik and Malik, 2009; Renganathan et al., 2006). Fungi are usually more susceptible to pH changes and can function better under acidic conditions, so the decolorization rate can be improved by maintaining pH in the favorable range for fungal growth (Erden, Kaymaz, and Pazarlioglu 2011). Addition of different additives such as: succinate, veratryl alcohol, Tween 80, and manganese ions can enhance the decolorization by inducing oxidative enzymes in fungi (Ghasemi et al. 2010; Ürek and Pazarlioğlu 2005) Moreover, the efficiency of process can be increased through fungal immobilization which reduces the effect of toxic substances, minimizes nutrition requirement and facilitates regeneration and reutilization for repeated cycles (Enayatzamir et al., 2010).

In addition to the live cultures, dead fungal biomass can also be utilized for dye waste treatment. Dead fungal biomass removes the dye through biosorption. Dead fungal biomass is advantageous in terms of no nutrient requirement, extended storage, easy operation and regeneration capability (Moreira et al. 2004). White rot fungi (basidiomycetes) are some of the most frequently explored fungi for textile degradation (Zhuo et al. 2011) of which *Phanerochaete chrysosporium* (Sedighi, Karimi, and Vahabzadeh 2009), *Ganoderma lucidum* IBL-05 (Asgher, Noreen, and Bhatti 2010), *Trametes versicolor* (Amaral et al. 2004), *Irpex lacteus* (Shin 2004), *Bjerkandera adusta* (Anastasi et al. 2011), are some most common examples. In addition to these various species of *Aspergillus* (Kadam et al. 2011; Karthikeyan et al. 2010) and other ascomycetes like some *Trichoderma* (Saravanakumar and Kathiresan 2014) species have also been investigated for dye degradation. Table 2.5 summarizes some of the fungal dye degradation studies in recent years. Despite the tremendous potential for

dye waste treatment, large scale application of fungi is hampered by the aeration requirement, sheer stress sensitivity, and long hydraulic retention times required for effective dye removal due to the slower fungal growth rates (Imran et al. 2014). Moreover, textile effluents are alkaline in nature which need to be acidified because fungi function best at acidic pH. Fungi also show antagonistic activities towards other useful organisms (Amir et al., 2006; Imran et al., 2014).

2.4.2.3.4 Bacteria

Bacteria are the most widely used microorganisms for textile dye degradation (Ali, 2010). Bacteria have several advantages over fungi (the second most important group of dye degrading microorganisms), such as: easier cultivation, faster growth rates, and ability to withstand harsh environmental conditions (Kodam et al., 2005; Dafale et al., 2008). The transformation process can be anaerobic, aerobic or facultative (Solís et al., 2012). Anaerobic [*Clostridium perfringes* (Semdé et al. 1998), *Bacteroides fragilis* (Bragger et al. 1997), *Acidaminococcus fermentans* (Malinauskiene 2012). etc.] and facultative [*Pseudomonas* sp. (Jadhav et al. 2011b), *E. coli* (Chang et al. 2000), *Citrobacter* sp. (Chan et al. 2012), *Micrococcus* sp. (Moosvi, Kher, and Madamwar 2007), *Klebsiella* sp. (Wong and Yuen 1998) *Staphylococcus* sp. (Pan et al. 2011), etc.] dye degrading bacteria contain different types of oxygen sensitive enzymes known as azo-reductases, for the reductive cleavage of azo dyes. Presence of oxygen inhibits the reductive breakdown of dye molecules by such anaerobic and facultative bacteria (Saratale et al., 2009; Solís et al., 2012). The process of anaerobic, microaerophilic or anoxic azo dye breakdown results in the production of aromatic amines, most of which have been reported as mutagens and carcinogens. Aromatic amines produced from the reductive cleavage can be further degraded in the presence of aerobic environment (Hosseini Koupaie, Alavi Moghaddam, and Hashemi 2011). Therefore, sequential anaerobic and aerobic treatment using two different types of bacteria presents an attractive solution for the toxic amine production issue (Jonstrup et al. 2011). Application of facultative bacteria that can survive under oxygen free and aerobic conditions provide a better solution in this regard as they require less stringent conditions for growth than strict anaerobes (Solís et al., 2012). Moreover, some aerobic (*Pseudomonas luteola*, *Bacillus* sp.) bacteria with oxygen insensitive reductive

enzymes have also been reported (Lin and Leu 2008; Ooi et al. 2007). In addition to the reductive enzymes, facultative and aerobic bacteria also contain oxidative enzymes such as: veratryl alcohol peroxidase, laccase, and tyrosinase (Saratale et al., 2011).

Most of the bacterial species reported in literature can survive under mesophilic temperature, neutral pH, and salinity free environment. Textile wastewaters are usually alkaline and have elevated temperature and salt concentrations (Solís et al., 2012), which necessitates pretreatment like cooling and dilution for making the effluent suitable for growth and functioning of such bacteria (Imran et al. 2014). Extremophilic bacteria [*Bacillus cohnii* (Prasad and Rao 2013), *Nesterenkonia lacusekhoensis* (Bhattacharya et al. 2017), *Aeromonas hydrophila* (Ogugbue, Sawidis, and Oranus 2012), *Shewanella* sp. (Khalid et al. 2008b), *Halomonas* sp. (Yang et al. 2010), *Geobacillus* sp. (Ambika Verma and Shirkot 2014), *Bacillus badius* (Misal et al. 2011)] can present a better solution for these kind of problems. Using pure bacterial cultures, for dye degradation can provide a detailed insight into the degradation pathways but pure cultures usually show a dye specific behavior. Moreover, the toxic and mutagenic aryl amines produced from the parent dye molecule resist further transformation by the same isolated bacterium (Saratale et al., 2011). The complex chemical composition of textile wastewaters, therefore demands some more comprehensive solutions such as mixed bacterial communities and cocultures (Nigam et al. 1996). Bacterial consortia (natural as well as developed ones) can efficiently transform the dye waste through collective activities of different species and/or genera (Chen and Chang 2007). Consortia based degradation process is usually faster due to involvement of multiple enzymes which can catalyze different steps in the degradation pathway in a synergistic manner (Forgacs, Cserhádi, and Oros 2004). Table 2.6 summarizes some of the studies on dye degradation by different types of bacteria.

Table 2.5 Studies on dye waste treatment by fungal cultures

Fungal strain(s)	Dye(s) and concentration	Conditions	Incubation Time	Decolorization performance	Reference
<i>Phanerochaete chrysosporium</i>	Multiple dyes (Reactive Black 5 (120 ppm), Direct Violet 51 (65 ppm), Ponceau Xylidine (100 ppm), and Bismark Brown R (100 ppm))	Minimal medium with Glucose (0.2%) and acetate (20mM), fungus immobilized on calcium alginate beads pH: 4.4, temperature: 30 °C, rpm: 150	72 hours	Up to 90% decolorization was observed for all dyes except Bismark Brown (86.7%)	(Enayatzamir et al. 2010)
<i>Fusarium oxysporum</i>	Glycoconjugate Azo Dye 150 ppm	Mineral salt medium with glucose (5g/L), bacto-peptone (1.5 g/L) and yeast extract (0.5 g/L), pH: 5.5, temperature: 25 °C, rpm: 160	24 hours	Up to 100% decolorization occurred, decolorization products showed reduced toxicity (92% detoxification) towards <i>Daphnia magna</i>	(Porri et al. 2011)
<i>Irpex lacteus</i>	Levafix Blue E-RA, 50-250 ppm	Malt extract medium, pH: 5.0-6.0, temperature: 35 °C, rpm: 200	96 hours	Up to 100% at all tested concentrations, degraded product showed non-toxic response towards <i>Vigna radiata</i> and <i>Brassica juncea</i>	(Kalpana et al. 2012)
<i>Thermomucor indicae-seudaticae</i>	Trypan Blue, Azure B, Remazol Brilliant Blue R,	Synthetic dye medium, pH: 6.0, Temperature 30-55 °C	24 hours	Up to 80% color removal was recorded with all	(Taha et al. 2014)

	and Congo Red mixture, (100-1000 ppm)			tested concentrations, color removal was slower at 55°C and reduced to 75%	
<i>Aspergillus terreus</i>	Procion Red MX-5B (200 ppm)	Aqueous solution, pH: 4.0, temperature: 30 °C, static cultures with fungal pellets	336 hours	98% color removal was recorded, metabolites were found to be toxic towards <i>L. sativa</i> seeds and <i>Artemia salina</i> larvae due to incomplete degradation	(Almeida and Corso 2014)
<i>Haematonectria haematococca, Trichoderma harzianum</i>	Alizarin Blue Black (300 ppm), Carminic Acid (100 ppm)	Salt medium with 0.25% glucose, pH: 5.5, 20 °C	336 hours	50–60 % of Alizarin Blue Black and 55-85% of Carminic Acid dye was decolorized.	(Rybczyńska and Korniłowicz-Kowalska 2015)
<i>Chaetomium globosum</i> IMA1 KJ472923	Industrial effluent containing indigo dyes (COD: 700 mg/L)	pH: 5.0, temperature: 28 °C, static and shaking (150 rpm) conditions	240 hours	99.8% decolorization under agitated condition with 88.4% reduction in COD	(Manai et al. 2016)
<i>Aspergillus niger</i>	Crystal Violet (10-40 ppm)	Basal medium with 3% sucrose and corn steep liquor, pH: 5.5, temperature: 30 °C	240 hours	96% decolorization under static condition	(Ali, 2016)

<i>Trichoderma asperellum</i>	Methyl Violet, Crystal violet, (MV), Malachite Green (100 ppm) and cotton blue (50 ppm)	Potato dextrose broth at 25, 75 and 100% concentration (for fungal cultivation), temperature: 30 °C, rpm: 150	336 hours	Decolorization activity (up to 80%) was not affected by PDB concentrations for all tested dyes	(Marcharchand and Ting 2017)
<i>Marasmius</i> sp. BBKAV79	Navy blue HER (50 ppm)	Production medium with sucrose and peptone, pH: 5.0, temperature: 40 °C, incubated under shaking condition	24 hours	Up to 95% color removal was observed, degradation metabolites were detoxified following decolorization as indicated by less phytotoxicity	(Vantamuri and Kaliwal 2017)
Immobilized (<i>Pleurotus ostreatus</i> , <i>Gleophyllum odoratum</i> , and <i>Poly-porus picipes</i>).	Brilliant green, Evans blues	100 ppm	24 hours	Varying decolorization depending upon the support material	(Przystaś, Zabłocka-Godlewska, and Grabińska-Sota 2018)

Table 2.6 Studies on dye waste treatment by bacterial cultures

Bacterial strain(s)	Dye(s) and concentration	Conditions	Incubation Time	Decolorization performance	Reference
<i>Pseudomonas putida</i> SKG-1 (isolated from dairy sludge)	Orange II, 100 ppm and textile effluent	Minimal salt medium with glucose and ammonium sulfate (0.4 and 0.1% [w/v] respectively. pH: 8, temperature: 30 °C, static culture	96 hours	Under static condition up to 93 and 50.2% decolorization was observed with Orange II and supplemented textile effluent, respectively	(Kumar Garg et al. 2012)
<i>Pseudomonas</i> sp. (immobilized in sol-gel)	Methyl orange, Benzyl Orange, and Remazol Black 5 (25-100 ppm)	Salt medium supplemented with 0.1 % (w/v) glucose, pH: 7.0, temperature: 35 °C, static culture	24-48 hours	Highest color removal (up to 86%) was observed at 50 ppm concentration (under static condition) for the three dyes with slight reduction (~9-10%) at 100 ppm. Immobilized cells retained decolorization activity after repeated batches (4 cycles)	(Tuttolomondo et al. 2014)
<i>Enterococcus faecalis</i> YZ 66 (isolated from dye effluent)	Direct Red 81(50 ppm)	Synthetic salt medium with 1% (w/v) lactose and peptone, temperature 37°C, static culture	1.5 hours	Complete decolorization at 50 ppm concentration, retained decolorization activity in repeated batches, within pH range of 5.0-8.0. Color removal ability was	(Sahasrabudhe et al. 2014)

					inhibited at higher dye concentrations (600-700 ppm)
<i>Micrococcus luteus</i> strain SSN2 (isolated from textile effluent)	Direct Orange 16 (100 ppm)	LB broth, NaCl: 3%, pH: 8.0, temperature: 37°C, static culture	6 hours	96% decolorization was observed and metabolites were less phytotoxic than parent dye.	(Singh et al., 2015)
<i>Marinobacter</i> sp. strain HBRA (moderately halophilic, isolated from seawater)	Direct Blue 1 (100 ppm)	LB broth, NaCl: 7% (w/v), pH: 8.0, temperature: 37 °C, static culture	6 hours	Complete decolorization, detoxification was indicated by <i>A. cepa</i> genotoxicity and phytotoxicity studies	(Arun Prasad et al. 2013)
<i>Bacillus cohnii</i> (obligate alkaliphile)	Direct Red-22 (5000 ppm)	Salt medium with 0.2% (w/v) yeast extract, NaCl: 5% (w/v) pH: 9.0, temperature: 37 °C, static	4 hours	95% decolorization, cytotoxicity and genotoxicity of the dye was reduced following bacterial treatment	(Prasad and Rao 2013)
Bacterial consortium (moderately alkaliphilic, isolated from saline soil)	Direct Blue 151 (200 ppm) and Direct Red 31 (200 ppm)	Mineral salt medium with sucrose and yeast extract, pH: 9.5, temperature: 36 °C, static	120 hours	94% decolorization, of the dye mixture was observed	(Lalnunhlmi and Veenagayathri 2016)
<i>Nesterenkonia lacusekhoensis</i> EMLA3 (alkaliphilic and halotolerant bacterium isolated from alkaline textile effluent)	Methyl Red (50 ppm), and textile effluent	Nutrient broth medium for MR degradation, pH: 11.5, Temperature: 35 °C, static and shaking conditions (200 rpm)	24 hours	97% color reduction was recorded for MR dye, 83% color and 49% COD reduction was observed (after 120 hours). Following sequential treatment (shaking: 200 rpm) COD reduction was improved (76%)	(Bhattacharya et al. 2017)

Natural bacterial consortium (from dye contaminated soil)	Dye mixture (8 different dyes) and textile effluent	Nutrient broth for dye mixture degradation study, pH: 5.0, temperature 50 °C, static condition	3-3.5 hours	89 and 67% color reduction in dye mixture and effluent respectively. BOD and COD reduction: 62, 66 and 43, 42% respectively.	(Joshi et al. 2010)
<i>Novibacillus thermophilus</i> SG-1 (isolated from soil)	Orange I (0.3 mM)	Salt medium wit acetate (0.17 mM) as electron donor, pH: 8.0, temperature 50 °C, anaerobic		Complete decolorization of Orange I	(Yu et al. 2015)
Five different pure bacterial cultures and their consortium	Reactive dye mixture	Amended BH medium with 100 ppm dye mixture, 37 °C, static		Faster color removal by the bacterial consortium than the pure cultures (75% in 6 days)	(Karim, Dhar, and Hossain 2018)

2.4.2.4 Biological reactors for dye waste treatment

Bioreactors used for textile dye waste treatment can be broadly classified into two major types: suspended and attached growth reactors (Erkurt and Arshad 2010; Riffat 2013)

2.4.2.4.1 Bioreactors based on suspension cultures

Suspended growth reactors are based on thoroughly mixed microbial suspension cultures. The treatment can be aerobic, aerobic or a combination of both (Davis and Cornwell 2013).

2.4.2.4.1.1 Activated sludge process

Activated sludge process, sequencing batch reactors, anaerobic and aerobic digesters are some of the common examples of suspended bioreactors systems (Ebrahimi and Najafpour, 2016). The conventional activated sludge process is based on microbial flocs formed in a high mixed liquor suspended solid (MLSS) containing effluents. Textile dyes are adsorbed to the microbial flocs which can be further transformed by the microbial cells. Major constituents of activated sludge flocs are bacteria. Some other microorganisms such as different types of protozoa are also found (Kumar et al. 2014). Differential distribution of oxygen in microbial flocs, facilitates a combined aerobic and anaerobic transformation process (Wagner and Amann, 1996). However, due to the high oxygen content in the system and elevated cost, conventional activated sludge system is not a considered as good option for textile waste treatment (Nawaz and Ahsan 2014).

2.4.2.4.1.2 Sequencing batch reactor (SBR) and upflow anaerobic sludge blanket (UASB) reactor

A modified form of the activated sludge process is a sequencing batch reactor (SBR), (operates in cycles of five main steps *i.e.*, fill, react, settling, decant and standby) which has low cost, operational flexibility, improved resistance to shock loading, reduced space requirement and ability to treat different type of textile effluents (Velmurugan, Clarkson, and Veenstra 2010). They can consist of activated sludge or potential dye degrading bacteria, isolated for wastewater treatment facilities and other niches

(Sathian et al. 2014). SBRs can be based on strict anaerobic or aerobic process but combined anaerobic-aerobic systems have showed better results (Kapdan and Oztekin 2006). In addition to these, upflow anaerobic sludge blanket reactors (UASB) have also been used for textile waste treatment (Baêta et al. 2012). Such reactors can resist the effect of toxic dye compounds through maintenance of high microbial biomass as they have longer solid retention time (SRT) as compared to the hydraulic retention times (Gnanapragasam et al. 2010).

2.4.2.4.1.3 Stirred tank bioreactor for fungi

Stirred tank bioreactor have the most suitable configuration for fungal suspension cultures (Andleeb et al. 2010). In suspension cultures fungi can grow as dispersed mycelia or as pellets. Pellet formation is a form self-immobilization in fungi, resulting from entangled and aggregated mycelia (Prosser and Tough 1991). This growth pattern can limit the nutrient and substrate utilization by fungi in larger hyphal aggregates, therefore, the pellet size and hyphal extension needs to be controlled through proper stirring (Moreira et al. 2004). Agitation speed is a crucial factor for controlling the pellet size as increased agitation can deleteriously affect the hyphal structure which in turn disturbs the enzyme secretion (Allen and Robinson 1989). To maintain a suitable pellet size for effective fungal biomass performance for treating the wastewater, jet and pulsing bioreactors can be used. Such bioreactors employ pellet shaving process for maintenance of proper pellet size (Cabral et al. 2001).

2.4.2.4.2 Bioreactors based on attached growth process

In attached growth process, microbial cells are immobilized through entrapment in porous structures or by attachment to inert support materials (immobilization) and grow in the form of layer that is known as biofilm (Tyagi and Ghose 1982). The influent wastewater comes in contact with the biofilm, where the solid and soluble contents are taken up by the microbial biomass and get transformed (Qureshi et al. 2005). Rock, gravel, slag and different types synthetic materials can be used as inert supports in immobilized microbial reactors (Kadam et al. 2013). Attached growth process has many advantages over suspended growth systems (Ebrahimi and Najafpour, 2016). Use of different types of support media helps in enhancing the reactor performance by

maintaining high biomass concentration through reduced cell washout (Iza 1991). Microbial regeneration and reutilization for repeated cycles is also facilitated through immobilization (Barceló, Petrović, and Armengol 2011; Przystaś et al. 2018). Additionally, attached growth reactors show improved resistance to shock loadings, toxic recalcitrant compounds and have long operation lifetime due to more stabilized microbial biomass (Qureshi et al. 2005).

2.4.2.4.2.1 Immobilized bioreactors

Depending upon the microorganism, immobilized reactors can be aerobic, anaerobic or combined systems which employ spatial separation of the two treatment conditions or use integrated approach i.e. sequential anaerobic-aerobic process in single reaction vessel (Davis and Cornwell, 2013) Bacteria can be immobilized by adsorption, covalent interactions, microencapsulation, and matrix entrapment. Bacterial immobilization through entrapment in polyvinyl alcohol (PVA) gel beads is the most commonly used method due to its low cost and high operational performance and stability (Cheng et al., 2012; Kim et al., 2013). Important reactor configurations based on immobilized bacterial cells include Packed bed (PBR), trickle bed (trickling filter systems), fluidized bed reactors (FBR), membrane bioreactors and rotating biological contactors (Hai et al. 2011; Hassard et al. 2015; Irum et al. 2015; Islam 2016; Lin et al. 2010). Entrapment and attachment are the two main methods for fungal immobilization. Both natural and artificial inert support materials such as: seeds, wheat straw, corncobs, wood shavings and chips, jute, collagen and alginate beads, nylon and stainless-steel sponge etc. can be utilized for fungal immobilization (Rodríguez Couto 2009). Fed-batch fluidized bed and continuous packed bed reactor systems based on immobilized fungal cultures have been tested for dye decolorization process (Moreira et al. 2004).

2.4.2.4.2.2 Biofilm reactors

Biofilm based reactors present a better alternative for azo dye transformation due to the presence of multiple species which can accelerate the treatment process by achieving high cell density and through community degradation process (Qureshi et al. 2005). Cell aggregation improves the reactor stability towards shock loadings and toxic

substances in the high strength influent (Naresh Kumar et al. 2014). Simultaneous anaerobic and aerobic dye conversion is achieved in such reactors as an oxygen gradient is established due to the differential oxygen distribution through the biofilm (Tan 2001). The anoxic and aerobic microenvironments in the biofilm help in the spatial distribution of microbes by creating a competition for oxygen, space and nutrients. So, the interior of the biofilm usually harbors anaerobic and microaerophilic bacteria, while aerobic bacteria colonize the exterior lining of biofilm (Venkata Mohan et al. 2012). Due to the endogenous metabolic phase, growth of anaerobic bacteria is relatively slower which can control the overall biofilm density (Lanthier, Gregory, and Lovley 2008). Rotating biological contactors (RBCs) are the most commonly employed biofilm reactors (Hassard et al. 2015). Other forms include fluidized bed and membrane bioreactors (Kumar and Singh 2011; You et al. 2007). Moreover, hybrid reactor systems that combine the suspended and attached growth process have also been tested. This can be done by augmenting the activated sludge process using different support materials, so that benefits of both suspended and attached growth process can be utilized (Riffat, 2013). This practice improves the reactor stability and the reactors can withstand higher hydraulic rates (Venkata Mohan et al. 2013). Moving bed biofilm reactor (MBBR) and fluidized bed bioreactor (FBBR) are common examples of hybrid systems (Hosseini Koupaie, Alavi Moghaddam, and Hashemi 2012; Papadia et al. 2011).

Chapter 3: Organismic level acute toxicology profiling of reactive azo dyes

Malik, N.H., Zain, H. & Ali, N. *Environ Monit Assess* (2018) 190: 612. <https://doi.org/10.1007/s10661-018-6986-7>

3.1 Introduction

Azo dyes represent an important group of organic colorants with a wide range of applications in different industries such as textile, plastic, food, and paper manufacturing (Zollinger 1987). Among these, textile industries are one of the major consumers of azo dyes (Ollgaard et al. 1998). During the process of fabric dyeing, profuse quantities (up to 50%) of the applied dyes are wasted due to incomplete adherence to the fabrics and thus released into the waste stream (O'Neill et al. 1999). The wastage percentage depends upon the class of dyes and is highest for the reactive azo dyes (Ali, 2010). Reactive azo dyes are the most extensively used dyeing agents in the textile industry, because of their bright hues, high fastness property, and easier application. They are used for coloring cellulose, wool, and viscose rayon fibers (Aksu, 2005; Wang et al. 2009). Chlorotriazine, trichloropyrimidine, vinyl sulfone, and difluorochloropyrimidine are the major functional groups found in different types of reactive azo dyes (Tunç et al. 2009). Reactive azo dyes containing sulfonic acid derivatives are more persistent in the aquatic environments due to their high-water solubility and complex polyaromatic nature (Levine 1991).

The discharge of colored textile effluents into the open water systems is one of the major causes of aquatic environmental havoc (Solís et al. 2012). These effluents not only are a cause of esthetic mutilation but also endanger the aquatic communities, due to the reduction in the dissolved oxygen levels resulting from lesser sunlight penetration and diminished photosynthetic activity (Lalnunhlimi and Veenagayathri, 2016). Different types of intrinsic and extrinsic factors affect the ecological fate of azo dyes. Intrinsic factors include the chemical structure of dyes and their interaction with the metabolic machinery of the living systems. Extrinsic factors include different environmental factors such as oxygen availability, moisture content, availability of light, and inorganic electron shuttles (Rawat et al. 2016). Toxicity evaluation is an important procedure for gaining an insight into the role of xenobiotics in the

environment (Akhtar et al. 2016). It is based on the response of different test organisms towards varying concentrations of a given toxicant, which manifests its effects following reaction with the cellular machinery and/or its microenvironment (Klemola et al., 2007). The data collected from such studies can be utilized to get a generalized idea about the possible effects of such chemicals in an ecological milieu. Reactive Blue 221 (RB 221), Reactive Red 195 (RR 195), and Reactive Yellow 145 (RY 145) are the commonly used reactive dyes in the textile industries, but their acute toxicological information is scarce. The present study focuses on the organismic-level acute toxicology profiling of these dyes in pure and mixture form (to document any synergistic chemical action). To determine, whether the toxicity of a given dye is determined by the dye's structural nature or the type of the target organism, effect of the reactive azo dyes was tested on microbial (bacteria and fungi), plant, and aquatic representatives and effective toxic concentrations of the dyes and their mixture were measured.

3.1.1 Aims and Objectives

The aim of this study was to develop organismic level toxicology profile of reactive azo dyes (RB 221, RR 195, RY 145 and reactive azo dye mixture) via microbial growth inhibition, acute toxicity and phytotoxicity assays. Following were the specific objectives of the present study:

- To determine the effect of reactive azo dyes on the growth of different bacteria and fungi through spectrophotometric analysis and growth diameter measurement, respectively.
- To ascertain the toxic response of dyes on different plants by measuring the seed germination rate.
- To investigate the effect of reactive azo dyes on *Artemia salina* larvae and *Daphnia magna* neonates, mortality rate.
- To compute the EC₂₀, EC₅₀, and EC₈₀ values through dose response analysis using Origin Pro 8 software.

3.2 Materials and Methods

3.2.1 Chemicals

All microbiological growth media and analytical grade chemicals were acquired from Sigma-Aldrich (Sigma- Aldrich, St. Louis, MO, USA) and Oxoid (Oxoid Limited, Hampshire, UK). Reactive azo dyes (RB 221: λ_{max} 615 nm, RR 195: λ_{max} 545 nm, and RY 145: λ_{max} 422 nm) (Table 3.1) were provided by a textile unit in Lahore, Pakistan, and used without further purification. Aqueous stock solutions of the dyes (individual dyes and mixture; 1000 ppm of each) were prepared, filter sterilized (0.2- μm nylon membrane; Corning Inc., Corning, NY, USA), and stored at room temperature.

Table 3.1 Chemical structures of reactive azo dyes

Dyes	Structures	λ_{max} (nm)	Reference
Reactive Blue 221		615	(Pajot, de Figueroa, and Fariña 2007)
Reactive Red 195		545	(Aguedach et al. 2005)
Reactive Yellow 145		422	(Nawahwi 2013)

3.2.2 Microbial growth inhibition assays

3.2.2.1 Effect on different bacteria

3.2.2.1.2 Bacterial specimens

Six bacterial specimens viz. *Pseudomonas aeruginosa* (ATCC® 15442™), *Escherichia coli* (ATCC ® 8739™), *Klebsiella pneumoniae* (ATCC® BAA-1705™), *Staphylococcus aureus* (ATCC ® 6538™), *Listeria monocytogenes* (ATCC® 13932™), and *Bacillus subtilis* (ATCC® 6633™) were obtained from American Type Culture Collection (ATCC), Manassas, VA, USA.

3.2.2.1.3 Medium for bacterial culture maintenance and growth inhibition assay

Nutrient broth was used for pure bacterial cultures growth and inocula preparation, while nutrient agar was used for culture storage (4 °C) (Lapage, Shelton, and Mitchell 1970). Growth inhibition assays were carried out in a slightly modified mineral salt medium, consisting of macronutrient and micronutrients solutions (Khehra et al. 2005). For macronutrient solutions, salts were mixed in the following composition (g/L): 0.09 MgSO₄·7H₂O; 0.54 (NH₄)₂SO₄; 0.0009 MnSO₄; 0.00013 FeSO₄·2H₂O; 0.018 CaCl₂·2H₂O; and 1.224 K₂HPO₄. To this solution, 10 mL/L of the micronutrient solution with the following composition was added (mg/L): 10.0 ZnSO₄·7H₂O; 1.0 CoCl₂·6H₂O; 20.0 NiCl₂·6H₂O; 30.0 Na₂MoO₄·2H₂O; and 1.0 CuCl₂·2H₂O. Glucose and yeast extract (0.001% [w/v] each) were added as additional carbon and nitrogen sources, respectively. pH of the medium was adjusted to 7.0 ± 0.2 with the help of 1 N solutions of HCl and NaOH.

3.2.2.1.4 Procedure

Pure bacterial colonies were picked and aseptically transferred to the nutrient broth medium. Test tubes were incubated at 37 °C. Dose-related effect of the Tubes were incubated at 37°C for 24 hours. reactive azo dyes on bacterial growth was tested in 100-mL Erlenmeyer flasks. Different dye concentrations were prepared by adding the filter-sterilized stock dye solutions (individual dyes and mixture) to the prepared salt medium as per final dye concentration, i.e., 50, 100, 150, 200, 250, 300, 350, 400, 450, 500, and 1000 ppm (final volume, 45 mL). Each flask was inoculated with 5.0 mL of the bacterial suspension in mid-log phase (OD₆₀₀, 0.6). Flasks were incubated under shaking (140 rpm) at 37 °C for 48 h. Dye-free inoculated medium was used as control. Samples were aseptically withdrawn and vortexed, and optical density (OD) was recorded at 600 nm, using a UV-Vis spectrophotometer (Agilent 8453; Agilent Technologies, Santa Clara, CA, USA) at the start of experiments and after 48 h of incubation, using culture-free

(centrifuged) dye containing salt medium samples as blank. The readings were then compared with that of control. For RB 221, due to the possible interference of its absorbance maxima (A615 nm) with that of bacterial growth absorbance wavelength (A600), prior to the optical density measurement, bacterial cultures were centrifuged for 10 min at 10,000×g, washed twice with sterile distilled water and resuspended in sterile saline solution. Growth inhibition ratio (%) was calculated using the following formula (Hendricks, Christman, and Roberts 2017):

$$\text{Growth inhibition ratio (\%)} = \frac{(\text{OD in control sample} - \text{OD in dye sample})}{\text{OD in control sample}} \times 100 \text{ (Eq 3.1)}$$

3.2.2.2 Effect of reactive azo dyes on the growth of fungi

Fungal strains, viz. *Trichoderma asperellum*, *Aspergillus flavus*, *Fusarium fujikuroi*, and *Rhizoctonia solani*, were obtained from Microbiology Research Laboratory, Quaid-i-Azam University, Islamabad, Pakistan.

3.2.2.2.1 Medium for fungal culture maintenance and growth inhibition assay

Dye-free and dye-amended Sabouraud dextrose agar media were used for culture storage and dose-response analysis, respectively.

3.2.2.2.2 Procedure

Dose-related effect of the reactive azo dyes and their mixture on fungal growth was monitored by growth diameter determination. One-hundred-microliter aliquots of the aqueous dye solutions (individual dyes and their mixture) at different concentrations (50, 100, 200, 300, 400, 500, 1000, and 2000 ppm) were added and spread on Sabouraud dextrose agar (SDA) medium containing Petri plates followed by inoculation with the respective fungal hyphae. The plates were incubated at 30 °C for a period of 5 days. Dye-free SDA plates were kept as control. Fungal growth diameter was measured in two perpendicular directions and the values were averaged. Results were then compared with the control (dye-free inoculated medium). Fungal growth inhibition ratio was computed using the following formula (Hendricks et al. 2017):

$$\text{Inhibition ratio (\%)} = \frac{\text{Average diameter in control} - \text{Average diameter in dye sample}}{\text{Average diameter in control}} \times 100$$

(Eq 3.2)

3.2.3 Effect of reactive azo dyes on the plant seed germination potential

To determine the plant seed germination rate in response to the different reactive azo dye (individual dyes and mixture) concentrations, i.e., 100, 200, 300, 400, 500, 600, 700, 800, 900, 1000, and 2000 ppm, *Raphanus sativus* (radish), *Triticum aestivum* (wheat), *Sorghum biocolor* (milo), and *Phaseolus mungo* (black gram) seeds were used according to Turker and Camper, (2002).

3.2.3.1 Seed pretreatment

Prior to the phytotoxicity assay, the plant seeds were rinsed with autoclaved distilled water and subjected to surface sterilization by soaking in a mixture of 10% sodium hypochlorite solution and few drops of Tween 80 for 5 min. Following that, the seeds were thoroughly washed with autoclaved distilled water and dried on a sterilized filter paper.

3.2.3.2 Procedure

Surface-sterilized plant seeds were transferred to the autoclaved Petri plates lined with sterilized filter papers. Five-milliliter aliquots of the aqueous dye solutions with different concentrations were poured in Petri plates. Plates were covered and stored under dim light at 25 °C for a period of 5 days. Petri plates were regularly checked and kept moistened. Alongside, a control was maintained in which the seeds were watered with sterile distilled water. On the fifth day, the number of germinated seeds was counted, and germination inhibition was calculated using the following formula:

$$\text{Germination inhibition ratio (\%)} = \frac{\text{Number of non-germinated seeds}}{\text{Number of seeds added}} \times 100 \text{ (Eq 3.3)}$$

3.3)

3.2.4 Effect of reactive azo dyes on aquatic invertebrate organisms

Acute toxicity of the reactive azo dyes (individual and mixture) towards *Artemia salina* larvae and *Daphnia magna* neonates was investigated according to Meyer et al., (1982) and OECD (2004), respectively.

3.2.4.1 *Artemia salina* larval mortality assay

Artificial seawater (pH 8.0 ± 0.2) was prepared by dissolving 34.0 g/L of commercial sea salt (Harvest Co. H. K.) in distilled water followed by aeration on a magnetic stirrer for 2 h. The seawater was then transferred to an unequally partitioned container (32 × 22 cm). *A. salina* cysts were added to the bigger compartment of the container, which was then covered with aluminum foil to keep that side in dark. The other smaller portion of the container was kept under illumination (with the help of a lamp). This setup was placed in an incubator at 28 °C for a period of 24 h. Following that, the active phototropic *A. salina* larvae (nauplii) were collected in the illuminated section. Different aliquots of the dye solutions (as per required final concentration, i.e., 50, 100, 200, 300, 400, 500, 600, 700, 800, 900, 1000, and 2000 ppm) were added to the small glass vials and ten (10) *A. salina* larvae, picked from the illuminated section of the container with the help of a Pasteur pipette, were transferred to the glass vials and volume was adjusted to 5.0 mL with the prepared seawater solution. Control was maintained by using dye-free seawater solution. The vials were incubated under illumination at 28 °C for 24 h. Dead larvae were counted following incubation and larval mortality percentage was calculated using the following formula:

$$\text{Larval Mortality (\%)} = \frac{\text{Number of } A.\text{salina} \text{ larvae dead}}{\text{Number of } A.\text{salina} \text{ larvae added}} \times 100 \quad (\text{Eq 3.4})$$

3.2.4.1 *Daphnia magna* immobilization assay

D. magna, obtained from a local pet store, were maintained in aerated M4 medium (OECD, 2004), in 2.0-L glass beakers at 20 ± 2 °C under a controlled photoperiod (16:8 h; light/ dark). The cultures were fed with baker's yeast supplemented algal food (*Chlorella vulgaris*). pH (7 ± 1) and hardness (150 ± 20 mg/L) of the culture medium were also maintained. For the acute toxicity analysis, neonates (< 24 h old) were separated from the adults and shifted (five each) to 50-mL glass beakers containing

different dye concentrations, i.e., 25, 50, 100, 200, 300, 400, 500, 1000, and 2000 ppm. The final volume was adjusted to 20 mL. Dye-free M4 medium served as control and the test was performed in quadruplicate for a period of 48 h. Mobility of the daphnids under illumination was tested after 24 and 48 h of exposure. The daphnids unable to swim even in response to gentle agitation were considered as immobile/dead. Immobilized daphnids were counted and immobilization percentage was calculated according to the following formula:

$$\text{Daphnid immobilization (\%)} = \frac{\text{Number of daphnids immobilized}}{\text{Number of daphnids added}} \times 100 \quad (\text{Eq 3.5})$$

3.2.5 Determination of effective concentration for reactive azo dyes

Effective concentrations (EC), i.e., EC20, EC50, and EC80, were calculated through dose-response analysis in Origin Pro 8 (OriginLab, Northampton, MA, USA). The following nonlinear regression equation was used for EC computation:

$$y = A1 + \frac{A2 - A1}{1 + 10^{(LOGx0 - x)p}} \quad (\text{Eq 3.6})$$

Where A1 is the bottom asymptote, A2 is the top asymptote, $LOGx0$ is the center, and p is the hill slope of the sigmoidal curve.

3.2.6 Statistical analysis

All the experiments were performed in triplicate and quadruplicate (*Daphnia* acute immobilization assay). Mean values and standard error of means were calculated using Microsoft Excel 2016. Multivariate analysis of variance (MANOVA) followed by Tukey's honest significant difference test (Tukey's HSD) at the significance level of $\alpha = 0.05$ ($p < 0.05$) was done using SPSS (IBM SPSS Statistics for Windows, Version 20.0., Armonk, NY, USA).

3.3 Results

3.3.1 Microbial growth inhibition assays

3.3.1.1 Effect of reactive azo dyes on different bacteria

Six bacterial specimens (three gram-negative and three gram-positive), i.e., *P. aeruginosa*, *E. coli*, *K. pneumoniae*, *S. aureus*, *L. monocytogenes*, and *B. subtilis*, were used to determine the antimicrobial effect of reactive azo dyes (RB 221, RR 195, RY 145, and reactive azo dye mixture). Effective concentrations corresponding to 20, 50, and 80% reduction in bacterial growth were computed. *P. aeruginosa* showed a dose-dependent response towards the reactive azo dyes (Fig. 3.1 and Table A1 [Appendix 1]). *P. aeruginosa* was found to be more sensitive towards the reactive azo dye mixture and RY 145 dye. The EC20, EC50, and EC80 values for reactive azo dye mixture were 58.42, 110.56, and 209.22 ppm, while for RY 145, 20, 50, and 80% growth inhibition was observed at 58.49, 120.04, and 246.33 ppm dye concentrations, respectively. RB 221 was found to be relatively less toxic towards *P. aeruginosa* and the effective concentration (EC20, EC50, and EC80) values for this dye were 79.45, 146.58, and 270.41 ppm, respectively. RR 195 was found to be the least toxic dye for *P. aeruginosa* and 20, 50, and 80% growth inhibition was recorded at 248.1, 328.08, and 433.85 ppm, respectively (Fig. 3.7a).

In the dose-response growth analysis for *E. coli* (Fig. 3.2 and Table A2 [Appendix 1]), RY 145 exhibited the most toxic effect. The respective EC20, EC50, and EC80 values were 52.47, 121.41, and 280.86 ppm. This was followed by the dye mixture (EC20, EC50, and EC80: 80.64, 185.58, and 427.02 ppm) and RB 221 (EC20, EC50, and EC80: 92.13, 205.41, and 457.98 ppm). Least toxic response was observed in the case of RR 195. With RR 195 dye, 20, 50, and 80% reduction in optical density was observed at 161.87, 270.59, and 452.35 ppm, respectively (Fig. 3.7b). Dose-response analysis of *K. pneumoniae* (Fig. 3.3 and Table A3 [Appendix 1]) showed RB 221 as the most toxic dye (EC20, EC50, and EC80: 31.92, 136.83, and 306.53 ppm) followed by RR 195 (EC20, EC50, and EC80: 57.81, 147.32, and 375.41 ppm). RY 145 showed a relatively lesser inhibitory effect on the growth of *K. pneumoniae* as 20, 50, and 80% growth reduction was observed at 64.96, 152.49, and 357.96 ppm dye concentrations, respectively. Dye mixture was found to be the least toxic for *K. pneumoniae*. The respective EC20, EC50, and EC80 were 138.09, 240.51, and 418.89 ppm (Fig. 3.7c).

For *S. aureus*, dose-response analysis (Fig. 3.4 and Table A4 [Appendix 1]) showed the dye mixture to be more toxic in comparison to the individual dyes, with EC20, EC50, and EC80 values of 123.43, 154.45, and 193.28 ppm, respectively. This was followed

by RB 221 that caused 20, 50, and 80% reduction in the optical density at 157.27, 176.27, and 197.56 ppm dye concentrations, respectively. The other two dyes were relatively less toxic. For RY 145, EC20, EC50, and EC80 were, 83.61, 219.06, and 573.91 ppm, while for RR 195, 20, 50, and 80% inhibition was recorded at 182.47, 303.58, and 505.09 ppm, respectively (Fig. 3.7d). In the dose-response analysis of *L. monocytogenes* (Fig. 3.5 and Table A5 [Appendix 1]), RR 195 showed higher toxicity than other dyes and the dye mixture. EC20, EC50, and EC80 were recorded at 40.54, 79.13, and 154.45 ppm dye concentrations, respectively. With the dye mixture, a relatively lesser toxic response was observed (EC20, EC50, and EC80: 56.96, 97.76, and 167.79 ppm, respectively). For RB 221, the respective EC20, EC50, and EC80 values were 71.13, 120.15, and 202.95 ppm. RY 145 was least toxic dye for *L. monocytogenes* as the 20, 50, and 80% growth inhibition was observed at 163.66, 240.26, and 352.69 ppm, respectively (Fig. 3.7e). For *B. subtilis*, RR 195 and RB 221 showed more inhibitory effect in the dose-response analysis (Fig. 3.6 and Table A6 [Appendix 1]). For RR 195, 20, 50, and 80% bacterial growth reduction was observed at 79.24, 136.42, and 244.09 ppm; whereas for RB 221 dye, the EC20, EC50, and EC80 values were 86.39, 146.39, and 258.35 ppm, respectively. Dye mixture and RY145, on the other hand, showed a slight lesser inhibitory effect on *B. subtilis* growth. For the dye mixture, the respective EC20, EC50, and EC80 values were 93.11, 161.32, and 373.07 ppm, while with RY 145, 20, 50, and 80% bacterial growth reduction was recorded at 90.16, 184.03, and 381.82 ppm, respectively (Fig. 3.7f).

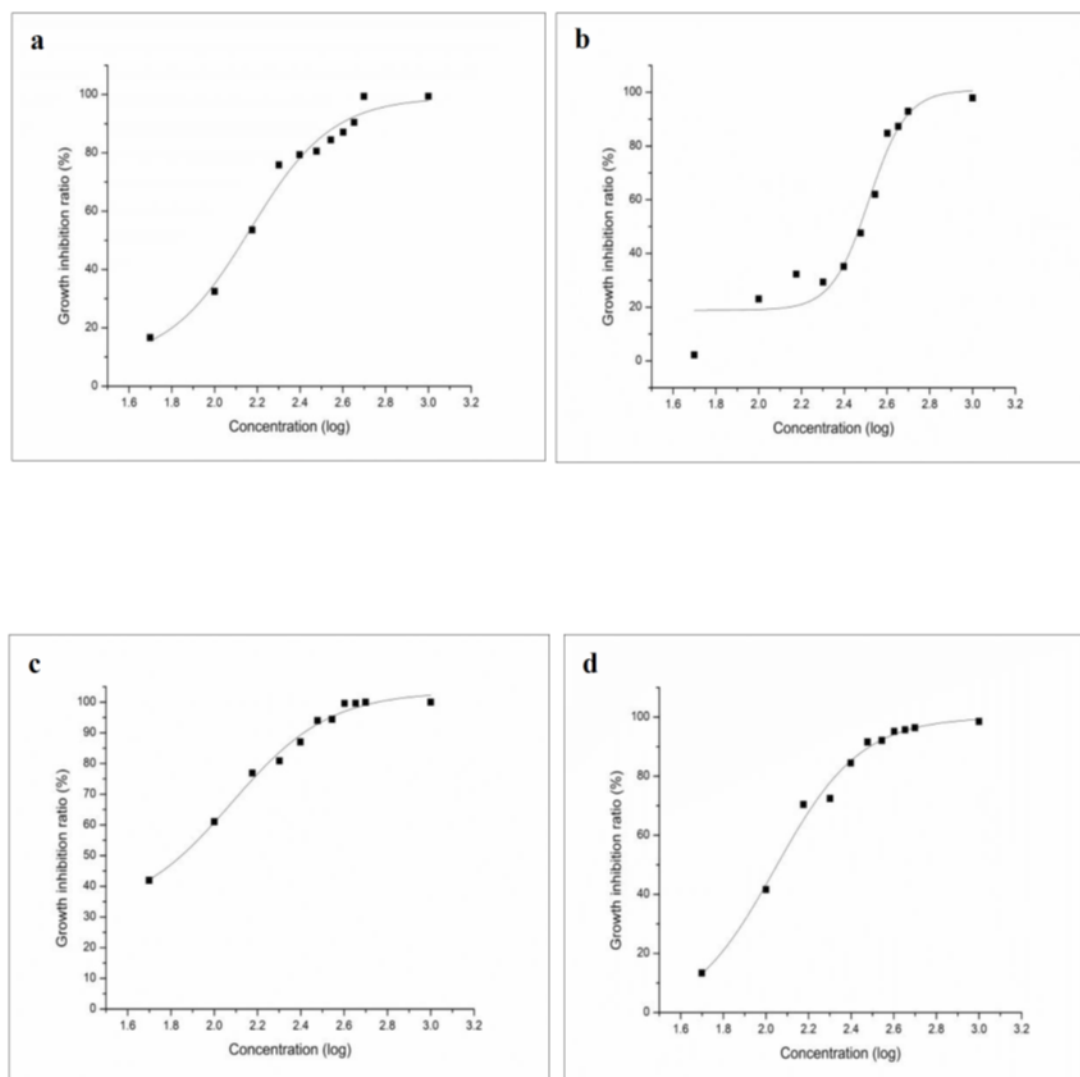


Fig. 3.1 Dose response curves for *P. aeruginosa* with (a) RB 221, (b) RR 195, (c) RY 145, and (d) Dyes mixture. Squares and lines represent the bacterial growth inhibition and fit curves, respectively

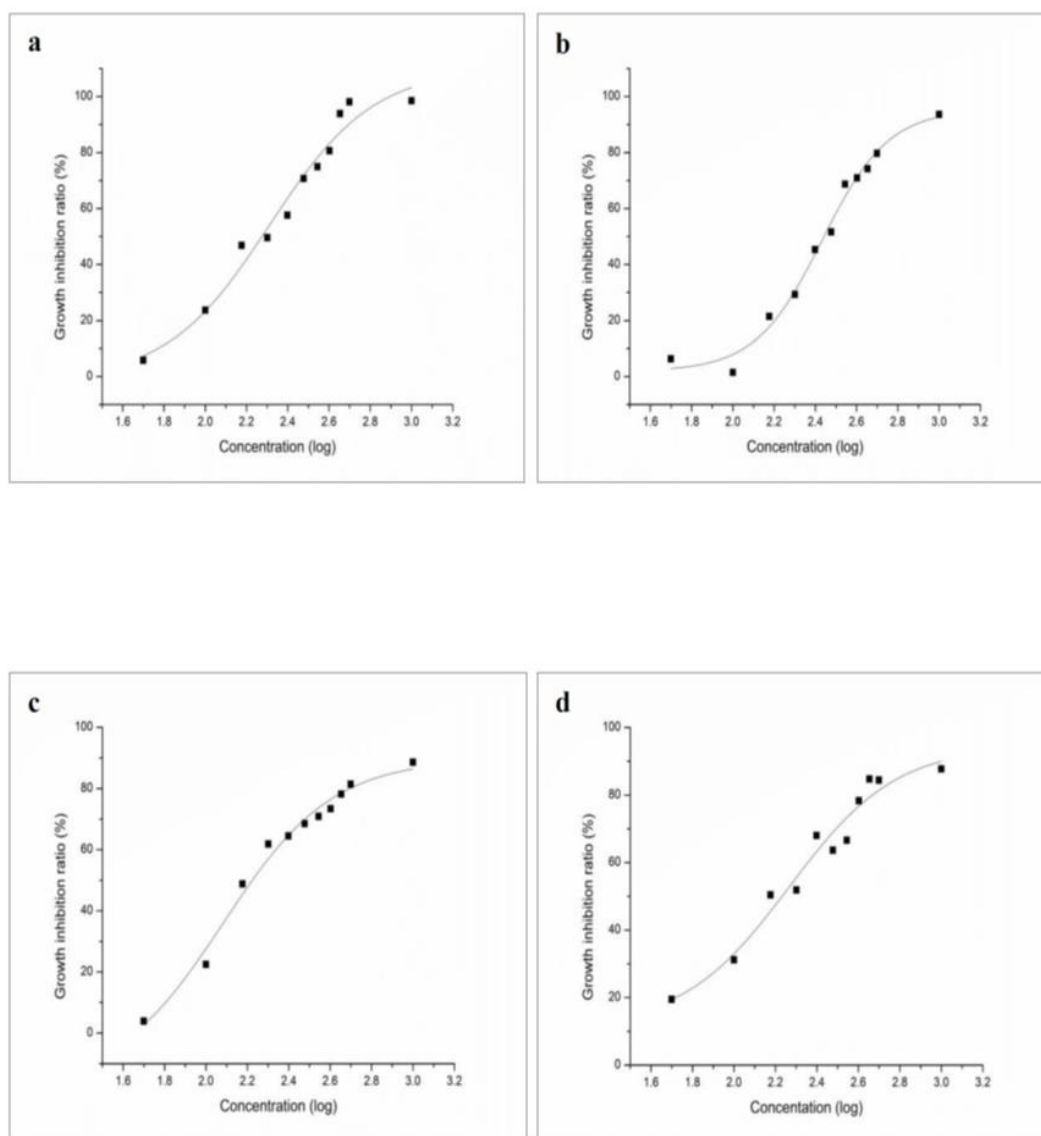


Fig. 3.2 Dose response curves for *E. coli* with (a) RB 221, (b) RR 195, (c) RY 145, and (d), Dyes mixture. Squares and lines represent the bacterial growth and fit curves, respectively

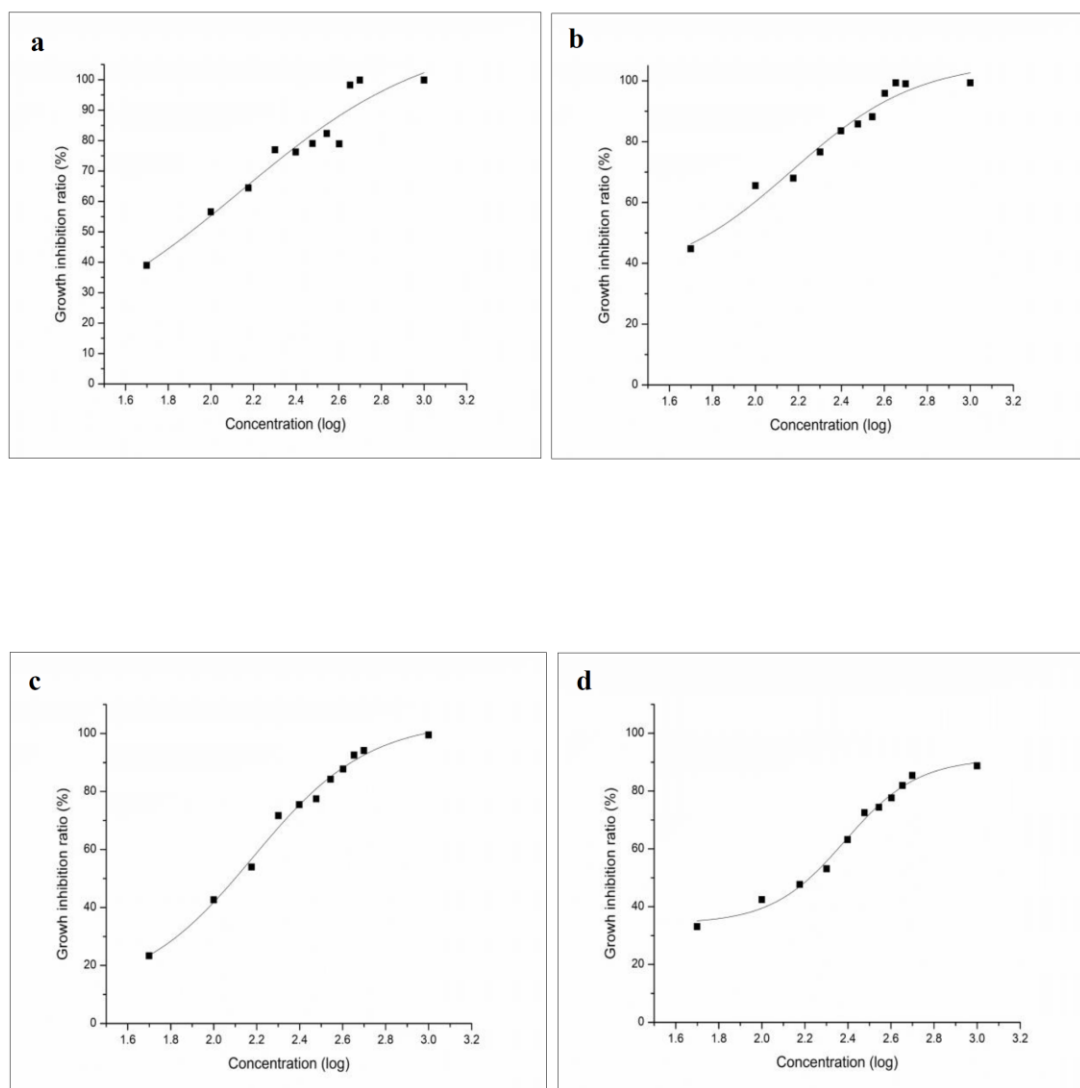


Fig. 3.3 Dose response curves for *K. pneumoniae* with (a) RB 221, (b) RR 195, (c) RY 145, and (d) Dyes mixture. Squares and lines represent the bacterial growth inhibition and fit curves, respectively

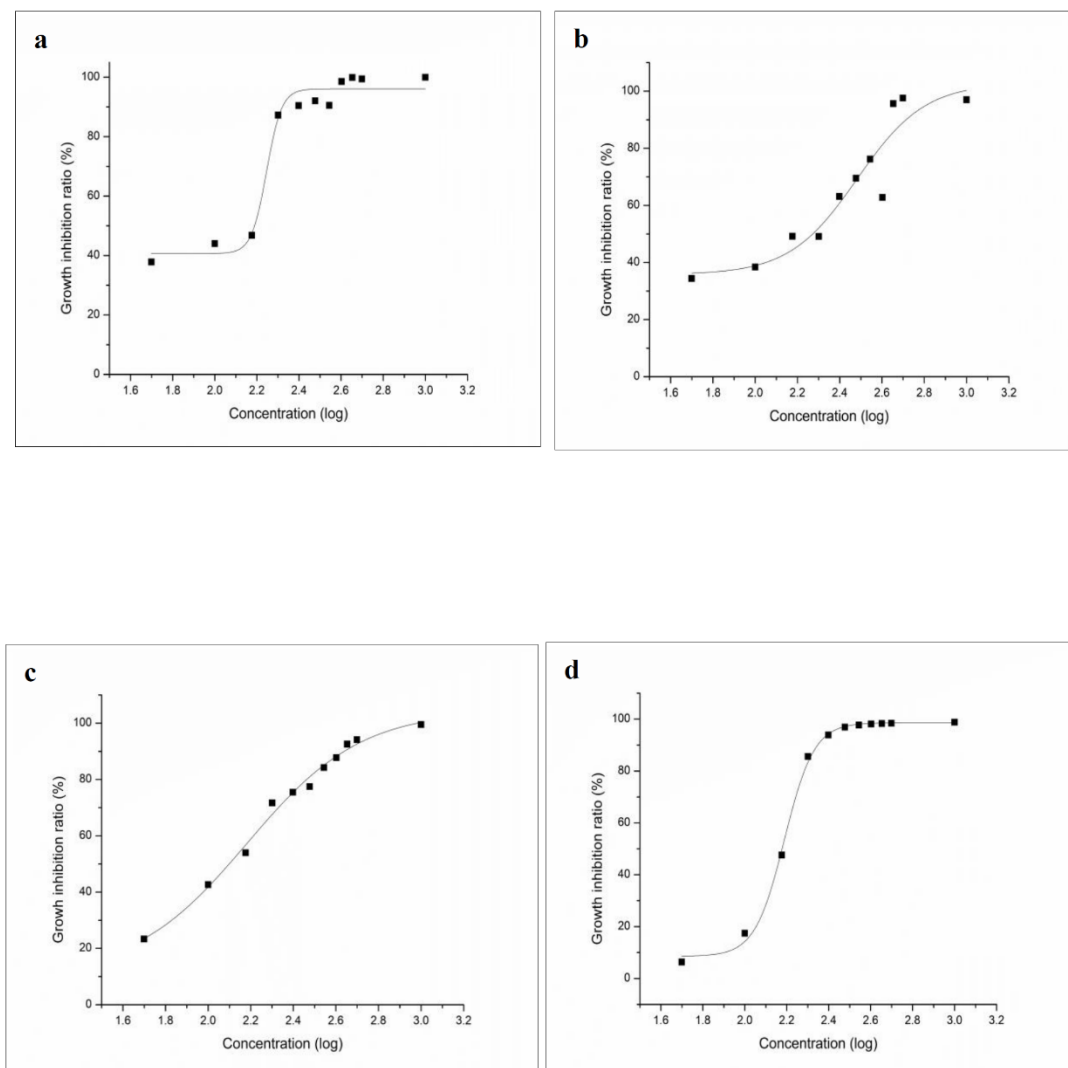


Fig. 3.4 Dose response curves for *S. aureus* with (a) RB 221, (b) RR 195, (c) RY 145, and (d) Dyes mixture. Squares and lines represent the bacterial growth inhibition and fit curves, respectively

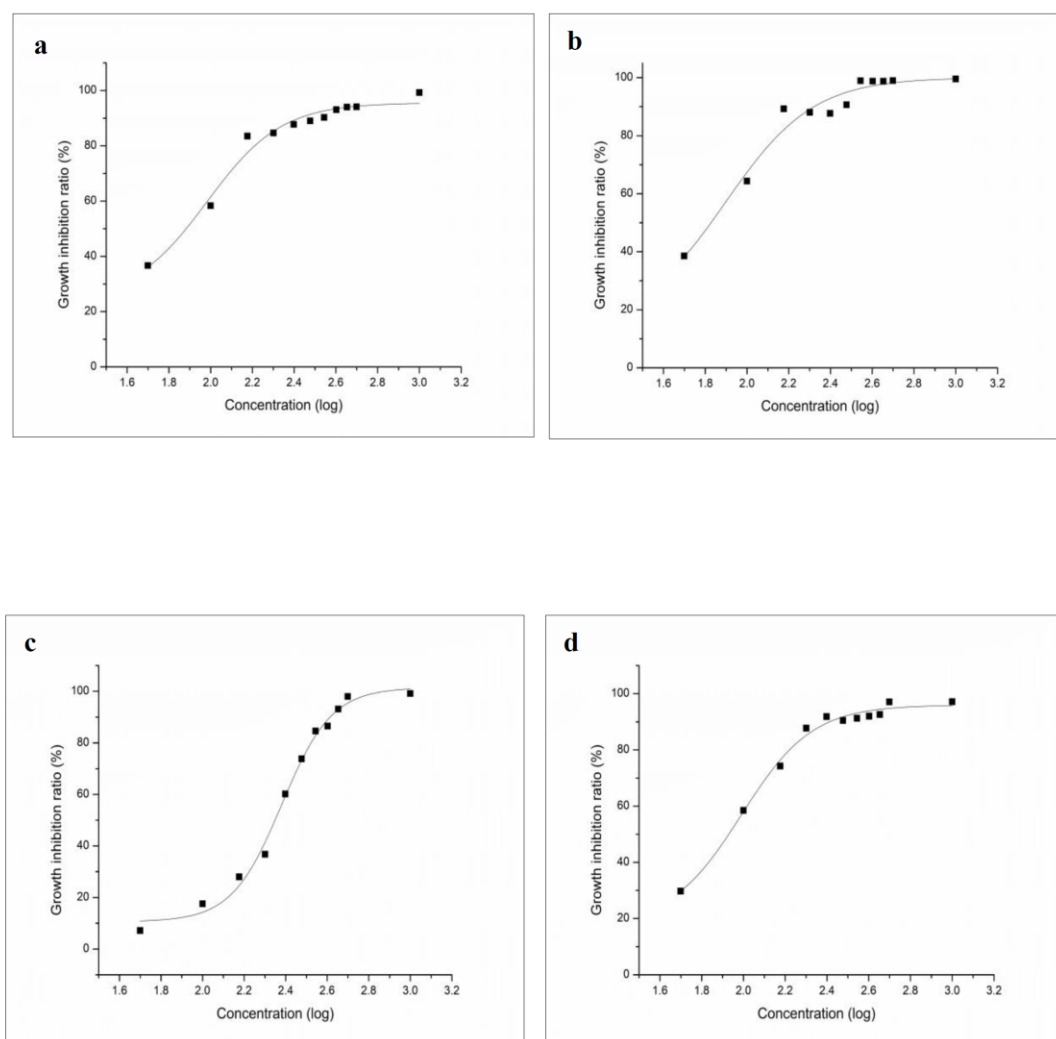


Fig. 3.5 Dose response curves for *L. monocytogenes* with (a) RB 221, (b) RR 195, (c) RY 145, and (d) Dyes mixture. Squares and lines represent the bacterial growth inhibition and fit curves, respectively

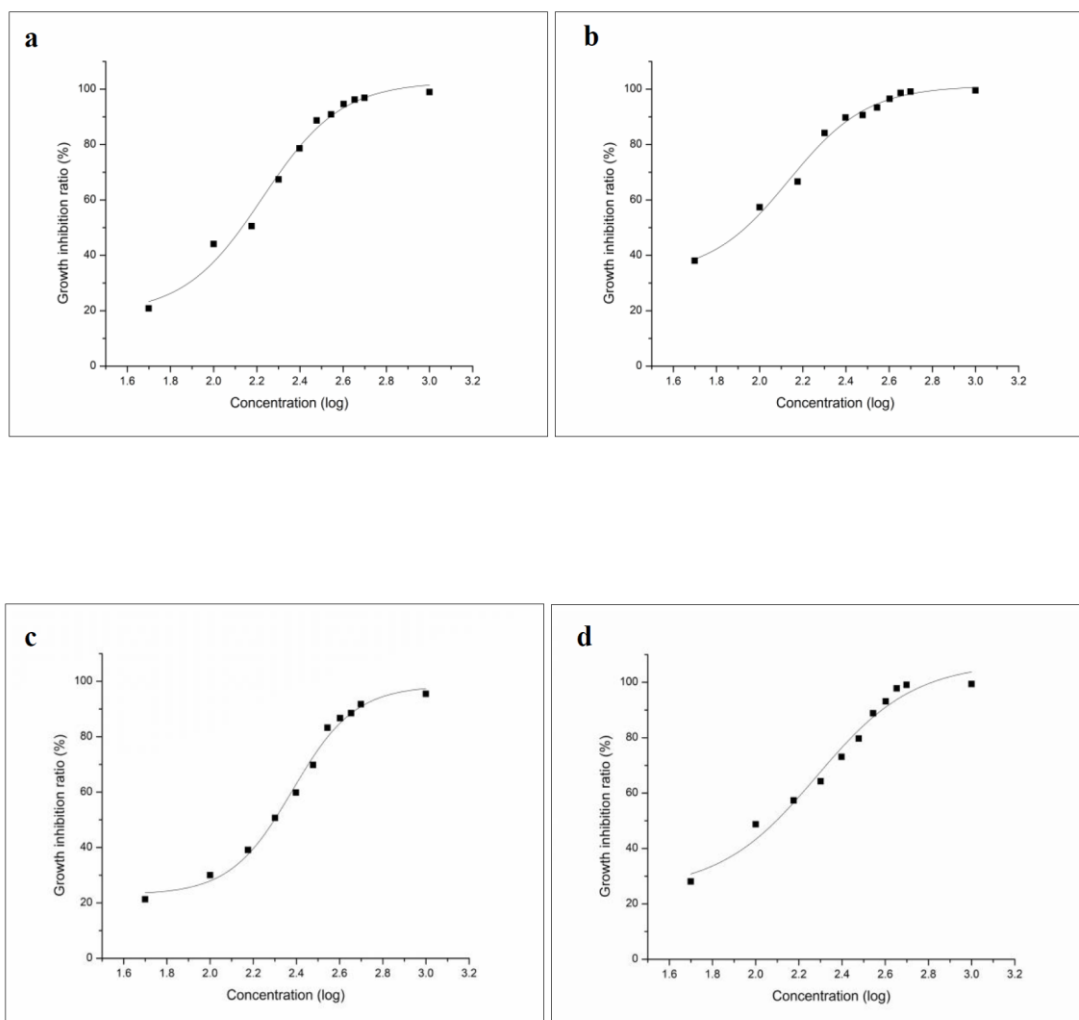


Fig. 3.6 Dose response curves for *B. subtilis* with (a) RB 221, (b) RR 195, (c) RY 145 and (d) Dyes mixture. Squares and lines represent the bacterial growth inhibition and fit curves, respectively

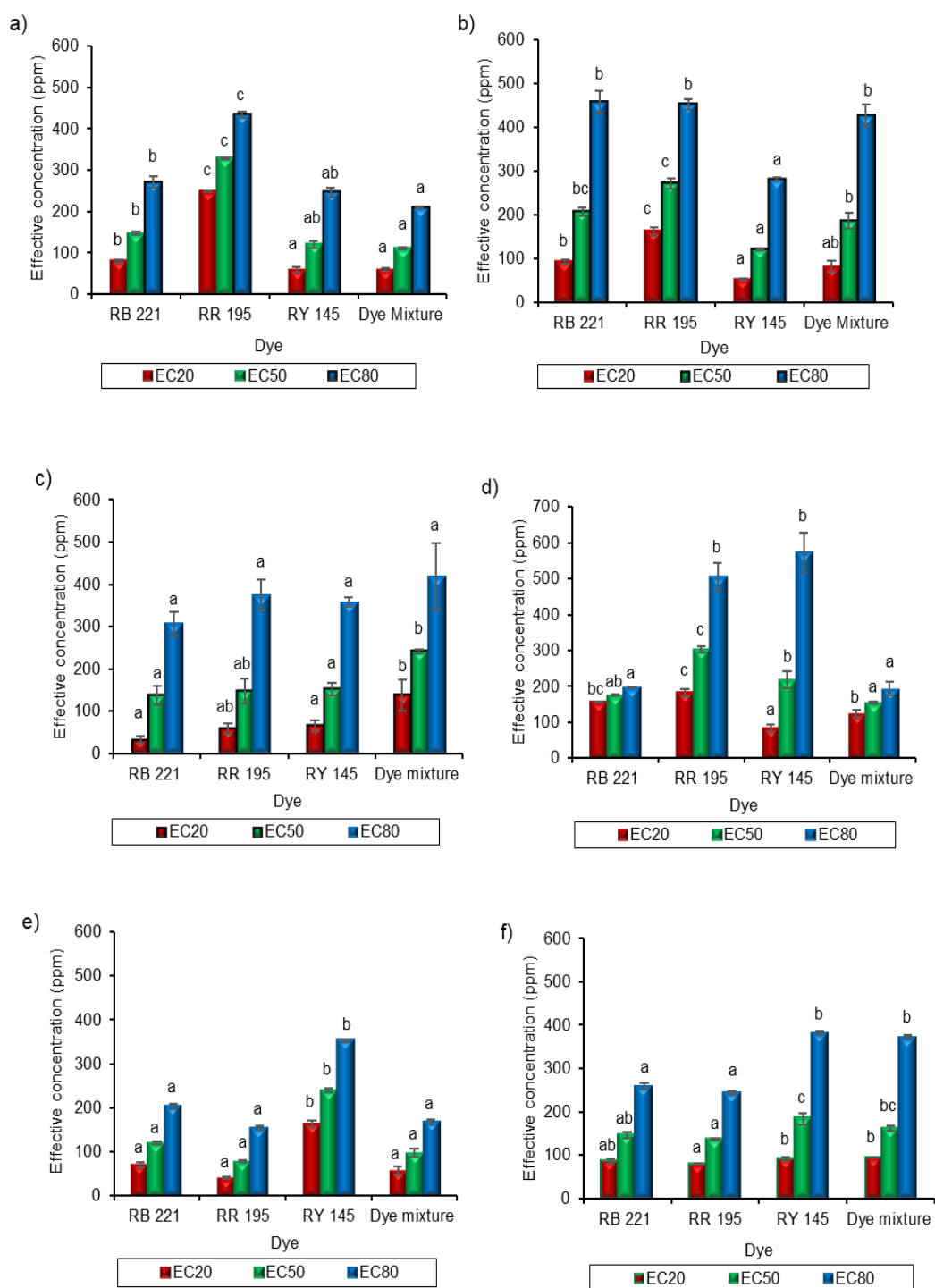


Fig. 3.7 Effective dye concentrations (EC20, EC50, and EC80) for (a) *P. aeruginosa*; (b) *E. coli*; (c) *K. pneumoniae*; (d) *S. aureus*; (e) *L. monocytogenes*; and (f) *B. subtilis*. Different letters within a series indicate significantly different values ($\alpha=0.05$, Tukey's HSD)

3.3.1.2 Effect of reactive azo dyes on the growth of fungi

Four fungal strains, i.e., *T. asperellum*, *A. flavus*, *F. fujikuroi*, and *R. solani*, were used to determine dose-related effect of reactive azo dyes (RB 221, RR 195, RY 145, and reactive azo dye mixture) (Figs. 3.8–3.11 and Tables A7–A10 [Appendix 1]). For *T. asperellum*, RB 221 was found to be the most toxic dye. Twenty, 50, and 80% reduction in growth diameter was observed at 38.59, 137.19, and 441.81 ppm dye concentrations, respectively. This was followed by the dye mixture (EC20, EC50, and EC80: 42.64, 145.09, and 551.98 ppm) and RY 145 (EC20, EC50, and EC80: 62.62, 148.88, and 553.99 ppm). With the RR 195 dye, 20, 50, and 80% growth inhibition was recorded at 66.59, 175.18, and 617.86 ppm dye concentrations, respectively (Fig. 3.12a). *A. flavus* was found to be more sensitive towards RR 195 dye. The respective EC20, EC50, and EC80 values were 17.65, 142.49, and 761.02 ppm. RB 221 (EC20, EC50, and EC80: 61.59, 226.32, and 631.56 ppm, respectively) and the dye mixture (EC20, EDC50, and EC80: 87.01, 227.42, and 594.38 ppm, respectively) were relatively less toxic for the tested organism. *A. flavus* was found to be a little more resistant to RY 145, with the respective EC20, EC50, and EC80 values of 78.51, 356.33, and 784.28 ppm (Fig. 3.12b).

F. fujikuroi was found to be more resistant to all the tested dyes. Twenty, 50, and 80% reduction in growth diameter with RB221 was observed at 338.81, 911.61, and 2570.03 ppm, respectively. This was followed by RY 145 (EC20, EC50, and EC80: 350.95, 1076.69, and 1921.65 ppm, respectively) and RR 195 (EC20, 50 and 80: 399.36, 1827.74, and 2964.86 ppm, respectively). With the dye mixture, 20, 50, and 80% inhibition was recorded at 552.64, 2108.92, and 2951.45 ppm dye concentrations, respectively (Fig. 3.12c). Similarly, *R. solani* showed very less sensitivity towards the reactive azo dyes and their mixture. Comparable inhibitory effects were recorded for the dye mixture (EC20, EC50, and EC80: 333.11, 539.75, and 1880.53 ppm, respectively) and RR 195 dye (EC20, EC50 and EC80: 330.27, 739.38, and 2184.51733 ppm, respectively). With RY 145, the respective EC20, EC50, and EC80 values were 413.23, 708.51, and 1714.79 ppm. RB 221 showed the least inhibitory effect, with the 20, 50, and 80% fungal growth diameter reduction observed at 445.19, 2276.49, and 2989.98 ppm dye concentrations, respectively (Fig. 3.12d).

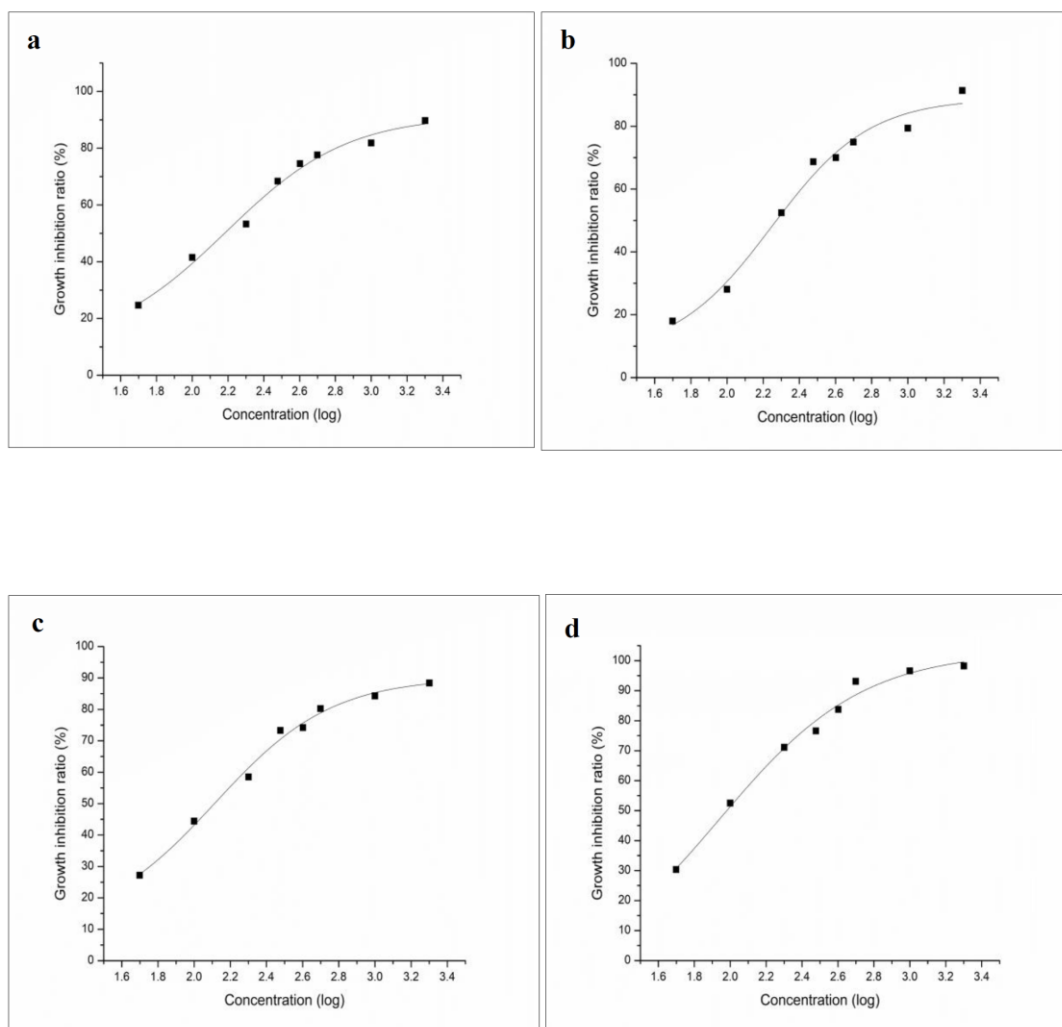


Fig. 3.8 Dose response curves for *T. asperellum* with (a) RB 221, (b) RR 195, (c) RY 145, and (d) Dyes mixture. Squares and lines represent the fungal growth inhibition and fit curves, respectively

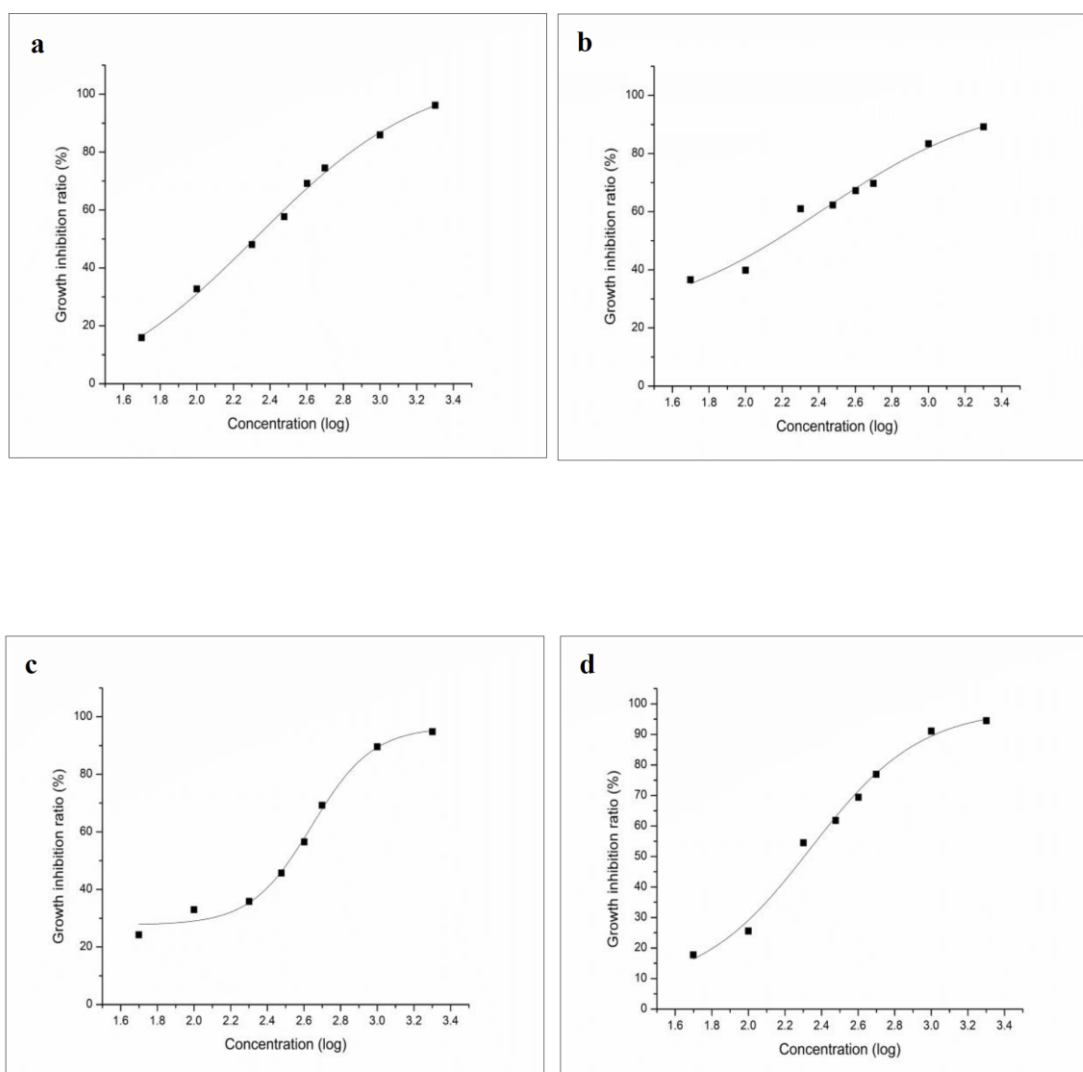


Fig. 3.9 Dose response curves for *A. flavus* with (a) RB 221, (b) RR 195, (c) RY 145, and (d), Dyes mixture. Squares and lines represent the fungal growth inhibition and fit curves, respectively

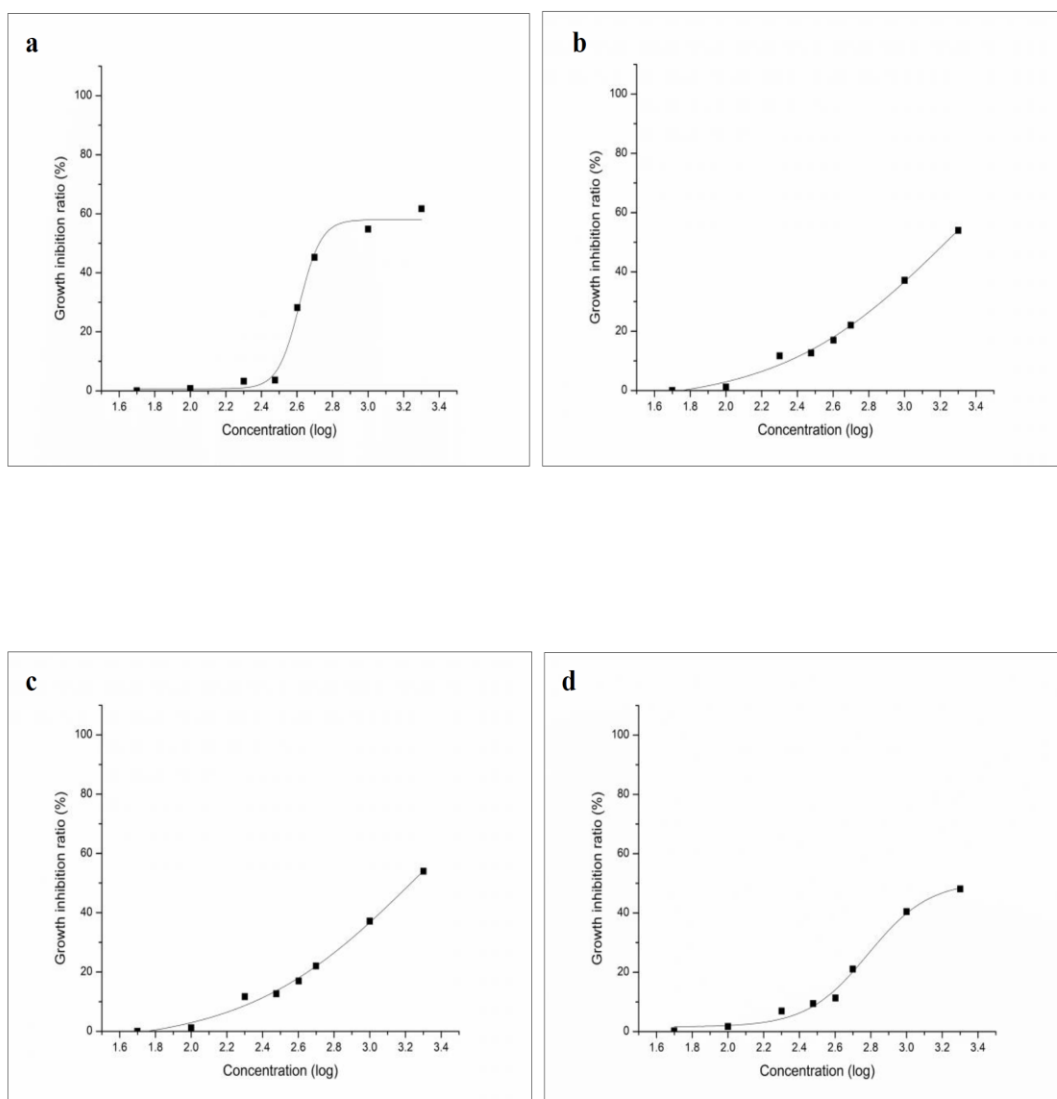


Fig. 3.10 Dose response curves for *F. fujikuroi* with (a) RB 221, (b) RR 195, (c) RY 145, and (d), Dyes mixture. Squares and lines represent the fungal growth inhibition and fit curves, respectively

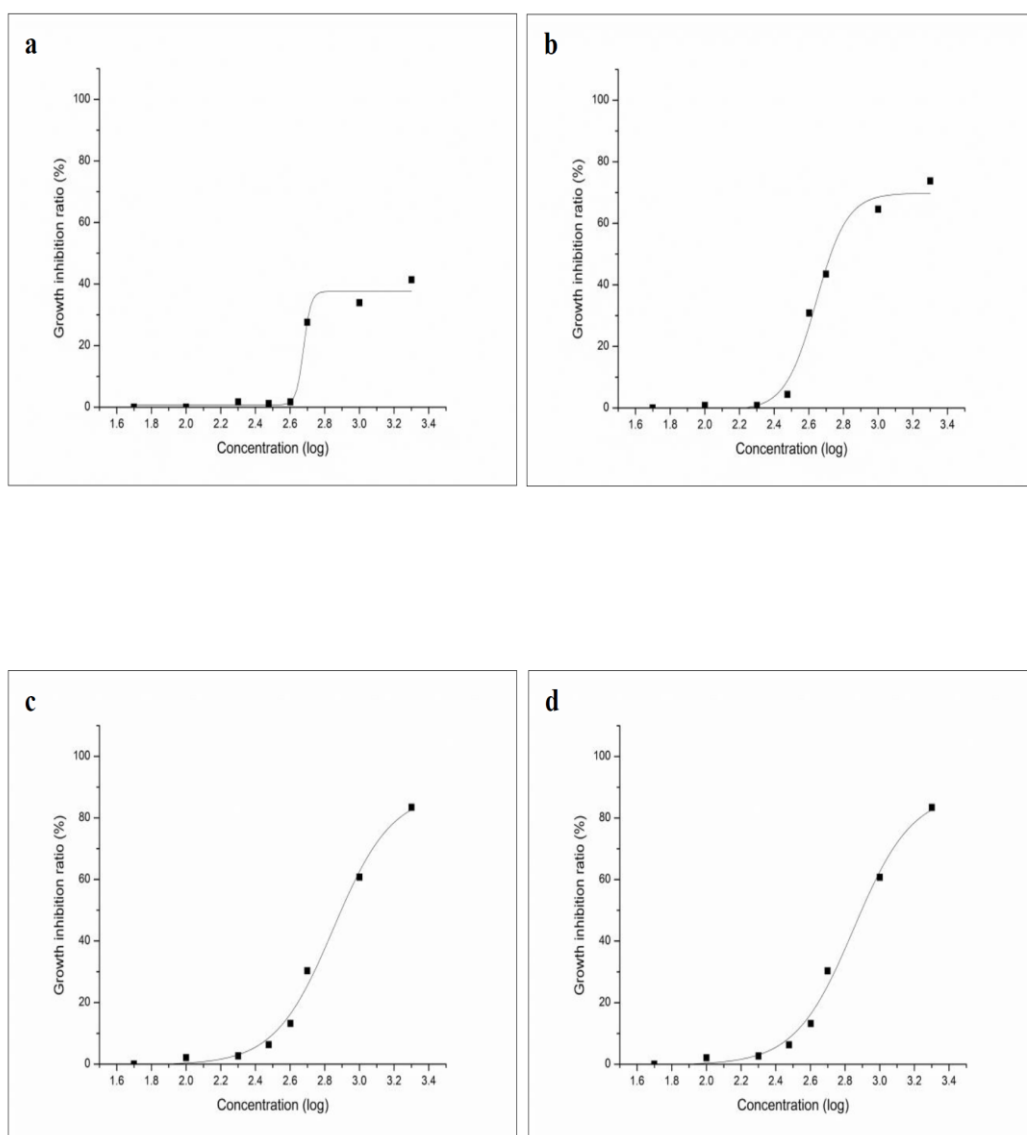


Fig. 3.11 Dose response curves for *R. solani* with (a) RB 221, (b) RR 195, (c) RY 145, and (d), Dyes mixture. Squares and lines represent the fungal growth inhibition and fit curves, respectively

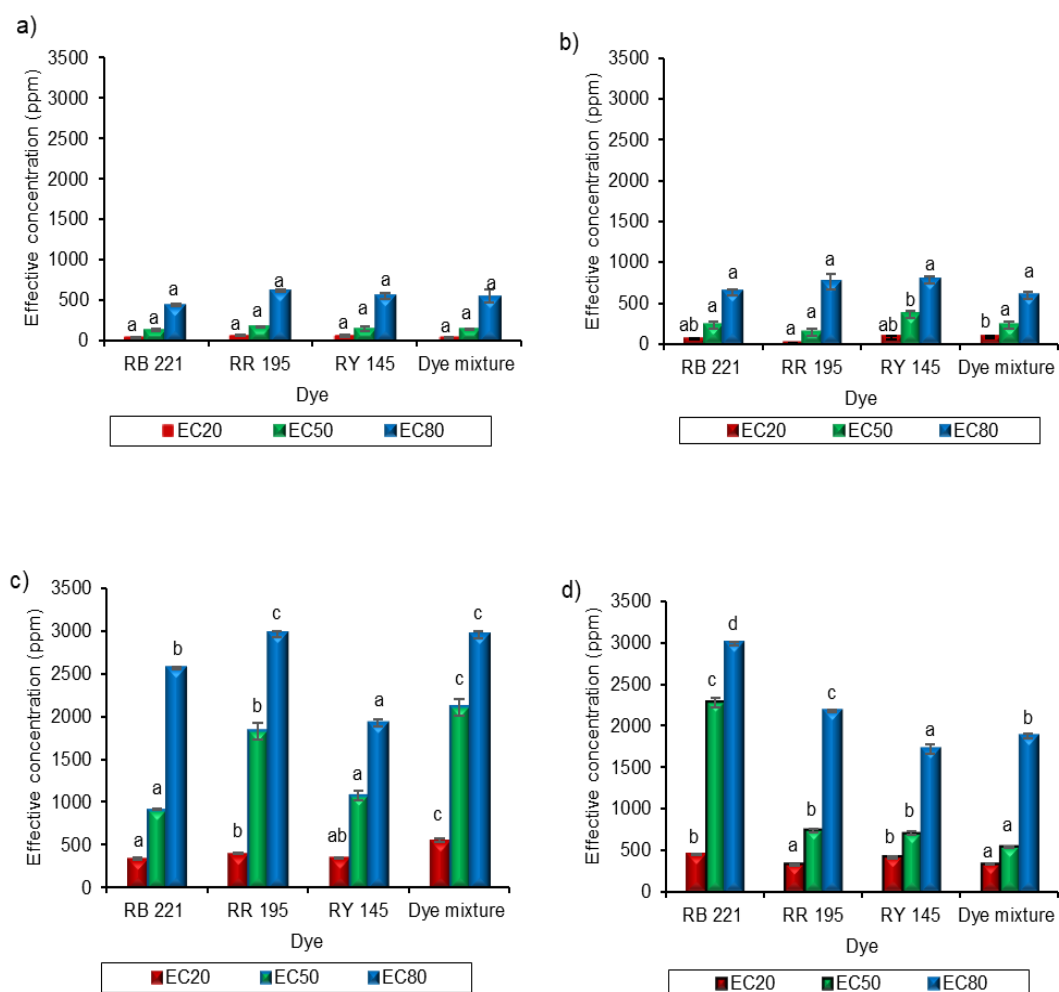


Fig. 3.12 Effective dye concentrations (EC20, EC50, and EC80) for (a) *T. asperellum*; (b) *A. flavus*; (c) *F. fujikuroi*; and (d) *R. solani*. Different letters within a series indicate significantly different values ($\alpha=0.05$, Tukey's HSD)

3.3.2 Effect of reactive azo dyes on the plant seed germination potential

R. sativus, *T. aestivum*, *S. bicolor*, and *P. mungo* seeds were used to determine the phytotoxicity of reactive azo dyes (RB 221, RR 195, RY 145, and reactive azo dye mixture). Seed germination inhibition was calculated, and the dose-response analysis was carried out (Figs. 3.13–3.16 and Tables A11–A14). For all the plant seeds, effective concentrations of the dyes corresponding to the 20 and 50% germination inhibition were calculated, but EC80 values were not determined for the tested range. For radish seeds, reactive azo dye mixture showed more phytotoxic effect than the individual dyes. Twenty percent seed germination inhibition was observed at 203.37 ppm while at 956.11 ppm, 50% germination inhibition was recorded. This was followed by RY 145 dye with which 20 and 50% germination inhibition was observed at 445.13 and 983.25 ppm dye concentrations respectively. The relatively less toxic dyes for *R. sativus* were RR 195 (EC20 and EC50: 461.41 and 2144.31 ppm) and RB 221 (EC20 and EC50: 395.78 and 2760.04 ppm) (Fig. 3.17a).

Like radish seeds, *T. aestivum* seeds were more sensitive towards the azo dye mixture (EC20 and EC50: 450.51 and 1984.65 ppm). Relatively lesser toxic response was observed with the individual dyes RY 145 (EC20 and EC50: 644.22 and 2015.66 ppm), RR 195 (EC20 and EC50: 668.34 and 2556.99 ppm), and RB 221 (EC20 and EC50: 762.16 and 2590.22 ppm) (Fig. 3.17b). In the case of *S. bicolor* seeds, RR 195 dye showed more toxic effect than the other dyes and mixture. Twenty and 50% germination inhibition was observed at 282.15 and 2141.11 ppm dye concentrations, respectively. This was followed by RY 145 as the respective EC20 and EC50 values were 337.74 and 2689.62 ppm. Comparable response was observed with RB 221 (EC20 and EC50: 409.75 and 2786.49 ppm) and the dye mixture (EC20 and EC50: 436.01 and 2799.42 ppm) (Fig. 3.13c). *P. mungo* showed a relatively more resistant response towards the tested dyes and mixture. EC20 and EC50 values for the dye mixture were 858.62 and 2732.97 ppm; for RR 195, the 20 and 50% inhibition was determined at 855.37 and 2929.79 ppm, whereas for RB 221, the respective values were 919.62 and 2864.49 ppm. *P. mungo* seeds were more resistant to RY 145 dye (EC20 and EC50: 1974.98 and 3566.73 ppm) (Fig. 3.17d).

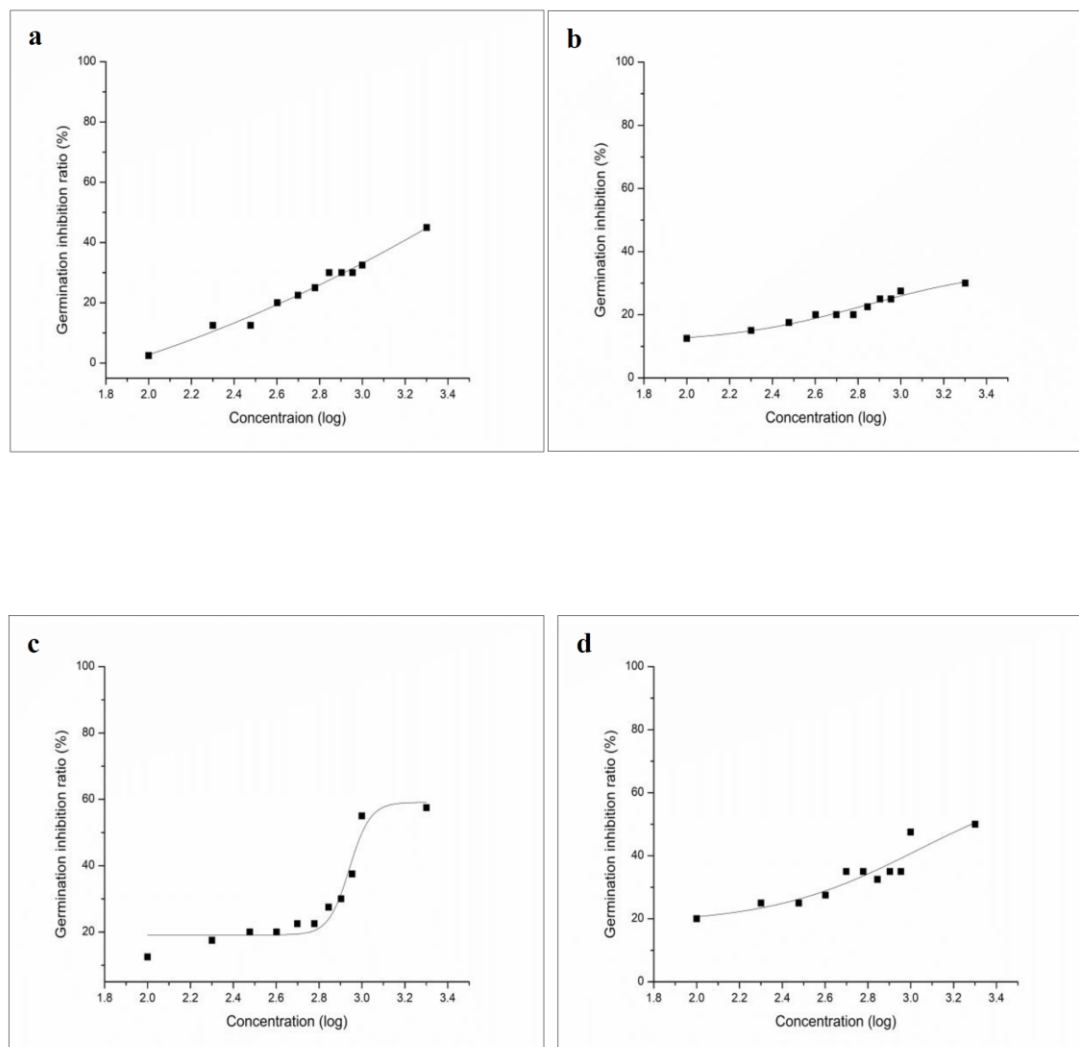


Fig. 3.13 Dose response curves for *R. sativus* seeds with (a) RB 221, (b) RR 195, (c) RY 145, and (d), Dyes mixture. Squares and lines represent the percent germination inhibition and fit curves, respectively

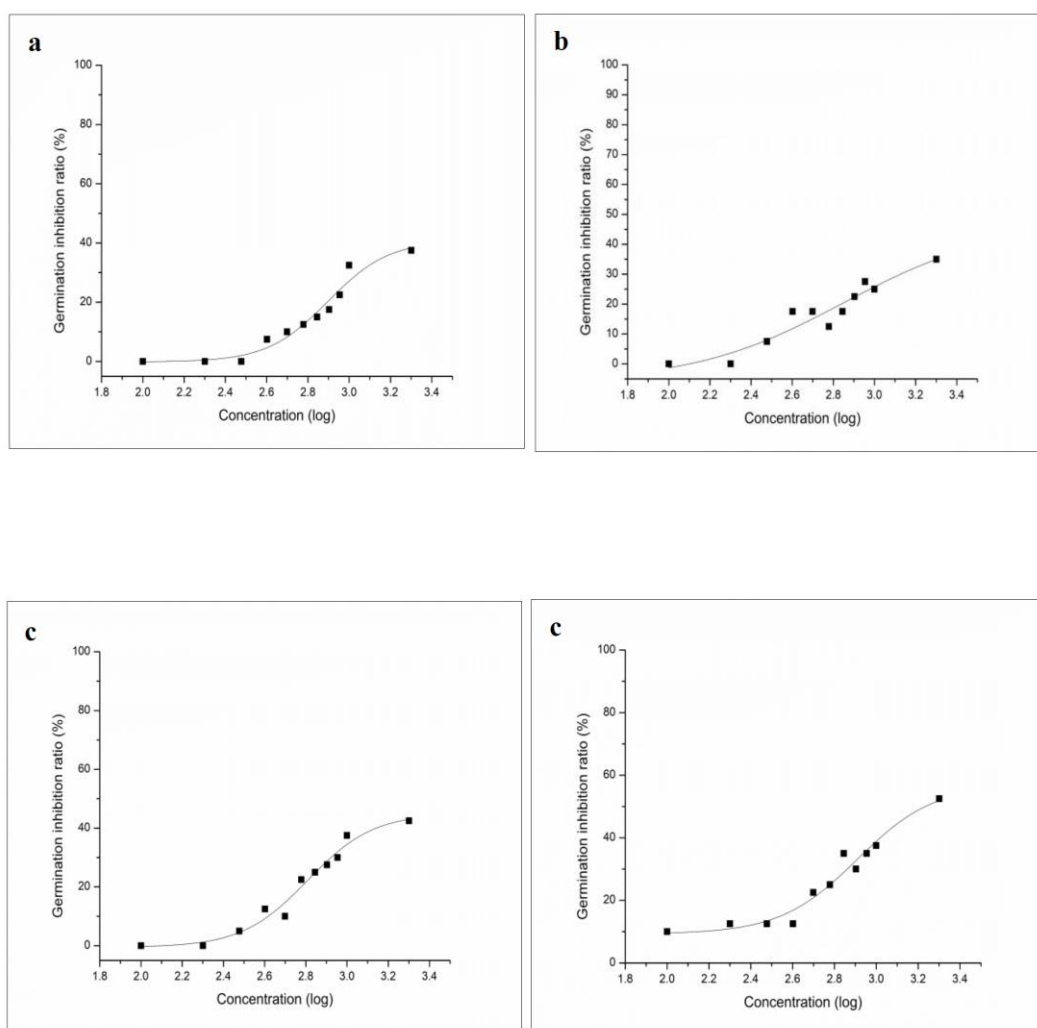


Fig. 3.14 Dose response curves for *T. aestivum* seeds with (a) RB 221, (b) RR 195, (c) RY145, and (d) Dyes mixture. Squares and lines represent the percent germination inhibition and fit curves, respectively

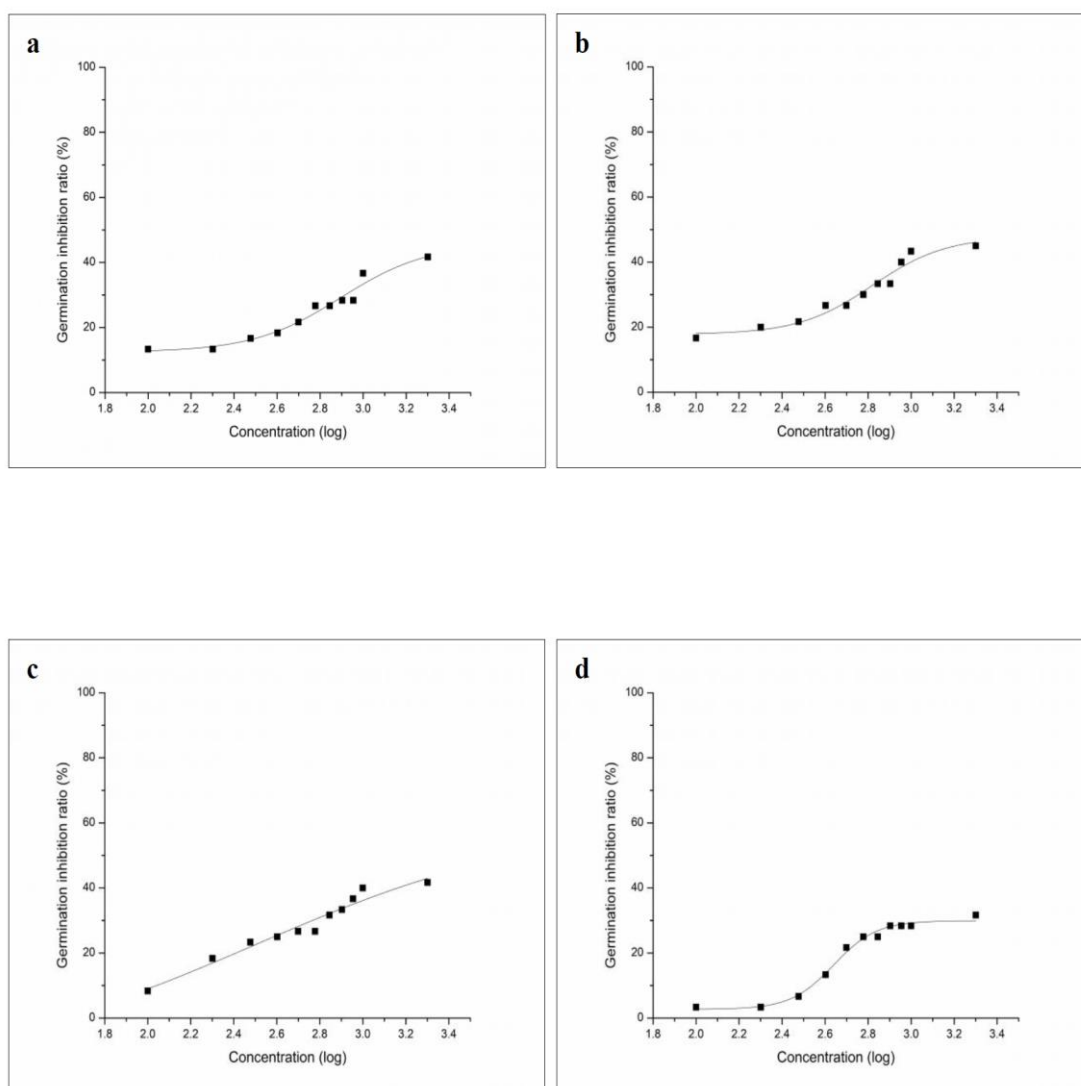


Fig. 3.15 Dose response curves for *S. bicolor* seeds with (a) RB 221, (b) RR 195, (c) RY 145, and (d) Dyes mixture. Squares and lines represent the percent germination inhibition and fit curves, respectively

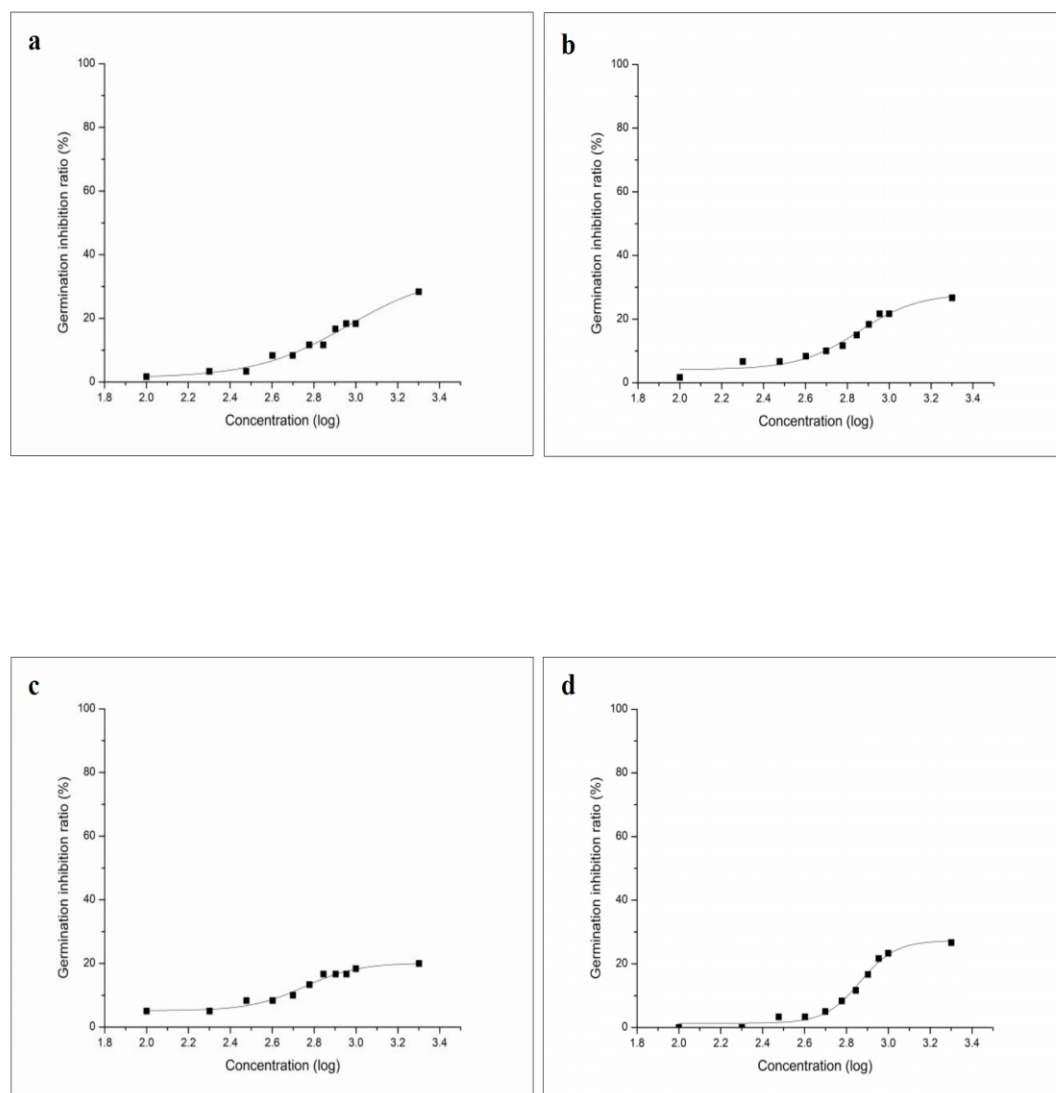


Fig. 3.16 Dose response curves for *P. mungo* seeds with (a) RB 221, (b) RR 195, (c) RY 145, and (d) Dyes mixture. Squares and lines represent the percent germination inhibition and fit curves, respectively

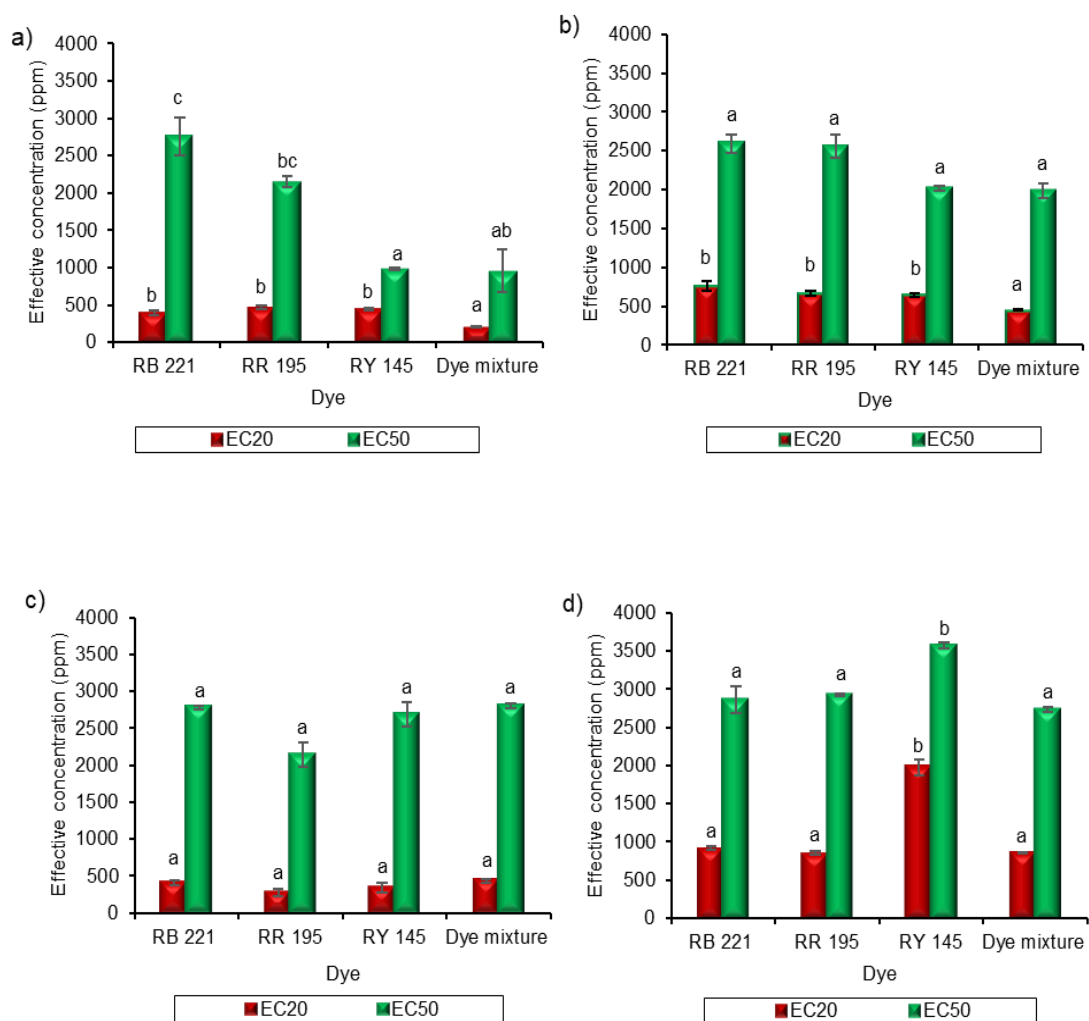


Fig. 3.17 Effective dye concentrations (EC20 and EC50) for (a) *R. sativus*; (b) *T. aestivum*; (c) *S. bicolor*; and (d) *P. mungo*. Different letters within a series indicate significantly different values ($\alpha= 0.05$, Tukey's HSD)

3.3.3 Effect of reactive azo dyes on aquatic invertebrate organisms

3.3.3.1 *Artemia salina* larval mortality assay

Acute toxicity of reactive azo dyes towards *A. salina* larvae was studied and dose-response analysis was done (Fig. 3.18 and Table A15 [Appendix 1]). Dye mixture was most toxic for brine shrimp larvae with the respective EC20, EC50, and EC80 values: 95.56, 503.93, and 877.71 ppm. With RB 221, 20, 50, and 80% mortality was recorded at 322.37, 639.31, and 967.85 ppm, respectively. The other two dyes, i.e., RR 195 (EC20, EC50, and EC80: 553.63, 906.22, and 1549.01 ppm) and RY 145 (EC20, EC50, and EC80: 691.01, 836.83, and 998.97 ppm), were relatively less toxic (Fig. 3.20a).

3.3.3.2 *Daphnia magna* immobilization assay

In the acute toxicity analysis of *D. magna* (Fig. 3.19 and Table A16 [Appendix 1]), no immobilization was observed after 24 h. After 48 h of exposure, a comparable toxic response was observed with the dye mixture (EC20, EC50, and EC80: 34.87, 108.77, and 180.46 ppm) and RR 195 (EC20, EC50, and EC80: 40.18, 137.44, and 166.77 ppm). EC20, EC50, and EC80 values for the RY 145 dye were 88.41, 172.63, and 297.13 ppm, respectively. RB 221 was found to be the least toxic dye for daphnids, as 20, 50, and 80% immobilization was observed at 172.73, 241.79, and 338.46 ppm, respectively (Fig. 3.20b).

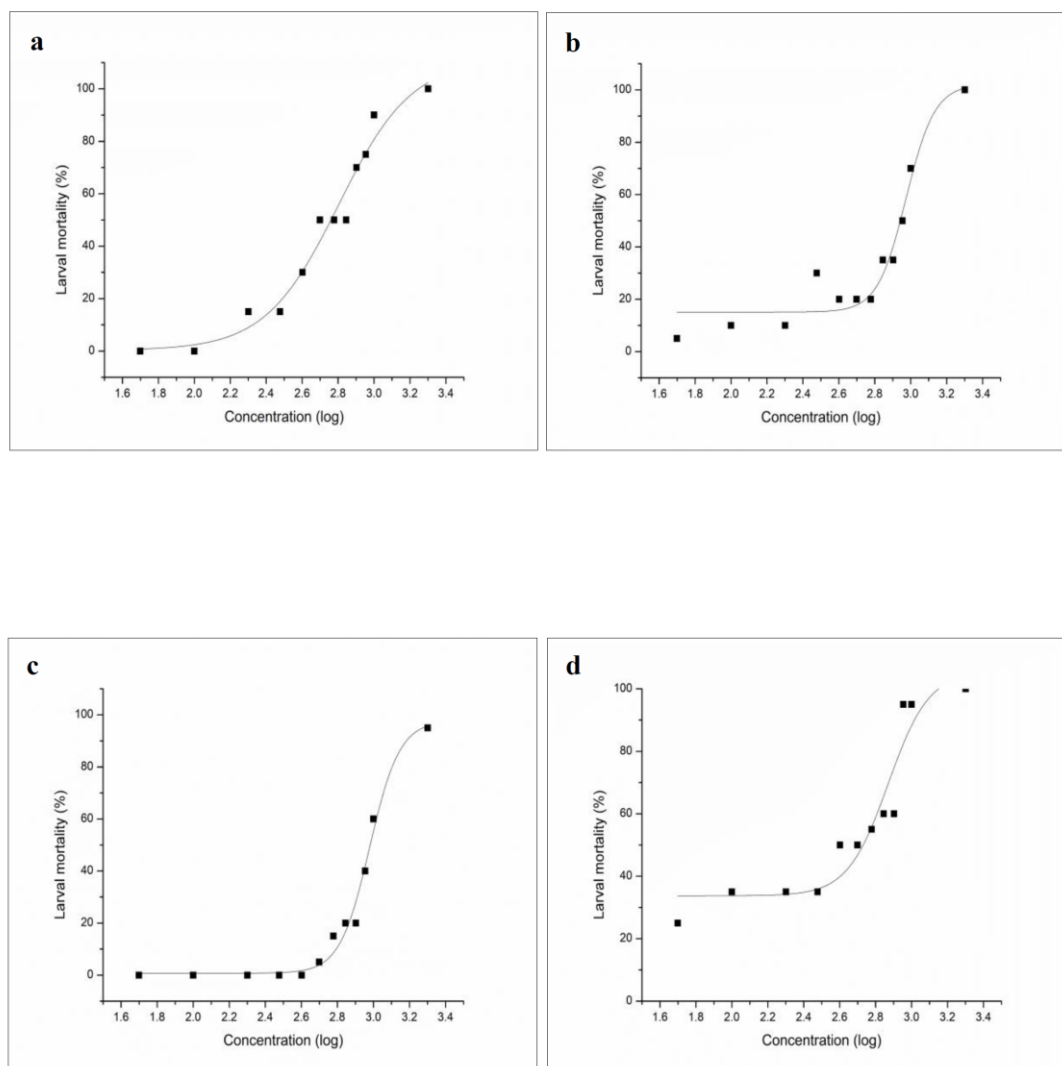


Fig. 3.18 Dose response curves for *A. salina* larvae with (a) RB 221, (b) RR 195, (c) RY 145, and (d) Dyes mixture. Squares and lines represent the percent mortality and fit curves, respectively

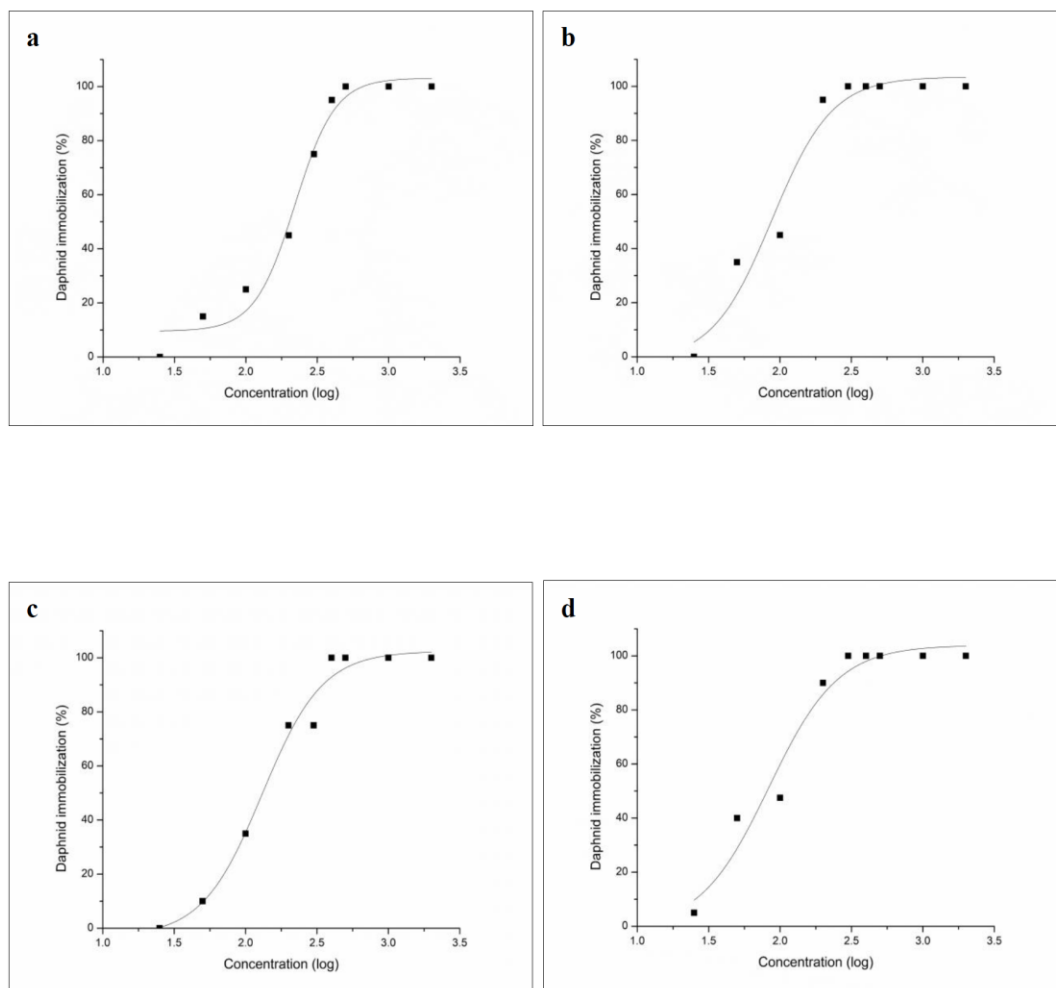


Fig. 3.19 Dose response curves for *D. magna* neonates with (a) RB 221, (b) RR 195, (c) RY 145, and (d) Dyes mixture. Squares and lines represent the percent mortality and fit curves, respectively

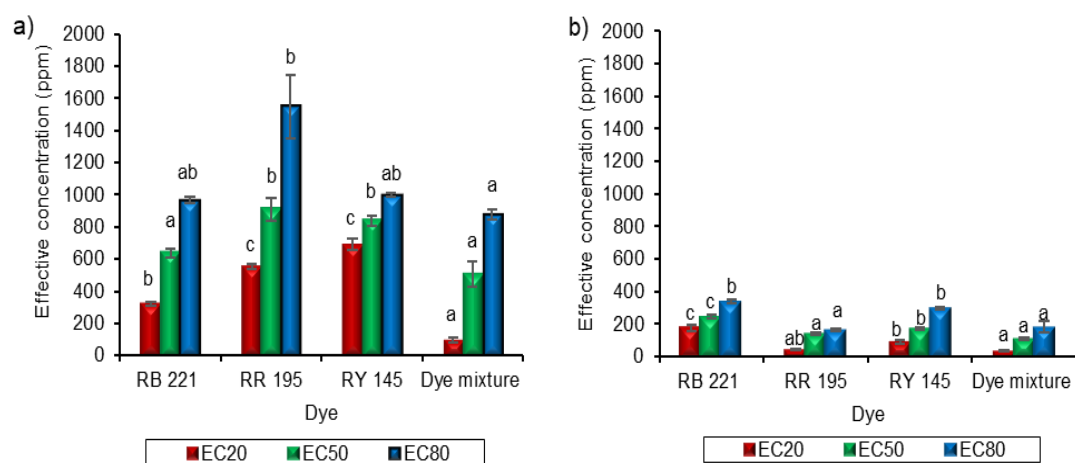


Fig. 3.20 Effective dye concentrations (EC20, EC50, and EC80) for (a) *A. salina* larvae; and (b) *D. magna*. Different letters within a series indicate significantly different values ($\alpha= 0.05$, Tukey's HSD)

3.4 Discussion

Toxicity assessment procedures for pollutants are based on the response of different test specimens towards sub-lethal concentrations of a given toxic compound (Rawat et al., 2016). Organismic-level acute toxicology profile of the sulfonated reactive azo dyes (RB 221, RR 195, RY 145, and the reactive azo dye mixture) was studied via microbial growth inhibition, phytotoxicity, and aquatic invertebrate toxicity assays. For the microbial level toxicity evaluation, bacterial and fungal specimens were used. In the antibacterial assay, three gram-negative (*P. aeruginosa*, *E. coli*, and *K. pneumoniae*) and three gram-positive bacteria (*S. aureus*, *L. monocytogenes*, and *B. subtilis*) were used. For all the bacterial specimens, no certain toxicity trend and gram-specific effect were observed for the reactive azo dyes (Fig. 3.7). In the case of *P. aeruginosa*, the dye mixture and RY 145 produced a comparable ($p > 0.05$) inhibitory effect in contrast to the other two dyes ($p < 0.05$). RY 145 was found to be the most toxic dye for *E. coli* ($p < 0.05$), while with *K. pneumoniae*, RB 221 showed the highest inhibitory effect, but the EC values were not significantly different from those observed with the red and yellow dyes ($p > 0.05$). For *S. aureus*, the dye mixture and RB 221 showed a relatively similar effect ($p > 0.05$) in comparison to the other two dyes ($p < 0.05$). With *L. monocytogenes*, RR 195 was found to be more toxic but statistically, the inhibitory response was like RB 221 and the dye mixture ($p > 0.05$). *B. subtilis* was found to be more sensitive to RR 195 and RB 221 than to the yellow dye and mixture ($p < 0.05$).

The non-specific behavior of dyes as well their mixture towards the gram-positive and gram-negative bacteria could be due to the varied interactions of dyes with the bacterial cytoplasmic membrane and/or their intracellular mechanisms (Yousefi et al. 2013). The inhibitory effect of the mixture of dyes was comparable to the individual dyes except in the case of *K. pneumoniae*, for which the mixture produced the least toxic effect. The increase or decrease in the toxicity of a mixture depends on how its individual components are interacting with each other in a metabolic machinery. This interaction can be synergistic (resulting in an enhanced toxic effect) or antagonistic (resulting in decreased toxicity) (Stine and Brown 1996). Generally, the bacterial specimens used in this study showed an appreciable sensitivity towards the reactive azo dyes as EC₂₀ values were in the range of 50–250 ppm and EC₅₀ values were in the range of 80–330 ppm, while the range for EC₈₀ was 200–580 ppm. The pronounced toxic effect of

reactive azo dyes on bacteria could be a result of sulfonated groups present in their structure (Khan et al., 2013). Contrary to this, Novotný et al., (2006) reported much higher EC50 values (more than 1000 ppm) for Reactive Orange 16 and Congo Red dye by using *Vibrio fischeri*.

The reactive azo dyes also exhibited a dose-dependent inhibitory effect on *T. asperellum*, *A. flavus*, *F. fujikuroi*, and *R. solani*. Like the antibacterial assay, antifungal response of reactive azo dye did not follow a specific trend in terms of the type of dyes (Fig. 3.12). RB 221 was found to be more toxic towards *T. asperellum*, but the EC values were not significantly different from those obtained with the other dyes and mixture ($p > 0.05$). For *A. flavus*, RR 195 was more toxic but statistically, the response was not significantly different from that observed with RB221 and the dye mixture ($p > 0.05$). *F. fujikuroi* was more sensitive to RB 221 than to RR 195 and dye mixture ($p < 0.05$). For *R. solani*, RR 195 and the dye mixture showed a relatively more inhibitory effect ($p < 0.05$). Two of the four fungal specimens used, i.e., *T. asperellum* and *A. flavus*, showed a considerable sensitivity towards the reactive azo dyes as indicated by the EC20 (17–80 ppm), EC50 (135–360 ppm), and EC80 (440–785 ppm) values. The latter two fungi (*F. fujikuroi* and *R. solani*) displayed a more resistant behavior towards the dyes and their mixture. The ranges for EC20, EC50, and EC80 values were 330–550, 530–2300, and 1700–3000 ppm, respectively. Few reports are available on the use of fungi for toxicity estimation of dyes. Bawa and Alzaraide, (2005) studied the inhibitory effect of phenolic azo derivatives on *A. niger*. In another study, Mahata et al., (2014) reported the toxic effect of a cardanol-azo derivative on *C. albicans* with the MIC value of 16 ppm.

Plants serve as another important test specimens for monitoring textile dye toxicity (Ali, 2010). So, the effect of the reactive azo dyes and mixture on plant seed germination potential was investigated using *R. sativus*, *T. aestivum*, *S. bicolor*, and *P. mungo* seeds (Fig. 3.17). The dye mixture was found to be more toxic for *R. sativus* and *T. aestivum* seeds, but this observation was not statistically different for EC50 values ($p > 0.05$) (except for the blue dye in the case of radish seeds). For *S. bicolor* seeds, RR 195 dye produced a relatively more inhibitory effect but statistically, the response was not different from that observed with the other dyes and mixture ($p > 0.05$). For *P. mungo* seeds, dye mixture, RB 221, and RR 195 showed comparable effect ($p > 0.05$). This

was the least sensitive among the tested plant species. Generally, the dyes were not highly toxic for all the plant seeds as the EC20 and EC50 values were in the range of 250–2000 and 950–3500 ppm, respectively. The seed germination inhibition at higher dye concentrations could be a result of decreased water absorption and/or accumulation of dyes in the plant seeds which in turn interferes with the normal germination mechanism (Araújo and Monteiro, 2005). Likewise, Singh et al., (2015) observed decreased seed germination potential for *V. radiata* and *V. mungo* seeds when treated with 100 ppm of Direct Orange 16 azo dye. Moreover, similar type of findings was reported by Saratale et al. (2010), where a reduction in seed germination potential was observed for *P. mungo* seeds upon treatment with 300 ppm concentration of Green HE4BD.

Bioassays that are based on the invertebrate aquatic test organisms could provide additional help in the prescreening of chemicals. Moreover, the in vivo biotransformation of chemicals can provide a better understanding of the possible effect of given chemicals on higher level organisms (Klemola et al. 2007). Several advantages such as wide geographical distribution, a highly adaptive nature, easy storage, rapid, simple, and low-cost test procedure make *A. salina* an ideal candidate for toxicity analysis (Rajabi et al. 2015). *D. magna* is another important test organism like its marine counterpart, i.e., *A. salina*, and plays a key role in freshwater ecology (Liu et al., 2007). To assess the effect of reactive azo dyes and their mixture at invertebrate level, *A. salina* larvae and *D. magna* neonates were used (Fig. 3.20).

A. salina larvae were found to be more sensitive to the dye mixture (EC20, EC50, and EC80 values: 95.51, 503.93, and 877.71 ppm, respectively; $p < 0.05$). For the individual dyes, EC20, EC50, and EC80 values were in the range of 320–690, 640–900, and 870–1550 ppm, respectively. So, generally, the dyes were not acutely toxic for *A. salina* larvae. In another study, Ayed et al., (2011) reported a decrease in *A. salina* survival rate, following exposure to the different concentrations of methyl red. The increased mortality at higher dye concentrations could possibly result from the accumulation of dye molecules in the mid-gut of *A. salina* larvae which in turn can interfere with the normal physiological functions (Kokkali, Katramados, and Newman 2011). For *D. magna*, the dye mixture and RR 195 were found to be more toxic than the yellow and blue dyes ($p < 0.05$). Moreover, *Daphnia* showed more sensitivity towards the tested

dyes and their mixture in comparison to the *A. salina* larvae, as the EC20, EC50, and EC80 values ranged between 34 and 173, between 108 and 242, and between 166 and 340 ppm, respectively. But as the EC50 values were higher than 100 ppm, so the dyes were not acutely toxic for *D. magna* as well. Similarly, Leme et al. (2015) observed a non-toxic effect of reactive dyes on *A. salina* larvae and a *Daphnia* specie, with the latter showing a relatively more sensitive behavior.

3.4 Conclusion

The reactive azo dyes and their mixture showed a variable toxic effect on the tested organisms. Microbial specimens (except *F. fujikuroi* and *R. solani*) were relatively more sensitive to the dyes and their mixture in comparison to the plant seeds. In the case of aquatic specimens used in this study, *D. magna* showed more sensitivity (relatively similar to the microbial test specimens) towards the reactive azo dyes and their mixture than the other aquatic test organism (*A. salina*). In general, the tested dyes were not acutely toxic, as EC50 values were higher than 100 ppm (except for *L. monocytogenes* for which EC50 values were lower than 100 ppm with RR 195 and the dye mixture). Moreover, the effect of the dyes seemed to be more related to the type of the target organism instead of the dyes' molecular structure. This study provides a general overview of the organismic-level toxicity of reactive azo dyes, but a more detailed study, focusing on the cellular- and molecular-level effects (mutagenic effects) of these dyes, can help in a better understanding of the nature of interactions of these dyes with the different living systems and their possible role in different ecological levels.

Chapter 4: Comparison of Immobilized Fungal and Hybrid Activated Sludge Batch Reactors for the Treatment of Metal complex Reactive Azo Dye

4.1 Introduction

A number of specialized configurations of bioreactors have been developed (which employ microbes like bacteria and fungi) and investigated for the textile dyes and effluent treatment. They are based on suspended and/or immobilized microbial cells (Van Der Zee and Villaverde 2005). The commonly used systems are stirred tank reactor, fixed bed bioreactors, rotating disk reactors, and membrane reactors (Khouni et al., 2012; Saratale et al. 2011b; Šíma et al., 2012; Andaleeb et al. 2010; Mutamim et al. 2012). However, numerous problems are associated with suspended cell fungal bioreactors like; mycelial aggregates, fouling of electrodes, and clogging that can begin after a short time thereby necessitating the periodic removal of the fungal biomass from the bioreactors (Rodríguez Couto 2009). So, in that case, most efficient decolorization is achieved when fungi are immobilized in different inert support materials (natural as well as synthetic e.g. seeds, wheat straw, wood shavings. corn cobs, alginate beads, nylon sponge, plastics discs etc.) (Moreira et al. 2004). Fungal immobilization on such supports facilitates the repeated usage, recovery, and effective utilization of fungal biomass (Rodríguez Couto 2009).

Activated sludge systems that involves the incorporation of some support medium in the suspended growth reactor are known as hybrid systems (Riffat, 2013). Hybrids are the types of reactors that offer high reaction rates through biomass concentration. Such type of configurations enhance the activated sludge process capacity in smaller reactor systems; thereby alleviating the need for large sized containers to combat higher hydraulic loading rates through optimal utilization of biomass (Venkata Mohan et al. 2013). Moreover, biofilm operation also induces both aerobic and anoxic microenvironments along biofilm depth and thus creates a competition for space, oxygen and organic carbon among microbes, which leads to their spatial distribution within the biofilm (Venkata Mohan et al. 2012).

In view of these points, present study was conducted to compare the biotreatment efficiency of two different bioreactors. Immobilized fungal (*Trichoderma asperellum*; aerobic) and a hybrid activated sludge reactor (in batch mode), were designed using Scotch Brite™ sponge as support material to evaluate the treatment of sulfonated reactive azo dye i.e., Reactive Blue 221 (RB 221) containing simulated textile effluent at varying dye concentrations i.e., 25, 50, and 100 ppm. The reactors efficiency was evaluated by periodic (24 hours) monitoring of color, COD, and pH. Moreover, the cultivable bacterial population (CFU/mL and CFU/mL.cm²) in the hybrid activated sludge system was monitored for assessing the active attached and suspended biomass concentration in the reactor. The reduction in synthetic dye wastewater toxicity was monitored by performing the toxicity tests.

4.1.1 Aims and Objectives

The aim of the present study was to evaluate and compare the treatment efficiency of an immobilized fungal and a hybrid activated sludge reactor for reactive azo dye containing simulated textile effluent. The specific objectives of this study are as follows:

- To utilize the polyester and nylon sponge i.e., Scotch Brite™, as a support material for fungal immobilization and biofilm development in immobilized fungal and hybrid activated sludge reactors, respectively.
- To design, fabricate and operate the reactor setups in batch mode and test the treatment efficacy by periodic monitoring of color, pH and chemical oxygen demand (COD) using spectrophotometric and standard wastewater analytical protocols.
- To determine the comparative efficiency of the reactor systems at varying synthetic dye wastewater concentrations.
- To monitor the progression of active suspended and attached bacterial biomass, during the biotreatment process, through bacterial growth (CFU/mL; CFU/mL.cm²).
- To assess the treatment efficiency by FTIR spectroscopy.
- To assess the detoxification efficiency of the treatment systems using phytotoxicity and brine shrimp acute toxicity assays.

4.2 Materials and methods

4.2.1 Chemicals

Analytical grade chemicals and microbiological media for fungal and bacterial culturing, were acquired from Sigma-Aldrich (Sigma-Aldrich, St. Louis, MO, USA) and Oxoid (Oxoid Limited, Hampshire, United Kingdom). The textile dye, Reactive Blue 221 (RB 221: λ_{\max} 615 nm) was provided by a textile industry, located at Lahore, Pakistan and used without any further purification. Aqueous stock dye solution (1000 ppm) was prepared, filter sterilized (0.2 μm nylon membrane; Corning Inc., Corning, NY, USA), and stored at room temperature.

4.2.2 Simulated textile effluent preparation

4.2.2.1 Immobilized fungal reactor

For the immobilized fungal reactor, simulated textile effluent was prepared according to Luangdilok and Panswad, (2000) with slight modifications. It consisted of the following components (g/L): 0.15 mL acetic acid (99.9%); 0.108 $(\text{NH}_4)_2\text{SO}_4$; 0.067 KH_2PO_4 ; 0.840 NaHCO_3 ; 0.038 $\text{MgSO}_4 \cdot 7\text{H}_2\text{O}$; 0.021 CaCl_2 , 0.007 $\text{FeCl}_3 \cdot 6\text{H}_2\text{O}$; 0.45 NaCl and 5.0 glucose. pH of the effluent was adjusted to a final value of 5.0 ± 0.2 using 1N solutions of HCl and NaOH. Filter sterilized stock solutions of RB221 were added as per final concentration of the synthetic dye effluent i.e., 25, 50 and 100 ppm.

4.2.2.2 Hybrid activated sludge reactor

Simulated textile effluent for the hybrid activated sludge reactor was prepared by adding the following components (g/L): 3.6 Na_2HPO_4 ; 1.0 $(\text{NH}_4)_2\text{SO}_4$; 1.0 KH_2PO_4 ; 1.0 MgSO_4 ; 0.01 Fe (NH_4) citrate; 0.10 $\text{CaCl}_2 \cdot 2\text{H}_2\text{O}$; 0.45 NaCl , 1.0 glucose, and 10.0 mL/L of trace element solution. The trace element solution used was of following composition (mg/L): 10.0 $\text{ZnSO}_4 \cdot 7\text{H}_2\text{O}$; 3.0 $\text{MnCl}_2 \cdot 4\text{H}_2\text{O}$; 1.0 $\text{CoCl}_2 \cdot 6\text{H}_2\text{O}$; 2.0 $\text{NiCl}_2 \cdot 6\text{H}_2\text{O}$; 3.0 $\text{Na}_2\text{MoO}_4 \cdot 2\text{H}_2\text{O}$; 30.0 H_3BO_3 ; and 1.0 $\text{CuCl}_2 \cdot 2\text{H}_2\text{O}$. The final pH of the medium was adjusted to 7.0 ± 0.2 using 1N solutions of HCl and NaOH (Khehra et al., 2005). To this salt medium, filter sterilized stock solution of RB 221 was added according to the final concentration of the effluent i.e., 25, 50, and 100 ppm.

4.2.3 Inoculum for the reactors

4.2.3.1 Immobilized fungal reactor

Fungal strain i.e., *Trichoderma asperellum* SI14 (GenBank accession number: KJ432865) was acquired from the Microbiology research laboratory, Quaid-i-Azam University, Islamabad, Pakistan. For fungal acclimation to RB221 dye, it was grown in dye containing sabouraud dextrose agar medium (25 ppm, pH: 5.0, at 30 °C) for 5 days. Following 3-4 successive transfers to fresh dye amended medium, fungal spore suspension was prepared. For that, fungal spores were picked from a mature fungal colony with the help of a sterile inoculating loop. The spore containing loop was then transferred to autoclaved distilled water. This was repeated 15 to 20 times for 100 mL of water. That was then subjected to vigorous mixing. 1.0 µL of prepared spore suspension was then added to hemocytometer and observed under the microscope (Spore count: 3.3×10^4 /mL). After that, this spore suspension was kept in refrigerator at 4 °C and used for further experimentation.

4.2.3.1.1 Immobilization of fungus

Commercially available Scotch Brite™ sponges (12; 80% polyester and 20% nylon, size: 8.5x6 cm; thickness: 0.8 mm) were used as support material for fungal immobilization. The support material was washed with distilled water and then allowed to air dry. The dried supports were autoclaved at 121 °C. Following that, the support material was dipped in sabouraud dextrose agar medium for 3 to 5 minutes; when it was near to solidification. The pretreated sponges were transferred to the flasks containing sterilized sabouraud dextrose broth medium (pH: 5.0). To this, 6% (v/v) fungal spore suspension was added. The flasks were then kept in shaker incubator at 140 rpm at 30 °C for a period of 10 days, till a visible fungal mass was observed on the support material (Fig. A1, Appendix 2).

4.2.3.2 Hybrid activated sludge reactor

Inoculum for the hybrid reactor (for suspended as well as attached microbial growth) was prepared by adding 10% (v/v) aqueous suspension of activated sludge (collected from a sewage treatment plant, sector I-9 Islamabad, Pakistan) in 25 ppm RB221 containing nutrient broth medium pH 7.0 ± 0.2 , incubated at 37 °C for 20 days for sludge acclimation (successive transfers to fresh dye containing medium was done after every 5 days).

4.2.3.2 .1 Support preparation

Scotch Brite™ sponges (as described in section 4.2.3.1.1) were used as support material for attached biomass development (during the biotreatment). Firstly, the supports were washed with distilled water followed by drying and sterilization. The support material was then dipped in nutrient agar medium for 3-5 minutes, when it was near to solidification followed by incorporation into the reactor.

4.2.4 Configuration of reactors

The immobilized fungal and hybrid activated sludge reactors consisted of plastic containers with an overall capacity of 12 L. The height of reactors was 36 cm, width from top was 35 cm and at the base, it was 28 cm. Working volume was kept up to 6.5 L, while void volume was 5.5 L. These reactor configurations were provided with removable lids (sealed with parafilm to maintain the sterilized conditions) and effluent valves, attached near the base of reactor (5 cm from the base) for sample collection. In immobilized fungal reactor a network of perforated pipes was used, that was linked to an air pump through an air filter (0.2 µm nylon membrane; Corning Inc., Corning, NY, USA) with an airflow controller for upflow aeration and mixing; while in the hybrid activated sludge reactor, an aquarium air stone linked to an air pump through a 0.2 µm air filter with an air flow regulator was used for diffused upflow aeration and mixing. . In addition to that, the reactors were equipped with 6 fixed iron rods (10 cm from the top of the reactor) used for hanging the support material (2 on each rod). Additionally, thermostats were incorporated in both setups to maintain temperature at 30 and 37 °C for fungal and hybrid reactors, respectively (Figs. 4.1 a and b).

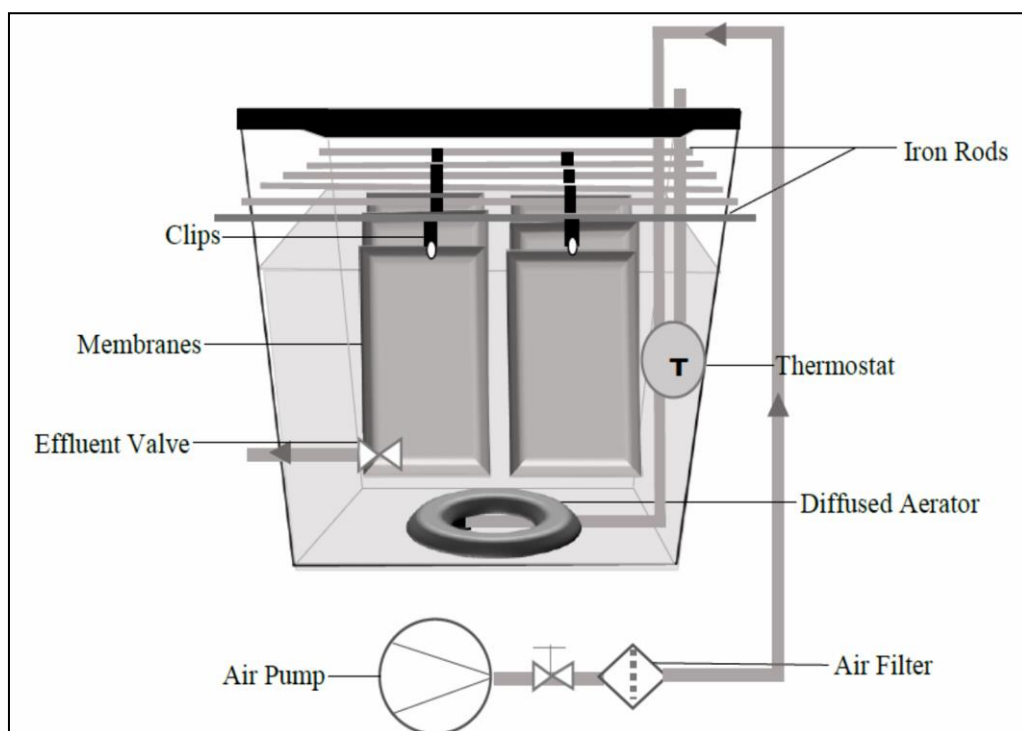
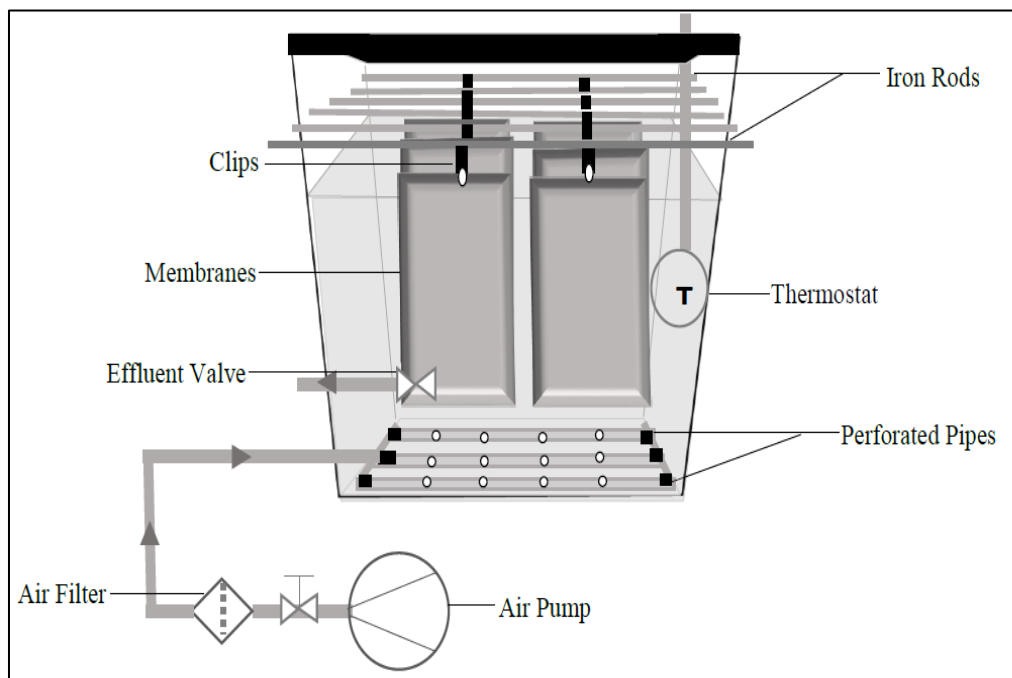


Fig. 4.1 a) Schematic diagram of immobilized fungal reactor; b) Schematic diagram of hybrid activated sludge reactor

4.2.5 Operation of reactors

Fungal immobilized and pretreated Scotch Brite supports were incorporated into the respective reactors (hanged with the help of clips on fixed iron rods). Hybrid activated sludge reactor was then seeded with the acclimated activated sludge inoculum. Bioreactors were then filled with the prepared synthetic dye wastewater. Following that, both containers were made air tight by sealing the lids with parafilm. Thermostat and air pump were then turned on. Both reactors were run in batch mode for a period of 144 hours. The reactors' efficiency was tested at different dye concentrations i.e., 25 (Batch 1), 50 (Batch 2) and 100 ppm (Batch 3) of RB 221. In the hybrid activated sludge reactor, aeration was turned off after the completion of a batch (for sludge settling) and 1/3 volume of the settled sludge was reused for the next batch. For periodic monitoring (after every 24 hours) of the reactors' performance, 10.0 mL of the samples were withdrawn from each reactor for color, pH and COD determination.

4.2.6 Analyses of treated effluent samples

4.2.6.1 Color

For monitoring the color removal, 1.5 mL of the reactors' samples were centrifuged at 12,000×g for 20 minutes at room temperature. The supernatant obtained after centrifugation was read at 615 nm i.e., absorbance maxima (λ_{\max}) of RB 221, using UV-Visible spectrophotometer (Agilent 8453; Agilent Technologies, Santa Clara, CA, USA). The uninoculated dye free salt medium was used as blank. The decolorization percentage was calculated by using the following formula (Sani and Banerjee 1999).

$$\text{Decolorization (\%)} = \frac{I - F}{I} \times 100 \quad \text{Eq 4.1}$$

Where I is initial absorbance of the colored sample and F is final absorbance of the treated sample.

4.2.6.2 Chemical Oxygen demand (COD)

COD of the untreated and treated synthetic dye wastewater samples, was determined by using COD kits (114541 COD Cell Test; 25-1500 mg/L, Merck KGaA, Darmstadt, Germany). Samples were diluted with distilled water if needed to adjust according to

the COD kit permissible range and calculated accordingly. Reduction in COD was calculated according to the following formula:

$$\text{COD reduction (\%)} = \frac{\text{Initial COD} - \text{Final COD}}{\text{Initial COD}} \times 100 \quad \text{Eq 4.2}$$

4.2.6.3 pH

pH of synthetic dye wastewater was measured after regular intervals with the help of pH probe (Sartorius professional meter PP15).

4.2.7 Biodegradation analysis through FTIR spectroscopy

Treated and untreated synthetic dye wastewater samples were analyzed through FTIR spectroscopy (spectrum 65 FTIR spectrometer equipped with ATR; Perkin Elmer, Waltham, MA, USA). The decolorized samples were centrifuged at 4000 rpm for 30 min and the supernatant was used for analysis. Dye metabolites were extracted with ethyl acetate followed by drying over anhydrous Na₂SO₄ and evaporation in a rotary evaporator. The analysis was performed (using dried residues dissolved in methanol) in the mid IR region of 600-4000 cm⁻¹ with 16 scan speed.

4.2.8 Bacterial community analysis of hybrid activated sludge reactor

Progression of active suspended and attached bacterial biomass, was monitored during the biotreatment process in each batch through bacterial growth (CFU/mL) measurement. Suspended and attached bacterial count was done to determine the ratio of attached to total bacterial count. For that, 1.0 mL of effluent samples were aseptically withdrawn on the final i.e., 6th day (144 hours) of each batch. For the attached biomass analysis, 1.0 cm² sections of the support material (on the 6th day of each batch) were washed thrice with sterile distilled water. The attached biomass was then detached from the Scotch Brite™ section, in sterile distilled water (1.0 mL in a sterile capped tube) by sonication for 60 seconds (Yamato 934). The suspended and attached biomass samples were subjected to serial dilution (10fold), followed by spread plating on nutrient agar medium. The Petri plates were incubated at 37 °C. After 24 hours, the colonies obtained on the nutrient agar medium were enumerated with the help of a

colony counter. CFU/mL and CFU/mL cm², as well as the ratio of attached to total bacterial count was computed.

4.2.9 Detoxification assessment for the reactors' samples

Detoxification efficiency of the treatment systems was measured using the untreated and treated synthetic dye wastewater, through phytotoxicity (Turker and Camper, 2002) and brine shrimp acute toxicity assays (Meyer et al., 1982) (Methods, as described in section 3.2.3 and 3.2.4).

4.2.9 Statistical analysis

Samples from each reactors' batch were analyzed in duplicate. Mean values and standard error of means were calculated using Microsoft Excel 2016. One-way analysis of variance (ANOVA) followed by Tukey's honest significant difference (Tukey's HSD) at the significance level of $\alpha=0.05$ ($p<0.05$), was done using SPSS 20 (IBM SPSS Statistics for Windows, Version 20.0., Armonk, NY, USA).

4.3. Results

The biotreatment efficiency of an immobilized fungal and a hybrid activated sludge reactor was evaluated and compared for RB 221 containing simulated textile wastewater. Both reactors were operated in batch mode for a period of 144 hours. The reactors' performance was tested by periodic monitoring of color, COD, and pH alterations, followed by biodegradation and detoxification assessment.

4.3.1 Analysis of treated effluent samples

4.3.1.1 Color

The reactors performance (at three different dye concentrations) in terms of decolorization of the synthetic textile wastewater was monitored by UV-Visible spectrophotometric analysis at 615 nm and decolorization efficiency was computed.

Immobilized fungal reactor

In the immobilized fungal reactor (Fig. 4.2a), a gradual decrease in color was observed in batch 1 (25 ppm dye) with a 93.28% reduction observed after 144 hours. In batch 2 (50 ppm dye), 92.32% color removal was observed after 24 hours of reactor operation,

following which it gradually increased to 96.88% after 144 hours. In the third batch (100 ppm dye), 98.03% color removal occurred after 96 hours of reactor's operation, following which it levelled off.

Hybrid activated sludge reactor

In the hybrid activated sludge reactor, a gradual decrease in the color of synthetic dye wastewater was observed in all batches (Fig. 4.2b). 90.21% decolorization was observed over a period of 144 hours in batch 1 (25 ppm dye). In the second batch i.e., at 50 ppm of dye concentration, 95.78% color removal was achieved after 144 hours, while in the third batch (100 ppm dye), 96.33% decolorization was observed at the final day of reactor operation.

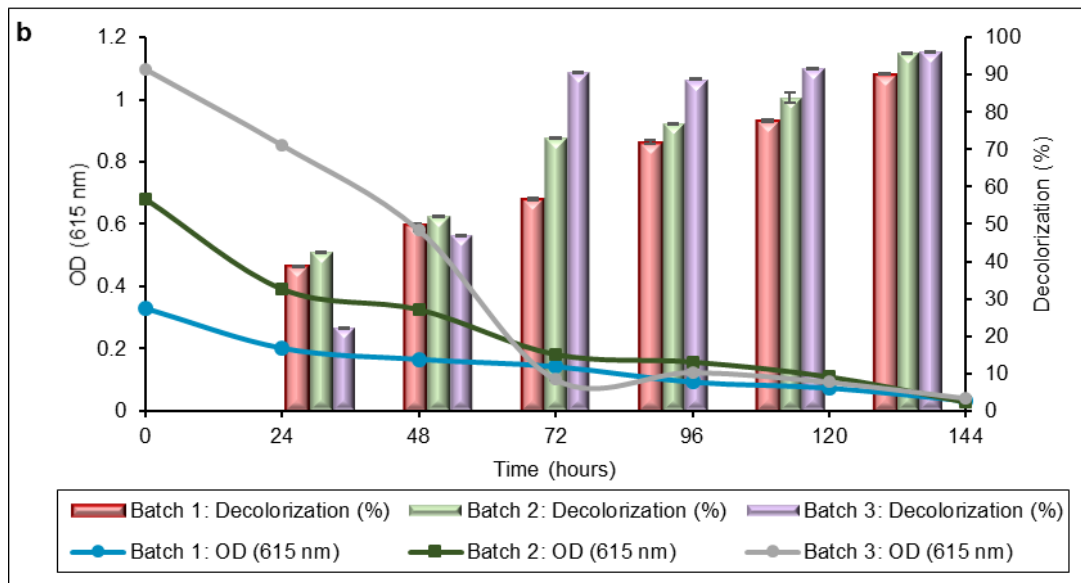
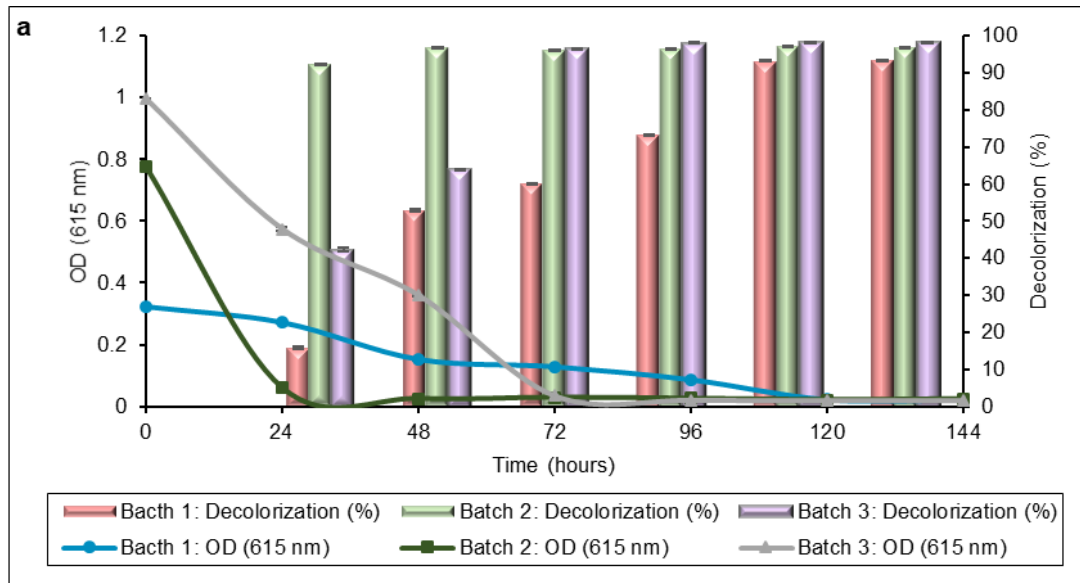


Fig. 4.2 Color removal performance of (a) Immobilized fungal reactor, (b) Hybrid activated sludge reactor

4.3.1.2 Chemical oxygen demand (COD)

COD removal efficiency of the reactors' batches (containing 25, 50 and 100 ppm of RB221) was monitored using commercial COD kits.

Immobilized fungal reactor

For the immobilized fungal reactor, treatment of the synthetic dye wastewater in all the three batches demonstrated a substantial reduction in COD on the final day of reactor operation (Fig 4.3a). However, the decrease did not follow a smooth pattern during the treatment process, as COD values kept on fluctuating in that period. For batch 1, 2 and 3, the overall COD reduction was 83.54%, 70.25%, and 73.17%, respectively, after 144 hours of treatment.

Hybrid activated sludge reactor

In the hybrid activated sludge reactor, a considerable reduction in COD of the synthetic dye wastewater was observed on the final day of reactor batches (Fig. 4.3b). For batch 1 (25 ppm dye), 55.18% COD removal was attained after 24 hours, which then gradually increased up to 92.49% after 144 hours of reactor operation. In batch 2 (50 ppm dye), 81.04% COD reduction was recorded on the final day of treatment. However, the COD values kept on fluctuating during the treatment process. With the third batch (100 ppm dye), 78.97% COD reduction was recorded after 144 hours of treatment. Like the second batch, COD reduction did not follow a smooth reduction pattern during the biotreatment.

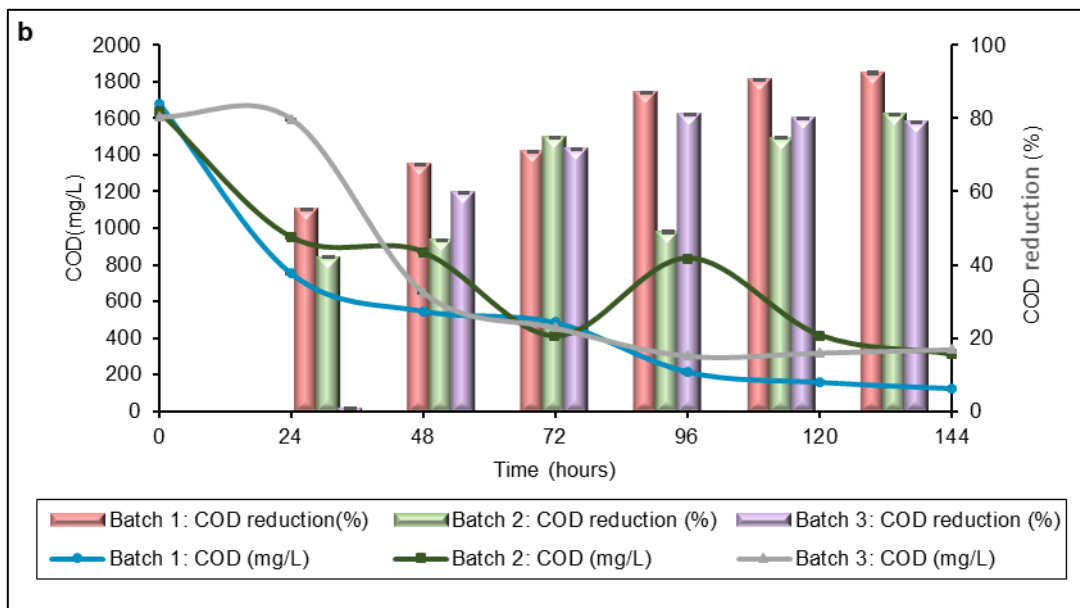
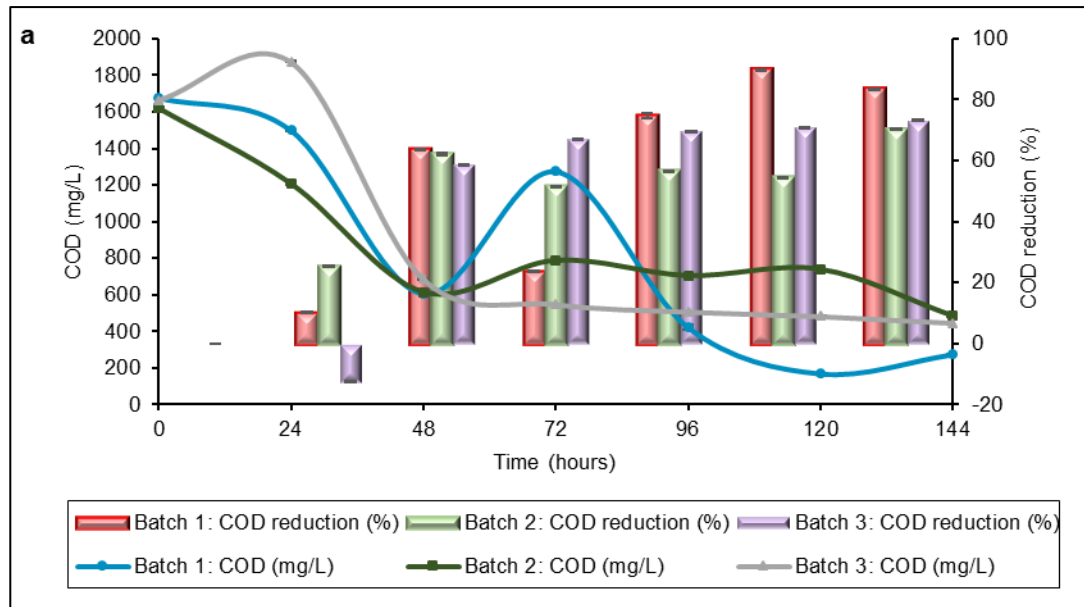


Fig. 4.3 COD removal performance of (a) Immobilized fungal reactor, (b) Hybrid activated sludge reactor

4.3.1.3 pH

Immobilized fungal reactor

The initial pH of the synthetic dye wastewater was 5.0 ± 0.2 . In batch 1 (25 ppm dye), pH was raised to 7.73 after 24 hours of reactor operation; following that it steadily increased to 8.64 till 120 hours. A slight drop to a pH value of 8.43 was recorded on the final day of biotreatment. In the second batch (50 ppm dye), a decrease in pH (4.73) of the synthetic dye wastewater was recorded till 48 hours of treatment, following which it raised with a slight fluctuation to a final pH of 5.04. In the third batch (100 ppm dye), an increase in pH to 5.75 was recorded after 24 hours, later it started declining, and reached a final value of 5.26 after 144 hours of reactor operation (Fig. 4.4a).

Hybrid activated sludge reactor

In the hybrid activated sludge reactor, initial pH of the synthetic dye wastewater was 7.0 ± 0.2 . In the first batch (25 ppm dye), the pH was decreased to value of 5.68 after 48 hours of biotreatment, and afterwards, with slight fluctuations, it reached to a value of 6.85 on the final day of reactor operation. In the second batch (50 ppm dye), a slight decrease to 6.94 was recorded over a period of 120 hours and later it raised up to 7.07 on the final day of second batch. In the third batch (100 ppm dye), with slight fluctuations, a slight increase in the pH was recorded and the final recorded pH was 7.05 (Fig. 4.4b).

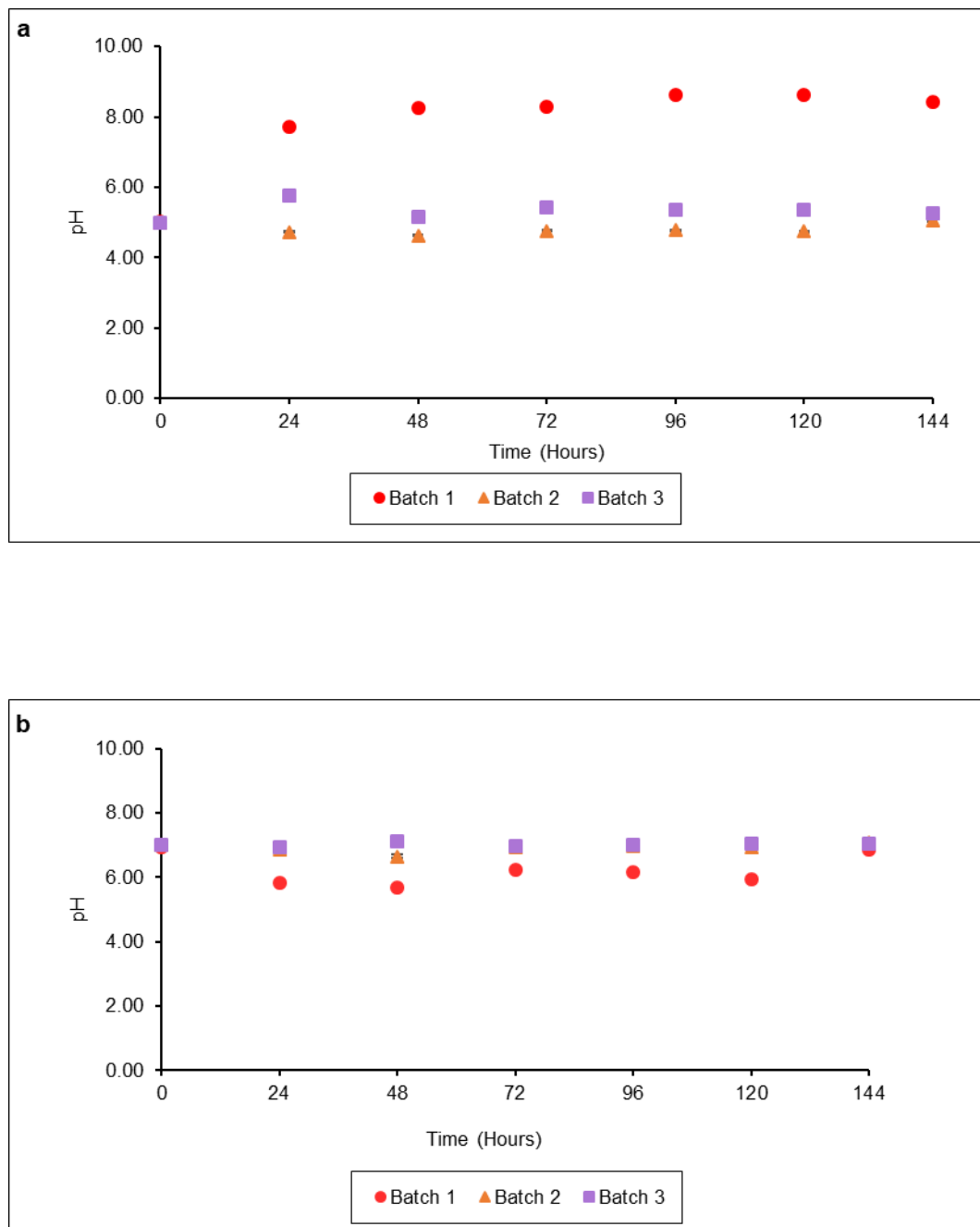


Fig. 4.4 pH variation in the synthetic dye wastewater (a) Immobilized fungal reactor, (b) Hybrid activated sludge reactor

4.3.2 Biodegradation analysis through FTIR spectroscopy

Immobilized fungal reactor

FTIR spectrum of the untreated synthetic dye wastewater for immobilized fungal reactor consisted of different bands at 1002.33 cm^{-1} , 1062.81 cm^{-1} , 1146.22 cm^{-1} , 1396.17 cm^{-1} , 1576.51 cm^{-1} , 1657.37 cm^{-1} , 2858.41 cm^{-1} , 2925.45 cm^{-1} , and 3519.30 cm^{-1} . In case of the FTIR spectrum of dye metabolites (obtained after fungal treatment), slight variations in the intensity of different bands were observed *e.g.* the bands at 2858.41 cm^{-1} , 1657.37 cm^{-1} , 1062.81 cm^{-1} , and 1002.33 cm^{-1} shifted to 2856.35 , 1654.39 , 1063.66 , and 1001.96 cm^{-1} , respectively. Some original dye peaks observed at 1396.17 cm^{-1} and 1576.51 cm^{-1} were disappeared. Moreover, new bands were observed at 3172.18 cm^{-1} and 3429.08 cm^{-1} (Fig. 4.5a).

Hybrid activated sludge reactor

FTIR spectrum of the untreated synthetic dye wastewater for the hybrid activated sludge reactor, showed different bands at 1003.46 cm^{-1} , 1062.23 cm^{-1} , 1113.88 cm^{-1} , 1396.17 cm^{-1} , 1576.51 cm^{-1} , 1513.12 cm^{-1} , 1659.25 cm^{-1} , 2857.50 cm^{-1} , 2971.61 cm^{-1} , 3190.62 cm^{-1} , and 3424.31 cm^{-1} . In case of the FTIR spectrum of dye metabolites (obtained after biotreatment), variation in the intensity of different bands was observed *e.g.* the bands at 3424.31 cm^{-1} , 3190.62 cm^{-1} , 2971.61 cm^{-1} , 2857.50 , 1659.25 cm^{-1} , 1113.88 cm^{-1} , 1062.23 cm^{-1} , and 1003.46 cm^{-1} shifted to 3417.56 , cm^{-1} , 3204.69 cm^{-1} , 2973.44 cm^{-1} , 2856.26 cm^{-1} , 1662.68 cm^{-1} , 1132.45 cm^{-1} , 1062.22 cm^{-1} and 1003.56 cm^{-1} , respectively. Some bands in the untreated sample observed at 1396.17 cm^{-1} , 1513.12 cm^{-1} , and 1576.51 cm^{-1} were disappeared after treatment. A new peak was observed at 628.41 cm^{-1} (Fig. 4.5b).

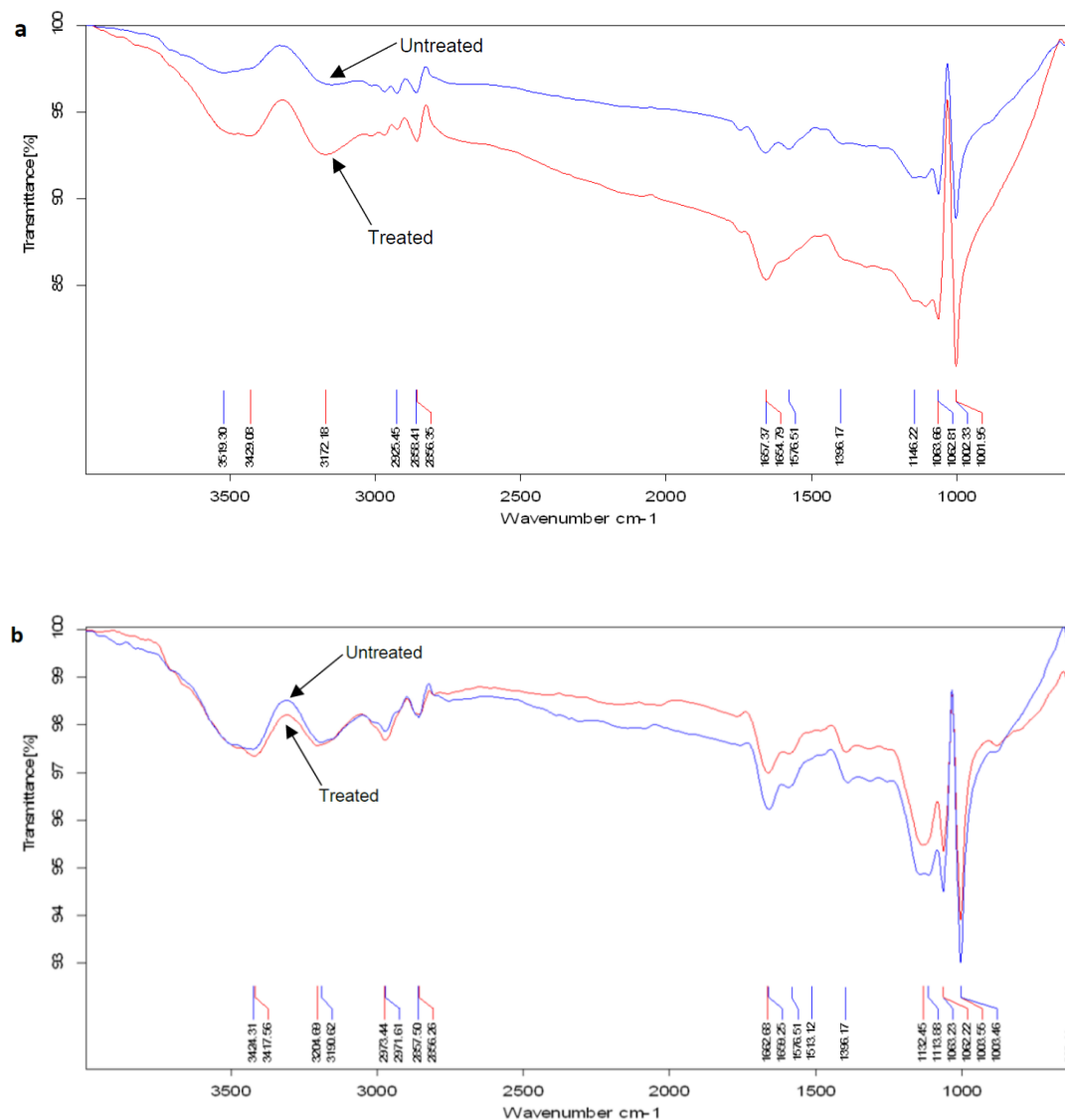


Fig. 4.5 FTIR overlay spectrum of synthetic dye wastewater (before and after treatment), (a) Immobilized fungal reactor, (b) Hybrid activated sludge reactor

4.3.3 Bacterial community analysis of hybrid activated sludge reactor

During the biotreatment process, progression of active, suspended and attached bacterial biomass was monitored via bacterial growth measurement (CFU/mL; CFU/mL.cm²) and the ratio of attached to total bacterial count was computed on the final day of each batch (Fig. 4.6a and b). In the first batch (25 ppm dye), the respective bacterial counts in suspended and attached forms were recorded as 2.03E+11 CFU/mL and 1.34E+11 CFU/mL.cm², while the attached to total bacterial count ratio was 39.69%. In the second batch (50 ppm dye), suspended and attached bacterial counts were 3.23E+11 CFU/mL and 7.05E+11 CFU/mL.cm², respectively. The ratio of attached to total count was 68.64%. In the final batch (100 ppm dye), the respective suspended and attached bacterial counts were 3.46E+11 CFU/mL and 6.68E+11 CFU/mL.cm² and the ratio of attached to total bacterial count was 65.89%.

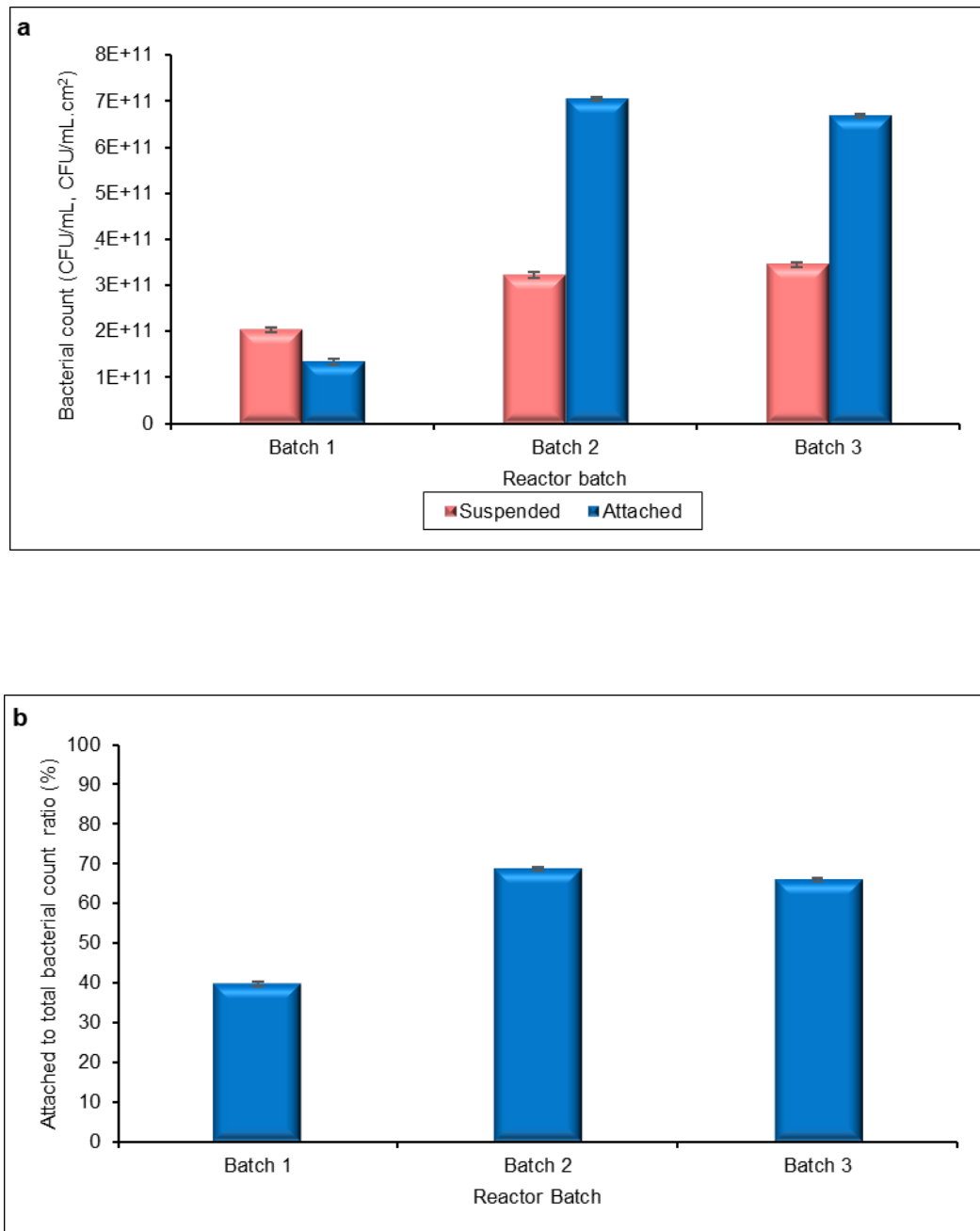


Fig. 4.6 (a) suspended and attached bacterial count in the hybrid activated sludge reactor batches, (b) Attached to total bacterial count ratio in the hybrid activated sludge reactor batches

4.3.4 Detoxification assessment of the reactors' samples

4.3.4.1 Phytotoxicity assay

4.3.4.1.1 Immobilized fungal reactor

Phytotoxic analysis of synthetic dye wastewater (before and after fungal treatment), was performed using *T. aestivum* (wheat) and *R. sativus* (radish) seeds. Dye free synthetic wastewater was used as negative control. In batch 1 (25 ppm dye), 100 percent seed germination was observed for *T. aestivum* seeds when watered with the untreated and treated synthetic dye wastewaters and a slight increase in root (2.44 cm [± 0.3] and 2.88 cm [± 0.22], respectively) and shoot lengths (3.31 cm [± 0.36] and 3.62 cm [± 0.19], respectively) was observed following fungal treatment. For batch 2 (50 ppm), 100 percent germination was recorded for the wastewater samples (before and after treatment). The respective root lengths recorded for untreated and treated samples were: 2.42 cm [± 0.29] and 2.53 cm [± 0.24], while the shoot lengths were 3.36 cm [± 0.29] and 3.49 cm [± 0.20], respectively. For Batch 3 (100 ppm), no germination inhibition was observed for treated and untreated synthetic dye wastewater samples and the respective observed root lengths were: 1.66 cm [± 0.28] and 1.85 [± 0.31]. The shoot lengths were 2.55 cm [± 0.30] and 2.71 cm [± 0.33], respectively.

For *R. sativus* seeds, 100 percent germination was observed before and after fungal treatment in the first batch, the root lengths recorded were 1.55 cm [± 0.17] and 1.76 cm [± 0.21], and the shoot lengths were 2.15 cm [± 0.20] and 2.25 cm [± 0.19], respectively. No germination inhibition was observed with the 50 ppm batch samples. Root lengths were 1.32 cm [± 0.16] and 1.34 cm [± 0.15] while the shoot lengths were 1.91 cm [± 0.21] and 2.04 cm [± 0.17], respectively. For the 100-ppm batch, 95% seeds germination was observed with untreated dye wastewater which increased to 100% following fungal treatment. Observed root lengths were 1.14 cm [± 0.16] and 1.34 cm [± 0.15] while the shoot lengths were 1.62 cm [± 0.22] and 1.91 cm [± 0.14], respectively (Table 4.1).

4.3.4.1.2 Hybrid activated sludge reactor

For the detoxification assessment of the hybrid activated sludge reactor, *T. aestivum* (wheat) and *R. sativus* (radish) seeds were used and phytotoxicity of the untreated and treated synthetic dye wastewater samples was measured. 85 percent germination of *T.*

aestivum seeds was recorded for untreated batch 1 sample while for the treated one, 100 percent seed germination was observed. The respective root lengths were: 1.62 cm [± 0.24] and 2.08 cm [± 0.13], and the shoot lengths were: 1.93 cm [± 0.22] and 2.32 cm [± 0.15]. For batch 2 (50 ppm), 85 and 100 percent seed germination was observed when watered with untreated and treated synthetic dye wastewater samples, respectively. The observed root lengths were 1.41 cm [± 0.21] and 1.91 cm [± 0.15], whereas the shoot lengths were 1.7 cm [± 0.24] and 2.03 cm [± 0.19], respectively. For the 100 ppm batch, 80 and 100 percent seed germination was observed before and after treatment with the activated sludge, respectively. The respective root lengths were: 1.13 cm [± 0.15] and 2.24 cm [± 0.14] while the shoot lengths were recorded as 1.26 cm [± 0.16] and 1.98 cm [± 0.12], respectively.

With *R. sativus* seeds, seed germination recorded with samples before and after biotreatment (batch 1) was 70 and 75%, respectively. The respective root lengths were 2.43 cm [± 0.28] and 3.4 cm [± 0.45], while the shoot lengths were 3.56 cm [± 0.46] and 3.88 cm [± 0.34]. For second batch, 60 and 65% seed germination was observed with the untreated and treated synthetic dye wastewater samples, respectively. Root lengths were 2.67 cm [± 0.32] and 3.86 cm [± 0.41]; and the shoot lengths were 2.72 cm [± 0.25] and 2.04 cm [± 0.17]. For the third batch, 45 percent seed germination was recorded before treatment, and following treatment, less germination inhibition was observed with 65% seed germination. The respective root lengths were 2.53 cm [± 0.34] and 3.31 cm [± 0.34]; and the shoot lengths were 2.47 cm [± 0.28] and 3.61 cm [± 0.33], respectively (Table 4.2).

Table 4.1 Phytotoxic analysis of immobilized fungal reactor samples

Batch		<i>T. aestivum</i>			<i>R. sativus</i>		
		Germination (%)	Root length (cm) \pm S.E.	Shoot length (cm) \pm S.E.	Germination (%)	Root length (cm) \pm S.E.	Shoot length (cm) \pm S.E.
	Control	100	2.85 \pm 0.29	3.79 \pm 0.29	100	1.90 \pm 0.16	2.56 \pm 0.16
Batch 1	STW	100	2.44 \pm 0.33	3.31 \pm 0.36	100	1.55 \pm 0.17	2.15 \pm 0.20
	TSTW	100	2.88 \pm 0.22	3.62 \pm 0.19	100	1.76 \pm 0.21	2.25 \pm 0.19
Batch 2	STW	100	2.42 \pm 0.29	3.36 \pm 0.29	100	1.32 \pm 0.16	1.91 \pm 0.21
	TSTW	100	2.53 \pm 0.24	3.49 \pm 0.20	100	1.39 \pm 0.14	2.04 \pm 0.17
Batch 3	STW	90	1.66 \pm 0.28	2.55 \pm 0.30	95	1.14 \pm 0.16	1.62 \pm 0.22
	TSTW	95	1.85 \pm 0.31	2.71 \pm 0.33	100	1.34 \pm 0.15	1.91 \pm 0.14

STW Synthetic textile wastewater, TSTW Treated synthetic textile wastewater, S.E., standard error

Table 4.2 Phytotoxic analysis for hybrid activated sludge reactor samples

Batch	<i>T. aestivum</i>			<i>R. sativus</i>			
	Germination (%)	Root length (cm) ± S.E.	Shoot length (cm) ± S.E.	Germination (%)	Root length (cm) ± S.E.	Shoot length (cm) ± S.E.	
Control	100	2.16 ± 0.18	2.38 ± 0.19	100	3.06 ± 0.34	4.0 ± 0.43	
Batch 1	STW	85	1.62 ± 0.24	1.93 ± 0.22	70	2.43 ± 0.28	3.56 ± 0.46
	TSTW	100	2.08 ± 0.13	2.32 ± 0.15	75	3.4 ± 0.45	3.88 ± 0.34
Batch 2	STW	85	1.41 ± 0.24	1.7 ± 0.21	60	2.67 ± 0.32	2.72 ± 0.25
	TSTW	100	1.91 ± 0.15	2.03 ± 0.19	65	3.86 ± 0.41	4.46 ± 0.47
Batch 3	STW	80	1.13 ± 0.15	1.26 ± 0.16	45	2.53 ± 0.34	2.47 ± 0.28
	TSTW	100	2.24 ± 0.14	1.98 ± 0.12	65	3.31 ± 0.34	3.61 ± 0.33

STW Synthetic textile wastewater, TSTW Treated synthetic textile wastewater, S.E., standard error

4.3.4.2 Acute toxicity assay

Acute toxicity of samples obtained from immobilized fungal and hybrid activated sludge reactors were assessed using *A. salina* larvae and thorough larval mortality ratio computation (Table 4.3).

4.3.4.2.1 Immobilized fungal reactor

For batch 1 (25 ppm dye) of immobilized fungal reactor, no larval mortality was observed before and after fungal treatment. For second batch (50 ppm dye), 10% mortality was observed with synthetic dye wastewater while with the samples obtained after biotreatment no larval mortality was observed. For the third batch (100 ppm dye), 20% larval mortality was recorded before treatment. Following fungal treatment of the synthetic dye wastewater, all brine shrimp larvae were found to be active.

4.3.4.2.2 Hybrid activated sludge reactor

For the 25-ppm batch of the hybrid activated sludge reactor, no larval mortality was observed before and after the biotreatment of the synthetic dye wastewater. In the second batch (50 ppm), 10% larval mortality was recorded which reduced to zero percent following biotreatment. In the 100-ppm batch, 25 and 10% larval mortality was observed before and after biotreatment, respectively.

Table 4.3 Acute toxicity analysis for immobilized fungal and hybrid activated reactor

Batch		Larval Mortality (%)	
		Immobilized fungal reactor	Hybrid activated sludge reactor
Control		0	0
Batch 1	STW	0	0
	TSTW	0	0
Batch 2	STW	10	10
	TSTW	0	0
Batch 3	STW	20	25
	TSTW	0	10

STW Synthetic textile wastewater, TSTW Treated synthetic textile wastewater

4.4 Discussion

An immobilized fungal and a hybrid activated sludge reactor were operated in batch mode for the treatment of RB 221 containing synthetic textile wastewater. The reactors' performance was evaluated by periodic monitoring (24 hours) of color, COD, and pH for 144 hours. In batch 1 (25 ppm dye) of the immobilized fungal reactor, a gradual increase in the color removal performance was observed. The very low color removal at the start of reactor operation might be result of fungal acclimation to the reactor volume and other operating conditions (Gao, Wen, and Qian 2006). Fastest color removal was observed in the second batch (50 ppm dye) where 92.32% decolorization was observed after 24 hours of reactor operation while in the third batch (100 ppm dye) color removal performance was in between of that observed in the first and second batch (Fig. 4.2a). Therefore, the repeated usage of the immobilized fungal biomass did not affect the *T. asperellum* activity as indicated by the complete color removal in each batch and statistically, the three batches demonstrated a significant difference in the color removal efficiency ($p < 0.05$). Moreover, colorless fungal mycelia indicated that the dye removal resulted from adsorption cum enzymatic degradation instead of solely adsorptive dye removal mechanism (Hossain et al. 2016). Similarly, Sierra Solache et al., (2016), observed complete color removal in food industry effluent within 5 hours using alginate beads immobilized *P. chrysosporium* in an airlift bioreactor. Conversely, Almeida and Corso, (2014) reported a relatively slower decolorization (98% in 336 hours) of Procion Red MX-5B dye by *A. terreus* in free form.

In the hybrid activated sludge reactor, a gradual color removal was observed in all the three batches, however in batch 1, a relatively lower (90.21% in 144 hours) color removal occurred as compared to the other two batches ($p < 0.05$). Comparable performance was observed in the second and third batch where up to 96% color reduction was observed after 144 hours of operation ($p > 0.05$) (Fig. 4.2b). At first, dye adsorption was observed, after which the activated sludge biomass gradually became colorless with the progression of first batch. This may be due to enzymatic degradative activity of the activated sludge community (Asad et al. 2007). Mirbolooki et al., (2017) reported 59.44% color removal of Remazol Brilliant Blue R (125 ppm), containing synthetic wastewater in a sequencing batch reactor with a cycle time of 24 hours. Comparison of the immobilized fungal and hybrid activated sludge reactor at each dye

concentration showed relatively faster and efficient removal by the immobilized *T. asperellum* than the activated sludge community ($p < 0.05$)

Chemical oxygen demand assessment of the immobilized fungal reactor during the synthetic textile wastewater treatment showed an azo dye independent behavior as the COD reduction pattern in all the three batches did not follow the same trend as that observed with the dye removal process, which is accordance with the literature (Cheriaa et al. 2012). A substantial overall COD reduction was observed in all the three batches with maximum decrease observed in the case of Batch 1 ($p < 0.05$) (Fig 4.3a). During the treatment process highs and lows were observed. The sudden increase following substantial decrease as observed at some points might have resulted due to the presence of some fungal and dye metabolites of higher recalcitrant nature. The extended treatment following considerable color removal (50-60%) might have helped in the adaptation of fungal biomass to the resulting metabolites that ultimately lead to 70-80% reduction in COD of the synthetic textile wastewater. In comparison to this, parallel findings were reported by Spina et al., (2012), where immobilized *Bjerkandera adusta* (MUT 2295) showed 91% reduction in COD in 5 days for real textile effluent. The reduction in COD value was indicative of biodegradation and formation of simpler compounds.

In the hybrid activated sludge reactor, 50-60% COD reduction was observed in in 24-48 hours and was slightly correlated with the color removal activity of the hybrid reactor. Batch 1 was found to be more efficient for COD reduction with up to 90% reduction recorded after 144 hours while in the other two batches, 79-81% reduction was recorded ($p < 0.05$) (Fig. 4.3b). Moreover, unlike the immobilized fungal reactor the hybrid activated sludge reactor showed a rather smooth decline (except for batch 2) in the chemical oxygen demand of the synthetic textile wastewater and was relatively more efficient for COD removal at each tested dye concentration ($p < 0.05$). Likewise, Naresh Kumar et al., (2014) reported 65% decrease in COD value in 48 hours, when real textile waste water was treated with enriched sludge in a suspended growth reactor.

The fungal and activated sludge treatment setups were run at different initial pH values, i.e. 5.0 and 7.0 for the fungal and hybrid systems, respectively. Due to different pH tolerance profiles for the fungi (acidic) and bacteria (neutral and/or basic) (Solís et al.,

2012), use of different initial pH was required to start the operations. As very low and high pH values are detrimental for many microorganisms, due to disruption of metabolic activities (Chang et al., 2001). As pH is a crucial factor for the dye wastewater treatment systems, pH of the two setups was regularly monitored to analyze the systems' dynamics. Periodic assessment of the pH in the immobilized fungal reactor demonstrated an overall increase for the three batches with the highest increase recorded in the first batch ($p < 0.05$) (Fig. 4.4a). The probable reason for alkalinity in the system could be the presence of aminated metabolites or the CO₂ stripping resulting from the aeration (Spagni et al. 2010). However, the fungal activity was not affected by the increased pH and retained ample efficacy in the successive batches where the synthetic dye wastewater was relatively more buffered and remained closer to the initial pH. This might have resulted from the release of simpler dye metabolites due to the improved fungal adaption and stability (Gao et al. 2006). Hai et al., (2009) reported somewhat similar findings where the pH was maintained in the range of 5.5-6.0 in continuous fungal membrane bioreactor. In the activated sludge reactor, the pH at the end of all the three batches stayed close to the reported optimum range for activated sludge i.e., 6.50-8.50 ($p > 0.05$) (Fig. 4.4b) (Almeida and Corso, 2014). However, substantial acidic pH was observed during the first 48 hours of batch 1 which might have resulted from the increased nitrification effect which later on became less pronounced due to continuous influx of oxygen and CO₂ stripping (Spagni et al. 2010). The hybrid activated sludge reactor showed less pH variation than the immobilized fungal reactor therefore suggesting a relatively stable system ($p < 0.05$).

FTIR spectrum of the untreated synthetic textile wastewater for immobilized fungal reactor consisted of different bands. Band at 3519.30 cm⁻¹ corresponded to O–H bond vibrations, while the bands at 2925.45 cm⁻¹ and 2858.41 cm⁻¹ corresponded to the aliphatic group C–H stretching (Yuen et al. 2005). The band at 1657.37 cm⁻¹ indicated the presence of C=N stretching vibrations (Jadhav et al., 2008). The absorption band observed at 1576.51 cm⁻¹ indicated the –N=N– stretching vibration (Jain et al. 2012). C–OH and S=O bond stretching were indicated by bands at 1146.22 and 1062.81 cm⁻¹, respectively, while the band at 1002.33 cm⁻¹ corresponded to the substituted aromatic ring structure (Lambert et al., 1998). In the FTIR spectrum of the dye metabolites (obtained after fungal treatment), some bands were found to be altered in intensity and

shifted from the positions observed in the untreated synthetic dye wastewater sample, such as the slight changes in the bands at 2858.41, 1657.37, and 1062.81 cm^{-1} might have occurred due to changes in other functional groups of the dye. Disappearance of peak at 1576.51 cm^{-1} indicated the possible cleavage of $-\text{N}=\text{N}-$ bond which explains the color removal from the synthetic dye wastewater (Mohammed and Mohammed, 2010; Olukanni et al., 2010).

FTIR spectrum of the untreated synthetic textile wastewater for the hybrid activated sludge reactor, showed different bands. Band at 3424.31 cm^{-1} corresponded to O–H bond vibrations. While the bands at 3190.62, 2971.61 and 2857.50 cm^{-1} corresponded to the aliphatic group C–H stretching. The band at 1659.25 cm^{-1} , indicated the presence of C=N stretching vibrations (Jadhav et al., 2008). The absorption bands observed at 1576.51 cm^{-1} indicated the $-\text{N}=\text{N}-$ stretching vibration (Jain et al. 2012). C–OH and S=O bond stretching were indicated by bands at 1113.88 and 1062.23 cm^{-1} , respectively, while the band at 1003.46 cm^{-1} corresponded to the substituted aromatic ring structure. In the FTIR spectrum of the dye metabolites (obtained after treatment in the hybrid reactor), some bands were found with a slightly changed intensity and shifted from the points seen in the untreated synthetic dye wastewater sample, such as the band at 2857.50 cm^{-1} , 1659.25, and 1062.23 cm^{-1} , that might have resulted from the changes occurred in other bonds of the dye molecules. Disappearance of peaks around 1513.12–1576.51 cm^{-1} indicated the of $-\text{N}=\text{N}-$ bond breakage which lead to the color removal from the synthetic dye wastewater (Mohammed and Mohammed, 2010; Olukanni et al., 2010). In both reactor setups changes in the characteristic bands indicated that the color removal was achieved as a result of biodegradation.

During the biotreatment in the hybrid activated sludge reactor, progression of active, suspended and attached bacterial biomass was monitored via bacterial growth measurement (CFU/mL; CFU/mL cm^2) and the ratio of attached to total bacterial count was calculated on the final day of each batch (Fig. 4.6a and b). At the completion of first batch (25 ppm dye), attached bacteria made only 39.69% of the total count as the activated sludge population was dominated by free form bacterial cells. Later, in the second batch, a marked improvement in the attached bacterial count was observed (making 68.64% of the total bacterial count) as compared to the first batch ($p < 0.05$). In the third and final batch, a slight decline in the attached bacterial count was recorded

(contributing 65.89% to the total count in the hybrid activated sludge population). The hybrid system proved to be efficient in terms of overall reactor performance for the treatment of synthetic dye wastewater through improved retention and stabilization of bacterial cells by combining and enhancing the properties of biofilm and suspended culture (Sirianuntapiboon and Sansak 2008). The vertical arrangement and utilization of Scotch Brite proved to be a suitable support for biofilm development and maintenance, as indicated by the marked increase in attached bacterial count over time despite the increasing dye concentrations. Likewise, Jianlong et al., (2000) developed a hybrid activated sludge system for the treatment of domestic wastewater and observed an improved treatment efficiency with biomass augmentation in comparison to conventional activated sludge treatment.

Phytotoxicity assessment of the synthetic textile wastewater (before and after biotreatment) in the immobilized fungal and hybrid activated sludge reactor was done using *T. aestivum* (wheat) and *R. sativus* (radish) seeds. In the first two batches of the immobilized fungal reactor, no germination inhibition was observed in wheat and radish seeds (before and after fungal treatment), however, in the third batch (100 ppm dye) a slight increase in the seed germination was observed (Table 4.1). The root and shoot length values were higher in all the three batches following fungal treatment, indicating a reduction in the toxicity of synthetic dye wastewater ($p < 0.05$). In the hybrid activated sludge reactor, an improvement in the seed germination, root, and shoot lengths was observed in all batches for both type of plant seeds used ($p < 0.05$) (Table 4.2).

Textile effluents are typically released into open water systems and despite the known threat associated with these waters, they are frequently used for irrigation (Jadhav et al. 2008). Although the harmful effects of textile waste can be reduced through treatment, it is vital to test the toxicity level of the waste following biotreatment (Kalyani et al. 2008). Both types of reactors were therefore, found to be good for detoxification of synthetic textile wastewater as indicated by the phytotoxicity assay. Likewise, reduction in toxicity of RB13 dye following biotreatment was reported by Olukanni *et al.*, (2010), where an improvement in seed germination rate, root and shoot length of *Z. mays* and *P. vulgaris* was observed when treated with degradation products of the RB13 dye. In another study, Buntić et al., (2017) reported improved germination rate, root

and shoot lengths of *T. aestivum* seeds when watered with decolorization products of Crystal violet and Safranin T dyes, obtained after treatment with *Streptomyces microflavus* CKS6. Acute toxicity assessment (using *A. salina* larvae) of the synthetic dye wastewater in both types of reactors indicated a decrease in toxicity in the second and third batch when compared to the untreated colored wastewater ($p < 0.05$), as the *A. salina* larval mortality rate was reduced (Table 4.3). The reduction in toxicity is indicative of the formation of milder and eco-friendly products following biotreatment in the reactor systems. Similarly, Palácio et al., (2009), Ayed et al., (2011), and Almeida and Corso, (2014) performed cytotoxicity tests, using *A. salina* larvae and reported decrease in toxicity of dyes following biotreatment.

4.5 Conclusion

Both the immobilized fungal reactor and hybrid activated sludge reactor were found to be effective for the treatment of synthetic textile wastewater. Scotch Brite™ was found to be a good support material for both fungal immobilization and biofilm development, as the repeated usage of the formulations did not affect their treatment efficiency. Immobilized fungal reactor was more efficient in the color removal, however, a better performance was shown by the hybrid activated sludge in terms of the COD reduction and system's stability (pH). The duality of the hybrid system (attached and suspended bacterial biomass) enhanced the reactor's efficacy. FTIR spectroscopic analysis showed characteristic band changes indicating the color removal a result of biodegradation. Moreover, the end products obtained following biotreatment were detoxified as indicated by the toxicity assays.

Chapter 5: Appraisal of different natural bacterial consortia for the treatment of reactive azo dyes

5.1 Introduction

Biological remediation techniques present an environmentally sustainable and relatively cost-effective solution for the textile wastewater treatment (Jadhav et al., 2010; Das and Mishra, 2017). Many different microorganisms have been reported for the textile dye waste treatment (Solís et al., 2012). Among the wide variety of dye decolorizing and/or degrading microbes, bacteria are considered as a more viable option due to their fast growth and adaptive nature (Dua et al. 2002). Bacteria are utilized for the dye waste treatment in pure, mixed, and/ or co-culture forms (Saratale et al. 2011). Mixed bacterial cultures are advantageous in this regard, due to their syntrophic metabolic activities that can result in complete dye removal through mineralization (Forgacs, 2004). Most of the available literature, is focused on designed consortia, consisting of isolated bacteria (usually from a textile originated sludge), capable of degrading single and/or multiple dyes (Sin et al. 2016). Such designed consortia can be used to bioaugment the natural biological treatment process (Hai et al. 2011). In addition to this, natural bacterial consortia are also used sometimes, but the constituents of a given consortium are usually left unexplored (Watanabe and Baker, 2000; Joshi et al., 2010). Gaining an insight into the community structure of such consortia can provide a better understanding of the complex bacterial communities. This can also help in the improvement of dye removal process by minimizing the drastic community shifts resulting from the changes in the treatment systems (Rgen Forss et al. 2017).

Textile effluents have a complex and heterogenic nature with multiple dyes, alkaline pH, elevated temperature, and high salinity (Amoozegar et al., 2011; Solís et al., 2012). Such conditions could limit the efficiency of most of the reported dye decolorizing bacteria and their consortia, that perform under neutral pH, mesophilic temperatures, and non-saline environments (Bhattacharya et al., 2017). Extremophilic bacterial consortia could provide a workable solution in such settings, as they are equipped with a more diverse metabolic profile that enables them to withstand harsh environmental conditions (Prasad and Rao, 2013). Many reports are available on the application of halotolerant and/ or halophilic, and alkaliphilic bacteria (mostly pure cultures) for the

textile dyes treatment; but the literature focusing on bacteria that can survive under combined high pH and salt pressure are rare (Asad et al. 2007; Khalid et al. 2008; Arun Prasad et al. 2013; Lalnunhlmi and Veenagayathri 2016; Bhattacharya et al. 2017). Furthermore, high temperature-dwelling mixed consortia are least explored for the textile dye degradation (Deive et al. 2010).

Keeping all these points in consideration, the present study was conducted to explore the efficacy of different natural (mesophilic [MBC], alkaliphilic and halotolerant [AHBC], and thermophilic [TBC]) bacterial consortia for the treatment of a reactive azo dye mixture (consisting of RB 221, RR 195, and RY 145) containing synthetic wastewater. The bacterial consortia were optimized by one factor optimization followed by Response surface methodology, using Box-Behnken design. Three (for MBC and TBC) and four (for AHBC) factor regression model designs were used to optimize the decolorization process. Response surface methodology (RSM) is one of the most useful approach for the optimization of a given biological process (Jadhav et al. 2013). It not only helps to identify and optimize the key factors influencing a process, but also provides an insight into their relationship in a multivariable system (Sharma, Singh, and Dilbaghi 2009). Moreover, the constituents of natural consortia were investigated using the high-throughput sequencing i.e., tag encoded 454-pyrosequencing. This next generation sequencing (NGS) technique is advantageous over the conventional sequencing methods, as it provides a detailed insight into the complex microbial communities by targeting and identifying both the high and low abundance individuals (Köchling et al. 2017). The treatment efficiency was assessed using FTIR and GC-MS analyses. Detoxification efficiency was monitored through toxicity assays.

5.1.1 Aims and Objectives

The aim of this study was to explore and optimize the treatment potential of different natural (MBC, AHBC, and TBC) bacterial consortia for a reactive azo dye mixture by using Response Surface Methodology (RSM). Specific objectives of the study were:

- To enrich the dye decolorizing bacterial consortia obtained from different sites.
- To carry out the preliminary optimization of the decolorization process through one-factor-at-a-time (OFAT) experimental technique.

- To further evaluate, validate the key parameters (based on the results of OFAT), and explore their interrelationship, using Box-Behnken (BBD) experimental design.
- To explore the bacterial community of natural dye decolorizing bacterial consortia using tag encoded 454-pyrosequencing.
- To investigate the treatment efficacy by periodic monitoring of color, pH and chemical oxygen demand (COD) using spectrophotometric and standard wastewater analytical protocols.
- To assess biodegradation thorough FTIR and GC-MS analyses.
- To assess the detoxification efficiency through plant and brine shrimp toxicity tests.

5.2 Materials and Methods

5.2.1 Dyes and chemicals

Reactive azo textile dyes viz. Reactive Blue 221 (RB 221, absorbance maxima: λ_{\max} 615 nm), Reactive Red 195 (RR 195, absorbance maxima: λ_{\max} 545 nm), and Reactive Yellow 145 (RY 145, absorbance maxima: λ_{\max} 422 nm) were generously given a textile industry in Lahore, Pakistan (Table 3.1). The dyes were used without any further purification. Filter sterilized (nylon membrane microfilters, 0.2 μm pore size, Corning Inc., Corning, NY, USA), 1000 ppm stock solutions of the individual dyes were prepared in distilled water. For the dye mixture (absorbance maxima: λ_{\max} 543 nm), equal proportions of each dye (333.33 ppm) were used. The stock solutions were stored at room temperature. Analytical grade chemicals, microbial growth, and storage media were acquired from Sigma-Aldrich (Sigma-Aldrich, St. Louis, MO, USA) and Oxoid (Oxoid Limited, Hampshire, UK).

5.2.2 Media for microbial growth and dye decolorization studies

Dye mixture amended nutrient broth medium was used for the enrichment of dye degrading bacterial consortia. Dye-free nutrient broth was used for bacterial culture growth, storage (at 4 °C), and preparation of fresh inocula. For the dye mixture decolorization studies, synthetic medium as described in section 4.2.2.2 was used. To that medium, filter sterilized stock solution of the dye mixture was added as per required final concentration of the simulated textile effluent. For mesophilic and thermophilic consortia, pH of the synthetic effluent was 7.0 ± 0.2 . For the alkaliphilic and halotolerant bacterial consortium, reactive azo dye containing synthetic effluent was amended with NaCl: 10% (w/v) and the final pH was 10.0 ± 0.2 .

5.2.3 Sampling

Sludge samples were collected from the waste disposal site of a textile industry in Lahore, Pakistan. The pH and temperature recorded at the site were 8 and 33.5 °C, respectively. Such temperature conditions usually facilitate the growth of mesophilic bacteria. Samples were taken in sterile plastic bags and transported on ice to Microbiology research lab, Quaid-i-Azam University, Islamabad, Pakistan. The

samples were then stored in refrigerator at 4 °C till further usage. For the alkaliphilic and halotolerant consortium, a humus rich soil sample was collected from the botanical garden at Quaid-i-Azam University in Islamabad, Pakistan. In plastic pots, 25 g of the soil sample was pretreated with 20 mL each of 10% (w/v) NaCl, NaOH at pH 10, and 1000 ppm azo dye mixture solution for the enrichment of alkaliphilic and halotolerant dye decolorizing bacteria in the soil media. With the addition of 20 mL each of the three solutions, the soil was completely flooded with water. For three months, the pots were stored in sunlight and regularly moistened with the three solutions every two days with approximately 5-10 mL of each solution added depending on the condition of the soil. The pretreated soil sample was then used as the inoculum for further enrichment of alkaliphilic and halotolerant dye decolorizing bacteria in liquid medium. To obtain potential thermophilic dye decolorizing bacteria, water samples were collected from a hot spring i.e., Moshkin Tato at Dashkin village, district Astore, Gilgit-Baltistan, Pakistan. pH and temperature of the water sample were 7.12 and ~70 °C, respectively. Samples were transported in sterile plastic bottles to Microbiology research lab, Quaid-i-Azam University, Islamabad, Pakistan and then stored in an incubator at 70 °C till further processing.

5.2.4 Enrichment of dye decolorizing consortia

For the mesophilic dye decolorizing bacterial consortium, aqueous suspension of the sludge sample (10% v/v) was inoculated into 90-mL of nutrient broth medium containing 25 ppm of dye mixture in 250-mL Erlenmeyer flask. Flasks were incubated at 35 °C under static and shaking (135 rpm) condition until complete decolorization. For the enrichment of alkaliphilic and halotolerant bacterial dye decolorizing bacteria consortium, 1.0 g of the pretreated soil was added to 100 mL (in 250-mL conical flasks) of nutrient broth medium containing 25 ppm azo dye mixture and 10% (w/v) NaCl, pH was adjusted to 10. The flasks were then incubated (35°C) under shaking (135 rpm) and static conditions until disappearance of color. The samples were incubated (35°C) until complete color removal occurred. For the enrichment of thermophilic bacteria, 10 mL of the hot spring water sample was added to 90 mL of nutrient broth containing 25 ppm of dye mixture following incubation at 50 °C under static and shaking (135 rpm) conditions till complete color removal. Ten (10 mL) of each of the decolorized samples (from the respective enrichment cultures) were subjected to successive transfers to fresh

dye mixture containing nutrient broth medium (25 and 50 ppm) and incubated at respective temperatures till complete color removal. Finally, the treated samples were added to synthetic textile wastewater and visually monitored till complete color loss.

5.2.5 Decolorization assessment

For the decolorization assessment, inoculum of each consortium, was prepared by transferring 5 mL of each of the treated (decolorized) sample to 45 mL of nutrient broth medium in 100-mL conical flasks followed by incubation at 35 °C (mesophilic and alkaliphilic-halotolerant) and 50 °C (thermophilic), respectively, until mid-log phase (OD₆₀₀: 0.6). Ten (10) mL of the prepared inocula were added to synthetic dye effluent (90 mL) containing 50 ppm azo dye mixture (pH: 10 and 10% NaCl for alkaliphilic and halotolerant consortium) and incubated under respective temperatures for 24 hours with and without agitation. The initial absorbance of each sample was recorded at 543 nm (λ_{max} of the dye mixture) with a UV-Vis Spectrophotometer (Agilent 8453; Agilent Technologies, Santa Clara, CA, USA). After 24 hours of incubation, 1.5 mL aliquots were aseptically withdrawn from each flask in centrifuge tubes. The samples were centrifuged at 10,000×g for 10 minutes and clear supernatant was read at 543 nm and absorbance was recorded. Uninoculated synthetic dye containing and dye-free effluent were used as abiotic control and blank for spectrophotometric analysis, respectively. The extent of decolorization was measured using the following formula (Sani and Banerjee, 1999).

$$\text{Decolorization (\%)} = \frac{(I - F)}{I} \times 100 \quad (\text{Eq 5.1})$$

where I is the initial absorbance of the colored sample and F is the final absorbance of the decolorized sample. The efficient dye decolorizing consortia were then maintained and preserved (as glycerol stocks) at 4 °C and -70 °C, respectively.

5.2.6 Optimization of culture conditions for dye mixture decolorization (OFAT)

Decolorization efficiency of the three consortia (for the dye mixture containing synthetic wastewater) was assessed under different culture conditions by modifying the carbon source (glucose, sorbitol, sucrose, lactose, and starch at 0.1% [(w/v)]), nitrogen source (yeast extract, peptone, sodium nitrite, potassium nitrate, and ammonium

sulfate, at 0.1% [(w/v)], temperature ([25, 30, 35, 40, 45 °C for MBC and AHBC consortium]; 45, 50, 55, 60, and 65 °C for TBC), dye concentration (50, 100, 150, 200, 250, 300, 400, 500, and 1000 ppm), pH ([5-9 for MBC and TBC]; and 9-14 for AHBC), and salt concentration (0, 2, 4, 6, 8, 10, 12% [w/v] NaCl). All experiments were carried out under static condition for 120 hours.

5.2.7 Response Surface Methodology (RSM)

RSM is a statistical procedure for investigation of interrelationship of independent factors and observed responses in a multivariable experimental system. There are three main steps of this optimization method: (i) execution of statistically designed set of experiments, (ii) estimation of coefficients in the mathematical model, and (iii) prediction of responses and model adequacy check (Box and Behnken 1960). Design-Expert version 7.0.0 (Stat-Ease) was used for applying the Box-Behnken design (BBD). Based on the results of the preliminary optimization experiments (OFAT), three design parameters viz. temperature (°C, designated as A), pH (designated as B), and dye (mixture) concentration (ppm, designated as C) were selected for two of the three consortia used in this study i.e., MBC and TBC. For AHBC consortium, four selected factors were: temperature (°C, designated as A), pH (designated as B), dye (mixture) concentration (ppm, designated as C), and salt concentration (% [w/v], designated as D). The three levels for the selected parameters were coded as -1, 0, and 1 for low, central point, and high levels, respectively (Tables 5.1-5.3). F test was used for evaluating the significance of the model. Determination coefficient (R^2 and adjusted R^2) was used for assessing the quality of the quadratic model. Model's statistical significance was evaluated by analysis of variance (ANOVA). With the help of regression equation and response surface plot, optimum values were obtained which were further confirmed through model validation experiments.

Table 5.1 Design factors and coded variables for MBC

Factor	Units	Coded levels		
		-1	0	1
Temperature (A)	°C	33	35	37
pH (B)	NA	6.0	7.0	8.0
Dye concentration (C)	ppm	50	100	150

Table 5.2 Design factors and coded variables for AHBC

Factor	Units	Coded levels		
		-1	0	1
Temperature (A)	°C	33	35	37
pH (B)	NA	9.5	10.0	10.5
Dye concentration (C)	ppm	50	100	150
Salt concentration (D)	%	8.0	10.0	12.0

Table 5.3 Design factors and coded variables for TBC

Factor	Units	Coded levels		
		-1	0	1
Temperature (A)	°C	48	50	52
pH (B)	NA	6.0	7.0	8.0
Dye concentration (C)	ppm	50	100	150

5.2.8 Molecular level analysis of natural bacterial consortia

5.2.8.1 DNA extraction from enriched broth cultures

The dye mixture decolorizing natural bacterial consortia (MBC, AHBC, and TBC), were grown in nutrient broth (5 mL inoculum, 45 mL nutrient broth) for 24 hours. The culture was used for inoculation of the synthetic dye (100 ppm) containing medium. The experiments were conducted under static condition till complete decolorization (72 hours for MBC and AHBC, 120 hours for TBC). The decolorized broth cultures were centrifuged at 10,000×g for 20 minutes, and the pelleted cells were used for isolation of genomic DNA according to Gao et al., (2010), with slight modifications. DNA extraction buffer: 13.5 mL (Tris-HCl [100 mmol/L, pH 8.0], 1.5 mol/L NaCl, and 1% CTAB) and proteinase K: 100 µL (10.0 mg/mL) were added to pellets. The centrifuge tubes placed in a shaker incubator (120 rpm) for half an hour at 37 °C. Then sodium dodecyl sulfate (SDS, 20%) was added followed by 2-hour incubation in a water bath at 65 °C. The samples were centrifuged at 6000×g for 10 minutes (room temperature) and supernatants were added to the fresh centrifuge tubes (50 mL). Equal volumes of phenol-chloroform-isoamyl alcohol (25:24:1) solution, were added, thoroughly mixed

and centrifuged (8,000×g for 20 min, room temperature). Aqueous layer was shifted to new centrifuge tube and re-extracted with phenol-chloroform-isoamyl alcohol solution. The upper aqueous phase was shifted to new tube and extracted finally with chloroform-isoamyl alcohol (24:1). Finally, the aqueous phase was precipitated by adding isopropanol (0.6 volume) and potassium acetate (0.5 M). The tubes were then incubated overnight at -20 °C. Following incubation, centrifugation was done at 12,000×g for 15 min, liquid phase was removed, and DNA was washed ethanol (70%, chilled). Centrifugation was done at 10,000×g for 5 min, ethanol was removed and 100 µL of Tris HCl-EDTA (T.E) buffer was added. Through agarose gel (1.0%) electrophoresis, stability of the DNA samples was confirmed. DNA concentration quantification (in 2µL of extracted samples) was done using Nanodrop spectrophotometer. The genomic DNA samples were stored at -20 °C till further processing.

5.2.8.2 Bacterial Tag-Encoded FLX Amplicon Pyrosequencing (bTEFAP®)

DNA samples, extracted from broth cultures of natural consortia were shipped to MR DNA Lab (MR DNA, Shallowater, TX, USA). Universal bacterial primers spanning V1-V3 region of the 16S rRNA gene, i.e., 27 F (5'-AGAGTTTGATCCTGGCTCAG-3') and 519 R (5'-GWATTACCGCGGCKGCTG-3') were used. For DNA amplification, PCR was performed by using HotStarTaq Plus Master Mix Kit (Qiagen, Valencia, CA). following were the optimized conditions for DNA amplification: 94 °C (3 minutes), 94 °C (30 seconds, 28 cycles), 53 °C (40 seconds), and 72 °C (1 minute), followed by 72 °C (5 minutes, final elongation step). After initial amplification, secondary PCR was performed using the above-mentioned conditions. This was done to incorporate specially designed primer sequences with barcodes and linkers (Table 5.4). Following that, amplicons of all samples were mixed in equal proportions followed by purification, using Agencourt Ampure beads (Agencourt Bioscience Corporation, MA, USA). The samples were then subjected to bTEFAP FLX parallel pyrosequencing, by using Roche 454 FLX titanium instruments and reagents according to the manufacturer's instructions.

Table 5.4 Barcode and linkers for the natural bacterial consortia

Sample	Barcode sequence	Linker Primer sequence
MBC	TCAGGTCC	AGRGTTCGATCMTGGCTCAG
AHBC	TCATGCGA	AGRGTTCGATCMTGGCTCAG
TBC	TCATCGTC	AGRGTTCGATCMTGGCTCAG

5.2.8.3 Processing and analytical steps for bTEFAP data

The sequencing data was further processed through the MR DNA analysis pipeline (www.mrdnalab.com, MR DNA, Shallowater, TX). Barcodes and primers were removed, and sequences with < 200bp were removed during the quality trimming. Moreover, the sequences with unclear base calls and homopolymer runs greater than 6bp were also removed. After that denoising was done and operational taxonomic units (OTUs) showing 97% similarity were defined. Finally, singletons and chimeras were erased using Uchime (Dowd et al. 2008; Edgar 2010). Following that, taxonomic classification of the final OTUs was done using BLASTn through NCBI (www.ncbi.nlm.nih.gov), GreenGenes (DeSantis et al. 2006) and RDP-II (<http://rdp.cme.msu.edu>) derived database. For the diversity analysis in the consortia samples, bacterial diversity and richness were determined through alpha diversity indices i.e., Shannon diversity index, Simpson index, Chao 1 estimator, observed species and phylogenetic distance whole tree and rarefaction curves were generated. The sequences were submitted to SRA archive in NCBI (<http://www.ncbi.nlm.nih.gov/Traces/sra/>)

5.2.9 Determination of Color, pH and COD during the treatment

The treatment efficiency of natural bacterial consortia for the synthetic dye effluent was tested under the optimized conditions. Experiments were conducted in large volume flasks, i.e., 1000 mL. Color, COD, and pH were determined at regular intervals (24 hours) for a period of 144 hours. (methods as described in section (5.2.4, 4.2.6.2, and 4.2.6.3, respectively).

5.2.9 Biodegradation assessment through FTIR and GC-MS

Treated and untreated synthetic dye effluent samples were analyzed through FTIR spectroscopy (spectrum 65 FTIR spectrometer equipped with ATR; Perkin Elmer, Waltham, MA, USA). The samples were centrifuged at 4000 rpm for 30 min, and the pelleted biomass was removed. Dye metabolites were extracted with ethyl acetate followed by drying over anhydrous Na₂SO₄ and evaporation in a rotary evaporator. The analysis was performed (using dried residues dissolved in methanol) in the mid IR region of 400-4000 cm⁻¹ with 16 scan speed. For GC-MS analysis Shimadzu 2010MS system was equipped with a HP1 column (30m, 0.25mm, 0.25 μm). Samples (1.0 uL) were auto injected. Carrier gas was Helium (flow rate: 1mL/min). Temperature of the injector was 280 °C. The oven temperature was kept at 80 °C (2 min), Then the temperature was raised up to 280 °C at the rate of 10 °C/ min. Mass spectra obtained were compared and identified with the help of NIST library.

5.2.10 Detoxification assessment of the synthetic dye effluent metabolites

Detoxification efficiency of the natural consortia was measured using the untreated and treated synthetic dye wastewater, through phytotoxicity (Turker and Camper, 2002) and brine shrimp acute toxicity tests (Meyer et al., 1982) (Methods, as described in section 3.2.3, and 3.2.4).

5.2.11 Statistical analyses

OFAT and detoxification experiments were performed in duplicates. Mean values and standard error of means were calculated using Microsoft Excel 2016. For the effect of different cultural parameters and toxicity reduction, one-way analysis of variance (ANOVA) followed by Tukey's honest significant difference (Tukey's HSD) at the significance level of $\alpha = 0.05$ ($p < 0.05$), was done using SPSS (IBM SPSS Statistics for Windows, Version 20.0., Armonk, NY, USA). The statistical procedures involved in response surface methodology (done in triplicates), were performed using Design-Expert version 7.0.0 (Stat-Ease).

5.3 Results

Natural bacterial consortia (mesophilic [MBC], alkaliphilic and halotolerant [AHBC], and thermophilic [TBC]), obtained from different origins were enriched and explored for the treatment of reactive azo dye mixture (consisting of RB 221, RR 195, and RY 145) containing synthetic textile effluent. Enriched natural bacterial consortia showed up to 85-88% color reduction after 24 hours under static incubation condition. However, the color reduction under shaking conditions was much less pronounced (> 50%) (Fig. 5.1). All further experiments were therefore performed under static incubation.

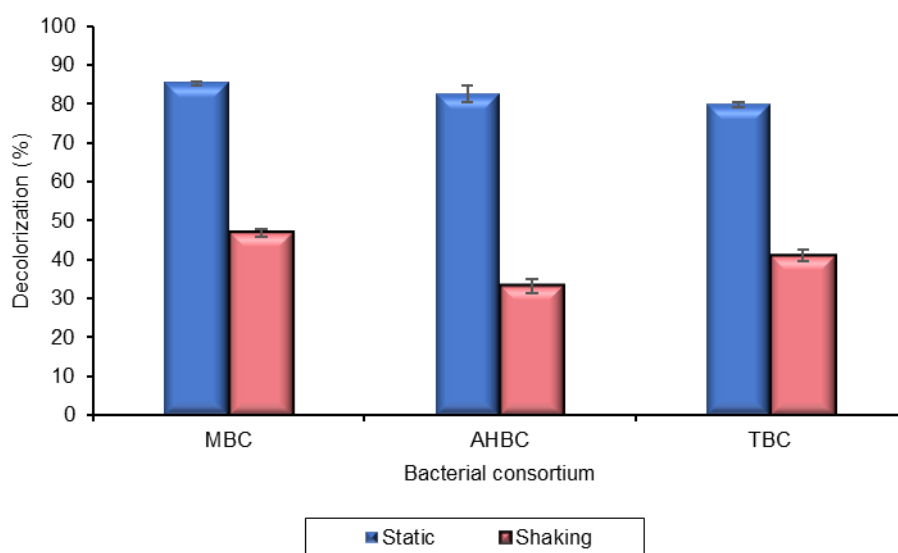


Fig. 5.1 Decolorization performance of the natural consortia under static and shaking conditions

5.3.1 Optimization of culture conditions for dye mixture decolorization (OFAT)

5.3.1.1 Carbon sources

Decolorization potential of natural bacterial consortia was assessed in the presence of different carbon sources (Fig. 5.2). Glucose was found to be the most suitable carbon source for MBC and AHBC, resulting in 97.89 and 92.28% decolorization (after 120 hours), respectively. While, the thermophilic bacterial consortium (TBC), showed 96.68, 99.9, and 98.24% color removal with glucose, sucrose, and lactose, respectively. For MBC, lactose was the second-best carbon source, as 64.83% decolorization was observed after 120 hours. With the other three carbon sources i.e., sorbitol, sucrose, and starch, MBC showed 55-57% decolorization. For AHBC, sucrose and lactose resulted in up to 54% color reduction. Sorbitol and starch were the least effective carbon sources for AHBC, with 40.09 and 34.23% decolorization observed after 120 hours. TBC showed 79.35 and 31.69% decolorization in the presence of sorbitol and starch, respectively.

5.3.1.2 Nitrogen sources

Decolorization efficacy of the natural bacterial consortia was tested by the addition of different nitrogen sources (Fig. 5.3). The organic nitrogen source i.e., yeast extract was found to be the most effective for the decolorization of synthetic dye wastewater by all the three natural bacterial consortia, as MBC, AHBC, and TBC showed 89.56, 94.19, and 98.34% decolorization, respectively. MBC showed 71.59, 64.64, 51.21, and 49.31% color removal with ammonium sulphate, potassium nitrate, peptone, and sodium nitrite, respectively. In the case of AHBC, 54.59, 49.29, 48.15, and 46.33% decolorization was recorded with potassium nitrate, peptone, sodium nitrite, and ammonium sulphate, respectively. While TBC showed 58.44, 57.51, 54.15, and 43.68% color reduction in the presence of sodium nitrite, peptone, potassium nitrate, and ammonium sulphate, respectively.

5.3.1.3 Temperature

Decolorization potential of the natural bacterial consortia for the synthetic dye effluent was investigated at different temperatures (Fig. 5.4). For the mesophilic bacterial consortium, an improved color removal performance was observed with the increase in

temperature i.e., 25-35 °C. The best suited temperature for MBC was 35 °C, as 89% decolorization occurred after 24 hours, reaching a final value of 99.72 after 120 hours. Further increase in temperature, resulted in a decline in color removal ability as after 120 hours, 53.71 and 16.87% decolorization was recorded at 40 and 45 °C, respectively. Alkaliphilic and halotolerant bacterial consortium also showed an improved color removal ability with the rise in temperature from 25-35 °C, with the highest color removal recorded at 35 °C i.e., 89.90% after 24 hours with a final value of 99.94% decolorization after 120 hours. At 40 °C, 76.97% color reduction was observed, while at 45 °C, decolorization ability was reduced to 26.89%. The thermophilic bacterial consortium showed maximum color removal at 50 °C, with 92.61 and 97.78% decolorization observed after 24 and 120 hours, respectively. At 55°C, 72.36% decolorization was recorded after 120 hours. Decolorization percentage was reduced upon further increase in temperature past 55 °C, as 57.37 and 28.57 decolorization was recorded at 60 and 65 °C, respectively.

5.3.1.4 pH

Effect of the different initial pH values on the color removal efficiency of the natural bacteria consortia, was investigated (Fig. 5.5). The optimum pH for MBC was 7.0, with a 95.24 and 99.79% color removal recorded after 48 and 120 hours, respectively. At pH 8.0, decolorization percentage was 80.55% after 120 hours. Moreover, under acidic (5.0 and 6.0) and basic pH (9.0) conditions, very low (< 50%) color removal was observed. For AHBC, optimum initial pH range was 10.0, as 99.01 % color reduction occurred after 72 hours. At pH 11.0, 92.84% decolorization was recorded after 120 hours of incubation. However, a marked decrease in the decolorization potential (< 50%) was observed at higher pH values, i.e., 12-14. TBC also showed maximum decolorization efficiency at neutral pH i.e. 7.0 with 97.21% decolorization after 72 hours. When the initial pH was raised to 8.0, a relatively slower decolorization was observed reaching a final value of 74.69%, after 120 hours. Acidic and basic conditions were not suitable for the color removal process as less than 50 percent color reduction was recorded at pH 5, 6, and 9.

5.3.1.5 Dye concentration

Color removal performance of the natural bacterial consortia for the synthetic dye effluent was studied at different initial dye concentrations (Fig. 5.6). MBC showed up to 99% decolorization at 50 (within 48 hours), 100, and 150 ppm (within 96 hours) initial dye concentrations. With an initial concentration of 200 ppm, 76.52% decolorization was achieved after 120 hours. However, a substantial decrease in the color removal performance was seen at higher initial dye concentrations, i.e., 250, 300, 500, and 1000 ppm. AHBC demonstrated a somewhat similar dye tolerance profile, as it showed up to 99% color reduction with initial dye concentrations of 50, 100 (within 72 hours), and 150 ppm (within 96 hours). At 200 and 250 ppm, 87.86% and 58.79% color removal occurred, respectively. Decolorization percentage considerably diminished at higher dye concentrations, i.e., 300, 500, and 1000 ppm. In the case of TBC, up to 98% color was reduced with an initial concentration of 50 and 100 ppm after 72 and 120 hours, respectively. With initial concentrations of 150 and 200 ppm, color removal percentages were 60.7 and 43.21%, respectively (after 120 hours). However, the decolorization percentage was reduced below 30% at higher initial dye concentrations.

5.3.1.6 NaCl concentration

Decolorization performance of the natural bacterial consortia was monitored in the presence of different NaCl concentrations (Fig. 5.7). Color removal ability of the mesophilic bacterial consortium (MBC), was considerably affected by the addition of salt to the medium, with a 54.11 and 42.45% decolorization observed in the presence of 2 and 4% NaCl, respectively. At higher NaCl concentrations, i.e., 6, 8, 10, and 12%, decolorization percentage was further reduced (< 40%). The alkaliphilic and halotolerant bacterial consortium (AHBC) retained a substantial decolorization ability over the whole tested NaCl concentrations range, i.e., 0-12% as it showed 82-98% color reduction. Most efficient color removal was recorded at 10 and 12% NaCl concentrations, with a 95.18 and 90.29% decolorization recorded after 72 and 96 hours, respectively. In the case of the thermophilic bacterial consortium (TBC), decolorization efficiency was substantially diminished in response to the addition of NaCl, as only 54.82 and 40.87% decolorization was recorded at 2 and 4% NaCl concentrations, respectively. The color removal ability was greatly inhibited in the presence of higher

NaCl concentrations. The varying co-substrate utilization, pH, temperature, dye, and salt tolerance profiles of the natural bacterial consortia are summarized in the Table 5.5.

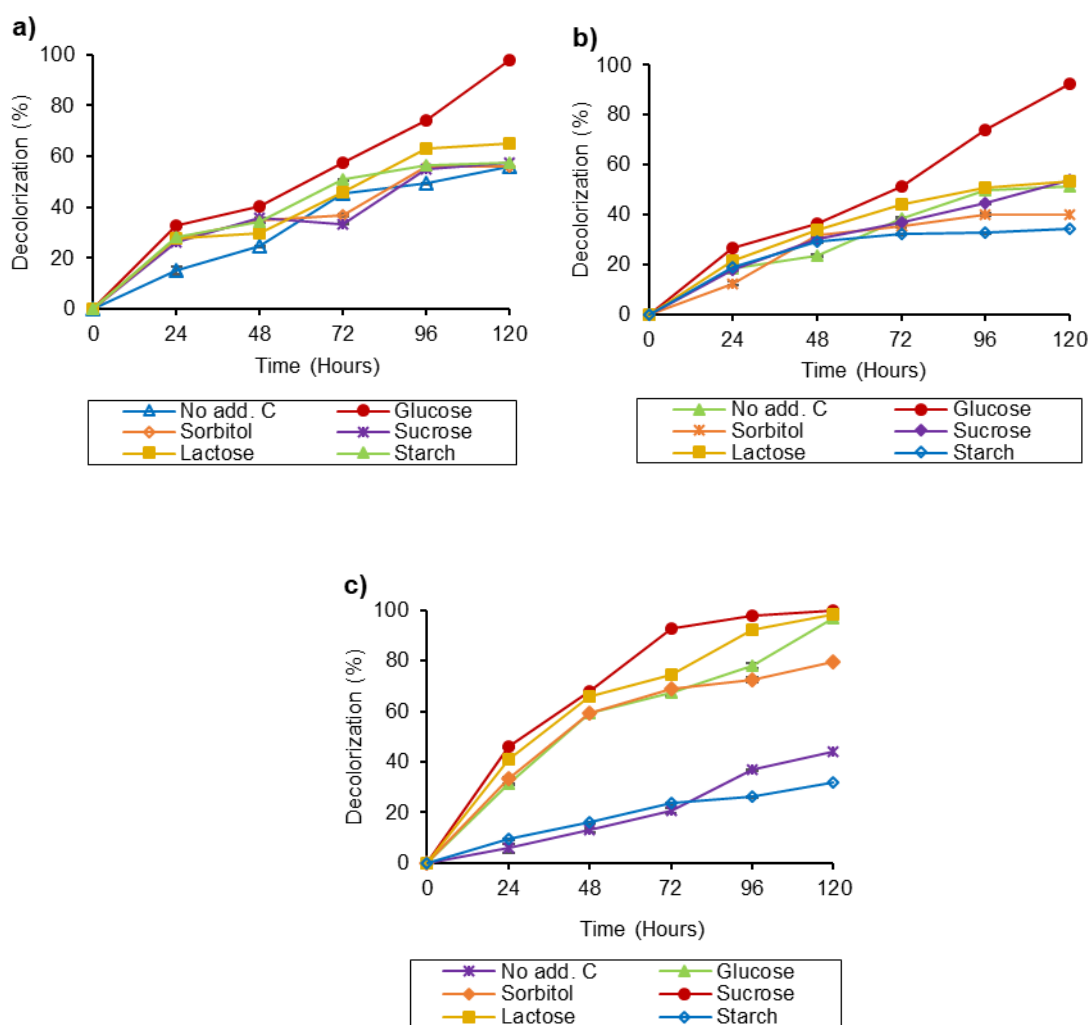


Fig. 5.2 Decolorization performance of (a) MBC (pH 7.0, 35°C); (b) AHBC (10% [w/v] NaCl, pH 10, 35°C); and (c) TBC (pH 7.0, 50°C) for the synthetic dye effluent, in the presence of different carbon sources (0.1% [w/v])

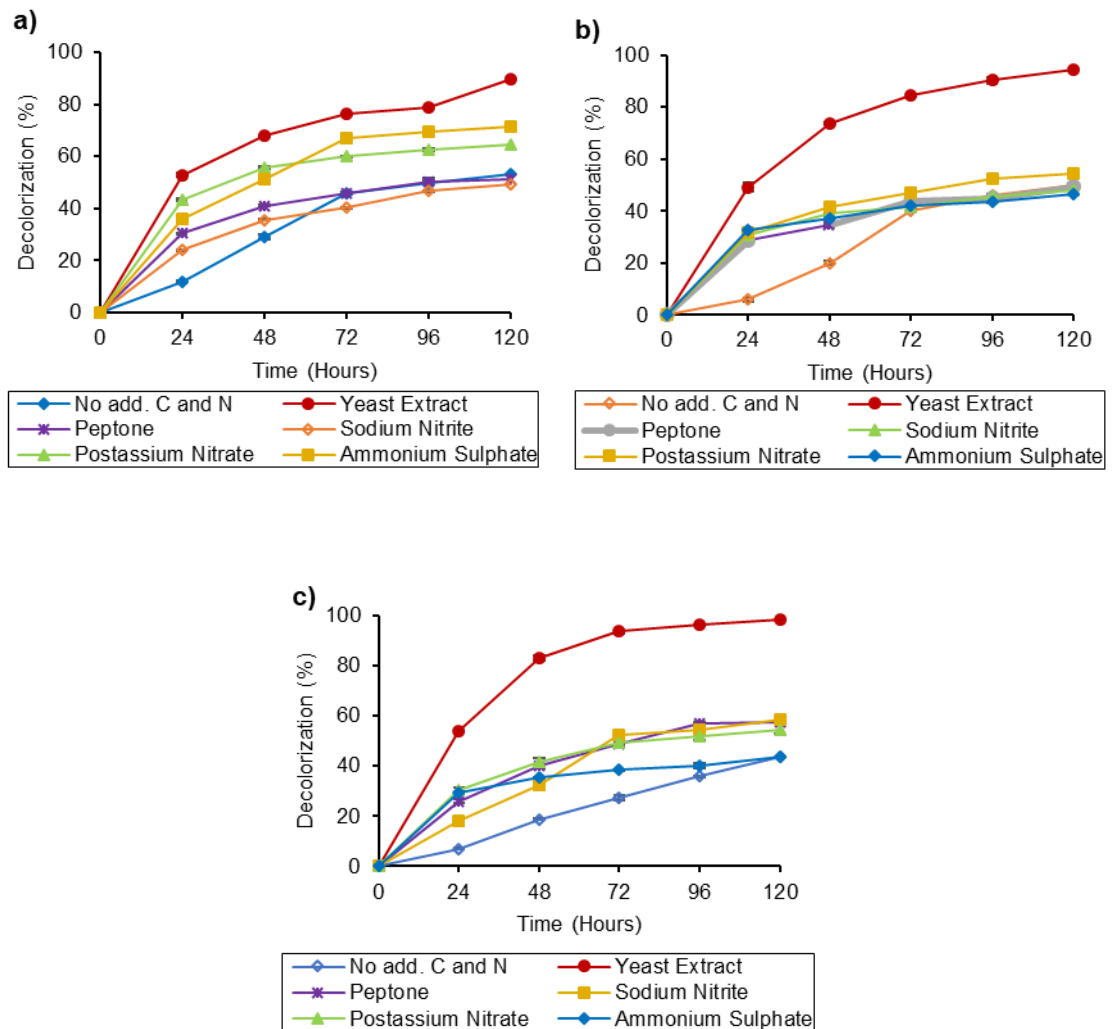


Fig. 5.3 Decolorization performance of (a) MBC (pH 7.0, 35°C); (b) AHBC (10% [w/v] NaCl, pH 10, 35°C); and (c) TBC (pH 7.0, 50°C) for the synthetic dye effluent, in the presence of different nitrogen sources (0.1% [w/v])

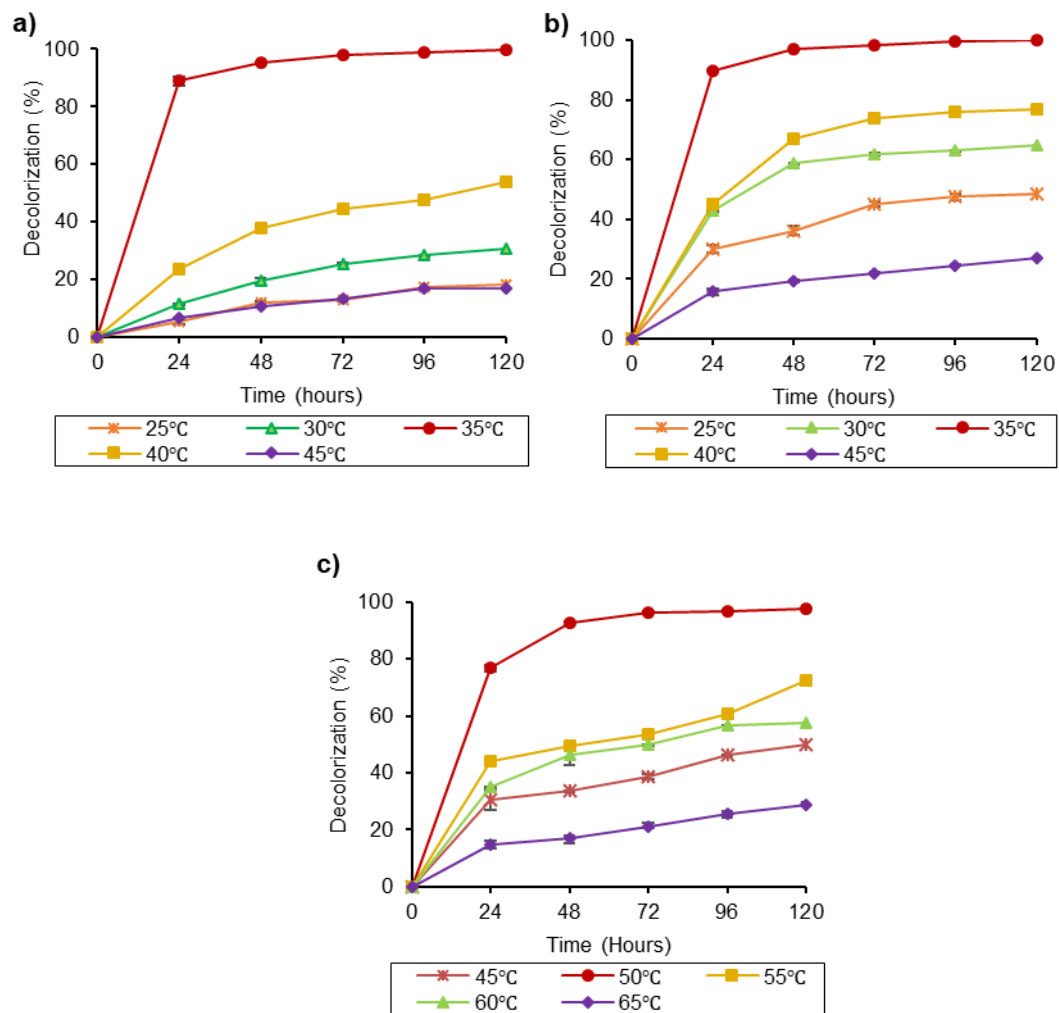


Fig. 5.4 Decolorization performance of (a) MBC (50 ppm, pH 7.0, glucose and yeast extract 0.1% [w/v] each); (b) AHBC (50 ppm dye mixture, 10% [w/v] NaCl, pH 10, glucose and yeast extract 0.1% [w/v] each); and (c) TBC (50 ppm, pH 7.0, sucrose and yeast extract 0.1% [w/v] each); for the synthetic dye effluent, at different temperatures

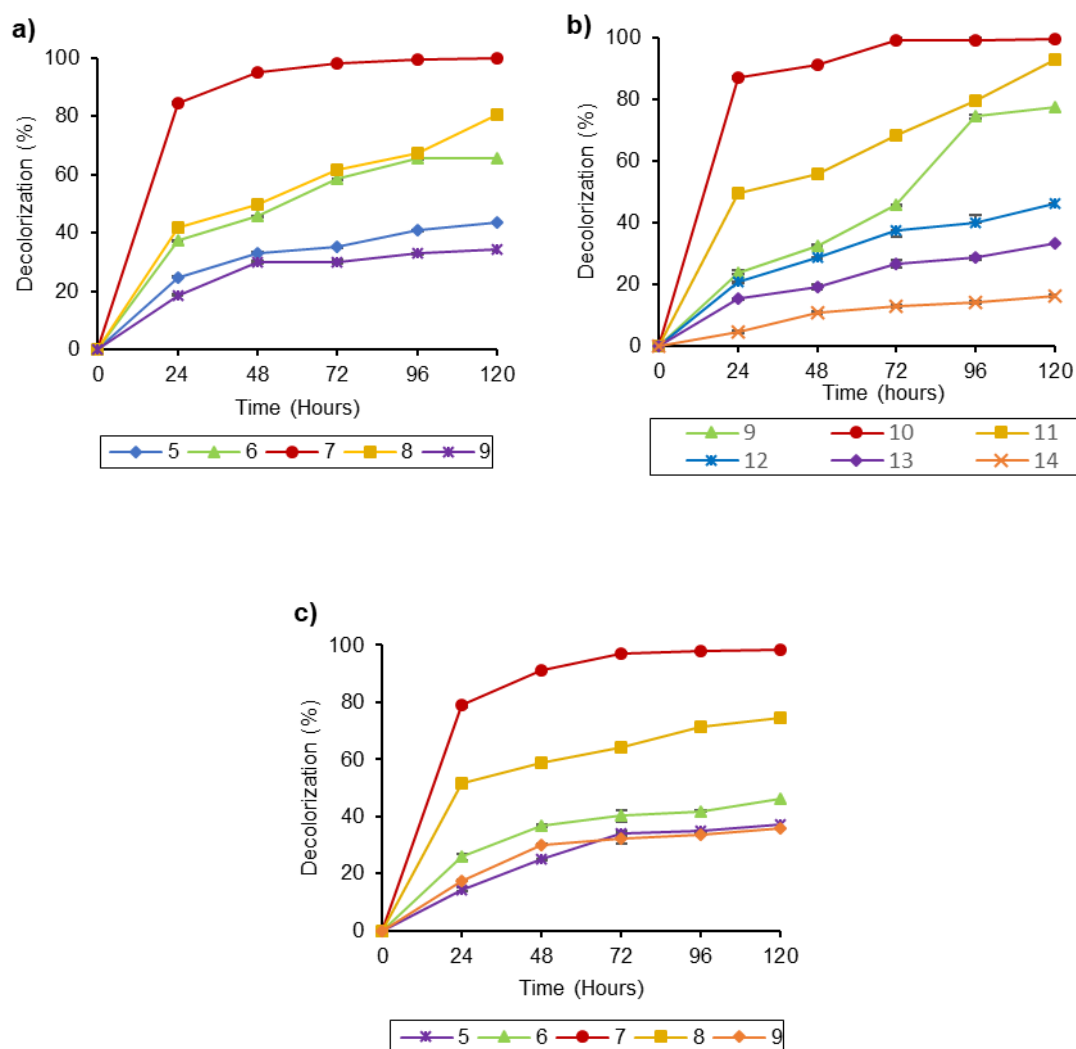


Fig. 5.5 Decolorization performance of (a) MBC (50 ppm, 35°C, glucose and yeast extract 0.1% [w/v] each); (b) AHBC (50 ppm, 35°C, 10% [w/v] NaCl, glucose and yeast extract 0.1% [w/v] each); and (c) TBC (50 ppm, 50°C, sucrose and yeast extract 0.1% [w/v] each); for the synthetic dye effluent, at different initial pH

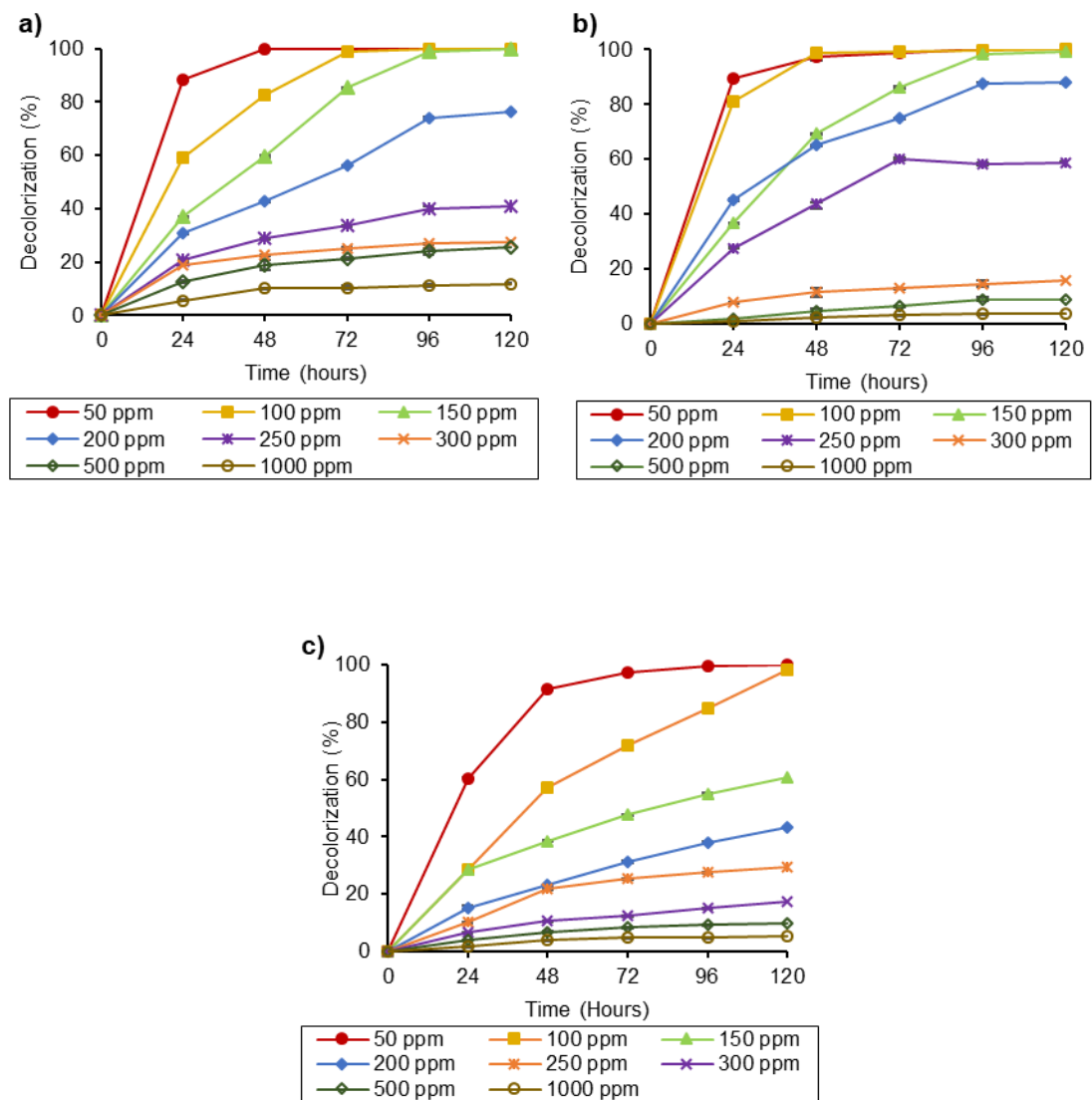


Fig. 5.6 Decolorization performance of (a) MBC (pH 7.0, 35°C, glucose and yeast extract 0.1% [w/v] each); (b) AHBC (pH 10, 35°C, 10% [w/v] NaCl, glucose and yeast extract 0.1% [w/v] each); and (c) TBC (pH 7.0, 50°C, sucrose and yeast extract 0.1% [w/v] each); for the synthetic dye effluent, at different initial dye concentrations (ppm)

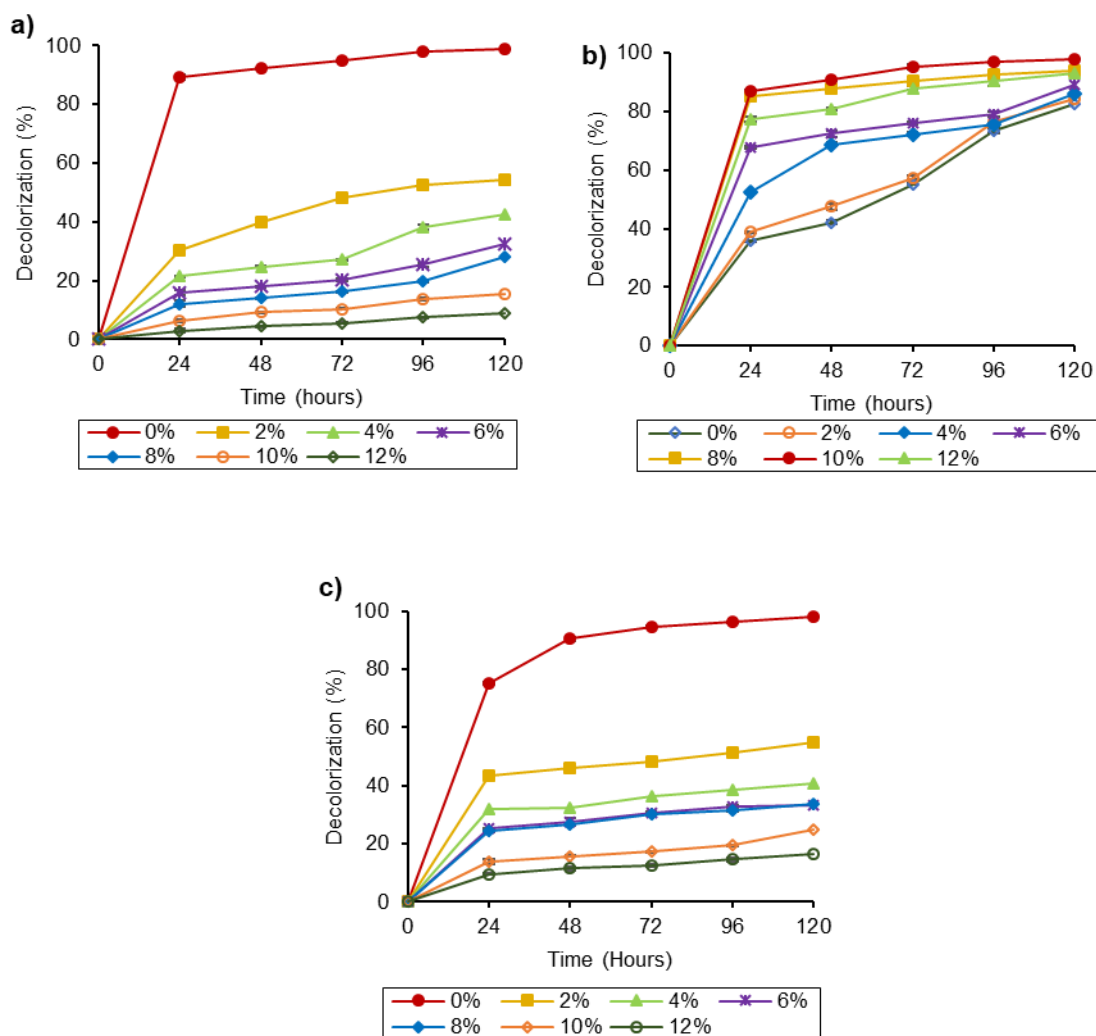


Fig. 5.7 Decolorization performance of (a) MBC (100 ppm, pH 7.0, 35°C, glucose and yeast extract 0.1% [w/v] each); (b) AHBC (100 ppm, pH 10, 35°C, glucose and yeast extract 0.1% [w/v] each); and (c) TBC (100 ppm, pH 7.0, 50°C, sucrose and yeast extract 0.1% [w/v] each); for the synthetic dye effluent, at different NaCl concentrations (% [w/v])

Table 5.5 Co-substrate utilization, pH, temperature, dye, and salt tolerance profiles of the natural bacterial consortia

Factor	Mesophilic bacterial consortium (MBC)	Alkaliphilic and halotolerant bacterial consortium (AHBC)	Thermophilic bacterial consortium (TBC)
Carbon sources			
(0.1% [w/v])			
No add. C	++	++	+
Glucose	++++	++++	++++
Sorbitol	++	+	+++
Sucrose	++	++	++++ ^b
Lactose	++	++	++++
Starch	++	+	+
Nitrogen Sources			
(0.1% [w/v])			
No add. C and N	++	++	+
Yeast extract	++++	++++	++++
Peptone	++	+	++
Sodium nitrite	+	+	++
Potassium nitrate	++	++	++
Ammonium sulfate	+++	+	+
Temperature (°C)			
25	–	+	nt
30	+	++	nt
35	++++ ^a	++++ ^a	nt
40	++	+++	nt
45	–	–/+	+
50	nt	nt	++++ ^a
55	nt	nt	+++
60	nt	nt	++
65	nt	nt	–/+
pH			
5	+	nt	+
6	++	nt	+
7	++++ ^a	nt	++++ ^a
8	+++	nt	+++
9	+	+++	+
10	nt	++++ ^a	nt
11	nt	++++	nt
12	nt	+	nt
13	nt	+	nt
14	nt	–	nt

Dye Concentration**(ppm)**

50	++++ ^a	++++ ^a	++++ ^a
100	++++ ^b	++++ ^a	++++
150	++++ ^b	++++ ^b	++
200	+++	+++	+
250	+	++	-/+
300	-/+	-	-
500	-/+	-	-
1000	-	-	-

NaCl concentration**(% [w/v])**

0	++++ ^a	+++	++++
2	++	+++	++
4	+	+++	+
6	+	+++	+
8	-/+	++++ ^b	+
10	-	++++ ^a	-/+
12	-	++++ ^b	-

++++ (90-99% color removal in 120 hours); +++ (70-89 color removal in 120 hours), ++ (50- 69% color removal in 120 hours); + (30-49% color removal in 120 hours); +/- (20-29 % color removal in 120 hours); - (less than 20% in 120 hours); ++++^a (85-95% color removal in 48 hours); ++++^b (85-95% color removal in 72 hours); nt (not tested)

5.3.2 Response Surface Methodology (RSM)

5.3.2.1 Statistical design and model

Decolorization efficiency of the natural bacterial consortia was further optimized by using statistical optimization procedure i.e., Response Surface Methodology through Box-Behnken design (BBD). The variable and levels were selected on the basis OFAT results. Triplicates experiments for the quadratic model were performed according to BBD layout, with 17 runs (for the mesophilic and thermophilic consortia) and 29 runs (for the alkaliphilic and halotolerant consortium), the center points for each were 5. Experiments were conducted for 72 (for MBC and AHHBC) and 120 hours (for TBC). The respective designs with the predicted and experimental response (decolorization %) values are given in Tables 5.6-5.8. Through regression analysis, the software calculated Y (the response) in terms of coded and actual factors. The equation with coded factors for the MBC is as follows:

$$Y = +98.62 + 7.12 \times A + 4.03 \times B - 6.43 \times C + 3.19 \times A \times B + 2.50 \times A \times C + 1.37 \times B \times C - 10.31 \times A^2 - 28.16 \times B^2 - 16.09 \times C^2 \quad \text{Eq (5.2)}$$

The equation with actual factors for the MBC is as follows:

$$\text{Decolorization (\%)} = -4145.22425 + 170.29250 \times \text{Temperature} + 339.76200 \times \text{pH} + 0.091340 \times \text{Dye Concentration} + 1.59375 \times \text{Temperature} \times \text{pH} + 0.025025 \times \text{Temperature} \times \text{Dye Concentration} + 0.027300 \times \text{pH} \times \text{Dye Concentration} - 2.57700 \times \text{Temperature}^2 - 28.16050 \times \text{pH}^2 - 6.43420\text{E-}003 \times \text{Dye Concentration}^2 \quad \text{Eq (5.3)}$$

The equation with coded factors for the AHBC is as follows:

$$Y = +98.62 + 3.14 \times A + 2.32 \times B - 3.42 \times C - 0.19 \times D + 0.17 \times A \times B + 1.14 \times A \times C - 1.30 \times A \times D - 0.53 \times B \times C + 0.75 \times B \times D - 0.80 \times C \times D - 13.15 \times A^2 - 10.37 \times B^2 - 6.37 \times C^2 - 6.65 \times D^2 \quad \text{Eq (5.4)}$$

The equation with actual factors for the AHBC is as follows:

$$\text{Decolorization (\%)} = -8328.08588 + 232.04208 \times \text{Temperature} + 822.68833 \times \text{pH} + 0.33164 \times \text{Dye Concentration} + 37.83667 \times \text{Salt Concentration} + 0.17500 \times$$

$$\begin{aligned} & \text{Temperature} \times \text{pH} + 0.011450 \times \text{Temperature} \times \text{Dye Concentration} - 0.32500 \times \\ & \text{Temperature} \times \text{Salt Concentration} - 0.021200 \times \text{pH} \times \text{Dye Concentration} + 0.75000 \times \\ & \text{pH} \times \text{Salt Concentration} - 7.95000\text{E-}003 \times \text{Dye Concentration} \times \text{Salt Concentration} - \\ & 3.28738 \times \text{Temperature}^2 - 41.47800 \times \text{pH}^2 - 2.54680\text{E-}003 \times \text{Dye Concentration}^2 \\ & -1.66300 \times \text{Salt Concentration}^2 \end{aligned} \quad \text{Eq (5.5)}$$

The equation with coded factors for the TBC is as follows:

$$Y = +99.01 + 3.46 \times A + 10.51 \times B - 7.89 \times C + 4.00 \times A \times B - 7.13 \times A \times C - 3.51 \times B \times C - 14.82 \times A^2 - 26.97 \times B^2 - 15.97 \times C^2 \quad \text{Eq (5.6)}$$

The equation with actual factors for the TBC is as follows:

$$\begin{aligned} \text{Decolorization (\%)} = & -10400.53800 + 365.41375 \times \text{Temperature} + 295.19950 \times \text{pH} + \\ & 5.17794 \times \text{Dye Concentration} + 1.99875 \times \text{Temperature} \times \text{pH} - 0.071325 \times \\ & \text{Temperature} \times \text{Dye Concentration} - 0.070250 \times \text{pH} \times \text{Dye Concentration} - 3.70544 \times \\ & \text{Temperature}^2 - 26.97175 \times \text{pH}^2 - 6.38870\text{E-}003 \times \text{Dye Concentration}^2 \end{aligned} \quad \text{Eq (5.7)}$$

Table 5.6 Box-Behnken design layout with observed and actual response values for MBC

Runs	Factor A (Temperature, °C)	Factor B (pH)	Factor C (Dye concentration, ppm)	Actual values decolorization (Y, %)	Predicted values for decolorization (Y1, %)	Externally studentized residuals
1	33	6	100	51.43	52.19	-2.506
2	37	6	100	59.54	60.06	-1.370
3	33	8	100	54.38	53.86	1.370
4	37	8	100	75.24	74.48	2.506
5	33	7	50	74.21	74.03	0.426
6	37	7	50	83.21	83.27	-0.136
7	33	7	150	56.23	56.17	0.136
8	37	7	150	75.24	75.42	-0.426
9	35	6	50	58.71	58.14	1.587
10	35	8	50	62.76	63.46	-2.149
11	35	6	150	43.25	42.55	2.149
12	35	8	150	52.76	53.34	-1.587
13	35	7	100	99.44	98.62	1.185
14	35	7	100	98.83	98.62	0.279
15	35	7	100	98.31	98.62	-0.402
16	35	7	100	98.29	98.62	-0.429
17	35	7	100	98.21	98.62	-0.538

Table 5.7 Box-Behnken design layout with observed and actual response values for AHBC

Runs	Factor A (Temperature, °C)	Factor B (pH)	Factor C (Dye concentration, ppm)	Factor D (Salt concentration, % [w/v])	Actual values decolorization (Y, %)	Predicted values for decolorization (Y1, %)	Externally studentized residuals
1	33	9.5	100	10	69.87	69.82	0.179
2	37	9.5	100	10	75.91	75.75	0.580
3	33	10.5	100	10	73.86	74.10	-0.936
4	37	10.5	100	10	80.60	80.74	-0.517
5	35	10	50	8	88.04	88.42	-1.525
6	35	10	150	8	83.26	83.16	0.359
7	35	10	50	12	89.45	89.64	-0.703
8	35	10	150	12	81.49	81.20	1.123
9	33	10	100	8	74.28	74.57	-1.112
10	37	10	100	8	83.18	83.45	-1.042
11	33	10	100	12	76.88	76.79	0.319
12	37	10	100	12	81.49	80.48	0.381
13	35	9.5	50	10	82.32	82.46	-0.539
14	35	10.5	50	10	88.48	88.16	1.263
15	35	9.5	150	10	76.17	76.68	-2.197
16	35	10.5	150	10	80.21	80.25	-0.151
17	33	10	50	10	80.79	80.53	0.980
18	37	10	50	10	84.66	84.53	0.494
19	33	10	150	10	71.54	71.40	0.533

20	37	10	150	10	79.99	79.97	0.071
21	35	9.5	100	8	80.73	80.22	2.197
22	35	10.5	100	8	83.69	83.36	1.315
23	35	9.5	100	12	78.29	78.35	-0.219
24	35	10.5	100	12	84.25	84.48	-0.885
25	35	10	100	10	98.12	98.62	-1.449
26	35	10	100	10	98.73	98.62	0.284
27	35	10	100	10	99.32	98.62	2.166
28	35	10	100	10	98.37	98.62	-0.690
29	35	10	100	10	98.58	98.62	-0.117

Table 5.8 Box-Behnken design layout with observed and actual response values for TBC

Runs	Factor A (Temperature, °C)	Factor B (pH)	Factor C (Dye concentration, ppm)	Actual values decolorization (Y, %)	Predicted values for decolorization (Y1, %)	Externally studentized residuals
1	48	6	100	47.21	47.25	-0.076
2	52	6	100	45.28	46.17	-3.100
3	48	8	100	61.15	60.27	3.100
4	52	8	100	75.21	75.17	0.076
5	48	7	50	65.21	65.51	-0.682
6	52	7	50	87.24	86.69	1.360
7	48	7	150	63.45	64.00	-1.360
8	52	7	150	56.95	56.65	0.682
9	50	6	50	50.27	49.93	0.768
10	50	8	50	77.39	77.97	-1.477
11	50	6	150	41.76	41.18	1.477
12	50	8	150	54.83	55.17	-0.768
13	50	7	100	99.68	99.01	0.868
14	50	7	100	98.56	99.01	-0.555
15	50	7	100	98.99	99.01	-0.019
16	50	7	100	98.14	99.01	-1.164
17	50	7	100	99.66	99.01	0.839

The statistical evaluation of the models through F test and ANOVA (Tables 5.9-5.11) showed that all the three models for MBC, AHBC, and TBC consortia were highly significant as indicated by the low probability values of the Fisher's F test ($[P_{\text{model}} > F] = 0.0001$). Moreover, the non-significant values of the lack-of-fit test i.e., $F = 4.14$ with $p = 0.10$, $F = 0.71880$ with $p = 0.69$, and $F = 2.37$ with $p = 0.2113$ for MBC, AHBC, and TBC, respectively, further demonstrate the adequacy of model designs for the selected response for each type of consortium. Furthermore, the models' goodness was assessed through determination and multiple correlation coefficients R^2 and R . The predicted R^2 values for all the three models were in reasonable agreement with the adjusted R^2 values ([MBC: Adj. $R^2 = 0.9984$ and Pred. $R^2 = 0.991$]; [AHBC: Adj. $R^2 = 0.9977$; Pred. $R^2 = 0.9951$]; and [TBC: Adj. $R^2 = 0.9984$; Pred. $R^2 = 0.9926$]). Signal to noise ratio was determined through adeq. Precision. The ratios for MBC, AHBC, and TBC models were 91.441, 99.179, and 88.430, respectively, which indicate adequate signal (a value greater than 4 is considered as a desirable signal). Normal probability plots of the internally studentized residuals showed a straight line (Fig. 5.8) and the values of externally studentized residuals were in range $[-3$ to $+3$ (Bhattacharya and Banerjee 2008)] (Tables 5.5-5.7) with no outliers for the three models. Box-Cox plots for the three models showed that no transformation was required as the current λ values were close to that of model design values for all the three models (Fig. 5.9).

Table 5.9 ANOVA for Quadratic Model of synthetic dye wastewater decolorization by MBC

Source	Sum of Squares	df	Mean Square	F Value	p-value	Prob > F
Model	6271.358	9	696.8176	1090.422	< 0.0001	significant
A-Temperature	405.8401	1	405.8401	635.0827	< 0.0001	
B-pH	129.6855	1	129.6855	202.9396	< 0.0001	
C-Dye Concentration	330.3735	1	330.3735	516.9881	< 0.0001	
AB	40.64062	1	40.64062	63.59687	< 0.0001	
AC	25.05003	1	25.05003	39.19977	0.0004	
BC	7.4529	1	7.4529	11.66274	0.0112	
A ²	447.3889	1	447.3889	700.1008	< 0.0001	
B ²	3339.005	1	3339.005	5225.074	< 0.0001	
C ²	1089.446	1	1089.446	1704.829	< 0.0001	
Residual	4.473245	7	0.639035			
Lack of Fit	3.383725	3	1.127908	4.140937	0.1017	not significant
Pure Error	1.08952	4	0.27238			
Cor Total	6275.832	16				

df = degree of freedom; Std. Dev. = 0.80; Mean = 72.94; C.V. = 1.10; PRESS = 55.84; R² = 0.9993; Adj. R² = 0.9984; Pred. R² = 0.991; Adeq. Precision = 91.441

Table 5.10 ANOVA for Quadratic Model of synthetic dye wastewater decolorization by AHBC

Source	Sum of Squares	df	Mean Square	F Value	p-value	Prob > F
Model	1974.72	14	141.0515	865.0861	< 0.0001	significant
A-Temperature	118.4408	1	118.4408	726.4123	< 0.0001	
B-pH	64.40333	1	64.40333	394.9936	< 0.0001	
C-Dye Concentration	140.6305	1	140.6305	862.5045	< 0.0001	
D-Salt Concentration	0.418133	1	0.418133	2.564464	0.1316	
AB	0.1225	1	0.1225	0.751308	0.4007	
AC	5.2441	1	5.2441	32.16271	< 0.0001	
AD	6.76	1	6.76	41.45992	< 0.0001	
BC	1.1236	1	1.1236	6.891178	0.0200	

BD	2.25	1	2.25	13.79953	0.0023	
CD	2.5281	1	2.5281	15.50515	0.0015	
A ²	1121.574	1	1121.574	6878.753	< 0.0001	
B ²	697.4694	1	697.4694	4277.666	< 0.0001	
C ²	262.9537	1	262.9537	1612.727	< 0.0001	
D ²	287.0212	1	287.0212	1760.337	< 0.0001	
Residual	2.282687	14	0.163049			
Lack of Fit	1.466567	10	0.146657	0.7188	0.6949	not significant
Pure Error	0.81612	4	0.20403			
Cor Total	1977.003	28				

df = degree of freedom; Std. Dev. = 0.40; Mean = 83.50; C.V. = 0.48; PRESS = 9.72; R² = 0.9988; Adj. R² = 0.9977; Pred. R² = 0.9951; Adeq. Precision = 99.179

Table 5.11 ANOVA for Quadratic Model of synthetic dye wastewater decolorization by TBC

Source	Sum of Squares	<i>df</i>	Mean Square	<i>F</i> Value	<i>p</i> -value Prob > <i>F</i>	
Model	7387.833	9	820.8703	1129.127	< 0.0001	significant
A-Temperature	95.63445	1	95.63445	131.5475	< 0.0001	
B-pH	883.2605	1	883.2605	1214.946	< 0.0001	
C-Dye Concentration	498.0168	1	498.0168	685.034	< 0.0001	
AB	63.92003	1	63.92003	87.92352	< 0.0001	
AC	203.4902	1	203.4902	279.9057	< 0.0001	
BC	49.35063	1	49.35063	67.88297	< 0.0001	
A ²	924.9864	1	924.9864	1272.341	< 0.0001	
B ²	3063.054	1	3063.054	4213.304	< 0.0001	
C ²	1074.092	1	1074.092	1477.439	< 0.0001	
Residual	5.08897	7	0.726996			
Lack of Fit	3.25785	3	1.08595	2.372209	0.2113	not significant
Pure Error	1.83112	4	0.45778			
Cor Total	7392.922	16				

df = degree of freedom; Std. Dev = 0.85; Mean = 71.82; C.V. = 1.19; PRESS = 54.99; R² = 0.9993; Adj. R² = 0.9984; Pred. R² = 0.9926; Adeq. Precision = 88.430

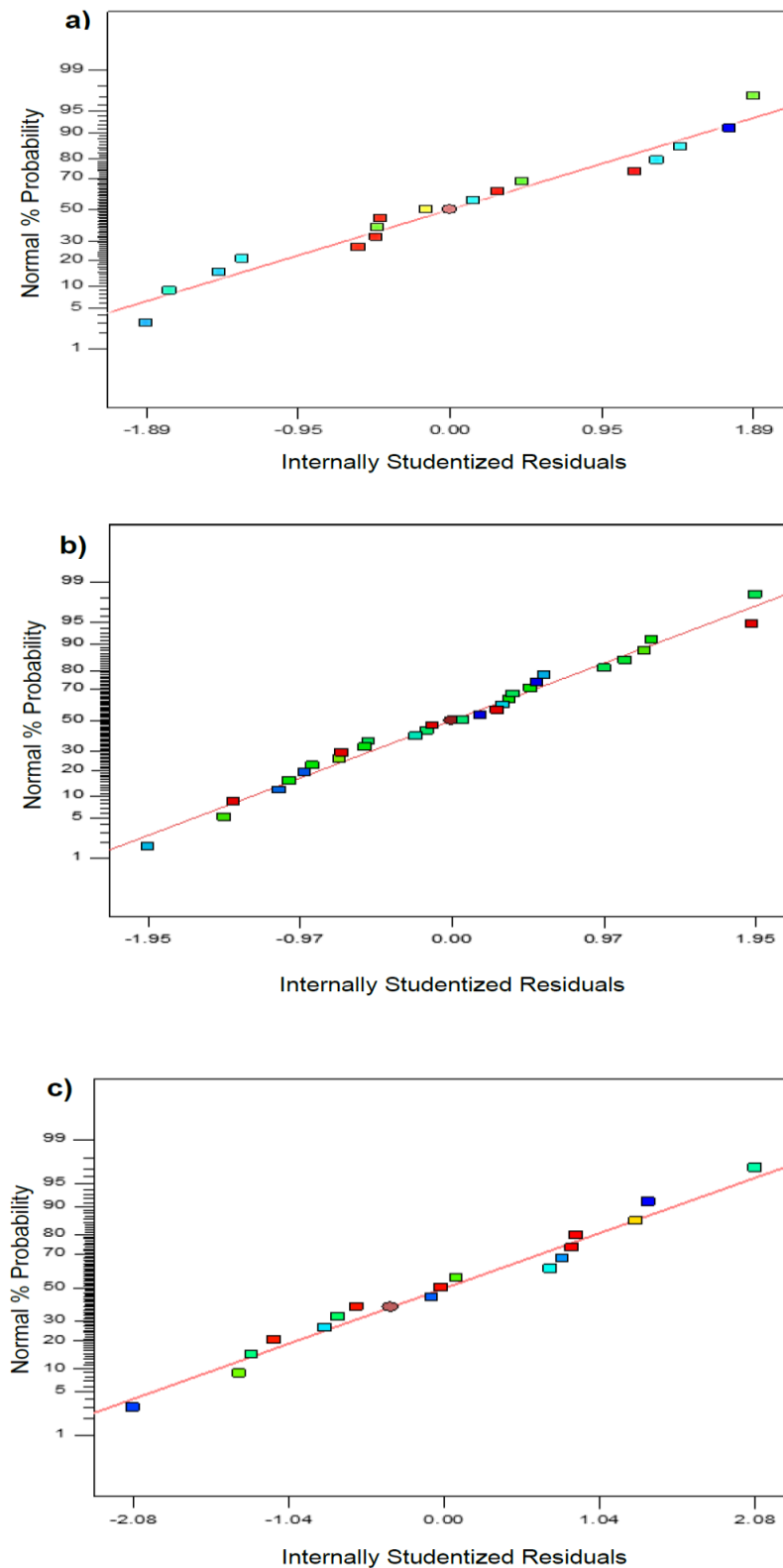


Fig. 5.8 The normal % probability vs. studentized residuals plots for (a) MBC, (b) AHBC, and (c) TBC

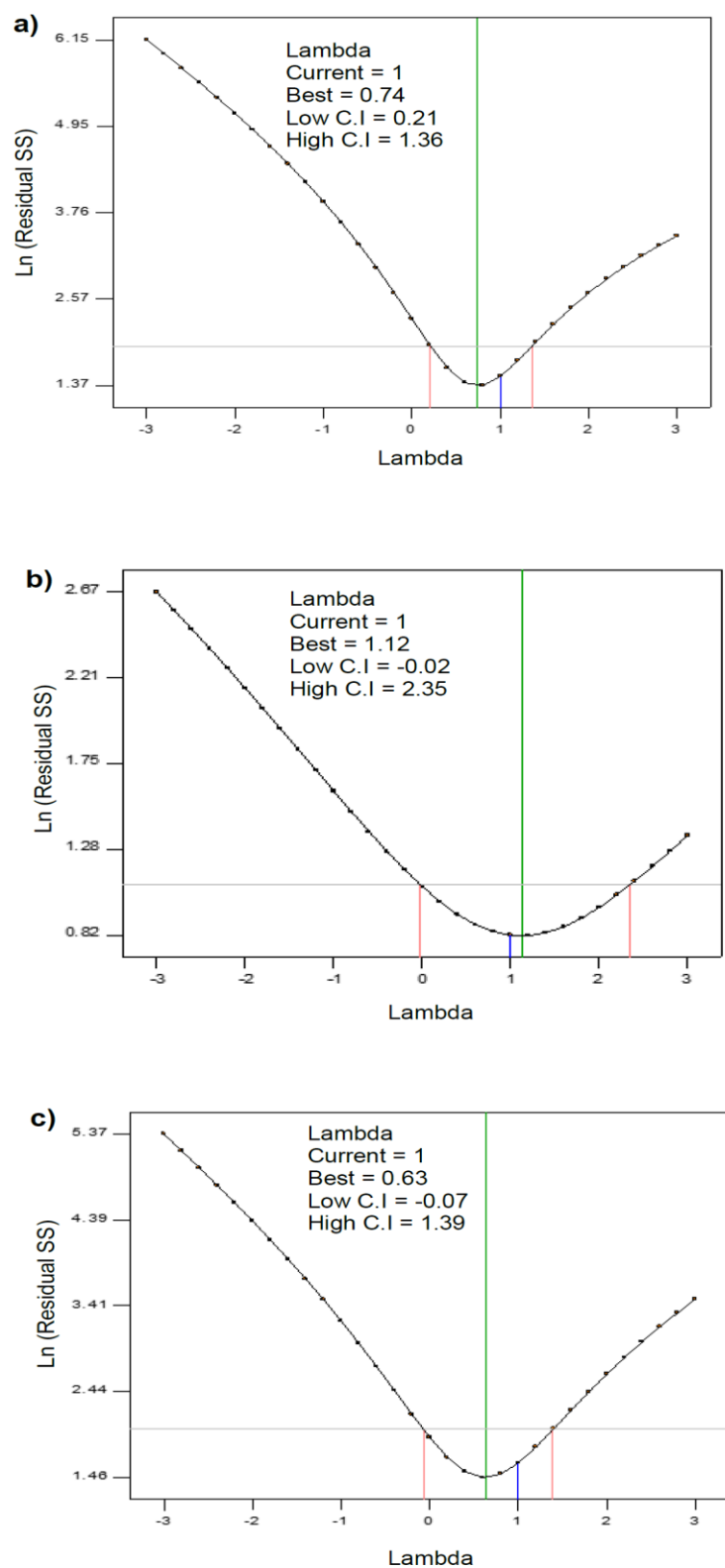


Fig. 5.9 Box-Cox plots of model transformation for the decolorization of synthetic dye wastewater by (a) MBC, (b) AHBC, and (c) TBC

5.3.2.2 Analysis of the factors affecting the decolorization process by the natural consortia

The 2D contour and 3D response surface plots help in understanding the interrelation of individual factors in a process. In the case of MBC, Fig. 5.10a and b, show the contour and 3D surface plots, respectively, for pH and temperature (with the dye concentration kept at constant). The decolorization percentage increased from about 60 to 99% as the pH and temperature raised from 6.0-7.0 and 33-35 °C. Further increase in pH, however resulted in a decline in decolorization percentage, while further rise in temperature seemed to have less pronounced effect than the pH. The contour plot for pH and temperature in this case is elliptical indicating a significant interaction between the two variables. The interaction between dye concentration and temperature (with the pH kept at constant) is shown in Fig. 5.11a and b. Increase in dye concentration past 100 ppm had a negative effect on the decolorization percentage (about 30 percent decrease observed). As observed previously, rise temperature in temperature beyond 35 °C did not produce major effect on the color removal percentage. The shape of that plot was elliptical indicating a significant interaction of the studied variables. The interaction between the dye concentration and pH is shown in Fig. 5.12a and b. In this case effect of pH was somewhat more evident as color removal percentage diminished upon decrease and increase in pH and was found to be more centralized near the neutral value. Moreover, dye concentrations up to 100 ppm as positive impact on decolorization percentage. The shape of the plot was slightly elliptical in that case.

For AHBC, the interaction between pH and temperature (keeping the dye and salt concentration constant) is shown in Fig. 5.13a and b. The decolorization percentage increased about 74 to 99% when the pH and temperature values raised from 9.5-10.00 and 33-35 °C. Maximum decolorization was observed around pH 10.0 and 35 °C. In that case, pH and temperature showed a similar effect, as indicated by the circular plot shape. The contour and 3D plots for the interaction of dye concentration and temperature (pH and salt concentration) are given in Fig. 5.14a and b. The temperature had a most noticeable effect than dye concentration on the decolorization of synthetic dye wastewater and highest removal was observed around 35 °C. In case of dye concentration, 50-100 ppm seemed to be the more suitable concentrations. The shape of this plot was also elliptical. Fig. 5.15a and b show the interaction between salt concentration and temperature (pH and dye concentration constant). The shape of the

that plot was also elliptical and the influence of temperature was more evident than the salt concentration with the maximum decolorization around 35 °C over a range of salt concentration 9-11%. The interactive effects between dye concentration and pH (temperature and salt concentration constant) are shown in Fig. 5.16a and b. In that case the response was more centralized around pH as compared to the dye concentration with the maximum (up to 99%) decolorization observed around pH 10.00, over a range of dye concentration i.e. 50-100 ppm. The plots shape was elliptical in that case. Fig. 5.17a and b show the effect of salt concentration and pH, and as observed earlier i.e. pH acting as a more influencing factor with the highest color removal observed around pH 10.00 over a range of salt concentration (9-11%). In the case of dye and salt concentration (pH and temperature constant), the two factors seemed to have negligible interaction as indicated by the circular shape of the plot (Fig. 5.18a and b).

For TBC, the contour and 3D surface plots showing the interaction between pH and temperature are given in Fig. 5.19a and b. The response in that case is more centralized around pH as compared to the temperature, with the maximum decolorization (up to 99%) observed around pH 7 and 50 °C temperature. The shape of the plot was elliptical. Fig. 5.20a and b show the interaction between the dye concentration and temperature. The elliptical plot shows that the dye concentration had a stronger influence on the decolorization efficiency of thermophilic bacterial consortium with the maximum removal observed around 50 °C temperature and a dye concentration of 100 ppm. The interaction between dye concentration and pH indicated a more pronounced influence of pH as compared to the dye concentration evident from the elliptical shape of the plot (Fig. 5.21a and b).

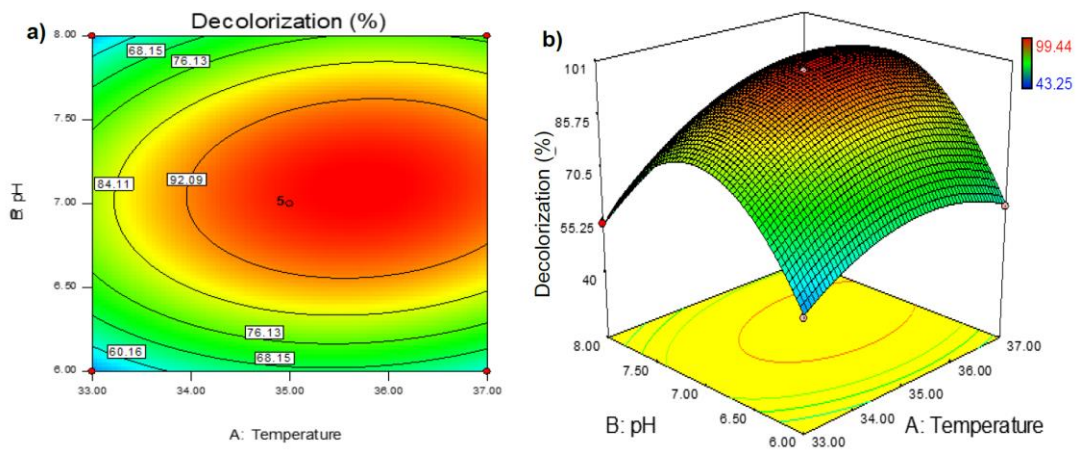


Fig. 5.10 Response surface plots showing interactions of pH and temperature for the synthetic dye wastewater decolorization by MBC (a) contour plot and (b) 3D surface plot

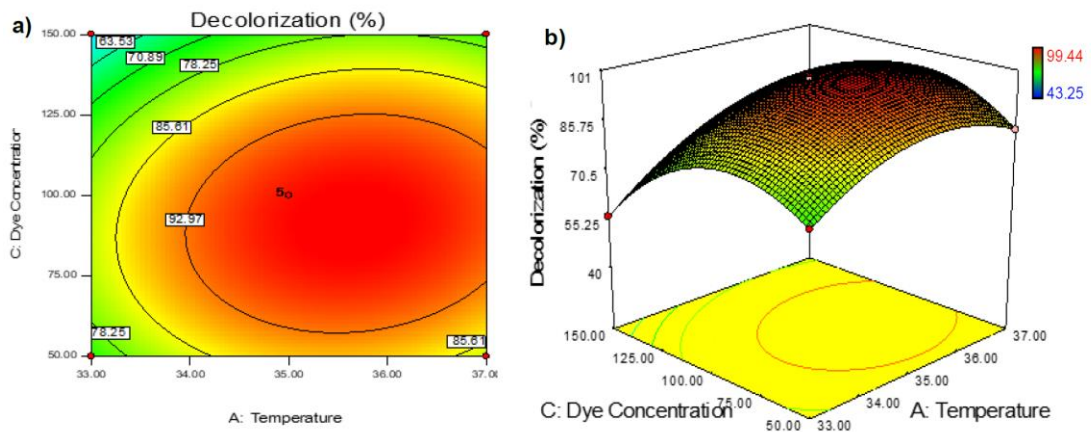


Fig. 5.11 Response surface plots showing interactions of dye concentration and temperature for the synthetic dye wastewater decolorization by MBC (a) contour plot and (b) 3D surface plot

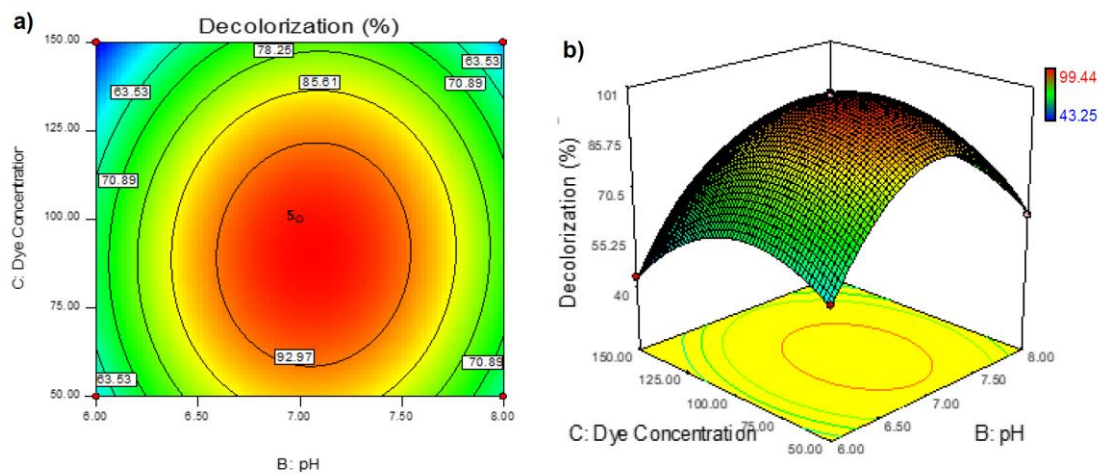


Fig. 5.12 Response surface plots showing interactions of dye concentration and pH for the synthetic dye wastewater decolorization by MBC (a) contour plot and (b) 3D surface plot

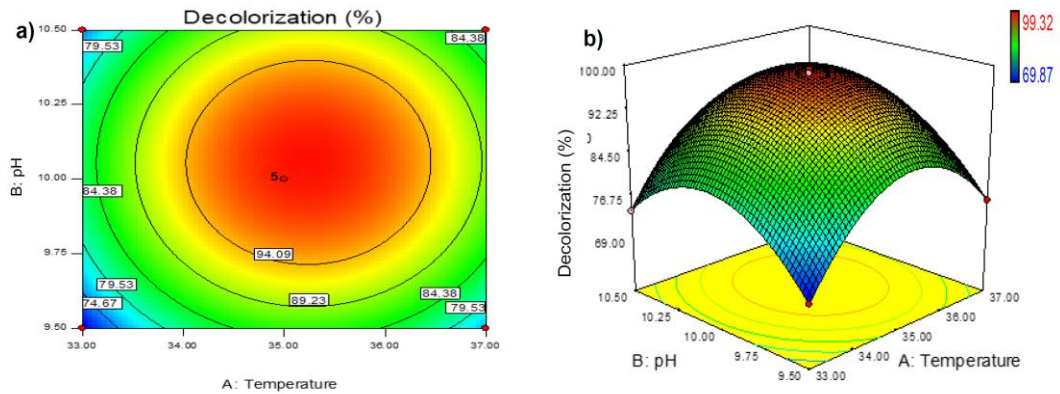


Fig. 5.13 Response surface plots showing interactions of pH and temperature for the synthetic dye wastewater decolorization by AHBC (a) contour plot and (b) 3D surface plot

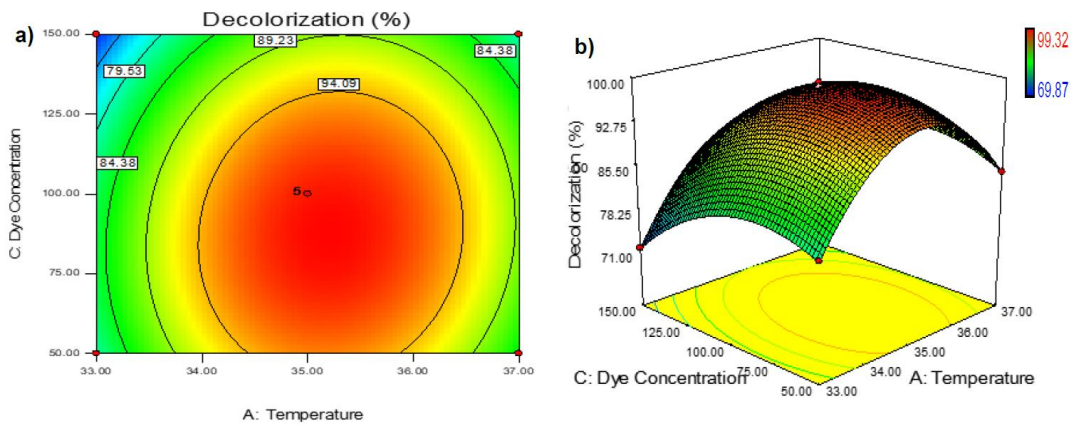


Fig. 5.14 Response surface plots showing interactions of dye concentration and temperature for the synthetic dye wastewater decolorization by AHBC (a) contour plot and (b) 3D surface plot

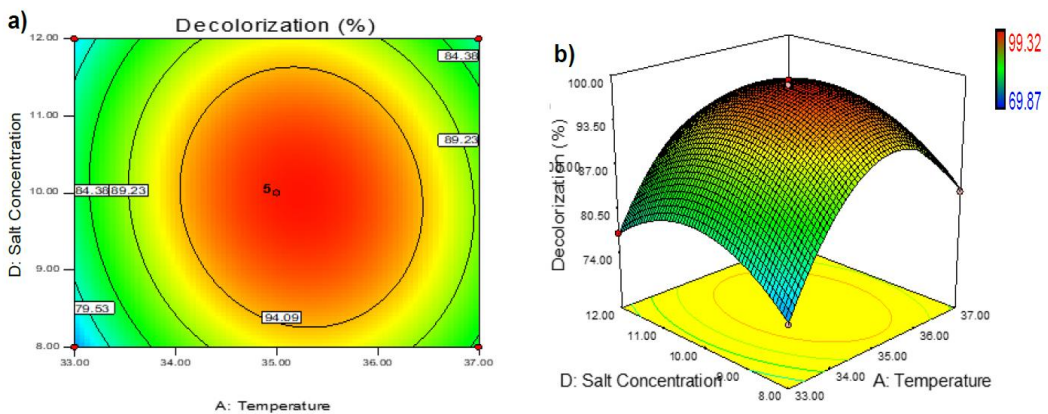


Fig. 5.15 Response surface plots showing interactions of salt concentration and temperature for the synthetic dye wastewater decolorization by AHBC (a) contour plot and (b) 3D surface plot

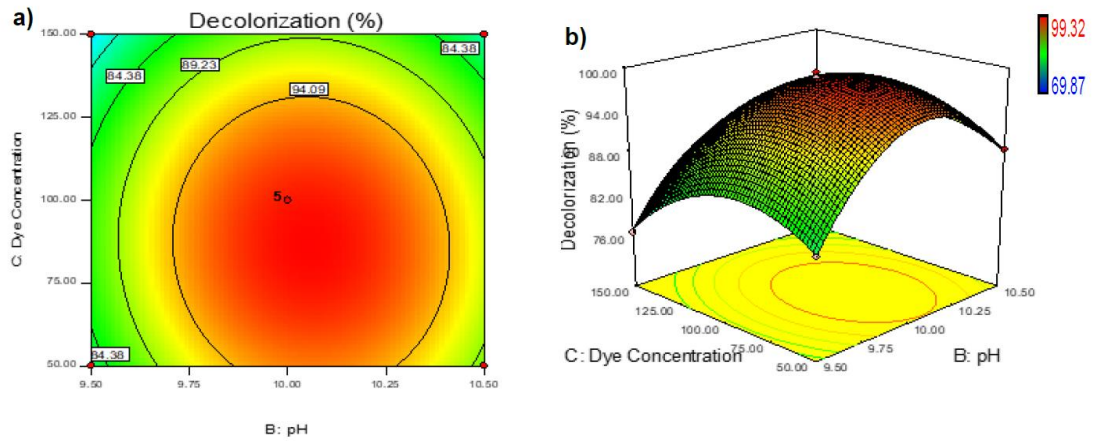


Fig. 5.16 Response surface plots showing interactions of dye concentration and pH for the synthetic dye wastewater decolorization by AHBC (a) contour plot and (b) 3D surface plot

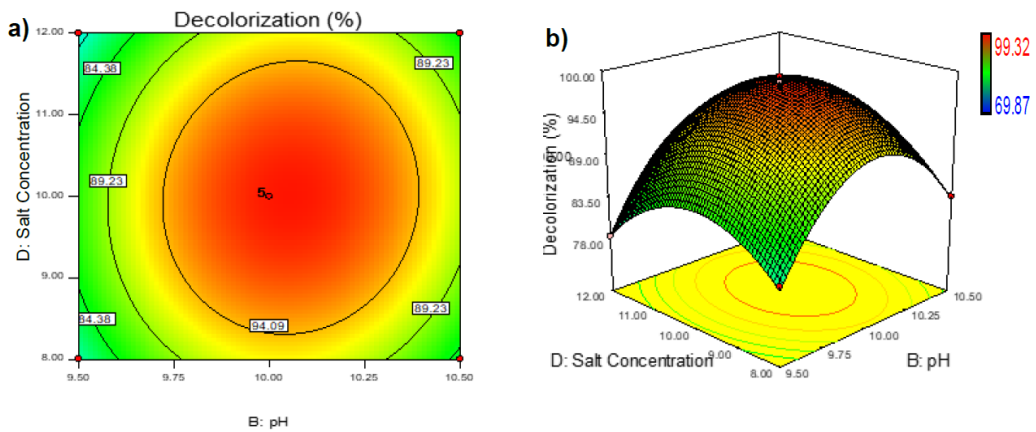


Fig. 5.17 Response surface plots showing interactions of salt concentration and pH for the synthetic dye wastewater decolorization by AHBC (a) contour plot and (b) 3D surface plot

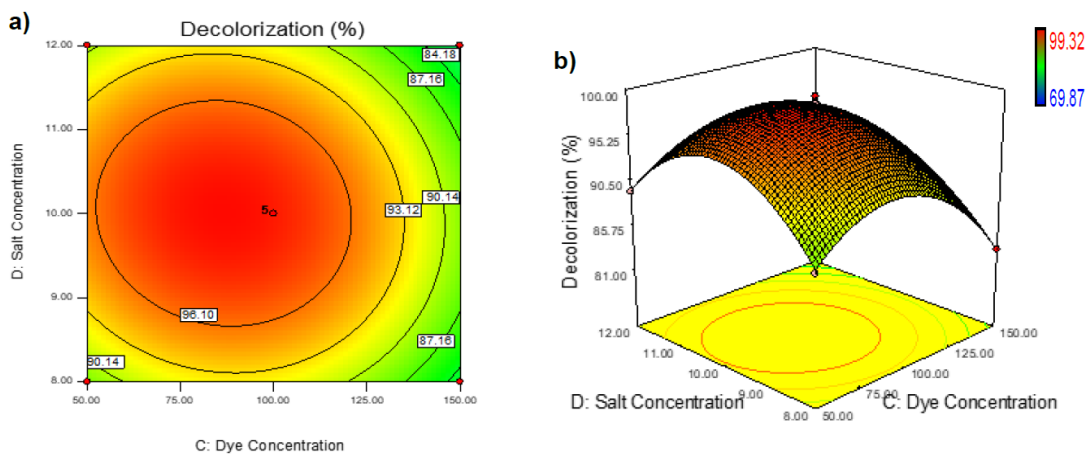


Fig. 5.18 Response surface plots showing interactions of salt concentration and dye concentration for the synthetic dye wastewater decolorization by AHBC (a) contour plot and (b) 3D surface plot

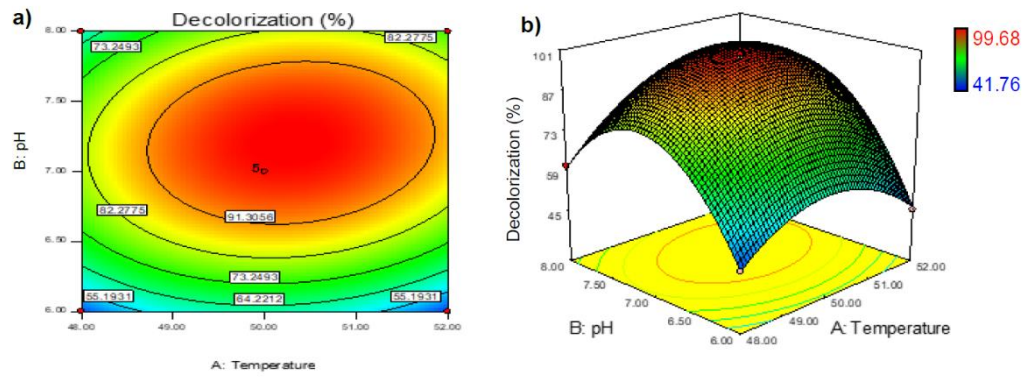


Fig. 5.19 Response surface plots showing interactions of pH and temperature for the synthetic dye wastewater decolorization by TBC (a) contour plot and (b) 3D surface plot

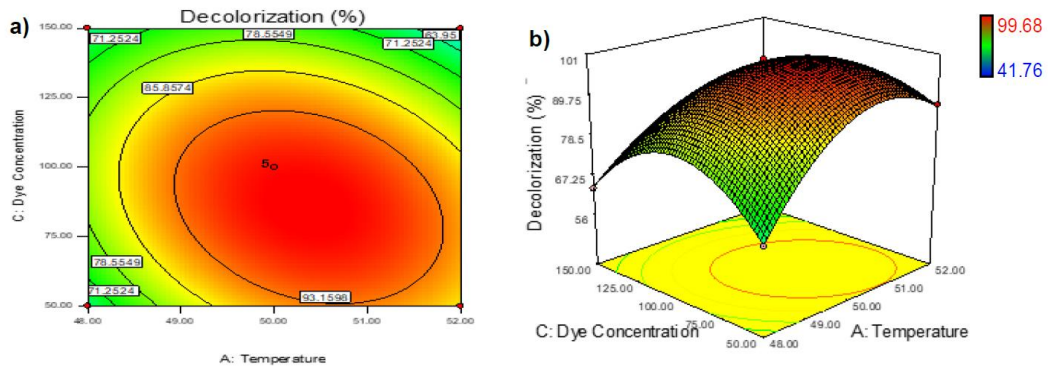


Fig. 5.20 Response surface plots showing interactions of dye concentration and temperature for the synthetic dye wastewater decolorization by TBC (a) contour plot and (b) 3D surface plot

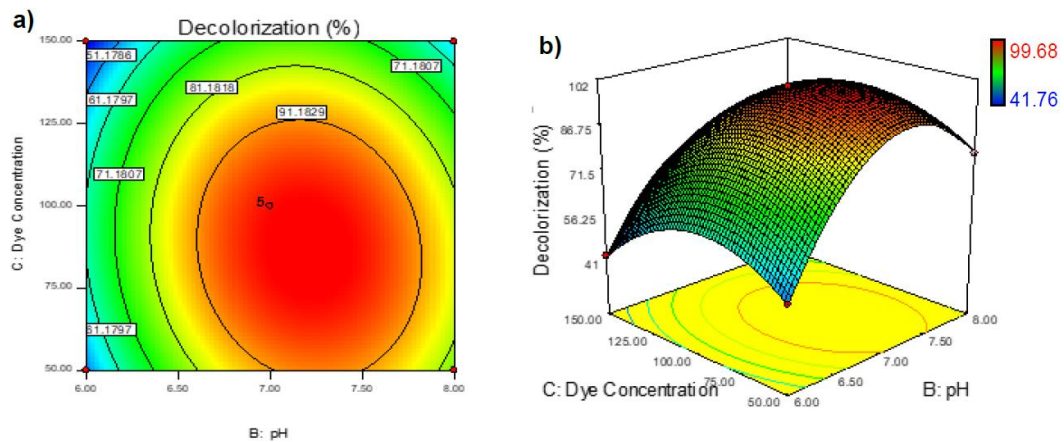


Fig. 5.21 Response surface plots showing interactions of dye concentration and pH for the synthetic dye wastewater decolorization by TBC (a) contour plot and (b) 3D surface plot

5.3.2.3 Model validation for the natural bacterial consortia

The optimum combinations of the factors affecting color removal by the natural consortia were further validated. Confirmatory experiments were performed using the selected combinations suggested by the software. The results were in accordance with the predicted values which indicate the adequacy of the three models. The selected combinations for the validation experiments are given in Tables 5.12a-c. The optimum combinations, giving highest color removal for each consortium are highlighted.

Table 5.12a Predicted solutions for model validation and confirmation for MBC

Solution	Temperature (°C)	pH	Dye concentration (ppm)	Predicted response (%)	Observed response (%)
1	34.67	6.96	75.48	96.52856	95.19
2	34.75	6.96	82.59	97.78216	98.14
3	35.51	6.89	103.54	98.38608	99.03
4	36.41	6.94	106.69	97.12115	93.22
5	35.51	7.35	112.19	95.7344	93.17

Table 5.12b Predicted solutions for model validation and confirmation for AHBC

Solution	Temperature (°C)	pH	Dye concentration (ppm)	Salt concentration (%)	Predicted response (%)	Observed response (%)
1	35.43	10.32	68.62	9.29	94.67917	95.22
2	35.43	10	124.6	10.92	93.79731	92.19
3	35.55	10.07	88.6	11.39	95.65364	95.03
4	34.93	10.08	104.06	10.65	97.55124	98.14
5	34.98	10.11	91.41	11.4	95.86601	96.28

Table 5.12c Predicted solutions for model validation and confirmation for TBC

Solution	Temperature (°C)	pH	Dye concentration (ppm)	Predicted response (%)	Observed response (%)
1	50.81	7.43	97	98.86422	98.02
2	49.36	7.56	70.24	91.97164	92.44
3	51.27	7.34	103.14	95.64291	96.11
4	51.13	7.49	90.12	97.99787	96.87
5	50.69	7.76	90.5	93.83208	94.16

5.3.3 Molecular level analysis of natural bacterial consortia

The bacterial community structure of the dye decolorizing natural bacterial consortia was investigated through next generation molecular analysis of 16 rRNA gene V1-V3 region. The total number of reads (> 200 bp) for the three samples obtained from the analysis pipeline were 36,823. The number of reads for MBC, AHBC, and TBC consortia samples were 14,248, 13,284, and 9,291, respectively.

5.3.3.1 Diversity analysis of the natural bacterial consortia

The bacterial diversity in the dye decolorizing natural bacterial consortia was assessed through different alpha diversity matrices, viz. phylogenetic diversity ((PD whole tree), observed species, and Chao 1 (for species richness estimation), Shannon (H') and Simpson index (D1) (for diversity estimation) and rarefaction plots were made. Fig. 5.22a and Table 5.13, show the observed species curves for the three natural bacterial consortia. The thermophilic bacterial consortium (TBC), showed the highest number of observed species, followed by the mesophilic dye decolorizing consortium (MBC). Lowest number of unique OTUs were observed in the case of the alkaliphilic and halotolerant bacterial consortium (AHBC). Moreover, the curve for AHBC had a gradual slope which almost reached plateau as compared to the other two samples. Similarly, the Chao 1 estimator indicated a higher specie richness in thermophilic consortium followed by MBC and AHBC (Fig. 5.22 b and Table 5.13). Phylogenetic diversity analysis of the consortia samples also showed that the thermophilic and mesophilic consortia had more distantly related bacteria as compared to the alkaliphilic, halotolerant consortium (Fig. 5.22c and Table 5.13). Both the Shannon and Simpson diversity indices indicated a higher diversity in mesophilic bacterial consortium followed by the thermophilic and alkaliphilic, halotolerant bacterial consortia (Fig. 5.22 d and e, Table 5.13).

Table 5.13 Statistical analysis of pyrosequencing data showing alpha diversity matrices

Samples	Sequences	Observed species	Chao 1	PD whole tree	Shannon index (H')	Simpson index (D1)
MBC	14,248	162.35	255.04	5.19	4.54	0.89
AHBC	13,284	81.22	118.29	4.33	2.43	0.64
TBC	9,291	156.09	327.74	8.24	3.47	0.73

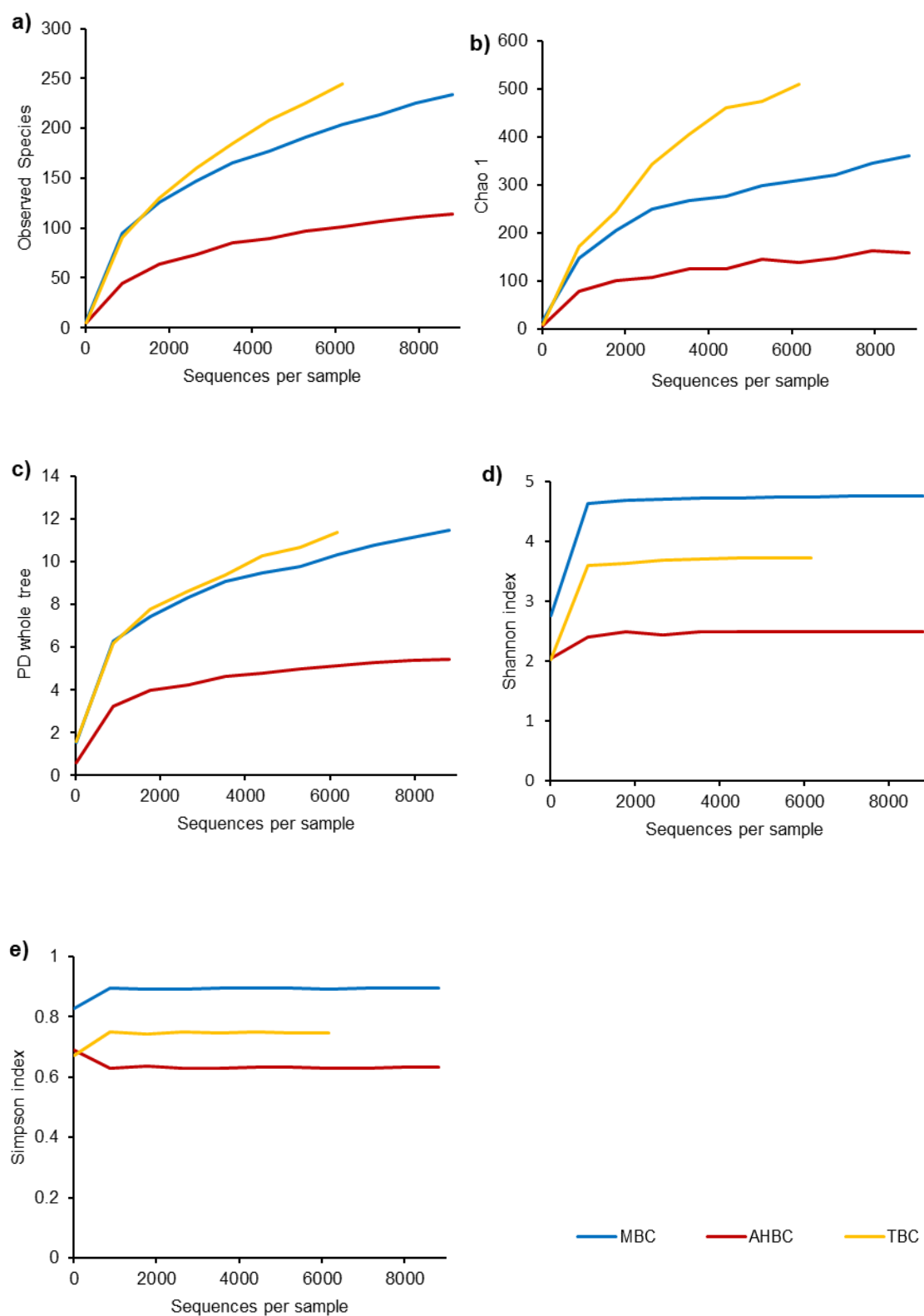


Fig. 5.22 Rarefaction plots for natural bacterial consortia (a) Observed species, (b) Chao 1, (c) PD whole tree, (d) Shannon index, and (e) Simpson index

5.3.3.2 Bacterial community analysis at different taxonomic levels

The bacterial community structure (relative abundance) of the natural consortia was studied at different taxonomic levels, i.e., phylum, class and genus level. In the mesophilic consortium, Firmicutes was the most abundant phylum with a relative abundance of 49.91%. The second major phylum was Bacteroidetes (29.81%) followed by Proteobacteria (19.12%). The other phyla observed were Actinobacteria, *Deinococcus_thermus*, and Verrucomicrobia, with the relative abundance values of 0.73, 0.40, and 0.04%, respectively. In the case of alkaliphilic, halotolerant bacterial consortium, Firmicutes was the major phylum as it made 67.26% of the total observed bacterial population in the AHBC sample. With a relative abundance of 26.79%, Bacteroidetes was second most abundant phylum. The remaining bacterial population belonged to Proteobacteria (5.13%) and Actinobacteria (0.82%). The thermophilic bacterial consortium was also dominated by the Firmicutes, contributing to 60.26% of the total observed bacterial OTUs. The percentage of Bacteroidetes and Proteobacteria was 23.74 and 14.79%, respectively, while the relative abundance of Actinobacteria, *Deinococcus_thermus*, and Verrucomicrobia was 0.84, 0.16, 0.03%, respectively (Fig. 5.23).

Bacteroidia was the most abundant class in MBC with a relative abundance of 29.57%. However, in the other two consortia it was the third most dominant class (26.73 and 23.68% for AHBC and TBC, respectively) after the representative classes of Firmicutes phylum. The two most dominant classes of Firmicutes in all the three consortia were Clostridia (25.14, 34.85, and 32.02% for MBC, AHBC, TBC, respectively) and Bacilli (24.76, 32.41, and 28.24% for MBC, AHBC, and TBC, respectively). Gammaproteobacteria (MBC, AHBC, and TBC: 10.174, 2.05, and 3.50%); Alphaproteobacteria (MBC and TBC: 5.87 and 5.79%); and Betaproteobacteria (MBC, AHBC, and TBC: 3.07, 2.94, and 5.67%) were some other important classes observed in the dye decolorizing natural bacterial consortia. (Fig. 5.24).

Genus level bacterial distribution analysis indicated that the mesophilic dye decolorizing bacterial consortium was dominated by *Dysgonomonas* (28.51%) and *Clostridium* (10.51%), followed by *Bacillus* (7.45%), *Proteus* (7.42%), *Lysinibacillus* (5.95%), *Brevundimonas* (5.41%), *Ureibacillus* (4.72%), *Anoxybacillus* (4.07%),

Caloramator (2.58%), *Romboutsia* (3.05%), *Brevibacillus* (1.55%), *Tissierella* (2.99%) and *Pseudomonas* (1.23%) (Fig.5.25a). The most abundant genera found in the alkaliphilic, halotolerant bacterial consortium (AHBC), were: *Dysgonomonas* (19.13%), *Ureibacillus* (10.08%), *Anoxybacillus* (10.49%), *Caloramator* (9.46%), *Bacteroides* (7.59%), *Paenibacillus* (5.62%), *Butyrivibrio* (2.84%), *Tissierella* (2.57%), *Lysinibacillus* (5.54%), *Fervidicella* (4.77%), *Desulfotomaculum* (3.74%), *Proteiniclasticum* (2.96%), *Terrisporobacter* (2.78%), *Alcaligenes* (2.65%), *Stenotrophomonas* (1.54%), and *Halomonas* (0.12%) (Fig. 5.25b). In the thermophilic bacterial consortium, the relative abundance of the major genera was: *Dysgonomonas* (23.62%), *Clostridium* (16.78%), *Ureibacillus* (10.17%), *Anoxybacillus* (8.02%), *Brevundimonas* (5.61%), *Anaerobranca* (5.87%), *Thauera* (4.29%), *Proteus* (2.55%), *Sedimentibacter* (2.46%), *Lysinibacillus* (2.31%), *Bacillus* (1.87%), and *Romboutsia* (1.57%) (Fig. 5.25c).

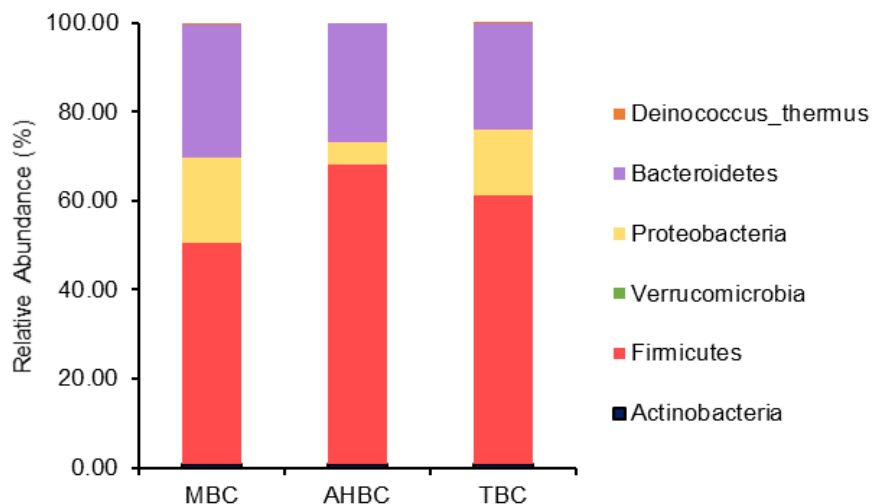


Fig. 5.23 Phylum level relative abundance (%) in natural bacterial consortia

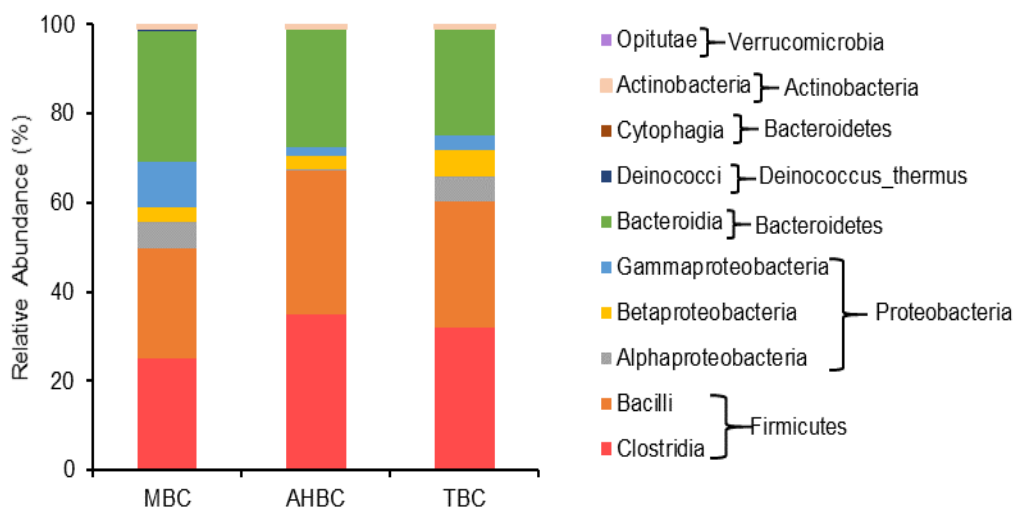


Fig. 5.24 Class level relative abundance (%) in natural bacterial consortia

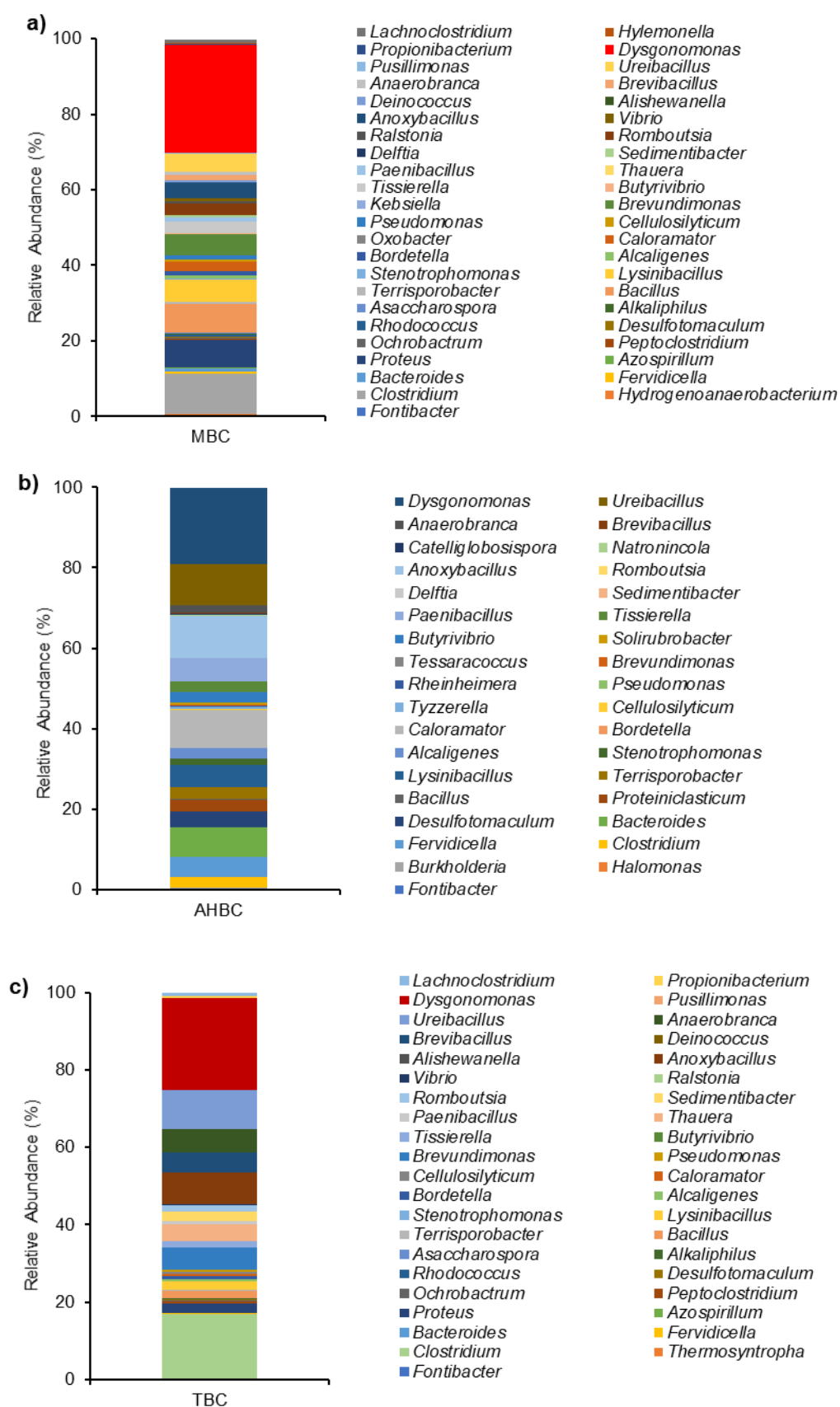


Fig. 5.25 Genus level relative abundance (%) in natural bacterial consortia (a) MBC, (b) AHBC, and (c) TBC

5.3.4 Color, COD and pH determination during the treatment

The treatment efficiency of the natural bacterial consortia for the synthetic textile wastewater was assessed in larger reactor volume i.e., 1000-mL flasks by periodic (24 hours) monitoring of color, COD, and pH. Mesophilic bacterial consortium (MBC) decolorized (98.31%) the synthetic dye effluent (100 ppm) within 72 hours, following which the decolorization percentage remained almost constant. With the alkaliphilic, halotolerant consortium (AHBC), 98.19% color reduction was recorded after 72 hours of incubation. In the case of the thermophilic bacterial consortium (TBC), 98.63% decolorization was observed after 96 hours of treatment (Fig. 5.26).

The COD of the synthetic dye effluent gradually decreased, upon treatment with the natural bacterial consortia. For the mesophilic bacterial consortium (MBC), COD of the synthetic dye effluent decreased by 68.49%, after 144 hours of bacterial treatment. With the alkaliphilic, halotolerant and thermophilic consortia, 70.35 and 71.63% COD reduction was recorded after 144 hours (Fig. 5.27). For the mesophilic consortium, initial pH of the synthetic dye effluent was 7.0 ± 0.2 . With slight fluctuations, the pH of the effluent was dropped to 6.75, on the final day of treatment. The initial pH of the synthetic effluent for the alkaliphilic, halotolerant consortium was 10 ± 0.2 , which dropped to 9.73 after 24 hours. Following that, with some fluctuations, it kept on declining to a final value of 8.41, after 144 hours. Similarly, pH drop was observed in the case of the thermophilic consortium treated synthetic effluent. The initial pH was 7.0 ± 0.2 , which decreased with some fluctuations to 6.10, after 144 hours (Fig. 5.28).

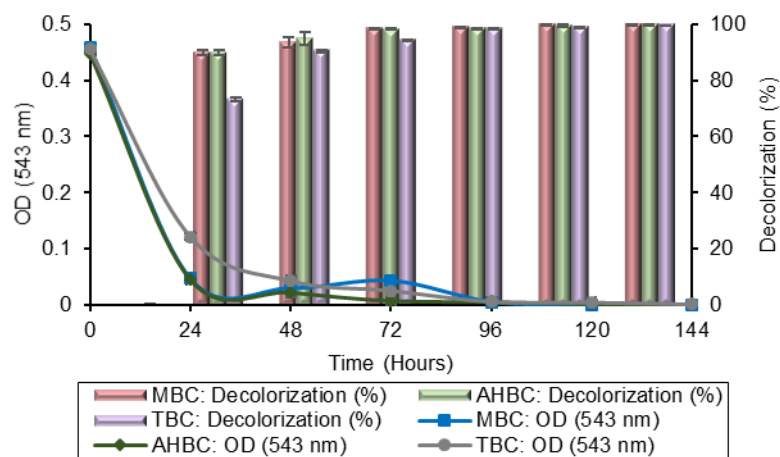


Fig. 5.26 Color reduction performance of the natural bacterial consortia

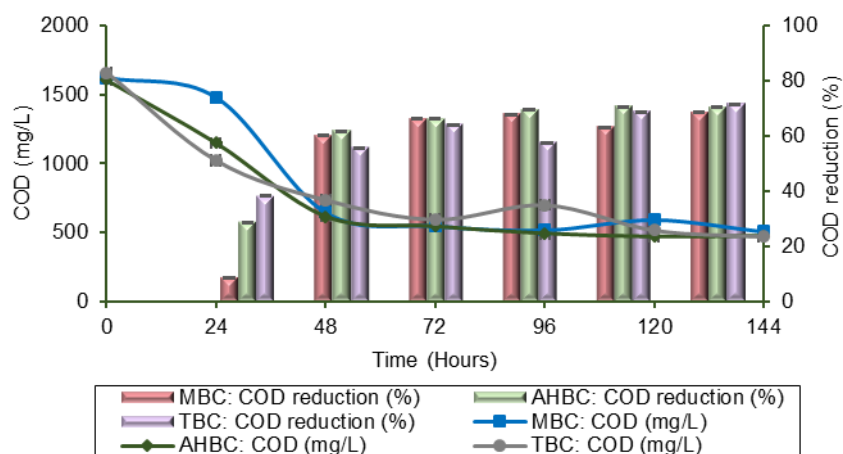


Fig. 5.27 COD reduction performance of the natural bacterial consortia

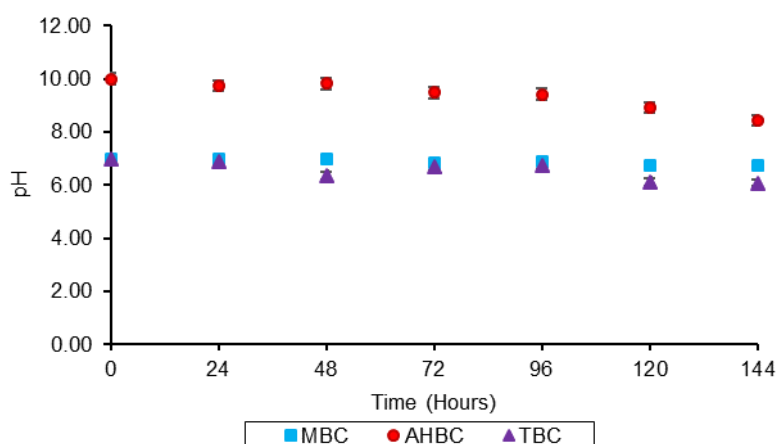
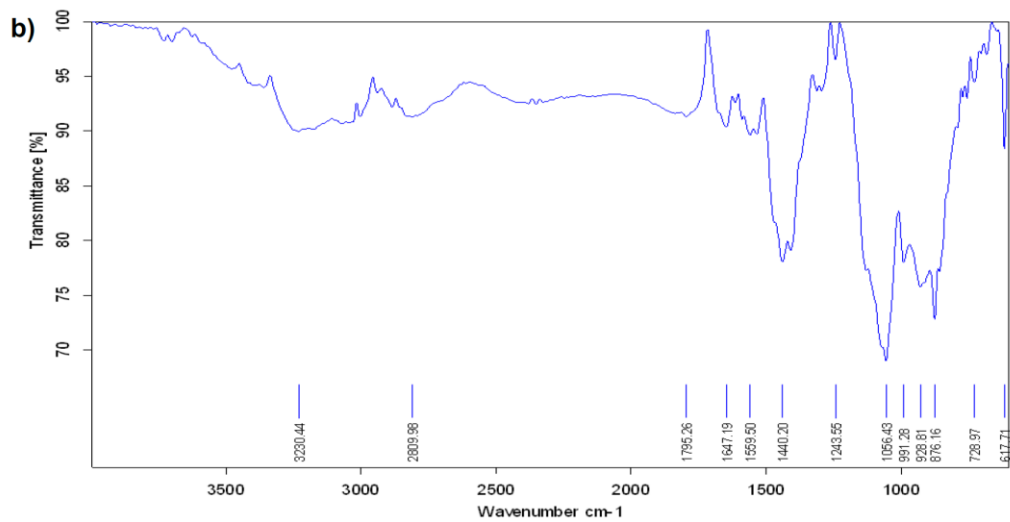
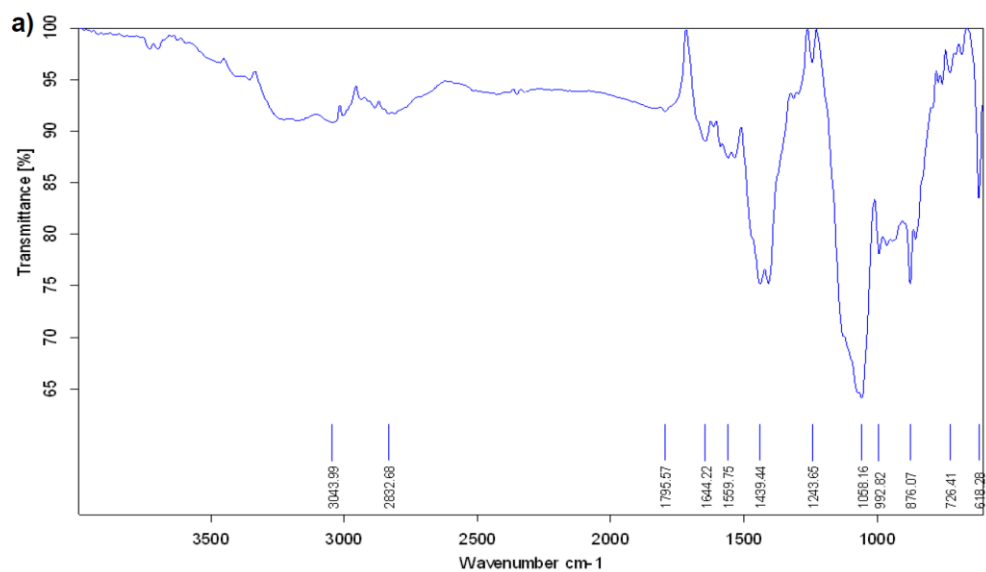


Fig. 5.28 pH variation in the synthetic dye wastewater treated by the natural bacterial consortia

5.3.5 Biodegradation assessment

5.3.5.1 FTIR analysis

FTIR analysis was done and spectra were recorded in the mid IR region (600-4000 cm^{-1}). In the FTIR spectrum of control (dye mixture), bands were observed at 618.28 cm^{-1} , 726.41 cm^{-1} , 876.07 cm^{-1} , 992.82 cm^{-1} , 1058.16 cm^{-1} , 1243.65 cm^{-1} , 1439.44 cm^{-1} , 1559.75 cm^{-1} , 1644.22 cm^{-1} , 1795.57 cm^{-1} , 2832.68 cm^{-1} , and 3043.39 cm^{-1} . FTIR analysis of the synthetic dye effluent samples, treated by the natural bacterial consortia (showed variations in the intensity of different bands as compared to the control (Fig. 5.29a-d). FTIR spectrum of the MBC, treated synthetic effluent samples, showed variations in the intensity and band shifts from 618.28 cm^{-1} -1644.22 cm^{-1} . The peaks in control spectrum, located at 2832.68 cm^{-1} and 3043.39 cm^{-1} were disappeared in the MBC treated sample. The FTIR spectrum for AHBC treated dye effluent sample, showed band variations in comparison to the control from 618.28-1058.16 cm^{-1} . The peaks observed in control at 1439.44 cm^{-1} , 1559.75 cm^{-1} , 1644.22 cm^{-1} , 2832.68 cm^{-1} , and 3043.39 cm^{-1} were disappeared in the AHBC treated sample. Moreover, new peaks were observed at 1435.10 cm^{-1} , 1531.84 cm^{-1} , 1681.59 cm^{-1} , and 3252.16 cm^{-1} . In the case of TBC treated dye effluent sample, FTIR spectrum showed slight band intensity variations from 618.28-876.07 cm^{-1} and 2832.68-3043.39 cm^{-1} , when compared to the control. Peaks observed in the control at 1439.44 cm^{-1} , 1559.75 cm^{-1} , and 1644.22 cm^{-1} were not observed in the FTIR spectrum of TBC treated effluent sample.



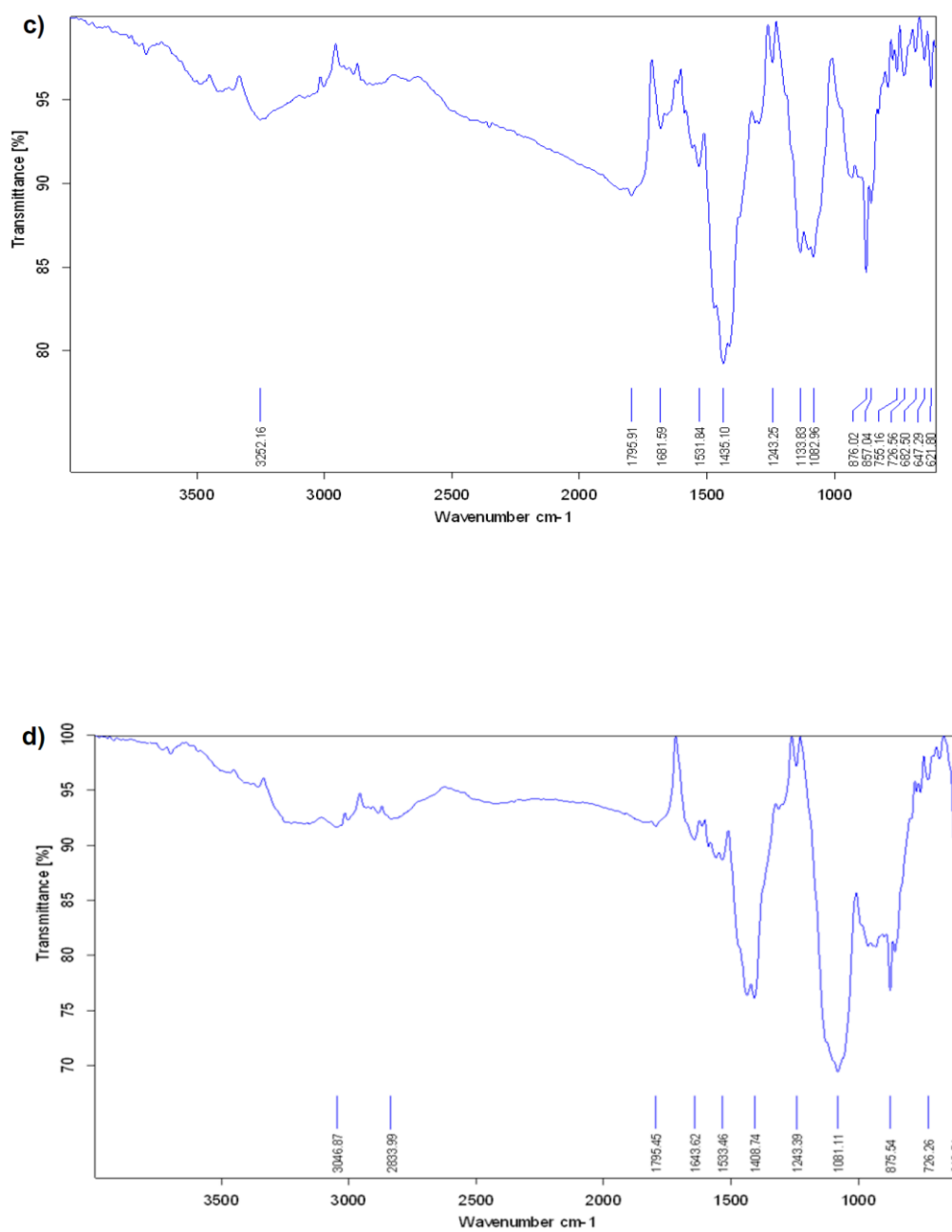

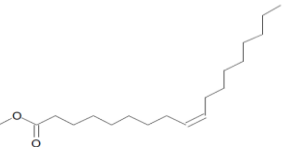


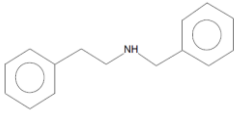


Fig. 5.29 FTIR spectra of synthetic dye wastewater (a) Control, metabolites obtained after treatment by the natural bacterial consortia, (b) MBC, (c) AHBC, and (d) TBC

5.3.5.2 GC-MS analysis

The dye mixture containing synthetic textile wastewater samples, obtained after decolorization by the natural bacterial consortia, were analyzed through GC-MS to find out the nature of products. The nature of the detected products was identified (by comparison with the NIST compounds library) on the basis of mass to charge ratio values, base and molecular ion peaks, and ionic fragmentation pattern (Fig.A1-A3, Appendix 3). In the case of MBC treated sample, the detected dye metabolites were: 1-Butanol (RT = 1.87, base peak at 56, and Mol. Ion peak at 264) and 9-Octadecenoic acid (Z)-, methyl ester (RT = 19.61, base peak at 55, and Mol. Ion peak at 73). With AHBC consortium, the dye mixture was converted to: 1-Butanol (RT = 1.92, base peak at 56, and Mol. Ion peak at 73) and n-Hexadecanoic acid (RT = 16.58, base peak at 43, and Mol. Ion peak at 256). The only detected dye degradation product in the TBC treated sample was N-Benzyl-2-phenethylamine (RT = 15.13, base peak at 91, and Mol. Ion peak at 209) (Table 5.14).

Table 5.14 Dye mixture metabolites detected in GC-MS analysis after treatment with the natural bacterial consortia

Bacterial consortium	R.T	B.P <i>m/z</i>	M.I peak <i>m/z</i>	Compound	Structure
MBC	1.87	56	73	1-Butanol	
	19.61	55	264	9-Octadecenoic acid (Z)-, methyl ester	
AHBC	1.92	56	73	1-Butanol	
	16.58	43	256	n-Hexadecanoic acid	
TBC	15.13	91	209	N-Benzyl-2-phenethylamine	

R.T., Retention time; B.P., Base peak, and M.I., Molecular ion

5.3.6 Detoxification assessment of the synthetic dye effluent metabolites

5.3.6.1 Phytotoxicity assay

Phytotoxicity analysis by using *T. aestivum* (wheat) and *R. sativus* (radish) seeds, was done for assessing the detoxification efficiency of the natural bacterial consortia for the synthetic dye wastewater (Table 5.15). For the *T. aestivum* seeds, 85% seed germination was observed with the positive control (colored wastewater). The root and shoot lengths were 5.91 cm [± 0.23] and 1.08 cm [± 0.07], respectively. In the case of the mesophilic bacterial consortium treated synthetic textile wastewater, an increase in the *T. aestivum* seed germination rate (87.5%), root (6.48 cm [± 0.33]), shoot lengths (1.71 cm [± 0.16]) was observed, as compared to the positive control. With the alkaliphilic-halotolerant and thermophilic bacterial consortia treated wastewater samples, the seed germination rates were the same as that observed, when watered with the control i.e., 85%. However, the root and shoot lengths were improved in comparison to that observed with the control. The respective root lengths were: 7.41 cm [± 0.14] and 7.51 cm [± 0.29]. The observed shoot lengths were: 1.92 cm [± 0.03] and 1.82 cm [± 0.14], respectively.

For the *R. sativus*, seed germination was 75%, when watered with the synthetic textile wastewater. The respective root and shoot lengths were: 1.43 cm [± 0.28] and 1.04 cm [± 0.28]. An increase in the seed germination rate was observed with all the three bacterial consortia treated synthetic textile wastewater samples i.e., 90, 77.5, and 80% for the mesophilic, alkaliphilic-halotolerant, and thermophilic bacterial consortia treated samples, respectively. The root and shoot lengths were also increased post bacterial treatment. The respective observed root lengths were: 2.48 cm [± 0.26], 1.98 cm [± 0.15], and 2.36 cm [± 0.15]. The shoot lengths were recorded as: 2.17 cm [± 0.14], 1.92 cm [± 0.09], and 1.55 cm [± 0.19], respectively.

Table 5.15 Phytotoxic analysis of the reactive azo dye mixture containing synthetic effluent (before and after bacterial treatment)

Sample	<i>T. aestivum</i>			<i>R. sativus</i>		
	Germination (%)	Root length (cm) ± S.E.	Shoot length (cm) ± S.E.	Germination (%)	Root length (cm) ± S.E.	Shoot length (cm) ± S.E.
Negative Control	95	7.59 ± 0.17	2.03 ± 0.09	100	2.39 ± 0.19	2.42 ± 0.18
Positive control	85	5.91 ± 0.23	1.08 ± 0.07	75	1.43 ± 0.28	1.04 ± 0.28
MBC-TSTW	87.5	6.48 ± 0.33	1.71 ± 0.16	90	2.48 ± 0.26	2.17 ± 0.14
AHBC-TSTW	85	7.41 ± 0.14	1.92 ± 0.03	77.5	1.98 ± 0.15	1.92 ± 0.09
TBC-TSTW	85	7.51 ± 0.29	1.82 ± 0.14	80	2.36 ± 0.15	1.55 ± 0.19

MBC-TSTW., Mesophilic bacterial consortium treated synthetic textile wastewater, AHBC-TSTW., Alkaliphilic, halotolerant bacterial consortium treated synthetic textile wastewater, TBC-TSTW., Thermophilic bacterial consortium treated synthetic textile wastewater, S.E., standard error

5.3.6.1 Acute toxicity assay

Brine shrimp larval mortality test was performed to assess the acute toxicity of the reactive azo dyes containing synthetic effluent (before and after treatment with the natural bacterial consortia (Fig. 5.30). Brine shrimp mortality ratio was reduced after bacterial treatment of the synthetic dye wastewater (control: 35% mortality). For the mesophilic and thermophilic bacterial consortia treated wastewater samples, 20% larval mortality was recorded, while in the case of alkaliphilic-halotolerant bacterial consortium treated sample larval mortality was 25%.

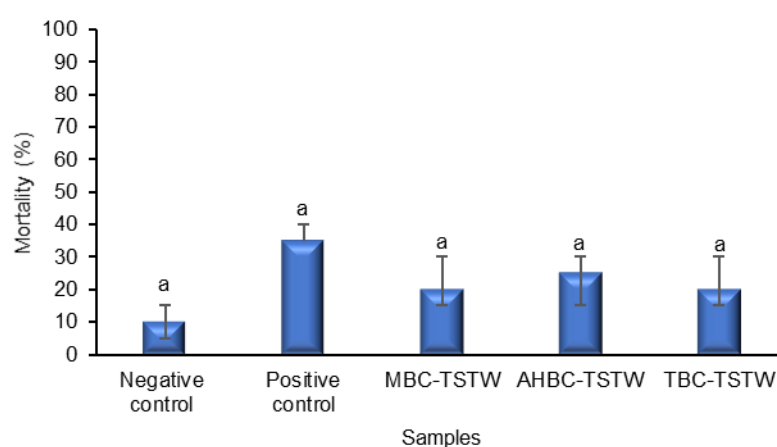


Fig. 5.30 Effect of the synthetic textile wastewater on Brine shrimp larvae (before and after bacterial treatment). Same letters on each column indicate statistically non-significant values ($\alpha=0.05$, One-way ANOVA followed by Tukey's HSD)

5.4 Discussion

In this study, natural bacterial consortia with different environmental conditions (pH, salt, and temperature) preferences, were used for the treatment of reactive azo dye mixture containing synthetic textile wastewater. Basically, the three types of consortia explored were; mesophilic (MBC), alkaliphilic-halotolerant (AHBC), and thermophilic in nature. The decolorization potential of the consortia was optimized. Biodegradation and detoxification efficiencies were also monitored. For all the three consortia, static condition was found to be more suitable for the color removal (80-85%) than the shaking condition (< 50%), $p < 0.05$ (Fig. 5.1). Likewise, different studies have reported an enhancement of bacterial dye decolorization efficacy under static and/or anoxic conditions (Işık and Sponza, 2003; Jadhav et al., 2008; Prasad and Rao, 2013). Shaking/aerobic conditions mostly lead to low color removal by bacteria, due to the interference of molecular oxygen (which is a strong terminal electron acceptor) with the azo bond reduction process by the redox mediator i.e., NADH (Chang et al., 2001). The natural consortia were then optimized for the synthetic dye wastewater decolorization through OFAT.

Additional carbon sources play a vital role in the bacterial dye decolorization process, by acting as energy source for the bacterial growth and electron donor for the azo bond reduction (McMullan et al., 2001; Kumar Garg et al., 2012). Therefore, effect of the different additional carbon sources on the decolorization efficiency of the natural bacterial consortia was investigated (Fig. 5.2). Except for sorbitol ($p > 0.05$), decolorization efficacy of MBC improved with the addition of secondary carbon sources ($p < 0.05$). Glucose was found as the most effective carbon source for the color removal by MBC, as the highest decolorization (up to 98%) was observed in comparison to the other tested carbon sources ($p < 0.05$). Similarly, AHBC, showed highest color removal with glucose ($p < 0.05$). Glucose, being one of the most easily utilizable carbon and energy source, usually serves as the most preferential additional carbon source for the azo dye decolorization. For example, Jain et al., (2012) reported glucose as an optimal carbon source (0.1% [w/v]), for the decolorization of Reactive Violet 5R (200 ppm) by a mixed culture of indigenous bacteria. In the case of TBC, the most suitable secondary carbon source was sucrose, with up to 93% decolorization observed in 72 hours ($p < 0.05$). Similarly, Lalnunhlimi and Veenagayathri, (2016)

observed sucrose as the most effective carbon source for the decolorization of mixed dyes (DB 151 and DR 31, 200 ppm).

Bacterial dye decolorization is also affected by the nitrogen source (Ali, 2010; Solís et al., 2012). So, different organic and inorganic nitrogen sources were used to assess their effect on the decolorization ability of natural bacterial consortia (Fig. 5.3). For all the three bacterial consortia, yeast extract was found as the optimal nitrogen source ($p < 0.05$). Likewise, Moosvi et al. (2007) and Jain et al., (2012) found yeast extract as the most effective nitrogen source for the decolorization of Reactive Violet 5R dye by different bacterial consortia. Yeast extract metabolism facilitates the azo bond reductive cleavage through the regeneration of electron carrier i.e., NADH (Chen et al. 2003).

Temperature influences the bacterial growth and enzymatic profile, which in turn can greatly affect the color removal ability of dye decolorizing bacteria (Imran et al., 2014). Therefore, the decolorization potential of natural bacterial consortia was assessed under different incubation temperatures (Fig. 5.4). Mesophilic temperature conditions were found to be more suitable for the color removal (50 ppm dye mixture) and growth (Fig. A4, Appendix 3) by MBC and AHBC consortia with the highest color removal (up to 98% in 72 hours) recorded at 35 °C ($p < 0.05$). Moreover, both type of consortia showed a linear increase in color removal efficiency that diminished at higher temperatures i.e., 40 and 45 °C ($p < 0.05$). Similarly, Wang et al., (2009) and Arun Prasad et al. (2013) observed best decolorization results at mesophilic temperatures, i.e., 32 (for Reactive Red 180: 50 ppm) and 37 °C (for Direct Blue 1: 100 ppm) by *Citrobacter* sp. CK3 and a moderately halophilic bacterium *Marinobacter* sp. strain HBRA, respectively. Additionally, higher temperatures (above 40 °C) were also found to be less suitable for the dye decolorization. Higher temperatures are usually detrimental to the cell viability of most mesophilic bacteria, and/or result in the denaturation of enzymes involved in dye decolorization (Çetin and Dönmez 2006). Unlike the other two consortia, the thermophilic consortium was more stable and active at higher temperatures. For TBC, the best decolorization temperature (for the 50-ppm dye mixture) was observed at 50 °C ($p < 0.05$) (growth profile given in Fig. A4, Appendix 3). Similar findings were reported by Yu et al., (2015), with 50 °C as the optimal temperature for decolorization of 0.3 mM Orange I, by *Novibacillus thermophilus* SG-1.

Decolorization ability of the natural bacterial consortia was studied with different initial pH values as it affects the bacterial enzymatic activity and/or dye adsorption process (Saratale et al. 2011) (Fig. 5.5). For MBC and TBC, compared to the acidic and basic pH values, neutral pH conditions were more suitable for color removal (dye mixture: 50 ppm). Moreover, considerable decolorization percentage (80.55 and 74.46 %, respectively) was observed at pH 8.0. These results are somewhat in accordance with those reported by Saratale et al. (2009b), where a consortium-GR decolorized 100 ppm of Scarlet R dye over a pH range of 6-8. For the alkaliphilic-halotolerant consortium optimal color removal activity (up to 99% in 72 hours) was recorded at pH 10.0 ($p < 0.05$), with a slightly slower decolorization observed at pH 11 reaching up to 92% dye removal in 120 hours. Similarly, Guadie et al., (2017) reported complete decolorization of 100 ppm Reactive Red 239 by *Bacillus* sp., at pH 10.0 in 48 hours. Contrary to that, Lalnunhlimi and Veenagayathri, (2016) observed the optimal decolorization activity of an alkaliphilic consortium for a 200-ppm dye mixture, at the pH value of 9.5 within 120 hours. Growth of the natural consortia also followed coinciding patterns in relation to the pH as given in Fig. A5 (Appendix 3).

Decolorization potential of the natural consortia was also examined with different initial dye concentrations (Fig. 5.6). MBC and AHBC showed the highest dye mixture tolerance with up to 76 and 58% decolorization observed at 200 and 250 ppm dye mixture concentrations, respectively. Moreover, complete decolorization was observed with both MBC and AHBC, at 50-150 ppm dye mixture concentrations, after 96 hours ($p > 0.05$). The dye tolerance limit for TBC was 150 ppm at which up to 60% dye removal (120 hours) was observed and maximum activity (98-99% in 120 hours) was recorded at 50-100 ppm dye mixture concentration. However, decolorization activity for all the three consortia was significantly diminished at higher dye concentrations i.e., 250-1000 ppm ($p < 0.05$). Similarly, Moosvi et al. (2007) observed a decrease in the decolorization efficiency of the consortium JW-2 for Reactive Violet 5R above the optimal concentration of 100 ppm. At higher concentrations, textile dyes are usually toxic for bacterial cells, and in the case of reactive dyes, the effect of sulfonic acid groups becomes more pronounced and hinders bacterial growth (Kalyani et al. 2008). Another possible explanation for the reduced decolorization activity is the resulting imbalance in the dye to cell ratio. This could lead to blockage of enzyme active sites

involved in color removal (Sani and Banerjee, 1999; Saratale et al. 2009a).

Textile wastewaters are usually saline in nature which can limit the decolorization potential of dye decolorizing bacteria. Therefore, salt tolerance of the natural bacterial consortia was tested (Fig. 5.7). Decolorization activities of MBC and TBC were greatly affected upon addition of the salt into the medium and were much reduced (> 40%) beyond 4% (w/v) NaCl ($p < 0.05$). The decreased activity at higher salt concentrations may have occurred due to cell death through plasmolysis (Peyton, Wilson, and Yonge 2002). AHBC however, showed considerable color reduction over 0-12% (w/v) NaCl concentrations. Moreover, decolorization activity improved with the increasing salt concentrations and the consortium also showed growth over a range of NaCl concentrations. Growth patterns for the natural consortia at different NaCl concentrations are given in Fig. A6 (Appendix 3). Khalid et al. (2012), reported similar findings with varying decolorization rates for different reactive dyes over a range of NaCl concentrations i.e., 0-10% (w/v) by *Psychrobacter alimentarius* and *Staphylococcus equorum*. In another study, Bhattacharya et al., (2017) observed up to 97% decolorization of Methyl Red by *N. lacusekhoensis* at 6% (w/v) NaCl concentration.

With the help OFAT results, important parameters affecting the decolorization activity of the natural bacterial consortia, were selected and further studied using Response Surface Methodology through the application of BBD method. All the statistical parameters indicated the adequacy of the quadratic model designs for the selected response i.e. decolorization (Tables 5.9-5.11). Moreover, depending upon the shapes of the contour plots, nature of interaction between the given factors can be inferred as significant (elliptical shape) or insignificant (circular shape) (Muralidhar et al. 2001). The 2D contour plots were mostly elliptical for the studied variables (pH, temperature, and initial dye mixture concentration for MBC and TBC; and pH temperature, salt, and dye mixture concentration for AHBC) for all the three consortia, indicating a significant interaction (Fig. 5.10-5.21). The validation experiments further confirmed the accuracy of the application of BBD method for process optimization (Tables 5.12a-c). Similarly, Sharma et al., (2009) optimized pH, temperature, and initial dye concentration, for the decolorization of Disperse Yellow 211 by *Bacillus subtilis*, using BBD method. In another study, Jadhav et al., (2013) used BBD to optimize the decolorization of

Remazol Orange by *P. aeruginosa* BCH. The studied parameters were pH, temperature, and cells mass concentration.

Next generation molecular analysis of the bacterial community structure of the dye decolorizing natural consortia was done. Statistical analysis and rarefaction plots made using richness estimates i.e., phylogenetic diversity, observed species, and Chao 1 indicated that the thermophilic consortium was richer (in unique OTUs) and diverse in terms of the phylogenetic diversity followed by MBC and AHBC (Fig. 5.22a-c). The diversity estimates i.e., Shannon (H') and Simpson ($D1$), consider specie richness and evenness with the later more sensitive to the rare species (Bibi and Ali 2013; Morris et al. 2014). The mesophilic consortium with the highest Shannon and Simpson index values, had higher diversity, followed by TBC and AHBC (Fig. 5.22d and e). In all the rarefaction plots, the gradual slope of the AHBC curve and early onset of plateau, indicate a more complete analysis. MBC curve also reached plateau, however the curve for TBC failed to reach the saturation limit which indicates the samples size was relatively small (Köchling et al., 2017).

The dominant genus found in the all the three consortia was *Dysgonomonas* (Phylum: Bacteroidetes, class Bacteroidia). Other major genera in MBC were, *Clostridium*, *Caloramator*, *Romboutsia*, and *Tissierella* (Phylum: Firmicutes, class Clostridia); *Bacillus*, *Lysinibacillus*, *Ureibacillus*, *Anoxybacillus*, and *Brevibacillus* (Phylum: Firmicutes, class: Bacilli); *Proteus* and *Pseudomonas* (Phylum: Proteobacteria, class: Gammaproteobacteria); and *Brevundimonas* (Phylum: Proteobacteria, class: Alphaproteobacteria). In AHBC, other dominant genera were, *Ureibacillus*, *Anoxybacillus*, *Paenibacillus*, and *Lysinibacillus* (Phylum: Firmicutes, class: Bacilli); *Caloramator*, *Fervidicella*, *Desulfotomaculum*, *Proteiniclasticum*, *Terrisporobacter*, *Butyrivibrio*, and *Tissierella* (Phylum: Firmicutes, class Clostridia); *Bacteroides* (Phylum: Bacteroidetes, class Bacteroidia), *Alcaligenes* (Phylum: Proteobacteria, class: Alphaproteobacteria); *Stenotrophomonas* and *Halomonas* (Phylum: Proteobacteria, class: Gammaproteobacteria). In TBC, other abundant genera were, *Clostridium*, *Anaerobranca*, *Sedimentibacter* and *Romboutsia* (Phylum: Firmicutes, class Clostridia); *Ureibacillus*, *Anoxybacillus*, *Lysinibacillus*, and *Bacillus* Phylum: Firmicutes, class: Bacilli); *Brevundimonas* and *Thauera* (Phylum: Proteobacteria, class: Alphaproteobacteria); and *Proteus* (Phylum: Proteobacteria, class:

Gammaproteobacteria) (Fig. 5.25a-c). Most of the observed genera in the three types of consortia i.e., *Clostridium* (Köchling et al., 2017), *Ureibacillus* (Samoylova et al. 2018), *Anoxybacillus* (Yh and Sg 2011), *Brevibacillus* (Kurade et al. 2013), *Bacillus* (Misal et al. 2011), *Alcaligenes* (Shah, Dave, and Rao 2012), *Stenotrophomonas* (Subashkumar et al., 2014), *Brevundimonas* (Yang et al. 2018), *Pseudomonas* (Joe et al. 2011), and *Halomonas* (Asad et al. 2007) have been reported in different studies for the textile dye and other xenobiotics degradation. The most dominant genus, *Dysgonomonas* has been reported earlier, for the biodegradation of complex aromatic compounds, such as lignin, antibiotics, textile dyes (Rgen Forss et al. 2017). Therefore, in general, a complex mixture of anaerobic, facultative anaerobic, and aerobic bacteria, was found in all the three consortia. All the cultures were incubated under static condition, and in such case, dissolved oxygen content is affected by the varied diffusion extent of the oxygen in the broth culture. Below 1.0 mm depth, most of the culture conditions turn microaerophilic and/or anaerobic. So, the growth of strict anaerobes and facultative anaerobes is facilitated by the oxygen-based zoning of the broth culture medium (Somerville and Proctor 2013). Members of Firmicutes, i.e., many types of Clostridia and Bacilli have been reported to exist in textile sludge and could also possess high salinity and/or pH tolerance, which explains their higher number in MBC and AHBC consortia (Köchling et al., 2017). Moreover, many members of these classes have also been reported to inhabit high temperature environments (Engle et al., 1995; Artzi et al., 2014; Kurade et al., 2013). Furthermore, members of Proteobacteria (Alphaproteobacteria, Betaproteobacteria, and Gammaproteobacteria) are metabolically more diverse and are generally facultative anaerobes in nature. They can harbor variety of different habitats and are mostly found in textile industry sludge e.g., *Alcaligenes*, *Proteus*, *Stenotrophomonas*, and *Pseudomonas* (Imran et al., 2014; Holkar et al., 2016).

The color and COD removal efficiency of the natural consortia was assessed in larger volume i.e. 1000-mL synthetic textile wastewater (Fig. 5.26 and 5.27). A substantial reduction in the color i.e., up to 98% was observed with all the three consortia (achieved in 72 hours by MBC and AHBC; and in 96 hours by TBC). With all the three consortia, a considerable COD reduction was observed after 144 hours of incubation. TBC was more efficient with 71.63% COD reduction, followed by AHBC (70.35% COD

reduction) and MBC (68.49% reduction) ($p < 0.05$). Moreover, a rather smooth decline in COD was observed with all the three consortia, and the removal process did not correlate with that of decolorization, which agrees with the literature (Cheriaa et al. 2012). A decline in the pH of synthetic dye wastewater was observed with all the three consortia (Fig. 5.28). Overall pH reduction was 15.65, 13.07, and 3.49% (after 144 hours) with AHBC, TBC, and MBC, respectively ($p < 0.05$). With all the three consortia, more reduction in pH was observed after substantial color reduction (up to 90%), i.e., towards the end of treatment. Similarly, Bhattacharya et al., (2017), reported a pH decline during the treatment of textile wastewater by *N. lacusekhoensis*.

In the FTIR spectrum of the control (untreated synthetic textile effluent), different bands were observed (Fig. 5.29a). The peaks observed at 3043.39 and 2832.68 cm^{-1} corresponded to C=C and C-H stretching vibrations, respectively. The band at 1795.57 cm^{-1} represented C=O stretching (Lambert et al, 1998). The bands observed in the range of 1439.44-1559.75 cm^{-1} indicated the presence of azo (-N=N-) linkages (Coates, 2006; Kumar Garg et al., 2012). The bands at 1644.22 and 1243.65 cm^{-1} corresponded to primary amide and C-N linkage, respectively (Jain et al., 2012). The band at 1058.16 cm^{-1} corresponded to S=O bond stretching (Joshi et al., 2010). The bands at 992.82 and 876.07 cm^{-1} indicated aromatic rings vibrations, while the band 726.41 cm^{-1} corresponded to C-Cl stretch (Lambert et al, 1998; Yuen et al., 2005).

In the FTIR spectrum of the treated samples (Fig. 5.29b-d), shifts (in MBC treated samples) and disappearance (in AHBC and TBC treated samples) of the bands at 1439.44-1559.75 cm^{-1} indicated distortions and cleavage of -N=N- bonds, respectively, explaining the color removal from the synthetic dye wastewater. Band variations (MBC and TBC) and disappearance (in AHBC spectrum) at 1644.22 cm^{-1} indicated changes in amide linkage (Jain et al., 2012). Variation in the band intensity at 2832.68 cm^{-1} MBC treated sample indicated C-H stretching fluctuation. The new peaks observed at 3230.44 and 3252.16 cm^{-1} in MBC and AHBC treated samples' spectra, respectively, indicated the presence of O-H linkages for alcohols in the metabolites (Franciscon et al. 2009). Changes in S=O positions were indicated by band variations at 1058.16 cm^{-1} , in the AHBC and TBC decolorized samples (Mohammed and Mohammed, 2010). Such bands with a slightly changed intensity and shifts from the points seen in the untreated synthetic dye wastewater sample, might have resulted from

the changes occurred in other bonds of the dye molecules. The characteristic FTIR band changes, observed after the bacterial treatment indicated that the decolorization was achieved because of biodegradation. Moreover, the GC-MS analysis of the decolorized samples produced by the natural bacterial consortia, showed the conversion of reactive azo dye mixture to a few low molecular weight aliphatic (in the case of MBC and AHBC treated dye mixture sample) and aromatic (TBC treated sample), compounds (Table 5.14). The detection of relatively lower weight products following treatment with the natural bacteria consortia further confirms the biodegradation of dyes. Production of similar natured low molecular weight compounds as a result of textile dyes biodegradation have been reported earlier (Muthunarayanan et al. 2011; Surti 2018).

Toxicity assessment of the microbially treated dye effluents, is a vital approach for the documentation of eco-safety of the treatment method (Kalyani et al., 2008). Therefore, the toxicity of metabolites obtained after the bacterial treatment of the reactive azo dyes containing synthetic textile effluent, was investigated through phytotoxicity and acute toxicity assays. Two types of plant seeds i.e., *T. aestivum* and *R. sativus*, were used for the phytotoxicity analysis (Table 5.15). In the case of MBC, a statistically non-significant ($p > 0.05$) improvement in the seed germination was observed for wheat seeds as compared to the control; while for AHBC and TBC, no change in seed germination was observed. However, with all the three treated samples, root and shoot lengths were higher than that observed in the control. For radish seeds, germination percentage was significantly ($p < 0.05$) improved (in comparison to the control) with MBC treated effluent sample, whereas with AHBC and TBC treated samples, radish seed germination was improved but the change was not statistically significant ($p > 0.05$). The root and shoot lengths were improved with all the three treated effluent samples, obtained after bacterial treatment ($p < 0.05$). Similarly, reduced phytotoxicity of textile dyes following bacterial treatment was reported in other studies, where seed germination rate, root, and shoot lengths were improved upon watering the plant seeds with the dye metabolites (Parshetti et al., 2006; Olukanni et al., 2010; Khelifi et al., 2009). Acute toxicity estimation using brine shrimp larvae also indicated a reduction in the toxicity of synthetic textile effluent following bacterial treatment, as shown by the decrease (statistically insignificant, $p > 0.05$) in brine shrimp larval mortality in

comparison to the control (Fig. 5.30). Likewise, Parsad and Rao, (2012) and Hafshejani et al., (2014), used *A. salina* larvae to investigate the bacterial (pure cultures) detoxification efficiency for the textile dyes and reported a decrease in larval mortality following bacterial treatment.

5.5 Conclusion

The natural bacterial consortia with different temperature, pH, and salt tolerance profiles (mesophilic, thermophilic, and alkaliphilic-halotolerant), were investigated for the treatment of a reactive azo dyes containing synthetic textile effluent. The consortia i.e., MBC, AHBC, and TBC, efficiently removed the dyes (100 ppm; provided with glucose and yeast extract, 0.1% [w/v] each) in 72 (MBC and AHBC) and 120 hours (TBC) from the synthetic effluent under different conditions, optimized through OFAT and RSM. MBC and AHBC were more efficient around mesophilic temperature conditions i.e. 35 °C, while ~50 °C was found as the suitable temperature for TBC. The optimal pH for both types of consortia was neutral. Moreover, AHBC effectively treated the dye mixture effluent, under high pH (~10.0) and salinity (10% [w/v]) conditions. The high pH, salt, and temperature stability of the extremophilic bacterial consortia makes them promising candidates for the treatment of heterogenic textile effluents under such conditions. Furthermore, substantial (up to 70%) COD reduction was observed with all the three consortia. Next generation sequencing following process optimization, showed that under a set of given conditions, all the three consortia consisted of a complex mixture of anaerobic, facultative and aerobic bacteria with some of the most efficient dye degrading genera. Biodegradation of the dye mixture was confirmed by the characteristic band changes observed in FTIR spectra, along with the smaller aromatic and long chained aliphatic compounds detected through GC-MS analysis. Moreover, the metabolites obtained after bacterial treatment were less toxic than the original dye mixture.

Chapter 6: Degradation optimization and kinetics studies for reactive azo dyes by mesophilic and thermophilic bacteria

6.1 Introduction

Bacterial mediated treatment of textile dye waste is one of the most widely researched topics (Chengalroyen and Dabbs, 2012; Holkar et al., 2016). Various pure and co-cultures of specialized dye decolorizing bacteria have been reported (Saratale et al. 2011). Despite the promising performance of individual bacterial isolates in dye decolorization, pure cultures may not be applicable for treatment of actual textile wastewaters with complex compositions, and the specificity of bacterial isolates to individual dyes (Khehra et al., 2005). Therefore, for effective and complete treatment of multiple dyes containing textile wastewaters, cocultures showing synergistic activities present a better alternative (Khouni et al. 2012). The available literature is mainly focused on indigenous bacterial cocultures (isolated and designed from textile sludge), as anthropogenic sites present one of the best sources of a given pollutant degraders (Jain et al., 2012 ; Balapure et al., 2015). In addition to these, application of thermophilic bacteria can also be beneficial, for the treatment of freshly released textile effluents with high temperature (40-60 °C) (Ali et al., 2009; Solís et al., 2012). Despite the extensive literature on thermophilic bacteria, very few reports are available on the application of thermophiles for the textile dye treatment (Deive et al. 2010; Kandelbauer et al. 2004).

Majority of the literature on bacterial dye treatment is focused on optimization of the color removal process (Ali, 2010). Optimization studies are vital to enhance the output of a given process, as they help to understand the tolerance limits and overall potential of microbes (Hassani et al., 2014). In addition to this, knowledge of bio-removal kinetics of pollutants is also very crucial. Basically, kinetics deals with the relationship of microbial growth and substrate/pollutant removal rates in stoichiometric terms (Kova and Egli, 1998; Gironi et al., 2008). The available literature on bacterial treatment kinetics for textile dyes is very scarce (Karunya et al., 2014; Das and Mishra, 2017; Sudha et al., 2018). Bio-removal kinetics data for pollutants, collected from a set of batch experiments helps in gaining a detailed insight into the interrelationship of

pollutant removal rates and bacterial growth dynamics. This information in turn can help in the upscaling of treatment processes (Plattes et al. 2006).

In view of these points, the present set of studies were conducted to explore the degradation potential of bacteria, isolated from two different niches, for the reactive azo dyes (RB 221, RR 195, and RY 145). One set of dye degrading bacteria (mesophilic) was isolated from a textile industry sludge sample while the second set of bacteria (thermophilic) was isolated from a hot-water spring sample. The isolated bacteria were screened for the selection of efficient dye decolorizers, and then characterized through biochemical and molecular analyses. Following that, the cocultures were designed and optimized for the dye mixture removal, through OFAT and RSM. Furthermore, growth and decolorization kinetics studies were carried out using single and mixed dyes, and decolorization performance of pure as well as cocultures was investigated. The growth and degradation rates were modeled using first order kinetics following data linearization and normalization. Dye degradation efficiency was monitored through FTIR and GC-MS analyses. Moreover, detoxification experiments were conducted on plant seeds and brine shrimp larvae.

6.1.1 Aims and Objectives

The aim of the present study was to explore the mesophilic and thermophilic bacteria for the treatment of reactive azo dyes. The specific objectives of the study were:

- To enrich and isolate the dye decolorizing bacteria obtained from two different sites with different temperature conditions.
- To screen the bacterial isolates for the selection of efficient dye decolorizing strains.
- To characterize the selected bacterial isolates through biochemical and molecular analyses.
- To design and screen the bacterial consortia (with different temperature tolerance profiles) for the selection of efficient cocultures capable of decolorizing individual reactive azo dyes and their mixture.
- To optimize the cocultures' decolorization potential through one-factor-at-a-time (OFAT) experimental technique.

- To further evaluate, validate the key parameters (based on the results of OFAT), and explore their interrelationship, using Box-Behnken (BBD) experimental design
- To investigate the dye removal kinetics with reference to the bacterial biomass growth rate and dye degradation rates using first order kinetics.
- To assess biodegradation efficiency thorough FTIR and GC-MS analyses.
- To investigate the detoxification potential of bacterial cocultures for the reactive azo dyes through plant and brine shrimp toxicity tests.

6.2 Materials and Methods

The details regarding the textile dyes viz. RB 221, RR 195, RY145 and their mixture, solution formulations are described in section 5.2.1. Media compositions for microbial growth and dye decolorization studies, sampling, and enrichment procedures for mesophilic and thermophilic bacteria are given in section 5.2.2-5.2.4.

6.2.1 Isolation and screening

The decolorized samples (1 mL of each, from the respective enriched cultures) were serially diluted, and 50 μ L each of the diluted samples were plated on mineral salt medium agar amended with 50 ppm azo dye mixture (pH 10, 10% NaCl). The plates were incubated for 24 hours at 35 and 50 $^{\circ}$ C, for mesophilic and thermophilic bacteria, respectively; then morphologically distinct bacterial colonies were picked and purified by the streak plate method. Pure cultures were then screened for their ability to efficiently decolorize the azo dye mixture containing synthetic wastewater. Inocula were prepared by transferring a single colony to nutrient broth medium using a sterile inoculation loop followed by incubation at the two respective temperatures, until mid-log phase (optical density at 600 nm [OD₆₀₀] was 0.6). Ten (10) mL of the prepared inocula were added to synthetic dye wastewater (90 mL) containing 50 ppm azo dye mixture (pH 7.0 \pm 0.2), and incubated for 24 hours under respective temperature conditions, with and without agitation. The initial absorbance of each sample was recorded at 543 nm (λ_{max} of the dye mixture) using a UV-Vis Spectrophotometer (Agilent 8453; Agilent Technologies, Santa Clara, CA, USA). After 24 hours, 1.5 mL of each treated sample was aseptically collected, centrifuged (12,000 rpm, 10 minutes, room temperature), and the absorbance was measured. The decolorization percentage was calculated using the following formula (Sani and Banerjee, 1999):

$$\text{Decolorization (\%)} = \frac{(I - F)}{I} \times 100 \quad (\text{Eq 6.1})$$

where I is the initial absorbance of the colored sample and F is the final absorbance of the decolorized sample. Uninoculated medium containing the dye was used as the abiotic control, and dye-free medium was used as the blank.

6.2.2 Microbial identification

The cultural and biochemical properties of the selected isolates were studied according to the standard protocols (Prescott, Harley, and Klein 2002). Details regarding the biochemical tests are given in section A4.1, Appendix 4. Isolates were further characterized by 16S rRNA gene sequencing. Genomic DNA of the Gram negative and positive isolates was extracted by the Phenol-Chloroform and CTAB methods, respectively (Andreou 2013; Howland 1996) (section A4.2, Appendix 4). For 16S rRNA gene sequencing, samples were sent to Macrogen Inc. (Seoul, Korea), and sequenced using 27F (5'-AGAGTTTGATCCTGGCTCAG-3') and 1492R (5'-CTACGGCTACCTTGTACGA-3') bacterial primers. Sequences were edited using BioEdit 7.2.6, and analyzed for similarity by submission to the NCBI BLAST database (<http://www.ncbi.nlm.nih.gov/BLAST/>). Sequences were aligned, and phylogenetic analysis was carried out using the neighbor joining method in MEGA7.0 software (Kumar, Stecher, and Tamura 2016).

6.2.3 Consortia development and screening

To ascertain the effect of the mixed cultures on the decolorization efficiency (50 ppm dye mixture), equal volumetric proportions of the selected mesophilic and thermophilic isolates in the mid-log growth phase were mixed in different combinations (Tables 6.1-6.2) and incubated under static condition at 35 and 50 °C, for the respective cultures for 24 hours. The decolorization percentage was computed using Equation 1. The two most efficient combinations were then subjected to further investigation.

Table 6.1 Bacterial combinations for consortia screening for mesophilic isolates

Combination	Bacterial isolates
M. coculture-1	NHS1-NHS2
M. coculture-2	NHS1-NHS3
M. coculture-3	NHS1-NHS4
M. coculture-4	NHS2-NHS3
M. coculture-5	NHS2-NHS4
M. coculture-6	NHS3-NHS4
M. coculture-7	NHS1-NHS2-NHS3
M. coculture-8	NHS1-NHS2-NHS4
M. coculture-9	NHS2-NHS3-NHS4
M. coculture-10	NHS1-NHS2-NHS3-NHS4

Table 6.2 Bacterial combinations for consortia screening for thermophilic isolates

Combination	Bacterial isolates
T. coculture-1	NHT1-NHT2
T. coculture-2	NHT1-NHT3
T. coculture-3	NHT1-NHT4
T. coculture-4	NHT2-NHT3
T. coculture-5	NHT2-NHT4
T. coculture-6	NHT3-NHT4
T. coculture-7	NHT1-NHT2-NHT3
T. coculture-8	NHT1-NHT2-NHT4
T. coculture-9	NHT2-NHT3-NHT4
T. coculture-10	NHT1-NHT2-NHT3-NHT4

6.2.4 Optimization of culture conditions for dye mixture decolorization (OFAT)

Decolorization activity of the two selected cocultures (for the dye mixture containing synthetic effluent) was monitored under different culture conditions by modifying the carbon source (lactose, sucrose, sorbitol, glucose, starch at 0.1% [(w/v)], nitrogen source (peptone, yeast extract, ammonium sulfate, sodium nitrite, potassium nitrate at 0.1% [(w/v)], temperature (25, 30, 35, 40, 45 °C for the mesophilic bacterial coculture; 40, 45, 50, 55, and 60 °C for the thermophilic bacterial coculture), dye concentration (50, 100, 150, 200, 250, 300, 400, 500 ppm), pH (5-9 for mesophilic; 5-10 for thermophilic coculture), and salt concentration (0, 2, 4, 6, 8, 10 % [(w/v)] NaCl). All experiments were conducted without agitation for 120 hours.

6.2.5 Response Surface Methodology (RSM)

Box-Behnken design (BBD) was applied using the Design-Expert version 7.0.0 (Stat-Ease). The results of the preliminary optimization experiments (OFAT) for the synthetic dye wastewater, by the two bacterial cocultures, were used to apply the statistical optimization technique i.e., RSM. For the two cocultures, three design parameters, viz. temperature (°C, denoted as A), pH (denoted as B), and dye (mixture) concentration (ppm, denoted as C) were selected. Codes for the three parameters levels were set as: -1, 0, and 1 (indicating the lowest, central, and highest tested values, respectively) (Tables 6.3 and 6.4). For the model significance assessment, F test was used. Determination coefficient (R^2 and adjusted R^2) was used for assessing the quality of the quadratic model. Model's statistical significance was evaluated through analysis of variance (ANOVA). With the help of regression equation and response surface plot, and model validation experiments, optimum values were obtained and confirmed.

Table 6.3 Design factors and coded variables for mesophilic bacterial coculture

Factor	Units	Coded levels		
		-1	0	1
Temperature (A)	°C	30	35	40
pH (B)	NA	6.0	7.0	8.0
Dye concentration (C)	ppm	100	175	250

Table 6.4 Design factors and coded variables for thermophilic bacterial coculture

Factor	Units	Coded levels		
		-1	0	1
Temperature (A)	°C	45	50	55
pH (B)	NA	7.0	8.0	9.0
Dye concentration (C)	ppm	50	100	150

6.2.6 Growth and degradation/decolorization batch experiments for kinetics studies

Inocula of the selected bacterial isolates were prepared by adding loopful of the cultures to LB broth medium, then incubated until mid-log phase (OD = 0.6 for mesophilic and 0.18 for thermophilic bacteria at 600 nm). Following that, 10% (v/v) of the bacterial cultures (pure as well as the cocultures) were transferred to synthetic textile wastewater containing the individual (25 and 50 ppm for thermophilic and mesophilic bacteria, respectively) and mixed dyes (50 ppm for both types of bacteria). The flasks were incubated at 35° C under static condition. To monitor the bacterial growth and color removal, samples were aseptically collected at different time points from the batch flasks and divided into two portions. One portion was centrifuged for 10 minutes at 10,000×g, and the supernatant was used for the spectrophotometric determination of color intensity (at the respective wavelengths for the dyes and their mixture) using an uninoculated dye-free salt medium as a blank. The second portion of the collected sample was used for spectrophotometric measurement of biomass. Samples were vortexed, and biomass was measured at 600 nm, using the centrifuged portion (supernatant) as a blank to account for changes in the culture color. Uninoculated, dye-containing medium was kept as an abiotic control. Spectrophotometry was conducted using a Hach DR/4000U, Loveland, CO, USA.

6.2.6.1 Growth and degradation kinetics

6.2.6.1.1 Growth kinetics calculations

Bacterial growth rates were modeled using first order kinetics.

$$\frac{dX}{dt} = k_g X$$

Where X was the biomass concentration, measured as optical density at 600 nm, t was time, k_g was the reaction rate constant for growth. The equation was differentiated and linearized for the initial condition of $t=0$.

$$\ln(X) = k_g t + \ln(X_0) \quad \text{Eq (6.2)}$$

Graphical solutions of this equation were used to determine k_g for the growth of bacteria in batch cultures. In some experiments a two-phase based growth analysis yielded more accurate results as compared to the single-phase growth analysis. For that, graphical solutions of equation 6. were used to determine k_g for the 1st phase of growth experiments for each culture. To determine k_g for later experimental phases, Equation 6.1 was solved for the initial condition when $t=t_1$ and $X=X_1$.

$$\ln(X_2) = k_g(t_2 - t_1) + \ln(X_1) \quad \text{Eq (6.3)}$$

Graphical solutions of this equation were used to determine k_g for the 2nd phase of the two-phase growth experiments.

6.2.6.1.2 Dye degradation kinetics calculations

Dye degradation was modeled using first order kinetics

$$\frac{dC}{dt} = rC$$

where C is the concentration of the dye (measured as optical density at the respective wavelengths for the dyes and their mixture), and r was the reaction rate.

For single phase dye degradation, substituting $r = k_c' X$ where k_c' was the reaction rate constant for biodegradation and X was biomass concentration (measured as optical density at 600 nm), and $X = X_0 e^{k_g t}$.

$$\frac{dC}{dt} = -k_c' X_0 e^{k_g t} C$$

Or

$$\ln(C) = \frac{-k_c'X_o}{k_g}(1 + e^{k_g t}) + \ln(C_o) \quad \text{Eq (6.4)}$$

Graphical solutions to this equation were obtained by graphing x as $(1 + e^{k_g t})$ and y as $\ln(C)$. The slope of the result line is m_2 which can be used to solve for k_c' .

The degradation constant k_c' , can be calculated as:

$$k_c' = \frac{m_2 \cdot m_1}{X_o}$$

Where $m_2 = k_c$, $m_1 = k_g$, and X_o is the bacterial biomass at $t=0$.

For the two-phase dye degradation process, the calculations are as follows:

$$\frac{dC}{dt} = rC$$

Substituting $r = k_c X$ where k_c was the reaction rate constant for biodegradation and X was biomass concentration (measured as optical density at 600 nm), and $X = X_o e^{k_g t}$.

$$\frac{dC}{dt} = k_c X_o e^{k_g t} C$$

In this equation, everything except C and t are constants. Separating the variables to integrate,

$$\int \frac{dC}{C} = k_c X_o \int (e^{k_g t}) dt$$

results in an equation where the right side of the equation is in the form that can be integrated as follows (Lide 1996):

$$\int e^{ax} dx = \frac{1}{a} e^{ax}$$

which, when integrated with the initial condition is $t=0$, can be solved as:

$$\int_{t=0}^{t=t} e^{k_g t} dt = \frac{1}{k_g} (e^{k_g t} - e^0)$$

So, integrating both sides when $X(t=0)=X_o$ results in:

$$\ln(C) = \frac{k_c X_0}{k_g} (e^{k_g t} - 1) - \ln(C_0) \quad \text{Eq (6.5)}$$

$$C = C_0 \times \exp \left[\frac{k_c X_0}{k_g} (e^{k_g t} - 1) \right]$$

where $C(t=0) = C_0$.

Integrating instead when the initial condition is $t=t_1$ and $X(t=t_1) = X_1$, the equation can be solved as:

$$\frac{dC}{C} = k_c X_1 e^{k_g(t-t_1)} dt$$

where everything except C and t are constants; so, the right side of the equation is in the form (Lide, 1996):

$$\int e^{a(x-b)} dx = \frac{1}{e^{ab}} \int e^{ax} = \frac{e^{ax}}{a(e^{ab})} = \frac{1}{a} e^{a(x-b)}$$

Integrating the right-side results in:

$$\int_{t=t_1}^t e^{k_g(t-t_1)} dt = \frac{1}{k_g} (e^{k_g t} - e^{k_g t_1})$$

and integrating both sides results in

$$\ln(C) = \frac{k_c X_1}{k_g} (e^{k_g t} - e^{k_g t_1}) - \ln(C_1) \quad \text{Eq (6.6)}$$

Graphical solutions to this equation are obtained by graphing x as $(e^{k_g t} - 1)$ or $(e^{k_g t} - e^{k_g t_1})$, and y as $\ln(C)$. The slope of the result line is $\frac{k_c X_0}{k_g}$; or $\frac{k_c X_1}{k_g}$, and can be used to solve for k_c . The intercept for the graphical solution is $\ln(C_0)$ or $\ln(C_1)$.

6.2.7 Biodegradation assessment through FTIR and GC-MS

6.2.7.1 Fourier transform Infrared (FTIR) spectral analysis

Samples, taken before and after treatment of the dye mixture containing synthetic textile wastewater by the two bacterial cocultures, were subjected to FTIR analysis (spectrum 65 FTIR spectrometer equipped with ATR; Perkin Elmer, Waltham, MA, USA) and the transmission spectra were studied. Samples were centrifuged at 4000 rpm for 30 min to obtain the biomass free supernatant. Dye metabolites were extracted using ethyl acetate followed by drying over anhydrous Na_2SO_4 and evaporation in a rotary evaporator. The dried residues were dissolved in methanol and the analysis was carried out in the mid IR region of $600\text{-}4000\text{ cm}^{-1}$ with 16 scan speed.

6.2.7.2 GC-MS analysis

The decolorized solutions (obtained after treatment of the individual and mixed reactive azo dyes by the bacterial cocultures) were centrifuged at 4000 rpm for 30 min to remove the biomass. Extraction of metabolites from the supernatants was carried out using equal volumes of HPLC grade ethyl acetate, followed by evaporation using nitrogen evaporator. The residues were then dissolved in HPLC grade methanol and used for GC-MS analysis. The GC-MS system used in this study was Shimadzu GCMS-QP2010 Plus, equipped with DB-5ms UI column (30.0-meter, 0.25 μm , 0.25 mm). 1.0 μL of the samples were auto injected into the system. The flow rate of the carrier gas i.e., helium was 1mL/min. Temperature of the injector was 280 °C. The oven temperature was raised up to 300 °C at the rate of 5 °C/ min. The scanning range for the mass spectrum was 30-600 m/z . The mass spectra obtained were compared and identified with the help of NIST library.

6.2.8 Toxicity analyses for the synthetic dye wastewater metabolites

Toxicity of the control and decolorized dye mixture containing synthetic wastewater samples (obtained after treatment with the cocultures), was determined through phytotoxicity (Turker and Camper, 2002) and brine shrimp acute toxicity assays (Meyer et al., 1982) (Methods, as described in section 3.2.3, and 3.2.4).

6.2.9 Statistical analyses

Duplicate experiments were performed for the screening, OFAT, and detoxification analyses. Mean values and standard error of means were computed using Microsoft

Excel 2016. For the significance analysis, one-way analysis of variance (ANOVA) followed by Tukey's honest significant difference (Tukey's HSD) at the significance level of $\alpha = 0.05$ ($p < 0.05$), was done using SPSS (IBM SPSS Statistics for Windows, Version 20.0., Armonk, NY, USA). All the statistical procedures for response surface methodology (done in triplicates) were performed using Design-Expert version 7.0.0 (Stat-Ease). For the growth and degradation analysis (performed in duplicates), data linearization, normalization and regression analyses were performed in Microsoft Excel 2016.

6.3 Results

Reactive azo dyes (RB 221, RR 195, and RY145) decolorizing bacteria with varying temperature tolerance, were isolated and screened from two separate locations i.e., textile industry sludge dumping site and hot- water spring. Bacterial cocultures were designed and optimized for the treatment of dye mixture containing synthetic textile wastewater. Moreover, the dye removal kinetics and degradation products were studied.

6.3.1 Isolation and screening of dye decolorizing mesophilic and thermophilic bacteria

Dye decolorizing bacteria were isolated using culture enrichment method. A total of 64 (mesophilic) and 23 (thermophilic) isolates were obtained from the sludge and hot spring enriched broth cultures, respectively. To select efficient decolorizers, isolates were screened by incubating for 24 hours under static and shaking conditions (50 ppm dye mixture containing synthetic effluent), and all the mesophilic and thermophilic isolates showed more efficient color reduction without agitation. Of the 64 mesophilic isolates, 5 showed 60-69 and less than 50% color removal under static and shaking conditions, respectively. 6 isolates showed 50-59 and less than 50% decolorization with and without agitation, respectively. With the 49 isolates less than 50% color removal was observed under both incubation conditions. The remaining 4 isolates i.e., isolate number S1, S6, S14, and S19, demonstrated 73-83 and 17-60% color reduction under static and shaking incubation conditions, respectively (Fig. 6.1). These four isolates were then selected for further investigations carried out under static condition. The isolates were then designated using the codes as given in Table 6.5.

Of the 23 thermophilic bacterial isolates, 15 showed less than 50% color reduction under static and shaking incubation. 4 isolates demonstrated 67-73 and less than 50 percent color removal, with and without agitation, respectively. The remaining 4 isolates viz. T14, T15, T18, and T23 efficiently decolorized the dye mixture effluent under both static and shaking incubation condition, with a former being a little more effective for the color reduction. With these 4 isolates, 82-85 and 53-71% decolorization was recorded under static and shaking conditions, respectively (Fig. 6.2). These four isolates were then selected for further experimentation under static

condition. The strain names used for the designation of the selected isolates are given in Table 6.5.

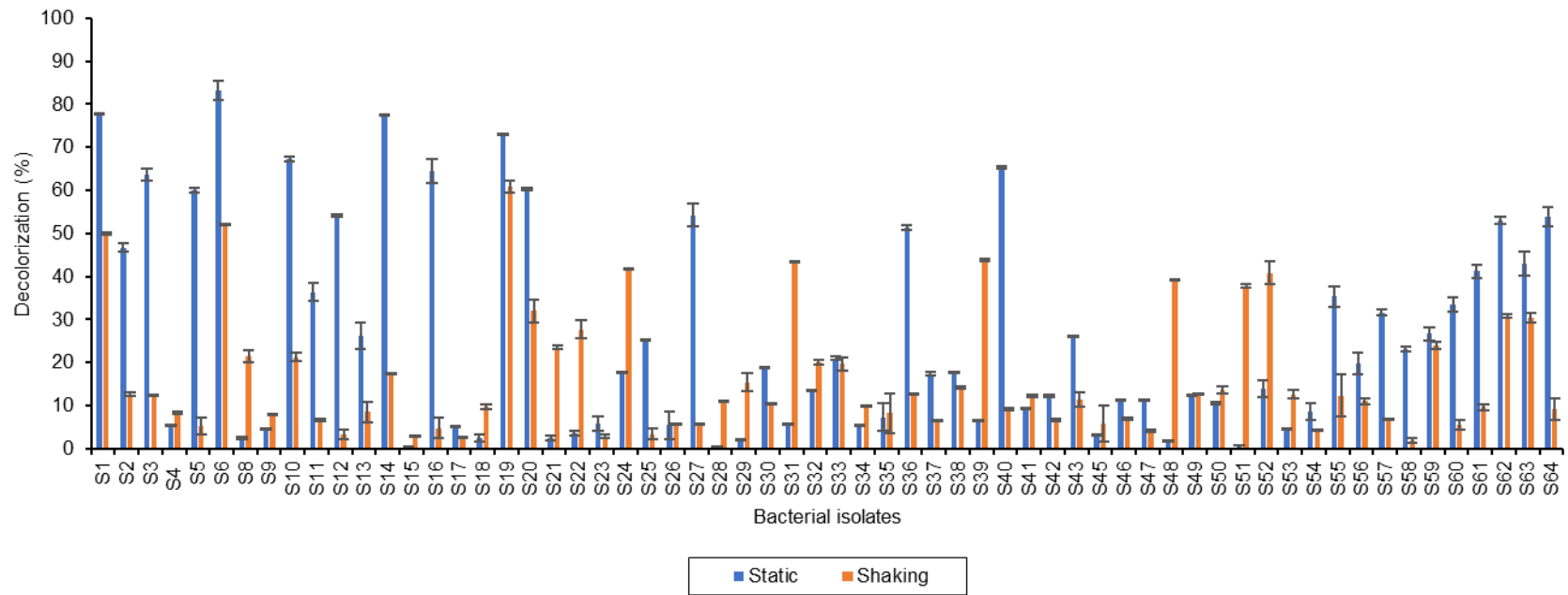


Fig. 6.1 Comparison of mesophilic bacterial isolates for the decolorization of a reactive azo dye mixture containing synthetic textile effluent under static and shaking conditions (24 hours)

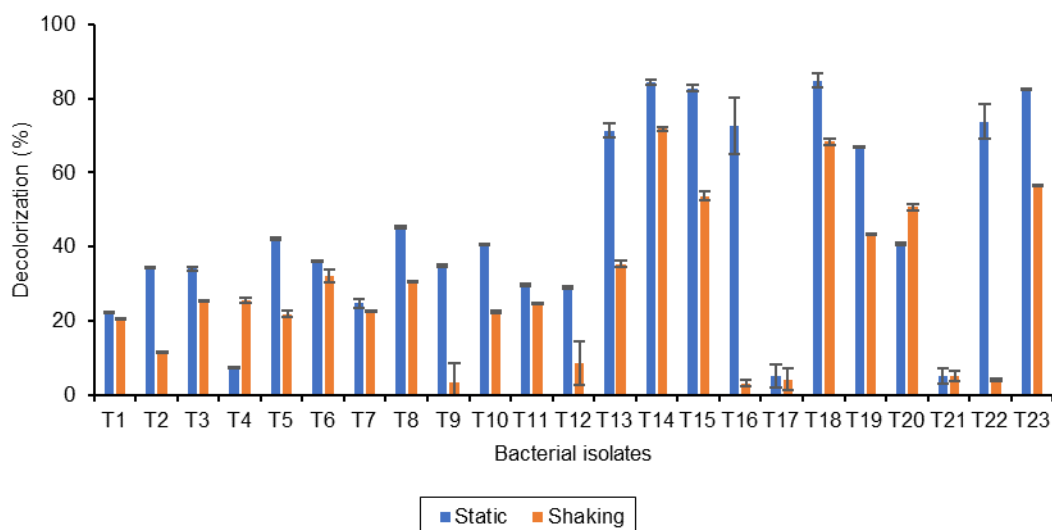


Fig. 6.2 Comparison of thermophilic bacterial isolates for the decolorization of a reactive azo dye mixture containing synthetic textile effluent under static and shaking conditions (24 hours)

Table 6.5 Strain names for the selected mesophilic and thermophilic isolates

Strain name used for the mesophilic isolate	Mesophilic Isolate number	Strain name used for the thermophilic isolate	Thermophilic isolate number
NHS1	S1	NHT1	T18
NHS2	S14	NHT2	T15
NHS3	S19	NHT3	T14
NHS4	S6	NHT4	T23

6.3.2 Microbial identification

Morphological and biochemical characteristics of the selected mesophilic and thermophilic isolates are summarized in the Table 6.6. Partial 16S rRNA gene sequence (Section 4.3, Appendix 4) similarity search of the selected mesophilic isolates i.e., NHS1, NHS2, NHS3, and NHS4, in NCBI BLAST showed 98-99% homology to *Pseudomonas aeruginosa*, *Pseudomonas* sp., *Escherichia* sp., and *Escherichia coli*, respectively. Evolutionary analysis of the isolates was done using Neighbor-joining method in MEGA7.0. The phylogenetic tree was drawn to scale with the sum of branch length = 0.56739624 (Fig. 6.3) The sequences were submitted to GenBank under the following accession IDs: MG984057, MG984058, MG984059, and MG984060 for *Pseudomonas aeruginosa* NHS1, *Pseudomonas* sp. NHS2, *Escherichia* sp. NHS3, and *Escherichia coli* NHS4, respectively.

For the thermophilic bacterial isolates i.e., NHT1, NHT2, NHT3, and NHT4, 16S rRNA gene sequences (Section 4.4, Appendix 4) similarity analysis demonstrated 99% homology to *Aeribacillus pallidus*, *Aeribacillus* sp., *Geobacillus* sp., and *Brevibacillus borstelensis*, respectively. Neighbor-joining method was used for the evolutionary analysis. The phylogenetic tree was drawn to scale, with the sum of branch length = 0.25952423, in MEGA7.0 (Fig. 6.4). Sequences were submitted to Genbank and the accession IDs i.e., MG984061, MG984062, MG984063, and MG984064 were assigned to *Aeribacillus pallidus* NHT1, *Aeribacillus* sp. NHT2, *Geobacillus* sp. NHT3, and *Brevibacillus borstelensis* NHT4, respectively.

Table 6.6 Morphological and biochemical properties of bacterial isolates

Sr. No.	Properties	Mesophilic bacterial isolates				Thermophilic bacterial isolates			
		NHS1	NHS2	NHS3	NHS4	NHT1	NHT2	NHT3	NHT4
1	Colonial characteristics	Small, round, mucoid, slightly raised, shiny colonies with green pigmentation	Small, round, moist, transparent colonies with greenish tinge	Round, mucoid shiny colonies with entire margins	Round, mucoid, whitish colonies with entire margins	Round pale, raised colonies with entire margins	Mucoid round colonies with curled margins	White, mucoid colonies with slightly curled margins	Slightly rough, colonies with creamy texture
2	Grams Reaction	–	–	–	–	+	+	+	+
3	Morphology	Coccobacilli	Coccobacilli	Coccobacilli	Coccobacilli	Rods	Rods	Rods	Rods
4	Glucose	±	±	+	+	+	+	+	±
5	Sucrose	–	–	+	±	–	+	–	+
6	Lactose	±	–	+	+	+	±	–	+
7	Citrate	+	±	±	–	+	+	±	+
8	H ₂ S production	–	–	–	–	–	–	–	–
9	Indole production	–	–	±	+	–	–	–	–
10	Methyl red	–	–	+	+	–	+	+	+
11	Voges Proskauer	–	–	–	–	–	±	+	–
12	Motility	+	+	+	+	+	±	±	+
13	Catalase	+	+	+	+	+	+	+	+
14	Oxidase	+	+	–	–	+	+	±	+
15	Endospore formation	–	–	–	–	+	+	–	+

+ Positive result, – Negative result, ± Variable response

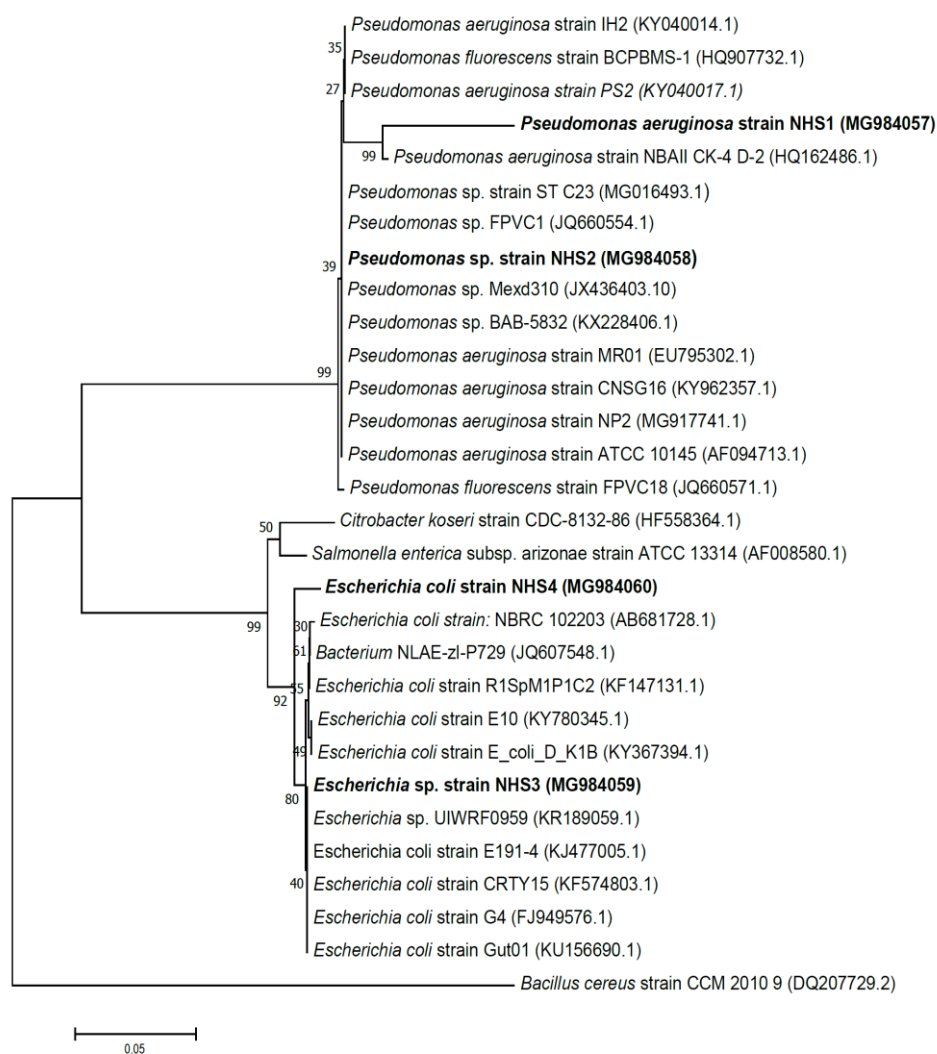


Fig. 6.3 Neighbor-joining phylogenetic tree of the mesophilic reactive azo dye mixture decolorizing bacterial isolates: *Pseudomonas aeruginosa* NHS1, *Pseudomonas* sp. NHS2, *Escherichia* sp. NHS3, and *Escherichia coli* NHS4, with the type strains and other representatives of closely related species of the genera: *Pseudomonas* and *Escherichia*. The numbers at the nodes indicate the bootstrap values obtained with 1000 replicates.

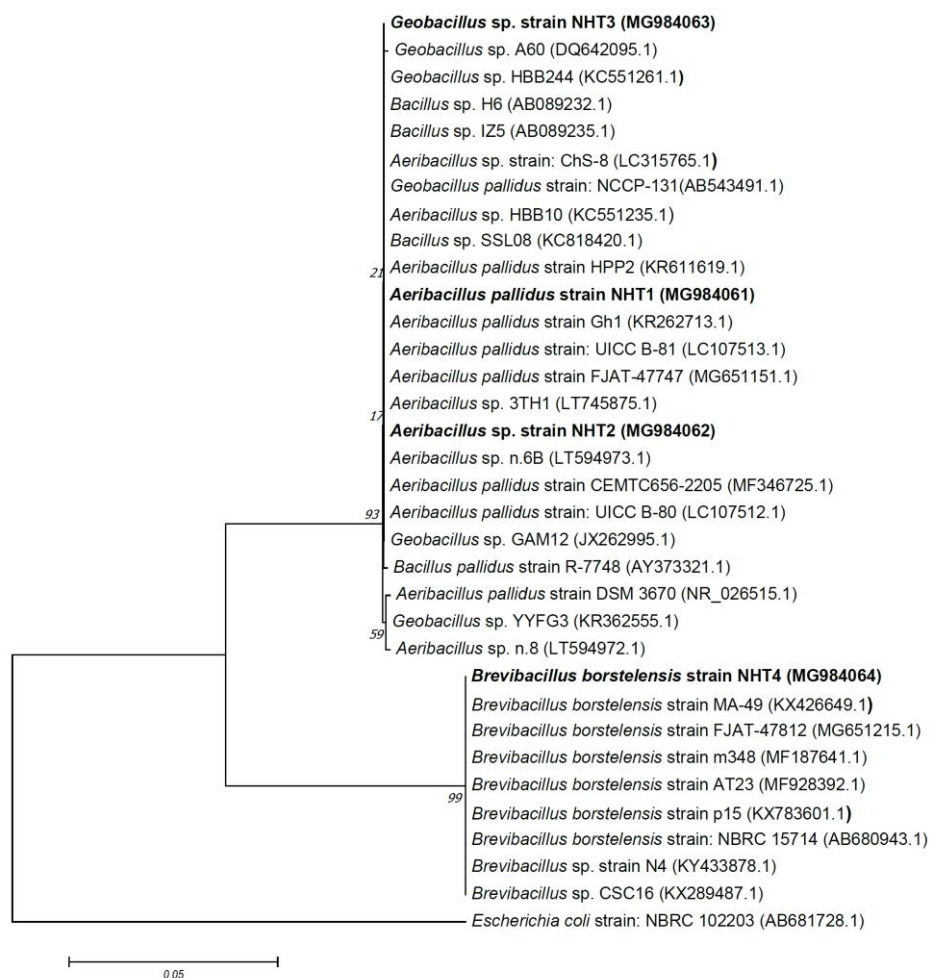


Fig. 6.4 Neighbor-joining phylogenetic tree of the thermophilic reactive azo dye mixture decolorizing bacterial isolates: *Aeribacillus pallidus* NHT1, *Aeribacillus* sp. NHT2, *Geobacillus* sp. NHT3, and *Brevibacillus borstelensis* NHT4, with the type strains and other representatives of closely related species of the genera: *Aeribacillus*, *Geobacillus*, and *Brevibacillus*. The numbers at the nodes indicate the bootstrap values obtained with 1000 replicates.

6.3.3 Consortia development and screening

The selected dye decolorizing isolates were mixed in different combinations to ascertain the effect of cocultures on the decolorization performance of bacteria for the synthetic textile wastewater. Ten different cocultures were tested for each of the two types of bacteria i.e., mesophilic and thermophilic (Tables 6.1 and 6.2). For the mesophilic bacteria, an improvement in the decolorization activity (3-19%) was observed with all the ten combinations, when compared to the color removal performance of the pure cultures. The best results were obtained when all the four mesophilic isolates were combined (M. coculture-10), as 11-22% rise in decolorization percentage was observed when compared to that of individual isolates. With that coculture, 93.42% decolorization was observed within 24 hours (Fig. 6.5a). For the thermophilic isolates, the color removal activity of the bacteria was also improved when they were mixed in different combinations with a 2-8% rise observed in the decolorization efficiency with the different cocultures in comparison to the pure cultures. The highest decolorization percentage was observed when all the four thermophilic isolates were mixed (T. coculture-10). With that, ~8-10% increase in the decolorization efficiency was observed when compared to the decolorization activity of the individual isolates. The coculture containing all the four thermophilic isolates showed 91.92% decolorization in 24 hours (Fig. 6.5b). The two most efficient cocultures (mesophilic and thermophilic) for each type of bacteria were then subjected to process optimization studies.

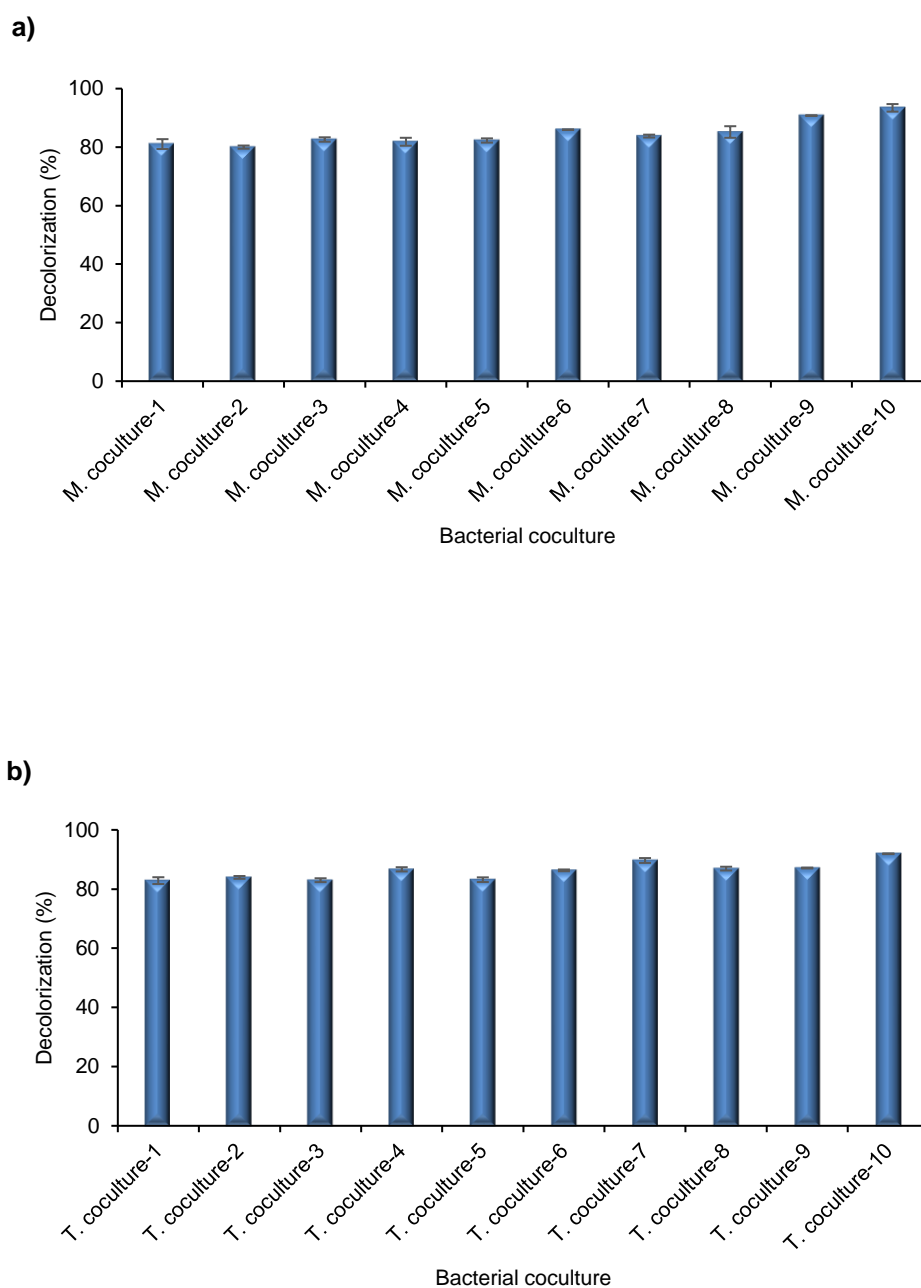


Fig. 6.5 Effect of different coculture combinations of the selected bacterial isolates on the decolorization of reactive azo dye mixture containing synthetic textile effluent under static condition (24 hours), (a) Mesophilic cocultures; (b) Thermophilic cocultures

6.3.4 Optimization of culture conditions for the dye mixture decolorization (OFAT) by the mesophilic and thermophilic bacterial cocultures

The decolorization potential of the two bacterial cocultures was investigated under different culture conditions through the use of different secondary carbon and nitrogen sources, incubation temperatures, initial pH, dye and salt concentrations.

6.3.4.1 Carbon sources

Decolorization activity of the mesophilic and thermophilic bacterial cocultures was examined in the presence of different additional carbon sources at 0.1% (w/v) (Fig. 6.6). Both types of cocultures showed best decolorization results with glucose. In the presence of glucose, mesophilic and thermophilic bacterial cocultures showed a 94.44 and 91.89% color reduction after 120 hours. The second most suitable carbon source was sucrose with 72.77% decolorization observed after 120 hours. However, with the other three tested carbon sources i.e., sorbitol, lactose, and starch, decolorization efficiency wasn't much improved in comparison to the dye as a sole carbon source, and 50.4, 54.85, and 51.95% color removal was recorded after 120 hours, respectively. For the thermophilic bacterial coculture, sorbitol and sucrose were found as the second and third best carbon sources, with a 68.16 and 61.34% decolorization observed after 120 hours of incubation, respectively. Lactose and starch were the least suitable carbon sources for the thermophilic coculture, as 58.28 and 52.96% decolorization was observed after 120 hours, respectively.

6.3.4.2 Nitrogen sources

Decolorization performance of the cocultures was investigated in the presence of two organic (yeast extract and peptone) and three inorganic (sodium nitrate, potassium nitrate, and ammonium sulfate) nitrogenous compounds at 0.1% (w/v) (Fig. 6.7). Both types of cocultures showed highest decolorization with the organic nitrogen source i.e., yeast extract, as 92.24 and 90.77% decolorization was shown by the mesophilic and thermophilic cocultures, respectively. With peptone as the second best organic nitrogen source, 79.76 and 73.21% color reduction, was demonstrated by the mesophilic and thermophilic cocultures, respectively. For the mesophilic coculture, the respective decolorization percentages observed with the inorganic nitrogen sources i.e.,

ammonium sulphate, potassium nitrate, and sodium nitrite were: 66.18, 57.71, and 53.79%. The thermophilic coculture showed 63.61, 58.68, and 56.44% color reduction with potassium nitrate, ammonium sulphate, and sodium nitrite, respectively.

6.3.4.3 Temperature

The color removal efficacy of the bacterial cocultures was assessed under different incubation temperatures (Fig. 6.8). The decolorization performance of the mesophilic bacterial coculture improved with the rise in temperature from 25-35 °C, with the highest color reduction (97.98% in 24 hours) recorded at 35 °C. At 40 °C, the color removal ability was reduced to 79.91% (120 hours). The decolorization efficiency was greatly affected by the further increase to 45 °C, as only 32.35% decolorization was recorded after 120 hours of treatment. The thermophilic bacterial coculture, showed best results at 50 °C, with a 90.73% decolorization observed after 24 hours. The color removal ability (95-99% in 120 hours) was retained over a range of temperature i.e., 45-55 °C. Further increase in temperature beyond 55 °C, resulted in a sharp decline in the color reduction to 31.32% after 120 hours.

6.3.4.4 pH

The color reduction efficiency of the cocultures was tested with different initial pH values (Fig. 6.9). The mesophilic coculture effectively removed the dye mixture over a range of pH i.e., 6-8 with up to 98% decolorization recorded after 24 hours. The color removal ability was slightly diminished at lower and higher tested initial pH values i.e., 5 and 9, as 80.73 and 83.73% decolorization was recorded after 120 hours, respectively. The thermophilic coculture also showed improved decolorization ability with the increasing pH values and showed up to 95% color reduction over the pH range of 7-9 in 48 hours. The decolorization potential of the coculture was considerably reduced at lower and higher pH values i.e., 5, 6, and 10, with a 48.99, 64.18, and 72.67% decolorization recorded after 120 hours.

6.3.4.5 Dye concentration

The dye tolerance profile of the cocultures was studied by using different initial dye

mixture concentrations (Fig. 6.10). The mesophilic bacterial coculture showed up to 98% decolorization at 50 and 100 ppm dye mixture concentrations within 24 hours. The decolorization performance was slightly slowed down at 150 ppm as 98 percent decolorization was achieved after 120 hours. The color removal potential was further reduced at 200 and 250 ppm dye mixture concentrations with 89.71 and 84.62% decolorization was observed after 120 hours. At higher dye mixture concentrations i.e., 300, 400, 500 the decolorization efficacy was reduced below 30%. In the case of the thermophilic coculture, highest efficiency was observed at 50 ppm, as 97.47% color reduction occurred after 48 hours of incubation. This was followed by 100 and 150 ppm dye mixture concentrations, at which 94.15 and 81.48% decolorization was recorded after 120 hours. However, at higher dye mixture concentrations very low color removal was observed (< 25%).

6.3.4.6 NaCl concentration

Dye decolorization potential of the two bacterial cocultures was tested in the presence of varying NaCl concentrations (Fig. 6.11). The mesophilic coculture showed 94-96% decolorization in the presence of 2 and 4% NaCl, within 24 hours. The color removal percentage was reduced at 6 and 8% NaCl concentrations, with 61.51 and 59.59% decolorization observed after 120 hours, respectively. At 10% NaCl, the mesophilic coculture showed 45.75% color reduction after 120 hours. The decolorization ability of the thermophilic bacterial coculture was considerably affected by the presence of salt in the medium. The coculture demonstrated 78.61 and 58.79% decolorization at 2 and 4% NaCl concentrations, respectively. Further increase in the salt concentration greatly reduced the color removal potential of the coculture, as only less than 40% dye removal was observed after 120 hours. Table 6.7 summarizes the co-substrate utilization, pH, temperature, dye, and salt tolerance profiles of the two bacterial cocultures.

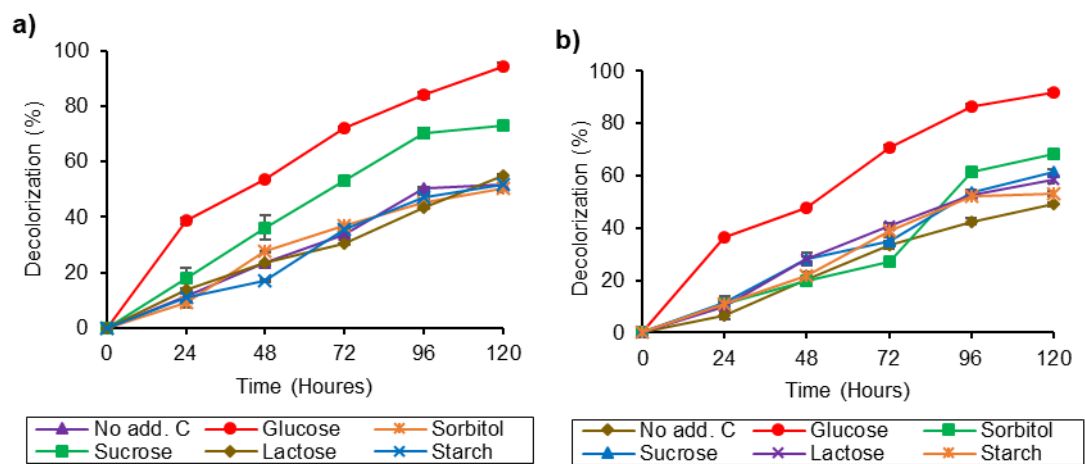


Fig. 6.6 Decolorization performance of (a) Mesophilic bacterial coculture (pH 7.0, 35°C); and (b) Thermophilic bacterial coculture (pH 7.0, 50°C) for the synthetic dye effluent, in the presence of different carbon sources (0.1% [w/v])

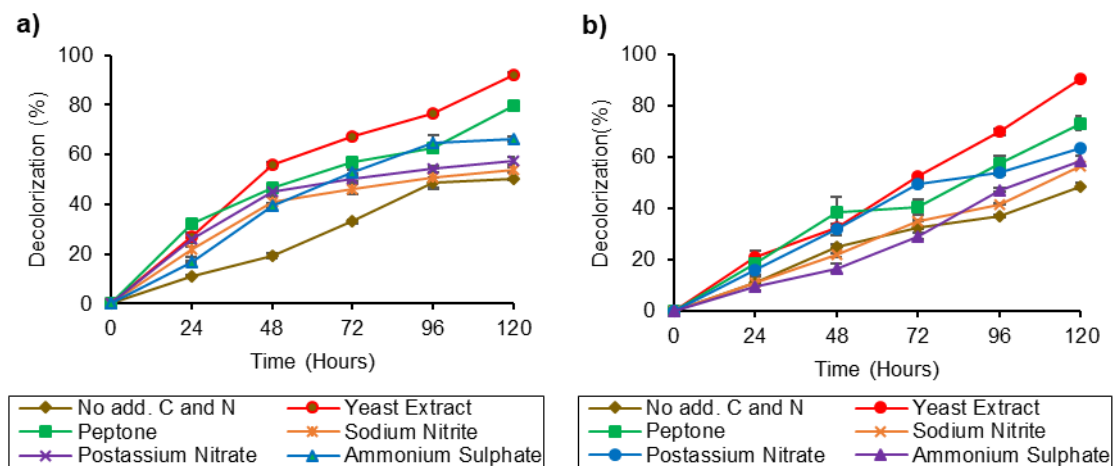


Fig. 6.7 Decolorization performance of (a) Mesophilic bacterial coculture (pH 7.0, 35); and (b) Thermophilic bacterial coculture (pH 7.0, 50°C) for the synthetic dye effluent, in the presence of different nitrogen sources (0.1% [w/v])

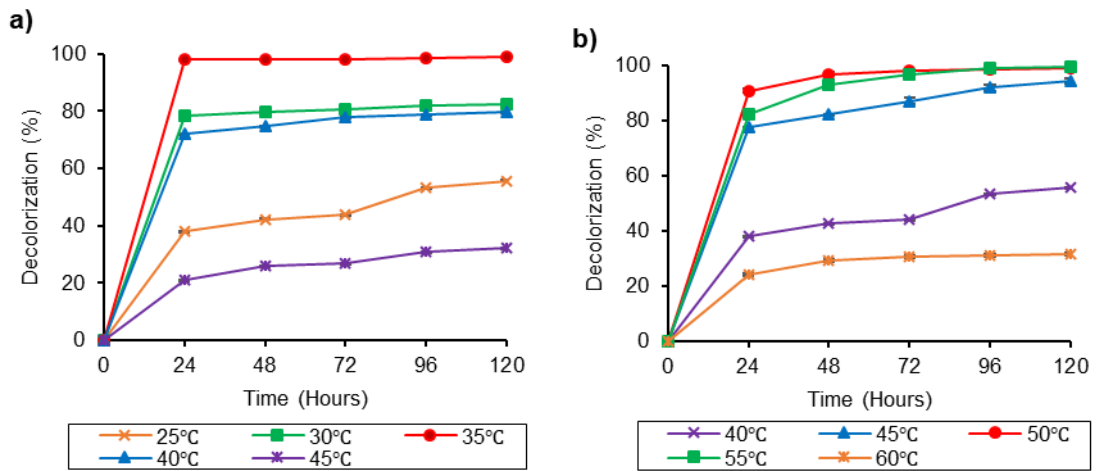


Fig. 6.8 Decolorization performance of (a) Mesophilic bacterial coculture (50 ppm, pH 7.0, glucose and yeast extract 0.1% [w/v] each); and (b) Thermophilic bacterial coculture (50 ppm, pH 7.0, glucose and yeast extract 0.1% [w/v] each); for the synthetic dye effluent, at different temperatures.

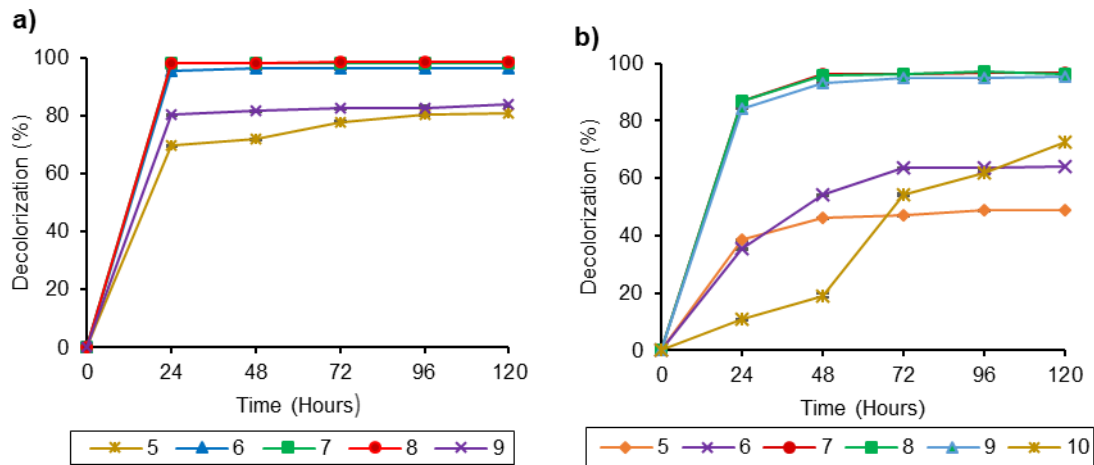


Fig. 6.9 Decolorization performance of (a) Mesophilic bacterial coculture (50 ppm, 35°C, glucose and yeast extract 0.1% [w/v] each); and (b) Thermophilic bacterial coculture (50 ppm, 50°C, glucose and yeast extract 0.1% [w/v] each); for the synthetic dye effluent, at different initial pH

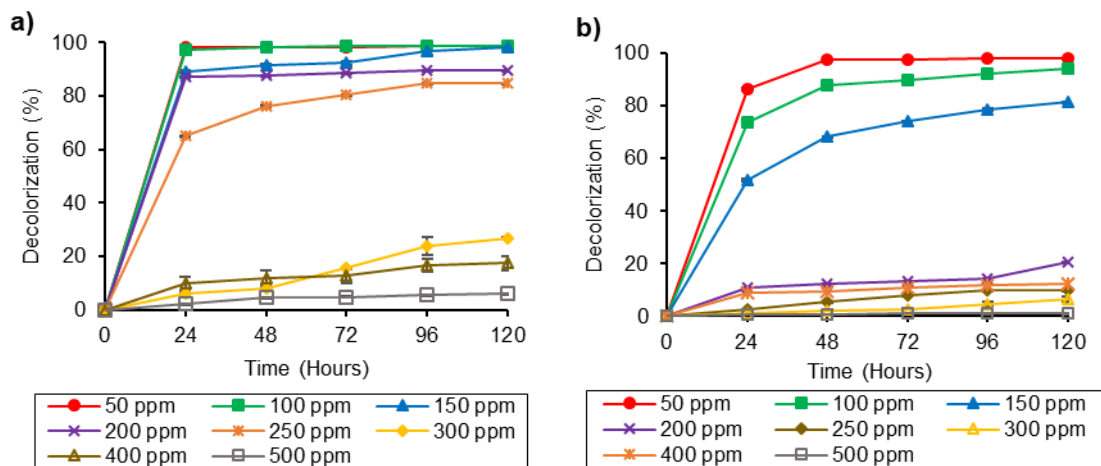


Fig. 6.10 Decolorization performance of (a) Mesophilic bacterial coculture (pH 7.0, 35°C, glucose and yeast extract 0.1% [w/v] each); and (b) Thermophilic bacterial coculture (pH 7.0, 50°C, glucose and yeast extract 0.1% [w/v] each); for the synthetic dye effluent, at different initial dye concentrations (ppm)

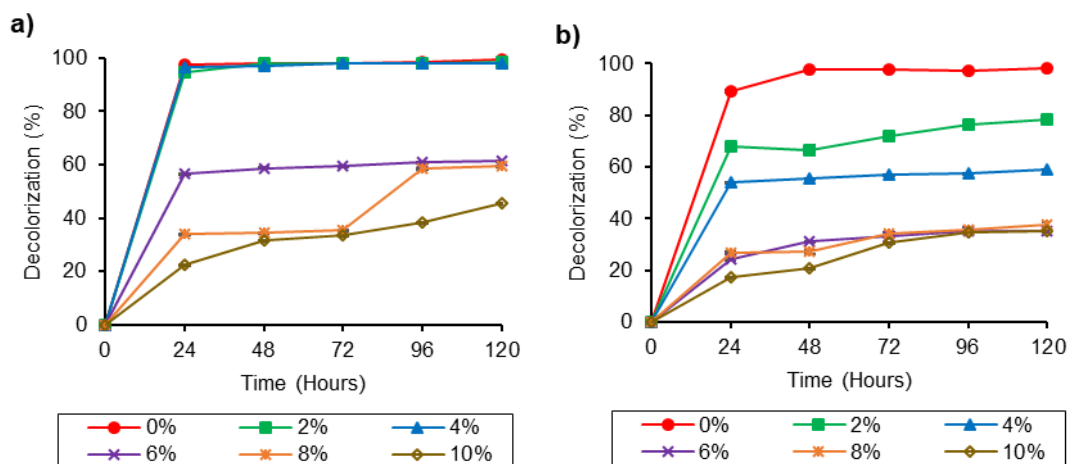


Fig. 6.11 Decolorization performance of (a) Mesophilic bacterial coculture (100 ppm, pH 7.0, 35°C, glucose and yeast extract 0.1% [w/v] each and (b) Thermophilic bacterial coculture (50 ppm, pH 7.0, 50°C, glucose and yeast extract 0.1% [w/v] each); for the synthetic dye effluent, at different NaCl concentrations (% [w/v])

Table 6.7 Co-substrate utilization, pH, temperature, dye, and salt tolerance profiles of the mesophilic and thermophili bacterial cocultures

Factor	Mesophilic bacterial coculture	Thermophilic bacterial coculture
Carbon sources		
(0.1% [w/v])		
No add. C	++	+
Glucose	++++	++++
Sorbitol	++	++
Sucrose	+++	++
Lactose	++	++
Starch	++	++
Nitrogen Sources		
(0.1% [w/v])		
No add. C and N	++	+
Yeast extract	++++	++++
Peptone	+++	+++
Sodium nitrite	++	++
Potassium nitrate	++	++
Ammonium sulfate	++	++
Temperature (°C)		
25	++	nt
30	+++	nt
35	++++ ^a	nt
40	+++	++
45	+	++++
50	nt	++++ ^a
55	nt	++++ ^b
60	nt	+
pH		
5	+++	+
6	++++ ^a	++
7	++++ ^a	++++ ^a
8	++++ ^a	++++ ^a
9	+++	++++ ^b
10	nt	+++
Dye Concentration		
(ppm)		
50	++++ ^a	++++ ^a
100	++++ ^a	++++ ^b
150	++++ ^b	+++
200	++++ ^b	-/+

250	+++	-
300	-	-
500	-	-

NaCl concentration

(% [w/v])

0	++++ ^a	++++ ^a
2	++++ ^a	+++
4	++++ ^a	++
6	++	+
8	++	+
10	+	+

++++ (90-99% color removal in 120 hours); +++ (70-89 color removal in 120 hours), ++ (50- 69% color removal in 120 hours); + (30-49% color removal in 120 hours); +/- (20-29 % color removal in 120 hours); - (less than 20% in 120 hours); +++^a (85-95% color removal in 24 hours); +++^b (85-95% color removal in 48 hours); nt (not tested)

6.3.5 Response Surface Methodology (RSM)

6.3.5.1 Box-Behnken statistical design

RSM was applied for the decolorization optimization by the bacterial cocultures. Key variables for color removal and their levels for the Box-Behnken design (BBD) were selected on the basis of OFAT findings. Averaged values from the triplicate experiments, performed using the BBD design layout (17 runs with 5 center points, for both types of cocultures) were used for the quadratic model. Experiments were conducted for 24 and 48 hours for the mesophilic and thermophilic bacterial cocultures, respectively. Tables 6.8-6.9 enlist the designs, predicted, and experimental response values for the respective the respective cocultures. The software calculated the response Y i.e., is the percent decolorization, in terms of the coded and actual factors.

The equation with coded factors for the mesophilic coculture is as follows:

$$Y = +86.38 - 5.62 \times A + 5.09 \times B - 13.95 \times C - 1.78 \times A \times B - 0.17 \times A \times C + 1.01 \times B \times C - 14.95 \times A^2 + 0.52 \times B^2 - 7.75 \times C^2 \quad \text{Eq (6.7)}$$

The equation with actual factors for the mesophilic coculture is as follows:

$$\text{Decolorization (\%)} = -699.62083 + 43.29142 \times \text{Temperature} + 7.84792 \times \text{pH} + 0.21810 \times \text{Dye Concentration} - 0.35500 \times \text{Temperature} \times \text{pH} - 4.46667\text{E-}004 \times \text{Temperature} \times \text{Dye Concentration} + 0.013433 \times \text{pH} \times \text{Dye Concentration} - 0.59790 \times \text{Temperature}^2 + 0.52250 \times \text{pH}^2 - 1.37867\text{E-}003 \times \text{Dye Concentration}^2 \quad \text{Eq (6.8)}$$

The equation with coded factors for the thermophilic coculture is as follows:

$$Y = +85.07 + 2.25 \times A - 2.25 \times B - 13.45 \times C - 0.29 \times A \times B - 2.42 \times A \times C + 0.19 \times B \times C - 6.40 \times A^2 + 0.73 \times B^2 - 6.08 \times C^2 \quad \text{Eq (6.9)}$$

The equation with actual factors for the thermophilic coculture is as follows:

$$\text{Decolorization (\%)} = -577.69650 + 27.46550 \times \text{Temperature} - 11.54475 \times \text{pH} + 0.67020 \times \text{Dye Concentration} - 0.057000 \times \text{Temperature} \times \text{pH} - 9.68000\text{E-}003 \times$$

$$\text{Temperature} \times \text{Dye Concentration} + 3.85000\text{E-}003 \times \text{pH} \times \text{Dye Concentration} - 0.25591 \times \text{Temperature}^2 + 0.73475 \times \text{pH}^2 - 2.43010\text{E-}003 \times \text{Dye Concentration}^2 \text{ Eq (6.10).}$$

Table 6.8 Box-Behnken design layout with observed and actual response values for the mesophilic coculture

Runs	Factor A (Temperature, °C)	Factor B (pH)	Factor C (Dye concentration, ppm)	Actual values decolorization (Y, %)	Predicted values for decolorization (Y1, %)	Externally studentized residuals
1	30	6	175	70.21	70.71	-0.648
2	40	6	175	62.28	63.02	-0.987
3	30	8	175	85.18	84.44	0.987
4	40	8	175	70.15	69.64	0.648
5	30	7	100	82.24	83.09	-1.163
6	40	7	100	71.56	72.17	-0.802
7	30	7	250	56.13	55.52	0.802
8	40	7	250	44.78	43.93	1.163
9	35	6	100	90.37	89.02	2.302
10	35	8	100	97.29	97.18	0.135
11	35	6	250	58.99	59.10	-0.135
12	35	8	250	69.94	71.29	-2.302
13	35	7	175	85.17	86.38	-0.894
14	35	7	175	86.94	86.38	0.394
15	35	7	175	87.88	86.38	1.150
16	35	7	175	87.32	86.38	0.677
17	35	7	175	84.59	86.38	-1.441

Table 6.9 Box-Behnken design layout with observed and actual response values for the thermophilic coculture

Runs	Factor A (Temperature, °C)	Factor B (pH)	Factor C (Dye concentration, ppm)	Actual values decolorization (Y, %)	Predicted values for decolorization (Y1, %)	Externally studentized residuals
1	45	7	100	78.67	79.12	-0.497
2	55	7	100	83.89	84.20	-0.333
3	45	9	100	75.49	75.18	0.333
4	55	9	100	79.57	79.12	0.497
5	45	8	50	80.58	81.37	-0.914
6	55	8	50	89.78	90.72	-1.112
7	45	8	150	60.25	59.31	1.112
8	55	8	150	59.77	58.98	0.914
9	50	7	50	96.87	95.62	1.605
10	50	9	50	91.22	90.73	0.538
11	50	7	150	67.85	68.34	-0.538
12	50	9	150	62.97	64.21	-1.605
13	50	8	100	83.42	85.07	-1.087
14	50	8	100	84.45	85.07	-0.377
15	50	8	100	87.16	85.07	1.471
16	50	8	100	83.43	85.07	-1.079
17	50	8	100	86.88	85.07	1.221

The ANOVA results indicated that the models for the mesophilic and thermophilic cocultures were highly significant as shown by the very low probability values of the Fisher's F test ($[P_{\text{model}} > F] = 0.0001$). Additionally, the values of lack of fit for both models were non-significant. For the mesophilic coculture: $F = 1.225$ ($p = 0.409$) and for the thermophilic coculture: $F = 0.713$ ($p = 0.593$). These non-significant values indicated the statistical adequacy of the models for the studied response i.e., dye decolorization. Determination and multiple correlation coefficients i.e., R^2 and R were used for the assessment of models' goodness for further analyses. For both models, predicted R^2 values showed reasonable agreement with the adjusted R^2 values. For mesophilic coculture the values were: $\text{Pred. } R^2 = 0.9600$; $\text{Adj. } R^2 = 0.9892$; and for the thermophilic coculture the values were: $\text{Pred. } R^2 = 0.9291$; $\text{Adj. } R^2 = 0.9754$. Through the adeq. Precision, signal to noise ratio was determined. The adeq. Precision values for the mesophilic and thermophilic cocultures were 46.544 and 27.832, respectively. These demonstrate adequate signals for the models (values greater 4 are considered workable). In the case of the normal probability plots of the internally studentized residuals, straight lines were obtained (Fig. 6.12). Moreover, the externally studentized residuals values were in the allowable range with no outliers (Tables 6.10-6.11). No model transformation was required in each case, as evident from the Box-Cox plots for the respective cocultures. The current λ values matched the design values for the models (Fig. 6.13).

Table 6.10 ANOVA for Quadratic Model of synthetic dye wastewater decolorization by Mesophilic coculture

Source	Sum of Squares	df	Mean Square	F Value	p-value	Prob > F
Model	3285.4451	9	365.049	164.074	< 0.0001	significant
A-Temperature	253.0125	1	253.012	113.718	< 0.0001	
B-pH	207.1630	1	207.163	93.111	< 0.0001	
C-Dye concentration	1557.378	1	1557.37	699.975	< 0.0001	
AB	12.6025	1	12.6025	5.6642	0.0489	
AC	0.11222	1	0.1122	0.05043	0.8287	
BC	4.06023	1	4.0602	1.8248	0.2188	
A ²	940.748	1	940.748	422.826	< 0.0001	
B ²	1.1495	1	1.1495	0.5166	0.4956	
C ²	253.2211	1	253.221	113.812	< 0.0001	
Residual	15.5743	7	2.2249			
Lack of Fit	7.4589	3	2.4863	1.2254	0.4095	not significant
Pure Error	8.1154	4	2.028			
Cor Total	3301.01	16				

df = degree of freedom; Std. Dev. = 1.49; Mean = 75.94; C.V. = 1.96; PRESS = 132.02; R² = 0.9953; Adj. R² = 0.9892; Pred. R² = 0.9600; Adeq. Precision = 46.544

Table 6.11 ANOVA for Quadratic Model of synthetic dye wastewater decolorization by Thermophilic coculture

Source	Sum of Squares	df	Mean Square	F Value	p-value Prob > F	
Model	1898.5521	9	210.95	71.5658	< 0.0001	significant
A-Temperature	40.59	1	40.59	13.7703	0.0075	
B-pH	40.63511	1	40.6351	13.7856	0.0075	
C-Dye concentration	1447.489	1	1447.489	491.0676	< 0.0001	
AB	0.3249	1	0.3249	0.1102	0.7496	
AC	23.4256	1	23.4256	7.9472	0.0258	
BC	0.148225	1	0.14822	0.0502	0.8290	
A ²	172.3419	1	172.3419	58.467	0.0001	
B ²	2.273	1	2.273	0.7711	0.4090	
C ²	155.4048	1	155.4048	52.7218	0.0002	
Residual	20.6334	7	2.9476			
Lack of Fit	7.1927	3	2.3978	0.7135	0.5931	not significant
Pure Error	13.4406	4	3.3601			
Cor Total	1919.186	16				

df = degree of freedom; Std. Dev. = 1.72; Mean = 79.54; C.V. = 2.16; PRESS = 136.09; R² = 0.9892; Adj. R² = 0.9754; Pred. R² = 0.9291; Adeq. Precision = 27.832

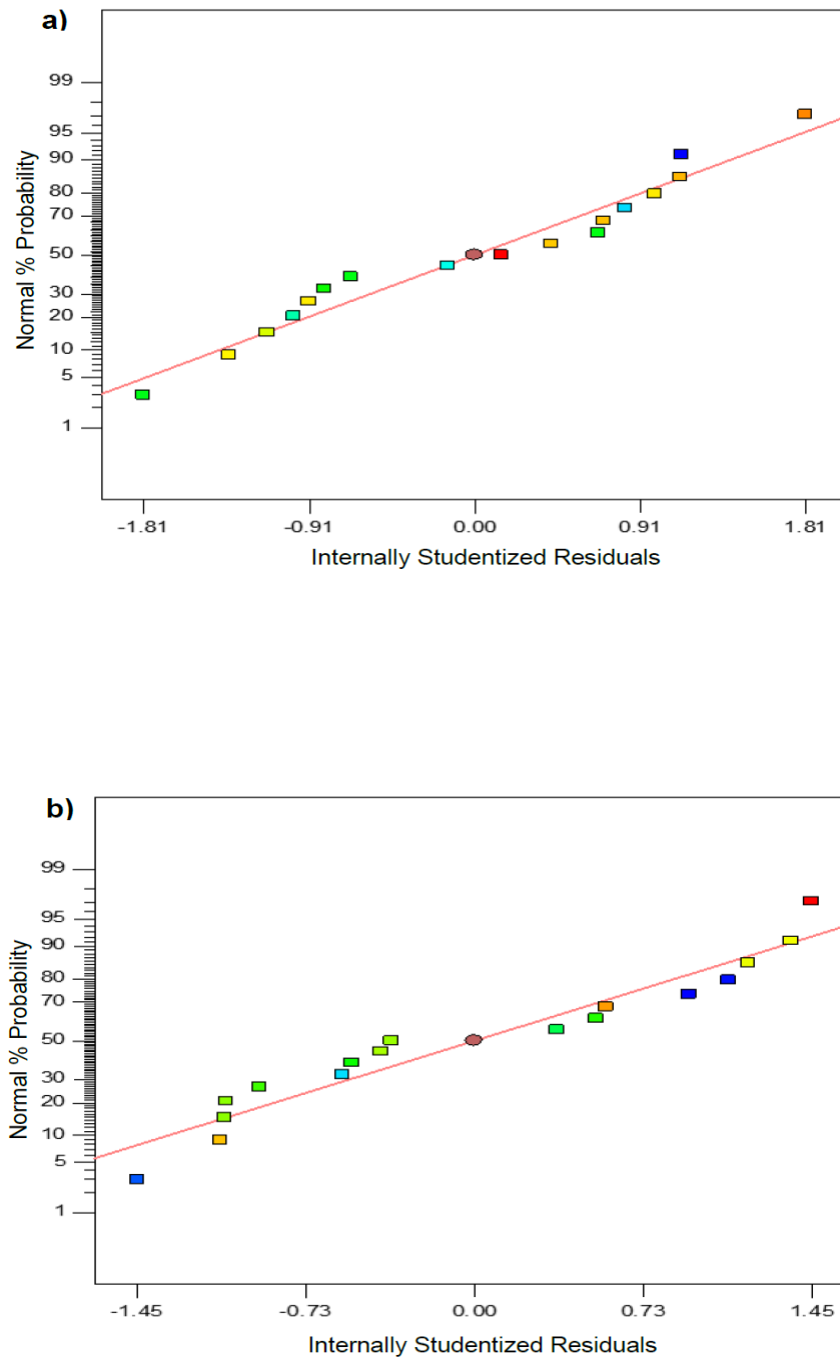


Fig. 6.12 The normal % probability vs. studentized residuals plots for (a) Mesophilic coculture, and (b) Thermophilic coculture

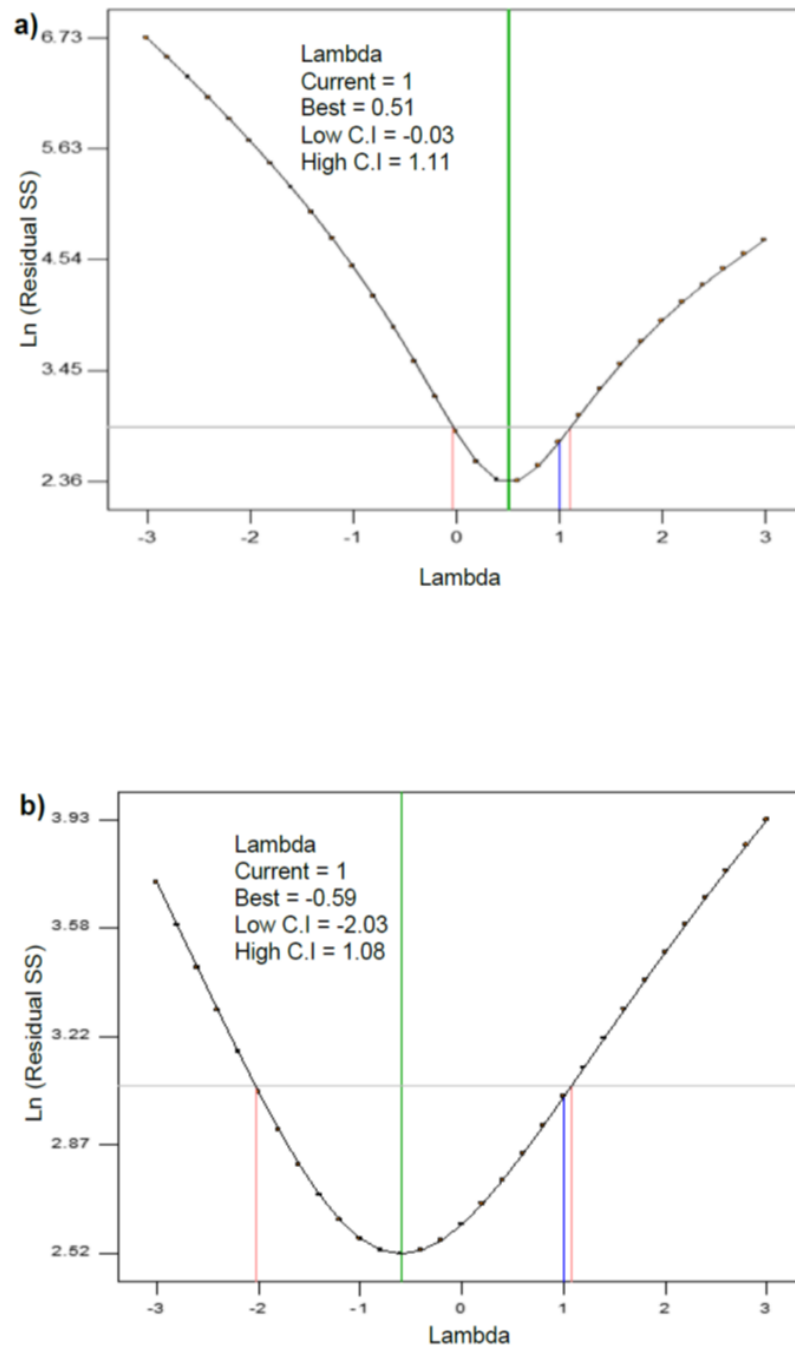


Fig. 6.13 Box-Cox plots of model transformation for the decolorization of synthetic dye wastewater by (a) Mesophilic coculture, and (b) Thermophilic coculture

6.3.5.2 Analysis of the factors and their interactions affecting the decolorization process by the cocultures

The interaction of variables and the response in a given model can be inferred from the 2D contour and 3D response surface plots. For the mesophilic coculture, the contour and 3D plots, demonstrating the interaction between pH and temperature, with third parameter i.e., the dye concentration held constant, are given in Fig. 6.14a and b, respectively. In that case, the decolorization percentage increased from 80-97% with the rise in temperature from 30-35 °C over the pH range of 6.0-8.0. The highest percentage removal was observed around 35 °C. The temperature had a dominating effect in that case, as the decolorization was reduced at lower and higher temperature values. This was also indicated by the elliptical shape of the contour plot. The interaction between temperature and dye concentration is shown in Fig. 6.15a and b. pH was the constant factor in case. As evident from the circular shape of the contour plot, the two variables didn't have apparent interaction and independently affected the decolorization. The dye concentration of 100 ppm and a temperature value of 35 °C gave the highest decolorization. Fig. 6.16a and b show the interaction between pH and the dye mixture concentration with temperature kept at a constant value. The dye concentration had a more pronounced effect than the pH on the decolorization, that was reduced beyond the dye concentration of 100 ppm, as indicated by the elliptical plot shape.

For the thermophilic coculture, Fig. 6.17a and b show the interaction between temperature and pH. The temperature had a greater effect on the decolorization efficacy as indicated by a more centralized response around temperature with the maximum removal observed around 50 °C. The shape of the contour plot was elliptical in that case. The interaction between the temperature and dye concentration are showed in Fig. 6.18a and b. The slightly elliptical shape of the contour plot indicates that the dye concentration had a stronger influence on the color removal as compared to the temperature. Similarly, the plots for the interaction between pH and dye concentration showed that the process was greatly affected by the changing dye concentrations as compared to the varying pH values for which the percentage removal was relatively less affected (Fig. 6.19a and b).

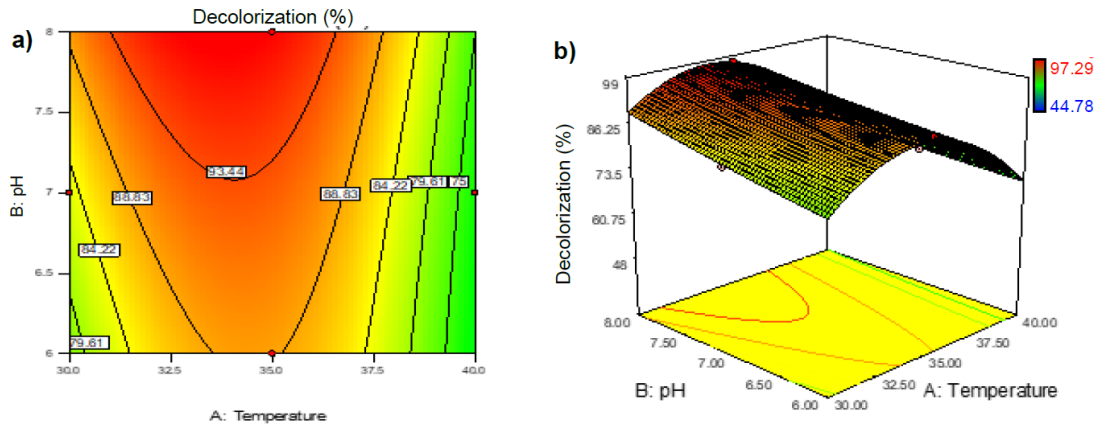


Fig. 6.14 Response surface plots showing interactions of pH and temperature for the synthetic dye wastewater decolorization by the Mesophilic coculture (a) contour plot and (b) 3D surface plot

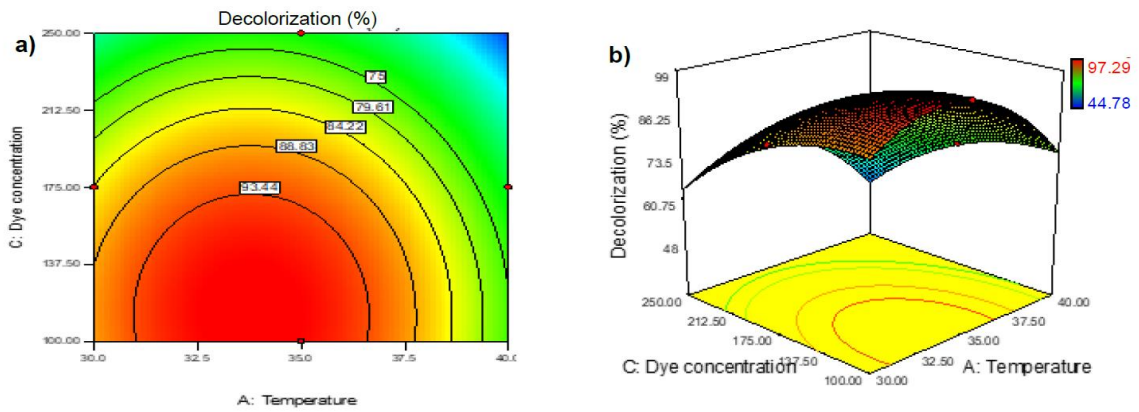


Fig. 6.15 Response surface plots showing interactions of dye concentration and temperature for the synthetic dye wastewater decolorization by the Mesophilic coculture (a) contour plot (b) 3D surface plot

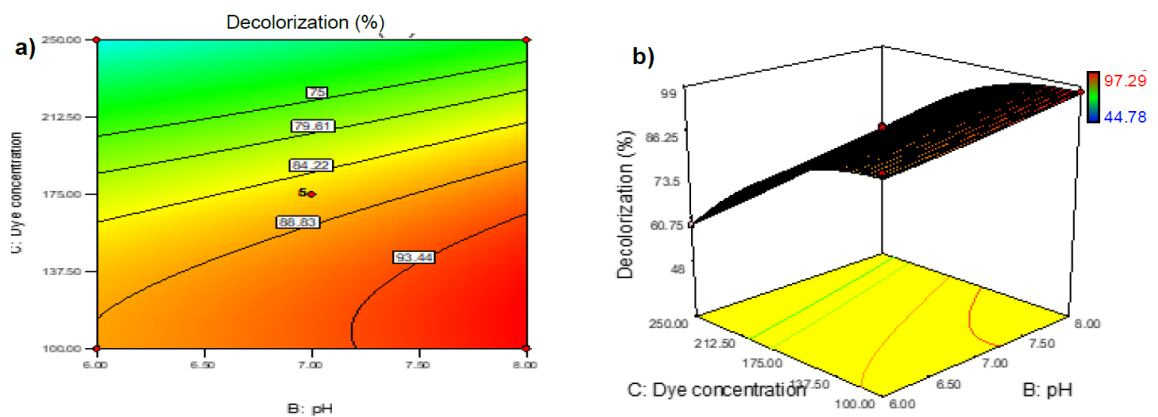


Fig. 6.16 Response surface plots showing interactions of dye concentration and pH for the synthetic dye wastewater decolorization by the Mesophilic coculture (a) contour plot and (b) 3D surface plot

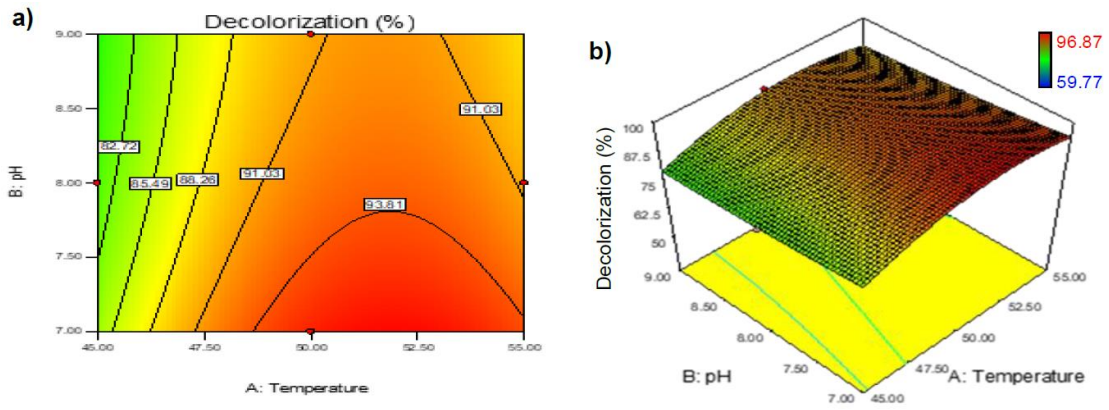


Fig. 6.17 Response surface plots showing interactions of pH and temperature for the synthetic dye wastewater decolorization by the thermophilic coculture (a) contour plot and (b) 3D surface plot

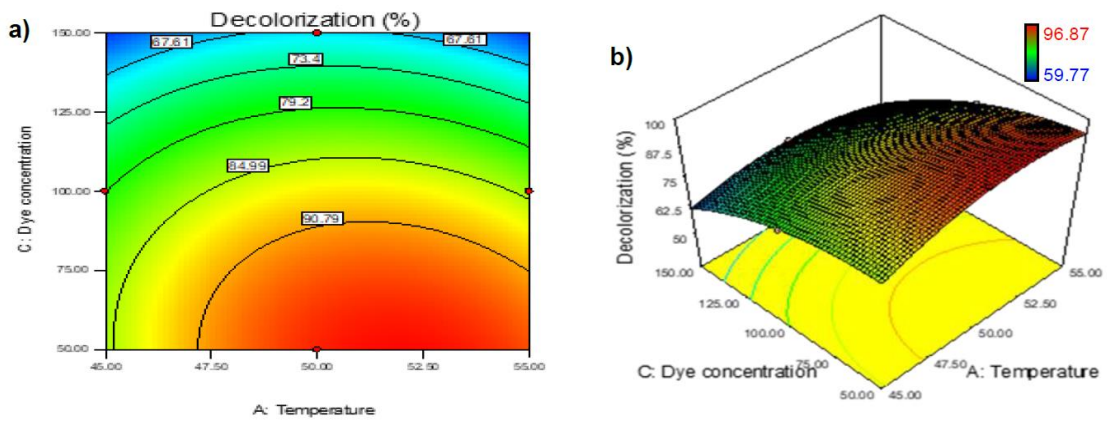


Fig. 6.18 Response surface plots showing interactions of dye concentration and temperature for the synthetic dye wastewater decolorization by the thermophilic coculture (a) contour plot and (b) 3D surface plot

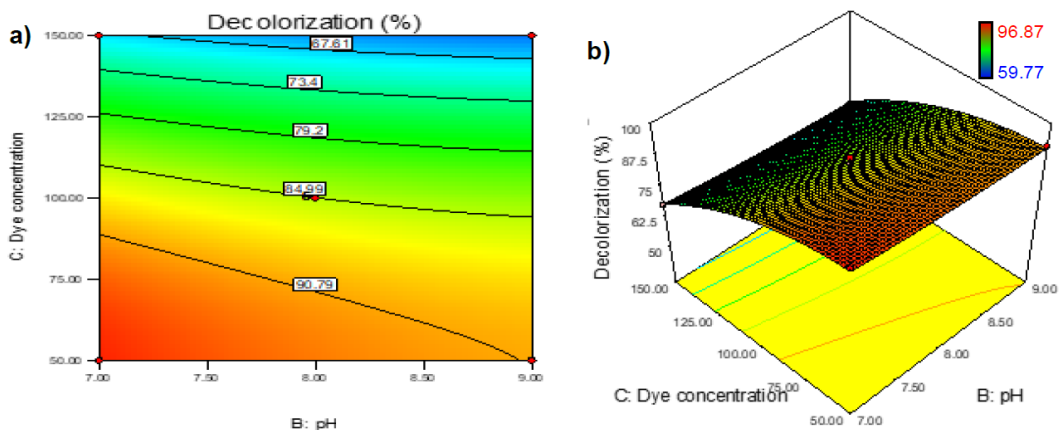


Fig. 6.19 Response surface plots showing interactions of dye concentration and pH for the synthetic dye wastewater decolorization by the thermophilic coculture (a) contour plot and (b) 3D surface plot

6.3.5.3 Model validation for the bacterial cocultures

To further validate the optimized combinations, confirmatory experiments were performed for the models designed for the two cocultures. This was done by selecting the factors combinations affecting the decolorization response as suggested by the software. The observed values were in accord with the predicted ones for each model. Tables 6.12-6.13 enlist the selected combinations for the validation studies. The optimum combinations, giving highest color removal for each coculture are highlighted.

Table 6.12 Predicted solutions for model validation and confirmation for the mesophilic coculture

Solution	Temperature (°C)	pH	Dye concentration (ppm)	Predicted response (%)	Observed response (%)
1	34.57	7.69	111.15	96.27	97.98
2	34.23	7.27	132.7	93.62	92.12
3	35.07	7.56	121.09	94.82	95.27
4	35.07	7.24	136.25	92.54	92.99
5	35.35	6.62	111.24	90.71	91.26

Table 6.13 Predicted solutions for model validation and confirmation for the thermophilic coculture

Solution	Temperature (°C)	pH	Dye concentration (ppm)	Predicted response (%)	Observed response (%)
1	51.52	7.15	99.75	87.73	86.94
2	51.85	7.14	80.25	92.38	91.25
3	50.25	7.31	60.07	94.15	93.11
4	51.77	7.96	58	92.89	91.71
5	51.43	8.31	60.59	91.86	89.22

6.3.6 Bacterial growth and dye decolorization/degradation studies

The kinetics of the dye removal process by the mesophilic and thermophilic bacteria was investigated. To gain a detailed insight, interrelation of the bacterial growth and dye removal rates (measured using the optical density), was investigated using first order kinetics. Through a set of batch experiments, degradation rates were studied for the individual dyes by the pure mesophilic and thermophilic bacterial cultures and the dye mixture by the pure as well as cocultures.

6.3.6.1 Kinetics studies for the individual dyes by the pure bacterial cultures

6.3.6.1.1 Mesophilic bacteria

Bacterial growth k_g and dye degradation k_c , rates were calculated using equations 6.2 and 6.4, respectively. Table 6.14 enlists the bacterial growth and dye degradation rate constants for the individual dyes (50 ppm) with their respective determination coefficient values R^2 , by the mesophilic pure bacterial cultures. *P. aeruginosa* NHS1 showed highest growth in the presence of RR 195 dye with a k_g value of 0.187 (hr^{-1}), this was followed by the RB 221 and RY 145 dyes with the k_g values of 0.103 (hr^{-1}) and 0.083 (hr^{-1}), respectively (Panel a in Fig. 6.20-6.22). However, the degradation rate was found to be higher for the blue dye with k_c value of -2.738 (hr^{-1}), followed by red and yellow dyes with k_c values of -1.963 (hr^{-1}) and -1.624 (hr^{-1}) (Panel b in Fig. 6.20-6.22). *Pseudomonas* sp. NHS2, also showed more growth with the red dye. The growth rate values observed with the blue and yellow dyes were however similar. The respective k_g values were 0.107 (hr^{-1}), 0.074 (hr^{-1}), and 0.08 (hr^{-1}), respectively (Panel a in Fig. 6.23-6.25). The degradation rate was higher for the blue dye followed by the red and yellow dye. The calculated k_c values for the respective dyes were: -1.359 (hr^{-1}), -0.534 (hr^{-1}), and -0.491 (hr^{-1}) (Panel b in Fig. 6.23-6.25).

In the case of *Escherichia* sp. NHS3, higher growth rate was observed with the yellow dye and the k_g value was 0.233 (hr^{-1}). The growth rate observed with the yellow and blue dyes were 0.225 and 0.049 (hr^{-1}), respectively (Panel a in Fig. 6.26-6.28). The removal rate was highest for the yellow dye as the k_c values was -1.711 (hr^{-1}). For the blue dye the lowest degradation rate was observed: $k_c = -0.226$ (hr^{-1}) and for the yellow dye, the removal rate was intermediate ($k_c = -0.405$ hr^{-1}) between the rates observed

for the other two dyes (Panel b in Fig. 6.26-6.28). For *E. coli* NHS4, higher growth rate was recorded in the presence of red dye followed by yellow and blue. The respective k_g values were 0.496, 0.397, and 0.058 (hr^{-1}), respectively (Panel a in Fig. 6.29-6.31). The degradation rate constant k_c for the red, yellow, and blue dyes were -0.991 , -0.592 , and -0.412 (hr^{-1}), respectively (Panel b in Fig. 6.29-6.31). Using the growth and degradation rates, growth and color dynamics were modeled for each type of culture. Growth and degradation were well predicted with the help of model for *P. aeruginosa* NHS1 for all the three dyes (Panel c in Fig. 6.20-6.22). In the case of *Pseudomonas* sp. NHS2, the more accurate degradation model was obtained for the red dye as compared to the other dyes, however the growth models were found to be good for all the three dyes (Panel c in Fig. 6.23-6.25). In the case of *Escherichia* sp. NHS3, both growth and degradation models were found to be good for the respective responses for the blue dye. The degradation models were good for the other two dyes, but the growth was not well predicted (Panel c in Fig. 6.26-6.28). Models for *E. coli* NHS4, only partially predicted the growth and color variation profiles (Panel c in Fig. 6.29-6.31).

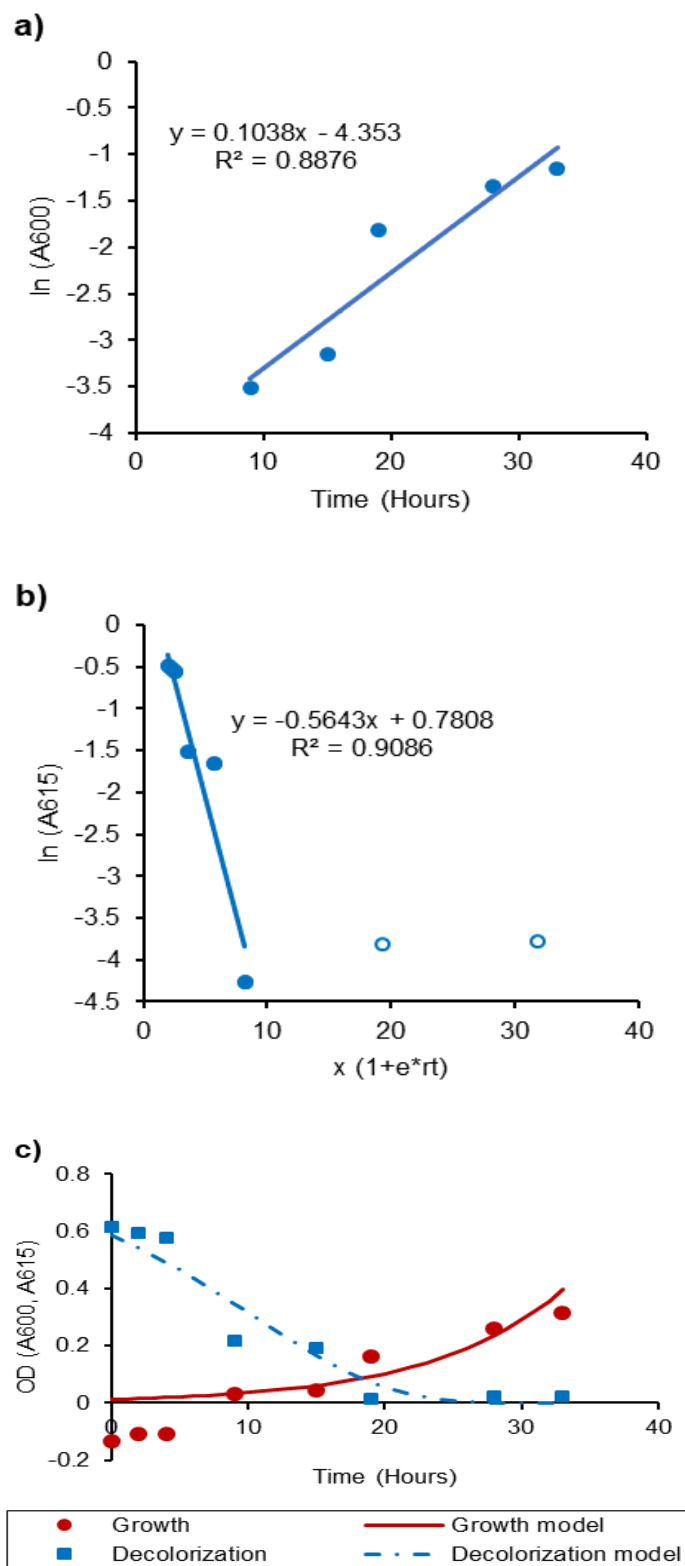


Fig. 6.20 Growth and degradation by *P. aeruginosa* NHS1 for RB 221 dye. Linear regression analysis for the rate constants determination for (a) Growth; (b) Dye degradation. Growth and degradation graphs (c) with the original and modeled data indicated by the squares and solid lines, respectively

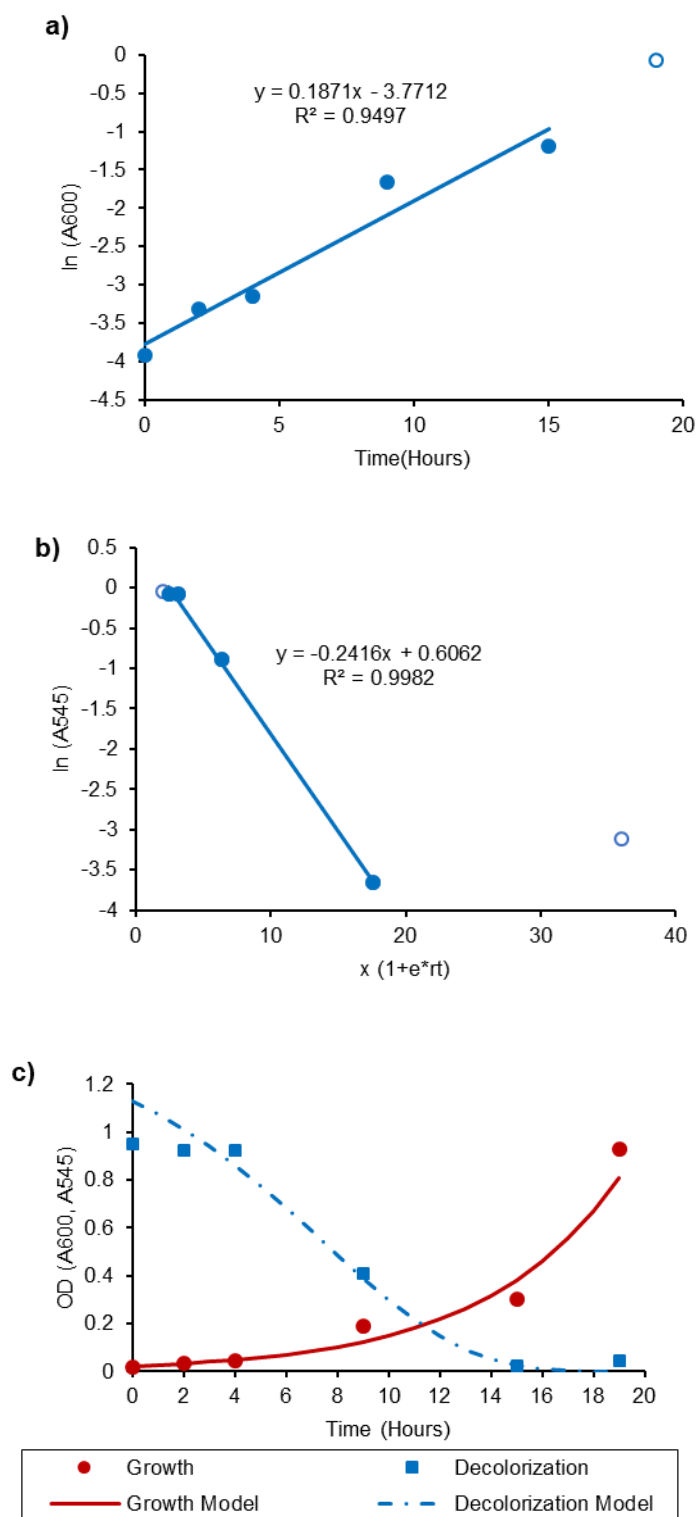


Fig. 6.21 Growth and degradation by *P. aeruginosa* NHS1 for RR 195 dye. Linear regression analysis for the rate constants determination for (a) Growth; (b) Dye degradation. Growth and degradation graphs (c) with the original and modeled data indicated by the squares and solid lines, respectively

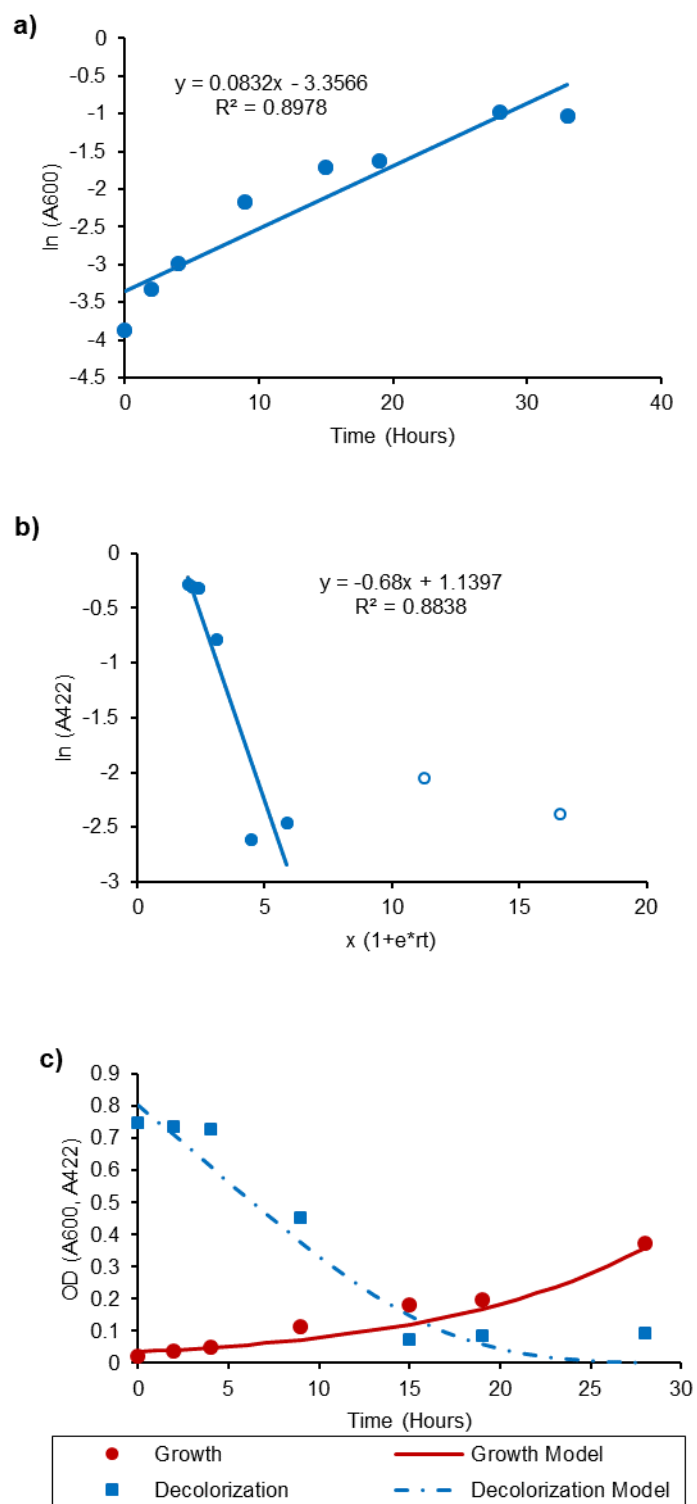


Fig. 6.22 Growth and degradation by *P. aeruginosa* NHS1 for RY 145 dye. Linear regression analysis for the rate constants determination for (a) Growth; (b) Dye degradation. Growth and degradation graphs (c) with the original and modeled data indicated by the squares and solid lines, respectively

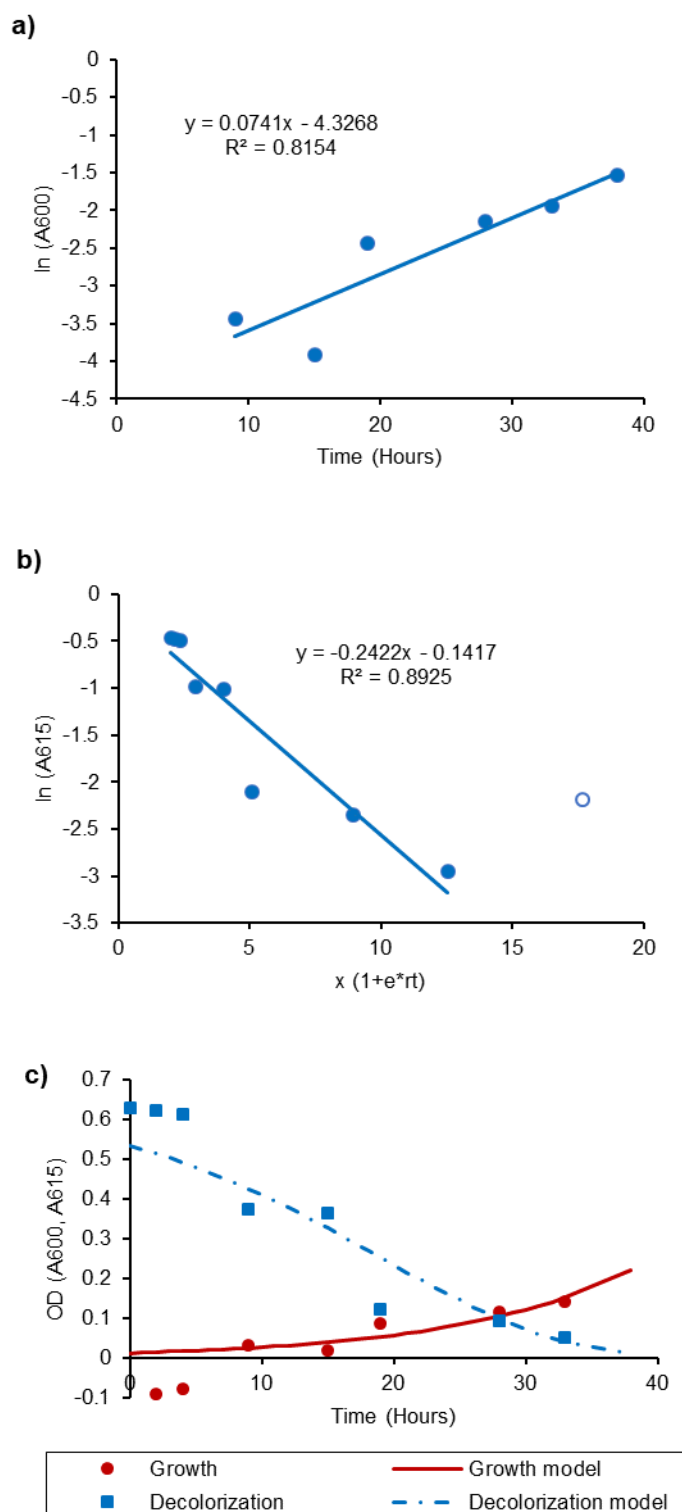


Fig. 6.23 Growth and degradation by *Pseudomonas* sp. NHS2 for RB 221 dye. Linear regression analysis for the rate constants determination for (a) Growth; (b) Dye degradation. Growth and degradation graphs (c) with the original and modeled data indicated by the squares and solid lines, respectively

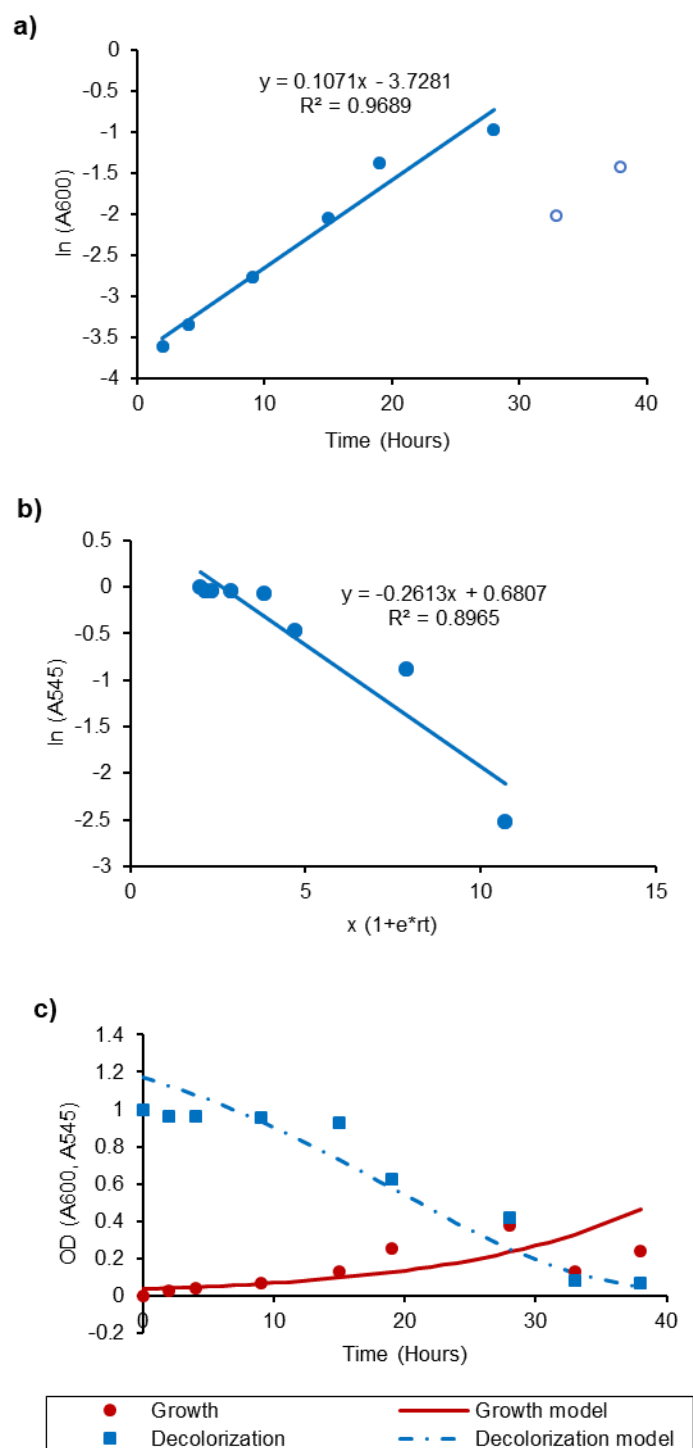


Fig. 6.24 Growth and degradation by *Pseudomonas* sp. NHS2 for RR 195 dye. Linear regression analysis for the rate constants determination for (a) Growth; (b) Dye degradation. Growth and degradation graphs (c) with the original and modeled data indicated by the squares and solid lines, respectively

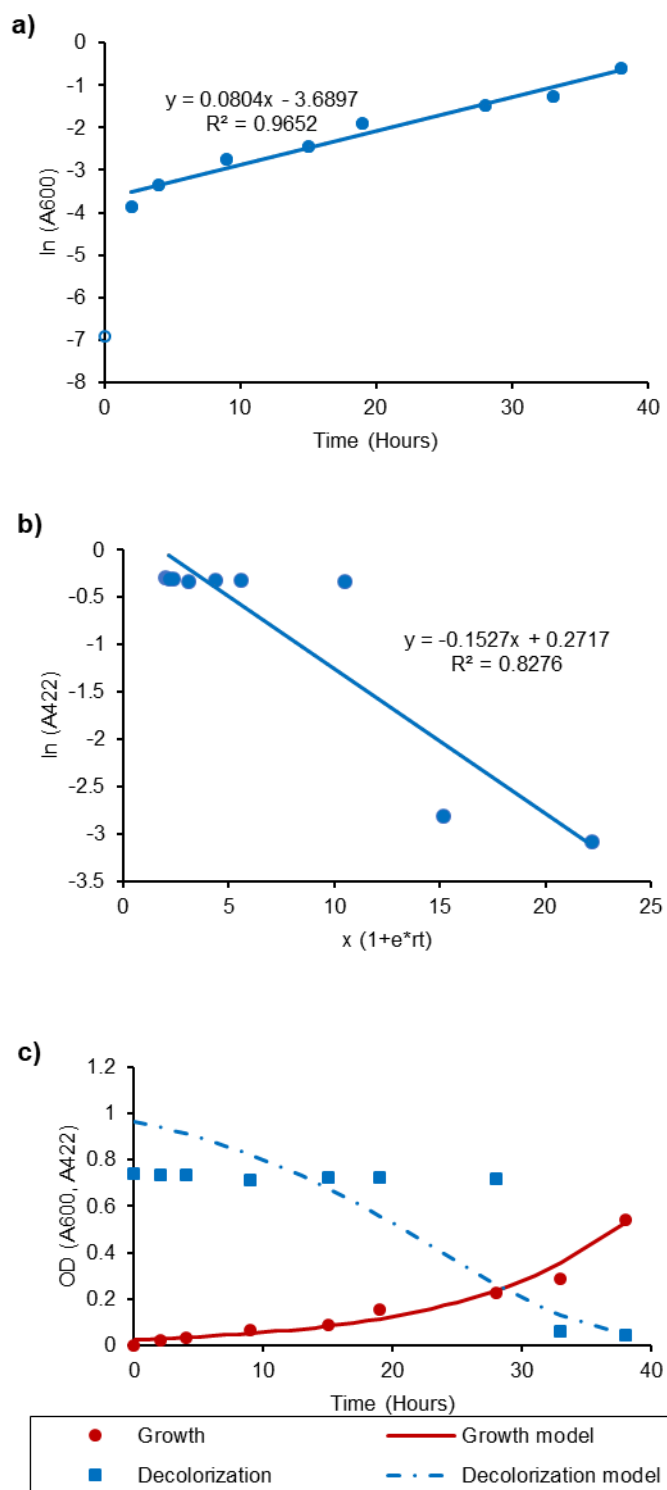


Fig. 6.25 Growth and degradation by *Pseudomonas* sp. NHS2 for RY 145 dye. Linear regression analysis for the rate constants determination for (a) Growth; (b) Dye degradation. Growth and degradation graphs (c) with the original and modeled data indicated by the squares and solid lines, respectively

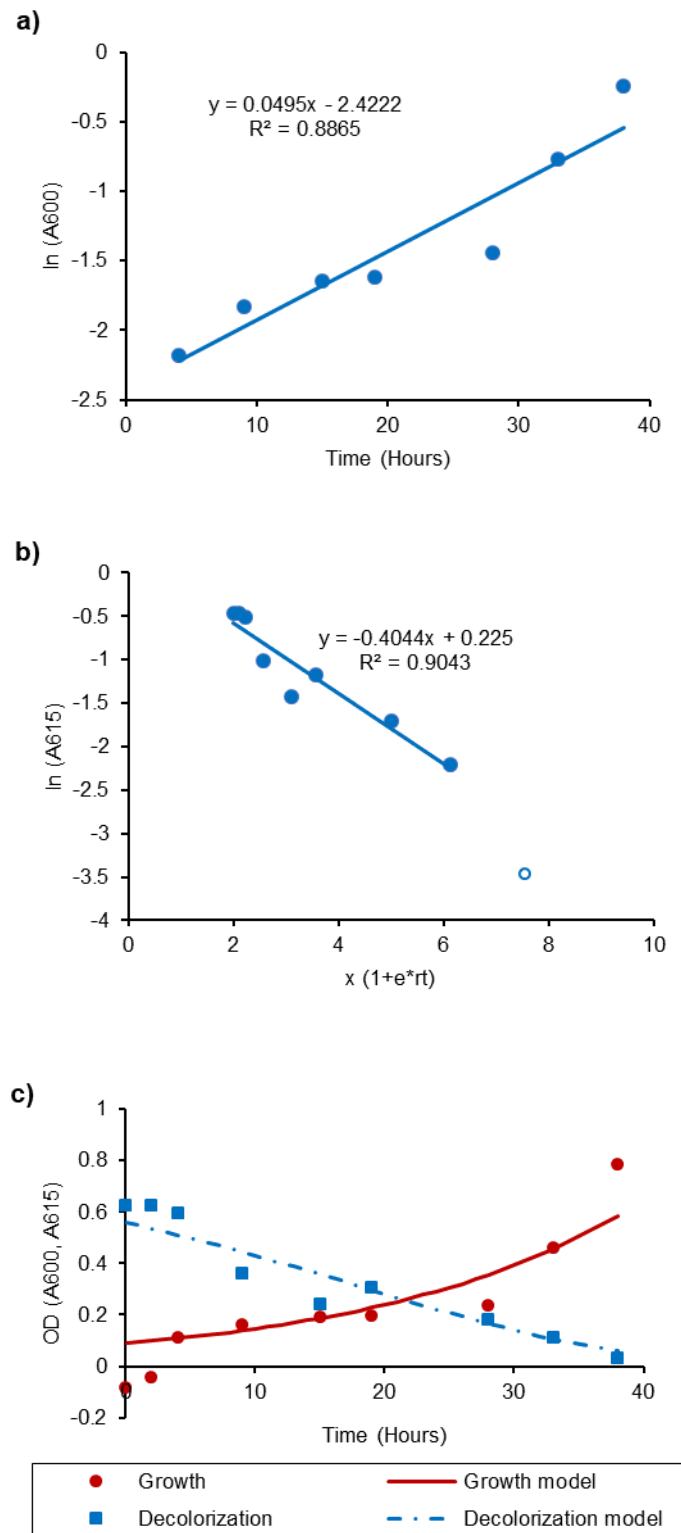


Fig. 6.26 Growth and degradation by *Escherichia* sp. NHS3 for RB 221 dye. Linear regression analysis for the rate constants determination for (a) Growth; (b) Dye degradation. Growth and degradation graphs (c) with the original and modeled data indicated by the squares and solid lines, respectively

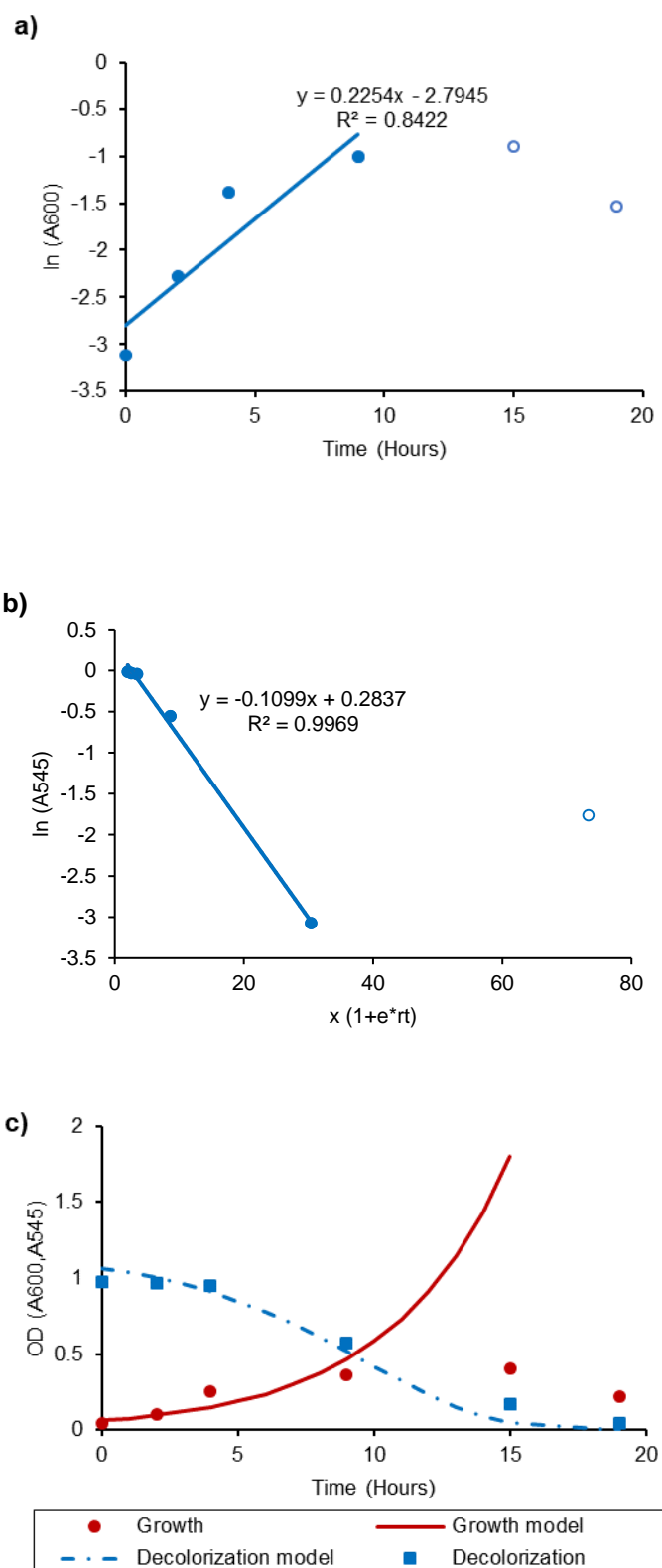


Fig. 6.27 Growth and degradation by *Escherichia* sp. NHS3 for RR 195 dye. Linear regression analysis for the rate constants determination for (a) Growth; (b) Dye degradation. Growth and degradation graphs (c) with the original and modeled data indicated by the squares and solid lines, respectively

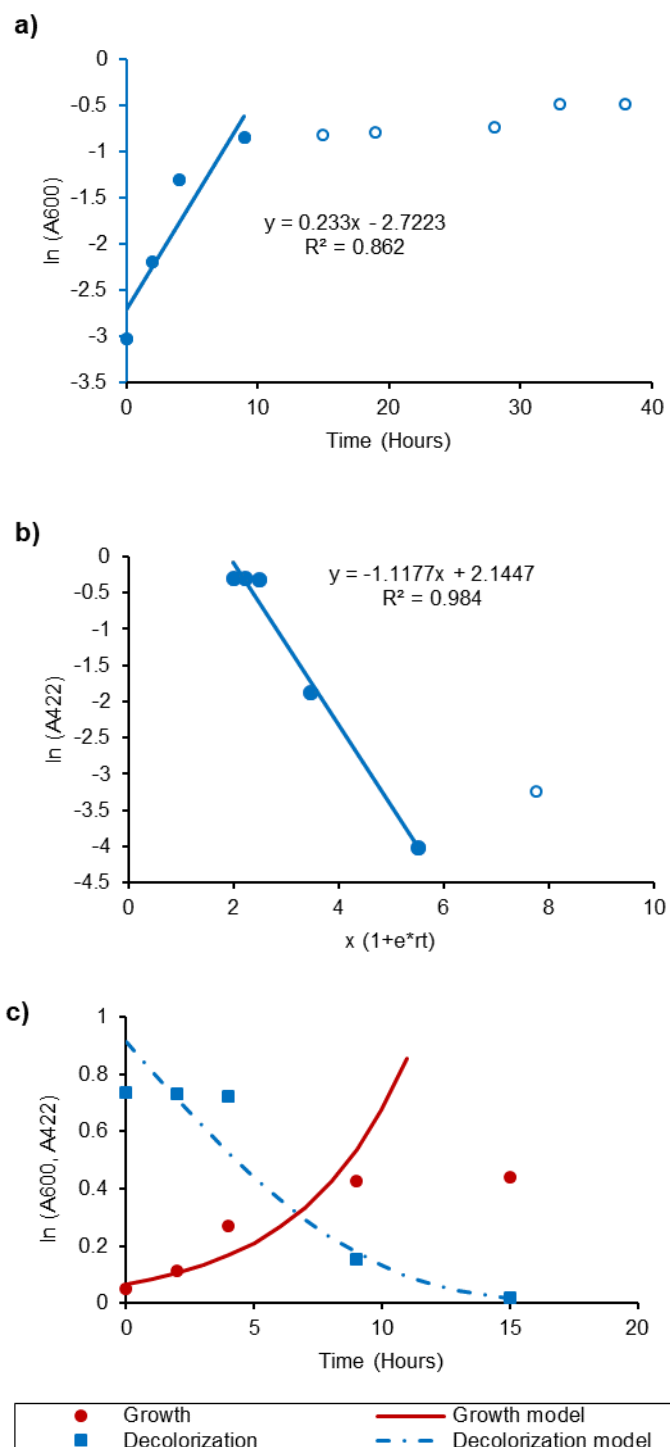


Fig. 6.28 Growth and degradation by *Escherichia* sp. NHS3 for RY 145 dye. Linear regression analysis for the rate constants determination for (a) Growth; (b) Dye degradation. Growth and degradation graphs (c) with the original and modeled data indicated by the squares and solid lines, respectively

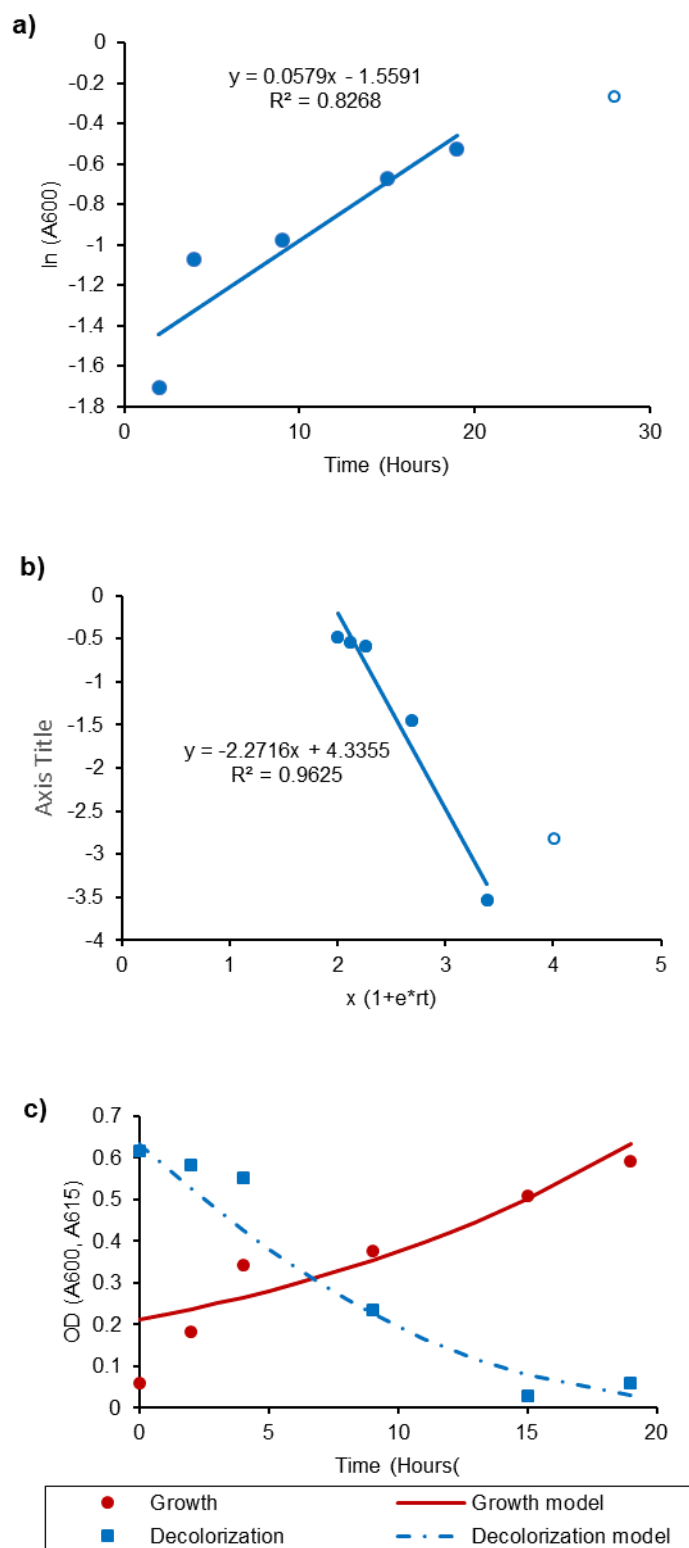


Fig. 6.29 Growth and degradation by *E. coli* NHS4 for RB 221 dye. Linear regression analysis for the rate constants determination for (a) Growth; (b) Dye degradation. Growth and degradation graphs (c) with the original and modeled data indicated by the squares and solid lines, respectively

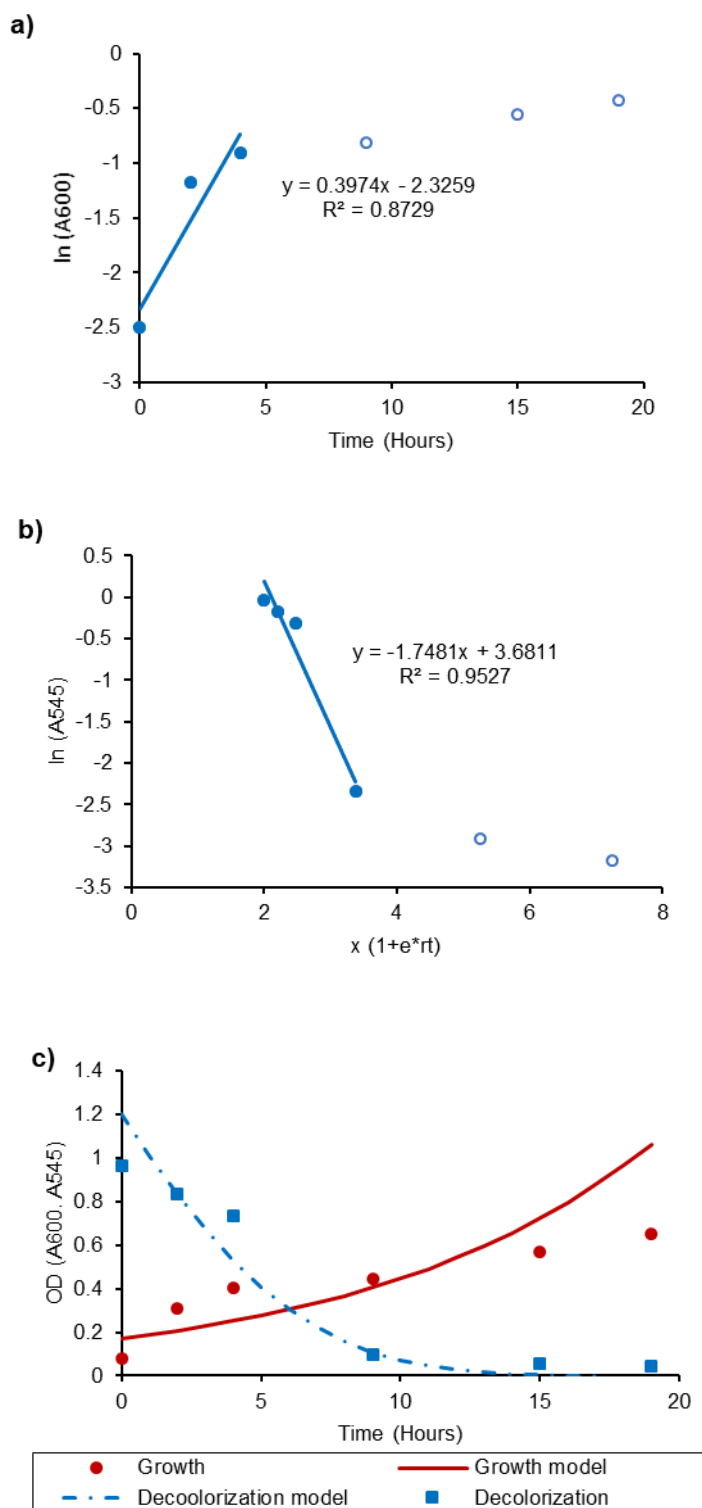


Fig. 6.30 Growth and degradation by *E. coli* NHS4 for RR 195 dye. Linear regression analysis for the rate constants determination for (a) Growth; (b) Dye degradation. Growth and degradation graphs (c) with the original and modeled data indicated by the squares and solid lines, respectively

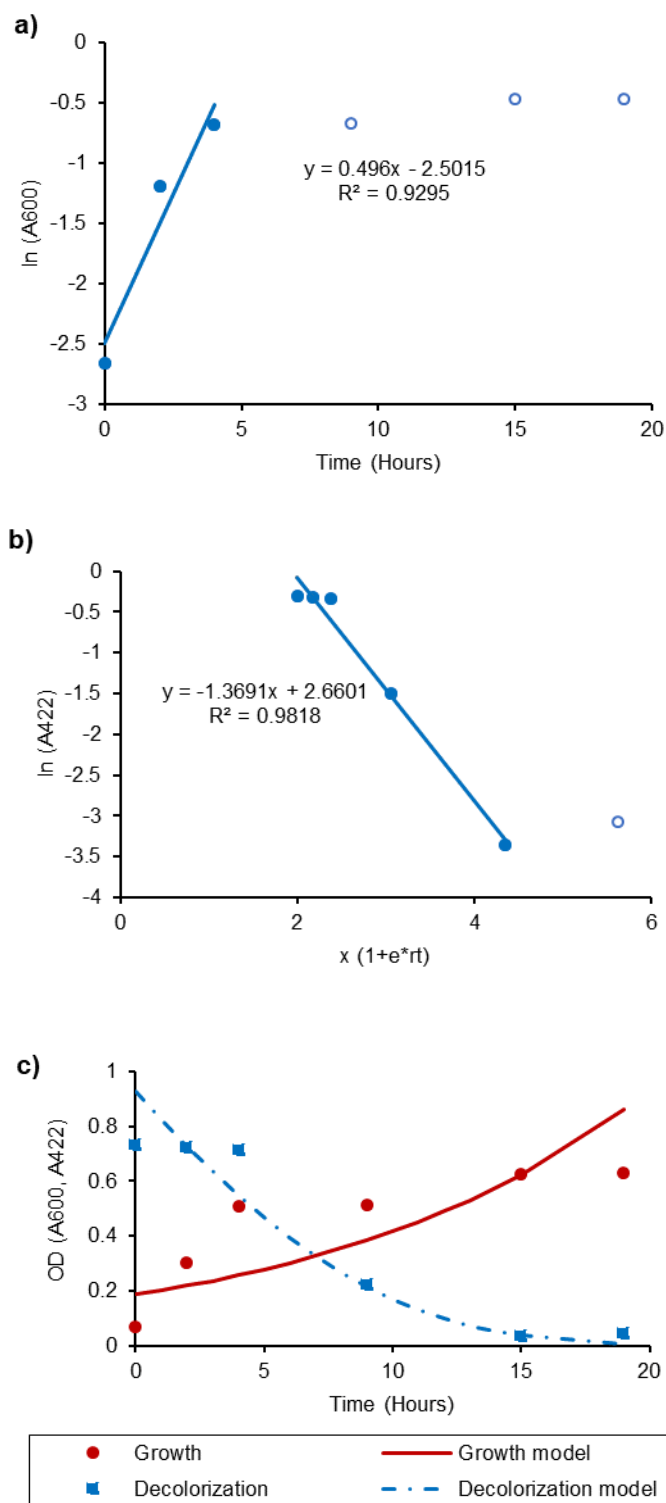


Fig. 6.31 Growth and degradation by *E. coli* NHS4 for RY 145 dye. Linear regression analysis for the rate constants determination for (a) Growth; (b) Dye degradation. Growth and degradation graphs (c) with the original and modeled data indicated by the squares and solid lines, respectively

Table 6.14 Bacterial Growth and dye degradation constants for the individual dye degradation by mesophilic bacteria

Bacterial culture	RB 221				RR 195				RY 145			
	Growth constant ^a k_g (hr ⁻¹)	R^2 for Growth	Deg. constant ^b $k_{c'}$ (hr ⁻¹)	R^2 for Deg.	Growth constant ^a k_g (hr ⁻¹)	R^2 for Growth	Deg. constant ^b $k_{c'}$ (hr ⁻¹)	R^2 for Deg.	Growth constant ^a k_g (hr ⁻¹)	R^2 for Growth	Deg. constant ^b $k_{c'}$ (hr ⁻¹)	R^2 for Deg.
<i>Pseudomonas aeruginosa</i> NHS1	0.103	0.887	-2.738	0.909	0.187	0.949	-1.963	0.998	0.083	0.898	-1.624	0.883
<i>Pseudomonas</i> sp. NHS2	0.074	0.815	-1.359	0.892	0.107	0.969	-0.534	0.896	0.080	0.965	-0.491	0.828
<i>Escherichia</i> sp. NHS3	0.049	0.887	-0.226	0.904	0.225	0.842	-0.405	0.996	0.233	0.862	-1.711	0.984
<i>Escherichia coli</i> NHS4	0.058	0.826	-0.412	0.962	0.397	0.873	-0.991	0.953	0.496	0.929	-0.592	0.982

^aGrowth rate calculated using Eq. 6.2; ^bDegradation constant calculated using Eq. 6.4

6.3.6.1.2 Thermophilic bacteria

By using equations 6.2 and 6.4, respectively, bacterial growth k_g and dye degradation k_c , rates for the individual dyes were calculated. Table 6.15 shows the kinetics constants for the individual dye degradation (25 ppm) by the thermophilic pure bacterial cultures. For *A. pallidus* NHT1, growth rate was higher with the yellow dye and the k_g value was 0.113 (hr^{-1}) (Panel a in Fig. 6.32-6.34). With the red and blue the respective growth rate constants were 0.064 and 0.074 (hr^{-1}). The degradation rate was higher for the red dye, followed by the yellow and blue dyes. The k_c values were -0.885 , -0.597 , and -0.432 (hr^{-1}) (Panel b in Fig. 6.32-6.34). The growth rate assessment for the *Aeribacillus* sp. NHT2 showed a higher value of k_g with the yellow dye i.e., 0.068 (hr^{-1}). The k_g values calculated in the presence of red and blue dyes were 0.041 and 0.028, respectively (Panel a in Fig. 6.35-6.37). This bacterium demonstrated similar degradation rates for the yellow and red dyes ($k_c = -0.798$ and -0.754 (hr^{-1}), respectively). For the blue dye the k_c was -0.341 (hr^{-1}) (Panel b in Fig. 6.35-6.37).

The growth rate for *Geobacillus* sp. NHT3 was also higher with the yellow dye with a k_g value of 0.114 (hr^{-1}), followed by k_g values of 0.099 and 0.044 (hr^{-1}), for the red and blue dyes, respectively (Panel a in Fig. 6.38-6.40). The k_c values for the blue, yellow, and red dyes were: -0.895 , -0.632 , and -0.592 (hr^{-1}), respectively (Panel b in Fig. 6.38-6.40). For *Brevibacillus borstelensis* NHT4, similar growth rates were observed for the blue and yellow dyes with k_g values of 0.029 and 0.033 (hr^{-1}), respectively, and for the red dye it 0.044 (hr^{-1}) (Panel a in Fig. 6.41-6.43). In that case, the respective k_c values for the yellow and blue dyes were: -0.321 and -0.245 (hr^{-1}). However, a very low removal rate was observed for the red dye ($k_c = -0.021\text{hr}^{-1}$) (Panel b in Fig. 6.41-6.43). The growth and degradation models were calculated using the respective rate constants. In most cases both responses were well predicted by the models for each dye type (Panel c in Fig. 6.32-6.43).

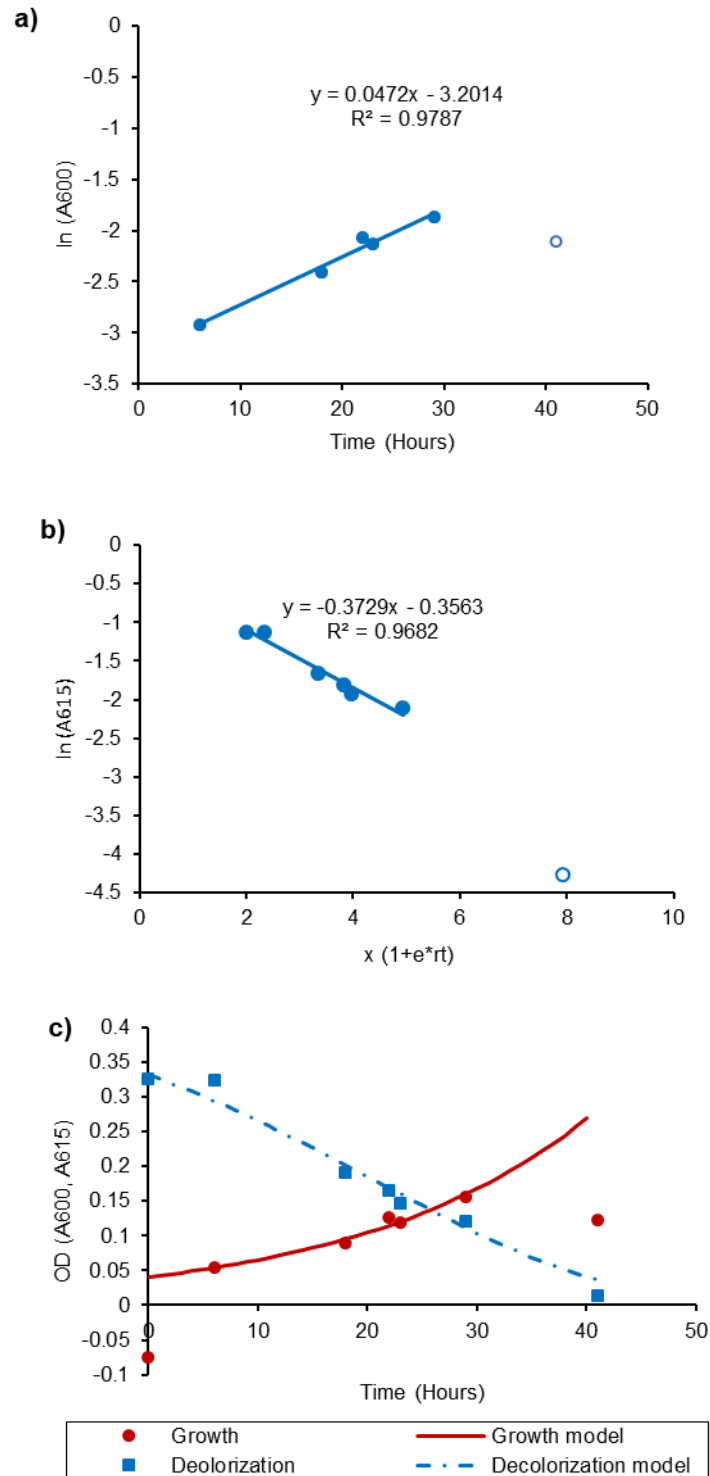


Fig. 6.32 Growth and degradation by *A. pallidus* NHT1 for RB 221 dye. Linear regression analysis for the rate constants determination for (a) Growth; (b) Dye degradation. Growth and degradation graphs (c) with the original and modeled data indicated by the squares and solid lines, respectively

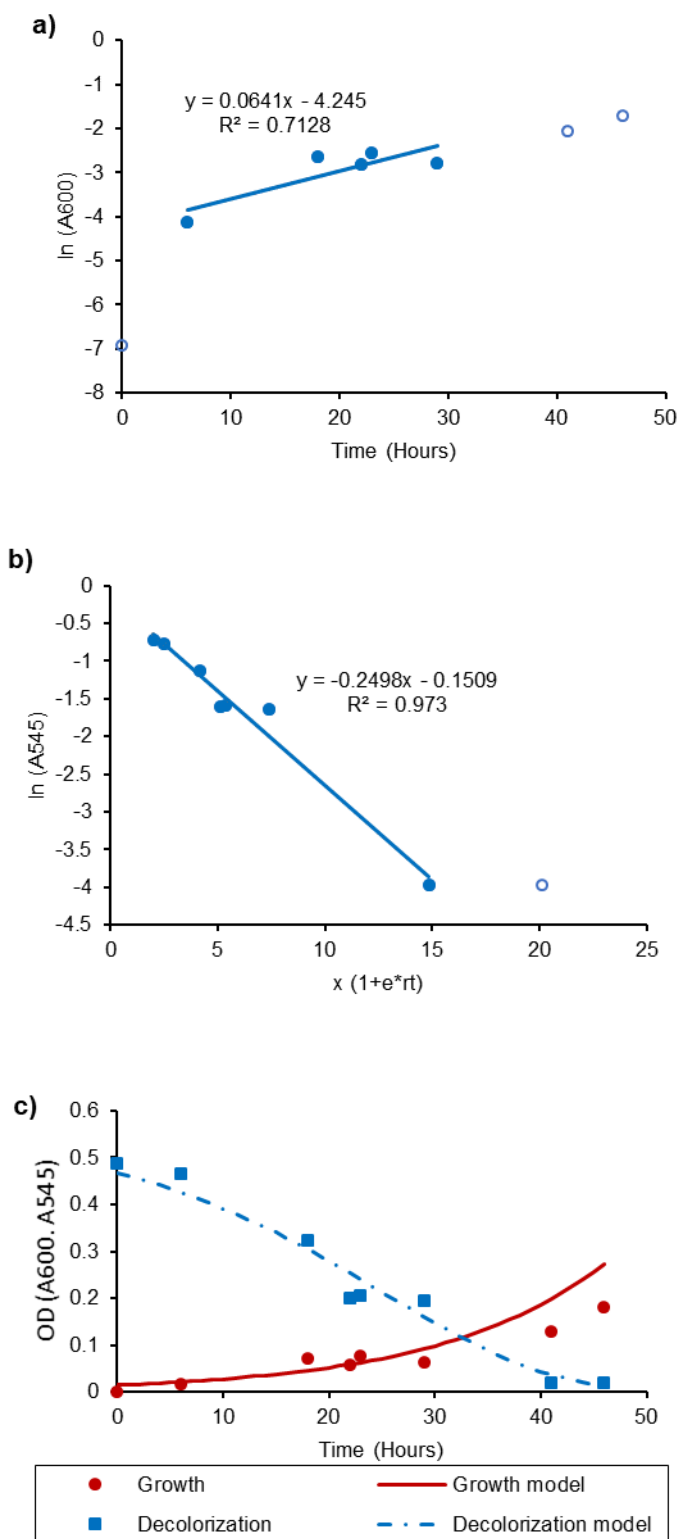


Fig. 6.33 Growth and degradation by *A. pallidus* NHT1 for RR 195 dye. Linear regression analysis for the rate constants determination for (a) Growth; (b) Dye degradation. Growth and degradation graphs (c) with the original and modeled data indicated by the squares and solid lines, respectively

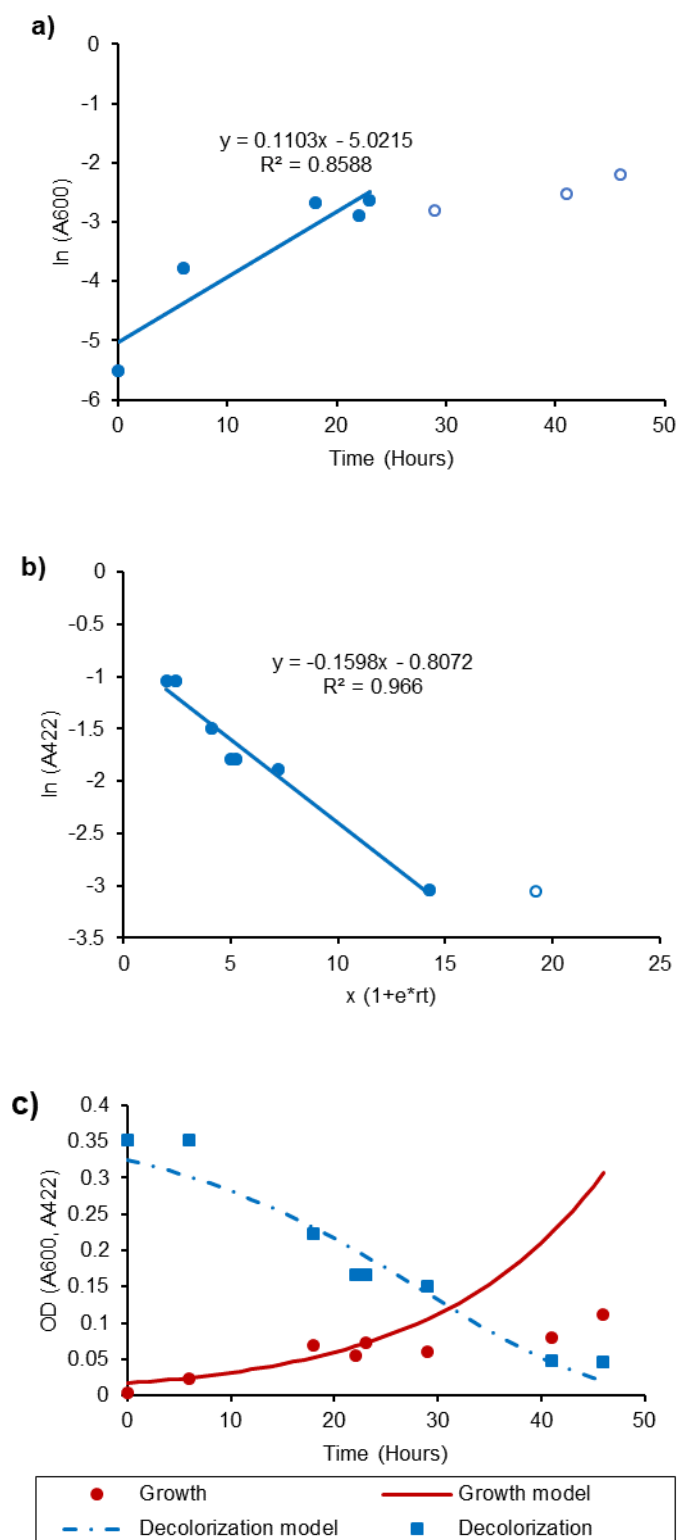


Fig. 6.34 Growth and degradation by *A. pallidus* NHT1 for RY 145 dye. Linear regression analysis for the rate constants determination for (a) Growth; (b) Dye degradation. Growth and degradation graphs (c) with the original and modeled data indicated by the squares and solid lines, respectively

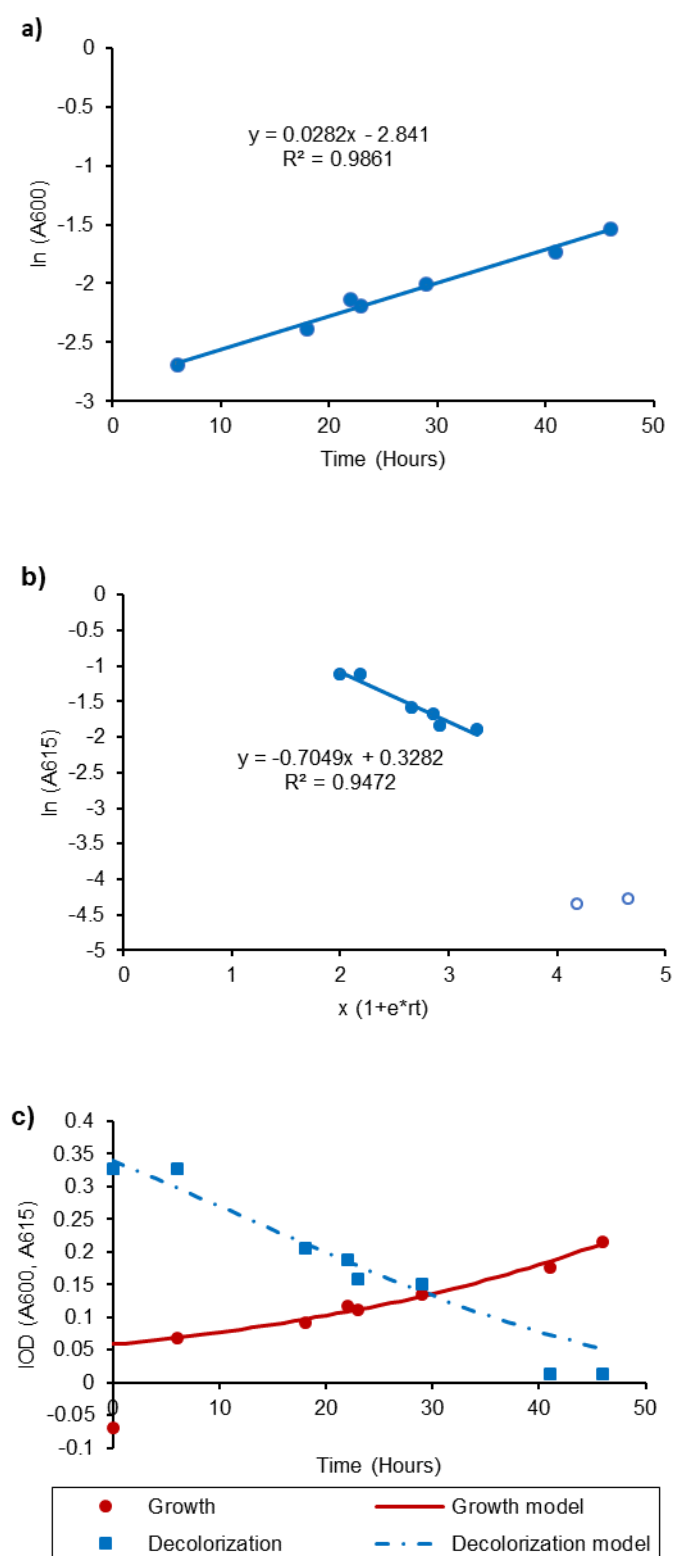


Fig. 6.35 Growth and degradation by *Aeribacillus* sp. NHT2 for RB 221 dye. Linear regression analysis for the rate constants determination for (a) Growth; (b) Dye degradation. Growth and degradation graphs (c) with the original and modeled data indicated by the squares and solid lines, respectively

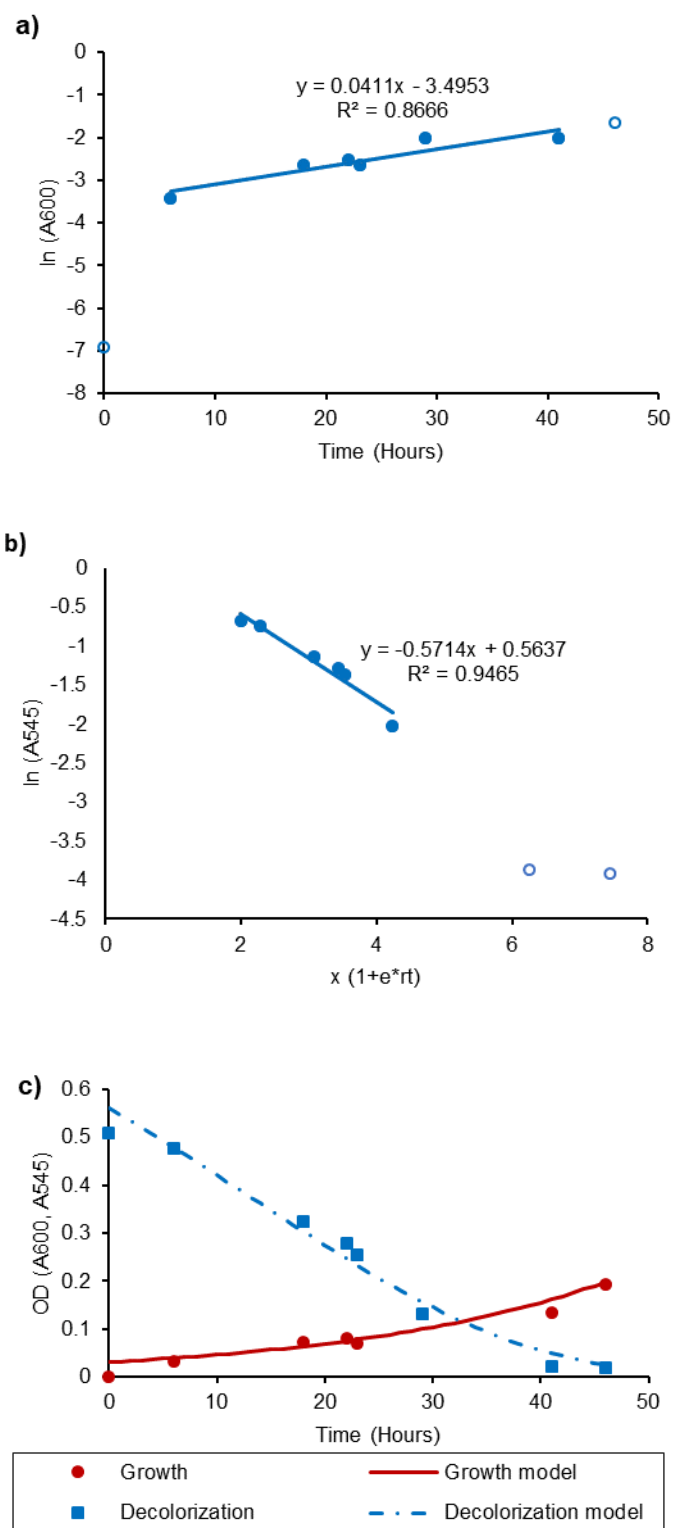


Fig. 6.36 Growth and degradation by *Aeribacillus* sp. NHT2 for RR 195 dye. Linear regression analysis for the rate constants determination for (a) Growth; (b) Dye degradation. Growth and degradation graphs (c) with the original and modeled data indicated by the squares and solid lines, respectively

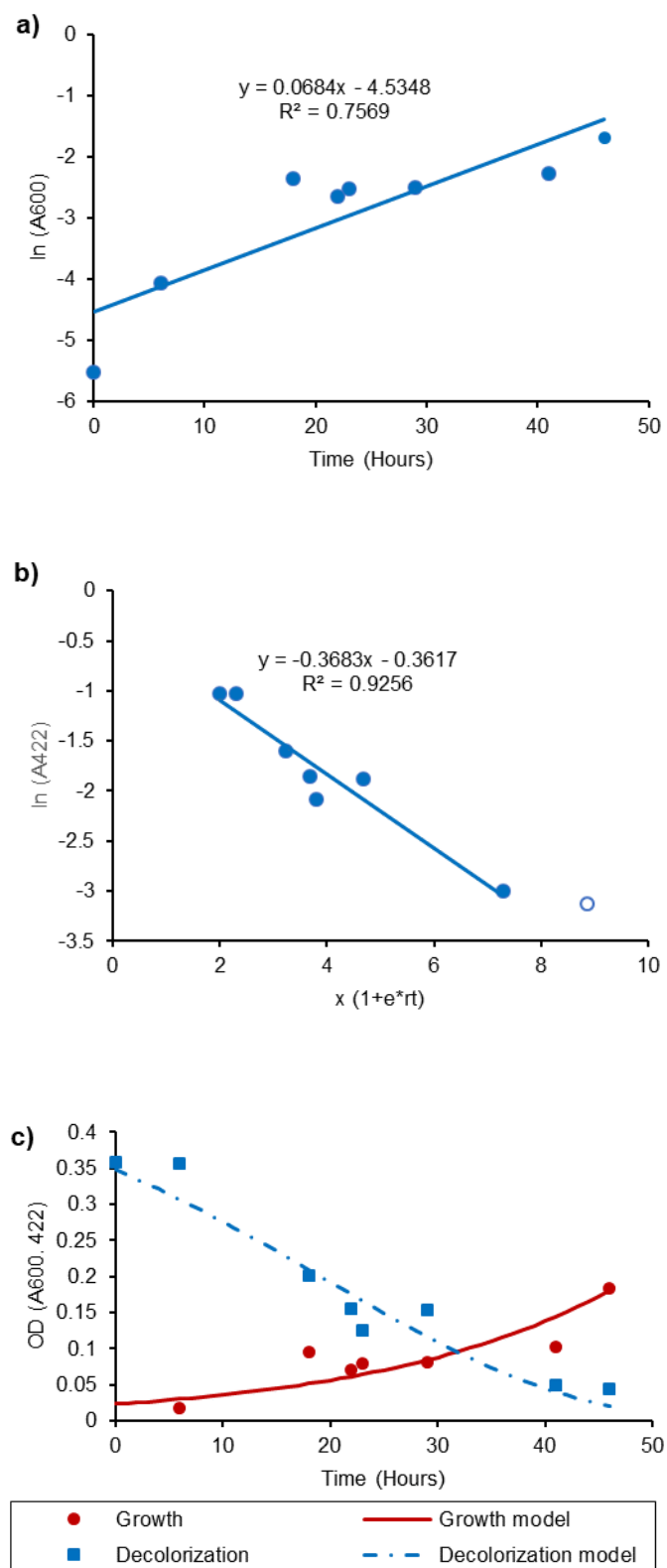


Fig. 6.37 Growth and degradation by *Aeribacillus* sp. NHT2 for RY 145 dye. Linear regression analysis for the rate constants determination for (a) Growth; (b) Dye degradation. Growth and degradation graphs (c) with the original and modeled data indicated by the squares and solid lines, respectively

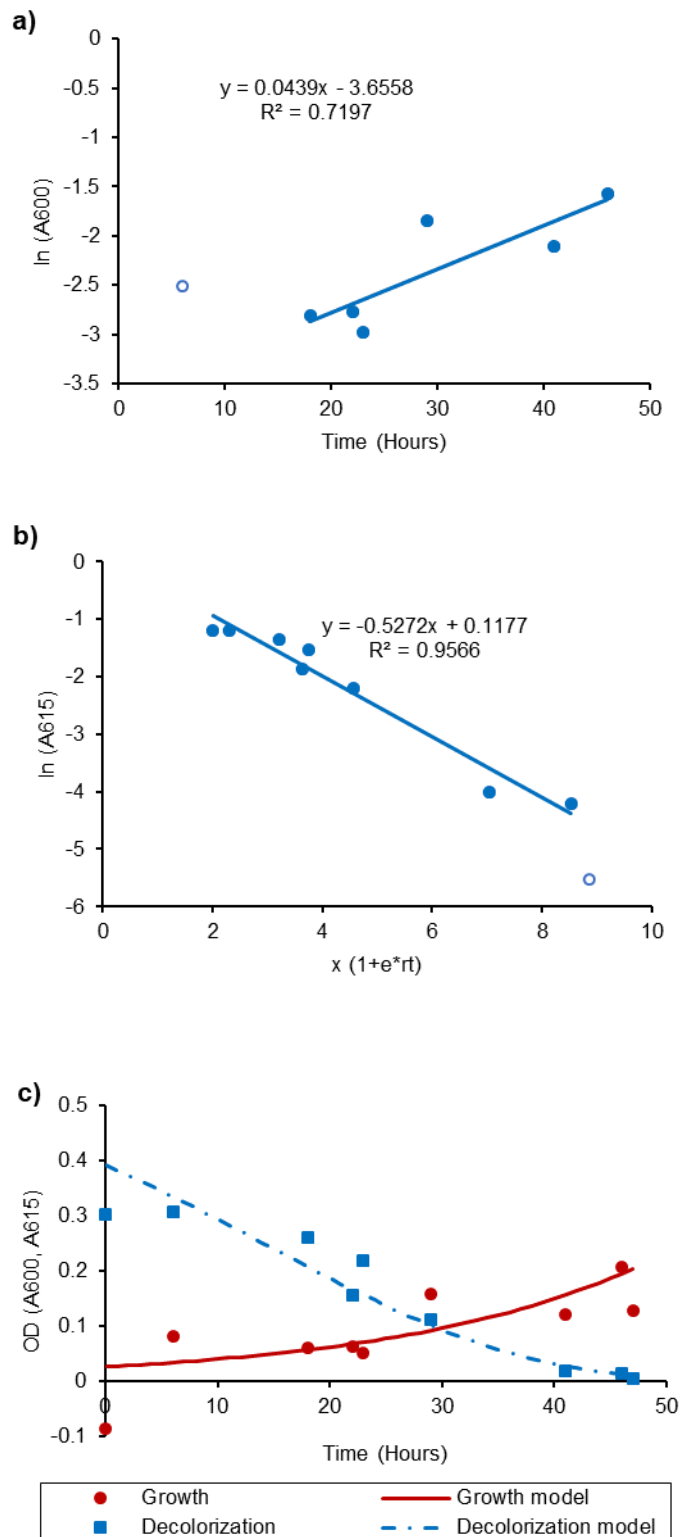


Fig. 6.38 Growth and degradation by *Geobacillus* sp. NHT3 for RB 221 dye. Linear regression analysis for the rate constants determination for (a) Growth; (b) Dye degradation. Growth and degradation graphs (c) with the original and modeled data indicated by the squares and solid lines, respectively

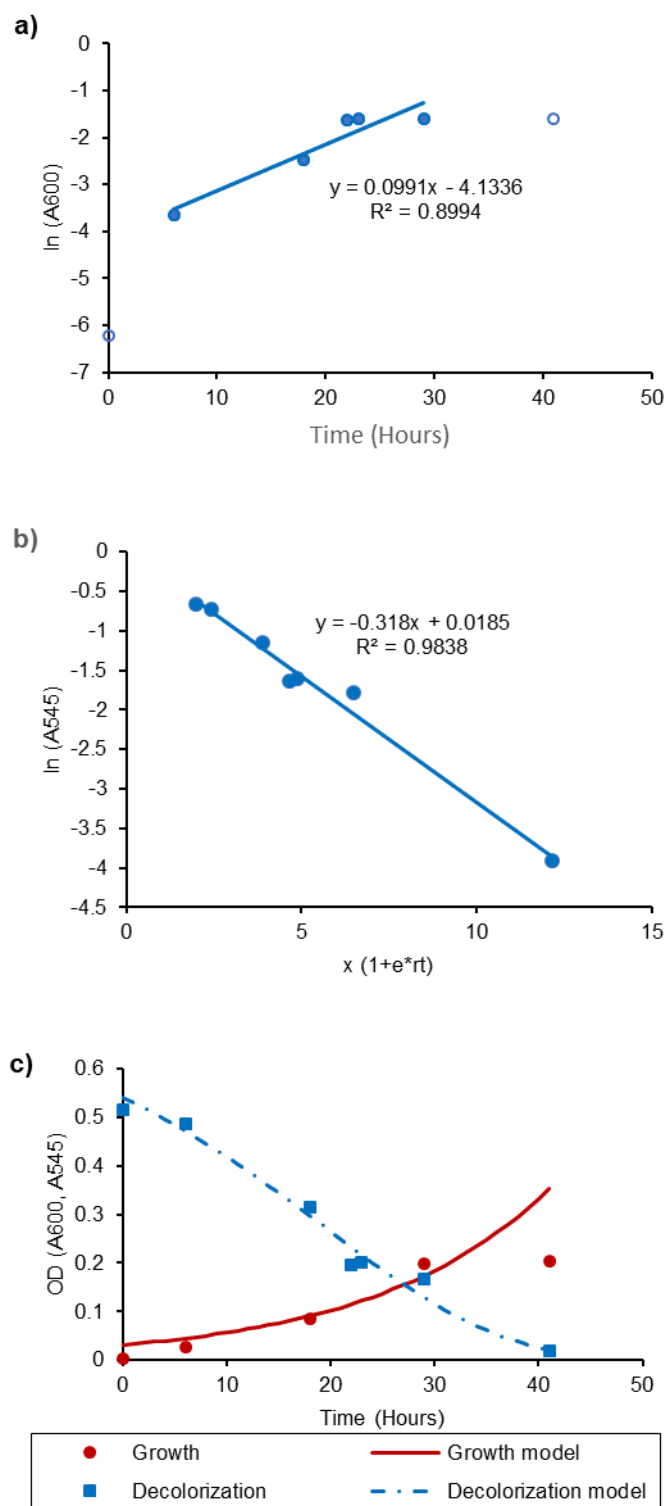


Fig. 6.39 Growth and degradation by *Geobacillus* sp. NHT3 for RR 195 dye. Linear regression analysis for the rate constants determination for (a) Growth; (b) Dye degradation. Growth and degradation graphs (c) with the original and modeled data indicated by the squares and solid lines, respectively

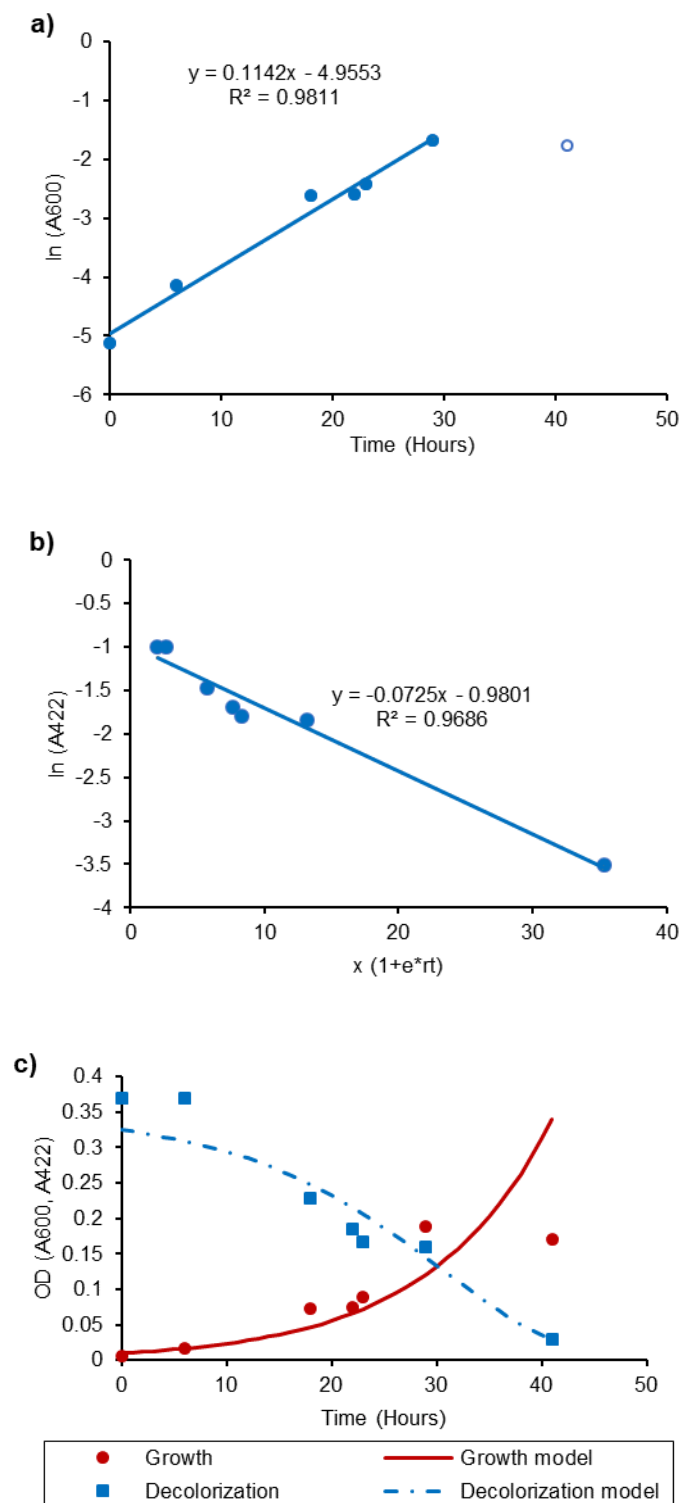


Fig. 6.40 Growth and degradation by *Geobacillus* sp. NHT3 for RY 145 dye. Linear regression analysis for the rate constants determination for (a) Growth; (b) Dye degradation. Growth and degradation graphs (c) with the original and modeled data indicated by the squares and solid lines, respectively

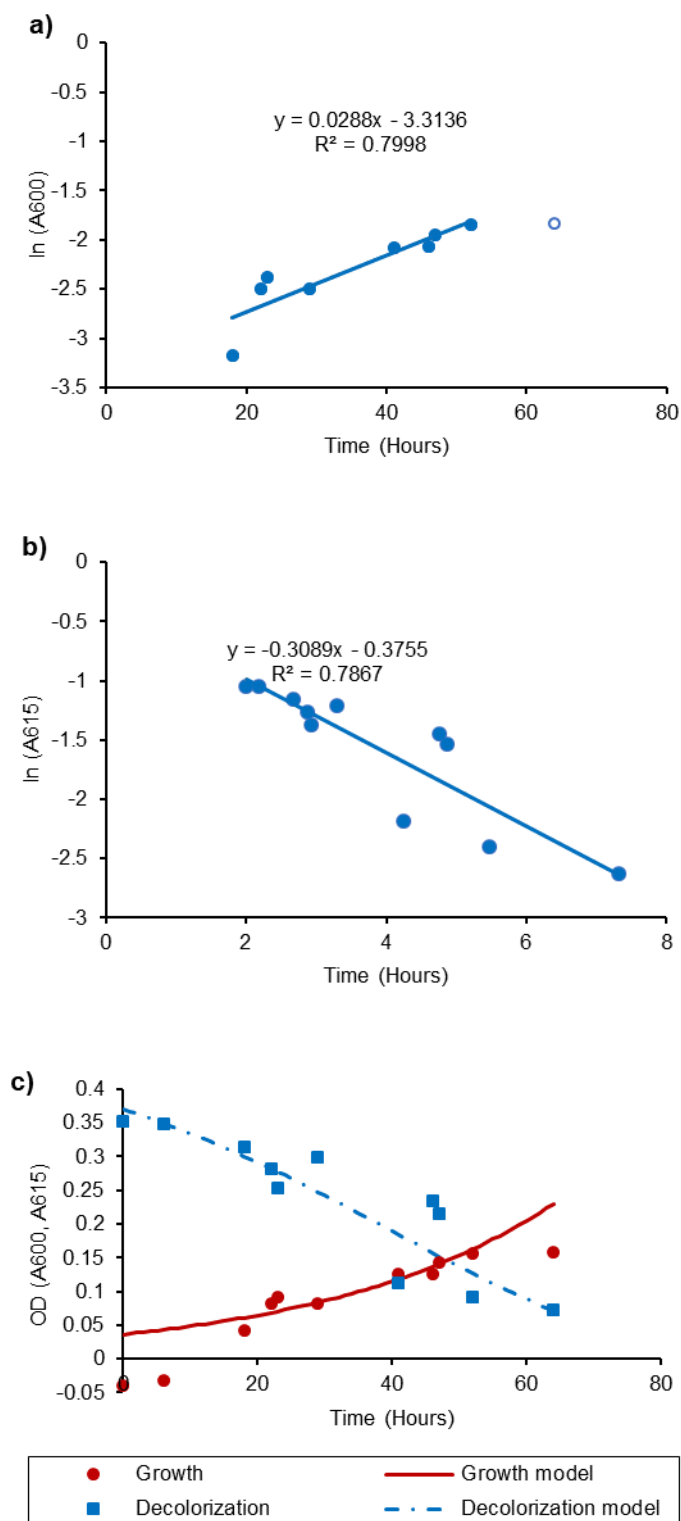


Fig. 6.41 Growth and degradation by *Brevibacillus borstelensis* NHT4 for RB 221 dye. Linear regression analysis for the rate constants determination for (a) Growth; (b) Dye degradation. Growth and degradation graphs (c) with the original and modeled data indicated by the squares and solid lines, respectively

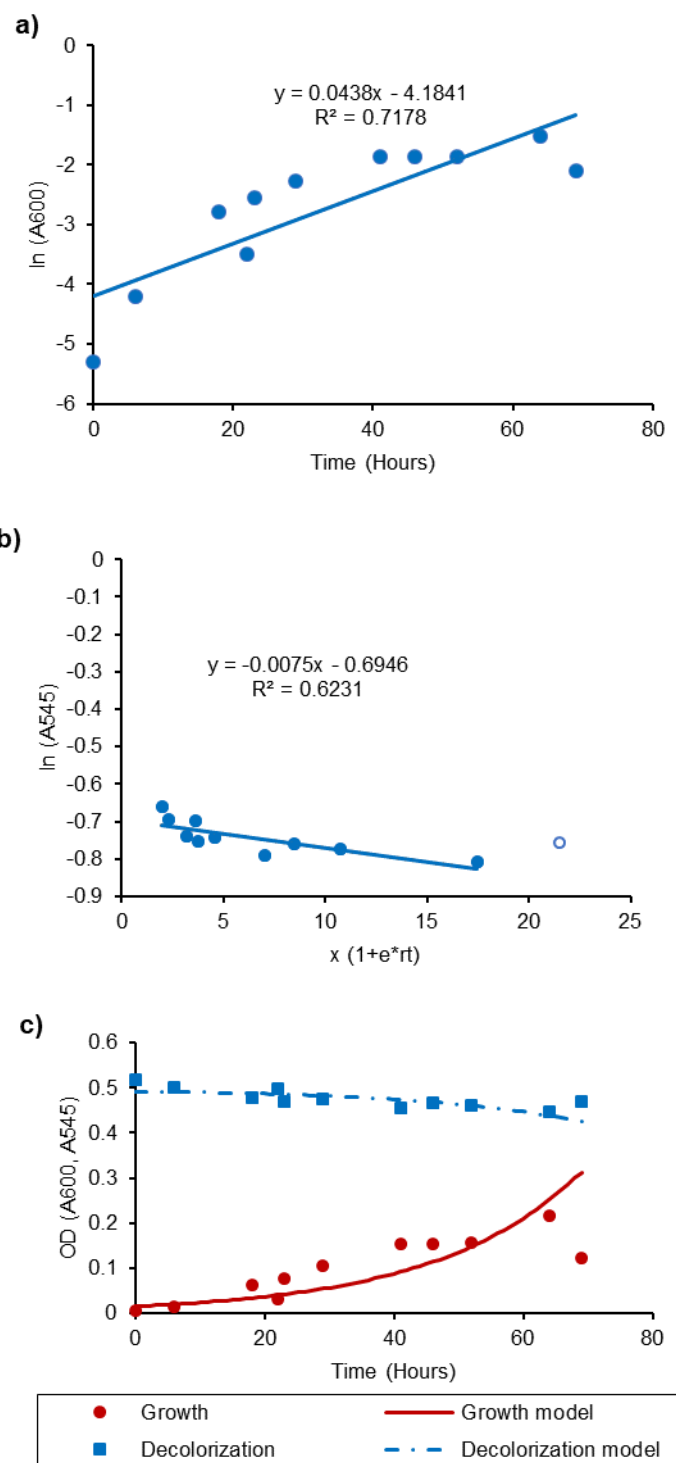


Fig. 6.42 Growth and degradation by *Brevibacillus borstelensis* NHT4 for RR 195 dye. Linear regression analysis for the rate constants determination for (a) Growth; (b) Dye degradation. Growth and degradation graphs (c) with the original and modeled data indicated by the squares and solid lines, respectively

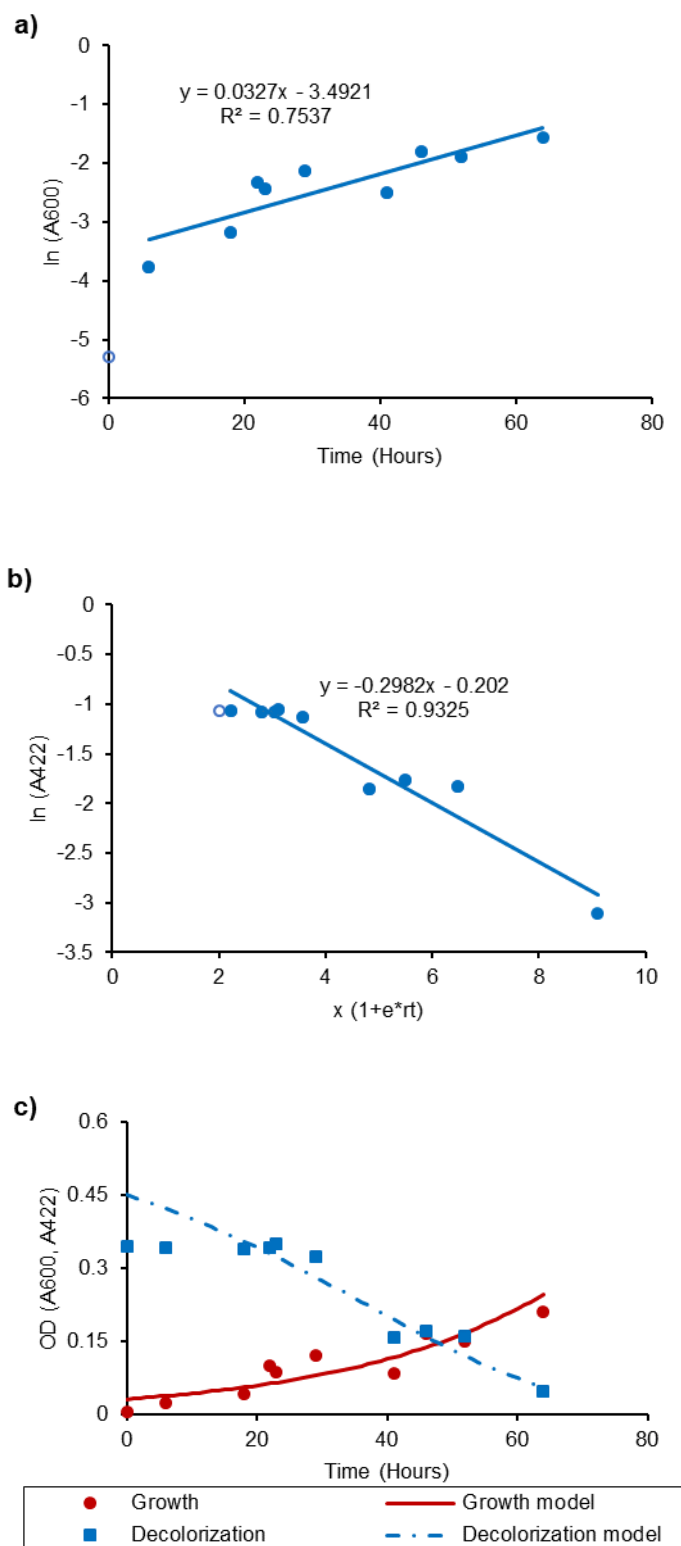


Fig. 6.43 Growth and degradation by *Brevibacillus borstelensis* NHT4 for RY 145 dye. Linear regression analysis for the rate constants determination for (a) Growth; (b) Dye degradation. Growth and degradation graphs (c) with the original and modeled data indicated by the squares and solid lines, respectively

Table 6.15 Bacterial Growth and dye degradation constants for the individual dye degradation by the thermophilic bacteria

Bacterial culture	RB 221				RR 195				RY 145			
	Growth constant ^a k_g (hr ⁻¹)	R^2 for Growth	Deg. constant ^b $k_{c'}$ (hr ⁻¹)	R^2 for Deg.	Growth constant ^a k_g (hr ⁻¹)	R^2 for Growth	Deg. constant ^b $k_{c'}$ (hr ⁻¹)	R^2 for Deg.	Growth constant ^a k_g (hr ⁻¹)	R^2 for Growth	Deg. constant ^b $k_{c'}$ (hr ⁻¹)	R^2 for Deg.
<i>Aeribacillus Pallidus</i> NHT1	0.047	0.978	-0.432	0.968	0.064	0.713	-0.885	0.973	0.113	0.858	-0.597	0.966
<i>Aeribacillus</i> sp. NHT2	0.028	0.986	-0.341	0.947	0.041	0.867	-0.754	0.946	0.068	0.757	-0.798	0.926
<i>Geobacillus</i> sp. NHT3	0.044	0.719	-0.895	0.957	0.099	0.899	-0.592	0.983	0.114	0.981	-0.632	0.967
<i>Brevibacillus borstelensis</i> NHT4	0.029	0.787	-0.245	0.787	0.044	0.712	-0.021	0.623	0.033	0.753	-0.321	0.932

^aGrowth rate calculated using Eq. 6.2; ^bDegradation constant calculated using Eq. 6.4

6.3.6.2 Kinetics studies for the dye mixture by the thermophilic bacterial cultures

The bacterial growth (k_g) and color removal (k_c) rates for the dye mixture (50 ppm) by the thermophilic bacteria (pure cultures and coculture) were calculated through the graphical solutions for the equations 6.2 and 6.4, respectively. The rate constant with the determination coefficients (R^2) are given in Table 6.16. For *A. pallidus* NHT1, the growth (k_g) and degradation (k_c) rate constants were calculated as 0.052 and -0.947 (hr^{-1}), respectively. Moreover, the growth and degradation rates were well predicted by the derived models except for the starting few hours (Fig. 6.44a-c). The growth and degradation rates for the *Aeribacillus* sp. NHT2 were slightly different than for NHT1: i.e., 0.056 and -0.735 (hr^{-1}), respectively. The growth and color changes were well described by the models as shown in Fig. 6.45a-c. *Geobacillus* sp. NHT3 showed a slightly higher growth rate ($k_g = 0.091$ hr^{-1}) but the color removal rate was lower as that observed with the other bacteria ($k_c = -0.679$ hr^{-1}). However, the growth and degradation were not well predicted by the models except for the few data points (Fig. 6.46a-c). For the *Brevibacillus borstelensis* NHT4, both the growth and color removal rates ($k_g = 0.041$ and $k_c = -0.241$ hr^{-1} , respectively) were found to be lower than the other isolates (Fig. 6.7a-c). With the coculture (containing all the four thermophilic bacterial isolates), the growth rate was higher than the individual isolates except for *Geobacillus* sp. NHT3, however, the degradation rate was found to be higher than all four pure cultures ($k_c = -1.522$). The model only partially predicted the coculture growth but for the degradation, the solid model line well fitted the data points for color removal (Fig. 6.48a-c).

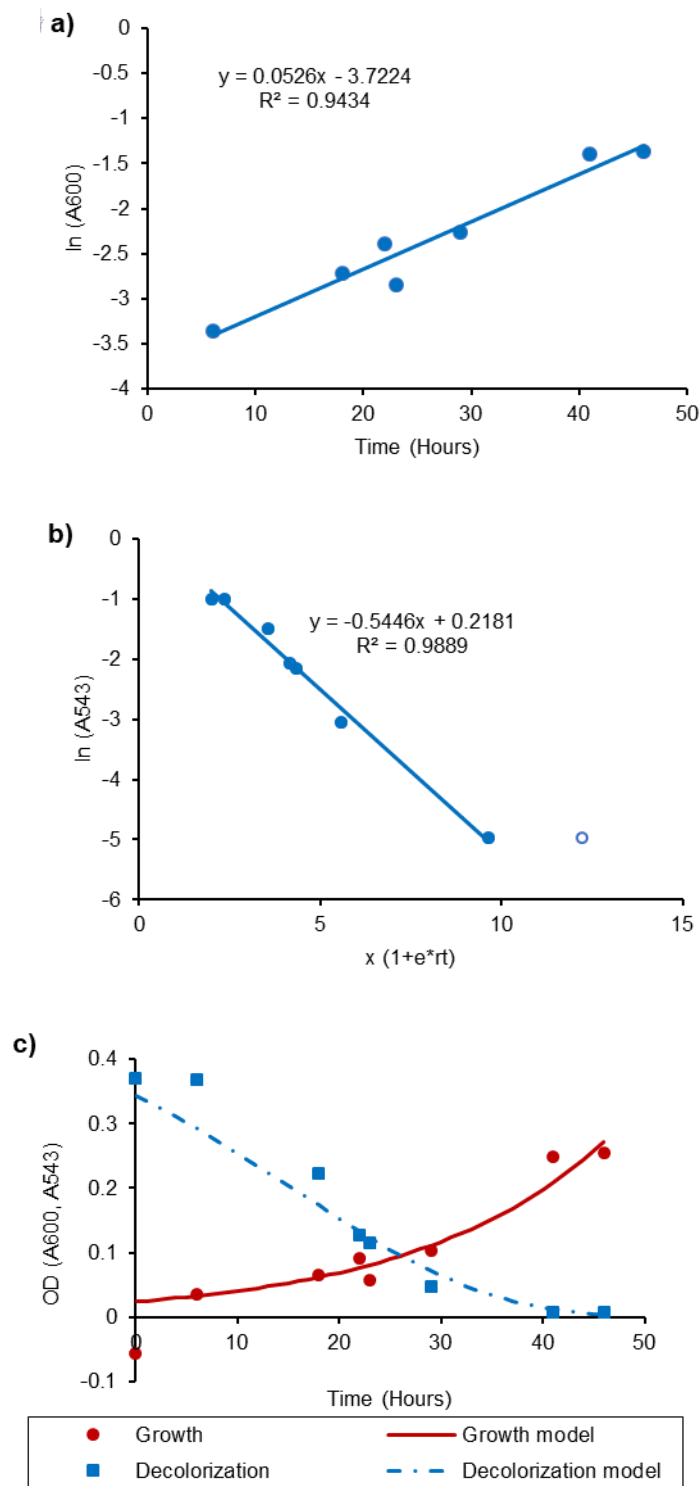


Fig. 6.44 Growth and degradation by *A. pallidus* NHT1 for the dye mixture. Linear regression analysis for the rate constants determination for (a) Growth; (b) Dye degradation. Growth and degradation graphs (c) with the original and modeled data indicated by the squares and solid lines, respectively

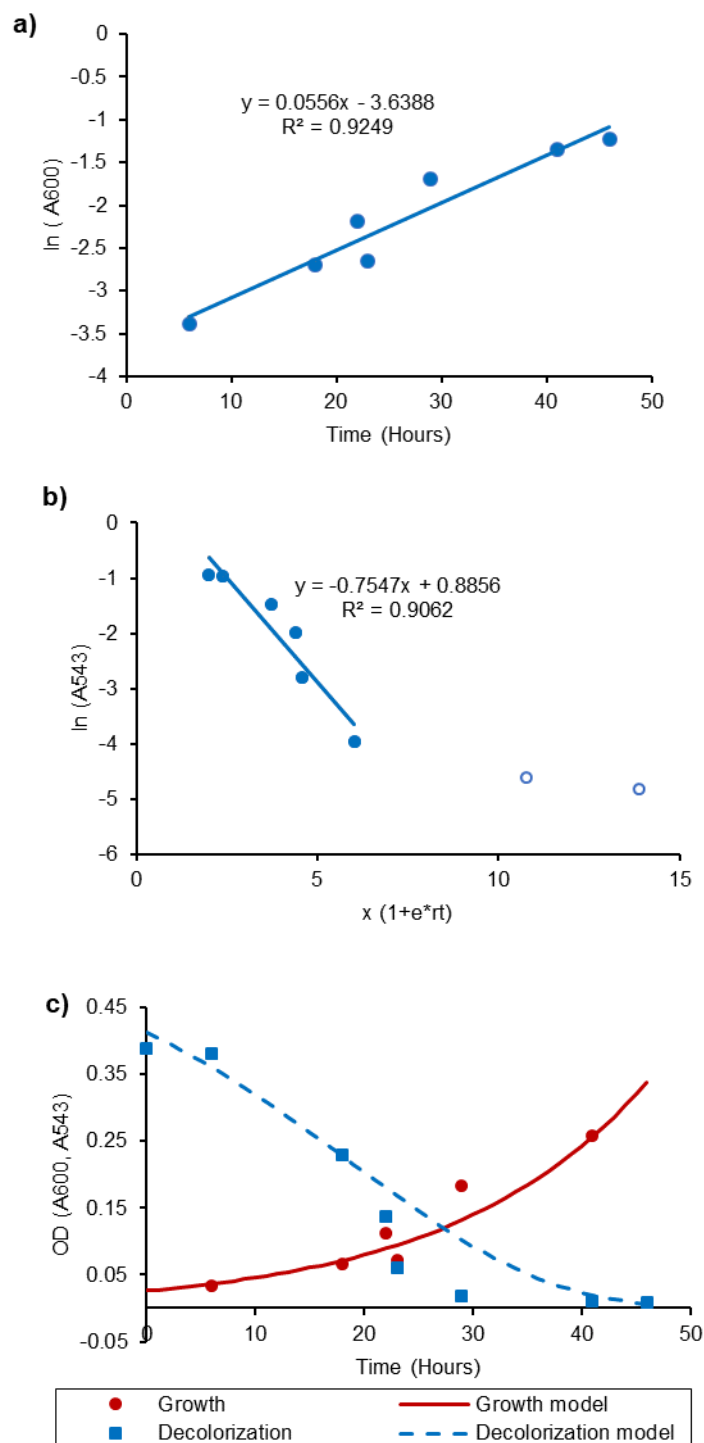


Fig. 6.45 Growth and degradation by *Aeribacillus* sp. NHT2 for the dye mixture. Linear regression analysis for the rate constants determination for (a) Growth; (b) Dye degradation. Growth and degradation graphs (c) with the original and modeled data indicated by the squares and solid lines, respectively

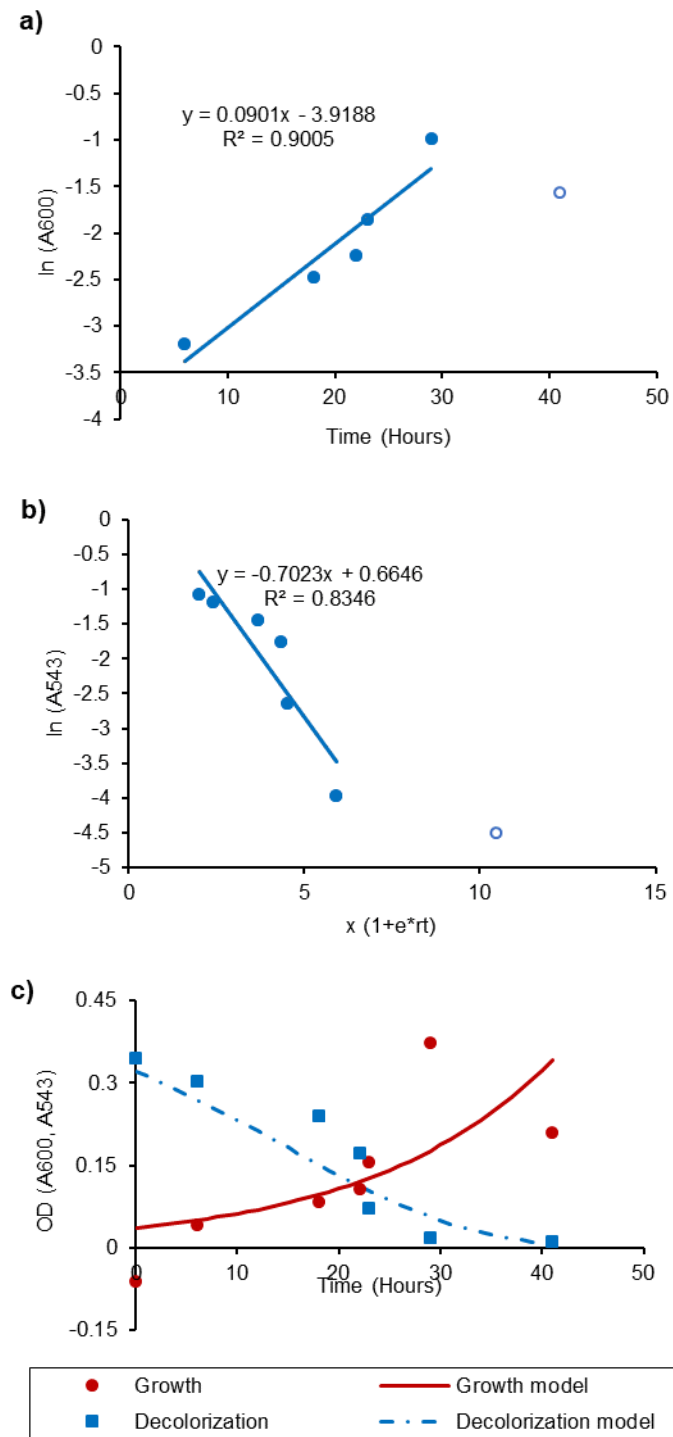


Fig. 6.46 Growth and degradation by *Geobacillus* sp. NHT3 for the dye mixture. Linear regression analysis for the rate constants determination for (a) Growth; (b) Dye degradation. Growth and degradation graphs (c) with the original and modeled data indicated by the squares and solid lines, respectively

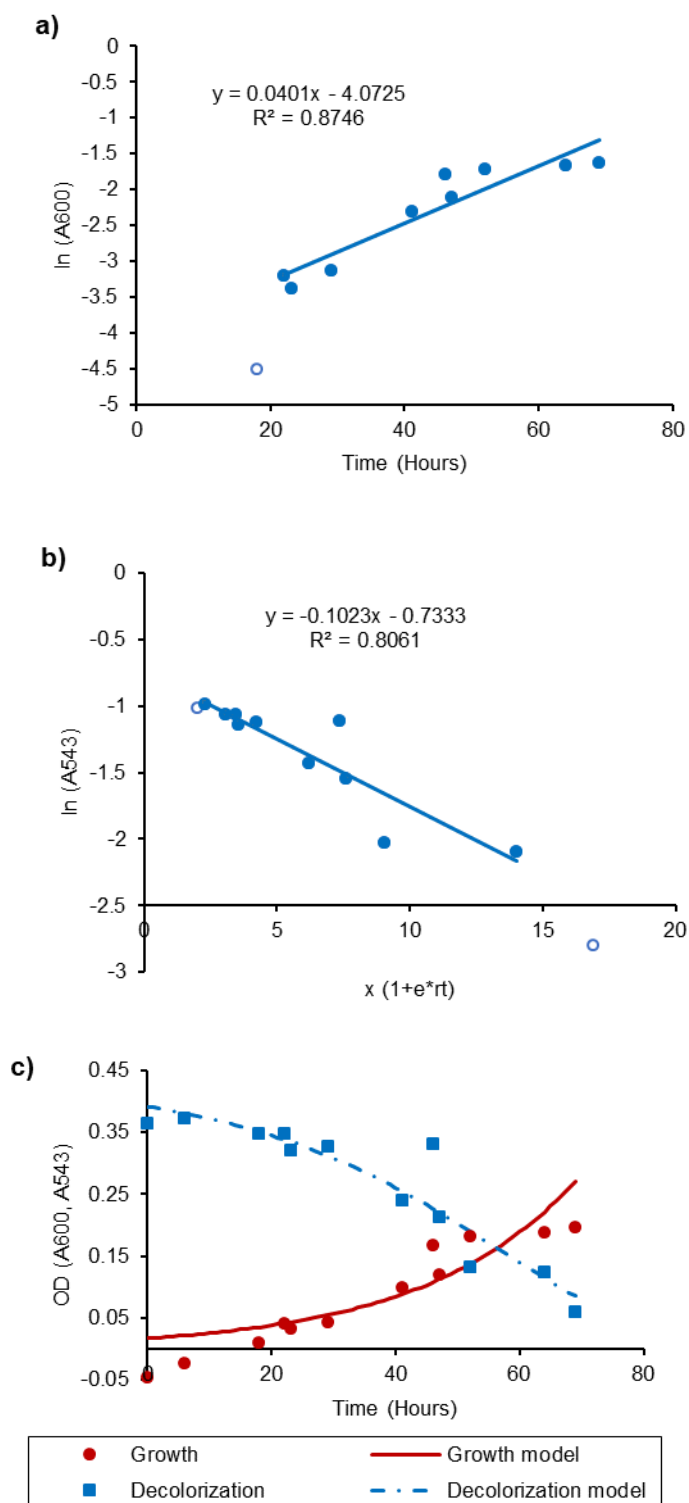


Fig. 6.47 Growth and degradation by *Brevibacillus borstelensis* NHT4 for the dye mixture. Linear regression analysis for the rate constants determination for (a) Growth; (b) Dye degradation. Growth and degradation graphs (c) with the original and modeled data indicated by the circles, squares and solid lines, respectively

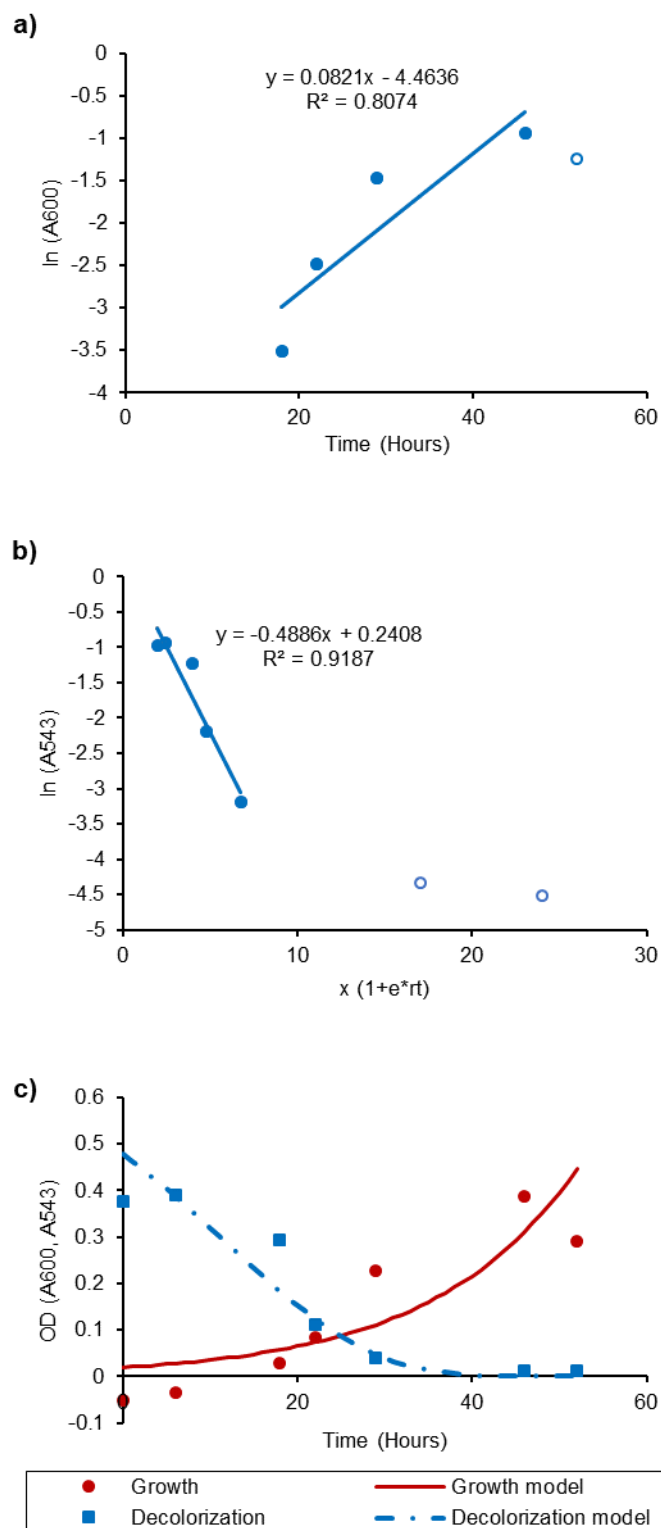


Fig. 6.48 Growth and degradation by the thermophilic coculture for the dye mixture. Linear regression analysis for the rate constants determination for (a) Growth; (b) Dye degradation. Growth and degradation graphs (c) with the original and modeled data indicated by the circles, squares and solid lines, respectively

Table 6.16 Bacterial Growth and dye degradation constants for dye mixture degradation by the thermophilic bacteria

Bacterial culture	Growth constant ^a k_g (hr ⁻¹)	R^2 for Growth	Degradation constant ^b k_c' (hr ⁻¹)	R^2 for Degradation
<i>Aeribacillus Pallidus</i> NHT1	0.052	0.943	-0.947	0.989
<i>Aeribacillus</i> sp. NHT2	0.056	0.943	-0.735	0.906
<i>Geobacillus</i> sp. NHT3	0.091	0.905	-0.679	0.835
<i>Brevibacillus borstelensis</i> NHT4	0.041	0.875	-0.241	0.806
Coculture	0.082	0.807	-1.522	0.919

^a Growth rate calculated using Eq. 6.2; ^b Degradation constant calculated using Eq. 6.4

6.3.6.3 Kinetics studies for the dye mixture degradation by the mesophilic bacterial cultures

Detailed analysis of the dye mixture removal process by the mesophilic bacterial cultures (pure as well as cocultures) indicated a two-phase growth and degradation mechanism. Change in the growth rate constant during the dye removal process (measured at $\lambda = 600$) was supported by the non-linear fitting of the whole data sets from the actively growing bacterial culture when Equation 6.2 was used for growth rate calculation (Panel a in Fig. 6.49-6.53). For the two-phase growth system, two different equations i.e., Equation 6.2 and 6.3 were used to find the growth rate constants k_g for each phase (Panels b in Fig. 6.49-6.53). The time and biomass concentration at the shift between the two phases were calculated when the two equations (6.2 and 6.3) were simultaneously solved. The outcome indicated considerably lower Phase-2 growth rates for all the four pure cultures and the coculture.

Table 6.17 shows a comparison of rate constants for the mesophilic bacteria. During the phase-1 *E. coli* NHS4, showed highest growth rate ($k_g = 0.669 \text{ hr}^{-1}$) followed by the coculture, *Escherichia* sp. NHS3, *P. aeruginosa* NHS1, and *Pseudomonas* sp. NHS2 with k_g values of 0.522, 0.251, 0.177, and 0.145 (hr^{-1}), respectively. For the phase-2, the rank order was not the same as observed in the phase-1. The growth rates for the higher for *P. aeruginosa* NHS1 and *Pseudomonas* sp. NHS2 ($k_g = 0.080$ and 0.077 hr^{-1} , respectively) followed by the coculture, *Escherichia* sp. NHS3, and *E. coli* NHS4 ($k_g = 0.029$, 0.027 , and 0.026 hr^{-1} , respectively). *E. coli* NHS4 and the coculture showed both the highest growth rates and earlier shifts (as compared to *Escherichia* sp. NHS3) to the second phase (after 3.3 and 3.6 hours, respectively). However, *P. aeruginosa* NHS1 despite showing a higher growth rate than *Pseudomonas* sp. NHS2, shifted to phase-2 later (time of shift = 11.7 and 7.8 hours, respectively).

The dye mixture removal (measured at $\lambda = 543$) from the synthetic textile wastewater by the mesophilic bacteria, also followed a two-phase system. Due to the simultaneous changes in growth and color, Equations 6.5 and 6.6 were derived to calculate the rate constants k_c for the two phases. Graphical analysis of the color intensity in experimental samples, through the derived equation demonstrated that the color reduction rate constant altered in the batch reactors (Panel c in Fig. 6.49-6.53). The rate constants for

the two-phase color removal by each culture are given in Table 6.17. Like the growth rates, degradation rates were higher in phase-1 for the all the cultures with k_c values of -0.926 , -0.569 , -0.425 , -0.393 , and -0.303 (hr^{-1}) for the coculture, *E. coli* NHS4, *Pseudomonas* sp. NHS2, *P. aeruginosa* NHS1, and *Escherichia* sp. NHS3, respectively. For phase-2, k_c was higher for the *E. coli* NHS4 and coculture ($k_c = -0.223$ and -0.205 hr^{-1} , respectively). This was followed by *Pseudomonas* sp. NHS2, *P. aeruginosa* NHS1, and *Escherichia* sp. NHS3 ($k_c = -0.124$, -0.116 , and -0.070 hr^{-1} , respectively). When the growth and color intensity were modeled using the growth and dye removal constants for each bacterial culture, growth was well predicted for the all culture types. In the case of dye, phase-1 degradation wasn't well predicted for *P. aeruginosa* NHS1, *Pseudomonas* sp. NHS2, and coculture as the color reduced faster than the derived model. However, it was well predicted for *Escherichia* sp. NHS3 and *E. coli* NHS4. In the case of *E. coli* NHS4, however a sharp decline in color occurred at the time point between the two phases which could not be predicted well as indicated by a break in the solid model line (Panel d in Fig. 6.49-6.53)

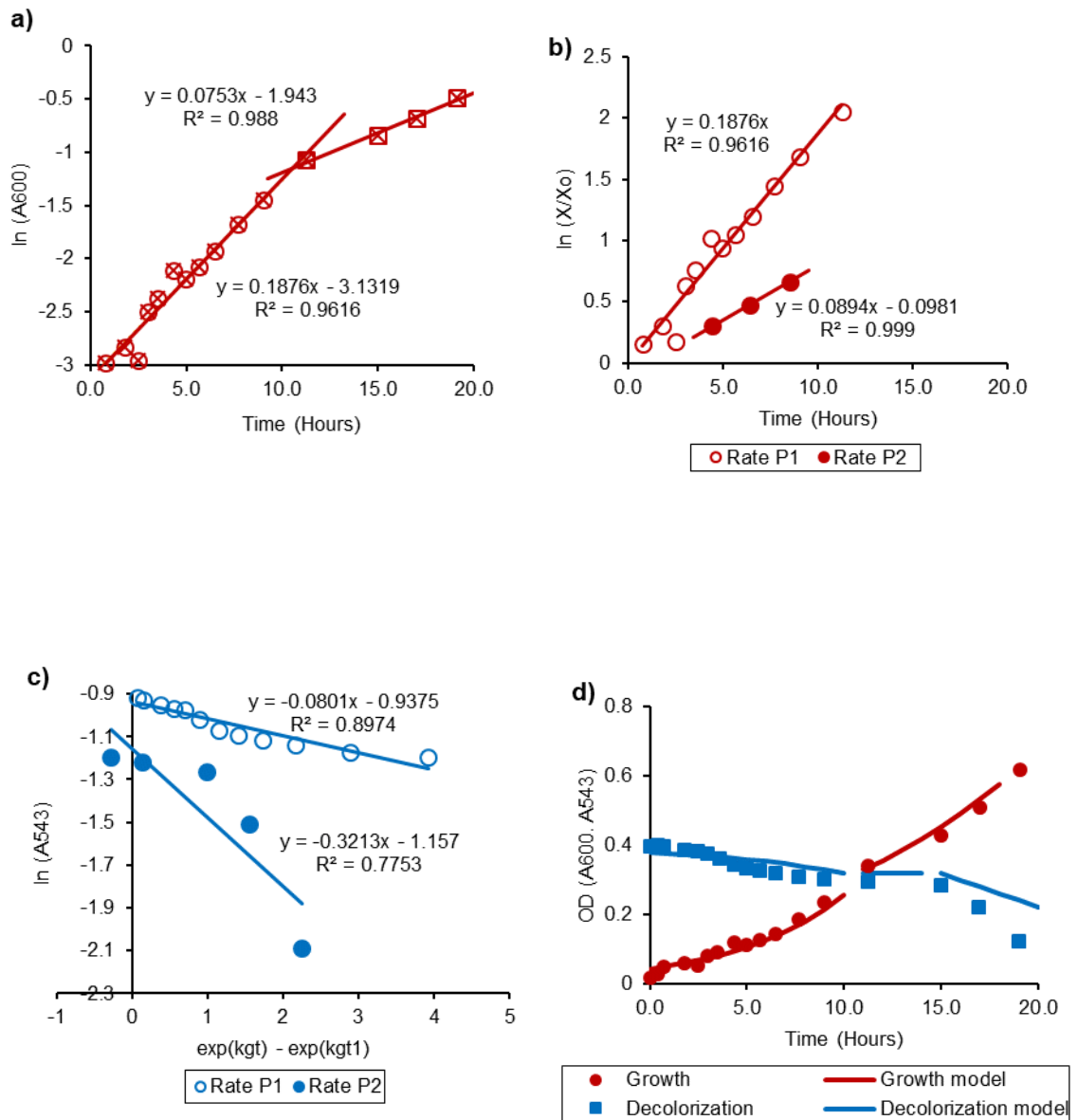


Fig. 6.49 Growth and degradation by *P. aeruginosa* NHS1 for the dye mixture. Linear regression analysis for the two-phase rate constants determination for (a) and (b) Growth, (c) Dye degradation. Growth and degradation graphs (d) with the original and modeled data indicated by the dots, squares and solid lines, respectively

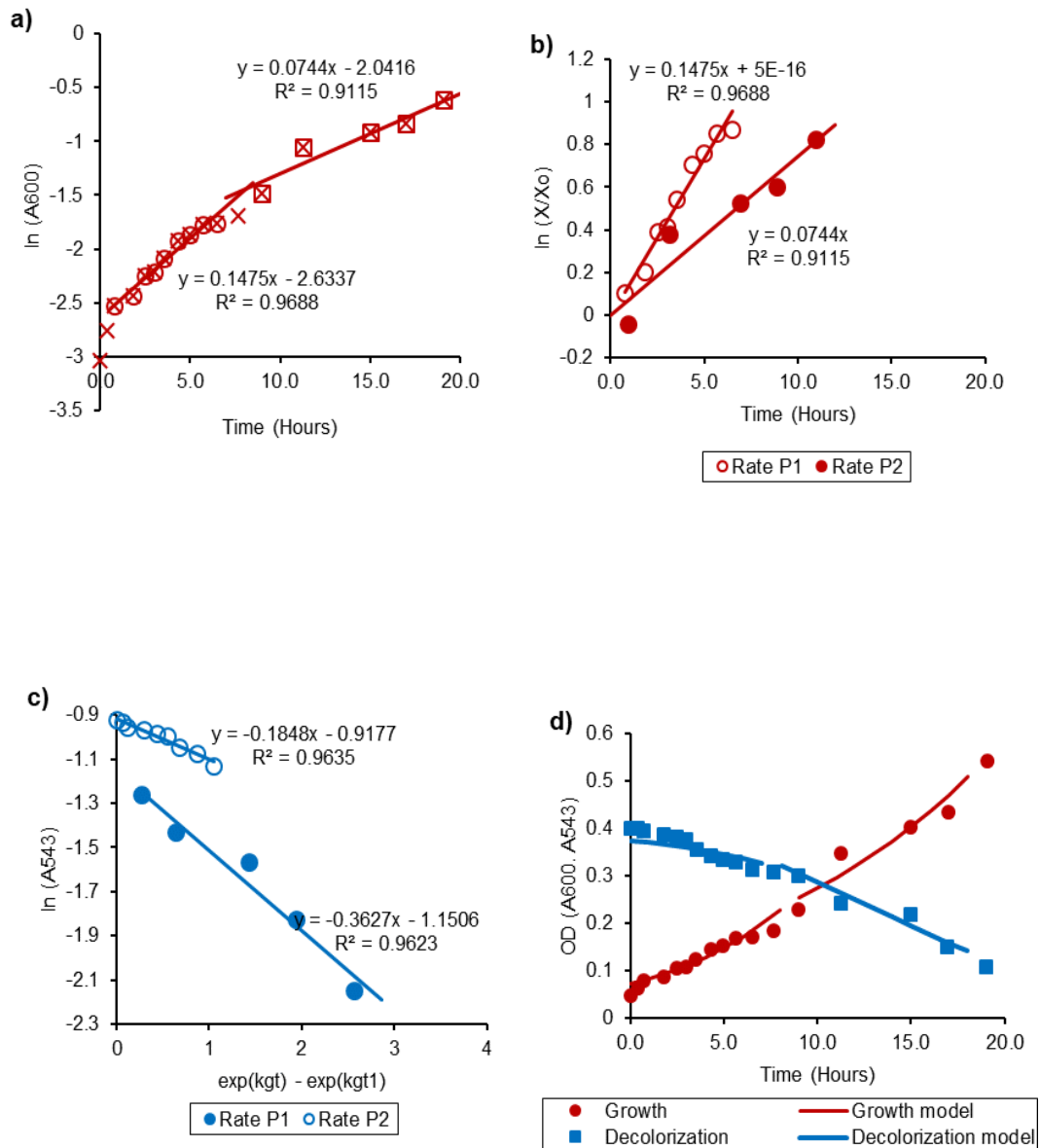


Fig. 6.50 Growth and degradation by *Pseudomonas* sp. NHS2 for the dye mixture. Linear regression analysis for the two-phase rate constants determination for (a) and (b) Growth, (c) Dye degradation. Growth and degradation graphs (d) with the original and modeled data indicated by the dots, squares and solid lines, respectively

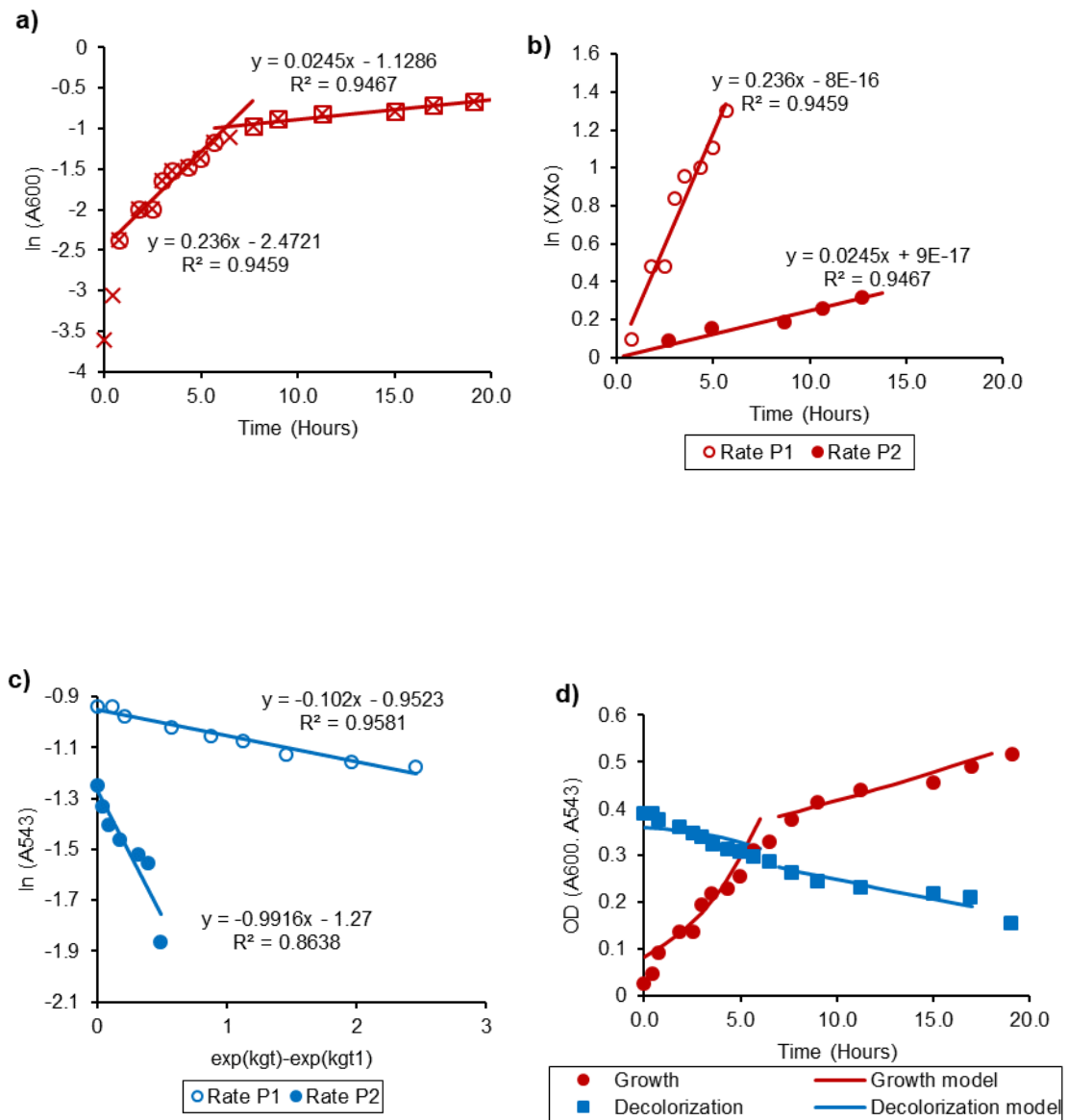


Fig. 6.51 Growth and degradation by *Escherichia* sp. NHS3 for the dye mixture. Linear regression analysis for the two-phase rate constants determination for (a) and (b) Growth, (c) Dye degradation. Growth and degradation graphs (d) with the original and modeled data indicated by the dots, squares and solid lines, respectively

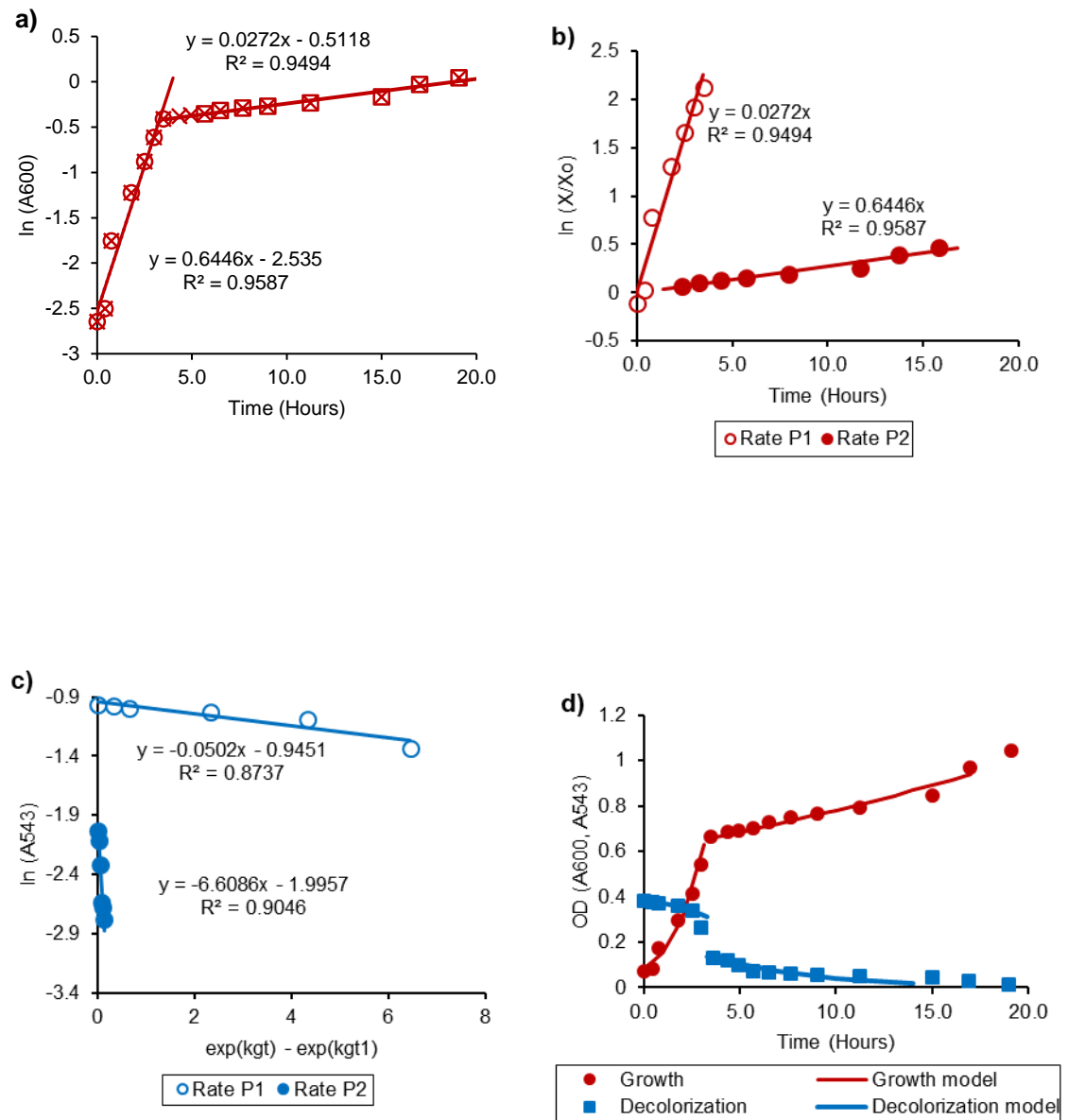


Fig. 6.52 Growth and degradation by *E. coli* NHS4 for the dye mixture. Linear regression analysis for the two-phase rate constants determination for (a) and (b) Growth, (c) Dye degradation. Growth and degradation graphs (d) with the original and modeled data indicated by the dots, squares and solid lines, respectively

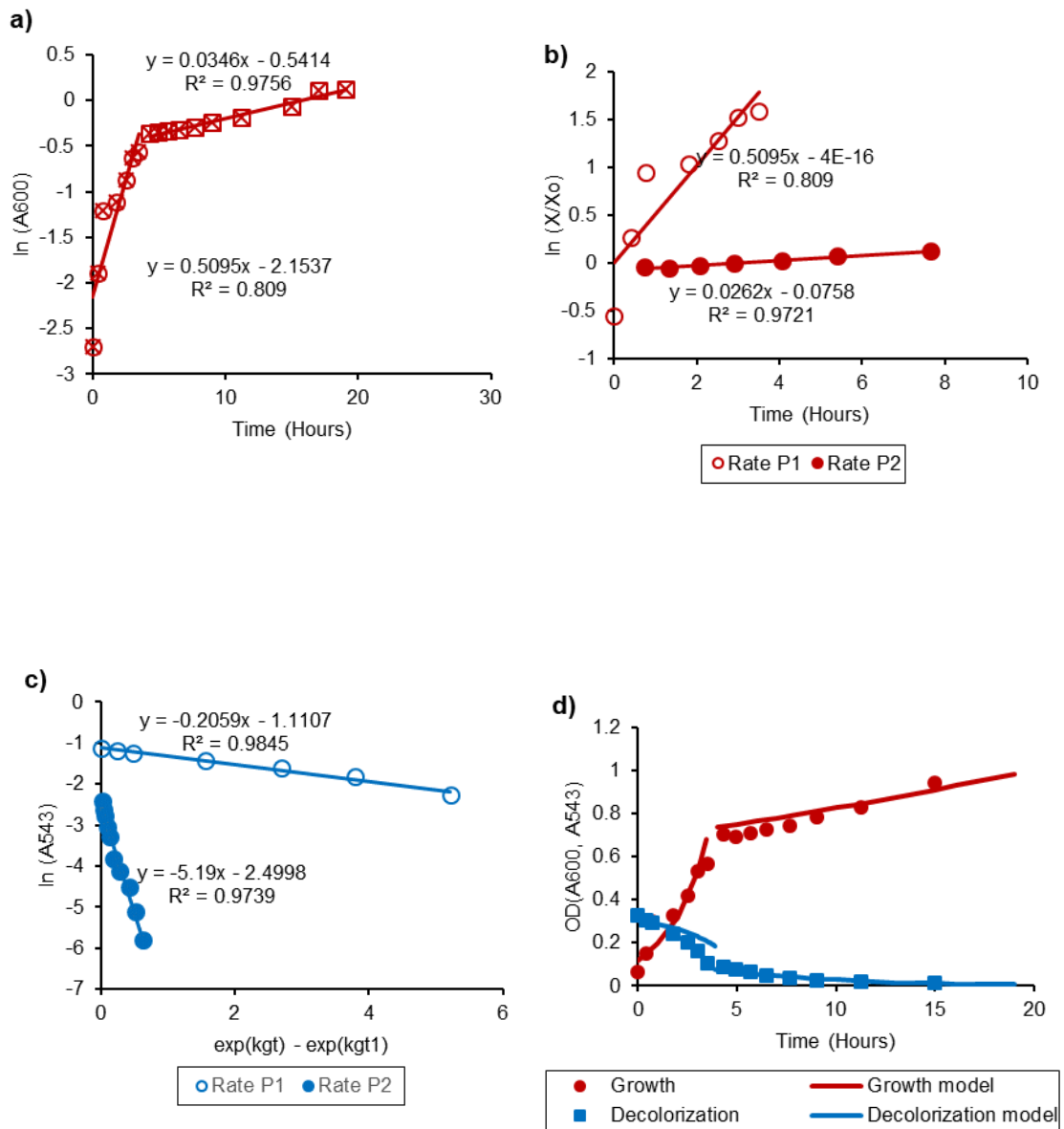


Fig. 6.53 Growth and degradation by the mesophilic coculture for the dye mixture. Linear regression analysis for the two-phase rate constants determination for (a) and (b) Growth, (c) Dye degradation. Growth and degradation graphs (d) with the original and modeled data indicated by the dots, squares and solid lines, respectively

Table 6.17 Bacterial Growth and dye degradation constants for dye mixture degradation by the mesophilic bacteria

Bacterial culture	Bacterial Growth				Dye degradation						
	Growth constant ^a k_g (hr ⁻¹) for phase-1	R^2 for phase-1 Growth	Growth constant ^b k_g (hr ⁻¹) for phase 2	R^2 for phase-1 Growth	Modeled values at Phase Shift in terms of OD			Degradation constant ^c k_c (hr ⁻¹) for phase 1	R^2 for phase-1 Degradation	Degradation constant ^d k_c (hr ⁻¹) for phase 2	R^2 for phase-2 Degradation
					Time (hr)	Bioma-ss (X)	Dye				
<i>Pseudomonas aeruginosa</i> NHS1	0.177	0.961	0.080	0.999	11.7	0.318	0.314	-0.393	0.897	-0.116	0.775
<i>Pseudomonas</i> sp. NHS2	0.145	0.968	0.077	0.911	7.8	0.237	0.321	-0.425	0.963	-0.124	0.962
<i>Escherichia</i> sp. NHS3	0.251	0.946	0.027	0.947	6.0	0.378	0.281	-0.303	0.958	-0.070	0.863
<i>Escherichia coli</i> NHS4	0.669	0.949	0.026	0.959	3.3	0.655	0.135	-0.569	0.873	-0.223	0.904
Coculture	0.522	0.809	0.029	0.972	3.6	0.731	0.082	-0.926	0.984	-0.205	0.973

^aGrowth rate for phase-1, calculated using Eq. 6.2; ^bGrowth rate for phase-2, calculated using Eq. 6.3; ^cDegradation rate constant for phase-1, calculated using Eq. 6.5; ^dDegradation rate constant for phase-2, calculated using Eq. 6.6

6.3.7 Biodegradation assessment through FTIR and GC-MS

6.3.7.1 Fourier transform Infrared (FTIR) spectral analysis

FTIR analysis was done and spectra were recorded in the mid IR region (600-4000 cm^{-1}). In the FTIR spectrum of the control (dye mixture), bands were observed at 618.28 cm^{-1} , 726.41 cm^{-1} , 876.07 cm^{-1} , 992.82 cm^{-1} , 1058.16 cm^{-1} , 1243.65 cm^{-1} , 1439.44 cm^{-1} , 1559.75 cm^{-1} , 1644.22 cm^{-1} , 1795.57 cm^{-1} , 2832.68 cm^{-1} , and 3043.39 cm^{-1} . In the FTIR spectra of the synthetic dye wastewater samples, treated by the bacterial cocultures, band intensity variations and shifts were observed in comparison to the control (Fig. 6.54a-c). For the mesophilic coculture, the peak in control spectrum located at 2832.68 cm^{-1} , disappeared, while the intensity of the peak at 3043.39 cm^{-1} altered in the FTIR spectrum of the dye wastewater sample treated by the coculture. Peaks observed at 1559.75 cm^{-1} and 1644.22 cm^{-1} were disappeared in the treated sample. Moreover, band shifts and intensity changes were observed from 1243.65 cm^{-1} , 1439.44 cm^{-1} . Some new peaks were observed at 3697.89 cm^{-1} and 3389.49 cm^{-1} . For the thermophilic coculture treated dye wastewater sample, intensity of the peaks from 1243.65 cm^{-1} -1644.22 cm^{-1} and 2832.68 cm^{-1} were altered. Moreover, new peaks were observed at 1403.94 cm^{-1} and 3228.61 cm^{-1} .

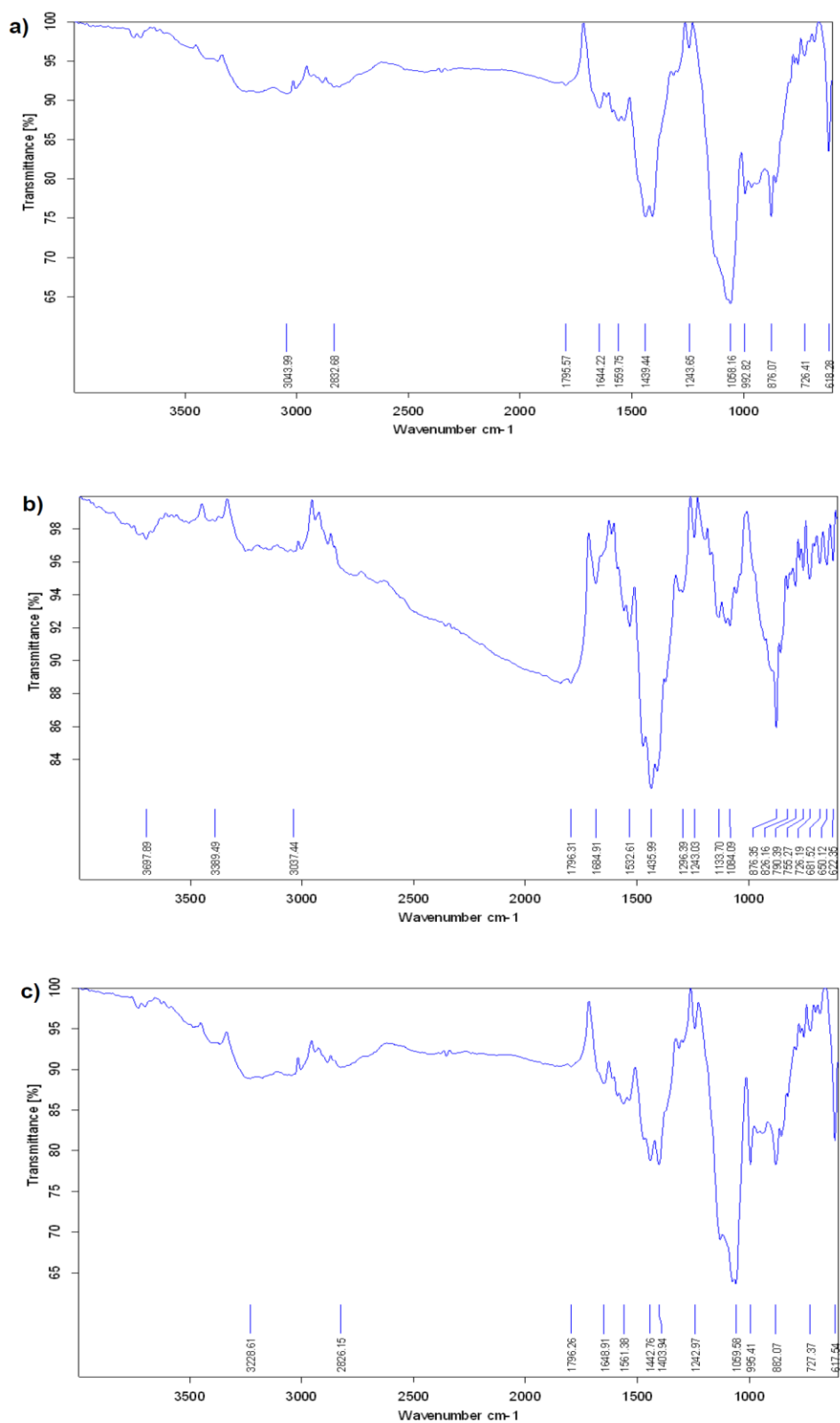


Fig. 6.54 FTIR spectra of synthetic (dye mixture containing) wastewater (a) Control; metabolites obtained after treatment by the bacterial cocultures, (b) Mesophilic; (c) Thermophilic

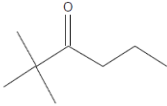
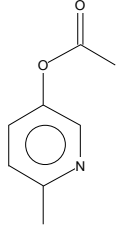
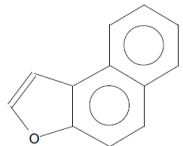
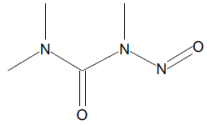
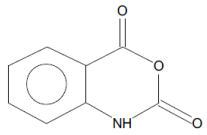
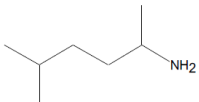
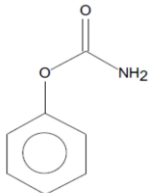
6.3.7.1 GC-MS analysis of the dye metabolites

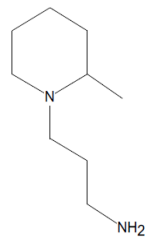
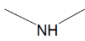
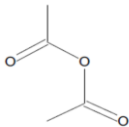
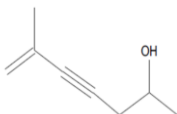
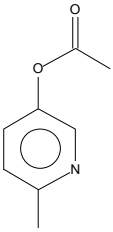
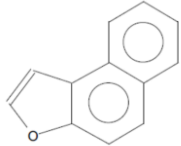
The colorless samples of the individual dyes and their mixture obtained after treatment with the mesophilic and thermophilic bacterial cocultures were analyzed through GC-MS. Based on the fragmentation patterns, base and molecular ion peaks, the structures of the products were elucidated thorough the NIST library structure comparison and detection tool.

6.3.7.1.1 GC-MS analysis of the dye metabolites produced by the mesophilic coculture

In the case of the RB 221 the detected metabolites were: 2,2-Dimethyl-3-hexanone (RT = 16.01, base peak at 57, and Mol. Ion peak at 128), 2-Methyl-5-acetoxypyridine (RT = 16.58, base peak at 109, and Mol. Ion peak at 151), and Naphtho [2,1-b] furan (RT = 20.39, base peak at 168, and Mol. Ion peak at 168) (Fig. A1, Appendix 4). RR 195 dye was found to be converted to N-Nitrosotrimethylurea (RT = 18.28, base peak at 72, and Mol. Ion peak at 131) and 2H-3,1-Benzoxazine-2,4(1H)-dione (RT = 19.35, base peak at 119, and Mol. Ion peak at 163) (Fig. A2, Appendix 4). For the RY 145 dye, the detected products were: 1,4-Dimethylpentylamine (RT = 6.08, base peak at 44, and Mol. Ion peak at 114), Carbamic acid, phenyl ester (RT = 7.45, base peak at 94, and Mol. Ion peak at 137), and N-(3-Aminopropyl)-2-pipecoline (RT = 13.96, base peak at 98, and Mol. Ion peak at 156) (Fig. A3, Appendix 4). The dye mixture was also found to be converted to a set of different products i.e., Dimethylamine (RT = 5.76, base peak at 44, and Mol. Ion peak at 45), Acetic anhydride (RT = 11.75, base peak at 43, and Mol. Ion peak at 102), 6-Methyl-6-hepten-4-yn-2-ol (RT = 12.72, base peak at 79, and Mol. Ion peak at 124), 2-Methyl-5-acetoxypyridine (RT = 16.01, base peak at 109, and Mol. Ion peak at 151), and Naphtho [2,1-b] furan (RT = 20.56, base peak at 168, and Mol. Ion peak at 168) (Fig. A4, Appendix 4). Table 6.18 enlists the detected metabolites structures and relative information for each type of dye.

Table 6.18 Dye metabolites detected in GC-MS analysis after treatment with the mesophilic coculture

Dye	R.T	B.P <i>m/z</i>	M.I peak <i>m/z</i>	Compound	Structure
Reactive Blue 221	16.01	57	128	2,2-Dimethyl-3-hexanone	
	16.58	109	151	2-Methyl-5-acetoxypyridine	
	20.39	168	168	Naphtho [2,1-b] furan	
Reactive Red 195	18.28	72	131	N-Nitrosotrimethylurea	
	19.35	119	163	2H-3,1-Benzoxazine-2,4(1H)-dione	
Reactive Yellow 145	6.08	44	114	1,4-Dimethylpentylamine	
	7.45	94	137	Carbamic acid, phenyl ester	

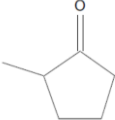
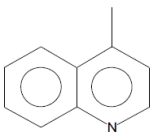
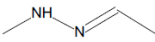
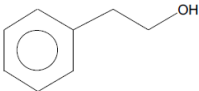
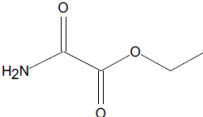
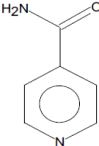
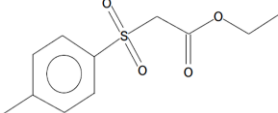
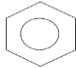
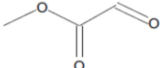
	13.96	98	156	N-(3-Aminopropyl)-2-pipecoline	
Dye Mixture	5.76	44	45	Dimethylamine	
	11.75	43	102	Acetic anhydride	
	12.72	79	124	6-Methyl-6-hepten-4-yn-2-ol	
	16.01	109	151	2-Methyl-5-acetoxypyridine	
	20.56	168	168	Naphtho [2,1-b] furan	

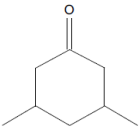
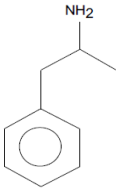
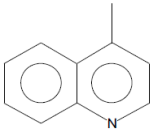
R.T = Retention time; B.P = Base peak, and M.I = Molecular ion

6.3.7.1.2 GC-MS analysis of the dye metabolites produced by the thermophilic coculture

For the RB 221 dye, the detected products were: 2-Methylcyclopentanone (RT = 15.51, base peak at 42, and Mol. Ion peak at 98) and p-Methylquinoline (RT = 18.51, base peak at 143, and Mol. Ion peak at 143) (Fig. A5, Appendix 4). In the case of RR 195 dye, the detected products were: Acetaldehyde, N-methylhydrazone (RT = 8.8, base peak at 72, and Mol. Ion peak at 72) and Phenylethyl Alcohol (RT = 12.75, base peak at 91, and Mol. Ion peak at 122) (Fig. A6, Appendix 4). The metabolites observed for the RY 145 dye were: Ethyl oxamate (RT = 4.77, base peak at 44, and Mol. Ion peak at 117), Pyridine-4-carboxylic acid amide (RT = 16.38, base peak at 122, and Mol. Ion peak at 122), and Acetic acid, (p-tolylsulfonyl)-, ethyl ester (RT = 21.35, base peak at 91, and Mol. Ion peak at 242) (Fig. A7, Appendix 4).. The analysis of dye mixture after bacterial treatment showed conversion to: Benzene (RT = 6.98, base peak at 78, and Mol. Ion peak at 78)Methyl glyoxylate (RT = 7.45, base peak at 29, and Mol. Ion peak at 88), 3,5-Dimethyl cyclohexanone (RT = 12.14, base peak at 69, and Mol. Ion peak at 126), Dextroamphetamine (RT = 16.01, base peak at 44, and Mol. Ion peak at 135), and p-Methylquinoline (RT = 18.49, base peak at 143, and Mol. Ion peak at 143) (Fig. A8, Appendix 4) . Table 6.19 enlists the detected metabolites structures and relative information for each type of dye.

Table 6.19 Dye metabolites detected in GC-MS analysis after treatment with the thermophilic coculture

Dye	R.T	B.P <i>m/z</i>	M.I peak <i>m/z</i>	Compound	Structure
Reactive Blue 221	15.51	42	98	2-Methylcyclopentanone	
	18.51	143	143	p-Methylquinoline	
Reactive Red 195	8.8	72	72	Acetaldehyde, N-methylhydrazone	
	12.75	91	122	Phenylethyl Alcohol	
Reactive Yellow 145	14.77	44	117	Ethyl oxamate	
	16.38	122	122	Pyridine-4-carboxylic acid amide	
	21.35	91	242	Acetic acid, (p-tolylsulfonyl)-, ethyl ester	
Dye Mixture	6.98	78	78	Benzene	
	7.45	29	88	Methyl glyoxylate	

12.14	69	126	3,5-Dimethyl cyclohexanone	
16.01	44	135	Dextroamphetamine	
18.49	143	143	p-Methylquinoline	

R.T = Retention time; B.P = Base peak, and M.I = Molecular ion

6.3.8 Toxicity analyses for the synthetic dye wastewater metabolites

6.3.8.1 Phytotoxicity assay

The detoxification potential of the bacterial cocultures for the dye mixture containing synthetic textile wastewater, was investigated through phytotoxicity analysis by using *T. aestivum* (wheat) and *R. sativus* (radish) seeds (Table 6.20). *T. aestivum* seeds showed 85% seed germination, root length = 1.58 cm [± 0.005], and shoot length = [1.07 cm \pm 0.37], when watered with the colored wastewater sample i.e., the positive control. With the mesophilic coculture treatment dye wastewater, 100% seed germination was observed for the *T. aestivum* seeds. The root (1.99 cm [± 0.41]) and shoot (1.86 cm [± 0.11]) lengths were also improved. With the thermophilic coculture treated wastewater, no improvement in the seed germination was observed, however root and shoot lengths were increased, the respective values were: 4.91cm [± 1.02] and 3.68 cm [± 1.44], respectively.

In the case of *R. sativus* seeds, 80% seed germination was recorded with the colored effluent sample (control). The root and shoot lengths were 2.17 cm [± 1.28] and 1.45 cm [± 0.87], respectively. When watered with the mesophilic coculture treated synthetic wastewater sample, seed germination, root, and shoot lengths were increased. The respective values were: 100%, 4.5 cm [± 1.31], and 2.78 cm [± 0.08]. When the radish seeds were watered with the thermophilic coculture treated sample, seed germination was similar as that observed with control. However, root (2.81 cm [± 1.24]) and shoot [2.02 cm [± 0.88]] lengths were higher.

Table 6.20 Phytotoxic analysis of the reactive azo dye mixture containing synthetic effluent (before and after bacterial treatment)

Sample	<i>T. aestivum</i>			<i>R. sativus</i>		
	Germination (%)	Root length (cm) ± S.E.	Shoot length (cm) ± S.E.	Germination (%)	Root length (cm) ± S.E.	Shoot length (cm) ± S.E.
Negative Control	100	3.18 ± 0.43	2.83 ± 0.36	100	2.69 ± 0.12	2.68 ± 0.96
Positive control	85	1.58 ± 0.005	1.07 ± 0.37	80	2.17 ± 1.28	1.45 ± 0.87
MC-TSTW	100	1.99 ± 0.41	1.86 ± 0.11	100	4.5 ± 1.31	2.78 ± 0.08
TC-TSTW	85	4.91 ± 1.02	3.68 ± 1.44	80	2.81 ± 1.24	2.02 ± 0.88

M.C-TSTW., Mesophilic coculture treated synthetic textile wastewater, T.C-TSTW., Thermophilic coculture treated synthetic textile wastewater, S.E., standard error

6.3.8.2 Acute toxicity assay

Through the brine shrimp larval mortality analysis, the acute toxicity of the synthetic dye (azo dye mixture containing) wastewater was assessed and compared with the response recorded with the decolorized wastewater obtained after treatment with the cocultures. With the positive control, i.e., the colored synthetic wastewater 35% larval mortality was recorded. Following treatment with the mesophilic and thermophilic cocultures, the larval mortality was reduced in comparison to the control. The respective values were: 25 and 30% (Fig. 6.55).

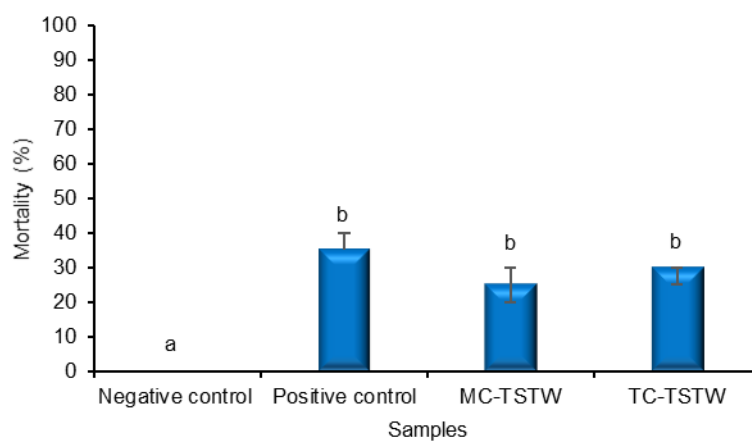


Fig. 6.55 Effect of the synthetic textile wastewater on Brine shrimp larvae (before and after bacterial treatment). Same letters on the bars indicate statistically non-significant values ($\alpha= 0.05$, One-way ANOVA followed by Tukey's HSD)

6.4 Discussion

In the present study, reactive azo dyes (RB 221, RR 195, and RY145) decolorizing bacteria with different temperature tolerance abilities (mesophilic and thermophilic) were isolated from two different niches, i.e., the textile sludge and hot water spring sample, respectively. Following bacterial identification procedures, the decolorization efficiency of the designed cocultures was assessed and optimized for the reactive azo dye mixture containing synthetic textile wastewater. Additionally, the dye treatment kinetics for individual and mixed dyes were studied, and nature of the dye metabolites was investigated through analytical methods. Toxicity analyses were also performed to assess the detoxification potential of the bacteria.

Reactive azo dyes decolorizing bacteria were isolated through the culture enrichment protocol. Of the 64 mesophilic bacterial isolates, 4 showed 73-83 and 17-60% color removal (50 ppm dye mixture) under static and shaking incubation, respectively. In the case of the thermophilic isolates, 4 isolates (out of 23) demonstrated 82-85 and 53-71% decolorization of the 50-ppm dye mixture, with and without agitation, respectively. So, these most efficient mesophilic and thermophilic isolates were used for further experimentation, and the experiments were conducted under static conditions. In general, the static condition was found to be relatively more suitable for the decolorization process by all the tested isolates ($p < 0.05$) (Fig. 6.1-6.2). The more efficient color reduction seen under the static condition is in accordance with the available literature. For example, Jain et al. (2012) reported complete decolorization of 200-ppm Reactive Violet 5R in 18 hours by an indigenous mixed bacterial culture under static condition. Additionally, Kumar Garg et al. (2012) observed 69% decolorization of 100 ppm Orange II (100 ppm) in 96 hours by *Pseudomonas putida* SKG-1 under static condition, and 36.5% decolorization with shaking. Meerbergen et al., (2018), also reported efficient decolorization (up to 80%) of Reactive Orange 16 and Reactive Green 19 dyes under static incubation. The ability of the most efficient isolates (except for one mesophilic isolate) to grow and decolorize under both aerobic/shaking and anoxic/static conditions, indicates the facultative nature of the bacteria (Solís et al., 2012). Similar findings were reported by Ghodake et al., (2011), while studying the treatment of Amaranth dye by using *A. calcoaceticus* NCIM 2890, where the tested bacterium showed 91 and 68% dye removal with and without agitation. The low color

removal efficiency under aerobic conditions could be attributed to the competition between oxygen (a strong terminal electron acceptor) and the azo bond for the oxidation of NADH (Chang et al., 2001).

Through the biochemical and partial 16S rRNA gene analyses (Table 6.6; Fig.6.3-6.4), two of the selected mesophilic isolates (NHS1 and NHS2) were found to be phylogenetically related and identified as *Pseudomonas aeruginosa* NHS1 and *Pseudomonas* sp. NHS2. The other two isolates (NHS3 and NHS4) were also related and identified as *Escherichia* sp. NHS3, and *Escherichia coli* NHS4. Both *Pseudomonas* and *Escherichia* have previously been reported for the decolorization of different types of dyes (Chang et al., 2000; Işik and Sponza, 2003; Jadhav et al., 2013; Cerboneschi et al., 2015). In the case of the thermophilic bacterial isolates, NHT1 and NHT2 were from the same genus and identified as *Aeribacillus pallidus* and *Aeribacillus* sp., respectively. The other two viz. NHT3 and NHT4 showed sequence homology to *Geobacillus* sp., and *Brevibacillus borstelensis*, respectively. Members of the genus *Aeribacillus* and *Geobacillus* have only been reported in a few studies for the treatment of some anthraquinone and azo dyes (Tastimi et al., 2013; Ambika Verma and Shirkot, 2014). Moreover, *Brevibacillus borstelensis* have been explored for the plastic degradation (Arya, Mishra, and Sharma 2016). Except for *Pseudomonas*, all other genera, reported in this study have not been explored before for the treatment of the reactive azo dyes used in the current study.

Following identification, mesophilic and thermophilic bacterial cocultures were designed by mixing the isolates in different combinations (Table 6.1-6.2). The mesophilic (with all the four mesophilic isolates, M. coculture-10) and thermophilic (combination of all four thermophilic bacterial isolates, T. coculture-10) cocultures showed a significantly higher decolorization of the dye mixture (50-ppm) containing synthetic textile wastewater when compared to the individual isolates with an 11-22 and 8-10% increase, respectively ($p < 0.05$). With the mesophilic and thermophilic cocultures, 93.42 and 91.92% color reduction occurred, in 24 hours respectively (Fig. 6.5). As this consortium was found to be more efficient for color removal, it was subjected to optimization experiments. Previous studies have also reported enhancement of color removal capability when using mixed cultures. Khehra et al., (2005) observed faster decolorization of 20 ppm Acid Red 88 by a consortium of four

bacteria (*Bacillus cereus*, *Pseudomonas putida*, *Pseudomonas fluorescence* (BN-5) and *Stenotrophomonas acidaminiphila*) when compared to the individual isolates. To achieve the same level of decolorization that the consortium achieved in 24 hours, individual isolates required 60 hours. et al. (2009) also reported similar findings, with the decolorization of 50 ppm Scarlet R at a faster rate when using consortium-GR than when using the pure cultures *Proteus vulgaris* NCIM-2027 and *Micrococcus glutamicus*. The improvement in the color removal could be due to synergistic activities of the bacteria in mixed communities where different enzymes are available to carry out a given function in the degradation pathway (Ali, 2010).

The decolorization activity of the two bacterial cocultures was optimized through OFAT. The color removal efficiency (50-ppm dye mixture) of the cocultures was tested in the presence of additional carbon sources at 0.1% (w/v), as they provide the bacteria with required energy and serve as electron donors for azo bond cleavage (McMullan et al., 2001) (Fig. 6.6), The color removal ability of both the mesophilic and thermophilic bacterial cocultures was significantly enhanced in the presence of glucose as compared to the other carbon sources, with up to 94 and 91% decolorization recorded after 120 hours, respectively. ($p < 0.05$). Glucose has been reported as the most suitable carbonaceous co-substrate in different studies (Singh et al., 2014; Meerbergen et al., 2018). Additionally, the effect of nitrogenous co-substrates at 0.1% (w/v) on the decolorization performance, was investigated for both cocultures (Fig. 6.7). Organic nitrogen sources were found to be more effective than the inorganic ones ($p < 0.05$) with the yeast extract resulted in the highest decolorization i.e., 92 and 90% (120 hours) by the mesophilic and thermophilic cocultures, respectively ($p < 0.05$). Yeast extract is one of the most widely reported nitrogenous co-substrate for the dye decolorization process (Bhavsar, Dudhagara, and Tank 2018).

The color (50-ppm dye mixture effluent) removal ability of the mesophilic and thermophilic cocultures was investigated at different incubation temperatures (Fig. 6.8). The mesophilic coculture showed a considerable activity over a temperature range of 30-40 °C and was found to be more efficient at 35 °C with up to 98% decolorization recorded after 24 hours ($p < 0.05$). However, at lower and higher temperature values, a sharp decline in the color reduction was observed ($p < 0.05$) that might have resulted from the reduced enzymatic activity outside the optimal range and/or low cell viability

(Çetin and Dönmez 2006). The growth of the coculture also followed a somewhat similar pattern (Fig. A9, Appendix 4). Similarly, Vijayalakshmi and Muthukumar, (2015) observed best treatment efficiency by a bacterial coculture for the dye effluent at 37 °C. Contrary to that, Chang et al. (2000) reported a mutant strain of *E. coli* that could decolorize 200 ppm Reactive Red 22 dye at 28 °C. In the case of the thermophilic bacterial coculture, substantial activity and stability (growth given in Fig. A10 Appendix 4) was observed over a higher temperature range of 45-55 °C with the optimal temperature value of 50 °C (up to 90% decolorization in 24 hours) ($p < 0.05$). Likewise, in another study 50 °C was found as the optimal temperature for the decolorization of 0.3 mM Orange I, by *Novibacillus thermophilus* SG-1 (Yu et al., 2015). Contrary to that Tastimi et al., (2013) and Ambika Verma and Shirkot, (2014) reported best decolorization results by the pure cultures of *Aeribacillus pallidus* and *Geobacillus thermocatenulatus* at 60 °C.

The cocultures' dye mixture (50-ppm) decolorization potential was investigated in relation to varying initial pH values (Fig. 6.9). The mesophilic coculture, showed optimal decolorization performance over the pH range of 6-8 with up to 98% color reduction recorded after 24 hours ($p > 0.05$). Although, lower and higher pH values i.e., 5 and 9 influenced the color removal efficiency when compared to the optimal pH range ($p < 0.05$) but the coculture retained a substantial decolorization activity i.e., up to 80% (120 hours). Similarly, Mate and Pathade, (2012) observed decolorization of Reactive Red 195 dye by a strain of *E. faecalis* over a pH range of 5-8. For the thermophilic coculture, a pH range of 7-9 was found to be the optimal for the reactive azo dye mixture decolorization (93-96% in 48 hours) ($p > 0.05$). However, at lower and higher pH values i.e., 5, 6, and 10, the color reduction was significantly reduced ($p < 0.05$) which might have occurred due to diminished activity of enzymes involved in the color removal process. Contrary to that, Deive et al., (2010) developed thermophilic consortia that showed maximum activity under neutral pH conditions.

The dye tolerance profile was studied by using varying initial dye mixture concentrations in the synthetic effluent (Fig. 6.10). The mesophilic coculture showed optimal activity at 50-100 ppm dye mixture concentration with up to 98% decolorization recorded in 24 hours. Moreover, the coculture retained a substantial decolorization efficacy (up to 84% in 120 hours) at a dye mixture concentration of 250

ppm. However, a sharp decline (< 30) was observed upon further increase in the effluent strength ($p < 0.05$). The decolorization activity of the thermophilic cocultures was optimal at 50-ppm dye mixture concentration, as up to 97% decolorization was observed in 48 hours ($p < 0.05$). The coculture showed considerable color reduction at 150 ppm (up to 81% in 120 hours). Additionally, the decolorization activity was drastically affected (reduced below 25%) beyond 150 ppm ($p < 0.05$). Likewise, a decrease in the color removal extent at higher dye concentrations was reported in other studies (Khehra et al., 2005; Jirasripongpun et al., 2007; Joe et al. 2011; Lv et al., 2013). The low bacterial activity in the presence of higher dye concentration results from the imbalanced dye to cell ratio and more pronounced toxicity, inflicted by the sulfonic acid groups in the reactive azo dyes (Kalyani et al., 2008).

To assess the salt tolerance of the cocultures, their decolorization ability was assessed in the presence of different NaCl concentrations (Fig. 6.11). The color (100 ppm dye mixture) removal efficiency of the mesophilic coculture was significantly affected by the NaCl beyond 4% concentration (about 35% reduction, $p < 0.05$). Moreover, the coculture tolerated up to 8% NaCl concentration with ~60% decolorization recorded after 120 hours, which makes it a promising candidate for the treatment of real textile effluents containing high salt load. There are few studies that have reported similar salt tolerance levels for the dye degrading bacteria (Ogugbue et al., 2011; Meerbergen et al., 2018). The thermophilic coculture's dye (50-ppm mixture) removal ability was greatly affected by the NaCl load in the medium and showed tolerance up to 4% NaCl beyond which only less than 40% dye removal was observed ($p < 0.05$). The reduced bacterial activity at high NaCl concentrations results from the increased osmotic pressure leading to cell lysis (Peyton et al., 2002).

The key factors (pH, temperature, and dye mixture concentration) affecting the decolorization performance of the bacterial cocultures were selected and levels were assigned according to the OFAT findings to apply the Response Surface methodology for the statistical optimization thorough BBD. Both quadratic models for the decolorization response were statistically supported (Tables 6.10-6.11). For the mesophilic and thermophilic coculture, the 2D contour and 3D surface plot were mostly elliptical, indicating a significant interaction of the studied parameters. Moreover, two of the three studied parameters, i.e., temperature and dye concentration seemed to have

a greater effect on the response. The cocultures as observed in the one factor experiments were relatively stable to pH variations (Fig. 6.14-6.19). Furthermore, the validation experiments confirmed the models' accuracy and optimal combinations giving the highest response were obtained. For the mesophilic coculture, the optimum temperature, pH, and dye concentration values were 34.75 °C, 7.69 and 111 ppm, respectively. For the thermophilic coculture. 50.25, 7.31, and 60 ppm were the optimal values of temperature, pH, and dye concentration, respectively (Table 6.12-6.13). Similarly, Das and Mishra, (2017), used BBD design to optimize the decolorization of Reactive Green 19 dye. The three parameters used to optimize the decolorization response were temperature, pH and yeast extract concentration.

To investigate the interrelationship of microbial growth and dye removal rates in stoichiometric terms, kinetics studies were carried out using first order kinetics equations. Through the growth and color reduction data, collected from a set of batch reactor vessels, degradation rates were studied for the individual dyes by the pure mesophilic and thermophilic bacterial cultures and the dye mixture by the pure as well as cocultures. For the mesophilic and thermophilic bacteria, bacterial growth k_g and dye degradation k_c (for individual dyes), rates were calculated using equations 6.2 and 6.4, respectively (Tables 6.14-6.15). Mesophilic bacteria showed relatively higher growth and degradation rates than the thermophilic isolates. In general, no characteristic trend was observed in terms of the dye type and bacterial growth and its degradation response, even in the case of phylogenetically related bacteria. Moreover, the degradation rates (k_c) were usually independent of the bacterial growth rate constant k_g values. Similarly, in the case of the dye mixture, degradation rates were not directly related to the growth rates and the increased toxic effect of the mixture was also not evident as described in another study (Malik et al., 2018). Furthermore, the coculture (despite a relatively similar growth rate to its individual components i.e., the pure cultures), showed a higher degradation rate which conforms to the theory of concerted metabolic activity of bacteria in combined form (Khehra et al., 2005; Joshi et al., 2010) (Table 6.16). The growth and dye removal were well predicted in most cases as indicated by the determination coefficients and the respective models (Panels c Fig. 6.20-6.48). These findings are in accord with the literature, where dye removal process for different types

of dyes, followed first order kinetics model (Karunya et al., 2014; Das and Mishra, 2017).

When dye mixture removal by the mesophilic bacteria (pure and cocultures) was studied in detail, a two-phase growth and degradation process was observed. The two-phasic growth rates (k_g) were calculated using the Equations: 6.2 and 6.3. The simultaneous solution of these two equations gave the time and biomass values at the shift between the two phases. For all bacterial cultures phase-2 growth rates were substantially lower than the phase-1. The shift in the growth phase could be explained by the change in bacterial metabolism because of the utilization of varying electron donors present in the synthetic dye wastewater (Yu et al., 2015). The phase-1 growth rates were in the following order *E. coli* NHS4 > coculture > *Escherichia* sp. NHS3 > *P. aeruginosa* NHS1 > *Pseudomonas* sp. NHS2. However, the phase-2 did not show the same rank order (Table 6.17). The two-phase dye degradation constants (k_c) were calculated using Equations 6.5 and 6.6. Like growth, the degradation rates were higher for the phase-1 with the rank order of: coculture > *E. coli* NHS4 > *Pseudomonas* sp. NHS2, > *P. aeruginosa* NHS1 > *Escherichia* sp. NHS3. Hence as expected, the combination of bacteria in the coculture resulted in a faster dye removal as reported earlier (Sin et al., 2016) (Table 6.17). The models derived using the two-phase growth constant well predicted the growth for each culture type, however the degradation was modeled with varying accuracy (Panel d in Fig. 6.49-6.53). First-order degradation kinetics with two different successive phases, with the latter showing considerably lower dye removal rate constant values, have been reported earlier for the mono (Brilliant Violet 5R) and diazo (Remazol Black B) reactive dyes (Lourenço, Novais, and Pinheiro 2006)

For the biodegradation analysis, FTIR spectroscopy was performed and different bands were observed in the FTIR spectrum of control (untreated dye mixture containing synthetic textile water) (Fig. 6.55a). The peaks observed at 3043.39 and 2832.68 cm^{-1} corresponded to C=C and C-H stretching vibrations, respectively. The band at 1795.57 cm^{-1} represented C=O stretching (Lambert et al., 1998). The presence of azo (-N=N-) linkages was indicated by the bands observed in the range of 1439.44-1559.75 cm^{-1} indicated (Coates, 2006; Kumar Garg et al., 2012).. The bands at 1644.22 and 1243.65 cm^{-1} corresponded to primary amide and C-N linkage, respectively (Jain et al., 2012).

The band at 1058.16 cm^{-1} corresponded to S=O bond stretching (natural cons). The bands at 992.82 and 876.07 cm^{-1} indicated aromatic rings vibrations, while the band 726.41 cm^{-1} corresponded to the C–Cl stretch (Lambert et al, 1998; Yuen et al., 2005).

FTIR spectra of the decolorized textile wastewater samples, treated by the bacterial cocultures, showed band intensity variations and shifts in comparison to the control (Fig. 6.55b-c). Intensity variation (in the thermophilic coculture treated sample) and peak disappearance (in the case of the mesophilic coculture treated sample) at 2832.68 cm^{-1} , indicated fluctuations and breakage of some C–H linkages. Some C=C bond fluctuations (in the mesophilic coculture treated sample) were shown by the altered intensity of the peak at 3043.39 cm^{-1} . The appearance of new peaks in mesophilic and thermophilic coculture treated samples, at 3389.49 cm^{-1} and 3228.61 cm^{-1} , respectively indicated the presence O–H and N–H linkages (Franciscon et al., 2012; Kumar Garg et al., 2012). Moreover, the new peak observed at 3697.89 cm^{-1} (mesophilic coculture treated sample) indicated the amide N–H stretch (Kumar Garg et al., 2012). In the mesophilic coculture treated sample, band shift and disappearance around 1439.44 cm^{-1} and 1559.75 cm^{-1} , respectively, indicated the distortion of –N=N– bonds, that in turn signify the removal of color from the synthetic wastewater. Similarly –N=N– bonds variations were observed in the thermophilic coculture treated sample, indicated by the intensity variations in the designated regions (Jain et al., 2012).

The decolorized synthetic textile effluent samples (containing the individual and mixed dyes), obtained after treatment with the bacterial cocultures were further analysed through GC-MS. The mass spectra of the original reactive azo dyes and their mixture could not be obtained due to the complex, non-volatile, and multisulfonated aromatic structures, which make them incompatible with the GC-MS instrument (Riu et al. 1997; Zhao et al. 2007). The GC-MS analysis of degradation products produced by both cocultures showed that the individual dyes (RB 221, RR 195, and RY 145) and their mixture were converted to smaller compounds with lower molecular masses in comparison to the parent molecules, which in turn confirms that the decolorization was a result of biodegradation (Jadhav et al., 2008; Jain et al., 2012). Using the base peak, molecular ion peak and fragmentation pattern data, different types of single and double ringed aromatic compounds along with some aliphatic products were identified through the NIST library comparison tool (Tables 6.18-6.19). Likewise, the conversation of RB

221, RR 195, and RY 145 (in individual forms) to low molecular weight ringed and straight chained organic compounds have been reported earlier (Savizi, Kariminia, and Bakhshian 2012; Shuang et al. 2008; Song et al. 2010). Mineralization of the ringed metabolites for further detoxification could be achieved through harnessing other microbial combinations.

To assess the ecoefficiency of the biotreatment by using bacterial cocultures, toxicity of the decolorized samples obtained after biodegradation was assessed through phytotoxicity and brine shrimp acute toxicity tests. In the phytotoxicity assay, *T. aestivum* and *R. sativus* seeds were used. The germination rates, root and shoot lengths of both seeds were significantly higher with the samples obtained after treatment with the mesophilic coculture ($p < 0.05$). However, when the wheat and radish seeds were watered with the samples obtained after biodegradation by the thermophilic coculture, statistically significant improvement was observed only in the root and shoot lengths ($p < 0.05$). The germination rate wasn't improved in comparison to the control ($p > 0.05$) (Table 6.20). Likewise, reduced phytotoxicity of textile dyes following biodegradation by bacterial cocultures have been reported earlier (Ali, 2010). In the invertebrate acute toxicity assay, brine shrimp viability was improved following treatment with both cocultures, however the results were not statistically significant ($p > 0.05$). So, in general the low molecular weight metabolites obtained after biodegradation showed a relatively less toxicity than the original dye mixture.

6.5 Conclusion

Bacteria capable of decolorizing reactive azo dyes containing synthetic textile wastewater, with different temperature tolerance abilities (mesophilic and thermophilic) were isolated from two separate locations i.e., textile sludge and hot water spring samples, respectively. Through 16S rRNA gene analysis, most efficient mesophilic isolates were identified as: *Pseudomonas aeruginosa* NHS1, *Pseudomonas* sp. NHS2, *Escherichia* sp. NHS3, and *Escherichia coli* NHS4. The thermophiles were identified as: *Aeribacillus pallidus*, *Aeribacillus* sp., *Geobacillus* sp. NHT3 and *Brevibacillus borstelensis* NHT4. The decolorization potential of the designed cocultures was optimized through OFAT followed by statistical process optimization RSM. The mesophilic and thermophilic cocultures efficiently removed the dye mixture

when supplied with the co-substrates (0.1% [w/v) yeast extract and glucose, each). Through BBD method, the mesophilic coculture showed optimal activity at temperature: 34.75 °C, pH: 7.69, and dye concentration: 111 ppm. For the thermophilic coculture, 50.25, 7.31, and 60 ppm, were the optimal values for temperature, pH, and dye concentration, respectively. The growth and degradation rates for the individual and mixed dyes were modeled using first order kinetics through data linearization and normalization. In most cases one phasic growth and degradation was observed except for the dye mixture removal by the mesophilic pure cultures and coculture. In that case a two-phasic growth and dye removal strategy better explained the treatment systems. The kinetics data obtained from this study will demonstrate the approach needed to enable modelling required to move biotreatment of azo dyes towards industrial application. Furthermore, mesophilic bacteria were relatively more efficient than the thermophiles. FTIR spectra and GC-MS analysis confirmed the formation of low molecular weight products by both cocultures. The metabolites were relatively less toxic towards plants seeds and brine shrimp larvae, which further documents the eco-safety of the treatment methods used in this study.

Generally, the following major conclusions can be drawn from the sets of studies conducted:

- Toxicity profile investigation of reactive azo dyes (RB 221, RR 195, RY 145, and their mixture) at organismic-level (using a set of test specimens), indicated a variable toxic effect of dyes and their mixture. The microbial test specimens (except *F. fujikuroi* and *R. solani*) were relatively more sensitive. Moreover, *D. magna* showed a relatively similar response to the microbes. The dyes and their mixture did not show acute toxicity, as the EC50 values were higher than 100 ppm in almost all cases.
- The immobilized fungal reactor and hybrid activated sludge reactor (with Scotch Brite™ as support material) were found to be effective for the treatment of synthetic textile wastewater. The repeated usage of the immobilized microbial formulations did not affect the treatment efficiency. Immobilized fungal reactor was more efficient in the color removal, however, a better performance was shown by the hybrid activated sludge in terms of the COD reduction and system's stability (pH). The duality of the hybrid system (attached and suspended bacterial biomass) enhanced the reactor's efficacy.
- The natural bacterial consortia with different temperature, pH, and salt tolerance profiles (mesophilic [MBC], thermophilic [TBC], and alkaliphilic-halotolerant [AHBC]) efficiently removed the dyes (100 ppm; provided with glucose and yeast extract, 0.1% [w/v] each) in 72 (MBC and AHBC) and 120 hours (TBC). MBC and AHBC were more efficient around mesophilic temperature conditions i.e. 35 °C, while ~50 °C was found as the suitable temperature for TBC. The optimal pH for both types of consortia was neutral. Moreover, AHBC effectively treated the dye mixture effluent, under high pH (~10.0) and salinity (10% [w/v]) conditions.
- The dye tolerance limits for MBC, AHBC, and TBC were 200, 250, and 150 ppm, respectively. The natural bacterial consortia also showed a substantial (up to 70%) COD reduction. Next generation sequencing following process optimization, showed that under a set of given conditions, all the three consortia consisted of a complex mixture of anaerobic, facultative and aerobic bacteria with some of the most efficient dye degrading genera.

- The designed mesophilic and thermophilic cocultures efficiently removed the dye mixture when supplied with the co-substrates (0.1% [w/v] yeast extract and glucose, each). Through BBD method, the mesophilic coculture showed optimal activity at temperature: 34.75 °C, pH: 7.69, and dye concentration: 111 ppm. For the thermophilic coculture, 50.25, 7.31, and 60 ppm, were the optimal values for temperature, pH, and dye concentration, respectively.
- The designed cocultures showed more stability to the initial pH, with the decolorization observed over a range of 6-8 and 7-9 for mesophilic and thermophilic cocultures, respectively. The dye tolerance limits were 250 and 150 ppm, respectively.
- The growth and degradation rates for the individual and mixed dyes were modeled using first order kinetics through data linearization and normalization. In most cases one phasic growth and degradation was observed except for the dye mixture removal by the mesophilic pure cultures and coculture. In that case a two-phasic growth and dye removal strategy better explained the treatment systems.
- FTIR band changes observed in all the studies indicated that decolorization was achieved as a result of biodegradation. Moreover, the GC-MS analyses showed the conversion of reactive azo dyes to low molecular weight aliphatic and aromatic compounds by both types of consortia (natural and designed). Toxicity analyses post microbial dye treatment procedures further showed the eco-safety of the methods used, as the metabolites did not show phytotoxic and acute toxic effects.
- The different treatment strategies (with a major focus on bacteria except one study involving the application of fungus) employed in the present sets of studies for the reactive azo dye waste, showed varying levels of efficacy. The fungal and activated sludge reactor systems presented overall favourable treatment options with the latter as more suitable reactor setup as explained earlier in this section. Application of natural and designed consortia with different physiological properties for the dye waste treatment showed the former ones somewhat more efficient than the latter. However, maintenance of a mixed culture requires more stringent conditions. Contrary to this, designed coculture with known organisms are relatively easier to maintain and could help to gain a more detailed insight into the treatment dynamics by applying some more sophisticated real time analytical techniques.

- Studies focusing on cellular and molecular level effects (mutagenic effects) of the dyes could be carried out to gain an insight into the interactions of dyes with the different living systems and their possible role in different ecological levels.
- The efficiency of the batch reactors configurations based on the fungal and hybrid systems, could be tested for different types of dyes in other operational modes i.e. sequential batch and continuous.
- The natural and designed bacterial consortia could be tested for their bioaugmentation capabilities using real textile wastewater.
- The kinetics data for the mesophilic, thermophilic bacteria, and their cocultures could be used to design and model the pilot scale treatment options.
- For a more detailed posttreatment toxicity analysis, the dye concentrations could be further optimized and/or some other test organisms, such Zebrafish and *Caenorhabditis elegans* could be utilized that might help in the determination of acute as well chronic toxic effects of dyes and their metabolites.
- Enzymatic and functional genetic analysis could be carried out to broaden the understanding of the mechanisms involved in the removal of dyes.
- Detailed GC-MS analysis of samples collected at multiple time points could help in deriving the degradation pathways for the dyes. Moreover, isotopic labelling of dyes could also be suitable option in this regard.
- Mineralization of the ringed metabolites obtained after treatment with the cocultures (for further detoxification) could be achieved through harnessing other microbial combinations.

- Aghaie-Khouzani, M., H. Forootanfar, M. Moshfegh, M. R. Khoshayand, and M. A. Faramarzi. 2012. "Decolorization of Some Synthetic Dyes Using Optimized Culture Broth of Laccase Producing Ascomycete *Paraconiothyrium Variabile*." *Biochemical Engineering Journal* 60:9–15.
- Agrawal, Shweta, Devayani Tipre, Bhavesh Patel, and Shailesh Dave. 2014. "Optimization of Triazo Acid Black 210 Dye Degradation by *Providencia* Sp. SRS82 and Elucidation of Degradation Pathway." *Process Biochemistry* 49(1):110–19.
- Aguedach, Abdelkahhar, Stephan Brosillon, Jean Morvan, and El Kbir Lhadi. 2005. "Photocatalytic Degradation of Azo-Dyes Reactive Black 5 and Reactive Yellow 145 in Water over a Newly Deposited Titanium Dioxide." *Applied Catalysis B: Environmental* 57(1):55–62.
- Akhtar, Muhammad Furqan, Muhammad Ashraf, Aqeel Javeed, Aftab Ahmad Anjum, Ali Sharif, Ammara Saleem, Bushra Akhtar, Abdul Muqeet Khan, and Imran Altaf. 2016. "Toxicity Appraisal of Untreated Dyeing Industry Wastewater Based on Chemical Characterization and Short Term Bioassays." *Bulletin of Environmental Contamination and Toxicology* 96(4):502–7.
- Aksu, Z??mriye. 2005. "Application of Biosorption for the Removal of Organic Pollutants: A Review." *Process Biochemistry* 40(3–4):997–1026.
- Al-Amrani, Waheeba Ahmed, Poh Eng Lim, Chye Eng Seng, and Wan Saime Wan Ngah. 2014. "Factors Affecting Bio-Decolorization of Azo Dyes and COD Removal in Anoxic-Aerobic REACT Operated Sequencing Batch Reactor." *Journal of the Taiwan Institute of Chemical Engineers* 45(2):609–16.
- Ali, Hazrat. 2010. "Biodegradation of Synthetic Dyes - A Review." *Water, Air, and Soil Pollution* 213(March):251–73.
- Ali, Naeem, Abdul Hameed, and Safia Ahmed. 2009. "Physicochemical Characterization and Bioremediation Perspective of Textile Effluent, Dyes and Metals by Indigenous Bacteria." *Journal of Hazardous Materials* 164:322–28.
- Allen, D. Grant and Campbell W. Robinson. 1989. "Hydrodynamics and Mass Transfer In *Aspergillus Niger* Fermentations in Bubble Column and Loop Bioreactors." *Biotechnology and Bioengineering* 34(6):731–40.
- Almeida, E. J. R. and C. R. Corso. 2014. "Comparative Study of Toxicity of Azo Dye Procion Red MX-5B Following Biosorption and Biodegradation Treatments with the Fungi *Aspergillus Niger* and *Aspergillus Terreus*." *Chemosphere* 112:317–22.
- Amaral, P. F. F., D. L. a Fernandes, a P. M. Tavares, a B. M. R. Xavier, M. C. Cammarota, J. a P. Coutinho, and M. a Z. Coelho. 2004. "Decolorization of Dyes from Textile Wastewater by *Trametes Versicolor*." *Environmental Technology* 25(11):1313–20.
- Ambika Verma and Poonam Shirkot. 2014. "Purification and Characterization of Thermostable Laccase from Thermophilic *Geobacillus Thermocatenulatus* MS5 and Its Applications in Removal of Textile Dyes." *Scholars Academic Journal of BiosciencesOnline) Sch. Acad. J. Biosci* 2(8):2321–6883.
- Amoozegar, Mohammad Ali, Mahbod Hajighasemi, Javad Hamedi, Sedigheh Asad, and Antonio Ventosa. 2011. "Azo Dye Decolorization by Halophilic and

- Halotolerant Microorganisms.” *Annals of Microbiology* 61:217–30.
- An, Yu, Liping Jiang, Jun Cao, Chengyan Geng, and Laifu Zhong. 2007. “Sudan I Induces Genotoxic Effects and Oxidative DNA Damage in HepG2 Cells.” *Mutation Research/Genetic Toxicology and Environmental Mutagenesis* 627(2):164–70.
- Anastasi, Antonella, Barbara Parato, Federica Spina, Valeria Tigini, Valeria Prigione, and Giovanna Cristina Varese. 2011. “Decolourisation and Detoxification in the Fungal Treatment of Textile Wastewaters from Dyeing Processes.” *New Biotechnology* 29(1):38–45.
- Andleeb, Saadia, Naima Atiq, Muhammad Ishtiaq Ali, Raja Razi-Ul-Hussnain, Maryam Shafique, Bashir Ahmad, Pir Bux Ghumro, Masroor Hussain, Abdul Hameed, and Safia Ahmad. 2010. “Biological Treatment of Textile Effluent in Stirred Tank Bioreactor.” *International Journal of Agriculture and Biology* 12:256–60.
- Andreou, Lefkothea-Vasiliki. 2013. “Preparation of Genomic DNA from Bacteria.” Pp. 143–51 in *Methods in enzymology*. Vol. 529.
- Anjaneyulu, Y., N. Sreedhara Chary, and D. Samuel Suman Raj. 2005. “Decolourization of Industrial Effluents – Available Methods and Emerging Technologies – A Review.” *Reviews in Environmental Science and Bio/Technology* 4(4):245–73.
- Araújo, Ademir Sérgio Ferreira and Regina Teresa Rosim Monteiro. 2005. “Plant Bioassays to Assess Toxicity of Textile Sludge Compost.” *Scientia Agricola* 62(3):286–90.
- Aravind, U. K., B. George, M. S. Baburaj, S. Thomas, A. P. Thomas, and C. T. Aravindakumar. 2010. “Treatment of Industrial Effluents Using Polyelectrolyte Membranes.” *Desalination* 252(1–3):27–32.
- Artzi, Lior, Bareket Dassa, Ilya Borovok, Melina Shamshoum, Raphael Lamed, and Edward A. Bayer. 2014. “Cellulosomics of the Cellulolytic Thermophile *Clostridium Clariflavum*.” *Biotechnology for Biofuels* 7:100.
- Arun Prasad, a. S. and K. V. Bhaskara Rao. 2010. “Physico Chemical Characterization of Textile Effluent and Screening for Dye Decolorizing Bacteria.” *Global Journal of Biotechnology & Biochemistry* 5:80–86.
- Arun Prasad, A. S., V. S. V Satyanarayana, and K. V. Bhaskara Rao. 2013. “Biotransformation of Direct Blue 1 by a Moderately Halophilic Bacterium *Marinobacter* Sp. Strain HBRA and Toxicity Assessment of Degraded Metabolites.” *Journal of Hazardous Materials* 262:674–84.
- Arya, Ridhima, Navnit Kumar Mishra, and Anil K. Sharma. 2016. “*Brevibacillus Borstelensis* and *Streptomyces Albogriseolus* Have Roles to Play in Degradation of Herbicide, Sulfosulfuron.” *3 Biotech* 6(2):1–7.
- Asad, S., M. A. Amoozegar, A. A. Pourbabae, M. N. Sarbolouki, and S. M. M. Dastgheib. 2007. “Decolorization of Textile Azo Dyes by Newly Isolated Halophilic and Halotolerant Bacteria.” *Bioresource Technology* 98(11):2082–88.
- Asgher, Muhammad, Sadia Noreen, and Haq Nawaz Bhatti. 2010. “Decolorization of Dye-Containing Textile Industry Effluents Using *Ganoderma Lucidum* IBL-05 in Still Cultures.” *Water Environment Research : A Research Publication of the*

- Water Environment Federation* 82(4):357–61.
- Ayed, Lamia, Abdelkarim Mahdhi, Abdelkarim Cheref, and Amina Bakhrouf. 2011. “Decolorization and Degradation of Azo Dye Methyl Red by an Isolated *Sphingomonas Paucimobilis*: Biototoxicity and Metabolites Characterization.” *Desalination* 274(1–3):272–77.
- Ayyaru, Sivasankaran and Sangeetha Dharmalingam. 2014. “Enhanced Response of Microbial Fuel Cell Using Sulfonated Poly Ether Ether Ketone Membrane as a Biochemical Oxygen Demand Sensor.” *Analytica Chimica Acta* 818:15–22.
- Babu, B. Ramesh, a K. Parande, S. Raghu, and T. Prem Kumar. 2007. “Cotton Textile Processing : Waste Generation and Effluent Treatment.” *The Journal of Cotton Science* 153:141–53.
- Bae, Jin Seok and Harold S. Freeman. 2007. “Aquatic Toxicity Evaluation of Copper-Complexed Direct Dyes to the *Daphnia Magna*.” *Dyes and Pigments* 73:126–32.
- Baêta, B. E. L., S. F. Aquino, S. Q. Silva, and C. a. Rabelo. 2012. “Anaerobic Degradation of Azo Dye Drimaren Blue HFRL in UASB Reactor in the Presence of Yeast Extract a Source of Carbon and Redox Mediator.” *Biodegradation* 23:199–208.
- Bafana, Amit, Minakshi Jain, Gaurav Agrawal, and Tapan Chakrabarti. 2009. “Bacterial Reduction in Genotoxicity of Direct Red 28 Dye.” *Chemosphere* 74(10):1404–6.
- Bakshi, D. K., S. Saha, I. Sindhu, and P. Sharma. 2006. “Use of *Phanerochaete Chrysosporium* Biomass for the Removal of Textile Dyes from a Synthetic Effluent.” *World Journal of Microbiology and Biotechnology* 22(8):835–39.
- Balapure, Kshama, Nikhil Bhatt, and Datta Madamwar. 2015. “Mineralization of Reactive Azo Dyes Present in Simulated Textile Waste Water Using down Flow Microaerophilic Fixed Film Bioreactor.” *Bioresource Technology* 175:1–7.
- Baldrian, Petr. 2006. “Fungal Laccases – Occurrence and Properties.” *FEMS Microbiology Reviews* 30(2):215–42.
- Barceló, Damià., M. (Mira) Petrović, and J. Armengol. 2011. *The Ebro River Basin*. Springer.
- Barsing, Prashant, Arti Tiwari, Taruna Joshi, and Sanjeev Garg. 2011. “Application of a Novel Bacterial Consortium for Mineralization of Sulphonated Aromatic Amines.” *Bioresource Technology* 102(2):765–71.
- Basha, C. Ahmed, K. V. Selvakumar, H. J. Prabhu, P. Sivashanmugam, and Chang Woo Lee. 2011. “Degradation Studies for Textile Reactive Dye by Combined Electrochemical, Microbial and Photocatalytic Methods.” *Separation and Purification Technology* 79(3):303–9.
- Beall, Jeffrey. 2011. “Internet Scientific Publications.” *The Charleston Advisor* 12:39–41.
- Bhattacharya, Amrik, Nidhi Goyal, and Anshu Gupta. 2017. “Degradation of Azo Dye Methyl Red by Alkaliphilic, Halotolerant *Nesterenkonia Lacusekhoensis* EMLA3: Application in Alkaline and Salt-Rich Dyeing Effluent Treatment.” *Extremophiles* 21(3):479–90.
- Bhattacharya, S. S. and R. Banerjee. 2008. “Laccase Mediated Biodegradation of 2,4-

- Dichlorophenol Using Response Surface Methodology.” *Chemosphere* 73(1):81–85.
- Bhavsar, Sunil, Pravin Dudhagara, and Shantilal Tank. 2018. “R Software Package Based Statistical Optimization of Process Components to Simultaneously Enhance the Bacterial Growth, Laccase Production and Textile Dye Decolorization with Cytotoxicity Study.” *PLoS ONE* 13(5):1–18.
- Bibi, F. and Z. Ali. 2013. “Measurement of Diversity Indices of Avian Communities at Taunsa Barrage Wildlife Sanctuary, Pakistan.” *Journal of Animal and Plant Sciences* 23(2):469–74.
- Box, G. E. P. and D. W. Behnken. 1960. “Some New Three Level Designs for the Study of Quantitative Variables.” *Technometrics* 2(4):455.
- Bragger, J. ..., A. .. Lloyd, S. .. Soozandehfar, S. .. Bloomfield, C. Marriott, and G. .. Martin. 1997. “Investigations into the Azo Reducing Activity of a Common Colonic Microorganism.” *International Journal of Pharmaceutics* 157(1):61–71.
- Brown, Mark A. and John E. Casida. 1988. “Daminozide: Oxidation by Photochemically Generated Singlet Oxygen to Dimethylnitrosamine and Succinic Anhydride.” *Journal of Agricultural and Food Chemistry* 36(5):1064–66.
- Brown, Mark A. and Stephen C. De Vito. 1993. “Predicting Azo Dye Toxicity.” *Critical Reviews in Environmental Science and Technology* 23(3):249–324.
- BuntiĆ, Aneta V., Marija D. Pavlović, Dušan G. Antonović, Slavica S. Šiler-Marinković, and Suzana I. Dimitrijević-Branković. 2017. “A Treatment of Wastewater Containing Basic Dyes by the Use of New Strain *Streptomyces Microflavus* CKS6.” *Journal of Cleaner Production* 148:347–54.
- Bürger, Sibylle and Andreas Stolz. 2010. “Characterisation of the Flavin-Free Oxygen-Tolerant Azoreductase from *Xenophilus Azovorans* KF46F in Comparison to Flavin-Containing Azoreductases.” *Applied Microbiology and Biotechnology* 87(6):2067–76.
- Cabral, Joaquim M. S., Manuel Mota, Johannes Tramper, Manuel Mota, and Johannes Tramper. 2001. “PULSING BIOREACTORS.” 343–67.
- Carmen, Zaharia and Suteu Daniel. 2012. “Textile Organic Dyes – Characteristics, Polluting Effects and Separation/Elimination Procedures from Industrial Effluents – A Critical Overview.” in *Organic Pollutants Ten Years After the Stockholm Convention - Environmental and Analytical Update*. InTech.
- Castro, Francine D., João Paulo Bassin, and Márcia Dezotti. 2017. “Treatment of a Simulated Textile Wastewater Containing the Reactive Orange 16 Azo Dye by a Combination of Ozonation and Moving-Bed Biofilm Reactor: Evaluating the Performance, Toxicity, and Oxidation by-Products.” *Environmental Science and Pollution Research* 24(7):6307–16.
- Cerboneschi, Matteo, Massimo Corsi, Roberto Bianchini, Marco Bonanni, and Stefania Tegli. 2015. “Decolorization of Acid and Basic Dyes: Understanding the Metabolic Degradation and Cell-Induced Adsorption/Precipitation by *Escherichia Coli*.” *Applied Microbiology and Biotechnology* 99(19):8235–45.
- Çetin, Demet and Gönül Dönmez. 2006. “Decolorization of Reactive Dyes by Mixed Cultures Isolated from Textile Effluent under Anaerobic Conditions.” *Enzyme*

- and Microbial Technology* 38(7):926–30.
- Chacko, Joshni T. and Kalidass Subramaniam. 2011. *Enzymatic Degradation of Azo Dyes-A Review*. Vol. 1.
- Chan, Giek Far, Noor Aini Abdul Rashid, Lee Suan Chua, Norzarini Ab.lilah, Rozita Nasiri, and Mohamed Roslan Mohamad Ikubar. 2012. “Communal Microaerophilic–Aerobic Biodegradation of Amaranth by Novel NAR-2 Bacterial Consortium.” *Bioresource Technology* 105:48–59.
- Chan, Yi Jing, Mei Fong Chong, Chung Lim Law, and D. G. Hassell. 2009. “A Review on Anaerobic-Aerobic Treatment of Industrial and Municipal Wastewater.” *Chemical Engineering Journal* 155:1–18.
- Chang, Jo Shu, Chien Chou, Yu Chih Lin, Ping Jei Lin, Jin Yen Ho, and Tai Lee Hu. 2001. “Kinetic Characteristics of Bacterial Azo-Dye Decolorization by *Pseudomonas Luteola*.” *Water Research* 35(12):2841–50.
- Chang, Jo Shu, Tai Shin Kuo, Yun Peng Chao, Jin Yen Ho, and Ping Jei Lin. 2000. “Azo Dye Decolorization with a Mutant *Escherichia Coli* Strain.” *Biotechnology Letters* 22(9):807–12.
- Charumathi, Dasarathan and Nilanjana Das. 2013. “Bioaccumulation of Synthetic Dyes by *Candida Tropicalis* Growing in Sugarcane Bagasse Extract Medium.”
- Chen, Bor-Yann and Jo-Shu Chang. 2007. “Assessment upon Species Evolution of Mixed Consortia for Azo Dye Decolorization.” *Journal of the Chinese Institute of Chemical Engineers* 38(3–4):259–66.
- Chen, Kuo Cheng, Jane Y. Wu, Dar J. Liou, and S. C. J. Hwang. 2003. “Decolorization of the Textile Dyes by Newly Isolated Bacterial Strains.” *Journal of Biotechnology* 101:57–68.
- Cheng, Ying, HongYan Lin, Zuliang Chen, Mallavarapu Megharaj, and Ravi Naidu. 2012. “Biodegradation of Crystal Violet Using *Burkholderia Vietnamensis* C09V Immobilized on PVA-Sodium Alginate-Kaolin Gel Beads.” *Ecotoxicology and Environmental Safety* 83:108–14.
- Chengalroyen, M. D. and E. R. Dabbs. 2012. “The Microbial Degradation of Azo Dyes: Minireview.” *World Journal of Microbiology and Biotechnology* 389–99.
- Cheriaa, Jihane, Monia Khaireddine, Mahmoud Rouabhia, and Amina Bakhrouf. 2012. “Removal of Triphenylmethane Dyes by Bacterial Consortium.” *The Scientific World Journal* 2012:1–9.
- Chollom, MN, S. Rathilal, VL Pillay, and D. Alfa. 2015. “The Applicability of Nanofiltration for the Treatment and Reuse of Textile Reactive Dye Effluent.” *Water SA* 41(3):398.
- Chu, Wan-Loy, Yike-Chu See, and Siew-Moi Phang. 2009. “Use of Immobilised *Chlorella Vulgaris* for the Removal of Colour from Textile Dyes.” *Journal of Applied Phycology* 21(6):641–48.
- Chung, K. T., Ssu-Ching Chen, Tit Yee Wong, Ying-Sing Li, Cheng-I. Wei, and Ming W. Chou. 2000. “Mutagenicity Studies of Benzidine and Its Analogs: Structure-Activity Relationships.” *Toxicological Sciences* 56(2):351–56.
- Coates, John. 2006. “Interpretation of Infrared Spectra, A Practical Approach.” in *Encyclopedia of Analytical Chemistry*. Chichester, UK: John Wiley & Sons, Ltd.

- Coughlin, Michael F., Brian K. Kinkle, and Paul L. Bishop. 2003. "High Performance Degradation of Azo Dye Acid Orange 7 and Sulfanilic Acid in a Laboratory Scale Reactor after Seeding with Cultured Bacterial Strains." *Water Research* 37(11):2757–63.
- Dafale, Nishant, N. Nageswara Rao, Sudhir U. Meshram, and Satish R. Wate. 2008. "Decolorization of Azo Dyes and Simulated Dye Bath Wastewater Using Acclimatized Microbial Consortium - Biostimulation and Halo Tolerance." *Bioresource Technology* 99(7):2552–58.
- Das, Adya and Susmita Mishra. 2017. "Removal of Textile Dye Reactive Green-19 Using Bacterial Consortium: Process Optimization Using Response Surface Methodology and Kinetics Study." *Journal of Environmental Chemical Engineering* 5(1):612–27.
- Das, Devlina, D. Charumathi, and Nilanjana Das. 2011. "Bioaccumulation of the Synthetic Dye Basic Violet 3 and Heavy Metals in Single and Binary Systems by *Candida Tropicalis* Grown in a Sugarcane Bagasse Extract Medium: Modelling Optimal Conditions Using Response Surface Methodology (RSM) and Inhibition Kinetics." *Journal of Hazardous Materials* 186(2–3):1541–52.
- Davis, Mackenzie Leo and David A. Cornwell. 2013. *Introduction to Environmental Engineering*. McGraw-Hill.
- Dawkar, Vishal V., Umesh U. Jadhav, Amar a. Telke, and Sanjay P. Govindwar. 2009. "Peroxidase from *Bacillus* Sp. VUS and Its Role in the Decolorization of Textile Dyes." *Biotechnology and Bioprocess Engineering* 14:361–68.
- Deive, F. J., A. Domínguez, T. Barrio, F. Moscoso, P. Morán, M. A. Longo, and M. A. Sanromán. 2010. "Decolorization of Dye Reactive Black 5 by Newly Isolated Thermophilic Microorganisms from Geothermal Sites in Galicia (Spain)." *Journal of Hazardous Materials* 182(1–3):735–42.
- DeSantis, T. Z., P. Hugenholtz, N. Larsen, M. Rojas, E. L. Brodie, K. Keller, T. Huber, D. Dalevi, P. Hu, and G. L. Andersen. 2006. "Greengenes, a Chimera-Checked 16S RRNA Gene Database and Workbench Compatible with ARB." *Applied and Environmental Microbiology* 72(7):5069–72.
- Dowd, Scot E., Todd R. Callaway, Randall D. Wolcott, Yan Sun, Trevor McKeehan, Robert G. Hagevoort, and Thomas S. Edrington. 2008. "Evaluation of the Bacterial Diversity in the Feces of Cattle Using 16S RDNA Bacterial Tag-Encoded FLX Amplicon Pyrosequencing (BTEFAP)." *BMC Microbiology* 8(1):125.
- Dua, M., A. Singh, N. Sethunathan, and A. Johri. 2002. "Biotechnology and Bioremediation: Successes and Limitations." *Applied Microbiology and Biotechnology* 59(2–3):143–52.
- Durruty, Ignacio, Diana Fasce, Jorge F. roilá. González, and Erika A. lejandr. Wolski. 2015. "A Kinetic Study of Textile Dyeing Wastewater Degradation by *Penicillium Chrysogenum*." *Bioprocess and Biosystems Engineering* 38(6):1019–31.
- Edgar, Robert C. 2010. "Search and Clustering Orders of Magnitude Faster than BLAST." *Bioinformatics* 26(19):2460–61.
- El-Sheekh, Mostafa M., M. M. Gharieb, and G. W. Abou-El-Souod. 2009.

- “Biodegradation of Dyes by Some Green Algae and Cyanobacteria.”
International Biodeterioration & Biodegradation 63(6):699–704.
- Electrochemical Science Group., Norazzizi, Siti Fathrita Mohd Amir, Riyanto, and Mohamed Rozali Othman. 2006. *International Journal of Electrochemical Science*. Vol. 8. Electrochemical Science Group.
- Enayatzamir, Kheirghadam, Hossein a. Alikhani, Bagher Yakhchali, Fatemeh Tabandeh, and Susana Rodríguez-Couto. 2010. “Decolouration of Azo Dyes by Phanerochaete Chrysosporium Immobilised into Alginate Beads.”
Environmental Science and Pollution Research 17:145–53.
- Enayatzamir, Kheirghadam, Hossein A. Alikhani, Bagher Yakhchali, Fatemeh Tabandeh, and Susana Rodríguez-Couto. 2010. “Decolouration of Azo Dyes by Phanerochaete Chrysosporium Immobilised into Alginate Beads.”
Environmental Science and Pollution Research 17(1):145–53.
- Engle, Marcella, Carl Woese, and Juergen Wiegel. 1995. Isolation and Characterization of a Novel. *International Journal of Systematic Bacteriology*.
- Erden, Emre, Yasin Kaymaz, and Nurdan Kasikara Pazarlioglu. 2011. “Biosorption Kinetics of a Direct Azo Dye Sirius Blue K-CFN by *Trametes Versicolor*.”
Electronic Journal of Biotechnology 14(2).
- Erkurt, Hatice Atacag. and Muhammad Arshad. 2010. *Biodegradation of Azo Dyes*. Springer.
- Fernandes, Henrique, Luiz Ventura, Cunha Menezes, Jhennifer Rebecca Fernandes-cal, Marcos Roberto, De Mattos Fontes, Carla C. Munari, F. Kummrow, Gisela De Arag, Daisy Maria, São Paulo, São Paulo, and São Paulo. 2018. “Research Article InVivo Genotoxicity of a Commercial C . I . Disperse Red1Dye.” (June):1–7.
- Ferraz, Elisa R. A., Zhaohui Li, Olga Boubriak, and Danielle P. de Oliveira. 2012. “Hepatotoxicity Assessment of the Azo Dyes Disperse Orange 1 (DO1), Disperse Red 1 (DR1,) and Disperse Red 13 (DR13) in HEPG2 Cells.” *Journal of Toxicology and Environmental Health, Part A* 75(16–17):991–99.
- Forgacs, Esther, Tibor Cserháti, and Gyula Oros. 2004. “Removal of Synthetic Dyes from Wastewaters: A Review.” *Environment International* 30:953–71.
- Franciscon, Elisangela, Matthew James Grossman, Jonas Augusto Paschoal, Felix Guillermo Reyes, and Lucia Regina Durrant. 2012. “Decolorization and Biodegradation of Reactive Sulfonated Azo Dyes by a Newly Isolated Brevibacterium Sp. Strain VN-15.” *SpringerPlus* 1:37.
- Franciscon, Elisangela, Andrea Zille, Fabiana Fantinatti-Garboggini, Isis Serrano Silva, Artur Cavaco-Paulo, and Lucia Regina Durrant. 2009. “Microaerophilic-Aerobic Sequential Decolourization/Biodegradation of Textile Azo Dyes by a Facultative *Klebsiella* Sp. Strain VN-31.” *Process Biochemistry* 44:446–52.
- Galán, J., A. Rodríguez, J. M. Gómez, S. J. Allen, and G. M. Walker. 2013. “Reactive Dye Adsorption onto a Novel Mesoporous Carbon.” *Chemical Engineering Journal* 219:62–68.
- Gao, Da-Wen, Xiang-Hua Wen, and Yi Qian. 2006. “Decolorization of Reactive Brilliant Red K-2BP by White Rot Fungus under Sterile and Non-Sterile Conditions.” *Journal of Environmental Sciences (China)* 18(3):428–32.

- Gao, Yang, Pei Zhou, Liang Mao, Yueer Zhi, Chunhua Zhang, and Wanjun Shi. 2010. "Community Structure under Cd and Pb Combined Pollution Je Sc Sc." *22(7):1040–48.*
- Ghasemi, F., F. Tabandeh, B. Bambai, and K. R. S. Sambasiva Rao. 2010. "Decolorization of Different Azo Dyes by Phanerochaete Chrysosporium RP78 under Optimal Condition." *International Journal of Environmental Science & Technology* 7(3):457–64.
- Ghodake, Gajanan, Umesh Jadhav, Dhawal Tamboli, Anuradha Kagalkar, and Sanjay Govindwar. 2011. "Decolorization of Textile Dyes and Degradation of Mono-Azo Dye Amarant by Acinetobacter Calcoaceticus NCIM 2890." *Indian Journal of Microbiology* 51(4):501–8.
- Gironi, F., V. Piemonte, I. Petric, V. Selimbašić, and Jens Nielsen. 2008. "Number 35." *Engineering* 139(February):4225–70.
- Gnanapragasam, G., M. Senthilkumar, V. Arutchelvan, P. Sivarajan, and S. Nagarajan. 2010. "Recycle in Upflow Anaerobic Sludge Blanket Reactor on Treatment of Real Textile Dye Effluent." *World Journal of Microbiology and Biotechnology* 26(6):1093–98.
- Gonçalves, Isolina Cabral, Susana Penha, Manuela Matos, Amélia Rute Santos, Francisco Franco, and Helena Maria Pinheiro. 2005. "Evaluation of an Integrated Anaerobic/Aerobic SBR System for the Treatment of Wool Dyeing Effluents: Purification of Wool Dyeing Effluent in a SBR." *Biodegradation* 16:81–89.
- Gottlieb, Anna, Chris Shaw, Alan Smith, Andrew Wheatley, and Stephen Forsythe. 2003. "The Toxicity of Textile Reactive Azo Dyes after Hydrolysis and Decolourisation." *Journal of Biotechnology* 101(1):49–56.
- Griffiths, J. 1990. "Introduction: The Evolution of Present-Day Dye Technology." Pp. 1–16 in *The Chemistry and Application of Dyes*. Boston, MA: Springer US.
- Grinevicius, Valdelúcia M. A. S., Reginaldo Geremias, Rogério Laus, Karina F. Bettega, Mauro C. M. Laranjeiras, Valfredo T. Fávere, Danilo Wilhelm Filho, and Rozangela C. Pedrosa. 2009. "Textile Effluents Induce Biomarkers of Acute Toxicity, Oxidative Stress, and Genotoxicity." *Archives of Environmental Contamination and Toxicology* 57(2):307–14.
- Guadie, Awoke, Samson Tizazu, Meseretu Melese, Wenshan Guo, Huu Hao Ngo, and Siqing Xia. 2017. "Biodecolorization of Textile Azo Dye Using Bacillus Sp. Strain CH12 Isolated from Alkaline Lake." *Biotechnology Reports* 15(January):92–100.
- Hafshejani, Maryam Khosravi, Chimezie Jason Ogugbue, and Norhashimah Morad. 2014. "Application of Response Surface Methodology for Optimization of Decolorization and Mineralization of Triazo Dye Direct Blue 71 by Pseudomonas Aeruginosa." *3 Biotech* 4(6):605–19.
- Hai, Faisal Ibney, Kazuo Yamamoto, Fumiuyuki Nakajima, and Kensuke Fukushi. 2009. "Factors Governing Performance of Continuous Fungal Reactor during Non-Sterile Operation - The Case of a Membrane Bioreactor Treating Textile Wastewater." *Chemosphere* 74(6):810–17.
- Hai, Faisal Ibney, Kazuo Yamamoto, Fumiuyuki Nakajima, and Kensuke Fukushi. 2011. "Bioaugmented Membrane Bioreactor (MBR) with a GAC-Packed Zone

- for High Rate Textile Wastewater Treatment.” *Water Research* 45(6):2199–2206.
- Hamza, Rania Ahmed, Oliver Terna Iorhemen, and Joo Hwa Tay. 2016. “Advances in Biological Systems for the Treatment of High-Strength Wastewater.” *Journal of Water Process Engineering* 10:128–42.
- Hassani, a., L. Alidokht, a. R. Khataee, and S. Karaca. 2014. “Optimization of Comparative Removal of Two Structurally Different Basic Dyes Using Coal as a Low-Cost and Available Adsorbent.” *Journal of the Taiwan Institute of Chemical Engineers* 45(4):1597–1607.
- Hassani, A., L. Alidokht, A. R. Khataee, and S. Karaca. 2014. “Optimization of Comparative Removal of Two Structurally Different Basic Dyes Using Coal as a Low-Cost and Available Adsorbent.” *Journal of the Taiwan Institute of Chemical Engineers* 45(4):1597–1607.
- Hassard, Francis, Jeremy Biddle, Elise Cartmell, Bruce Jefferson, Sean Tyrrel, and Tom Stephenson. 2015. “Rotating Biological Contactors for Wastewater Treatment - A Review.” *Process Safety and Environmental Protection* 94(C):285–306.
- Hendricks, Katherine E., Mary C. Christman, and Pamela D. Roberts. 2017. “A Statistical Evaluation of Methods of In-Vitro Growth Assessment for *Phyllosticta Citricarpa*: Average Colony Diameter vs. Area.” *PLoS ONE* 12(1):1–7.
- Hensley, K., K. A. Robinson, S. P. Gabbita, S. Salsman, and R. A. Floyd. 2000. “Reactive Oxygen Species, Cell Signaling, and Cell Injury.” *Free Radical Biology & Medicine* 28(10):1456–62.
- Holkar, Chandrakant R., Ananda J. Jadhav, Dipak V. Pinjari, Naresh M. Mahamuni, and Aniruddha B. Pandit. 2016. “A Critical Review on Textile Wastewater Treatments: Possible Approaches.” *Journal of Environmental Management* 182:351–66.
- Holkar, Chandrakant R., Aniruddha B. Pandit, and Dipak V. Pinjari. 2014. “Kinetics of Biological Decolorisation of Anthraquinone Based Reactive Blue 19 Using an Isolated Strain of *Enterobacter* Sp.F NCIM 5545.” *Bioresource Technology* 173:342–51.
- Holme, Ian. 2006. “Sir William Henry Perkin: A Review of His Life, Work and Legacy.” *Coloration Technology* 122(5):235–51.
- Hossain, Kaizar, Shlrene Quaik, Norli Ismail, Mohd Rafatullah, Maruthi Avasan, and Rameeja Shaik. 2016. “Bioremediation and Detoxification of the Textile Wastewater with Membrane Bioreactor Using the White-Rot Fungus and Reuse of Wastewater.” *Iranian Journal of Biotechnology* 14(3):154–62.
- Hosseini Koupaie, E., M. R. Alavi Moghaddam, and S. H. Hashemi. 2011. “Post-Treatment of Anaerobically Degraded Azo Dye Acid Red 18 Using Aerobic Moving Bed Biofilm Process: Enhanced Removal of Aromatic Amines.” *Journal of Hazardous Materials* 195:147–54.
- Hosseini Koupaie, E., M. R. Alavi Moghaddam, and S. H. Hashemi. 2012. “Investigation of Decolorization Kinetics and Biodegradation of Azo Dye Acid Red 18 Using Sequential Process of Anaerobic Sequencing Batch

- Reactor/Moving Bed Sequencing Batch Biofilm Reactor.” *International Biodeterioration and Biodegradation* 71:43–49.
- Howland, J. L. 1996. “Short Protocols in Molecular Biology, Third Edition: Edited by F Ausubel, R Brent, R E Kingston, D D Moore, J G Seidman, J A Smith and K Struhl. P 836. John Wiley & Sons, New York. 1995. \$74.95. ISBN 0-471-13781-2.” *Biochemical Education* 24(1):68–68.
- Hsueh, Chung-Chuan, Bor-Yann Chen, and Chia-Yi Yen. 2009. “Understanding Effects of Chemical Structure on Azo Dye Decolorization Characteristics by *Aeromonas Hydrophila*.” *Journal of Hazardous Materials* 167(1–3):995–1001.
- Hunger, Klaus and Applications Wiley-vch. 2003. *Industrial Dyes*: Vol. 125.
- Imran, Muhammad, David E. Crowley, Azeem Khalid, Sabir Hussain, Muhammad Waseem Mumtaz, and Muhammad Arshad. 2014. “Microbial Biotechnology for Decolorization of Textile Wastewaters.” *Reviews in Environmental Science and Biotechnology* 14(1):73–92.
- Irum, A., S. Mumtaz, A. Rehman, I. Naz, and S. Ahmed. 2015. “Treatment of Simulated Textile Wastewater Containing Reactive Azo Dyes Using Laboratory Scale Trickling Filter.” 9(1):1–7.
- Isik, Mustafa and Delia Teresa Sponza. 2003. “Effect of Oxygen on Decolorization of Azo Dyes by *Escherichia Coli* and *Pseudomonas Sp.* and Fate of Aromatic Amines.” *Process Biochemistry* 38(8):1183–92.
- Islam, Mohammad Tajul. 2016. “Environment-Friendly Reactive Dyeing Process for Cotton to Substitute Dyeing Additives.” *Clean Technologies and Environmental Policy* 18(2):601–8.
- Iza, J. 1991. “Fluidized Bed Reactors for Anaerobic Wastewater Treatment.” *Water Science and Technology* 24(8):109–32.
- Jadhav, J. P., D. C. Kalyani, A. A. Telke, S. S. Phugare, and S. P. Govindwar. 2010. “Evaluation of the Efficacy of a Bacterial Consortium for the Removal of Color, Reduction of Heavy Metals, and Toxicity from Textile Dye Effluent.” *Bioresource Technology* 101(1):165–73.
- Jadhav, S. B., S. N. Surwase, S. S. Phugare, and J. P. Jadhav. 2013. “Response Surface Methodology Mediated Optimization of Remazol Orange Decolorization in Plain Distilled Water by *Pseudomonas Aeruginosa* BCH.” *International Journal of Environmental Science and Technology* 10(1):181–90.
- Jadhav, S. U., U. U. Jadhav, V. V. Dawkar, and S. P. Govindwar. 2008. “Biodegradation of Disperse Dye Brown 3REL by Microbial Consortium of *Galactomyces Geotrichum* MTCC 1360 and *Bacillus Sp.* VUS.” *Biotechnology and Bioprocess Engineering* 13(2):232–39.
- Jadhav, Shekhar B., Swapnil S. Phugare, Pratibha S. Patil, and Jyoti P. Jadhav. 2011a. “Biochemical Degradation Pathway of Textile Dye Remazol Red and Subsequent Toxicological Evaluation by Cytotoxicity, Genotoxicity and Oxidative Stress Studies.” *International Biodeterioration & Biodegradation* 65(6):733–43.
- Jadhav, Shekhar B., Swapnil S. Phugare, Pratibha S. Patil, and Jyoti P. Jadhav. 2011b. “Biochemical Degradation Pathway of Textile Dye Remazol Red and Subsequent Toxicological Evaluation by Cytotoxicity, Genotoxicity and

- Oxidative Stress Studies.” *International Biodeterioration and Biodegradation* 65(6):733–43.
- Jadhav, Shekhar B., Shripad N. Surwase, Dayanand C. Kalyani, Ranjit G. Gurav, and Jyoti P. Jadhav. 2012. “Biodecolorization of Azo Dye Remazol Orange by *Pseudomonas Aeruginosa* BCH and Toxicity (Oxidative Stress) Reduction in *Allium Cepa* Root Cells.” *Applied Biochemistry and Biotechnology* 168(5):1319–34.
- Jadhav, Umesh U., Vishal V. Dawkar, Gajanan S. Ghodake, and Sanjay P. Govindwar. 2008. “Biodegradation of Direct Red 5B, a Textile Dye by Newly Isolated *Comamonas* Sp. UVS.” *Journal of Hazardous Materials* 158:507–16.
- Jäger, Ismene, Klaus Schneider, Petr Janak, and Michael Huet. 2005. “Mutagenic Dyes in Textile Finishing.” *Melliand International* 11(March):52–55.
- Jain, Kunal, Varun Shah, Digantkumar Chapla, and Datta Madamwar. 2012. “Decolorization and Degradation of Azo Dye - Reactive Violet 5R by an Acclimatized Indigenous Bacterial Mixed Cultures-SB4 Isolated from Anthropogenic Dye Contaminated Soil.” *Journal of Hazardous Materials* 213–214:378–86.
- Jianlong, Wang, Shi Hanchang, and Qian Yi. 2000. “Wastewater Treatment in a Hybrid Biological Reactor (HBR): Effect of Organic Loading Rates.” 36:297–303.
- Jin, Xian-Chun, Gao-Qiang Liu, Zheng-Hong Xu, and Wen-Yi Tao. 2007. “Decolorization of a Dye Industry Effluent by *Aspergillus Fumigatus* XC6.” *Applied Microbiology and Biotechnology* 74(1):239–43.
- Jirasripongpun, Kalyanee, Rujikan Nasanit, Jongiira Niruntasook, and Boonsiri Chotikasatian. 2007. “Decolorization and Degradation of CI Reactive Red 195 by *Enterobacter* Sp.” *Thammasat Int J Sci Technol* 12(6):6–11.
- Joe, J., R. K. Kothari, C. M. Raval, C. R. Kothari, V. G. Akbari, and S. P. Singh. 2011. “Decolorization of Textile Dye Remazol Black B by *Pseudomonas Aeruginosa* CR-25 Isolated from the Common Effluent Treatment Plant.” *Journal of Bioremediation and Biodegradation* 2(2):1–6.
- Johnson, G. E., E. L. Quick, E. M. Parry, and J. M. Parry. 2010. “Metabolic Influences for Mutation Induction Curves after Exposure to Sudan-1 and Para Red.” *Mutagenesis* 25(4):327–33.
- Jonstrup, M., N. Kumar, M. Murto, and B. Mattiasson. 2011. “Sequential Anaerobic-Aerobic Treatment of Azo Dyes: Decolourisation and Amine Degradability.” *Desalination* 280(1–3):339–46.
- Joshi, Swati M., Shrirang A. Inamdar, Amar A. Telke, Dhawal P. Tamboli, and Sanjay P. Govindwar. 2010. “Exploring the Potential of Natural Bacterial Consortium to Degrade Mixture of Dyes and Textile Effluent.” *International Biodeterioration and Biodegradation* 64(7):622–28.
- Kabra, Akhil N., Rahul V. Khandare, Tatoba R. Waghmode, and Sanjay P. Govindwar. 2011. “Differential Fate of Metabolism of a Sulfonated Azo Dye Remazol Orange 3R by Plants *Aster Amellus* Linn., *Glandularia Pulchella* (Sweet) Tronc. and Their Consortium.” *Journal of Hazardous Materials* 190(1–3):424–31.

- Kadam, Avinash a., Jeevan D. Kamatkar, Rahul V. Khandare, Jyoti P. Jadhav, and Sanjay P. Govindwar. 2013. "Solid-State Fermentation: Tool for Bioremediation of Adsorbed Textile Dyestuff on Distillery Industry Waste-Yeast Biomass Using Isolated *Bacillus Cereus* Strain EBT1." *Environmental Science and Pollution Research* 20:1009–20.
- Kadam, Avinash a., Ashwini N. Kulkarni, Harshad S. Lade, and Sanjay P. Govindwar. 2014. "Exploiting the Potential of Plant Growth Promoting Bacteria in Decolorization of Dye Disperse Red 73 Adsorbed on Milled Sugarcane Bagasse under Solid State Fermentation." *International Biodeterioration and Biodegradation* 86:364–71.
- Kadam, Avinash A., Amar A. Telke, Sujit S. Jagtap, and Sanjay P. Govindwar. 2011. "Decolorization of Adsorbed Textile Dyes by Developed Consortium of *Pseudomonas* Sp. SUK1 and *Aspergillus Ochraceus* NCIM-1146 under Solid State Fermentation." *Journal of Hazardous Materials* 189(1–2):486–94.
- Kalpna, Duraisamy, Natarajan Velmurugan, Jae Hong Shim, Byung Taek Oh, Kalaiselvi Senthil, and Yang Soo Lee. 2012. "Biodecolorization and Biodegradation of Reactive Levafix Blue E-RA Granulate Dye by the White Rot Fungus *Irpex Lacteus*." *Journal of Environmental Management* 111:142–49.
- Kalyani, D. C., P. S. Patil, J. P. Jadhav, and S. P. Govindwar. 2008. "Biodegradation of Reactive Textile Dye Red BLI by an Isolated Bacterium *Pseudomonas* Sp. SUK1." *Bioresource Technology* 99(11):4635–41.
- Kandelbauer, Andreas, Angelika Erlacher, Artur Cavaco-paulo, and Georg M. Gu. 2004. "A New Alkali-Thermostable Azoreductase From." *Society* 70(2):837–44.
- Kapdan, Ilgi Karapinar and Rukiye Oztekin. 2006. "The Effect of Hydraulic Residence Time and Initial COD Concentration on Color and COD Removal Performance of the Anaerobic-Aerobic SBR System." *Journal of Hazardous Materials* 136:896–901.
- Karim, Ekramul, Kartik Dhar, and Towhid Hossain. 2018. "Journal of Genetic Engineering and Biotechnology Decolorization of Textile Reactive Dyes by Bacterial Monoculture and Consortium Screened from Textile Dyeing Effluent." *Journal of Genetic Engineering and Biotechnology* 16(2):375–80.
- Karim, Zoheb, Rohana Adnan, and Qayyum Husain. 2012. "A ??-Cyclodextrin-Chitosan Complex as the Immobilization Matrix for Horseradish Peroxidase and Its Application for the Removal of Azo Dyes from Textile Effluent." *International Biodeterioration and Biodegradation* 72:10–17.
- Karthikeyan, K., K. Nanthakumar, K. Shanthi, and P. Lakshmanaperumalsamy. 2010. "Response Surface Methodology for Optimization of Culture Conditions for Dye Decolorization by a Fungus, *Aspergillus Niger* HM11 Isolated from Dye Affected Soil." *Iranian Journal of Microbiology* 2(4):213–22.
- Karunya, A., C. Rose, and C. Valli Nachiyar. 2014. "Biodegradation of the Textile Dye Mordant Black 17 (Calcon) by *Moraxella Osloensis* Isolated from Textile Effluent-Contaminated Site." *World Journal of Microbiology and Biotechnology* 30(3):915–24.
- Kaushik, P. and A. Malik. 2009. "Fungal Dye Decolourization: Recent Advances and Future Potential." *Environment International* 35(1):127–41.

- Khalid, Azeem, Muhammad Arshad, and David E. Crowley. 2008a. "Decolorization of Azo Dyes by *Shewanella* Sp. under Saline Conditions." *Applied Microbiology and Biotechnology* 79(6):1053–59.
- Khalid, Azeem, Muhammad Arshad, and David E. Crowley. 2008b. "Decolorization of Azo Dyes by *Shewanella* Sp. under Saline Conditions." *Applied Microbiology and Biotechnology* 79:1053–59.
- Khalid, Azeem, Farzana Kausar, Muhammad Arshad, Tariq Mahmood, and Iftikhar Ahmed. 2012. "Accelerated Decolorization of Reactive Azo Dyes under Saline Conditions by Bacteria Isolated from Arabian Seawater Sediment." *Applied Microbiology and Biotechnology* 96(6):1599–1606.
- Khan, Razia, P. Bhawana, and M. H. Fulekar. 2013. "Microbial Decolorization and Degradation of Synthetic Dyes: A Review." *Reviews in Environmental Science and Biotechnology* 12:75–97.
- Khehra, Manjinder Singh, Harvinder Singh Saini, Deepak Kumar Sharma, Bhupinder Singh Chadha, and Swapandeep Singh Chimni. 2005. "Decolorization of Various Azo Dyes by Bacterial Consortium." *Dyes and Pigments* 67:55–61.
- Khelifi, Eltaief, Lamia Ayed, Hassib Bouallagui, Youssef Touhami, and Moktar Hamdi. 2009. "Effect of Nitrogen and Carbon Sources on Indigo and Congo Red Decolourization by *Aspergillus Alliaceus* Strain 121C." *Journal of Hazardous Materials* 163(2–3):1056–62.
- Khouni, Imen, Benoît Marrot, and Raja Ben Amar. 2012. "Treatment of Reconstituted Textile Wastewater Containing a Reactive Dye in an Aerobic Sequencing Batch Reactor Using a Novel Bacterial Consortium." *Separation and Purification Technology* 87:110–19.
- Kim, Moonil, Dukkyu Han, Fenghao Cui, and Wookeun Bae. 2013. "Recalcitrant Organic Matter Removal from Textile Wastewater by an Aerobic Cell-Immobilized Pellet Column." *Water Science & Technology* 67:2124.
- Klemola, Kaisa, John Pearson, Atte von Wright, Jyrki Liesivuori, and Pirjo Lindström-Seppä. 2007. "Evaluating the Toxicity of Reactive Dyes and Dyed Fabrics with the Hepa-1 Cytotoxicity Test." *Autex Research Journal* 7(September):224–30.
- Köchling, Thorsten, Antônio Djalma Nunes Ferraz, Lourdinha Florencio, Mario Takayuki Kato, and Sávia Gavazza. 2017. "454-Pyrosequencing Analysis of Highly Adapted Azo Dye-Degrading Microbial Communities in a Two-Stage Anaerobic–Aerobic Bioreactor Treating Textile Effluent." *Environmental Technology (United Kingdom)* 38(6):687–93.
- Kodam, K. M., I. Soojhawon, P. D. Lokhande, and K. R. Gawai. 2005. "Microbial Decolorization of Reactive Azo Dyes under Aerobic Conditions." *World Journal of Microbiology and Biotechnology* 21(3):367–70.
- Kojima, M., M. Degawa, Y. Hashimoto, and M. Tada. 1994. "The Carcinogenicity of Methoxyl Derivatives of 4-Aminoazobenzene: Correlation between DNA Adducts and Genotoxicity." *Environmental Health Perspectives* 102(suppl 6):191–94.
- Kokkali, Varvara, Ioannis Katramados, and Jeffrey D. Newman. 2011. "Monitoring the Effect of Metal Ions on the Mobility of *Artemia Salina* Nauplii." *Biosensors*

- 1(2):36–45.
- Kova, Karin and Thomas Egli. 1998. “Growth Kinetics of Suspended Mixed Cultures.” *Microbiology and Molecular Biology Reviews* 62(3):646–66.
- Koyuncu, Ismail and Kenan Güney. 2013. “Membrane-Based Treatment of Textile Industry Wastewaters.” Pp. 1–12 in *Encyclopedia of Membrane Science and Technology*. Hoboken, NJ, USA: John Wiley & Sons, Inc.
- Kuberan, T., J. Anburaj, C. Sundaravadivelan, and P. Kumar. 2011. “Biodegradation of Azo Dye by *Listeria* Sp.” *International Journal of Environmental Sciences* 1(7):1760–70.
- Kumar Garg, Satyendra, Manikant Tripathi, Santosh Kumar Singh, and Jitendra Kumar Tiwari. 2012. “Biodecolorization of Textile Dye Effluent by *Pseudomonas Putida* SKG-1 (MTCC 10510) under the Conditions Optimized for Monoazo Dye Orange II Color Removal in Simulated Minimal Salt Medium.” *International Biodeterioration and Biodegradation* 74:24–35.
- Kumar, Kapil, Gaurav Kumar Singh, M. G. Dastidar, and T. R. Sreekrishnan. 2014. “Effect of Mixed Liquor Volatile Suspended Solids (MLVSS) and Hydraulic Retention Time (HRT) on the Performance of Activated Sludge Process during the Biotreatment of Real Textile Wastewater.” *Water Resources and Industry* 5:1–8.
- Kumar, Koel, Sivanesan Saravana Devi, Kannan Krishnamurthi, Dipanwita Dutta, and Tapan Chakrabarti. 2007. “Decolorisation and Detoxification of Direct Blue-15 by a Bacterial Consortium.” *Bioresource Technology* 98(16):3168–71.
- Kumar Saha, Sushanta, Palanisami Swaminathan, C. Raghavan, Lakshmanan Uma, and Gopalakrishnan Subramanian. 2010. “Ligninolytic and Antioxidative Enzymes of a Marine Cyanobacterium *Oscillatoria Willei* BDU 130511 during Poly R-478 Decolourization.”
- Kumar, Sudhir, Glen Stecher, and Koichiro Tamura. 2016. “MEGA7: Molecular Evolutionary Genetics Analysis Version 7.0 for Bigger Datasets.” *Molecular Biology and Evolution* 33(7):1870–74.
- Kumar, Suresh and Pawan Kumar Singh. 2011. “Degradation of AZO Dye in Fixed Film Bioreactors : A Bench Scale Study.” 2(2):686–95.
- Kumara, K. G. S. U., M. G. Dastidara, and T. R. Sreekrishnanb. 2012. “Effect of Process Parameters on Aerobic Decolourization of Reactive Azo Dye Using Mixed Culture.”
- Kurade, Mayur B., Tatoba R. Waghmode, Akhil N. Kabra, and Sanjay P. Govindwar. 2013. “Degradation of a Xenobiotic Textile Dye, Disperse Brown 118, by *Brevibacillus Laterosporus*.” *Biotechnology Letters* 35:1593–98.
- Kwan, K. K. and B. J. Dutka. 1992. “A Novel Bioassay Approach: Direct Application of the Toxi-Chromotest and the SOS Chromotest to Sediments.” *Environmental Toxicology & Water Quality* 7:49–60.
- Lalnunhlimi, Sylvine and Krishnaswamy Veenagayathri. 2016. “Decolorization of Azo Dyes (Direct Blue 151 and Direct Red 31) by Moderately Alkaliphilic Bacterial Consortium.” *Brazilian Journal of Microbiology* 47(1):39–46.
- Lanthier, Martin, Kelvin B. Gregory, and Derek R. Lovley. 2008. “Growth with High

- Planktonic Biomass in *Shewanella Oneidensis* Fuel Cells.” *FEMS Microbiology Letters* 278(1):29–35.
- Lapage, SP, JE Shelton, and TG Mitchell. 1970. “Chapter I Media for the Maintenance and Preservation of Bacteria.” *Methods in Microbiology*.
- Leme, Daniela Morais, Gisele Augusto Rodrigues De Oliveira, Gabriela Meireles, Lara Barroso Brito, Laís De Brito Rodrigues, and Danielle Palma De Oliveira. 2015. “Eco- and Genotoxicological Assessments of Two Reactive Textile Dyes.” *Journal of Toxicology and Environmental Health - Part A: Current Issues* 78(5):287–300.
- Levine, Walter G. 1991. “Metabolism of AZO Dyes: Implication for Detoxication and Activation.” *Drug Metabolism Reviews* 23(3–4):253–309.
- Lide, David R. 1996. *CRC Handbook of Chemistry and Physics : A Ready-Reference Book of Chemical and Physical Data*. CRC Press.
- Liers, Christiane, Caroline Bobeth, Marek Pecyna, René Ullrich, and Martin Hofrichter. 2010. “DyP-like Peroxidases of the Jelly Fungus *Auricularia Auricula-Judae* Oxidize Nonphenolic Lignin Model Compounds and High-Redox Potential Dyes.” *Applied Microbiology and Biotechnology* 85(6):1869–79.
- Lim, Sing-Lai, Wan-Loy Chu, and Siew-Moi Phang. 2010. “Use of *Chlorella Vulgaris* for Bioremediation of Textile Wastewater.” *Bioresource Technology* 101(19):7314–22.
- Lin, Jun, Xingwang Zhang, Zhongjian Li, and Lecheng Lei. 2010. “Biodegradation of Reactive Blue 13 in a Two-Stage Anaerobic/Aerobic Fluidized Beds System with a *Pseudomonas* Sp. Isolate.” *Bioresource Technology* 101(1):34–40.
- Lin, Yen-Hui and Jyh-Yih Leu. 2008. “Kinetics of Reactive Azo-Dye Decolorization by *Pseudomonas Luteola* in a Biological Activated Carbon Process.” *Biochemical Engineering Journal* 39(3):457–67.
- Liu, Guangfei, Jiti Zhou, Hong Lv, Xuemin Xiang, Jing Wang, Mi Zhou, and Yuanyuan Qv. 2007. “Azoreductase from *Rhodobacter Sphaeroides* AS1.1737 Is a Flavodoxin That Also Functions as Nitroreductase and Flavin Mononucleotide Reductase.” *Applied Microbiology and Biotechnology* 76(6):1271–79.
- Liu, Hongling, Hongxia Yu, John P. Giesy, Yuanyuan Sun, and Xiaorong Wang. 2007. “Toxicity of HC Orange No. 1 to *Daphnia Magna*, Zebrafish (*Brachydanio Rerio*) Embryos, and Goldfish (*Carassius Auratus*).” *Chemosphere* 66(1):2159–65.
- Lourenço, Nídia D., Júlio M. Novais, and Helena M. Pinheiro. 2006. “Kinetic Studies of Reactive Azo Dye Decolorization in Anaerobic/Aerobic Sequencing Batch Reactors.” *Biotechnology Letters* 28:733–39.
- Lv, Guo Ying, Jian Hui Cheng, Xiao Yang Chen, Zuo Fa Zhang, and Lei Fa Fan. 2013. “Biological Decolorization of Malachite Green by *Deinococcus Radiodurans* R1.” *Bioresource Technology* 144:275–80.
- Mahata, Denial, Santi M. Mandal, Rashmi Bharti, Vinay Krishna Gupta, Mahitosh Mandal, Ahindra Nag, and Golok B. Nando. 2014. “Self-Assembled Cardanol Azo Derivatives as Antifungal Agent with Chitin-Binding Ability.” *International Journal of Biological Macromolecules* 69:5–11.

- Majeau, Josée-Anne, Satinder K. Brar, and Rajeshwar Dayal Tyagi. 2010. "Laccases for Removal of Recalcitrant and Emerging Pollutants." *Bioresource Technology* 101(7):2331–50.
- Malik, Noshaba Hassan, Hajira Zain, and Naeem Ali. 2018. "Organismic-Level Acute Toxicology Profiling of Reactive Azo Dyes." *Environmental Monitoring and Assessment* 190(10).
- Malinauskiene, Laura. 2012. *Contact Allergy to Textile Dyes. Clinical and Experimental Studies on Disperse Azo Dyes.*
- Manai, Imène, Baligh Miladi, Abdellatif El Mselmi, Issam Smaali, Aida Ben Hassen, Moktar Hamdi, and Hassib Bouallagui. 2016. "Industrial Textile Effluent Decolourization in Stirred and Static Batch Cultures of a New Fungal Strain *Chaetomium Globosum* IMA1 KJ472923." *Journal of Environmental Management* 170:8–14.
- Ben Mansour, Hedi, Daniel Barillier, David Corroler, Kamel Ghedira, Leila Chekir-Ghedira, and Ridha Mosrati. 2009. "IN VITRO STUDY OF DNA DAMAGE INDUCED BY ACID ORANGE 52 AND ITS BIODEGRADATION DERIVATIVES." *Environmental Toxicology and Chemistry* 28(3):489.
- Mansour, Hedi Ben, Kamel Ghedira, Daniel Barillier, Leila Chekir Ghedira, and Ridha Mosrati. 2011. "Degradation and Detoxification of Acid Orange 52 by *Pseudomonas Putida* Mt-2: A Laboratory Study." *Environmental Science and Pollution Research* 18(9):1527–35.
- Marcharchand, Samriti and Adeline Su Yien Ting. 2017. "Trichoderma Asperellum Cultured in Reduced Concentrations of Synthetic Medium Retained Dye Decolourization Efficacy." *Journal of Environmental Management* 203:542–49.
- Martorell, María M., Hipólito F. Pajot, and Lucía I. C. de Figueroa. 2012. "Dye-Decolourizing Yeasts Isolated from Las Yungas Rainforest. Dye Assimilation and Removal Used as Selection Criteria." *International Biodeterioration & Biodegradation* 66(1):25–32.
- Mate, Madhuri Sahasrabudhe and Girish Pathade. 2012. "Biodegradation of C.I. Reactive Red 195 by *Enterococcus Faecalis* Strain YZ66." *World Journal of Microbiology and Biotechnology* 28(3):815–26.
- Mathur, N., P. Bhatnagar, and P. Bakre. 2006. "Assessing Mutagenicity of Textile Dyes from Pali (Rajasthan) Using Ames Bioassay." *Applied Ecology and Environmental Research* 4(1):111–18.
- Mathur, Nupur, Pradeep Bhatnagar, and Pratibha Sharma. 2012. "Review of the Mutagenicity of Textile Dye Products Abstract : 1 . 2 Mutagenicity of Benzidine , Benzidine Analogues , and Benzidine-Based Dyes : " 2(2):1–18.
- McMullan, G., C. Meehan, a. Conneely, N. Kirby, T. Robinson, P. Nigam, I. M. Banat, R. Marchant, and W. F. Smyth. 2001. "Microbial Decolourisation and Degradation of Textile Dyes." *Applied Microbiology and Biotechnology* 56:81–87.
- Meerbergen, Ken, Kris A. Willems, Raf Dewil, Jan Van Impe, Lise Appels, and Bart Lievens. 2018. "Isolation and Screening of Bacterial Isolates from Wastewater Treatment Plants to Decolorize Azo Dyes." *Journal of Bioscience and Bioengineering* 125(4):448–56.

- Meyer, B., N. Ferrigni, J. Putnam, L. Jacobsen, D. Nichols, and J. McLaughlin. 1982. "Brine Shrimp: A Convenient General Bioassay for Active Plant Constituents." *Planta Medica* 45(05):31–34.
- Mirbolooki, Hanieh, Reza Amirnezhad, and Ali Reza Pendashteh. 2017. "Treatment of High Saline Textile Wastewater by Activated Sludge Microorganisms." *Journal of Applied Research and Technology* 15(2):167–72.
- Misal, Santosh A., Devendra P. Lingojar, Ravindra M. Shinde, and Kachru R. Gawai. 2011. "Purification and Characterization of Azoreductase from Alkaliphilic Strain *Bacillus Badius*." *Process Biochemistry* 46(6):1264–69.
- Mohammed, Issam Ahmed and Asniza Mohammed. 2010. "Synthesis of New Azo Compounds Based on N-(4-Hydroxyphenyl)Maleimide and n-(4-Methylphenyl)Maleimide." *Molecules* 15(10):7498–7508.
- Mohan, S. Venkata, S. V. Ramanaiah, and P. N. Sarma. 2008. "Biosorption of Direct Azo Dye from Aqueous Phase onto *Spirogyra* Sp. I02: Evaluation of Kinetics and Mechanistic Aspects." *Biochemical Engineering Journal* 38(1):61–69.
- Monsinjon, Tiphaine and Thomas Knigge. 2007. "Proteomic Applications in Ecotoxicology." *PROTEOMICS* 7(16):2997–3009.
- Moosvi, Safia, Xama Kher, and Datta Madamwar. 2007. "Isolation, Characterization and Decolorization of Textile Dyes by a Mixed Bacterial Consortium JW-2." *Dyes and Pigments* 74(3):723–29.
- Moreira, M. T., G. Feijoo, and J. M. Lema. 2004. "Fungal Bioreactors : Applications to White-Rot Fungi." *Environmental Science and Bio/Technology* 2:247–59.
- Morris, E. Kathryn, Tancredi Caruso, François Buscot, Markus Fischer, Christine Hancock, Tanja S. Maier, Torsten Meiners, Caroline Müller, Elisabeth Obermaier, Daniel Prati, Stephanie A. Socher, Ilja Sonnemann, Nicole Wäschke, Tesfaye Wubet, Susanne Wurst, and Matthias C. Rillig. 2014. "Choosing and Using Diversity Indices: Insights for Ecological Applications from the German Biodiversity Exploratories." *Ecology and Evolution* 4(18):3514–24.
- Muralidhar, R. ..., R. ... Chirumamila, R. Marchant, and P. Nigam. 2001. "A Response Surface Approach for the Comparison of Lipase Production by *Candida cylindracea* Using Two Different Carbon Sources." *Biochemical Engineering Journal* 9(1):17–23.
- Mutamim, Noor Sabrina Ahmad, Zainura Zainon Noor, Mohd Ariffin Abu Hassan, and Gustaf Olsson. 2012. "Application of Membrane Bioreactor Technology in Treating High Strength Industrial Wastewater: A Performance Review." *Desalination* 305:1–11.
- Muthunayanan, Vasanthy, Santhiya M, Swabna M, and Geetha A. 2011. "Phytodegradation of Textile Dyes by Water Hyacinth (*Eichhornia Crassipes*) from Aqueous Dye Solutions." *International Journal of Environmental Sciences* 1(7):1702–17.
- Naresh Kumar, A., C. Nagendranatha Reddy, R. Hari Prasad, and S. Venkata Mohan. 2014. "Azo Dye Load-Shock on Relative Behavior of Biofilm and Suspended Growth Configured Periodic Discontinuous Batch Mode Operations: Critical Evaluation with Enzymatic and Bio-Electrocatalytic Analysis." *Water Research* 60:182–96.

- Nawahwi, Mohd Zaini. 2013. "Degradation of the Azo Dye Reactive Red 195 by *Paenibacillus* Spp. R2." *Journal of Bioremediation and Biodegradation* 04(1):1–7.
- Nawaz, Muhammad Saqib and Muhammad Ahsan. 2014. "Comparison of Physico-Chemical, Advanced Oxidation and Biological Techniques for the Textile Wastewater Treatment." *Alexandria Engineering Journal* 53:717–22.
- Nguyen, Thai Anh and Ruey Shin Juang. 2013. "Treatment of Waters and Wastewaters Containing Sulfur Dyes: A Review." *Chemical Engineering Journal* 219:109–17.
- Nigam, Poonam, Ibrahim M. Banat, Darel Singh, and Roger Marchant. 1996. "Microbial Process for the Decolorization of Textile Effluent Containing Azo, Diazo and Reactive Dyes." *Process Biochemistry* 31(5):435–42.
- Novotný, Čeněk, Nicolina Dias, Anu Kapanen, Kateřina Malachová, Marta Vádrovcová, Merja Itävaara, and Nelson Lima. 2006. "Comparative Use of Bacterial, Algal and Protozoan Tests to Study Toxicity of Azo- and Anthraquinone Dyes." *Chemosphere* 63:1436–42.
- O'Neill, Cliona, Freda R. Hawkes, Dennis L. Hawkes, Nidia D. Lourenço, Helena M. Pinheiro, and Wouter Delée. 1999. "Colour in Textile Effluents - Sources, Measurement, Discharge Consents and Simulation: A Review." *Journal of Chemical Technology and Biotechnology* 74(11):1009–18.
- Ogugbue, C. J., T. Sawidis, and N. A. Oranusi. 2011. "Evaluation of Colour Removal in Synthetic Saline Wastewater Containing Azo Dyes Using an Immobilized Halotolerant Cell System." *Ecological Engineering* 37(12):2056–60.
- Ogugbue, Chimezie Jason, Thomas Sawidis, and Nathaniel A. Oranusi. 2012. "Bioremoval of Chemically Different Synthetic Dyes by *Aeromonas Hydrophila* in Simulated Wastewater Containing Dyeing Auxiliaries." *Annals of Microbiology* 62(3):1141–53.
- de Oliveira, Gisele Augusto Rodrigues, Joaquín de Lapuente, Elisabet Teixidó, Constança Porredón, Miquel Borràs, and Danielle Palma de Oliveira. 2016. "Textile Dyes Induce Toxicity on Zebrafish Early Life Stages." *Environmental Toxicology and Chemistry* 35(2):429–34.
- Ollgaard, H., L. Frost, J. Galster, and O. C. Hensen. 1998. "Survey of Azo-Colorants in Denmark: Consumption, Use, Health and Environmental Aspects." (Xx):147–290.
- Olukanni, O. D., A. A. Osuntoki, and G. O. Gbenle. 2009. "Decolourization of Azo Dyes by a Strain of *Micrococcus* Isolated from a Refuse Dump Soil." *Biotechnology(Faisalabad)* 8(4):442–48.
- Olukanni, O. D., a. a. Osuntoki, D. C. Kalyani, G. O. Gbenle, and S. P. Govindwar. 2010. "Decolorization and Biodegradation of Reactive Blue 13 by *Proteus Mirabilis* LAG." *Journal of Hazardous Materials* 184(1–3):290–98.
- Omar, Hanan Hafez. 2008. "Algal Decolorization and Degradation of Monoazo and Diazo Dyes." *Pakistan Journal of Biological Sciences : PJBS* 11(10):1310–16.
- Ong, Siew-Teng, Pei-Sin Keng, Weng-Nam Lee, Sie-Tiong Ha, and Yung-Tse Hung. 2011. "Dyes Waste Treatments." *Water* 3(Vi):157–76.

- Ooi, Toshihiko, Takeshi Shibata, Reiko Sato, Hiroaki Ohno, Shinichi Kinoshita, Tran Linh Thuoc, and Seiichi Taguchi. 2007. "An Azoreductase, Aerobic NADH-Dependent Flavoprotein Discovered from *Bacillus* Sp.: Functional Expression and Enzymatic Characterization." *Applied Microbiology and Biotechnology* 75(2):377–86.
- Pajot, Hipólito F., Osvaldo D. Delgado, L. I. C. De Figueroa, and Julia I. Fariña. 2011. "Unraveling the Decolourizing Ability of Yeast Isolates from Dye-Polluted and Virgin Environments: An Ecological and Taxonomical Overview." *Antonie van Leeuwenhoek, International Journal of General and Molecular Microbiology* 99:443–56.
- Pajot, Hipólito F., L. I. C. de Figueroa, and Julia I. Fariña. 2007. "Dye-Decolorizing Activity in Isolated Yeasts from the Ecoregion of Las Yungas (Tucumán, Argentina)." *Enzyme and Microbial Technology* 40:1503–11.
- Pajot, Hipólito Fernando, Julia Inés Fariña, and Lucía Inés Castellanos de Figueroa. 2011. "Evidence on Manganese Peroxidase and Tyrosinase Expression during Decolorization of Textile Industry Dyes by *Trichosporon Akiyoshidainum*." *International Biodeterioration & Biodegradation* 65(8):1199–1207.
- Palácio, Soraya M., Fernando R. Espinoza-Quiñones, Aparecido N. Módenes, Cláudio C. Oliveira, Fernando H. Borba, and Fernando G. Silva. 2009. "Toxicity Assessment from Electro-Coagulation Treated-Textile Dye Wastewaters by Bioassays." *Journal of Hazardous Materials* 172:330–37.
- Pan, Hongmiao, Jinhui Feng, Carl E. Cerniglia, and Huizhong Chen. 2011. "Effects of Orange II and Sudan III Azo Dyes and Their Metabolites on *Staphylococcus Aureus*." *Journal of Industrial Microbiology & Biotechnology* 38(10):1729–38.
- Pandey, Anjali, Poonam Singh, and Leela Iyengar. 2007. "Bacterial Decolorization and Degradation of Azo Dyes." *International Biodeterioration and Biodegradation* 59:73–84.
- Papadia, Simone, Giorgio Rovero, Fabio Fava, and Diana Di Gioia. 2011. "Comparison of Different Pilot Scale Bioreactors for the Treatment of a Real Wastewater from the Textile Industry." *International Biodeterioration and Biodegradation* 65(3):396–403.
- Parikh, Amit and Datta Madamwar. 2005. "Textile Dye Decolorization Using Cyanobacteria." *Biotechnology Letters* 27(5):323–26.
- Parshetti, Ganesh, Satish Kalme, Ganesh Saratale, and Sanjay Govindwar. 2006. "Biodegradation of Malachite Green by *Kocuria Rosea* MTCC 1532." *Acta Chimica Slovenica* 53(4):492–98.
- Pearce, C. I., J. R. Lloyd, and J. T. Guthrie. 2003. "The Removal of Colour from Textile Wastewater Using Whole Bacterial Cells: A Review." *Dyes and Pigments* 58(3):179–96.
- Peyton, Brent M., Tomás Wilson, and David R. Yonge. 2002. "Kinetics of Phenol Biodegradation in High Salt Solutions." *Water Research* 36(19):4811–20.
- Phugare, Swapnil S., Dayanand C. Kalyani, Asmita V. Patil, and Jyoti P. Jadhav. 2011. "Textile Dye Degradation by Bacterial Consortium and Subsequent Toxicological Analysis of Dye and Dye Metabolites Using Cytotoxicity, Genotoxicity and Oxidative Stress Studies." *Journal of Hazardous Materials*

- 186(1):713–23.
- Pielesz, a, I. Baranowska, a Rybakt, and a Włochowicz. 2002. “Detection and Determination of Aromatic Amines as Products of Reductive Splitting from Selected Azo Dyes.” *Ecotoxicology and Environmental Safety* 53:42–47.
- Pinheiro, H. M., E. Touraud, and O. Thomas. 2004. “Aromatic Amines from Azo Dye Reduction: Status Review with Emphasis on Direct UV Spectrophotometric Detection in Textile Industry Wastewaters.” *Dyes and Pigments* 61(2):121–39.
- Plattes, M., E. Henry, P. M. Schosseler, and A. Weidenhaupt. 2006. “Modelling and Dynamic Simulation of a Moving Bed Bioreactor for the Treatment of Municipal Wastewater.” *Biochemical Engineering Journal* 32(2):61–68.
- Ponraj, M., K. Gokila, and Vasudeo Zambare. 2011. “Bacterial Decolorization of Textile Dye-Orange 3R.” *International Journal of ...* 2(1):168–77.
- Porri, Aimone, Riccardo Baroncelli, Lorenzo Guglielminetti, Sabrina Sarrocco, Lorenzo Guazzelli, Maurizio Forti, Giorgio Catelani, Giorgio Valentini, Agostino Bazzichi, Massimiliano Franceschi, and Giovanni Vannacci. 2011. “Fusarium Oxysporum Degradation and Detoxification of a New Textile-Glycoconjugate Azo Dye (GAD).” *Fungal Biology* 115(1):30–37.
- Prasad, A. S. Arun and K. V. Bhaskara Rao. 2013. “Aerobic Biodegradation of Azo Dye by *Bacillus Cohnii* MTCC 3616; An Obligately Alkaliphilic Bacterium and Toxicity Evaluation of Metabolites by Different Bioassay Systems.” *Applied Microbiology and Biotechnology* 97(16):7469–81.
- Prescott, Lansing M., John P. Harley, and Donald A. Klein. 2002. *Microbiology*. McGraw-Hill.
- Priya, Balakrishnan, Lakshmanan Uma, Abdul Khaleel Ahamed, Gopalakrishnan Subramanian, and Dharmar Prabakaran. 2011a. “Ability to Use the Diazo Dye, C.I. Acid Black 1 as a Nitrogen Source by the Marine Cyanobacterium *Oscillatoria Curviceps* BDU92191.” *Bioresource Technology* 102(14):7218–23.
- Priya, Balakrishnan, Lakshmanan Uma, Abdul Khaleel Ahamed, Gopalakrishnan Subramanian, and Dharmar Prabakaran. 2011b. “Ability to Use the Diazo Dye, C.I. Acid Black 1 as a Nitrogen Source by the Marine Cyanobacterium *Oscillatoria Curviceps* BDU92191.” *Bioresource Technology* 102(14):7218–23.
- Prosser, J. I. and A. J. Tough. 1991. “Growth Mechanisms and Growth Kinetics of Filamentous Microorganisms.” *Critical Reviews in Biotechnology* 10(4):253–74.
- Przystaś, Wioletta, Ewa Zabłocka-Godlewska, and Elżbieta Grabińska-Sota. 2018. “Efficiency of Decolorization of Different Dyes Using Fungal Biomass Immobilized on Different Solid Supports.” *Brazilian Journal of Microbiology* 49(2):285–95.
- Puvaneswari, N., J. Muthukrishnan, and P. Gunasekaran. 2006. “Toxicity Assessment and Microbial Degradation of Azo Dyes.” *Indian Journal of Experimental Biology* 44(8):618–26.
- Qureshi, Nasib, Bassam a Annous, Thaddeus C. Ezeji, Patrick Karcher, and Ian S. Maddox. 2005. “Biofilm Reactors for Industrial Bioconversion Processes: Employing Potential of Enhanced Reaction Rates.” *Microbial Cell Factories* 4:24.

- Rahman, Md Mahfuzur, Md Fazlur Rahman, and Khondokar Nasirujjaman. 2017. "A Study on Genotoxicity of Textile Dyeing Industry Effluents from Rajshahi, Bangladesh, by the Allium Cepa Test." *Chemistry and Ecology* 33(5):434–46.
- Rajabi, Somayeh, Ali Ramazani, Mehrdad Hamidi, and Tahereh Najji. 2015. "Artemia Salina as a Model Organism in Toxicity Assessment of Nanoparticles." *DARU, Journal of Pharmaceutical Sciences* 23(1):1–6.
- Rawat, Deepak, Vandana Mishra, and Radhey Shyam Sharma. 2016. "Detoxification of Azo Dyes in the Context of Environmental Processes." *Chemosphere* 155:591–605.
- Renganathan, S., W. Richard Thilagaraj, Lima Rose Miranda, P. Gautam, and M. Velan. 2006. "Accumulation of Acid Orange 7, Acid Red 18 and Reactive Black 5 by Growing Schizophyllum Commune." *Bioresource Technology* 97(16):2189–93.
- Rgen Forss, Jö, Markus V Lindh, Jarone Pinhassi, and Ulrika Welander. 2017. "Microbial Biotreatment of Actual Textile Wastewater in a Continuous Sequential Rice Husk Biofilter and the Microbial Community Involved."
- Riffat, Rumana. 2013. *Fundamentals of Wastewater Treatment and Engineering*. CRC Press/Taylor & Francis.
- Riu, J., I. Schönsee, D. Barceló, and C. Ràfols. 1997. "Determination of Sulphonated Azo Dyes in Water and Wastewater." *TrAC - Trends in Analytical Chemistry* 16(7):405–19.
- Rodríguez Couto, Susana. 2009. "Dye Removal by Immobilised Fungi." *Biotechnology Advances* 27(3):227–35.
- Roy, R., ANM Fakhruddin, R. Khatun, and MS Islam. 1970. "Reduction of COD and PH of Textile Industrial Effluents by Aquatic Macrophytes and Algae." *Journal of Bangladesh Academy of Sciences* 34(1):9–14.
- Ruiz-Arias, Alfredo, Cleotilde Juárez-Ramírez, Daniel De Los Cobos-Vasconcelos, Nora Ruiz-Ordaz, Angélica Salmerón-Alcocer, Deifilia Ahuatzi-Chacón, and Juvencio Galíndez-Mayer. 2010. "Aerobic Biodegradation of a Sulfonated Phenylazonaphthol Dye by a Bacterial Community Immobilized in a Multistage Packed-Bed BAC Reactor." *Applied Biochemistry and Biotechnology* 162:1689–1707.
- Rybczyńska, Kamila and Teresa Kornilłowicz-Kowalska. 2015. "Evaluation of Dye Compounds' Decolorization Capacity of Selected H. Haematococca and T. Harzianum Strains by Principal Component Analysis (PCA)." *Water, Air, and Soil Pollution* 226(7).
- Sadhasivam, Subramaniam, Sivasubramanian Savitha, Krishnasamy Swaminathan, and Feng-Huei Lin. 2009. "Metabolically Inactive Trichoderma Harzianum Mediated Adsorption of Synthetic Dyes: Equilibrium and Kinetic Studies." *Journal of the Taiwan Institute of Chemical Engineers* 40(4):394–402.
- Sahasrabudhe, M. M. and G. R. Pathade. 2011. "Decolourization of C . I . Reactive Yellow 145 by Enterococcus Faecalis." *Science* 3(3):403–14.
- Sahasrabudhe, Madhuri M., Rijuta G. Saratale, Ganesh D. Saratale, and Girish R. Pathade. 2014. "Decolorization and Detoxification of Sulfonated Toxic Diazo Dye C.I. Direct Red 81 by Enterococcus Faecalis YZ 66." *Journal of*

- Environmental Health Science & Engineering* 12(1):151.
- Samoylova, Yuliya, Ksenia Sorokina, Alexander Piligaev, Valentin Parmon, Yuliya V. Samoylova, Ksenia N. Sorokina, Alexander V. Piligaev, and Valentin N. Parmon. 2018. "Preparation of Stable Cross-Linked Enzyme Aggregates (CLEAs) of a *Ureibacillus Thermosphaericus* Esterase for Application in Malathion Removal from Wastewater." *Catalysts* 8(4):154.
- Sani, Rajesh Kumar and Uttam Chand Banerjee. 1999. "Decolorization of Triphenylmethane Dyes and Textile and Dye-Stuff Effluent by *Kurthia* Sp." *Enzyme and Microbial Technology* 24(7):433–37.
- dos Santos, A. B., F. J. Cervantes, and J. B. van Lier. 2004. "Azo Dye Reduction by Thermophilic Anaerobic Granular Sludge, and the Impact of the Redox Mediator Anthraquinone-2,6-Disulfonate (AQDS) on the Reductive Biochemical Transformation." *Applied Microbiology and Biotechnology* 64(1):62–69.
- Saratale, Ganesh D., Rijuta G. Saratale, Jo Shu Chang, and Sanjay P. Govindwar. 2011. "Fixed-Bed Decolorization of Reactive Blue 172 by *Proteus Vulgaris* NCIM-2027 Immobilized on *Luffa Cylindrica* Sponge." *International Biodeterioration & Biodegradation* 65(3):494–503.
- Saratale, R. G., G. D. Saratale, J. S. Chang, and S. P. Govindwar. 2009. "Decolorization and Biodegradation of Textile Dye Navy Blue HER by *Trichosporon Beigelii* NCIM-3326." *Journal of Hazardous Materials* 166:1421–28.
- Saratale, R.G., G. D. Saratale, J. S. Chang, and S. P. Govindwar. 2009. "Ecofriendly Degradation of Sulfonated Diazo Dye C.I. Reactive Green 19A Using *Micrococcus Glutamicus* NCIM-2168." *Bioresource Technology* 100(17):3897–3905.
- Saratale, R. G., G. D. Saratale, J. S. Chang, and S. P. Govindwar. 2010. "Decolorization and Biodegradation of Reactive Dyes and Dye Wastewater by a Developed Bacterial Consortium." *Biodegradation* 21:999–1015.
- Saratale, R. G., G. D. Saratale, J. S. Chang, and S. P. Govindwar. 2011. "Bacterial Decolorization and Degradation of Azo Dyes: A Review." *Journal of the Taiwan Institute of Chemical Engineers* 42(1):138–57.
- Saratale, R. G., G. D. Saratale, D. C. Kalyani, J. S. Chang, and S. P. Govindwar. 2009. "Enhanced Decolorization and Biodegradation of Textile Azo Dye Scarlet R by Using Developed Microbial Consortium-GR." *Bioresource Technology* 100(9):2493–2500.
- Saratale, Rijuta G., Soniya S. Gandhi, Madhavi V. Purankar, Mayur B. Kurade, Sanjay P. Govindwar, Sang Eun Oh, and Ganesh D. Saratale. 2013. "Decolorization and Detoxification of Sulfonated Azo Dye C.I. Remazol Red and Textile Effluent by Isolated *Lysinibacillus* Sp. RGS." *Journal of Bioscience and Bioengineering* 115(6):658–67.
- Saratale, Rijuta G., Ganesh D. Saratale, Jo Shu Chang, and Sanjay P. Govindwar. 2011. "Decolorization and Degradation of Reactive Azo Dyes by Fixed Bed Bioreactors Containing Immobilized Cells of *Proteus Vulgaris* NCIM-2027." *Biotechnology and Bioprocess Engineering* 16:830–42.
- Saravanakumar, Kandasamy and Kandasamy Kathiresan. 2014. "Bioremoval of the

- Synthetic Dye Malachite Green by Marine Trichoderma Sp.” *SpringerPlus* 3(1):1–12.
- Sarayu, K. and S. Sandhya. 2012. “Current Technologies for Biological Treatment of Textile Wastewater-A Review.” *Applied Biochemistry and Biotechnology* 167:645–61.
- Sathian, S., M. Rajasimman, G. Radha, V. Shanmugapriya, and C. Karthikeyan. 2014. “Performance of SBR for the Treatment of Textile Dye Wastewater: Optimization and Kinetic Studies.” *Alexandria Engineering Journal* 53(2):417–26.
- Savizi, Iman Shahidi Pour, Hamid Reza Kariminia, and Sahar Bakhshian. 2012. “Simultaneous Decolorization and Bioelectricity Generation in a Dual Chamber Microbial Fuel Cell Using Electropolymerized-Enzymatic Cathode.” *Environmental Science and Technology* 46:6584–93.
- Sedighi, M., A. Karimi, and F. Vahabzadeh. 2009. “Involvement of Ligninolytic Enzymes of Phanerochaete Chrysosporium in Treating the Textile Effluent Containing Astrazon Red FBL in a Packed-Bed Bioreactor.” *Journal of Hazardous Materials* 169(1–3):88–93.
- Semdé, R., D. Pierre, G. Geuskens, M. Devleeschouwer, and A. .. Moës. 1998. “Study of Some Important Factors Involved in Azo Derivative Reduction by Clostridium Perfringens.” *International Journal of Pharmaceutics* 161(1):45–54.
- Shah, Parin D., Shailesh R. Dave, and M. S. Rao. 2012. “Enzymatic Degradation of Textile Dye Reactive Orange 13 by Newly Isolated Bacterial Strain Alcaligenes Faecalis PMS-1.” *International Biodeterioration and Biodegradation* 69:41–50.
- Sharma, K. P., S. Sharma, Subhasini Sharma, P. K. Singh, S. Kumar, R. Grover, and P. K. Sharma. 2007. “A Comparative Study on Characterization of Textile Wastewaters (Untreated and Treated) Toxicity by Chemical and Biological Tests.” *Chemosphere* 69(1):48–54.
- Sharma, Praveen, Lakhvinder Singh, and Neeraj Dilbaghi. 2009. “Optimization of Process Variables for Decolorization of Disperse Yellow 211 by Bacillus Subtilis Using Box-Behnken Design.” *Journal of Hazardous Materials* 164(2–3):1024–29.
- Sharma, Subhasini, V. Suryavathi, Pawan K. Singh, and K. P. Sharma. 2008. “Toxicity Assessment of Textile Dye Wastewater Using Swiss Albino Rats.” 81–85.
- Shin, Kwang-Soo. 2004. “The Role of Enzymes Produced by White-Rot Fungus Irpex Lacteus in the Decolorization of the Textile Industry Effluent.” *Journal of Microbiology (Seoul, Korea)* 42(1):37–41.
- Shuang, Song, Xu Xing, Xu Lejin, He Zhiqiao, Ying Haiping, Chen Jianmeng, and Yan Bing. 2008. “Mineralization of CI Reactive Yellow 145 in Aqueous Solution by Ultraviolet-Enhanced Ozonation.” *Industrial and Engineering Chemistry Research* 47(5):1386–91.
- Sierra Solache, Rosario Esmeralda, Claudia Muro-Urista, Rosa Elena Ortega Aguilar, Ainhoa Arana Cuenca, and Alejandro Téllez Jurado. 2016. “Application of Immobilized Fungi on Food Effluent Treatment Using Airlift Reactor.” *Desalination and Water Treatment* 57(27):12743–54.

- Šíma, J., J. Povedič, T. Roubíčková, and P. Hasal. 2012. "Rotating Drum Biological Contactor and Its Application for Textile Dyes Decolorization." *Procedia Engineering* 42(August):1579–86.
- Sin, Sui H., Jinjie Xu, Ka Y. Fung, Ka M. Ng, and Kathy Qian Luo. 2016. "Evaluation of Bacterial Consortium Construction Approaches for Anaerobic Decolorization." *Journal of Environmental Chemical Engineering* 4(1):1191–98.
- Singh, Ram Lakhan, Pradeep Kumar Singh, and Rajat Pratap Singh. 2015. "Enzymatic Decolorization and Degradation of Azo Dyes - A Review." *International Biodeterioration and Biodegradation* 104:21–31.
- Singh, RamLakhan, RajatPratap Singh, and PradeepKumar Singh. 2014. "Bacterial Decolorization of Textile Azo Dye Acid Orange by Staphylococcus Hominis RMLRT03." *Toxicology International* 21(2):160.
- Singh, S., S. Chatterji, P. T. Nandini, A. S. A. Prasad, and K. V. B. Rao. 2015. "Biodegradation of Azo Dye Direct Orange 16 by Micrococcus Luteus Strain SSN2." *International Journal of Environmental Science and Technology* 12(7):2161–68.
- Sirianuntapiboon, Suntud and Jutarat Sansak. 2008. "Treatability Studies with Granular Activated Carbon (GAC) and Sequencing Batch Reactor (SBR) System for Textile Wastewater Containing Direct Dyes." *Journal of Hazardous Materials* 159(2–3):404–11.
- Solís, Myrna, Aida Solís, Herminia Inés Pérez, Norberto Manjarrez, and Maribel Flores. 2012a. "Microbial Decolouration of Azo Dyes: A Review." *Process Biochemistry* 47(12):1723–48.
- Solís, Myrna, Aida Solís, Herminia Inés Pérez, Norberto Manjarrez, and Maribel Flores. 2012b. "Microbial Decolouration of Azo Dyes: A Review." *Process Biochemistry* 47:1723–48.
- Somerville, Greg A. and Richard A. Proctor. 2013. "Cultivation Conditions and the Diffusion of Oxygen into Culture Media: The Rationale for the Flask-to-Medium Ratio in Microbiology." *BMC Microbiology* 13(1).
- Song, Shuang, Jiaqi Fan, Zhiqiao He, Liyong Zhan, Zhiwu Liu, Jianmeng Chen, and Xinhua Xu. 2010. "Electrochemical Degradation of Azo Dye C.I. Reactive Red 195 by Anodic Oxidation on Ti/SnO₂-Sb/PbO₂ Electrodes." *Electrochimica Acta* 55(11):3606–13.
- Soriano, Jeriel J., Justine Mathieu-Denoncourt, Grant Norman, Shane R. de Solla, and Valérie S. Langlois. 2014. "Toxicity of the Azo Dyes Acid Red 97 and Bismarck Brown Y to Western Clawed Frog (*Silurana tropicalis*)." *Environmental Science and Pollution Research* 21(5):3582–91.
- Spagni, Alessandro, Selene Grilli, Stefania Casu, and Davide Mattioli. 2010. "Treatment of a Simulated Textile Wastewater Containing the Azo-Dye Reactive Orange 16 in an Anaerobic-Biofilm Anoxic-Aerobic Membrane Bioreactor." *International Biodeterioration and Biodegradation* 64(7):676–81.
- Sponza, Delia Teresa. 2006. "Toxicity Studies in a Chemical Dye Production Industry in Turkey." *Journal of Hazardous Materials* 138(April 2005):438–47.
- Srinivasan, Asha and Thiruvengkatachari Viraraghavan. 2010. "Decolorization of Dye Wastewaters by Biosorbents: A Review." *Journal of Environmental*

- Management* 91(10):1915–29.
- Stine, Karen. and Thomas M. (Thomas Miller) Brown. 1996. *Principles of Toxicology*. CRC Lewis Publishers.
- Stolz, A. 2001. “Basic and Applied Aspects in the Microbial Degradation of Azo Dyes.” *Applied Microbiology and Biotechnology* 56(1–2):69–80.
- Subashkumar R, Rajeswari K., Subashkumar R, and Vijayaraman K. 2014. “Degradation of Textile Dyes by Isolated *Lysinibacillus Sphaericus* Strain RSV-1 and *Stenotrophomonas Maltophilia* Strain RSV-2 and Toxicity Assessment of Degraded Product.” *Journal of Environmental & Analytical Toxicology* 04(04):1–5.
- Sudha, M., G. Bakiyaraj, A. Saranya, N. Sivakumar, and G. Selvakumar. 2018a. “Prospective Assessment of the *Enterobacter Aerogenes* PP002 in Decolorization and Degradation of Azo Dyes DB 71 and DG 28.” *Journal of Environmental Chemical Engineering* 6(1):95–109.
- Sudha, M., G. Bakiyaraj, A. Saranya, N. Sivakumar, and G. Selvakumar. 2018b. “Prospective Assessment of the *Enterobacter Aerogenes* PP002 in Decolorization and Degradation of Azo Dyes DB 71 and DG 28.” *Journal of Environmental Chemical Engineering* 6(1):95–109.
- Surti, A., Ansari, R.. 2018. “Characterization of dye degrading potential of suspended and nanoparticle immobilized cells of *Pseudomonas aeruginosa* AR-7. 774–80.
- Suryavathi, V., Subhasini Sharma, Shweta Sharma, Pratibha Saxena, Shipra Pandey, Ruby Grover, Suresh Kumar, and K. P. Sharma. 2005. “Acute Toxicity of Textile Dye Wastewaters (Untreated and Treated) of Sanganer on Male Reproductive Systems of Albino Rats and Mice.” *Reproductive Toxicology* 19:547–56.
- Sweeney, E. A., J. K. Chipman, and S. J. Forsythe. 1994. “Evidence for Direct-Acting Oxidative Genotoxicity by Reduction Products of Azo Dyes.” *Environmental Health Perspectives* 102(suppl 6):119–22.
- Szeberenyi, Jozsef. 2003. “The Ames Test.” *Biochemistry and Molecular Biology Education* 31:344–45.
- Taha, M., E. M. Adetutu, E. Shahsavari, a. T. Smith, and a. S. Ball. 2014. “Azo and Anthraquinone Dye Mixture Decolourization at Elevated Temperature and Concentration by a Newly Isolated Thermophilic Fungus, *Thermomucor Indicae-Seudaticae*.” *Journal of Environmental Chemical Engineering* 2(1):415–23.
- Tan, Nico C. G. 2001. *Integrated and Sequential Anaerobic / Aerobic Biodegradation of Azo Dyes*.
- Tastimi, Parham, H. Nadaroglu, A. Adiguzel, C. Bozoglu, and M. Gulluce. 2013. “Removal of Some Textile Dyes from Aqueous Solution by Using a Catalase-Peroxidase from *Aeribacillus Pallidus* (P26).” *Journal of Pure and Applied Microbiology* 7(4):2629–40.
- Tony, Bella Devassy, Dinesh Goyal, and Sunil Khanna. 2009. “Decolorization of Textile Azo Dyes by Aerobic Bacterial Consortium.” *International Biodeterioration and Biodegradation* 63(4):462–69.
- Tunç, Özlem, Hacer Tanacı, and Zümriye Aksu. 2009. “Potential Use of Cotton Plant

- Wastes for the Removal of Remazol Black B Reactive Dye.” *Journal of Hazardous Materials* 163(1):187–98.
- Turker, Arzu Ucar and N. .. Camper. 2002. “Biological Activity of Common Mullein, a Medicinal Plant.” *Journal of Ethnopharmacology* 82(2–3):117–25.
- Tuttolomondo, María Victoria, Gisela Solange Alvarez, Martín Federico Desimone, and Luis Eduardo Diaz. 2014. “Removal of Azo Dyes from Water by Sol-Gel Immobilized Pseudomonas Sp.” *Journal of Environmental Chemical Engineering* 2:131–36.
- Tyagi, R. D. and T. K. Ghose. 1982. “Studies on Immobilized Saccharomyces Cerevisiae. I. Analysis of Continuous Rapid Ethanol Fermentation in Immobilized Cell Reactor.” *Biotechnology and Bioengineering* 24(4):781–95.
- Ürek, Raziye Öztürk and Nurdan Kaşıkara Pazarlıoğlu. 2005. “Production and Stimulation of Manganese Peroxidase by Immobilized Phanerochaete Chrysosporium.” *Process Biochemistry* 40(1):83–87.
- Vacchi, Francine Inforçato, Josiane Aparecida de Souza Vendemiatti, Bianca Ferreira da Silva, Maria Valnice Boldrin Zanoni, and Gisela de Aragão Umbuzeiro. 2017. “Quantifying the Contribution of Dyes to the Mutagenicity of Waters under the Influence of Textile Activities.” *Science of the Total Environment* 601–602:230–36.
- Vandevivere, Philippe C., Roberto Bianchi, and Will Verstraete. 1998. “Review Treatment and Reuse of Wastewater from the Textile Wet-Processing Industry: Review of Emerging Technologies.”
- Vantamuri, Adivappa B. and Basappa B. Kaliwal. 2017. “Decolourization and Biodegradation of Navy Blue HER (Reactive Blue 171) Dye from Marasmius Sp. BBKAV79.” *3 Biotech* 7(1):48.
- Velmurugan, S., William W. Clarkson, and John N. Veenstra. 2010. “Model-Based Design of Sequencing Batch Reactor for Removal of Biodegradable Organics and Nitrogen.” *Water Environment Research* 82:462–74.
- Venkata Mohan, S., C. Nagendranatha Reddy, A. Naresh Kumar, and J. Annie Modestra. 2013. “Relative Performance of Biofilm Configuration over Suspended Growth Operation on Azo Dye Based Wastewater Treatment in Periodic Discontinuous Batch Mode Operation.” *Bioresource Technology* 147:424–33.
- Venkata Mohan, S., P. Suresh Babu, K. Naresh, G. Velvizhi, and Datta Madamwar. 2012. “Acid Azo Dye Remediation in Anoxic-Aerobic-Anoxic Microenvironment under Periodic Discontinuous Batch Operation: Bio-Electro Kinetics and Microbial Inventory.” *Bioresource Technology* 119:362–72.
- Ventura-camargo, Bruna De Campos and Maria Aparecida Marin-morales. 2013. “Azo Dyes : Characterization and Toxicity – A Review.” *Textiles and Light Industrial Science and Technology* 2(2):85–103.
- Vijayalakshmidivi, S. R. and Karuppan Muthukumar. 2015. “Improved Biodegradation of Textile Dye Effluent by Coculture.” *Ecotoxicology and Environmental Safety* 114:23–30.
- Vitor, Vivian and Carlos Renato Corso. 2008. “Decolorization of Textile Dye by Candida Albicans Isolated from Industrial Effluents.” *Journal of Industrial*

- Microbiology & Biotechnology* 35(11):1353–57.
- Waghmode, T. R., M. B. Kurade, A. N. Kabra, and S. P. Govindwar. 2012. “Biodegradation of Rubine GFL by *Galactomyces Geotrichum* MTCC 1360 and Subsequent Toxicological Analysis by Using Cytotoxicity, Genotoxicity and Oxidative Stress Studies.” *Microbiology* 158(Pt_9):2344–52.
- Waghmode, Tatoba R., Mayur B. Kurade, and Sanjay P. Govindwar. 2011. “Time Dependent Degradation of Mixture of Structurally Different Azo and Non Azo Dyes by Using *Galactomyces Geotrichum* MTCC 1360.” *International Biodeterioration and Biodegradation* 65(3):479–86.
- Waghmode, Tatoba R., Mayur B. Kurade, Rahul V. Khandare, and Sanjay P. Govindwar. 2011. “A Sequential Aerobic/Microaerophilic Decolorization of Sulfonated Mono Azo Dye Golden Yellow HER by Microbial Consortium GG-BL.” *International Biodeterioration and Biodegradation* 65(7):1024–34.
- Wang, Chunxia, Ayfer Yediler, Doris Lienert, Zijian Wang, and Antonius Kettrup. 2002. “Toxicity Evaluation of Reactive Dyestuffs, Auxiliaries and Selected Effluents in Textile Finishing Industry to Luminescent Bacteria *Vibrio Fischeri*.” *Chemosphere* 46:339–44.
- Wang, Hui, Jian Qiang Su, Xiao Wei Zheng, Yun Tian, Xiao Jing Xiong, and Tian Ling Zheng. 2009. “Bacterial Decolorization and Degradation of the Reactive Dye Reactive Red 180 by *Citrobacter* Sp. CK3.” *International Biodeterioration and Biodegradation* 63(4):395–99.
- Wang, Lei, Jian Yan, William Hardy, Charity Mosley, Shuguang Wang, and Hongtao Yu. 2005. “Light-Induced Mutagenicity in *Salmonella* TA102 and Genotoxicity/Cytotoxicity in Human T-Cells by 3,3'-Dichlorobenzidine: A Chemical Used in the Manufacture of Dyes and Pigments and in Tattoo Inks.” *Toxicology* 207(3):411–18.
- Wang, Qing-Xiang, Xuan Zhang, Jian-Cong Ni, Juan-Lan Shi, Feng Gao, Guo-Liang Chen, and Fei Gao. 2012. “Binding Mode and Photo-Cleavage of an Azo Dye, Acid Chrome Blue K, to Double-Stranded DNA.” *Journal of Solution Chemistry* 41(7):1185–96.
- Wang, Rong-Chi, Kuo-Shiuan Fan, and Jyh-Shyong Chang. 2009. “Removal of Acid Dye by ZnFe₂O₄/TiO₂-Immobilized Granular Activated Carbon under Visible Light Irradiation in a Recycle Liquid–Solid Fluidized Bed.” *Journal of the Taiwan Institute of Chemical Engineers* 40(5):533–40.
- Wang, Xiaodong, Cheng Sun, Shixiang Gao, Liansheng Wang, and Han Shuokui. 2001. “Validation of Germination Rate and Root Elongation as Indicator to Assess Phytotoxicity with *Cucumis Sativus*.” *Chemosphere* 44:1711–21.
- Wang, Zongping, Miaomiao Xue, Kai Huang, and Zizheng Liu. 2010. “Textile Dyeing Wastewater Treatment.” 91–116.
- Waring, David R. and G. (Geoffrey) Hallas. 1990. *The Chemistry and Application of Dyes*. Plenum Press.
- Watanabe, K. and P. W. Baker. 2000. “Environmentally Relevant Microorganisms.” *Journal of Bioscience and Bioengineering* 89(1):1–11.
- Willmott, Nicola Jane. 1997. “The Use of Bacteria-Polymer Composites for the Removal of Colour from Reactive Dye Effluents.”

- Wong, P. K. and P. Y. Yuen. 1998. "Decolourization and Biodegradation of N,N'-Dimethyl-p-Phenylenediamine by Klebsiella Pneumoniae RS-13 and Acetobacter Liquefaciens S-1." *Journal of Applied Microbiology* 85(1):79–87.
- Yang, Chunyu, Zhe Wang, Yang Li, Yu Niu, Miaofen Du, Xiaofei He, Cuiqing Ma, Hongzhi Tang, and Ping Xu. 2010. "Metabolic Versatility of Halotolerant and Alkaliphilic Strains of Halomonas Isolated from Alkaline Black Liquor." *Bioresource Technology* 101(17):6778–84.
- Yang, Yonggang, Ou Luo, Guannan Kong, Bin Wang, Xiaojing Li, Enze Li, Jianjun Li, Feifei Liu, and Meiyong Xu. 2018. "Deciphering the Anode-Enhanced Azo Dye Degradation in Anaerobic Baffled Reactors Integrating With Microbial Fuel Cells." *Frontiers in Microbiology* 9:2117.
- Yeap, Kiew Lee, Tjoon Tow Teng, Beng Teik Poh, Norhashimah Morad, and Khai Ern Lee. 2014. "Preparation and Characterization of Coagulation/Flocculation Behavior of a Novel Inorganic–Organic Hybrid Polymer for Reactive and Disperse Dyes Removal." *Chemical Engineering Journal* 243:305–14.
- Yh, Gursahani and Gupta Sg. 2011. "Decolourization of Textile Effluent by a Thermophilic Bacteria Anoxybacillus Rupiensis." *Journal of Petroleum & Environmental Biotechnology* 02(2):2–5.
- You, S. J., D. H. Tseng, S. H. Ou, and W. K. Chang. 2007. "PERFORMANCE AND MICROBIAL DIVERSITY OF A MEMBRANE BIOREACTOR TREATING REAL TEXTILE DYEING WASTEWATER." *Environmental Technology* 28(8):935–41.
- Yousefi, H., A. Yahyazadeh, E. O. Moradi Rufchahi, and M. Rassa. 2013. "Synthesis, Spectral Properties, Biological Activity and Application of New 4-(Benzyloxy)Phenol Derived Azo Dyes for Polyester Fiber Dyeing." *Journal of Molecular Liquids* 180:51–58.
- Yu, Zhen, Xuemei Zhou, Yueqiang Wang, Guiqin Yang, and Shungui Zhou. 2015. "Dissimilatory Azoreduction of Orange I by a Newly Isolated Moderately Thermophilic Bacterium, Novibacillus Thermophilus SG-1." *Biotechnology and Bioprocess Engineering* 20(6):1064–70.
- Yu, Zhisheng and Xianghua Wen. 2005. "Screening and Identification of Yeasts for Decolorizing Synthetic Dyes in Industrial Wastewater." *International Biodeterioration & Biodegradation* 56(2):109–14.
- Yuen, C. W. M., S. K. a Ku, P. S. R. Choi, C. W. Kan, and S. Y. Tsang. 2005. "Determining Functional Groups of Commercially Available Ink-Jet Printing Reactive Dyes Using Infrared Spectroscopy." 9(2):26–38.
- Van Der Zee, Frank P. 2002. *Anaerobic Azo Dye Reduction*.
- Van der Zee, Frank P. and Francisco J. Cervantes. 2009. "Impact and Application of Electron Shuttles on the Redox (Bio)Transformation of Contaminants: A Review." *Biotechnology Advances* 27(3):256–77.
- Van Der Zee, Frank P. and Santiago Villaverde. 2005. "Combined Anaerobic-Aerobic Treatment of Azo Dyes - A Short Review of Bioreactor Studies." *Water Research* 39:1425–40.
- Zhao, Xueheng, Yiping Lu, Dennis R. Phillips, Huey-Min Hwang, and Ian R. Hardin. 2007. "Study of Biodegradation Products from Azo Dyes in Fungal Degradation

- by Capillary Electrophoresis/Electrospray Mass Spectrometry.” *Journal of Chromatography A* 1159(1–2):217–24.
- Zhuo, Rui, Li Ma, Fangfang Fan, Yangmin Gong, Xia Wan, Mulan Jiang, Xiaoyu Zhang, and Yang Yang. 2011. “Decolorization of Different Dyes by a Newly Isolated White-Rot Fungi Strain *Ganoderma* Sp.En3 and Cloning and Functional Analysis of Its Laccase Gene.” *Journal of Hazardous Materials* 192(2):855–73.
- Zollinger, H. 1987. *Colour Chemistry—Synthesis, Properties and Applications of Organic Dyes and Pigments*. New York: VCH.

Table A1. Effect of reactive azo dyes on growth of *Pseudomonas aeruginosa*

Dye	Concentration (ppm)	Growth inhibition ratio (%) *	EC20 (ppm)**	EC50 (ppm)**	EC80 (ppm)**	Determination coefficient (R ²)
RB 221	Control	0.00 a	79.45 b	146.58 b	270.42b	0.97
	50	16.64 b				
	100	32.45 c				
	150	53.55 d				
	200	75.86 e				
	250	79.33 ef				
	300	80.58 ef				
	350	84.45 fg				
	400	87.07 g				
	450	90.46 g				
	500	99.33 h				
RR 195	Control	0.00 a	248.11 c	328.09 c	433.85 c	0.93
	50	2.21 a				
	100	23.01 b				
	150	32.27 bc				
	200	29.36 bc				
	250	35.16 c				
	300	47.56 d				
	350	62.02 e				
	400	84.75 f				
	450	87.32 fg				
	500	92.91 fg				
RY 145	Control	0.00 a	58.49 a	120.03 ab	246.33 ab	0.98
	50	41.92 b				
	100	61.04 c				
	150	76.93 d				
	200	80.86 d				
	250	87.04 e				
	300	93.98 f				
	350	94.41 f				
	400	99.55 g				
	450	99.62 g				
	500	99.97 g				
Mixture	Control	0.00 a	58.42 a	110.56 a	209.22 a	0.99
	50	13.35 b				
	100	41.59 c				
	150	70.41 d				
	200	72.45 d				
	250	84.49 e				
	300	91.59 f				
	350	92.09 fg				
	400	95.16 gh				
	450	95.67 hi				
	500	96.37 hi				
1000	98.51 i					

* Mean values with the different letters in each cell are significantly different (one-way ANOVA followed by Tukey's HSD, $\alpha = 0.05$)

** Mean values with the different letters in each column are significantly different (MANOVA followed by Tukey's HSD, $\alpha = 0.05$)

Table A2. Effect of reactive azo dyes on growth of *Escherichia coli*

Dye	Concentration (ppm)	Growth inhibition ratio (%) *	EC20 (ppm)**	EC50 (ppm)**	EC80 (ppm)**	Determination coefficient (R ²)
RB 221	Control	0.00 a	92.13 b	205.41 bc	457.98 b	0.96
	50	5.83 b				
	100	23.69 c				
	150	46.82 d				
	200	49.59 de				
	250	57.62 e				
	300	70.73 f				
	350	74.95 fg				
	400	80.63 g				
	450	93.86 h				
	500	98.10 h				
1000	98.48 h					
RR 195	Control	0.00 a	161.87 c	270.59 c	452.35 b	0.98
	50	6.30 a				
	100	1.50 a				
	150	21.49 b				
	200	29.29 b				
	250	45.32 c				
	300	51.63 c				
	350	68.71 d				
	400	70.96 de				
	450	74.21 de				
	500	79.69 e				
1000	93.59 f					
RY 145	Control	0.00 a	52.48 a	121.40 a	280.86 a	0.98
	50	3.96 b				
	100	22.45 c				
	150	48.78 d				
	200	61.82 e				
	250	64.49 f				
	300	68.48 g				
	350	70.85 h				
	400	73.41 h				
	450	78.17 i				
	500	81.39 i				
1000	88.57 i					
Mixture	Control	0.00 a	80.64 ab	185.57 b	427.02 b	0.95
	50	19.45 b				
	100	31.18 b				
	150	50.40 c				
	200	51.87 cd				
	250	68.13 cde				
	300	63.65 de				
	350	66.59 e				
	400	78.25 fg				
	450	84.74 g				
	500	84.42 g				
1000	87.73 g					

* Mean values with the different letters in each cell are significantly different (one-way ANOVA followed by Tukey's HSD, $\alpha=0.05$)

** Mean values with the different letters in each column are significantly different (MANOVA followed by Tukey's HSD, $\alpha=0.05$)

Table A3. Effect of reactive azo dyes on growth of *Klebsiella pneumoniae*

Dye	Concentration (ppm)	Growth inhibition ratio (%) *	EC20 (ppm)**	EC50 (ppm)**	EC80 (ppm)**	Determination coefficient (R ²)
RB 221	Control	0.00 a	31.92 a	136.83 a	306.54 a	0.89
	50	38.99 b				
	100	56.55 c				
	150	64.45 d				
	200	76.96 e				
	250	76.22 e				
	300	79.04 ef				
	350	82.31 f				
	400	78.93 ef				
	450	98.24 g				
	500	99.87 g				
	1000	99.89 g				
RR 195	Control	0.00 a	57.81 ab	147.31 ab	375.42 a	0.95
	50	44.76 b				
	100	65.55 b				
	150	67.95 c				
	200	76.59 c				
	250	83.55 e				
	300	85.82 ef				
	350	88.18 f				
	400	95.85 e				
	450	99.29 g				
	500	99.01 g				
	1000	99.34 g				
RY 145	Control	0.00 a	64.96 a	152.49 a	357.95 a	0.99
	50	23.31 b				
	100	42.65 c				
	150	53.96 d				
	200	71.69 e				
	250	75.45 ef				
	300	77.48 f				
	350	84.24 g				
	400	87.72 gh				
	450	92.54 hi				
	500	94.07 i				
	1000	99.49 j				
Mixture	Control	0.00 a	138.09 b	240.51 a	418.89 a	0.98
	50	32.62 b				
	100	42.63 bc				
	150	47.86 bcd				
	200	53.23 cde				
	250	63.32 def				
	300	72.64 efg				
	350	74.42 fg				
	400	77.69 fg				
	450	82.04 fg				
	500	85.45 g				
	1000	88.74 g				

* Mean values with the different letters in each cell are significantly different (one-way ANOVA followed by Tukey's HSD, $\alpha=0.05$)

** Mean values with the different letters in each column are significantly different (MANOVA followed by Tukey's HSD, $\alpha=0.05$)

Table A4. Effect of reactive azo dyes on growth of *Staphylococcus aureus*

Dye	Concentration (ppm)	Growth inhibition ratio (%) *	EC20 (ppm)**	EC50 (ppm)**	EC80 (ppm)**	Determination coefficient (R ²)
RB 221	Control	0.00 a	157.27 bc	176.27 ab	197.56 a	0.96
	50	37.81 b				
	100	44.01 c				
	150	46.81 c				
	200	87.21 d				
	250	90.39 e				
	300	92.02 e				
	350	90.49 e				
	400	98.53 f				
	450	99.87 f				
	500	99.38 f				
1000	99.92 f					
RR195	Control	0.00 a	182.47 c	303.58 c	505.09 b	0.84
	50	34.39 b				
	100	38.39 b				
	150	49.19 c				
	200	49.12 c				
	250	63.13 d				
	300	69.51 d				
	350	76.21 de				
	400	62.73 e				
	450	96.18 f				
	500	97.55 f				
1000	96.99 f					
RY145	Control	0.00 a	83.61 a	219.06 b	573.90 b	0.90
	50	29.87 b				
	100	34.61 b				
	150	59.61 c				
	200	63.02 cd				
	250	66.83 cd				
	300	70.01 cd				
	350	72.96 d				
	400	74.06 d				
	450	88.85 e				
	500	97.49 e				
1000	96.57 e					
Mixture	Control	0.00 a	123.43 b	154.45 a	193.28 a	0.99
	50	6.31 a				
	100	17.43 a				
	150	47.59 c				
	200	85.60 d				
	250	93.87 d				
	300	96.89 d				
	350	97.73 d				
	400	98.11 d				
	450	98.27 d				
	500	98.40 d				
1000	98.79 d					

* Mean values with the different letters in each cell are significantly different (one-way ANOVA followed by Tukey's HSD, $\alpha=0.05$)

** Mean values with the different letters in each column are significantly different (MANOVA followed by Tukey's HSD, $\alpha=0.05$)

Table A5. Effect of reactive azo dyes on growth of *Listeria monocytogenes*

Dye	Concentration (ppm)	Growth inhibition ratio (%) *	EC20 (ppm)**	EC50 (ppm)**	EC80 (ppm)**	Determination coefficient (R ²)
RB 221	Control	0.00 a	71.13 a	120.15 a	202.95 a	0.94
	50	37.26 b				
	100	58.41 c				
	150	83.22 d				
	200	84.30 de				
	250	87.34 def				
	300	88.59 def				
	350	89.88 defg				
	400	92.53 fgh				
	450	93.52 gh				
	500	93.53 gh				
1000	99.75 h					
RR 195	Control	0.00 a	40.54 a	79.13 a	154.45 a	0.95
	50	38.54 b				
	100	64.36 c				
	150	89.23 d				
	200	88.01 d				
	250	87.65 d				
	300	90.65 d				
	350	98.89 d				
	400	98.77 d				
	450	98.73 d				
	500	98.97 d				
1000	99.53 d					
RY 145	Control	0.00 a	163.67 b	240.26 b	352.69 b	0.99
	50	7.16 b				
	100	17.52 c				
	150	28.01 d				
	200	36.77 e				
	250	60.15 f				
	300	73.83 g				
	350	84.61 h				
	400	86.55 h				
	450	93.11 i				
	500	98.01 i				
1000	99.14 i					
Mixture	Control	0.00 a	56.96 a	97.76 a	167.79 a	0.99
	50	29.74 b				
	100	58.51 c				
	150	74.27 d				
	200	87.75 d				
	250	91.88 de				
	300	90.49 de				
	350	91.26 de				
	400	92.01 de				
	450	92.63 de				
	500	97.09 e				
1000	97.15 e					

* Mean values with the different letters in each cell are significantly different (one-way ANOVA followed by Tukey's HSD, $\alpha=0.05$)

** Mean values with the different letters in each column are significantly different (MANOVA followed by Tukey's HSD, $\alpha=0.05$)

Table A6. Effect of reactive azo dyes on growth of *Bacillus subtilis*

Dye	Concentration (ppm)	Growth inhibition ratio (%) *	EC20 (ppm)**	EC50 (ppm)**	EC80 (ppm)**	Determination coefficient (R ²)
RB 221	Control	0.00 a	86.39 ab	146.38 ab	258.35 a	0.98
	50	20.83 b				
	100	44.09 c				
	150	50.56 d				
	200	67.39 e				
	250	78.61 f				
	300	88.69 g				
	350	90.89 gh				
	400	94.62 hi				
	450	96.21 i				
	500	96.88 i				
1000	98.94 i					
RR 195	Control	0.00 a	79.24 a	136.42 a	244.09 a	0.98
	50	38.06 b				
	100	57.37 c				
	150	66.64 d				
	200	84.16 e				
	250	89.74 f				
	300	90.65 f				
	350	93.37 fg				
	400	96.49 gh				
	450	98.64 h				
	500	99.09 h				
1000	99.56 h					
RY 145	Control	0.00 a	90.16 b	184.02 c	381.82 b	0.99
	50	21.29 b				
	100	30.01 c				
	150	39.15 d				
	200	50.71 e				
	250	59.85 f				
	300	69.83 g				
	350	83.22 h				
	400	86.69 i				
	450	88.51 i				
	500	91.72 j				
1000	95.47 k					
Mixture	Control	0.00 a	93.12 b	161.32 bc	373.07 b	0.96
	50	28.07 b				
	100	48.75 c				
	150	57.35 d				
	200	64.28 e				
	250	73.07 f				
	300	79.71 f				
	350	88.82 h				
	400	93.11 i				
	450	97.79 j				
	500	99.07 j				
1000	99.41 j					

* Mean values with the different letters in each cell are significantly different (one-way ANOVA followed by Tukey's HSD, $\alpha = 0.05$)

** Mean values with the different letters in each column are significantly different (MANOVA followed by Tukey's HSD, $\alpha = 0.05$)

Table A7. Effect of reactive azo dyes on growth of *Trichoderma asperellum*

Dye	Concentration (ppm)	Growth inhibition ratio (%) *	EC20 (ppm)**	EC50 (ppm)**	EC80 (ppm)**	Determination coefficient (R ²)
RB 221	Control	0.00 a	38.59 a	137.19 a	441.81 a	0.95
	50	24.39 b				
	100	44.33 c				
	200	51.76 d				
	300	70.05 e				
	400	75.89 f				
	500	79.43 f				
	1000	80.93 f				
	2000	90.71 g				
RR 195	Control	0.00 a	66.59 a	175.18 a	617.86 a	0.96
	50	19.82 b				
	100	31.64 c				
	200	51.35 d				
	300	70.71 e				
	400	69.12 e				
	500	75.52 ef				
	1000	80.46 f				
	2000	91.98 g				
RY 145	Control	0.00 a	62.62 a	148.88 a	553.99 a	0.99
	50	19.08 b				
	100	36.66 c				
	200	56.17 d				
	300	72.62 e				
	400	74.92 ef				
	500	81.23 fg				
	1000	84.74 gh				
	2000	90.31 h				
Mixture	Control	0.00 a	42.63 a	145.09 a	551.98 a	0.98
	50	33.16 b				
	100	51.87 c				
	200	71.55 d				
	300	77.88 de				
	400	83.55 e				
	500	91.97 f				
	1000	97.01 f				
	2000	97.87 f				

* Mean values with the different letters in each cell are significantly different (one-way ANOVA followed by Tukey's HSD, $\alpha=0.05$)

** Mean values with the different letters in each column are significantly different (MANOVA followed by Tukey's HSD, $\alpha=0.05$)

Table A8. Effect of reactive azo dyes on growth of *Aspergillus flavus*

Dye	Concentration (ppm)	Growth inhibition ratio (%) *	EC20 (ppm)**	EC50 (ppm)**	EC80 (ppm)**	Determination coefficient (R ²)
RB 221	Control	0.00 a	61.59 ab	226.31 a	631.56 a	0.99
	50	15.97 b				
	100	32.41 c				
	200	47.67 d				
	300	57.61 d				
	400	70.48 e				
	500	74.11 e				
	1000	87.27 f				
	2000	95.96 f				
RR 195	Control	0.00 a	17.65 a	142.49 a	761.02 a	0.94
	50	37.18 b				
	100	39.62 b				
	200	62.49 c				
	300	61.55 cd				
	400	67.35 de				
	500	69.62 e				
	1000	82.01 f				
	2000	88.25 g				
RY 145	Control	0.00 a	78.51 ab	356.33 b	784.28 a	0.98
	50	27.36 b				
	100	35.03 b				
	200	37.71 b				
	300	48.39 c				
	400	56.03 c				
	500	68.40 d				
	1000	90.65 e				
	2000	94.83 e				
Mixture	Control	0.00 a	87.01 b	227.42 a	594.38 a	0.96
	50	21.33 b				
	100	25.59 b				
	200	57.36 c				
	300	61.35 c				
	400	69.49 cd				
	500	75.36 de				
	1000	91.98 e				
	2000	93.99 e				

* Mean values with the different letters in each cell are significantly different (one-way ANOVA followed by Tukey's HSD, $\alpha=0.05$)

** Mean values with the different letters in each column are significantly different (MANOVA followed by Tukey's HSD, $\alpha=0.05$)

Table A9. Effect of reactive azo dyes on growth of *Fusarium fujikuroi*

Dye	Concentration (ppm)	Growth inhibition ratio (%) *	EC20 (ppm)**	EC50 (ppm)**	EC80 (ppm)**	Determination coefficient (R ²)
RB 221	Control	0.00 a	338.81 a	911.61 a	2570.03 b	0.98
	50	0.00 a				
	100	0.76 a				
	200	3.26 a				
	300	3.64 a				
	400	28.16 b				
	500	45.21 c				
	1000	54.79 cd				
	2000	61.68 d				
RR 195	Control	0.00 a	399.36 b	1827.74 b	2964.86 c	0.98
	50	0.00 a				
	100	1.149 a				
	200	11.68 a				
	300	12.64 a				
	400	16.97 ab				
	500	22.03 ab				
	1000	37.16 bc				
	2000	54.02 c				
RY 145	Control	0.00 a	350.95 ab	1076.69 a	1921.65 a	0.96
	50	0.00 a				
	100	0.38 a				
	200	2.79 ab				
	300	3.64 ab				
	400	13.22 b				
	500	27.39 c				
	1000	46.74 d				
	2000	58.62 d				
Mixture	Control	0.00 a	552.64 c	2108.92 c	2951.45 c	0.98
	50	0.19 a				
	100	1.72 a				
	200	6.89 ab				
	300	9.38 b				
	400	11.31 b				
	500	21.07 c				
	1000	40.42 d				
	2000	48.08 e				

* Mean values with the different letters in each cell are significantly different (one-way ANOVA followed by Tukey's HSD, $\alpha = 0.05$)

** Mean values with the different letters in each column are significantly different (MANOVA followed by Tukey's HSD, $\alpha = 0.05$)

Table A10. Effect of reactive azo dyes on growth of *Rhizoctonia solani*

Dye	Concentration (ppm)	Growth inhibition ratio (%) *	EC20 (ppm)**	EC50 (ppm)**	EC80 (ppm)**	Determination coefficient (R ²)
RB 221	Control	0.00 a	445.19 b	2276.49 c	2989.98 d	0.97
	50	0.00 a				
	100	0.00 a				
	200	0.96 a				
	300	2.11 a				
	400	3.45 a				
	500	20.11 b				
	1000	30.84 c				
	2000	40.88 d				
RR 195	Control	0.00 a	330.28 a	739.38 b	2184.52 c	0.97
	50	0.00 a				
	100	0.76 a				
	200	0.76 a				
	300	4.41 a				
	400	30.84 b				
	500	43.49 c				
	1000	64.56 d				
	2000	73.75 e				
RY 145	Control	0.00 a	413.23 b	708.51 b	1714.79 a	0.98
	50	0.00 a				
	100	2.11 a				
	200	2.68 a				
	300	6.32 ab				
	400	13.22 b				
	500	30.34 c				
	1000	60.73 d				
	2000	83.41 e				
Mixture	Control	0.00 a	333.11 a	539.75 a	1880.53 b	0.96
	50	0.14 a				
	100	1.87 a				
	200	1.15 a				
	300	3.01 a				
	400	34.91 b				
	500	47.56 c				
	1000	69.39 d				
	2000	82.61 e				

* Mean values with the different letters in each cell are significantly different (one-way ANOVA followed by Tukey's HSD, $\alpha = 0.05$)

** Mean values with the different letters in each column are significantly different (MANOVA followed by Tukey's HSD, $\alpha = 0.05$)

Table A11. Effect of reactive azo dyes on germination of *Raphanus sativus* seeds

Dye	Concentration (ppm)	Germination inhibition (%) *	EC20 (ppm)**	EC50 (ppm)**	Determination coefficient (R ²)
RB 221	Control	0.00 a	395.78 b	2760.04 c	0.97
	100	3.33 ab			
	200	11.67 abc			
	300	13.33 bc			
	400	21.67 cd			
	500	23.33 cd			
	600	25.00 d			
	700	31.66 d			
	800	31.67 d			
	900	33.33 de			
	1000	33.33 de			
	2000	45.00 e			
RR 195	Control	0.00 a	461.40 b	2144.30 bc	0.96
	100	11.67 b			
	200	16.67 bc			
	300	16.67 bc			
	400	20.00 bcd			
	500	20.00 bcd			
	600	21.67 bcd			
	700	25.00 cde			
	800	25.00 cde			
	900	26.67 cde			
	1000	28.33 de			
	2000	33.33 e			
RY 145	Control	0.00 a	445.13 b	983.25 a	0.89
	100	13.33 b			
	200	15.00 bc			
	300	21.67 bcd			
	400	20.00 bcd			
	500	23.33 bcd			
	600	25.00 bcde			
	700	26.67 cde			
	800	31.67 de			
	900	36.67 e			
	1000	58.33 f			
	2000	60.00 f			
Mixture	Control	0.00 a	203.37 a	956.11 ab	0.84
	100	18.33 b			
	200	26.67 bc			
	300	28.33 bc			
	400	28.33 bc			
	500	33.33 bc			
	600	35.00 c			
	700	31.67 c			
	800	36.67 cd			
	900	38.33 cd			
	1000	50.00 de			
	2000	53.33 e			

* Mean values with the different letters in each cell are significantly different (one-way ANOVA followed by Tukey's HSD, $\alpha = 0.05$)

** Mean values with the different letters in each column are significantly different (MANOVA followed by Tukey's HSD, $\alpha = 0.05$)

Table A12. Effect of reactive azo dyes on germination of *Triticum aestivum* seeds

Dye	Concentration (ppm)	Germination inhibition (%) *	EC20 (ppm)**	EC50 (ppm)**	Determination coefficient (R ²)
RB 221	Control	0.00 a	762.16 b	2590.22 a	0.94
	100	0.00 a			
	200	0.00 a			
	300	0.00 a			
	400	5.00 ab			
	500	10.00 abc			
	600	13.33 bc			
	700	15.00 bc			
	800	20.00 c			
	900	20.00 c			
	1000	33.33 d			
	2000	36.67 d			
RR 195	Control	0.00 a	668.34 b	2556.99 a	0.96
	100	0.00 a			
	200	0.00 a			
	300	6.66 ab			
	400	15.00 bc			
	500	18.33 bc			
	600	15.00 cd			
	700	20.00 cd			
	800	21.67 cd			
	900	26.67 de			
	1000	26.67 de			
	2000	36.67 e			
RY 145	Control	0.00 a	644.22 b	2015.66 a	0.97
	100	0.00 a			
	200	0.00 a			
	300	5.00 a			
	400	11.67 ab			
	500	13.33 abc			
	600	23.33 bcd			
	700	25.00 bcde			
	800	26.67 cde			
	900	30.00 def			
	1000	38.33 ef			
	2000	41.67 f			
Mixture	Control	0.00 a	450.51 a	1984.65 a	0.96
	100	8.33 ab			
	200	13.33 bc			
	300	15.00 bcd			
	400	15.00 bcd			
	500	23.33 cde			
	600	25.00 def			
	700	35.00 ef			
	800	31.67 ef			
	900	36.67 f			
	1000	38.33 f			
	2000	56.67 g			

* Mean values with the different letters in each cell are significantly different (one-way ANOVA followed by Tukey's HSD, $\alpha = 0.05$)

** Mean values with the different letters in each column are significantly different (MANOVA followed by Tukey's HSD, $\alpha = 0.05$)

Table A13. Effect of reactive azo dyes on germination of *Sorghum bicolor* seeds

Dye	Concentration (ppm)	Germination inhibition (%) *	EC20 (ppm)**	EC50 (ppm)**	Determination coefficient (R ²)
RB 221	Control	0.00 a	409.76 a	2786.49 a	0.95
	100	13.33 b			
	200	13.33 b			
	300	16.66 bc			
	400	18.33 bcd			
	500	21.67 bcd			
	600	26.67 cde			
	700	26.66 cde			
	800	28.33 de			
	900	28.33 de			
	1000	36.67 ef			
	2000	41.66 f			
RR 195	Control	0.00 a	282.15 a	2141.11 a	0.94
	100	16.67 b			
	200	20.00 bc			
	300	21.66 bc			
	400	26.67 bcd			
	500	26.67 bcd			
	600	30 bcde			
	700	33.33 cdef			
	800	33.33 cdef			
	900	40 def			
	1000	43.33 ef			
	2000	45.00 f			
RY 145	Control	0.00 a	337.74 a	2689.61 a	0.94
	100	8.33 ab			
	200	18.33 bc			
	300	23.33 cd			
	400	25 cd			
	500	26.67 cde			
	600	26.66 cde			
	700	31.66 cdef			
	800	33.33 def			
	900	36.67 def			
	1000	40 .00ef			
	2000	41.67 f			
Mixture	Control	0.00 a	436.01 a	2799.42 a	0.98
	100	3.33 a			
	200	3.33 a			
	300	6.67 a			
	400	13.33 ab			
	500	21.67 bc			
	600	25 bc			
	700	25 bc			
	800	28.33 c			
	900	28.33 c			
	1000	28.33 c			
	2000	31.67 c			

* Mean values with the different letters in each cell are significantly different (one-way ANOVA followed by Tukey's HSD, $\alpha = 0.05$)

** Mean values with the different letters in each column are significantly different (MANOVA followed by Tukey's HSD, $\alpha = 0.05$)

Table A14. Effect of reactive azo dyes on germination of *Phaseolus mungo* seeds

Dye	Concentration (ppm)	Germination inhibition (%) *	EC20 (ppm)**	EC50 (ppm)**	Determination coefficient (R ²)
RB 221	Control	0.00 a	919.62 a	2864.49 a	0.97
	100	1.67 ab			
	200	3.33 ab			
	300	3.33 ab			
	400	8.33 bc			
	500	8.33 bc			
	600	11.67 cd			
	700	11.66 cd			
	800	16.67 d			
	900	18.33 d			
	1000	18.33 d			
	2000	28.33 e			
RR 195	Control	0.00 a	855.37 a	2929.79 a	0.96
	100	1.67 ab			
	200	6.67 abc			
	300	6.67 abc			
	400	8.33 abc			
	500	10 bcd			
	600	11.67 cd			
	700	15 cde			
	800	18.33 def			
	900	21.67 ef			
	1000	21.67 ef			
	2000	26.67 f			
RY 145	Control	0.00 a	1974.99 b	3566.73 b	0.96
	100	5.00 ab			
	200	5.00 ab			
	300	8.33 abc			
	400	8.33 abc			
	500	10.00 abc			
	600	13.33 bc			
	700	16.67 bc			
	800	16.67 bc			
	900	16.67 bc			
	1000	18.33 c			
	2000	20.00 c			
Mixture	Control	0.0 a	858.62 a	2732.97 a	0.98
	100	0.00 a			
	200	0.00 a			
	300	3.33 ab			
	400	3.33 ab			
	500	5.00 abc			
	600	8.33 bcd			
	700	11.67 cd			
	800	16.67 d			
	900	21.67 e			
	1000	23.33 e			
	2000	26.67 e			

* Mean values with the different letters in each cell are significantly different (one-way ANOVA followed by Tukey's HSD, $\alpha=0.05$); ** Mean values with the different letters in each column are significantly different (MANOVA followed by Tukey's HSD, $\alpha=0.05$)

Table A15. Effect of reactive azo dyes on *Artemia salina* larvae

Dye	Concentration (ppm)	Larval mortality (%) *	EC20 (ppm)**	EC50 (ppm)**	EC80 (ppm)**	Determination coefficient (R ²)
RB 221	Control	0.00 a	322.37 b	639.31 a	967.86 ab	0.95
	50	0.00 a				
	100	0.00 a				
	200	13.33 ab				
	300	16.67 ab				
	400	33.37 bc				
	500	46.66 cd				
	600	53.33 cd				
	700	53.33 cd				
	800	60.00 de				
	900	76.67 ef				
	1000	93.33 fg				
	2000	100 g				
	RR 195	Control				
50		3.33 ab				
100		6.66 ab				
200		13.33 abc				
300		26.67 abc				
400		20.00 abc				
500		23.33 bcd				
600		26.67 bcd				
700		33.33 cd				
800		36.67 cd				
900		50.00 de				
1000		70.00 e				
2000		100 f				
RY 145		Control	0.00 a	691.01 c	836.83 b	998.97 ab
	50	0.00 a				
	100	0.00 a				
	200	0.00 a				
	300	0.00 a				
	400	6.66 ab				
	500	16.67 bc				
	600	23.33 c				
	700	23.33 c				
	800	40.00 d				
	900	63.33 e				
	1000	96.66 f				
	2000	100 f				
	Mixture	Control	0.00 a			
50		20.00 ab				
100		36.67 bc				
200		33.33 bc				
300		46.67 cd				
400		50.00 cd				
500		50.00 cd				
600		56.67 cd				
700		63.33 d				
800		66.67 d				
900		96.67 e				
1000		96.67e				
2000		100 e				

Table A16. Effect of reactive azo dyes on *Daphnia magna*

Dye	Concentration (ppm)	Larval mortality (%) *	EC20 (ppm)**	EC50 (ppm)**	EC80 (ppm)**	Determination coefficient (R ²)
RB 221	Control	0.00 a	172.73 c	241.78 c	338.46 b	0.98
	25	0.00 a				
	50	15.00 ab				
	100	25.00 b				
	200	45.00 c				
	300	75.00 d				
	400	95.00 e				
	500	100 e				
	1000	100 e				
	2000	100 e				
RR 195	Control	0.00 a	40.19 ab	137.44 a	166.77 a	0.98
	25	0.00 a				
	50	35.00 b				
	100	45.00 b				
	200	95.00 c				
	300	100 c				
	400	100 c				
	500	100 c				
	1000	100 c				
	2000	100 c				
RY 145	Control	0.00 a	88.41 b	172.63 b	297.13 b	0.95
	25	0.00 a				
	50	10.00 a				
	100	35.00 b				
	200	75.00 c				
	300	75.00 c				
	400	100 d				
	500	100 d				
	1000	100 d				
	2000	100d				
Mixture	Control	0.00 a	34.87 a	108.77 a	180.45 a	0.98
	25	5.00 a				
	50	40.00 b				
	100	47.50 b				
	200	90.00 cd				
	300	100 d				
	400	100 d				
	500	100 d				
	1000	100 d				
	2000	100 d				

* Mean values with the different letters in each cell are significantly different (one-way ANOVA followed by Tukey's HSD, $\alpha=0.05$)

** Mean values with the different letters in each column are significantly different (MANOVA followed by Tukey's HSD, $\alpha=0.05$)



Fig. A1. Immobilized *T. asperellum* on Scotch Brite™ membrane

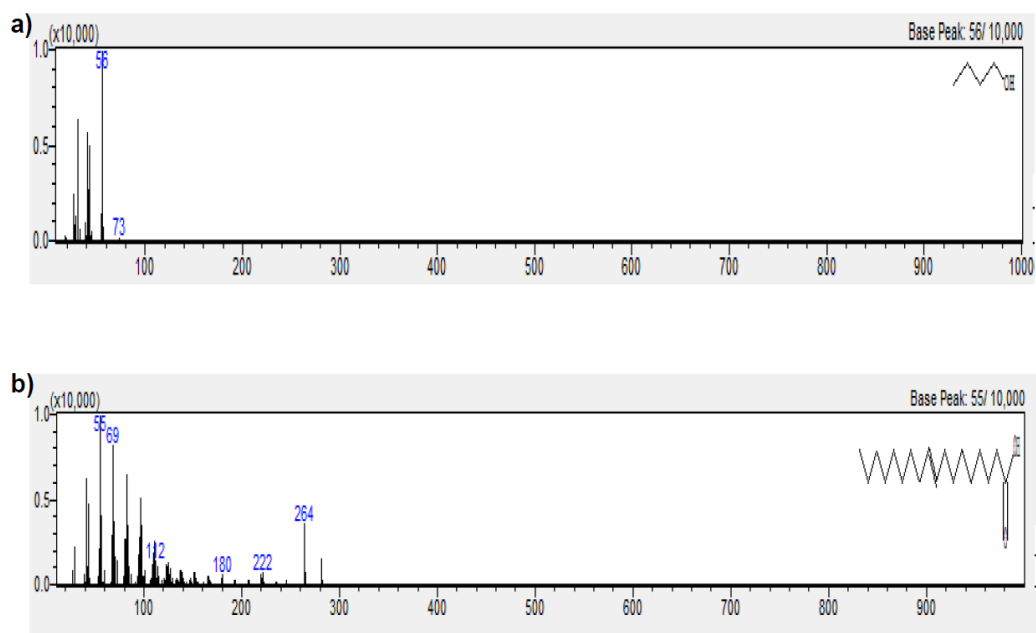


Fig. A1. Spectra of degradative metabolites of the dye mixture produced by MBC
a). 1-Butanol; b). 9-Octadecenoic acid (Z)-, methyl ester

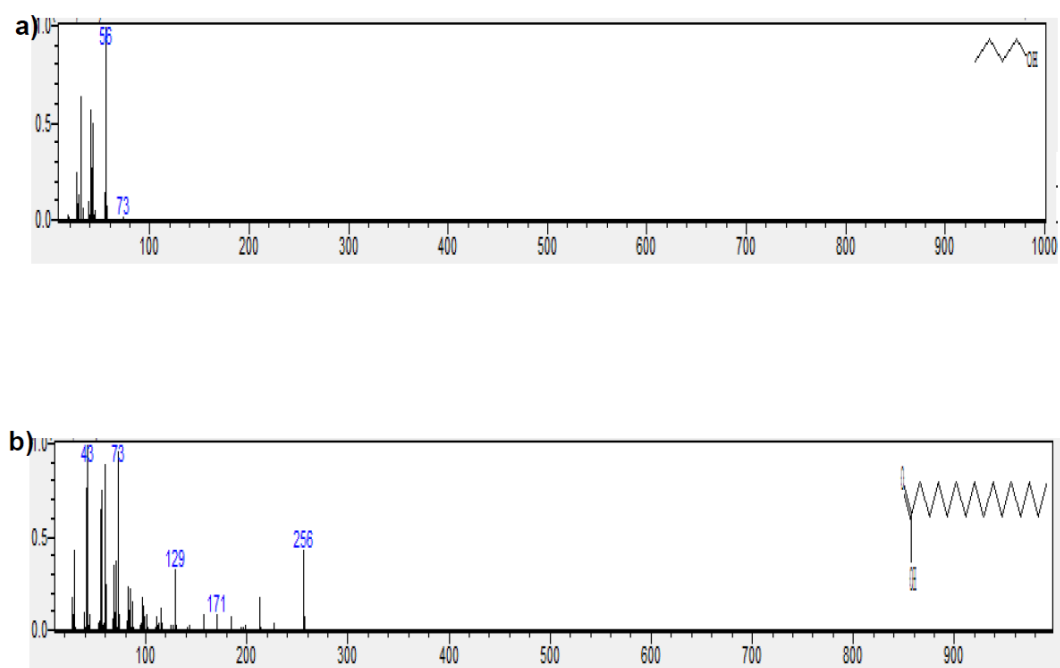


Fig. A2. Spectra of degradative metabolites of the dye mixture produced by AHBC
a). 1-Butanol; b). n-Hexadecanoic acid

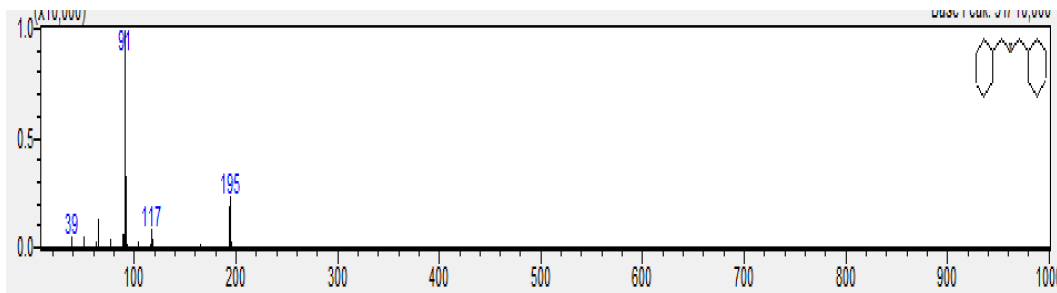


Fig. A3. Spectra of degradative metabolites of the dye mixture produced by MBC: N-Benzyl-2-phenethylamine

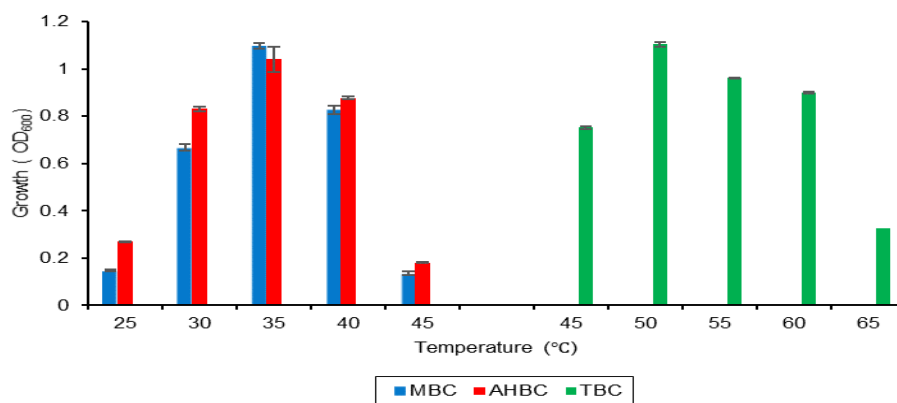


Fig. A4. Growth of natural bacterial consortia at different temperatures in dye free medium

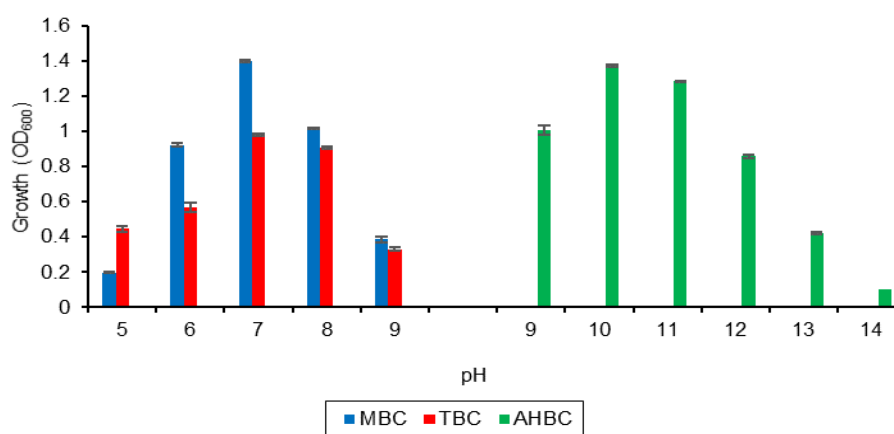


Fig. A5. Growth of natural bacterial consortia at different pH in dye free medium

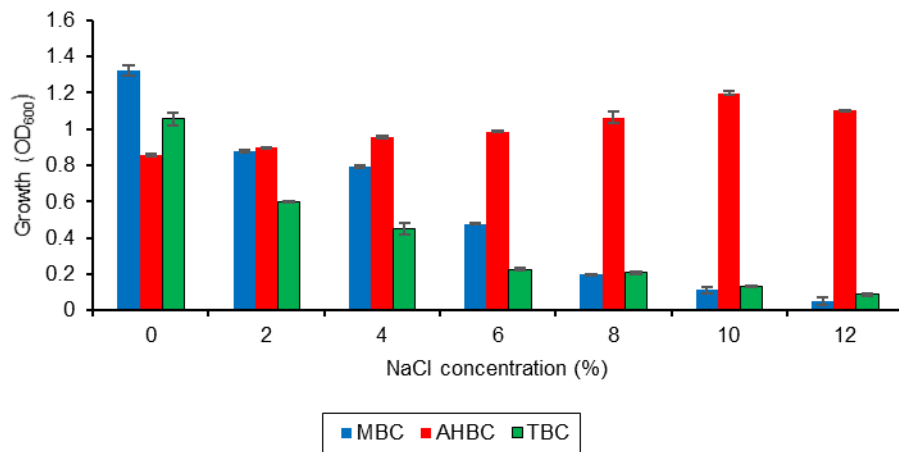


Fig. A6. Growth of natural bacterial consortia at different salt concentrations in dye free medium

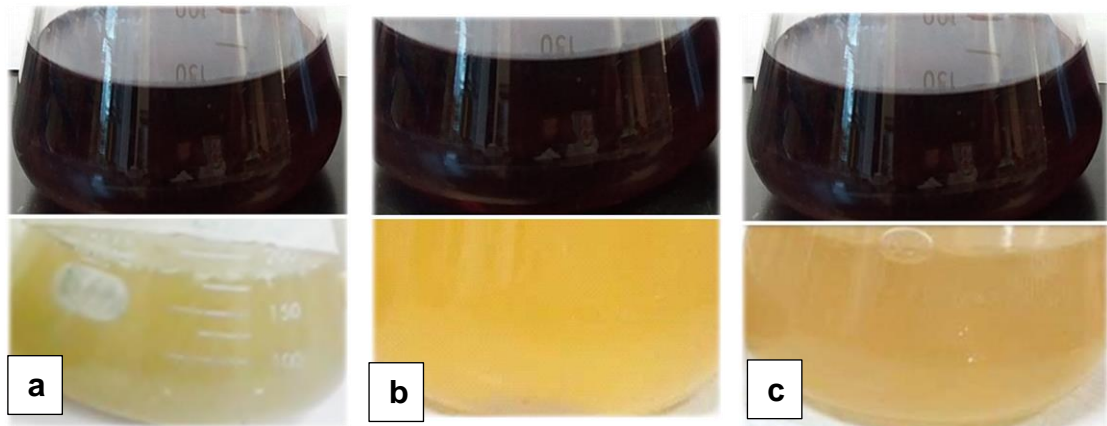


Fig. A7. Decolorization by natural consortia a) MBC; b) AHBC; and c) TBC

A4.1 Morphological and Biochemical identification

A4.1.1 Gram Staining

Gram staining was performed by sequential application of crystal violet (primary stain) for 30 sec and G. Iodine for min to heat fixed smears of isolated strains on glass slides. This was followed by decolorization with 95% ethanol for 10-15 sec and counterstaining with safranin for 45-60 sec (After each step the excessive stains and the decolorizer, were rinsed with water for 5 sec). The slides were blot dried and observed under oil immersion to study the morphology and staining reaction.

A4.1.2 Carbohydrate fermentation

Carbohydrate fermentation test is used to determine the fermentative and degradative ability of microbes for different type of carbohydrates. In order to detect the gas production, Durham tubes (inverted inner vials) were inserted into each of the fermentation broth tubes. After this the test was performed by loop inoculation of 24-48 hrs old cultures of the 6 selected isolates into 3 different types of sterilized broths i.e. phenol red containing lactose broth, dextrose broth and sucrose broth. These tubes were then incubated at 37°C for 24 hrs. After incubation the tubes were checked for appearance of yellow color due to acid production and formation of gas bubble in the Durham tube.

A4.1.3 IMVIC Test

The series of IMVIC tests i.e. Indole production, Methyl red, Voges-Proskauer and citrate utilization test were performed by following procedures:

A4.1.3.1 Indole production Test

Indole production test was performed by stab inoculation of 24-48 hrs old cultures of 6 selected bacterial strains into sterilized SIM agar deep tubes. The tubes were incubated at 37°C for 24 hrs. After incubation the tubes were observed to check for motility and H₂S production i.e. blackening of test tubes. Indole production indicated by formation of red colored layer was tested by addition of 5- drop o Kovac' reagent.

A4.1.3.2 Methyl Red Test

Methyl red test that is employed for determination of ability of microbes to oxidize glucose with acid production was performed by loop inoculation of 24-48 hrs old cultures of selected strains into sterilized MR-VP broth containing test tubes followed by incubation at 37°C for 24 hrs. Acid production was tested by addition of methyl red indicator and subsequent formation of red color.

A4.1.3.3 Voges-Proskauer Test

Voges-Proskauer test, that is used to establish the ability of microbes to produce neutral end products from glucose metabolism, was performed by loop inoculation of 24-48 hrs old cultures of selected bacterial strains into sterilized MR-VP broth containing test tubes. The test tubes were incubated at 37°C for 24 hrs. Production of acetylmethylcarbinol i.e. the neutral end product was tested by addition to Barritt' reagent and production of deep rose color after 15 min of addition of that reagent.

3.7.3.4 Citrate utilization Test

Citrate utilization test that is used to determine the citrate fermenting ability of microbes was performed by stab and streak inoculation of 24-48 hrs old cultures of selected bacterial strains into Simmons citrate agar slants followed by incubation at 37°C for 24 hrs. Formation of deep Prussian blue color following incubation indicated a positive citrate utilization test.

A4.1.4 Triple sugar Iron (TSI) Test

Triple sugar iron (TSI) test is used to study the carbohydrate fermentation patterns, H₂S and gas production by some microorganisms. This test was performed by stab and streak inoculation of 24-48 hrs old cultures of selected bacterial strains into TSI agar slants. The test tubes were incubated at 37°C for 24 hrs. Following incubation the test tubes were examined to check for gas production and presence or absence of blackening i.e. H₂S production. The colors of slant and butt were also observed to establish the reaction type i.e. acidic (colored yellow), alkaline (turned red) or none.

A4.1.5 Catalase test

Catalase test is used to test the ability of microbes to produce catalase enzyme that degrades hydrogen peroxide. For this test a small amount of growth was picked with a sterile inoculating loop from 24 hrs

old cultures of selected strains and mixed in a drop of 3% hydrogen peroxide on a glass slide. Immediate formation of bubbles indicated a positive catalase test.

A4.1.6 Oxidase test

Oxidase test is employed to establish the cytochrome oxidase production ability of bacteria. For this test, a small amount of growth was picked with the help of a sterile inoculating loop from 24 hrs old cultures of selected strains and transferred to a filter paper moistened with oxidase reagent. Formation of dark purple color within 20-30 sec indicated a positive test.

A4.1.7 Endospore staining

Prepare smears of organisms to be tested for presence of endospores on a clean microscope slide and air dry it. Heat fix the smear. Place a small piece of blotting paper over the smear and place the slide (smear side up) on a wire gauze on a ring stand. Heat the slide gently till it starts to evaporate (either by putting the slide on a staining rack that has been placed over a boiling water bath or via bunsen burner). Remove the heat and reheat the slide as needed to keep the slide steaming for about 3-5 minutes. As the paper begins to dry add a drop or two of malachite green to keep it moist, but don't add so much at one time that the temperature is appreciably reduced. The process is steaming and not baking. After 5 minutes carefully remove the slide from the rack using a clothespin. Remove the blotting paper and allow the slide to cool to room temperature for 2 minutes. Rinse the slide thoroughly with tap water (to wash the malachite green from both sides of the microscope slide). Stain the smear with safranin for 2 minutes. Rinse both side of the slide to remove the secondary stain and blot the slide/ air dry. The vegetative cells appear pink/red and the spores appear green.

A4.2 DNA extraction protocols

A.4.2.1 Phenol-chloroform extraction method

1. Loopful of cultures were inoculated in nutrient broth medium and incubated at 37°C for a period of 24-48 hrs.
2. 1.5 mL of each culture was then taken in eppendorf tubes and centrifuged at 13,000 rpm for 15 min. Pelleted cells were collected and supernatant was discarded.
3. The pellet was then resuspended in 450 µL Tris HCl-EDTA (T.E) buffer pH: 8.0, to that 45 µL of 10% Sodium dodecyl sulfate (SDS) and 5 µL of proteinase K (20 mg/mL) was added followed by incubation at 37°C for 1 hr.
4. Following incubation 500 µL of phenol-chloroform (1:1) solution was added to the cell suspension and mixed thoroughly. The tubes were then centrifuged at 10,000 rpm for 20 min.
5. After centrifugation three layers were formed, the upper aqueous layer was transferred to new eppendorf and 500 µL of phenol-chloroform solution was added again followed by centrifugation at 10,000 rpm for 5 min.
6. Aqueous layer was transferred to new tube. To that, 50 µL of 5M sodium acetate and 300 µL of isopropanol was added and thoroughly mixed until formation of precipitates.
7. Tubes were then then centrifuged at 10,000 rpm for 5 min, liquid phase was discarded and the pellet was washed with 1 mL of chilled ethanol (70%).
8. Centrifugation was done for 5 min at 10,000 rpm, ethanol was removed and 100 µL of T.E buffer was added followed by mixing and storage at -20°C.

A.4.2.1 CTAB Method

1. Loopful of culture was picked from 24-48 hrs old plates and resuspended in T.E buffer followed by centrifugation at 13,000 for 20 min.
2. Supernatant was discarded, and pellet was used for further process. To the cell pellet 900 µL of lysis buffer [2 % CTAB, 100 mM Tris-HCl (pH: 8.0), 20 mM EDTA (pH: 8.0), 1.5 NaCl, 5 µL of proteinase K (20 mg/mL) and 50 µL of 10% SDS].
3. The tubes were then incubated at 65°C for 1 hr. The contents of the tube were gently mixed from time to time during the incubation by inverting the microcentrifuge tube.

4. After incubation, 0.8 mL of phenol-chloroform-isoamyl alcohol (25:24:1) solution was added and mixed thoroughly followed by centrifugation at 12,000 rpm for 10 min.
5. The aqueous layer was then transferred to new tube and re-extracted with phenol-chloroform-isoamyl alcohol solution. Centrifugation was then performed at 12,000 rpm for 15 min.
6. The upper aqueous phase was shifted to new tube and extracted finally with chloroform-isoamyl alcohol (24:1). The tubes were centrifuged at 10,000 rpm for 15 min.
7. Aqueous phase was transferred to new tube, to that 450 μ L of isopropanol and 300 μ L of potassium acetate (0.5 M) was added.
8. The tubes were then incubated overnight at -20°C. Following incubation centrifugation was done at 12,000 rpm for 10 min, liquid phase was removed, and DNA was washed ethanol (70%, chilled).
9. Centrifugation was done at 10,000 rpm for 5 min, ethanol was removed and 100 μ L of T.E buffer was added and stored at -20°C till further processing.

4.3 Partial 16S rRNA gene sequences for the mesophilic isolates

NHS1:TGGATTACGCGGGACGGGTGAGTAATGCCTAGGAATCTGCCTGGTAGTGGGGGATAACGTCCGGAAACG GGCCTAATACCGCACACGTCTGAGGGAGAAAAGTGGGGGATCTTCGGACCTCAGGCTATCAGATGAGCCTATGT CGGATTACCTAGTTGGTGGGGTAAAGGCCTACCGGGGCCACGATCCCTAACTGGTCTGAGAGGATGATCAGTCAC AGTGGAACTGACACACTGTCCCTACTCCTACGGGAGGCATCCTTGGGGAATATTGGACAATGGGCCAAAAGCCTGA GCCAGCCATGCCGCGTGTGTGAAGAAGGTCTTCTGATTGTAGAGCACTTTAAGTTGGGATGAATGGCAGTGAGTTA ATACCTTGCTGTTTTGACGTTACCAACATAATAAGCACCGGCTAACTTCGTGCCAGCAGCCTCGGTGATACCAACG GTGCAAGCGTTAATCTGAATTACTGGGCGTAAAGCGCGGTACGTGGTTTACCAAGTTGGATGTGAAATCCCCGG ACTCAACCTGGGAACTGCATCCAAAACCTACTGAGCTAGAGTACGGTAGACGGTGGTGGAAATTTACTGTGTAGCAG TTAATATGCGTAGATATAAGAAGGAACACCATTGGCAAAAAGCGACCACCTGGACTGATACTGACTGATGTGCGA AAGCCTGAGGAGCAAACACGATTAGATACCCTGGTAGTCCACGCCGTGGACGATGTGCGACTAGCCGTTGGGATCC TTGAGATCTTAGTGGCGCAGCTCACGCGATAAGTCGACCGCCTGGGGAGTACCGCCGCGAGGTTAAACTCAAATG AATTGACGGGGCCCCGCACAAGCGGTG

NHS2:TCCTGGATTACGCGGGACGGGTGAGTAATGCCTAGGAATCTGCCTGGTAGTGGGGGATAACGTCCGGAA ACGGGCGCTAATACCGCATACTCCTGAGGGAGAAAAGTGGGGGATCTTCGGACCTCAGCCTATCAGATGAGCCTA GGTCCGATTAGCTAGTTGGTGGGGTAAAGGCCTACCAAGGCGACGATCCGTAACCTGGTCTGAGAGGATGATCAGT CACACTGGAACTGAGACACGGTCCAGACTCCTACGGGAGGCAGCAGTGGGGAATATTGGACAATGGGCCAAAAGC CTGATCCAGCCATGCCGCGTGTGTGAAGAAGGTCTTCCGATTGTAAAGCACTTTAAGTTGGGAGGAAGGGCAGTA AGTTAATACCTTGCTGTTTTGACGTTACCAACAGAATAAGCACCGGCTAACTTCGTGCCAGCAGCCGCGGTAATAC GAAGGGTGCAAGCGTTAATCGGAATTACTGGGCGTAAAGCGCGGTAGGTGGTTTACGAAGTTGGATGTGAAATC CCCGGGCTAACCTGGGAACTGCATCCAAAACCTACTGAGCTAGAGTACGGTAGACGGTGGTGGAAATTTCCCTGTGT AGCGGTGAAATGCGTAGATATAGGAAGGAACACCAGTGGCGAAGGCGACCACCTGGACTGATACTGACTGACTGAG GTGCGAAAGCGTGGGGAGCAAACAGGATTAGATACCCTGGTAGTCCACGCCGTAACAGATGTGCGACTAGCCGTTG GGATCCTTGAGATCTTAGTGGCGCAGCTAACCGGATAAGTTCGACCGCCTGGGGAGTACGGCCGCAAGGTTAAAAA TCAAATGAATTGACGGGGCCCCGCACAAGCGGTGGAGCATGTGGTTTTAATTCGAAGCAACGCGAAGAACCCTACC TGGCCTTGAGACTGTGAGAACTTTCCAGAGATGGATTGGTGCCTTCGGGAACTCAGACACAGGTGTGTCATGGCTG TCGTACGCTCGTGTGAGATGTTGGGTTAAGTCCCCTAACGAGCGCAACCCCTTGTCTTAGTTACCAGCACCTT CGG

NHS3:GCTTCTTTGCTGACGAGTGGCGGACGGGTGAGTAATGTCTGGGAAACTGCCTGATGGAGGGGATAACTAC TGGAACCGGTAGCTAATACCGCATAACGTCGCAAGACCAAAAGAGGGGACCTTCGGGCCTCTTGCCATCGGATGT GCCAGATGGGATTAGCTTGTGGTGGGGTAAAGGCCTACCTAGGCGACGATCCCTAGCTGGTCTGAGAGGATGA CCAGCCACACTGGAAGTGGAGACACGGTCCAGACTCCTACGGGAGGCAGCAGTGGGGAATATTGCACAATGGGCGC AAGCCTGATGCAGCCATGCCGCGTGTATGAAGAAGGCCTTCGGGTTGTAAAGTACTTTCAGCGGGGAGGAAGGGA GTAAAGTTAATACCTTTGCTCATTGACGTTACCCGCGAAGAAGCACCGGCTAACTCCGTGCCAGCAGCCGCGGTA ATACGGAGGGTGCAAGCGTTAATCGGAATTACTGGGCGTAAAGCGCACGACGCGGTTTGTAAAGTCAGATGTGA AATCCCCGGGCTCAACCTGGGAACTGCATCTGATACTGGCAAGCTTGTAGTCTCGTAGAGGGGGGTAGAATCCAG GTGTAGCGGTGAAATGCGTAGAGATCTGGAGGAATACCGTGGCGAAGGCGGCCCTGGACGAAGACTGACGC TCAGTGCAGAAAGCGTGGGGAGCAAACAGGATTAGATACCCTGGTAGTCCACGCCGTAACAGATGTGCGACTTGGA GGTGTGCCCCTGAGGCGTGCTTCCGGAGCTAACCGGTTAAGTCGACCGCCTGGGGAGTACGGCCGCAAGGTTA AAACCTCAAATGAATTGACGGGGCCCCGCACAAGCGGTGGAGCATGTGGTTTTAATTCGATGCAACGCGAAGAACC TACCTGGTCTTGACATCCACGGAAGTTTTAGAGATGAGAATGTGCCTTCGGGAAACCGTGAGACAGGTGTGTCATG GCTGTGTCAGCTCGTGTGTGAAATGTTGGGGTTAAGTCCCCTAACGAGCGCAACCCCTTATCTTTGTTGCCAGC GGTCCGGCCGGGAACCTCAA

NHS4:TGGCATAGGCTACGCTACCATGCAGTCAACGTTAACACGAAGAAGCTTGCTTCTTTGCTGACGAGTGGCG GACGGGTGAGTAATGTCTGGGAAACTGCCTGATGGAGGGGATAACTACTGGAACCGTAGCTAATACCGCATAA CGTCGCAAGACCAAGAGGGGGACCTTCGGGCCTCTTGCCATCGGATGTGCCATATGGGATTAGCTTGTGGGTG GGGTAACGGCTACCTAGGCGACGATCCCTAGCTGGTCTGAGAGGATGACCAGCCACACTGGAAGTGGAGACCGG TCCAGACTCCTACGGGAGGCAGCAGTGGGGAATATTGCACAATGGGCGCAAGCCTGATGCACCATGCCGCGTGT ATGAAGAAGGCCTTCGGGTTGTAAAGTACTTTCAGCGGGGAGGAAGGGAGTAAAGTTAATACCTTTGCTCATTGA

CGTTACCCGCAAAAAGAAGCACCGGCTAACTCCGTGCCAGCAGCCGCGGTAATACGGAGGGTGCAAGCGTTAATCG
GAATTACTGGGCGTAAAGCGCACGCAGGCGGTTTGTAAAGTCAGATGTGAAATCCCCGGGCTCAACCTGGGAACT
GCATCTGATACTGGCGAGCTAGAGTCTTGTAGAGGGGGGTAGAATTCCGTGTGTAGCGGTGAAATGCGTAGAGAT
CTGGAGGAATACCGGTGGCGAACGCGGCC

4.4 Partial 16S rRNA gene sequences for the thermophilic isolates

NHT1:GCTCCTTTAGGTTAGCGGCGGACGGGTGAGTAACACGTGGGCAACCTGCCCTGCAGACTGGGATAACTTCG
GGAAACCGGAGCTAATACCGGATAACACCGAAAACCGCATGGTTTTTCGGTTGAAAGGCGGCTTTTAGCTGCTACT
GCAGGATGGGCCCGCGGCGCATTAGCTAGTTGGTGAGGTAACGGCTCACCAAGGCGACGATGCGTAGCCGACCTG
AGAGGGTGACCGCCACACTGGGACTGAGACACGGCCAGACTCCTACGGGAGGCAGCAGTAGGGAATCTTCCG
CAATGGACGAAAGTCTGACGGAGCAACGCCGCGTGAGCGAAGAAGGTCTTCGGATCGTAAAGCTCTGTTGTCAGG
GAAGAACAAGTACCGTTCGAACAGGGCGGTACCTTGACGGTACCTGACGAGGAAGCCACGGCTAACTACGTGCCA
GCAGCCGCGGTAATACGTAGGTGGCAAGCGTTGTCGGAAATTATTGGGCGTAAAGCGCGCGCAGGCGGTTCCCTTA
AGTCTGATGTGAAATCTCGCGGCTCAACCGCGAGCGGCCATTGGAAACTGGGGAACCTTGAGTGCAGGAGAGGGGA
GCGGAATCCACGTGTAGCGGTGAAATGCGTAGAGATGTGGAGGAACACCAGTGGCGAAGGCGGCTCTCTGGCCT
GTAACTGACGCTGAGGCGCGAAAGCGTGGGAGCGAACAGGATTAGATACCCTGGTAGTCCACGCCGTAAACGAT
GAGTGCTAAGTGTAGAGGGTATCCACCCTTATGCTGTCAGCAAACGCATTAAGCACTCCGCCTGGGGAGTACG
GCCGCAAGGCTGAAACTCAAAGGAATTGACGGGGACCCGCAACAAGCGGTGGAGCATGTGGTTTAATTCGAAGCA
ACGCGA

NHT2:AACACGTGGGCAACCTGCCCTGCAGACTGGGATAACTTCGGGAAACCGGAGCTAATACCGGATAACACCG
AAAACCGCATGGTTTTTCGGTTGAAAGGCGGCTTTTAGCTGCTACTGCAGGATGGGCCCGCGGCGCATTAGCTAGTT
GGTGAGGTAACGGCTCACCAAGGCGACGATGCGTAGCCGACCTGAGAGGGTGACCGGCCACACTGGGACTGAGA
CACGGCCCAGACTCCTACGGGAGGCAGCAGTAGGGAATCTTCCGCAATGGACGAAAGTCTGACGGAGCAACGCC
GCGTGAGCGAAGAAGGTCTTCGGATCGTAAAGCTCTGTTGTCAGGGAAGAACAAGTACCGTTCGAACAGGGCGGT
ACCTTGACGGTACCTGACGAGGAAGCCACGGCTAACTACGTGCCAGCAGCCGCGGTAATACGTAGGTGGCAAGCG
TTGTCGGAAATTATTGGGCGTAAAGCGCGCGCAGGCGGTTCCCTAAGTCTGATGTGAAATCTCGCGGCTCAACCGC
GAGCGGCCATTGGAAACTGGGGAACCTTGAGTGCAGGAGAGGGGAGCGGAATTCCACGTGTAGCGGTGAAATGCG
TAGAGATGTGGAGGAACACCAGTGGCGAAGGCGGCTCTCTGGCCTGTAAGTGCAGCTGAGGCGCGAAAGCGTGG
GGAGCGAACAGGATTAGATACCCTGGTAGTCCACGCCGTAACAGCATGAGTGTAAAGTGTAGAGGGTATCCACC
TTTAGTGTGCTGAGCAAACGCATTAAGCACTCCGCTGGGGAGTACGGCCGCAAGGCTGAAACTCAAAGGAATTGA
CGGGGACCCGCAACAGCGGTGGAGCATGTGGTTTAATTCGAAGCAACGCGAA

NHT3:CCTTTAGGTTAGCGGCGGACGGGTGAGTAACACGTGGGCAACCTGCCCTGCAGACTGGGATAACTTCGGGA
AACCGGAGCTAATACCGGATAACACCGAAAACCGCATGGTTTTTCGGTTGAAAGGCGGCTTTTAGCTGTACTGCA
GGATGGGCCCGCGGCGCATTAGCTAGTTGGTGAGGTAACGGCTCACCAAGGCGACGATGCGTAGCCGACCTGAGA
GGGTGACCGGCCACACTGGGACTGAGACACGGCCCAGACTCCTACGGGAGGCAGCAGTAGGGAATCTTCCGCAAT
GGACGAAAGTCTGACGGAGCAACGCCGCGTGAGCGAAGAAGGTCTTCGGATCGTAAAGCTCTGTTGTCAGGGAAG
AACAAGTACCGTTCGAACAGGGCGGTACCTTGACGGTACCTGACGAGGAAGCCACGGCTAACTACGTGCCAGCAG
CCGCGGTAATACGTAGGTGGCAAGCGTTGTCCGGAATTATTGGGCGTAAAGCGCGCGCAGGCGGTTCCCTAAGTC
TGATGTGAAATCTCGCGGCTCAACCGCGAGCGGCCATTGGAAACTGGGGAACCTTGAGTGCAGGAGAGGGGAGCG
GAATTAGGCGGCTCTCTGGCCTGTAAGTGCAGCTGAGGCGCGAAAGCGTGGGAGCGAACAGGATTAGATACCCT
GGTAGTCCACCGCTAAACGATGAGTGTAAAGTGTAGAGGGTATCCACCCTTATGCTGTCAGCAAACGCATTA
AGCACTCCGCTGGGGAGTACGGCCGCAAGGCTGAAACTCAAAGGAATTGACGGGGACCCGCAACAAGCGGTGGA
GCATGTGGTTTAATTCGAAGCAACGCGAAGAACCCTACCAGGCTTGTACATCCCCTGACAACCCTAGAGATAGGG
CGTCCCCCTTCGGGGACAGGGTGACAGGTGGTGCATGGTTGTCTCAGCTCGTGTGAGATGTTGGGGTTAAG
TCCCCAACAAAGCGCAACCCTTGACCTTAG

NHT4:TAGCGGCGGACGGGTGAGTAACACGTAGGCAACCTGCCCGTAAGCTCGGGATAACATGGGGAAACTCATG
CTAATACCGGATAGGGTCTTCTCTCGCATGAGAGGAGACGGAAAGGTGGCGCAAGCTACCCTTACGGATGGGCC
TGCGGCGCATTAGCTAGTTGGTGGGGTAACGGCCTACCAAGGCGACGATGCGTAGCCGACCTGAGAGGGTGACCC
GCCACACTGGGACTGAGACACGGCCCAGACTCCTACGGGAGGCAGCAGTAGGGAATTTCCACAATGGACGAAA
GTCGTGAGGAGCAACGCCGCGTGAACGATGAAGGCTTTCGGATTGTAAAGTCTGTTGTCAGAGACGAACAAGTA
CCGTTTCGAACAGGGCGGTACCTTGACGGTACCTGACGAGAAAGCCACGGCTAACTACGTGCCAGCAGCCGCGTA
ATACGTAGGTGGCAAGCGTTGTCCGGAATTATTGGGCGTAAAGCGCGCAGGCGGCTATGTAAGTCTGGTGTTA
AAGCCCCGGGCTCAACCCCGGTTTCGATCGGAAACTGTGTAGCTTGTAGTGCAGAAGAGGAAAGCGGTATTCCACG
TGTAGCGGTGAAATGCGTAGAGATGTGGAGGAACACCAGTGGCGAAGGCGGCTTTCTGGTCTGTAAGTACGCTG
AGGCGCGAAAGCGTGGGAGCAAACAGGATTAGATACCCTGGTAGTCCACGCCGTAACAGATGAGTGTAGGTGT
TGGGGGTTTCAATACCCTCAGTGCCGCGACTAACGCAATAAGCACTCCGCCTGGGGAGTACGCTCGCAAGAGTGA
AACTCAAAGGAATTGACGGGGGCCCGCAACAAGCGGTGGAGCATGTGGTTTAATTCGAAGCAACGCGAAGAACCCT
ACCAGGCTTGTACATCCCCTGACCGTCTAGAGATAGGGCTTCCCTTCGGGGCAGCGGTGACAGGTGGTGCATG
GTTGTCGTACGCTCCTGTCTGAGATGTTGGGGTTAAGTCCCGCAACGAGCGCAACCCTTATCTTTAGTTGCCAGC
ATTGAGTTGGGCACTCAAAGAGACTGCCCTCCACAAAACGAAGAAAGGCGGGGG

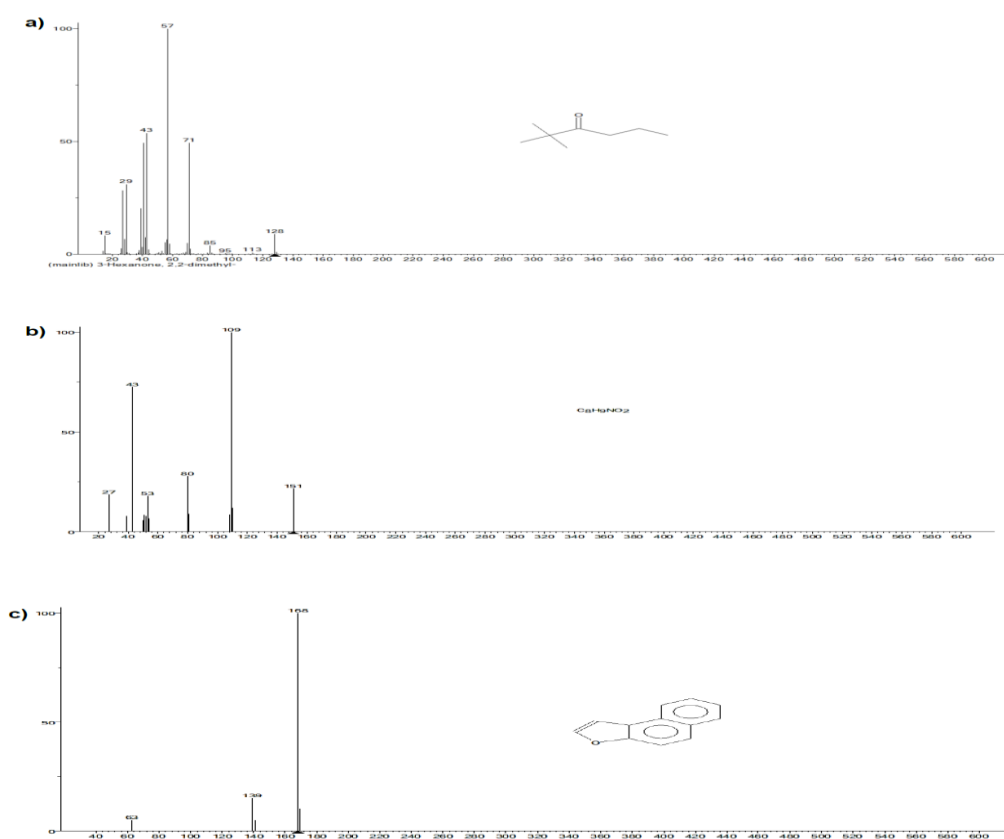


Fig. A1. Spectra of degradative metabolites of the RB 221 produced by Mesophilic coculture a). 2,2-Dimethyl-3-hexanone; b) 2-Methyl-5-acetoxypyridine; c) Naphtho [2,1-b] furan

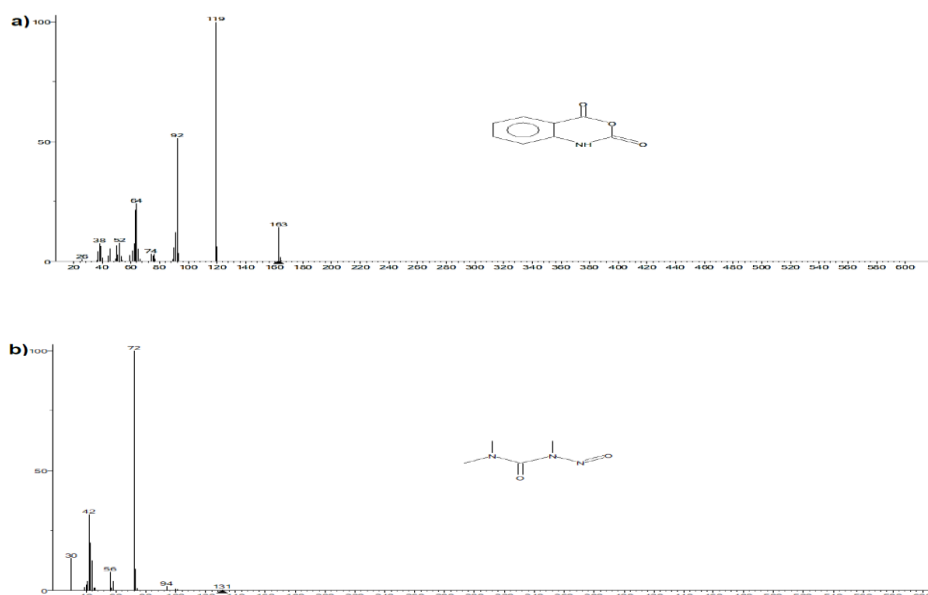


Fig. A2. Spectra of degradative metabolites of the RR 195 produced by Mesophilic coculture a). N-Nitrosotrimethylurea b) 2H-3,1-Benzoxazine-2,4(1H)-dione

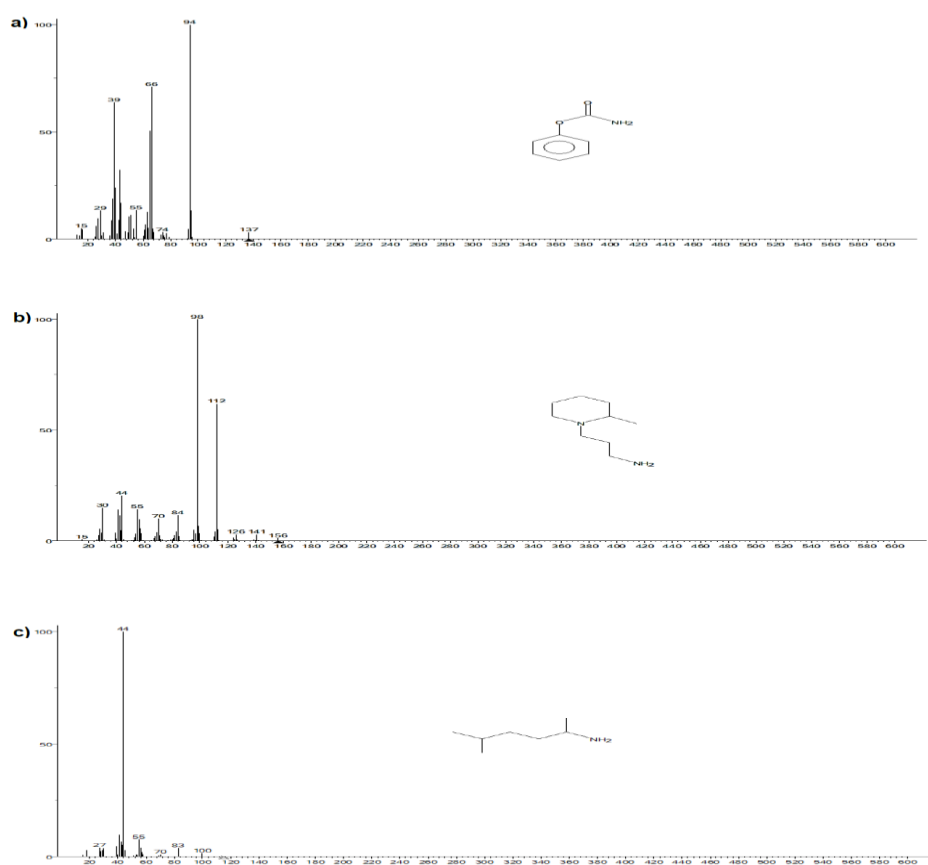


Fig. A3. Spectra of degradative metabolites of the RY 145 produced by Mesophilic coculture a). 1,4-Dimethylpentylamine; b) Carbamic acid, phenyl ester; c) N-(3-Aminopropyl)-2-pipecoline

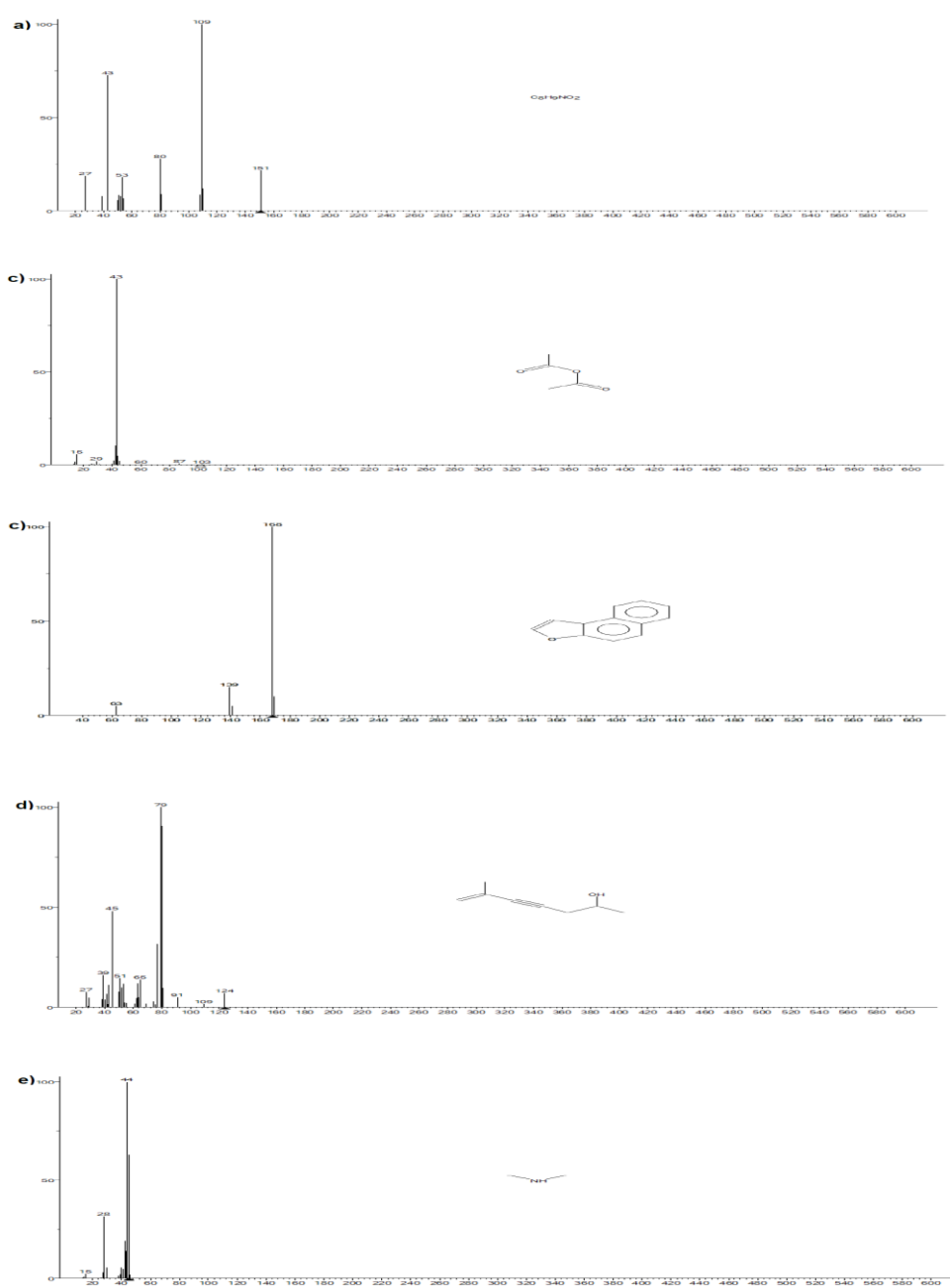


Fig. A4. Spectra of degradative metabolites of the dye mixture produced by Mesophilic coculture a) Dimethylamine; b) Acetic; c) 6-Methyl-6-hepten-4-yn-2-ol; d) 2-Methyl-5-acetoxypyridine; e) Naphtho [2,1-b] furan

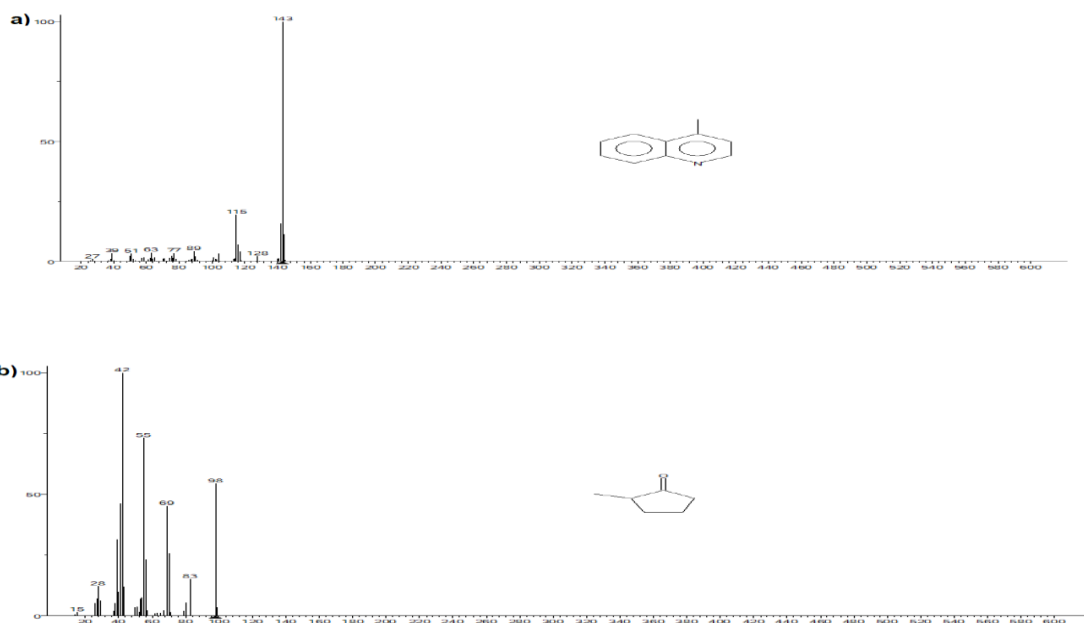


Fig. A5. Spectra of degradative metabolites of RB 221 produced by thermophilic coculture a) 2-Methylcyclopentanone b) p-Methylquinoline

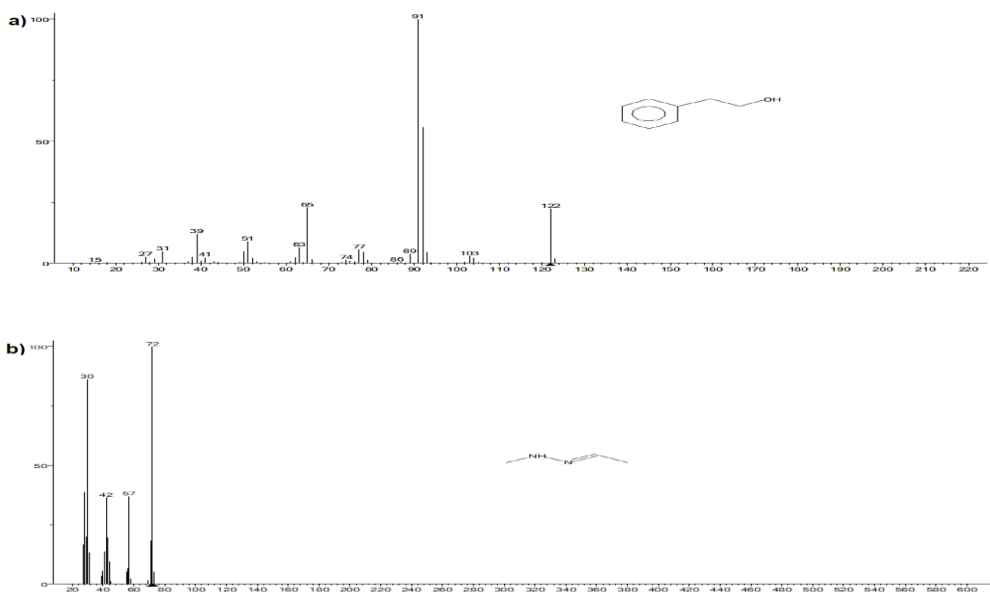


Fig. A6 Spectra of degradative metabolites of RR 195 produced by thermophilic coculture a) Acetaldehyde, N-methylhydrazone; b) Phenylethyl Alcohol

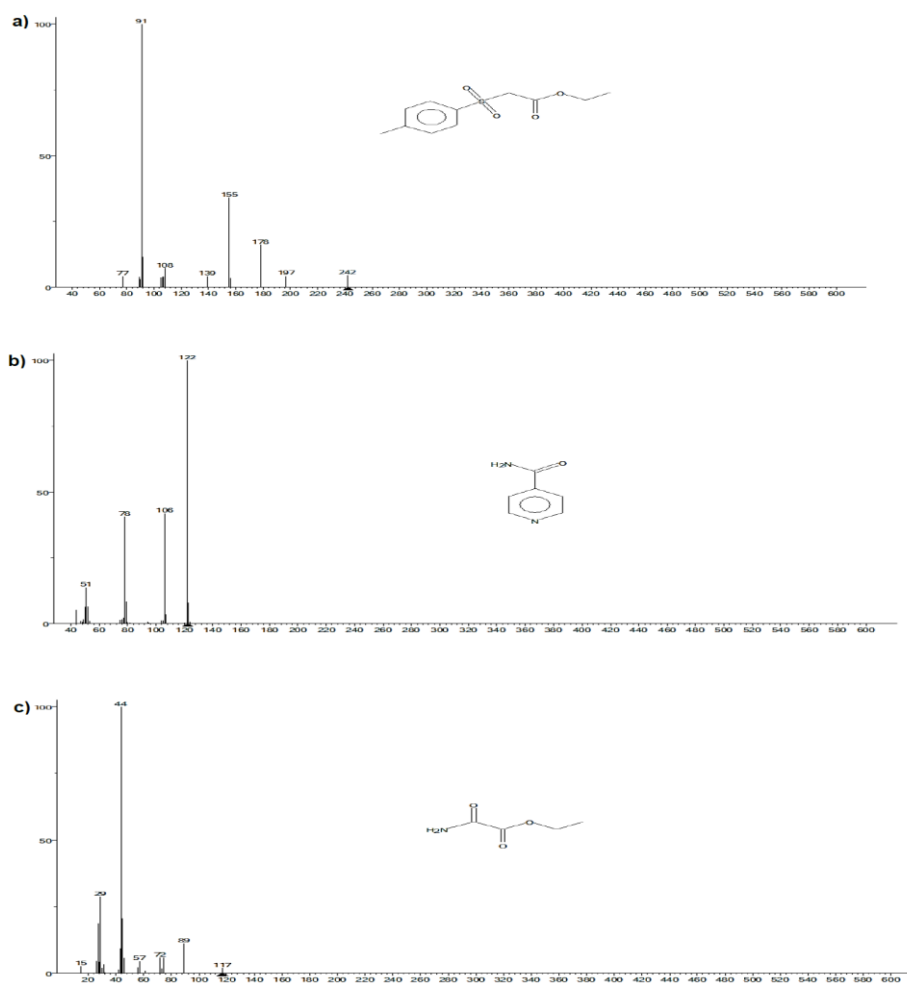


Fig. A7 Spectra of degradative metabolites of RY 145 produced by thermophilic coculture a) Ethyl oxamate; b) Pyridine-4-carboxylic acid amide; c) Acetic acid, (p-tolylsulfonyl)-, ethyl ester

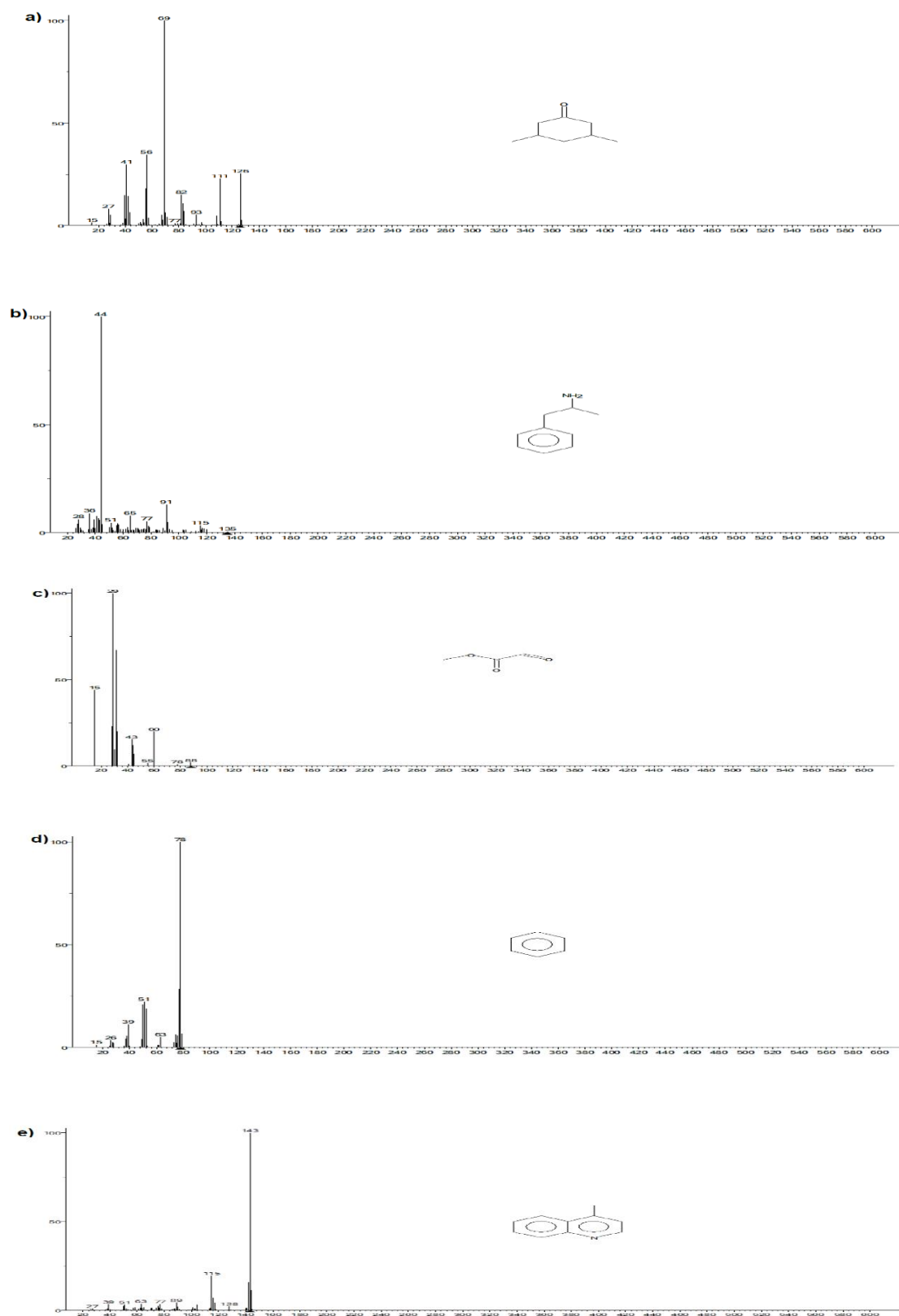


Fig. A8 Spectra of degradative metabolites of the dye mixture produced by thermophilic coculture a) Benzene; b) Methyl glyoxylate; c) 3,5-Dimethyl cyclohexanone; d) Dextroamphetamine peak; e) p-Methylquinoline

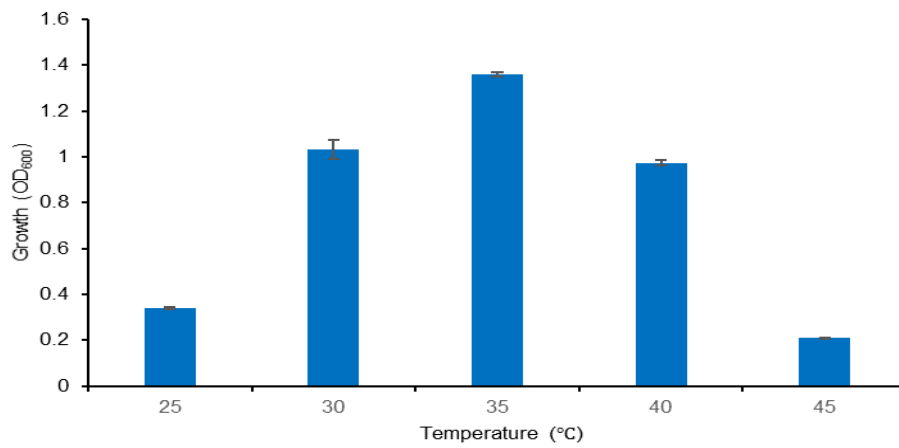


Fig. A9. Growth of mesophilic coculture at different temperatures in dye free medium

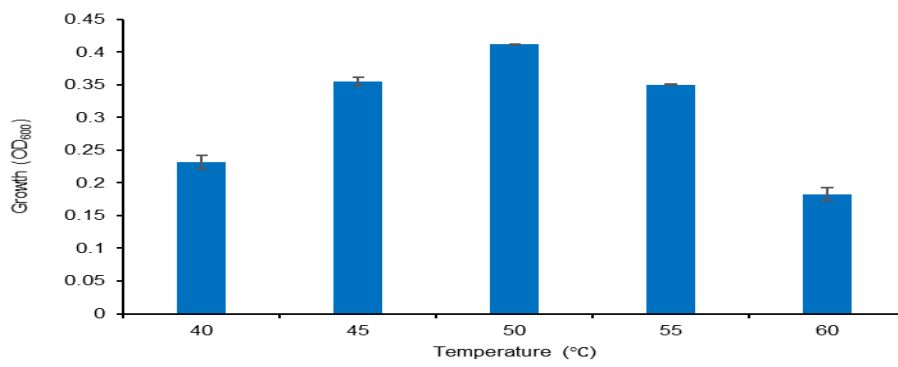


Fig. A10. Growth of thermophilic coculture at different temperatures in dye free medium

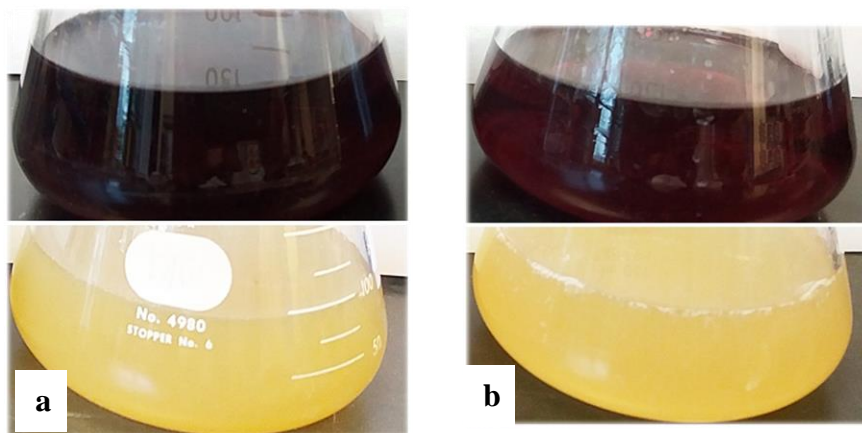


Fig. A11. Decolorization by cocultures a) mesophilic; b) thermophilic